

---

Computational Finite Elements  
and Methods of  
Static and Dynamic Analyses  
in MSC.NASTRAN and LS/DYNA

---

JULY 2011

Maverick United Consulting Engineers

**TABLE OF CONTENTS**

**ACKNOWLEDGEMENTS .....6**

**LIST OF SYMBOLS AND NOTATIONS .....7**

**1 INTRODUCTION.....10**

**2 CONCEPTS OF COMPUTATIONAL FINITE ELEMENT STRUCTURAL ANALYSIS .....11**

**2.1 OVERVIEW OF THE FINITE ELEMENT METHOD.....11**

2.1.1 **GL, ML Static Finite Element Elemental Formulation .....12**

2.1.1.1 The Principle of Virtual Displacements of The Principle of Virtual Work (Equivalent to the Variational Method or The Principle of Minimum Potential Energy) ..... 12

2.1.1.2 The Method of Weighted Residuals ..... 13

2.1.2 **GL, ML Static Finite Element Global Formulation .....15**

2.1.3 **GNL, MNL Static Finite Element Elemental Formulation.....18**

2.1.4 **GNL, MNL Static Finite Element Global Formulation .....23**

2.1.5 **How Nonlinear Analysis Varies From Linear Analysis .....26**

2.1.5.1 Geometric Nonlinearity ..... 26

2.1.5.2 Material Nonlinearity ..... 28

2.1.5.3 Contact and Boundary Conditions Nonlinearity ..... 28

2.1.6 **GL, ML and GNL, MNL Dynamic Finite Element Elemental and Global Formulation .....28**

**2.2 STATIC ANALYSIS CONCEPTS.....29**

2.2.1 **Overview of Methods of Structural Static Analyses .....29**

**2.3 DYNAMIC ANALYSIS CONCEPTS.....30**

2.3.1 **Overview of Methods of Structural Dynamic Analyses .....30**

2.3.1.1 Modal Analyses ..... 30

2.3.1.2 Forced Response Analyses ..... 30

2.3.2 **Nature of Trial Solution in Harmonic Frequency Vibrations .....32**

**2.4 STATIC AND DYNAMIC ANALYSES SEQUENCES.....33**

**3 METHODS OF STATIC ANALYSES .....36**

**3.1 GL, ML STATIC ANALYSIS BY THE IMPLICIT DIRECT STIFFNESS METHOD.....36**

3.1.1 **Mathematical Formulation of Analysis .....36**

3.1.2 **Concepts of Geometric Stiffness or P-Δ (K<sub>G</sub><sup>A</sup> From K<sub>E</sub><sup>A</sup>) Analysis .....37**

3.1.3 **Performing P-Δ (K<sub>G</sub><sup>A</sup> From K<sub>E</sub><sup>A</sup>) Linear Static Analysis – Direct Approach .....42**

3.1.4 **Performing P-Δ (K<sub>G</sub><sup>A</sup> From K<sub>E</sub><sup>A</sup>) Linear Static Analysis – Modal Approach; And Hence P-Δ Based Buckling .....44**

3.1.4.1 Objectives..... 44

3.1.4.2 Mathematical Formulation ..... 44

3.1.4.3 Critical Load Case Considerations ..... 46

3.1.4.4 Modelling (Modal) Imperfections ..... 47

3.1.4.5 Design ..... 51

3.1.4.6 Limitations ..... 52

3.1.4.7 Methodology ..... 53

3.1.5 **MSC.NASTRAN Decks .....56**

3.1.5.1 GL, ML Static Analysis..... 56

3.1.5.2 GL, ML P-Δ (K<sub>G</sub><sup>A</sup> From K<sub>E</sub><sup>A</sup>) Static Analysis ..... 65

3.1.5.3 GL, ML P-Δ (K<sub>G</sub><sup>A</sup> From Exact or Approximate K<sub>T</sub><sup>A</sup>) Static Analysis ..... 66

3.1.6 **Hand Methods Verification .....67**

3.1.6.1 Static Displacements by the Unit Load Method of the Virtual Work Principle ..... 67

3.1.6.2 BMD and SFD of Structures of Low Static Indeterminacies by Flexibility Analysis ..... 70

3.1.6.3 Bending Moments, Shear Force, and Displacements of Structural Elements by the Stiffness Method ..... 92

3.1.6.4 Bending Moments and Shear Force of Structures of Low Kinematic Indeterminacies by Moment Distribution ..... 93

3.1.6.5 Summary of Deflections and Effects ..... 117

3.1.6.6 Member Buckling Check Using The P-Δ Method To Incorporate Imperfections, Residual Stresses..... 158

3.1.6.7 Overall Portal Frame and Multi-Storey Building P-Δ Analysis Using The Amplified Sway Method..... 171

**3.2 GL, ML BUCKLING ANALYSIS BY THE IMPLICIT LINEARIZED EIGENVALUE ANALYSIS .....172**

3.2.1 **Linearization of Tangent Stiffness Matrix and Formulating The Linear Eigenvalue Problem..... 172**

<b>3.2.2</b>	<b>Problem Reduction and Trial Modes in Linear Buckling Analysis .....</b>	<b>178</b>
<b>3.2.3</b>	<b>Concepts of Linearized (<math>K_G^A</math> From <math>K_E^A</math>) Buckling Analysis .....</b>	<b>179</b>
<b>3.2.4</b>	<b>MSC.NASTRAN Decks .....</b>	<b>180</b>
3.2.4.1	GL, ML ( $K_G^A$ From $K_E^A$ ) Buckling Analysis.....	180
3.2.4.2	GL, ML ( $K_G^A$ From Exact or Approximate $K_T^A$ ) Buckling Analysis.....	186
<b>3.2.5</b>	<b>Hand Methods Verification .....</b>	<b>189</b>
3.2.5.1	Member or Local ( $K_G^A$ From $K_E^A$ ) Buckling.....	189
3.2.5.2	Overall System ( $K_G^A$ From $K_E^A$ ) Buckling.....	197
<b>3.3</b>	<b>GL, MNL PLASTIC COLLAPSE ANALYSIS BY THE IMPLICIT LINEAR SIMPLEX PROGRAMMING.....</b>	<b>208</b>
<b>3.3.1</b>	<b>Mathematical Formulation of Analysis .....</b>	<b>208</b>
<b>3.3.2</b>	<b>Mathematical Proof .....</b>	<b>211</b>
<b>3.3.3</b>	<b>Displacements and Rotations at Collapse.....</b>	<b>215</b>
<b>3.3.4</b>	<b>Plastic Limit Analysis of Simple Framed Structures.....</b>	<b>216</b>
3.3.4.1	Portal Frame.....	216
3.3.4.2	Parabolic Arch.....	222
3.3.4.3	Displacements and Rotations at Collapse.....	223
<b>3.3.5</b>	<b>Plastic Limit Analysis of Rectangular Multi-Storey Multi-Bay Frames with Improved Data Generation .....</b>	<b>225</b>
3.3.5.1	Two Storey Frame With Concentrated Loading.....	226
3.3.5.2	Three Storey Frame With Distributed Load.....	228
3.3.5.3	Multi-Bay Portal Frame.....	231
3.3.5.4	Vierendeel Truss.....	233
<b>3.3.6</b>	<b>Hand Methods Verification .....</b>	<b>234</b>
3.3.6.1	Plastic Collapse Analysis by Solving Equilibrium Equations.....	234
3.3.6.2	Plastic Collapse Analysis by Virtual Work (Hobbs).....	238
3.3.6.3	Plastic Collapse Analysis by Virtual Work (Chryssanthopoulos).....	240
<b>3.4</b>	<b>GNL, MNL, CONTACT NONLINEAR STATIC AND BUCKLING ANALYSIS BY THE IMPLICIT TRACING THE EQUILIBRIUM PATH METHOD .....</b>	<b>256</b>
<b>3.4.1</b>	<b>Mathematical Formulation of Tracing the Equilibrium Path .....</b>	<b>256</b>
<b>3.4.2</b>	<b>Newton-Raphson Load Control, Displacement Control or Arc-Length Control Algorithm .....</b>	<b>259</b>
<b>3.4.3</b>	<b>Equilibrium Paths, Stability of Equilibrium Paths, Critical Points, Stability of Critical Points .....</b>	<b>260</b>
<b>3.4.4</b>	<b>MSC.NASTRAN Decks .....</b>	<b>263</b>
3.4.4.1	GNL, MNL Load Control, Displacement Control or Arc-Length Control Static Analysis.....	263
3.4.4.2	Nonlinear Static and Linearized Eigenvalue Buckling Analysis.....	274
3.4.4.3	Nonlinear Static and Linear Eigenvalue Modal Dynamic Analysis.....	275
3.4.4.4	Restart From Nonlinear Static Analysis SOL 106 Into Nonlinear Static Analysis SOL 106.....	276
3.4.4.5	Restart From Nonlinear Static SOL 106 Into Linear Solution Schemes SOL 107 to SOL 112.....	276
3.4.4.6	Implicit Nonlinear Static (and Dynamic Analysis) SOL 400.....	276
3.4.4.7	Implicit Nonlinear Static (and Dynamic Analysis) SOL 600.....	276
<b>3.5</b>	<b>GNL, MNL STATIC AND BUCKLING ANALYSIS BY DYNAMIC RELAXATION .....</b>	<b>277</b>
<b>3.5.1</b>	<b>Dynamic Relaxation of the Explicit Finite Difference Scheme Solving Newton's Dynamic Equilibrium ODE (LS-DYNA).....</b>	<b>277</b>
<b>3.5.2</b>	<b>LS-DYNA (GNL, MNL Explicit Transient) Dynamic Relaxation Cards .....</b>	<b>280</b>
<b>4</b>	<b>METHODS OF DYNAMIC ANALYSES .....</b>	<b>282</b>
<b>4.1</b>	<b>GL, ML IMPLICIT REAL MODAL (EIGENVALUE) ANALYSIS .....</b>	<b>282</b>
<b>4.1.1</b>	<b>Mathematical Formulation of Analysis .....</b>	<b>282</b>
<b>4.1.2</b>	<b>MSC.NASTRAN Decks .....</b>	<b>286</b>
4.1.2.1	GL, ML Real Modal Analysis.....	286
4.1.2.2	GL, ML P- $\Delta$ ( $K_G^A$ From $K_E^A$ ) Real Modal Analysis.....	287
4.1.2.3	GL, ML P- $\Delta$ ( $K_G^A$ From Exact or Approximate $K_T^A$ ) Real Modal Analysis.....	289
<b>4.1.3</b>	<b>Hand Methods Verification .....</b>	<b>290</b>
4.1.3.1	Natural Frequency and Free Vibration Response of SDOF Systems.....	290
4.1.3.2	Natural Frequencies of MDOF Systems.....	293
4.1.3.3	Natural Frequencies of Distributed Systems.....	305
4.1.3.4	Natural Frequencies By Exactly Solving the Partial Differential Equilibrium Equation.....	306
4.1.3.5	Approximate Formulae.....	311
<b>4.2</b>	<b>GL, ML IMPLICIT DIRECT COMPLEX MODAL (EIGENVALUE) ANALYSIS.....</b>	<b>313</b>
<b>4.2.1</b>	<b>Mathematical Formulation of Analysis .....</b>	<b>313</b>
<b>4.2.2</b>	<b>Complexity of Modes of Vibration.....</b>	<b>314</b>
<b>4.2.3</b>	<b>Complex Modal Analysis To Determine Modal Damping Values.....</b>	<b>314</b>
<b>4.2.4</b>	<b>MSC.NASTRAN Decks .....</b>	<b>315</b>
4.2.4.1	GL, ML Complex Modal Analysis.....	315
4.2.4.2	GL, ML P- $\Delta$ ( $K_G^A$ From $K_E^A$ ) Complex Modal Analysis.....	317
4.2.4.3	GL, ML P- $\Delta$ ( $K_G^A$ From Exact or Approximate $K_T^A$ ) Complex Modal Analysis.....	319
<b>4.2.5</b>	<b>Hand Methods Verification .....</b>	<b>320</b>

4.2.5.1	Determination of Damped Natural Frequency and the Maximum Dynamic Displacement, $u_{max}$ for Free Damped Vibration Due to Initial Displacement and/or Initial Velocity by Classically Solving the SDOF Linear ODE and Maximizing the Solution .....	320
<b>4.3</b>	<b>GL, ML IMPLICIT (REAL) MODAL FREQUENCY RESPONSE ANALYSIS .....</b>	<b>323</b>
4.3.1	Nature of the Dynamic Loading Function .....	323
4.3.2	Mathematical Formulation of Analysis .....	323
4.3.3	Capability of A Finite Number of Modes To Model The Static and Dynamic Response of Structure .....	328
4.3.4	Complex Response $F(\omega)$ and Amplification $D(\omega)$ With Elemental and/or Modal Structural Damping .....	331
4.3.5	Representation of A MDOF System As A SDOF system .....	332
4.3.6	MSC.NASTRAN Decks .....	334
4.3.6.1	GL, ML Modal Forced Frequency Response Analysis .....	334
4.3.6.2	GL, ML P- $\Delta$ ( $K_G^A$ From $K_E^A$ ) Modal Forced Frequency Response Analysis .....	337
4.3.6.3	GL, ML P- $\Delta$ ( $K_G^A$ From Exact or Approximate $K_T^A$ ) Modal Forced Frequency Response Analysis .....	339
4.3.7	Hand Methods Verification .....	340
4.3.7.1	Determination of Maximum Dynamic Displacement for Deterministic Frequency Domain Loading by Transforming the Coupled MDOF Linear Damped ODEs To a Set of Independent (Uncoupled) SDOF ODEs and Solving the Independent Equations in a Manner Similar to Solving a SDOF ODE .....	340
<b>4.4</b>	<b>GL, ML IMPLICIT (COMPLEX) MODAL FREQUENCY RESPONSE ANALYSIS .....</b>	<b>349</b>
4.4.1	Mathematical Formulation of Analysis .....	349
<b>4.5</b>	<b>GL, ML IMPLICIT DIRECT FREQUENCY RESPONSE ANALYSIS .....</b>	<b>352</b>
4.5.1	Nature of the Dynamic Loading Function .....	352
4.5.2	Mathematical Formulation of Analysis .....	352
4.5.3	MSC.NASTRAN Decks .....	355
4.5.3.1	GL, ML Direct Forced Frequency Response Analysis .....	355
4.5.3.2	GL, ML P- $\Delta$ ( $K_G^A$ From $K_E^A$ ) Direct Forced Frequency Response Analysis .....	365
4.5.3.3	GL, ML P- $\Delta$ ( $K_G^A$ From Exact or Approximate $K_T^A$ ) Direct Forced Frequency Response Analysis .....	367
4.5.4	Hand Methods Verification .....	368
4.5.4.1	The Theory of the Dynamic Magnification Factor for Undamped Motion and Hence the Determination of Maximum Dynamic Displacement, $u_{max}$ for Deterministic Harmonic Loading by Classically Solving the SDOF Linear Undamped ODE and Maximizing the Solution .....	368
4.5.4.2	The Theory of the Dynamic Magnification Factor for Damped Motion and Hence Determination of Maximum Dynamic Displacement, $u_{max}$ for Deterministic Harmonic Loading by Classically Solving the SDOF Linear Damped ODE and Maximizing the Solution .....	370
4.5.4.3	The Theory of Vibration (Base) Isolation and the Force Transmitted Into Rigid Foundation by the Damped Structure Subjected to Deterministic Harmonic Loading .....	375
4.5.4.4	The Theory of Vibration (Base) Isolation and the Determination of Maximum Dynamic Displacement, $u_{max}$ for Deterministic Harmonic Support Motion (Displacement, Velocity or Acceleration) by Classically Solving the SDOF Linear Damped ODE (in Absolute and Relative Terms) and Maximizing the Solution .....	377
<b>4.6</b>	<b>GL, ML FREQUENCY DOMAIN ANALYSIS – DETERMINISTIC AND RANDOM DYNAMIC RESPONSE ANALYSIS .....</b>	<b>380</b>
4.6.1	Mathematical Preliminaries of Representing Dynamic Characteristics in the Frequency Domain .....	380
4.6.2	GL, ML Vibration Testing .....	381
4.6.2.1	Vibration Testing for Model Correlation .....	381
4.6.2.2	Vibrating Testing For Analysis Procedure Verification .....	384
4.6.3	GL, ML Steady-State Response of Deterministic Periodic (Not Necessarily Harmonic) Long Duration Excitation Utilizing Fourier Series (or Generally Utilizing Fast Fourier Transforms FFT) .....	385
4.6.3.1	Fourier Series .....	385
4.6.3.2	Discrete Fourier Series .....	386
4.6.3.3	Discrete Fourier Series in Complex Notation .....	387
4.6.3.4	Double Sided Discrete Fourier Series in Complex Notation .....	388
4.6.3.5	Normalized Double Sided Discrete Fourier Series in Complex Notation .....	389
4.6.3.6	Symmetrical Normalized Double Sided Discrete Fourier Series in Complex Notation .....	390
4.6.3.7	Symmetrical Normalized Single Sided Discrete Fourier Series in Complex Notation .....	391
4.6.3.8	Practicalities of the Specification of the Fast Fourier Transform (FFT) Representation .....	392
4.6.3.9	MSC.NASTRAN Fast Fourier Transform Analysis Methodology .....	394
4.6.4	GL, ML Steady-State Response of Random, Gaussian, and Stationary (and Ergodic) Excitations Utilizing Power Spectral Density (PSD) Functions .....	397
4.6.4.1	Statistic of Time Domain Function .....	397
4.6.4.2	Definition of the Power Spectral Density (PSD) .....	401
4.6.4.3	Validity of the PSD Representation .....	404
4.6.4.4	Generation and Specification of the PSD .....	405
4.6.4.5	Statistical Information Provided by the PSD .....	406
4.6.4.6	MSC.NASTRAN Random Analysis Methodology .....	409
<b>4.7</b>	<b>GL, ML IMPLICIT (REAL) MODAL TRANSIENT RESPONSE ANALYSIS .....</b>	<b>413</b>
4.7.1	Nature of the Dynamic Loading Function .....	413
4.7.2	Mathematical Formulation of Analysis .....	413
4.7.3	Capability of A Finite Number of Modes To Model The Static and Dynamic Response of Structure .....	418
4.7.4	Concepts of Equivalent Static Force .....	427
4.7.5	Structural Damping in Time Domain Analyses .....	429
4.7.6	MSC.NASTRAN Decks .....	431
4.7.6.1	GL, ML Modal Forced Transient Response Analysis .....	431
4.7.6.2	GL, ML P- $\Delta$ ( $K_G^A$ From $K_E^A$ ) Modal Forced Transient Response Analysis .....	434

4.7.6.3	GL, ML P- $\Delta$ ( $K_G^A$ From Exact or Approximate $K_T^A$ ) Modal Forced Transient Response Analysis .....	436
<b>4.7.7</b>	<b>Hand Methods Verification .....</b>	<b>437</b>
4.7.7.1	Determination of Maximum Dynamic Displacement for Deterministic Time Domain Loading by Transforming the Coupled MDOF Linear Undamped ODEs To a Set of Independent (Uncoupled) SDOF ODEs and Solving the Independent Equations in a Manner Similar to Solving a SDOF ODE 437	
4.7.7.2	Determination of Max Dynamic Displacement for Deterministic Time Domain Support Motion (Displacement, Velocity or Acceleration) by Transforming the Coupled MDOF Linear Undamped ODEs (In Relative Terms) To a Set of Independent (Uncoupled) SDOF ODEs (In Relative Terms) and Solving the Independent Equations in a Manner Similar to Solving a SDOF ODE .....	446
4.7.7.3	Determination of Maximum Dynamic Displacement for Deterministic Time Domain Loading by Transforming the Coupled Distributed System Linear Damped ODEs (from the governing PDE) To A Set of Independent (Uncoupled) SDOF ODEs and Solving the Independent Equations in a Manner Similar to Solving a SDOF ODE .....	450
<b>4.8</b>	<b>GL, ML IMPLICIT DIRECT TRANSIENT RESPONSE ANALYSIS.....</b>	<b>451</b>
<b>4.8.1</b>	<b>Nature of the Dynamic Loading Function.....</b>	<b>451</b>
<b>4.8.2</b>	<b>Mathematical Formulation of Analysis .....</b>	<b>451</b>
<b>4.8.3</b>	<b>MSC.NASTRAN Decks .....</b>	<b>454</b>
4.8.3.1	GL, ML Direct Forced Transient Response Analysis .....	454
4.8.3.2	GL, ML P- $\Delta$ ( $K_G^A$ From $K_E^A$ ) Direct Forced Transient Response Analysis.....	464
4.8.3.3	GL, ML P- $\Delta$ ( $K_G^A$ From Exact or Approximate $K_T^A$ ) Direct Forced Transient Response Analysis .....	466
<b>4.8.4</b>	<b>Hand Methods Verification .....</b>	<b>467</b>
4.8.4.1	Determination of Maximum Dynamic Displacement, $u_{max}$ by Solving the SDOF Undamped/Damped Linear Equation of Motion ODE for Deterministic Time Domain Loading With/Without Initial Conditions Using the Convolution Integral (Duhamel's integral) .....	467
4.8.4.2	Determination of Maximum Dynamic Displacement, $u_{max}$ by Solving the SDOF Undamped/Damped Linear Equation of Motion ODE (In Relative Terms) for Deterministic Time Domain Support Motion (Displacement, Velocity or Acceleration) With/Without Initial Conditions Using the Convolution Integral (Duhamel's integral).....	474
<b>4.9</b>	<b>GNL, MNL IMPLICIT AND EXPLICIT DIRECT TRANSIENT RESPONSE ANALYSIS .....</b>	<b>475</b>
<b>4.9.1</b>	<b>Nature of the Dynamic Loading Function.....</b>	<b>475</b>
<b>4.9.2</b>	<b>Deterministic Non-Periodic Short Duration Impulse (a.k.a. Blast) Loading Functions With Subsequent Wave Propagation 476</b>	
<b>4.9.3</b>	<b>Projectile Crash (a.k.a. Impact) (and Impulsive Blast) Analysis With Subsequent Wave Propagation .....</b>	<b>477</b>
<b>4.9.4</b>	<b>Brittle Snap or Redundancy Check Excitation.....</b>	<b>480</b>
<b>4.9.5</b>	<b>GNL, MNL Explicit Central FD Scheme for Newton's Dynamic Equilibrium ODE (LS-DYNA).....</b>	<b>485</b>
4.9.5.1	Solution of Partial or Ordinary Differential Equations Using Finite Difference (FD) Schemes .....	485
4.9.5.2	Mathematical Formulation of Analysis – Explicit Central Finite Difference Scheme .....	486
4.9.5.3	Stability .....	487
4.9.5.4	Accuracy .....	488
<b>4.9.6</b>	<b>GNL, MNL Implicit Newmark Scheme for Newton's Dynamic Equilibrium ODE (MSC.NASTRAN).....</b>	<b>489</b>
4.9.6.1	Mathematical Formulation of Analysis – Implicit Newmark Scheme .....	489
4.9.6.2	Stability .....	491
4.9.6.3	Accuracy .....	491
<b>4.9.7</b>	<b>Comparison Between Implicit and Explicit Time Integration Schemes .....</b>	<b>492</b>
<b>4.9.8</b>	<b>MSC.NASTRAN Decks .....</b>	<b>494</b>
4.9.8.1	GNL, MNL Direct Forced (Implicit) Transient Response Analysis .....	494
4.9.8.2	Nonlinear Static Analysis and Nonlinear Transient Analysis .....	498
4.9.8.3	Restart From Nonlinear Static Analysis SOL 106 Into Nonlinear Transient Analysis SOL 129 .....	498
4.9.8.4	Restart From Nonlinear Transient Analysis SOL 129 Into Nonlinear Transient Analysis SOL 129.....	498
4.9.8.5	Implicit Nonlinear (Static and) Dynamic Analysis SOL 400.....	499
4.9.8.6	Implicit Nonlinear (Static and) Dynamic Analysis SOL 600.....	499
4.9.8.7	Explicit Nonlinear Dynamic Analysis SOL 700.....	499
<b>4.9.9</b>	<b>LS-DYNA Decks.....</b>	<b>500</b>
4.9.9.1	GNL, MNL Direct Forced (Explicit) Transient Response Analysis .....	500
<b>4.9.10</b>	<b>Hand Methods Verification .....</b>	<b>502</b>
4.9.10.1	Determination of Displacement Response Time History by Solving the SDOF Nonlinear (in Stiffness, Damping and Displacement) Equation of Motion ODE for Deterministic Time Domain Loading With/Without Initial Conditions by Implicit Newmark- $\beta$ Time Integration Schemes .....	502
<b>BIBLIOGRAPHY.....</b>		<b>504</b>

## **ACKNOWLEDGEMENTS**

My humble gratitude to the Almighty, to Whom this and all work is dedicated.

A special thank you also to my teachers at Imperial College of Science, Technology and Medicine, London and my fellow engineering colleagues at Ove Arup and Partners London and Ramboll Whitbybird London.

**Maverick United Consulting Engineers**

## LIST OF SYMBOLS AND NOTATIONS

### Elemental Notations

$\{y\}$	=	displacement function
$[N]$	=	shape functions matrix
$\{f\}$	=	element forces in element axes including fixed end forces
$\{d\}$	=	element deformation in element axes
$\{b\}$	=	element body forces
$[k]$	=	element constitutive matrix
$[m]$	=	element mass matrix
$[c]$	=	element viscous damping matrix
$\{p\}$	=	element nodal loading vector
$[T]$	=	transformation matrix
$W$	=	work done by external loads

### SDOF, MDOF and Modal Dynamic Equation of Motion Notations

$m$	=	SDOF mass
$[M]$	=	Global MDOF mass matrix
$c$	=	SDOF viscous damping constant
$[C]$	=	Global MDOF viscous damping matrix
$k$	=	SDOF stiffness
$[K]$	=	Global MDOF stiffness matrix
$u$	=	SDOF displacement
$\{u\}, \{U\}$	=	Global MDOF displacement matrix
$\{P\}$	=	Global nodal loading vector
$M_i, [M]$	=	Modal (generalized) mass and modal (generalized) mass matrix
$C_i, [C]$	=	Modal (generalized) damping and modal (generalized) damping matrix
$K_i, [K]$	=	Modal (generalized) stiffness and modal (generalized) stiffness matrix
$\xi_i, \{\xi_i\}$	=	Modal displacement response and modal displacement response vector

### SDOF Dynamic Notations

$\omega_n$	=	Natural circular frequency, $(k/m)^{1/2}$
$\omega_d$	=	Damped natural circular frequency, $\omega_n(1-\zeta^2)^{1/2}$
$\omega$	=	Frequency of forcing function
$c$	=	Viscous damping constant
$c_{cr}$	=	Critical viscous damping constant, $2(km)^{1/2} = 2m\omega_n$
$\zeta$	=	Damping ratio (fraction of critical), $c/c_{cr}$
$\delta$	=	Logarithmic decrement

### SDOF Free Vibrational Notations

$G$	=	Complex starting transient response function, $G = G_R + iG_I$
-----	---	--

### SDOF Time Domain Loading and Transient and Steady-State Response Notations

$P(t)$	=	Loading function
$p_0$	=	Force excitation amplitude
$p_0/k$	=	Static displacement
$D(t)$	=	Dynamic amplification factor

$D_{\max}$	=	Maximum dynamic amplification factor
$u(t)$	=	Displacement response, $D(t)(p_0/k)$
$u_{\max}$	=	Maximum displacement response, $D_{\max}(p_0/k)$

### Modal Time Domain Loading and Transient and Steady-State Notations

$\{P(t)\}$	=	Loading function vector
$P_i(t)$	=	Modal loading function, $P_i(t) = \{\phi_i\}^T \{P(t)\}$
$\rho_{0i}$	=	Modal force excitation amplitude
$\rho_{0i}/K_i$	=	Modal static displacement
$D_i(t)$	=	Modal dynamic amplification factor
$D_{i \max}$	=	Modal maximum dynamic amplification factor
$\xi_i(t)$	=	Modal displacement response, $\xi_i(t) = D_i(t)\rho_{0i}/K_i$
$\xi_{i \max}$	=	Modal maximum displacement response, $\xi_{i \max} = D_{i \max} \rho_{0i}/K_i$
$\{u(t)\}$	=	Displacement response vector, $\{u(t)\} = [\Phi]\{\xi(t)\}$

### SDOF Frequency Domain Loading and Steady-State Response Notations

$P(t)$	=	SDOF Time domain harmonic loading function, $P(t) = \text{Real} [ P(\omega)e^{i\omega t} ]$
$P(\omega)$	=	SDOF frequency domain complex harmonic loading function
$p_0$	=	SDOF harmonic loading amplitude
$p_0/k$	=	SDOF static displacement
$D(\omega)$	=	SDOF (magnitude of the) dynamic amplification factor
$D_{\text{resonant}}$	=	SDOF (magnitude of the) dynamic amplification factor at resonance when $\omega = \omega_n$
$D_{\max}$	=	SDOF maximum (magnitude of the) dynamic amplification factor when $\omega = \omega_n(1-2\zeta^2)^{1/2}$
$F(\omega)$	=	SDOF complex displacement response function (FRF), $F(\omega) = D(\omega)(p_0/k)e^{-i\theta}$
$H(\omega)$	=	SDOF transfer function, $H(\omega) = D(\omega)(1/k)e^{-i\theta}$
$F_{\text{resonant}}$	=	SDOF complex displacement response function at resonance, $F_{\text{resonant}} = D_{\text{resonant}}(p_0/k)e^{-i\theta}$
$F_{\max}$	=	SDOF complex maximum displacement response function, $F_{\max} = D_{\max}(p_0/k)e^{-i\theta}$
$u(t)$	=	SDOF time domain displacement response, $u(t) = \text{Real} [ F(\omega)e^{i\omega t} ]$
$u_{\text{resonant}}$	=	SDOF time domain displacement response at resonance, $u(t) = \text{Real} [ F_{\text{resonant}} e^{i\omega t} ]$
$u_{\max}$	=	SDOF time domain maximum displacement response, $u(t) = \text{Real} [ F_{\max} e^{i\omega t} ]$
$T_r$	=	SDOF transmissibility of displacement, acceleration or force

### Modal Frequency Domain Loading and Steady-State Response Notations

$\{P(t)\}$	=	Time domain harmonic loading function vector, $\{P(t)\} = \text{Real} [ \{P(\omega)\} e^{i\omega t} ]$
$\{P(\omega)\}$	=	Frequency domain complex harmonic loading function vector
$P_i(\omega)$	=	Modal frequency domain complex harmonic loading function vector, $P_i(\omega) = \{\phi_i\}^T \{P(\omega)\}$
$\rho_{0i}$	=	Modal harmonic loading amplitude
$\rho_{0i}/K_i$	=	Modal static displacement
$D_i(\omega)$	=	Modal (magnitude of the) dynamic amplification factor
$D_{i \text{ resonant}}$	=	Modal (magnitude of the) dynamic amplification factor at resonance when $\omega = \omega_{ni}$
$D_{i \max}$	=	Modal maximum (magnitude of the) dynamic amplification factor when $\omega = \omega_{ni}(1-2\zeta_i^2)^{1/2}$
$\xi_i(\omega)$	=	Modal complex displacement response function (FRF), $\xi_i(\omega) = D_i(\omega)\rho_{0i}/K_i e^{-i\theta_i}$
$\xi_{i \text{ resonant}}$	=	Modal complex displacement response function at resonance, $\xi_{i \text{ resonant}} = D_{i \text{ resonant}} \rho_{0i}/K_i e^{-i\theta_i}$
$\xi_{i \max}$	=	Modal complex maximum displacement response function, $\xi_{i \max} = D_{i \max} \rho_{0i}/K_i e^{-i\theta_i}$
$\{u(t)\}$	=	Time domain displacement response vector, $\{u(t)\} = \text{Real} [ [\Phi]\{\xi(\omega)\}e^{i\omega t} ]$

### Additional Abbreviations

ML: Materially Linear  
MNL: Materially Nonlinear  
GL: Geometrically Linear  
GNL: Geometrically Nonlinear  
[] = matrix  
{ } = column vector  
< > = row vector

## **1 INTRODUCTION**

This paper serves as a guide to performing effective static and dynamic structural analyses with MSC.NASTRAN in particular, although the concepts described herein are also equally applicable to other analysis codes.

A disbeliever wonders if the answer provided by a finite element analysis is correct. The question is not whether the correct answer has been obtained, but rather if the correct question was asked, for the answer will always be correct.

## 2 CONCEPTS OF COMPUTATIONAL FINITE ELEMENT STRUCTURAL ANALYSIS

### 2.1 Overview of the Finite Element Method

An overview of the steps performed in the finite element method is presented as follows: -

*step 1: formulate element stiffness equations*

$$\{f\} = [k] \cdot \{d\}$$

Examples include the beam, plate, shell, brick and spring element formulations.

*step 2: transform [k] into global axes and merge all element formulations into the global stiffness matrix [K]*

$$[K] = [T]^T \cdot [k] \cdot [T]$$

*step 3: formulate the governing equation for the particular type of structural analysis*

$$\{P\} = [K] \cdot \{U\}$$

This above is described for the linear static analysis i.e.  $\{P\} = [K] \cdot \{U\}$ . For other analyses, although the governing equation differs, the method is similar. Other analyses for example are the linear modal analysis, linear buckling analysis, nonlinear static analysis and linear and nonlinear dynamic analyses.

*step 4: solve by Gaussian Elimination to obtain {U}*

$$\{U\} = [K]^{-1} \cdot \{P\}$$

This again is described for the linear static analysis for which the solution gives us the deflection plot  $\{U\}$ . Other forms of analyses will yield different results such as mode shapes  $\{\phi\}$ , acceleration  $\{\ddot{U}\}$  or velocity  $\{\dot{U}\}$ .

*step 5: transform {U} back to local axes and solve for element stresses*

$$\{d\} = [T] \cdot \{U\}$$

$$\{f\} = [k] \cdot \{d\} = [k] \cdot [T] \cdot \{U\}$$

This now gives us the element stresses  $\{f\}$ . The element stresses include the bending moments, shear forces, axial forces, torsional moments and all types of normal and shear stresses.

### 2.1.1 GL, ML Static Finite Element Elemental Formulation

The elemental stiffness formulation of the finite element describes the stiffness behavior of an element. The finite element elemental stiffness formulation describes the force-displacement relationship of a finite number of degrees of freedom of the element. This relationship can be formulated by one of two general methods as described below.

#### 2.1.1.1 The Principle of Virtual Displacements of The Principle of Virtual Work (Equivalent to the Variational Method or The Principle of Minimum Potential Energy)

The stiffness of a linear system is based on the stiffness at the initial undeformed state. Define state A as the initial undeformed state. The variation of displacement within a finite element can be presented as a function of the matrix of shape functions [N] and the discrete nodal degree of freedom displacement vector {d} as

$$\{y\} = [N]\{d\}$$

Vector {y} describes the general displacement function (interpolation function) within the finite element, {d} is the unknown nodal DOFs and [N] are their corresponding shape functions.

The general strain vector {ε} in terms of {d} can then be derived as the strain is some derivative function of the displacement function and hence the nodal DOFs {d}

$$\{\varepsilon\} = [B^A]\{d\}$$

The general stress vector {σ} can then be established in terms of the strains and hence be expressed in terms of the DOFs {d} amongst other terms

$$\{\sigma\} = [D^A][B^A]\{d\} + \{\sigma\}_i - [D^A]\{\varepsilon\}_i$$

The second term is due to the initial stresses (such as residual stresses within the element) and the third term is the initial strains due to **temperature shrinkage** or **lack of fit**.

**Two equivalent fundamental theorems of structural analysis are the principle of virtual displacements (virtual work) and the principle of minimum potential energy.** These theorems provide the fundamental Newton's equilibrium equations for the finite element. The principle of virtual displacements (virtual work) states that a structural system is in equilibrium in its deflected configuration if the external work performed by the applied loading over any possible infinitesimal displacement mode is equal to the internal work performed by the component forces over the corresponding compatible infinitesimal deformations. In other words, a system is in equilibrium when the external work done equates the internal work. The equivalent principle of minimum potential energy states that a structural system is in equilibrium in its deflected configuration if its total potential energy (V), consisting of the system strain energy (U) and the loading potential energy (-W), is stationary with respect to any infinitesimal variation in the possible deformation modes.

For a finite element, the equilibrium equation is thus derived by equating the external work to the internal energy for a virtual displacement set.

$$\begin{aligned} & (\text{Virtual Nodal Disp}) \times (\text{Real Nodal Forces}) + (\text{Virtual General Disp}) \times (\text{Real Distributed Forces}) \\ & = (\text{Virtual Strains Or Deformations}) \times (\text{Real Stresses Or Actions}) \end{aligned}$$

$$\delta\{d\}^T \{f\} + \int_{\Omega} \delta\{y\}^T \{b\} d\Omega = \int_{\Omega} \delta\{\varepsilon\}^T \{\sigma\} d\Omega$$

where  $\{f\}$  is the nodal force vector and  $\{b\}$  is the distributed body forces within the finite element. We have however established that

$$\begin{aligned}\{y\} &= [N]\{d\} & \text{hence} & \{y\}^T = \{d\}^T [N]^T \\ \{\varepsilon\} &= [B^A]\{d\} & \text{hence} & \{\varepsilon\}^T = \{d\}^T [B^A]^T \\ \{\sigma\} &= [D^A][B^A]\{d\} + \{\sigma\}_i - [D^A]\{\varepsilon\}_i\end{aligned}$$

hence

$$\delta\{d\}^T \{f\} + \int_{\Omega} \delta\{d\}^T [N]^T \{b\} d\Omega = \int_{\Omega} \delta\{d\}^T [B^A]^T [D^A][B^A]\{d\} d\Omega + \int_{\Omega} \delta\{d\}^T [B^A]^T \{\sigma\}_i d\Omega - \int_{\Omega} \delta\{d\}^T [B^A]^T [D^A]\{\varepsilon\}_i d\Omega$$

The above expression is valid for any virtual displacement  $\delta\{d\}$ . Choosing unity virtual displacements we arrive at the elemental equilibrium equations

$$\{f\} = \left\{ \int_{\Omega} [B^A]^T [D^A][B^A] d\Omega \right\} \{d\} + \left\{ \int_{\Omega} [B^A]^T \{\sigma\}_i d\Omega \right\} - \left\{ \int_{\Omega} [B^A]^T [D^A]\{\varepsilon\}_i d\Omega \right\} - \left\{ \int_{\Omega} [N]^T \{b\} d\Omega \right\}$$

This is the expression that is set up for each and every element. If the nodal force vector  $\{f\}$  is known, then the only remaining unknown within these equations are the nodal displacement vector  $\{d\}$ . Note that we have defined  $[B]$  the strain matrix,  $\{\sigma\}_i$  the initial stresses,  $[D]$  the material constitutive matrix,  $\{\varepsilon\}_i$  the initial strains,  $[N]$  = shape functions matrix,  $\{b\}$  = the elemental (external) body loads and of course  $\{d\}$  = nodal element displacement in element axes.

To summarize the terms in the above elemental static equilibrium equation expression

- (i) the term on the LHS is the nodal force vector in element axis
- (ii) the first term on the RHS is the instantaneous stiffness matrix
- (iii) the second, third and fourth terms on the RHS are the so-called **fixed end forces**

We note that the choice of the shape functions  $[N]$  affects the accuracy of

- (i) the elemental instantaneous stiffness matrix
- (ii) the fixed end forces

The important concept to grasp is that geometrically linear (GL) finite elements have linear strain-displacement relationships i.e. the  $[B^A]$  matrix would be constant and thus independent of the nodal displacements  $\{d\}$ . Materially linear (ML) finite elements have linear stress-strain relationships i.e. the  $[D^A]$  matrix would be constant and thus independent of the strain vector  $\{\varepsilon\}$ .

### 2.1.1.2 The Method of Weighted Residuals

We have seen that the principle of virtual displacements or the principle of minimum potential energy (variational approach) can be used to establish the element stiffness matrix. The shape function  $[N]$  is applied to the variational statement in the discretization.

Another method of establishing the elemental stiffness matrix is the method of weighted residuals. Here, instead of applying the shape functions  $[N]$  to the variational statement, it is applied to the so-called *weak* statement. The *weak* statement is a perfectly equivalent integral form of the *strong* statement which is the governing Newton's differential equation representing the equilibrium of the element internal and external forces. The *weak* statement of a differential equation (*strong* statement) can be stated as

$$\int_{\Omega} v(\text{Differential Equation}) d\Omega + \bar{v}(\text{Natural Boundary Conditions of the Differential Equation}) = 0$$

for any function of  $v$  and  $\bar{v}$ .

The weak statement is perfectly equivalent to the strong statement. The shape function  $[N]$  is applied to the differential equation. Any shape function  $[N]$  that satisfies the strong statement also satisfies the weak statement. The functions  $v$  and  $v$  are the weighting function for the error in the differential equation and the natural boundary conditions respectively. The weak statement is perfectly equivalent to the strong statement if the weak statement is satisfied for any weighting functions whatsoever. In words, the weak statement states that the residual errors in the approximation of the original differential equation and the natural boundary condition weighted by the weighting functions are zero, hence the name weighted residual methods. This does not mean that the error in the strong statement is zero, as there will still be approximations in the shape functions  $[N]$ . On top of that, usually, the weak statement will not be satisfied for all weighting functions. The choice of the finite weighting functions define the various different methods of weighted residuals.

Two common methods within the method of weighted residuals are the sub-domain collocation method and the popular Galerkin method (which is equivalent to the variational approach). The sub-domain collocation method divides the geometric domain into as many sub-domains as there are DOFs with the weighting functions having a value of unity in a particular sub-domain and zero in all other sub-domains leading to *one* equation from the weak statement. The weighting functions are also put to unity at other sub-domains in turn, leading to a set of simultaneous equations which formulate the elemental stiffness matrix.

In the Galerkin approach, the weighting functions are identical to the shape functions. Since there are as many shape functions as there as DOFs, each shape function is applied to the weak statement for an equation. This leads to a set of simultaneous equations which formulate the elemental stiffness matrix. The Galerkin approach is actually exactly equivalent to the variational approach.

### 2.1.2 GL, ML Static Finite Element Global Formulation

The following describes the assembly of the element stiffness matrices towards the formulation of the global system stiffness matrix by the use of the equilibrium, compatibility and constitutive laws. We have shown that the elemental equilibrium equations are

$$\begin{aligned} \{f\} &= \left\{ \int_{\Omega} [B^A]^T [D^A] [B^A] d\Omega \right\} \{d\} + \left\{ \int_{\Omega} [B^A]^T \{\sigma\}_i d\Omega \right\} - \left\{ \int_{\Omega} [B^A]^T [D^A] \{\varepsilon\}_i d\Omega \right\} - \left\{ \int_{\Omega} [N]^T \{b\} d\Omega \right\} \\ &= [k_E^A] \{d\} + \left\{ \int_{\Omega} [B^A]^T \{\sigma\}_i d\Omega \right\} - \left\{ \int_{\Omega} [B^A]^T [D^A] \{\varepsilon\}_i d\Omega \right\} - \left\{ \int_{\Omega} [N]^T \{b\} d\Omega \right\} \end{aligned}$$

Inherent within this expression is the material constitutive law. This expression is computed for each and every element in the element axes system. These contributions make up the nodal equilibrium equations at each and every node. In order to assemble that, we again employ the principle of virtual displacements

$$\begin{aligned} \delta W &= \delta \{d\}^T \{f\} \quad (\text{for all } \delta \{U\}) \\ \left\{ \frac{\partial W}{\partial \{U\}} \right\} &= \left[ \frac{\partial \{d\}}{\partial \{U\}} \right]^T \{f\} \\ \{P\} &= [T]^T \{f\} \end{aligned}$$

or the principle of minimum potential energy

$$\begin{aligned} \text{Total Potential Energy, } V &= U + (-W) \\ \delta V &= \delta U - \delta W = 0 \quad (\text{for all } \delta \{U\}) \\ U &= \frac{1}{2} \{d\}^T [k] \{d\} \quad (\text{for linear elastic material}) \\ \delta U &= \delta \{d\}^T [k] \{d\} = \delta \{d\}^T \{f\} \\ \delta V &= \delta \{d\}^T \{f\} - \delta W = \{0\} \\ \text{For equilibrium, } \left\{ \frac{\partial V}{\partial \{U\}} \right\} &= \left[ \frac{\partial \{d\}}{\partial \{U\}} \right]^T \{f\} - \left\{ \frac{\partial W}{\partial \{U\}} \right\} = \{0\} \\ \left\{ \frac{\partial W}{\partial \{U\}} \right\} &= \left[ \frac{\partial \{d\}}{\partial \{U\}} \right]^T \{f\} \\ \{P\} &= [T]^T \{f\} \end{aligned}$$

Both theorems result in the nodal equilibrium equations

$$\{P\} = [T^A]^T \{f\}$$

where  $\{P\}$  is the nodal external force vector in global axes system,  $\{f\}$  is the elemental nodal force vector in the element axes system and  $[T]$  is the transformation matrix. The vector  $\{P\}$  is thus the user-specified external loads which are known. The transformation matrix  $[T]$  transforms the elemental contribution to the static equilibrium equations such that compatibility is ensured. Also note that the displacement DOFs need also be transformed to ensure compatibility

$$\{d\} = [T^A] \{U\}$$

We thus obtain the nodal static equilibrium equations in the global axes system

$$\begin{aligned}
 \{P\} &= [T^A]^T \{f\} \\
 &= [T^A]^T \left\{ \int_{\Omega} [B^A]^T [D^A] [B^A] d\Omega \right\} [T^A] \{U\} + \left\{ \int_{\Omega} [B^A]^T \{\sigma\}_i d\Omega \right\} - \left\{ \int_{\Omega} [B^A]^T [D^A] \{\varepsilon\}_i d\Omega \right\} - \left\{ \int_{\Omega} [N]^T \{b\} d\Omega \right\} \\
 &= [T^A]^T [k_E^A] [T^A] \{U\} + [T^A]^T \left\{ \int_{\Omega} [B^A]^T \{\sigma\}_i d\Omega \right\} - [T^A]^T \left\{ \int_{\Omega} [B^A]^T [D^A] \{\varepsilon\}_i d\Omega \right\} - [T^A]^T \left\{ \int_{\Omega} [N]^T \{b\} d\Omega \right\} \\
 &= [K_E^A] \{U\} + [T^A]^T \left\{ \int_{\Omega} [B^A]^T \{\sigma\}_i d\Omega \right\} - [T^A]^T \left\{ \int_{\Omega} [B^A]^T [D^A] \{\varepsilon\}_i d\Omega \right\} - [T^A]^T \left\{ \int_{\Omega} [N]^T \{b\} d\Omega \right\} \\
 \text{as } [K_E^A] &= [T^A]^T [k_E^A] [T^A]
 \end{aligned}$$

The first term on the RHS in the nodal static equilibrium equation expression is the global instantaneous stiffness matrix. The second, third and fourth on the RHS are the **fixed end forces** in the global axes system. Note that the only unknowns in this expression are the global nodal displacement DOFs  $\{U\}$ . Hence in a linear static solutions scheme, this expression is solved for  $\{U\}$  after the essential boundary conditions are applied using a simultaneous equation solving algorithm such as Gaussian Elimination.

The stiffness matrix prior to application of the essential boundary conditions is known as the initial stiffness matrix whilst that after the application of the essential boundary conditions is known as the final stiffness matrix. The essential boundary conditions may be zero (constraints) or non-zero (**settlement or enforced displacement**). Applying zero essential boundary condition effectively refers to deleting both the row and column associated with the constrained DOF. Applying a **non-zero (settlement) essential boundary condition** refers to deleting the row but not the columns associated with the DOF with the settlement. The deletion of the row indicates that the additional equation defining the DOF as an unknown is not utilized within the simultaneous solver. And by not deleting the column, the remaining equations utilize the known displacement value, which becomes a part of the fixed end forces when the term is brought over the loading side of the equations. Hence the specification of the enforced displacement always requires the specification of a constraint to delete the row (SPC entry in MSC.NASTRAN) and the specification of an enforced displacement to account for the known displacement value for the column (SPCD entry in MSC.NASTRAN). For example if the following is the initial stiffness matrix where  $f$  now denotes the fixed end forces

$$\begin{Bmatrix} P_1 \\ P_2 \\ P_3 \\ P_4 \end{Bmatrix} - \begin{Bmatrix} f_1 \\ f_2 \\ f_3 \\ f_4 \end{Bmatrix} = \begin{bmatrix} K_{11} & K_{12} & K_{13} & K_{14} \\ K_{21} & K_{22} & K_{23} & K_{24} \\ K_{31} & K_{32} & K_{33} & K_{34} \\ K_{41} & K_{42} & K_{43} & K_{44} \end{bmatrix} \begin{Bmatrix} U_1 \\ U_2 \\ U_3 \\ U_4 \end{Bmatrix}$$

and if the displacement  $U_1$  is a settlement or an enforced displacement, and  $U_2$  is a constraint, then the final stiffness matrix

$$\begin{Bmatrix} P_1 \\ P_2 \\ P_3 \\ P_4 \end{Bmatrix} - \begin{Bmatrix} f_1 \\ f_2 \\ f_3 \\ f_4 \end{Bmatrix} = \begin{bmatrix} K_{11} & K_{12} & K_{13} & K_{14} \\ K_{21} & K_{22} & K_{23} & K_{24} \\ K_{31} & K_{32} & K_{33} & K_{34} \\ K_{41} & K_{42} & K_{43} & K_{44} \end{bmatrix} \begin{Bmatrix} U_1 \\ U_2 \\ U_3 \\ U_4 \end{Bmatrix}$$

giving

$$\begin{Bmatrix} P_3 \\ P_4 \end{Bmatrix} - \begin{Bmatrix} f_3 \\ f_4 \end{Bmatrix} - \begin{Bmatrix} K_{31} U_1 \\ K_{41} U_1 \end{Bmatrix} = \begin{bmatrix} K_{33} & K_{34} \\ K_{43} & K_{44} \end{bmatrix} \begin{Bmatrix} U_3 \\ U_4 \end{Bmatrix}$$

Notice the settlements now contribute to the fixed end forces. This expression is solved simultaneously for the unknown displacements  $U_3$  and  $U_4$ . Solving these final stiffness static equilibrium equations simultaneously then, effectively produces the deformed configuration of the structure.

Finally, element stress recovery is performed utilizing

$$\{\sigma\} = [D^A][B^A]\{d\} + \{\sigma\}_i - [D^A]\{\varepsilon\}_i$$

The reactions (obtained for both zero and non-zero essential boundary conditions) are obtained from the deleted rows of the initial stiffness matrix. For the above example, the reactions  $P_1$  (**at the settlement**) and  $P_2$  (at the zero constraint) are

$$\begin{Bmatrix} P_1 \\ P_2 \end{Bmatrix} - \begin{Bmatrix} f_1 \\ f_2 \end{Bmatrix} = \begin{bmatrix} K_{11} & K_{12} & K_{13} & K_{14} \\ K_{21} & K_{22} & K_{23} & K_{24} \end{bmatrix} \begin{Bmatrix} U_1 \\ U_2 \\ U_3 \\ U_4 \end{Bmatrix}$$

The reaction at the enforced displacement constrained should be checked after an analysis to ensure that the forces required to effect this displacement are realistic.

Note that a static analysis can be solved with solely applied displacements, i.e. loads are not mandatory, as long as the 6 rigid-body modes are constrained.

Again, it is important to grasp the concept that in geometrically linear (GL) global element stiffness formulations, the transformation matrix  $[T^A]$  is constant and thus independent of the global displacement vector  $\{U\}$ .

### 2.1.3 GNL, MNL Static Finite Element Elemental Formulation

The variation of displacement within a finite element can be presented as a function of the matrix of shape functions  $[N]$  and the discrete nodal degree of freedom displacement vector  $\{d\}$  as

$$\{y\} = [N]\{d\}$$

Vector  $\{y\}$  describes the general displacement function (interpolation function) within the finite element,  $\{d\}$  is the unknown nodal DOFs and  $[N]$  are their corresponding shape functions.

The general strain vector  $\{\varepsilon\}$  in terms of  $\{d\}$  can then be derived as the strain is some derivative function of the displacement function and hence the nodal DOFs  $\{d\}$

$$\{\varepsilon\} = [B]\{d\}$$

One of the differences with a nonlinear finite element stiffness formulation lies in the elemental strain expression  $\{\varepsilon\}$  which is no longer linearly related to the nodal displacement DOFs  $\{d\}$ . Hence the strain matrix  $[B]$  is no longer constant but instead a function of the nodal displacement vector  $\{d\}$ . This has further repercussions that will become apparent.

The general stress vector  $\{\sigma\}$  can then be established in terms of the strains and hence be expressed in terms of the DOFs  $\{d\}$  amongst other terms

$$\{\sigma\} = [D][B]\{d\} + \{\sigma\}_i - [D]\{\varepsilon\}_i$$

The second term is due to the initial stresses (such as residual stresses within the element) and the third term is the initial strains due to **temperature shrinkage** or **lack of fit**. For material nonlinearity, the constitutive matrix  $[D]$  is also dependent upon the strains  $\{\varepsilon\}$  which in turn is dependent upon the nodal displacement vector  $\{d\}$ .

For a variational finite element, the equilibrium equation is thus derived by equating the external work to the internal energy for a virtual displacement set or by minimizing the total potential energy (note that these theorems are equally applicable for nonlinear systems as they are for linear systems)

$$\begin{aligned} V &= U - W \\ \delta V &= \delta U - \delta W = 0 \quad \text{for equilibrium} \\ \delta V &= \int_{\Omega} \delta\{\varepsilon\}^T \{\sigma\} d\Omega - \delta\{d\}^T \{f\} - \int_{\Omega} \delta\{y\}^T \{b\} d\Omega = 0 \end{aligned}$$

where  $\{f\}$  is the nodal force vector and  $\{b\}$  is the distributed body forces within the finite element. We have however established that

$$\begin{aligned} \{y\} &= [N]\{d\} & \text{hence} & \quad \{y\}^T = \{d\}^T [N]^T \\ \{\varepsilon\} &= [B]\{d\} & \text{hence} & \quad \{\varepsilon\}^T = \{d\}^T [B]^T \\ \{\sigma\} &= [D][B]\{d\} + \{\sigma\}_i - [D]\{\varepsilon\}_i \end{aligned}$$

hence

$$\delta\{d\}^T \{f\} + \int_{\Omega} \delta\{d\}^T [N]^T \{b\} d\Omega = \int_{\Omega} \delta\{d\}^T [B]^T [D][B]\{d\} d\Omega + \int_{\Omega} \delta\{d\}^T [B]^T \{\sigma\}_i d\Omega - \int_{\Omega} \delta\{d\}^T [B]^T [D]\{\varepsilon\}_i d\Omega$$

The above expression is valid for any virtual displacement  $\delta\{d\}$ . Choosing unity virtual displacements we arrive at the elemental equilibrium equations

$$\{f\} = \left[ \int_{\Omega} [B]^T [D][B] d\Omega \right] \{d\} + \left\{ \int_{\Omega} [B]^T \{\sigma\}_i d\Omega \right\} - \left\{ \int_{\Omega} [B]^T [D]\{\varepsilon\}_i d\Omega \right\} - \left\{ \int_{\Omega} [N]^T \{b\} d\Omega \right\}$$

This is the expression that is set up for each and every element. If the nodal force vector  $\{f\}$  is known, then the only remaining unknown within these equations are the nodal displacement vector  $\{d\}$ . Note that we have defined  $[B]$  the strain matrix,  $\{\sigma\}_i$  = the initial stresses,  $[D]$  the material constitutive matrix,  $\{\varepsilon\}_i$  = the initial strains,  $[N]$  = shape functions matrix,  $\{b\}$  = the elemental (external) body loads and of course  $\{d\}$  = nodal element displacement in element axes.

To summarize the terms in the above elemental static equilibrium equation expression

- (i) the term on the LHS is the nodal force vector in element axis
- (ii) the first term on the RHS is the instantaneous stiffness matrix
- (iii) the second, third and fourth terms on the RHS are the so-called **fixed end forces**

We note that the choice of the shape functions  $[N]$  affects the accuracy of

- (i) the elemental instantaneous stiffness matrix
- (ii) the fixed end forces

This elemental static equilibrium expression seems exactly identical to that of the linear finite element. However, there are inherent fundamental differences that must be realized, i.e.

- (i) Firstly, the strain matrix  $[B]$  is no longer constant but instead dependent upon the nodal displacement vector  $\{d\}$ , this being a characteristic of geometric nonlinearity.
- (ii) Secondly, the constitutive matrix  $[D]$  is not constant but instead dependent upon the nodal displacement vector  $\{d\}$ , this being a characteristic of material nonlinearity.
- (iii) Thirdly, the body loading vector  $\{b\}$  is also dependent upon the nodal displacement vector  $\{d\}$ , this also being a characteristic of geometric nonlinearity

An extremely fundamental concept to grasp is that as a result of the dependence of  $[B]$ ,  $[D]$  and  $\{b\}$  on  $\{d\}$ , we can no longer solve for  $\{d\}$  using linear simultaneous equation solving algorithms. In the linear systems, we write the expression

$$\{f\} = [k_E]\{d\} + \text{Fixed End Forces}$$

and provided we know the applied nodal forces  $\{f\}$ , which we do, we can solve for  $\{d\}$  as the fixed end forces are independent of  $\{d\}$ . Now, in the nonlinear system, the equilibrium equations are nonlinear. We thus employ another technique based on the tangent stiffness in order to solve the nonlinear equilibrium equations for  $\{d\}$ .

The stiffness matrix of the nonlinear system is no longer constant. By definition the stiffness of the system is

$$[k] = \left[ \frac{\partial \{f\}}{\partial \langle d \rangle} \right]$$

For a linear finite element, since  $[B]$ ,  $[D]$  and  $\{b\}$  are independent of  $\{d\}$ , the second, third and fourth terms in the elemental equilibrium equation does not feature in the stiffness expression which simply is

$$[k] = \left[ \int_{\Omega} [B]^T [D] [B] d\Omega \right]$$

On the other hand, for a nonlinear finite element, there are remaining terms when the second, third and fourth terms of the elemental equilibrium equation are differentiated with respect to  $\{d\}$  to obtain the elemental tangent stiffness expression as shown below.

$$\begin{aligned}
 [\mathbf{k}_T] &= \left[ \frac{\partial^2 \mathbf{V}}{\partial \langle \mathbf{d} \rangle \partial \langle \mathbf{d} \rangle} \right] \\
 &= \left[ \frac{\partial^2 \mathbf{U}}{\partial \langle \mathbf{d} \rangle \partial \langle \mathbf{d} \rangle} \right] - \left[ \frac{\partial^2 \mathbf{W}}{\partial \langle \mathbf{d} \rangle \partial \langle \mathbf{d} \rangle} \right] \\
 &= \left[ \frac{\partial}{\partial \langle \mathbf{d} \rangle} \{ [\mathbf{B}]^T \{ \boldsymbol{\sigma} \} \} \right] - \left[ \frac{\partial^2 \mathbf{W}}{\partial \langle \mathbf{d} \rangle \partial \langle \mathbf{d} \rangle} \right] \quad \text{as } [\mathbf{B}] = \left[ \frac{\partial \langle \boldsymbol{\varepsilon} \rangle}{\partial \langle \mathbf{d} \rangle} \right] \\
 &= [\mathbf{B}]^T \left[ \frac{\partial \langle \boldsymbol{\sigma} \rangle}{\partial \langle \mathbf{d} \rangle} \right] + \left[ \frac{\partial [\mathbf{B}]^T}{\partial \langle \mathbf{d} \rangle} \{ \boldsymbol{\sigma} \} \right] - \left[ \frac{\partial^2 \mathbf{W}}{\partial \langle \mathbf{d} \rangle \partial \langle \mathbf{d} \rangle} \right] \quad \text{using the derivative of product rule} \\
 &= [\mathbf{B}]^T \left[ \frac{\partial \langle \boldsymbol{\sigma} \rangle}{\partial \langle \boldsymbol{\varepsilon} \rangle} \right] \left[ \frac{\partial \langle \boldsymbol{\varepsilon} \rangle}{\partial \langle \mathbf{d} \rangle} \right] + \left[ \frac{\partial [\mathbf{B}]^T}{\partial \langle \mathbf{d} \rangle} \{ \boldsymbol{\sigma} \} \right] - \left[ \frac{\partial^2 \mathbf{W}}{\partial \langle \mathbf{d} \rangle \partial \langle \mathbf{d} \rangle} \right] \quad \text{using the chain rule} \\
 &= [\mathbf{B}]^T [\mathbf{D}] [\mathbf{B}] + \left[ \frac{\partial [\mathbf{B}]^T}{\partial \langle \mathbf{d} \rangle} \{ \boldsymbol{\sigma} \} \right] - \left[ \frac{\partial^2 \mathbf{W}}{\partial \langle \mathbf{d} \rangle \partial \langle \mathbf{d} \rangle} \right] \quad \text{as } [\mathbf{D}] = \left[ \frac{\partial \langle \boldsymbol{\sigma} \rangle}{\partial \langle \boldsymbol{\varepsilon} \rangle} \right] \text{ and } [\mathbf{B}] = \left[ \frac{\partial \langle \boldsymbol{\varepsilon} \rangle}{\partial \langle \mathbf{d} \rangle} \right] \\
 &= [\mathbf{B}]^T [\mathbf{D}] [\mathbf{B}] + \left[ \frac{\partial}{\partial \langle \mathbf{d} \rangle} \left[ \frac{\partial \langle \boldsymbol{\varepsilon} \rangle}{\partial \langle \mathbf{d} \rangle} \right]^T \{ \boldsymbol{\sigma} \} \right] - \left[ \frac{\partial^2 \mathbf{W}}{\partial \langle \mathbf{d} \rangle \partial \langle \mathbf{d} \rangle} \right] \quad \text{as } [\mathbf{B}] = \left[ \frac{\partial \langle \boldsymbol{\varepsilon} \rangle}{\partial \langle \mathbf{d} \rangle} \right] \\
 &= [\mathbf{B}]^T [\mathbf{D}] [\mathbf{B}] + \left[ \frac{\partial^2 \langle \boldsymbol{\varepsilon} \rangle}{\partial \langle \mathbf{d} \rangle \partial \langle \mathbf{d} \rangle} \{ \boldsymbol{\sigma} \} \right] - \left[ \frac{\partial^2 \mathbf{W}}{\partial \langle \mathbf{d} \rangle \partial \langle \mathbf{d} \rangle} \right]
 \end{aligned}$$

Hence, we can conclude that the elemental tangent stiffness matrix is

$$\begin{aligned}
 [\mathbf{k}_T] &= [\mathbf{k}_E] + [\mathbf{k}_G] \\
 [\mathbf{k}_E] &= \int_{\Omega} [\mathbf{B}]^T [\mathbf{D}] [\mathbf{B}] d\Omega \\
 [\mathbf{k}_G] &= \int_{\Omega} \left[ \frac{\partial^2 \langle \boldsymbol{\varepsilon} \rangle}{\partial \langle \mathbf{d} \rangle \partial \langle \mathbf{d} \rangle} \{ \boldsymbol{\sigma} \}_n + \{ \boldsymbol{\sigma} \}_i - [\mathbf{D}] \{ \boldsymbol{\varepsilon} \}_i \right] d\Omega - \left[ \frac{\partial^2 \mathbf{W}_i}{\partial \langle \mathbf{d} \rangle \partial \langle \mathbf{d} \rangle} \right] - \lambda \left[ \frac{\partial^2 \mathbf{W}_n}{\partial \langle \mathbf{d} \rangle \partial \langle \mathbf{d} \rangle} \right] \\
 \{ \boldsymbol{\sigma} \}_n &= [\mathbf{D}] [\mathbf{B}] \{ \mathbf{d} \}
 \end{aligned}$$

It is apparent now that the stiffness of the nonlinear finite element (and by stiffness we mean the variation of resistance  $\{f\}$  with respect to the nodal displacement  $\{d\}$ ) is not just dependent upon the instantaneous stiffness  $[\mathbf{k}_E]$  but also includes *second order internal strain energy and external work terms* so-called the differential stiffness terms due to the initial and nominal stresses within the finite element and the initial and nominal external work done on the element.

To summarize, the primary differences with the nonlinear static stiffness formulation are

- (i) the elemental strain  $\{\boldsymbol{\varepsilon}\}$  have higher order (than linear) terms of the displacement DOFs  $\{d\}$  and hence the strain matrix  $[\mathbf{B}]$  is no longer constant but instead dependent upon the nodal displacement vector  $\{d\}$ , this being a characteristic of geometric nonlinearity. Hence, firstly, the  $[\mathbf{B}]$  term within  $[\mathbf{k}_E]$  is dependent upon the state of deflections  $\{d\}$  instead of being constant with respect to  $\{d\}$ , and secondly, the second derivative of the strain  $\{\boldsymbol{\varepsilon}\}$  with respect to  $\{d\}$  is not zero thus causing the addition of a geometric stiffness that is also a function of the prestress.

- (ii) the constitutive matrix  $[D]$  is not constant but instead dependent upon the nodal displacement vector  $\{d\}$ , this being a characteristic of material nonlinearity.
- (iii) the elemental loading vector  $\{b\}$  has higher order (than linear) terms of the displacement DOFs  $\{d\}$ , this also being a characteristic of geometric nonlinearity.

These differences produce stiffness terms that are not constant (or independent) with respect to  $\{d\}$  but instead dependent upon  $\{d\}$ . The nonlinearity of the stiffness expression thus requires the evaluation of an appropriately called tangent stiffness matrix.

Elements with GNL capabilities have thus the following additional capabilities: -

- (i) The instantaneous stiffness matrix  $[k_E]$  is dependent upon the deflected configuration. This is because the strain-displacement relationship is nonlinear i.e.  $[B]$  would be a function of  $\{d\}$ . Elements with the capability of nonlinear  $[B]$  matrices are termed large strain elements.
- (ii) The geometric (or differential) stiffness matrix is dependent upon the state of stresses (or forces for one-dimensional finite elements) as depicted by the  $\{\sigma_n + \sigma_i + D\varepsilon_i\}$  term where  $\{\sigma_i\}$  is the initial prestress and  $\{\varepsilon_i\}$  is the initial strain. Elements that are capable of modelling this effect are termed large strain elements.
- (iii) The geometric (or differential) stiffness matrix is dependent upon the second order variation of initial and nominal work done with respect to the local element DOFs. There will be no contribution from these terms if the applied external forces are work-conjugate with the element DOFs. By work-conjugate, we mean that these second-order work terms will produce equivalent nodal loading which are always in the direction of the local element nodal displacement DOFs  $\{d\}$ . GNL elements capable of modelling the 'follower force effect' where the force direction is dependent upon the deflected shape would make contributions to these terms as the equivalent nodal force contributions are then not work-conjugate.

Elements with MNL capabilities have the following additional capabilities: -

- (i) The stress-strain relationships is nonlinear i.e.  $[D]$  would be a function of  $\{\varepsilon\}$  which in turn is a function of the nodal displacement vector  $\{d\}$

These GNL, MNL elements reduce to GL, ML elements if  $[B]$ ,  $[D]$  and  $\{b\}$  are constant in which case the stiffness matrix will not be dependent upon the state of stress (or forces for one-dimensional finite elements) or the second order work variation. The stiffness matrix then corresponds to that of the instantaneous stiffness matrix at the initial undeflected configuration state, A.

GNL, MNL elements

$$[f] = [k_T] \{d\} \quad \text{but cannot be solved by linear simultaneous equation solving algorithms}$$

$$[k_T] = [k_E] + [k_G]$$

$$[k_E] = \int_{\Omega} [B]^T [D] [B] d\Omega$$

$$[k_G] = \int_{\Omega} \left[ \frac{\partial^2 \langle \varepsilon \rangle}{\partial \{d\} \partial \langle d \rangle} \{ \sigma \}_n + \{ \sigma \}_i - [D] \{ \varepsilon \}_i \right] d\Omega - \left[ \frac{\partial^2 W_i}{\partial \{d\} \partial \langle d \rangle} \right] - \lambda \left[ \frac{\partial^2 W_n}{\partial \{d\} \partial \langle d \rangle} \right]$$

$$\{ \sigma \}_n = [D] [B] \{d\}$$

GL, ML elements

$$[f] = [k_E^A] \{d\}$$

$$[f] = \left[ \int_{\Omega} [B^A]^T [D] [B^A] d\Omega \right] \{d\} \quad \text{can be solved by linear simultaneous equation solving algorithms}$$

In conclusion, nonlinear finite elements have the following additional capabilities

- (i) Large strain effect – Non constant instantaneous stiffness due to non-constant  $[B]$  and the effect of the geometric stiffness due to prestress and prestrain and nominal stress
- (ii) The follower-force effect
- (iii) Nonlinear stress-strain behavior

It is imperative to realize that the nonlinearity of  $[B]$  and the prominence of the element  $[k_G]$  matrix both reduce when the element length  $L$  (or other dimensions for two and three dimensional finite elements) reduces. This brings us to a very important conclusion, i.e. that GL elements (small strain elements) can be used to approximate GNL element (large strain element or hyperelastic elements) force-displacement response if a sufficient number of elements are utilized to model a single structural member. This however does not mean that a GL analysis solution scheme can be employed, instead a GNL solution technique must be used as the nonlinearities are accounted for in the global behaviour and not the local element behaviour.

### 2.1.4 GNL, MNL Static Finite Element Global Formulation

The following describes the assembly of the element stiffness matrices towards the formulation of the global system stiffness matrix by the use of the equilibrium, compatibility and constitutive laws. We have shown that the elemental equilibrium equations are

$$\{f\} = \left\{ \int_{\Omega} [B]^T [D] [B] d\Omega \right\} \{d\} + \left\{ \int_{\Omega} [B]^T \{\sigma\}_i d\Omega \right\} - \left\{ \int_{\Omega} [B]^T [D] \{\varepsilon\}_i d\Omega \right\} - \left\{ \int_{\Omega} [N]^T \{b\} d\Omega \right\}$$

Inherent within this expression is the material constitutive law. This expression is computed for each and every element in the element axes system. These contributions make up the nodal equilibrium equations at each and every node. In order to assemble that, we again employ the principle of minimum potential energy

$$\begin{aligned} \text{Total potential energy} \quad V &= U - W \\ \text{For equilibrium} \quad \left\{ \frac{\partial V}{\partial \{U\}} \right\} &= \{0\} \\ \left\{ \frac{\partial U}{\partial \{U\}} \right\} - \left\{ \frac{\partial W}{\partial \{U\}} \right\} &= \{0\} \\ \left[ \frac{\partial \{d\}}{\partial \{U\}} \right]^T \{f\} - \left\{ \frac{\partial W}{\partial \{U\}} \right\} &= \{0\} \\ [T]^T \{f\} - \left\{ \frac{\partial W}{\partial \{U\}} \right\} &= \{0\} \text{ as } [T] = \left[ \frac{\partial \{d\}}{\partial \{U\}} \right] \\ [T]^T \{f\} &= \{P\} \end{aligned}$$

Replacing the elemental contributions to the nodal equilibrium equations, we can assemble the nodal static equilibrium equation, which can be written in its full glory

$$\{P\} = [T]^T \left\{ \int_{\Omega} [B]^T [D] [B] d\Omega \right\} [T] \{U\} + \left\{ \int_{\Omega} [B]^T \{\sigma\}_i d\Omega \right\} - \left\{ \int_{\Omega} [B]^T [D] \{\varepsilon\}_i d\Omega \right\} - \left\{ \int_{\Omega} [N]^T \{b\} d\Omega \right\}$$

Note that  $[T]$  is the transformation matrix between the element DOF system  $\{d\}$  to the global DOF system  $\{U\}$ . This transformation matrix is dependent upon the global system parameters  $\{U\}$ . The local element axes system changes with respect to the global element axes as it is dependent upon the position of the DOFs in the deflected configuration, a so-called Eulerian system.

The equilibrium equations cannot be solved using a linear solution algorithm, as they are a set of nonlinear equations, nonlinearly related to  $\{U\}$ , which are the only unknowns. Of course a nonlinear simultaneous algorithm could in theory be applied, but this usually proves to be too computationally demanding, and inefficient. Hence, solutions schemes almost always utilize the tangent stiffness matrix approach. The tangent stiffness is independent of the unknowns  $\{U\}$ . Hence, for a small load or displacement step, the response of system can be approximated to be linear with respect to  $\{U\}$ . In other words, for a small load or displacement step, the response of the system will be linear and hence a linear simultaneous solution algorithm may be employed if the solution scheme is implicit. Knowing the tangent stiffness matrix, we can write that for a small change in  $\{U\}$  (small displacement step) or for a small change in  $\{P\}$  that

$$\delta\{P\} = [K_T] \delta\{U\}$$

This is a linear relationship for the nonlinear problem. Hence, any solution scheme (static or dynamic) that incorporates the variation of stiffness with deformation  $\{U\}$  i.e. nonlinear stiffnesses requires a stepping algorithm in order to change the value of the tangent stiffness as the solution progresses. This is required as from the equation

above, it is apparent that a particular linear equilibrium equation that represents the nonlinear problem is valid only for a small load or displacement step. For completion, it is worth mentioning that when  $\delta\{P\}$  is zero for a certain small  $\delta\{U\}$ , this means that  $[K_T]$  is zero. Physically, this means that the system is at an unstable equilibrium state, i.e. it is on the brink of buckling.

The expression for the tangent stiffness matrix in the global system will now be presented. We know from the principle of minimum potential energy that a system is in equilibrium when the first order derivative of the total potential energy with respect to  $\{U\}$  is zero. The tangent stiffness of the system is the second order derivative of the total potential energy function with respect to  $\{U\}$ , i.e.

$$\begin{aligned} [K_T] &= \left[ \frac{\partial^2 V}{\partial\{U\}\partial\langle U \rangle} \right] \\ &= \left[ \frac{\partial^2 U}{\partial\{U\}\partial\langle U \rangle} \right] - \left[ \frac{\partial^2 W}{\partial\{U\}\partial\langle U \rangle} \right] \\ &= \left[ \frac{\partial^2 U}{\partial\{U\}\partial\langle U \rangle} \right] - \left[ \frac{\partial\{P\}}{\partial\langle U \rangle} \right] \quad \text{as} \quad \{P\} = \left\{ \frac{\partial W}{\partial\langle U \rangle} \right\} \end{aligned}$$

But loads applied at nodes within a commercial finite element program are always in the direction of the global system throughout the analysis. This means that the nodal loading is work-conjugate with the global displacement vector  $\{U\}$  and thus there will be no second order variation in work. Thus the second term in the above expression is zero. Note that the second order variation of work terms due to loading within the finite elements is taken into account within the elemental formulations as described earlier. We thus arrive at

$$[K_T] = \left[ \frac{\partial^2 U}{\partial\{U\}\partial\langle U \rangle} \right]$$

which states that the tangent stiffness matrix is equal to the second order variation of internal strain energy. Performing some basic calculus

$$\begin{aligned} [K_T] &= \left[ \frac{\partial}{\partial\langle U \rangle} \{T\}^T \{f\} \right] \quad \text{as} \quad [T] = \left[ \frac{\partial\{d\}}{\partial\langle U \rangle} \right] \\ &= [T]^T \left[ \frac{\partial\{f\}}{\partial\langle U \rangle} \right] + \left[ \frac{\partial[T]^T}{\partial\langle U \rangle} \{f\} \right] \quad \text{using the derivative of product rule} \\ &= [T]^T \left[ \frac{\partial\{f\}}{\partial\langle d \rangle} \right] \left[ \frac{\partial\{d\}}{\partial\langle U \rangle} \right] + \left[ \frac{\partial[T]^T}{\partial\langle U \rangle} \{f\} \right] \quad \text{using the chain rule} \\ &= [T]^T [k_T] [T] + \left[ \frac{\partial[T]^T}{\partial\langle U \rangle} \{f\} \right] \quad \text{as} \quad [k_T] = \left[ \frac{\partial\{f\}}{\partial\langle d \rangle} \right] \text{ and } [T] = \left[ \frac{\partial\{d\}}{\partial\langle U \rangle} \right] \\ &= [T]^T [k_T] [T] + \left[ \frac{\partial}{\partial\langle U \rangle} \left[ \frac{\partial\{d\}}{\partial\langle U \rangle} \right]^T \{f\} \right] \quad \text{as} \quad [T] = \left[ \frac{\partial\{d\}}{\partial\langle U \rangle} \right] \\ &= [T]^T [k_T] [T] + \left[ \frac{\partial^2 \langle d \rangle}{\partial\{U\}\partial\langle U \rangle} \{f\} \right] \end{aligned}$$

To summarize global tangent stiffness matrix replacing terms from the elemental tangent stiffness matrix

$$\begin{aligned}
 \text{From above} \quad & [\mathbf{K}_T] = [\mathbf{T}]^T [\mathbf{k}_T] [\mathbf{T}] + \left[ \frac{\partial^2 \langle \mathbf{d} \rangle}{\partial \langle \mathbf{U} \rangle \partial \langle \mathbf{U} \rangle} \{ \mathbf{f} \} \right] \\
 \text{but} \quad & \{ \mathbf{f} \} = \left\{ \int_{\Omega} [\mathbf{B}]^T [\mathbf{D}] [\mathbf{B}] \mathbf{d} \Omega \right\} \mathbf{d} + \left\{ \int_{\Omega} [\mathbf{B}]^T \{ \sigma \}_i \mathbf{d} \Omega \right\} - \left\{ \int_{\Omega} [\mathbf{B}]^T [\mathbf{D}] \{ \varepsilon \}_i \mathbf{d} \Omega \right\} - \left\{ \int_{\Omega} [\mathbf{N}]^T \{ \mathbf{b} \} \mathbf{d} \Omega \right\} \\
 \text{and} \quad & [\mathbf{k}_T] = [\mathbf{k}_E] + [\mathbf{k}_G] \\
 \text{where} \quad & [\mathbf{k}_E] = \int_{\Omega} [\mathbf{B}]^T [\mathbf{D}] [\mathbf{B}] \mathbf{d} \Omega \\
 \text{and} \quad & [\mathbf{k}_G] = \int_{\Omega} \left[ \frac{\partial^2 \langle \varepsilon \rangle}{\partial \langle \mathbf{d} \rangle \partial \langle \mathbf{d} \rangle} \{ \{ \sigma \}_n + \{ \sigma \}_i - [\mathbf{D}] \{ \varepsilon \}_i \} \right] \mathbf{d} \Omega - \left[ \frac{\partial^2 \mathbf{W}_i}{\partial \langle \mathbf{d} \rangle \partial \langle \mathbf{d} \rangle} \right] - \lambda \left[ \frac{\partial^2 \mathbf{W}_n}{\partial \langle \mathbf{d} \rangle \partial \langle \mathbf{d} \rangle} \right] \\
 \text{for which} \quad & \{ \sigma \}_n = [\mathbf{D}] [\mathbf{B}] \{ \mathbf{d} \}
 \end{aligned}$$

$$\begin{aligned}
 \text{Thus} \quad & [\mathbf{K}_T] = [\mathbf{K}_E] + [\mathbf{K}_G] \\
 \text{where} \quad & [\mathbf{K}_E] = [\mathbf{T}]^T [\mathbf{k}_E] [\mathbf{T}] \\
 \text{for which} \quad & [\mathbf{k}_E] = \int_{\Omega} [\mathbf{B}]^T [\mathbf{D}] [\mathbf{B}] \mathbf{d} \Omega \\
 \text{and} \quad & [\mathbf{K}_G] = [\mathbf{T}]^T [\mathbf{k}_G] [\mathbf{T}] + \left[ \frac{\partial^2 \langle \mathbf{d} \rangle}{\partial \langle \mathbf{U} \rangle \partial \langle \mathbf{U} \rangle} \{ \mathbf{f} \} \right] \\
 \text{for which} \quad & [\mathbf{k}_G] = \int_{\Omega} \left[ \frac{\partial^2 \langle \varepsilon \rangle}{\partial \langle \mathbf{d} \rangle \partial \langle \mathbf{d} \rangle} \{ \{ \sigma \}_n + \{ \sigma \}_i - [\mathbf{D}] \{ \varepsilon \}_i \} \right] \mathbf{d} \Omega - \left[ \frac{\partial^2 \mathbf{W}_i}{\partial \langle \mathbf{d} \rangle \partial \langle \mathbf{d} \rangle} \right] - \lambda \left[ \frac{\partial^2 \mathbf{W}_n}{\partial \langle \mathbf{d} \rangle \partial \langle \mathbf{d} \rangle} \right] \\
 \text{and} \quad & \{ \sigma \}_n = [\mathbf{D}] [\mathbf{B}] \{ \mathbf{d} \} \\
 \text{and} \quad & \{ \mathbf{f} \} = \left\{ \int_{\Omega} [\mathbf{B}]^T [\mathbf{D}] [\mathbf{B}] \mathbf{d} \Omega \right\} \mathbf{d} + \left\{ \int_{\Omega} [\mathbf{B}]^T \{ \sigma \}_i \mathbf{d} \Omega \right\} - \left\{ \int_{\Omega} [\mathbf{B}]^T [\mathbf{D}] \{ \varepsilon \}_i \mathbf{d} \Omega \right\} - \left\{ \int_{\Omega} [\mathbf{N}]^T \{ \mathbf{b} \} \mathbf{d} \Omega \right\}
 \end{aligned}$$

Note that we have omitted the second order variation of work due to the external nodal loadings  $\{ \mathbf{P} \}$  from the above tangent stiffness matrix expression, i.e.

$$- \left[ \frac{\partial^2 \mathbf{W}}{\partial \langle \mathbf{U} \rangle \partial \langle \mathbf{U} \rangle} \right] = - \left[ \frac{\partial \{ \mathbf{P} \}}{\partial \langle \mathbf{U} \rangle} \right] \quad \text{as} \quad \{ \mathbf{P} \} = \left\{ \frac{\partial \mathbf{W}}{\partial \langle \mathbf{U} \rangle} \right\}$$

This is because, as mentioned, the externally applied loads at the nodes are in commercial codes always work-conjugate with the nodal DOFs  $\{ \mathbf{U} \}$ , failing which the above term must be incorporated. The second order variation of work due to loads applied on the finite elements is obviously still taken into account, namely in the terms

$$- \left[ \frac{\partial^2 \mathbf{W}_i}{\partial \langle \mathbf{d} \rangle \partial \langle \mathbf{d} \rangle} \right] - \lambda \left[ \frac{\partial^2 \mathbf{W}_n}{\partial \langle \mathbf{d} \rangle \partial \langle \mathbf{d} \rangle} \right]$$

Finally, the second-order work contribution of these elemental loadings to the internal energy of the global formulation is

$$- \left[ \frac{\partial^2 \langle \mathbf{d} \rangle}{\partial \langle \mathbf{U} \rangle \partial \langle \mathbf{U} \rangle} \left\{ \int_{\Omega} [\mathbf{N}]^T \{ \mathbf{b} \} \mathbf{d} \Omega \right\} \right]$$

## 2.1.5 How Nonlinear Analysis Varies From Linear Analysis

### 2.1.5.1 Geometric Nonlinearity

Geometric nonlinearity can be broken down into just four component, firstly nonlinearity due to the prominence of **HIGHER ORDER ELEMENT STRAIN TERMS** when local element deflections become large, secondly nonlinearity due to **HIGHER ORDER WORK TERMS (FOLLOWER FORCE EFFECT)** when global deflections become large, thirdly nonlinearity of the **LOCAL TO GLOBAL TRANSFORMATION MATRIX** when global deflections become large and fourthly the nonlinearity in the form of the global geometric stiffness matrix due to global **PRESTRESS** and large global displacements.

- I. **HIGHER ORDER ELEMENT STRAIN TERMS.** Higher order element strain terms have two effects upon the tangent stiffness matrix. Firstly, the local element instantaneous stiffness matrix  $[k_E]$  becomes dependent upon the local element deflected configuration and not the undeflected configuration.

$$[k_E] = \int_{\Omega} [B]^T [D] [B] d\Omega$$

This is because the strain-displacement relationship is nonlinear i.e.  $[B]$  would be a function of  $\{d\}$  instead of being constant and corresponding to the initial undeflected state  $[B^A]$  as in a linear analysis. If  $\{d\}$  is large, higher order terms in the strain-deflection  $\{\varepsilon\} = [B]\{d\}$  relationships become significant. Elemental small displacement theory does not produce correct results. This occurs because the inherent instantaneous stiffness of a structural element changes as its dimensions change as the analysis progresses. Elements with the capability of nonlinear  $[B]$  matrices are termed large strain or hyperelastic elements. In large strains elements, the strain matrix  $[B]$  varies with deflection  $\{d\}$ . Large strain effect occurs in metal forming, rubber and elastomer applications. The material could be elastic with linear  $[D]$  but still it may accommodate large strains within its elastic range, the higher order strains affecting its stiffness. Secondly, higher order element strain terms cause nonlinearity of the local element tangent stiffness with respect to local element deflections in the form of the element geometric stiffness due to prestress. In linear analysis, elemental  $[k_G]$  is not accounted for.

$$[k_G] = \int_{\Omega} \left[ \frac{\partial^2 \langle \varepsilon \rangle}{\partial \langle d \rangle \partial \langle d \rangle} \{ \{ \sigma \}_n + \{ \sigma \}_i - [D] \{ \varepsilon \}_i \} \right] d\Omega$$

$$\text{where } \{ \varepsilon \} = [B] \{ d \}$$

$$\{ \sigma \}_n = [D] [B] \{ d \}$$

An important observation is that the nonlinearity of  $[B]$  and the prominence of the element  $[k_G]$  matrix both reduce when the element length  $L$  (or other dimensions for two and three dimensional finite elements) reduces. This brings us to a very important conclusion, i.e. that GL elements (small strain elements) can be used to approximate GNL element (large strain element or hyperelastic elements) force-displacement response if a sufficient number of elements are utilized to model a single structural member. The smaller dimensions of the small strain finite elements ensure that they are not distorted too much ensuring that the internal strains are not too large so as to invalidate the linear  $[B]$  relationship. It is perfectly valid to allow the small strain elements to undergo large total deformation as in rigid body motion, however its relative deformation must be small for its linear  $[B]$  relationship to be valid. The nonlinearity of the system is then accounted for in the global behaviour within the GNL solution technique and not the local element behaviour.

- II. **HIGHER ORDER WORK TERMS (FOLLOWER FORCE EFFECT).** The follower force effect is the nonlinearity of the tangent stiffness with respect to deflections in the form of the geometric stiffness due to external forces, also known as the follower force effect. The geometric (or differential) stiffness matrix is dependent upon the second order variation of work done with respect to the local and global DOFs. The stiffness of the structure is dependent upon the magnitude and direction of the external element loads,

which again is dependent upon the current deflected configuration. This occurs when the applied force depends on the deformation (so-called follower force) in the case of hydrostatic loads on submerged or container structures, aerodynamic and hydrodynamic loads caused by the motion of aeriform and hydroform fluids (wind loads, wave loads, drag forces). Element loads often tend to follow the normal to the surface of the element. In linear analysis, these terms are not included.

$$-\left[\frac{\partial^2 \mathbf{W}_i}{\partial \langle \mathbf{d} \rangle \partial \langle \mathbf{d} \rangle}\right] - \lambda \left[\frac{\partial^2 \mathbf{W}_n}{\partial \langle \mathbf{d} \rangle \partial \langle \mathbf{d} \rangle}\right] = -\left[\frac{\partial^2 \langle \mathbf{d} \rangle}{\partial \langle \mathbf{U} \rangle \partial \langle \mathbf{U} \rangle} \left\{ \int_{\Omega} [\mathbf{N}]^T \{ \mathbf{b} \} d\Omega \right\}\right]$$

Nodal forces and accelerations are always in the direction of freedoms and hence are work conjugate and hence linear analysis is sufficient to model these. Hence, there will be no contribution from these terms if the applied external forces are work-conjugate with the element or global DOFs. GNL elements capable of modelling the ‘follower force effect’ where the force direction is dependent upon the deflected shape would make contributions to these terms as the force is then not work-conjugate.

$$-\left[\frac{\partial^2 \mathbf{W}}{\partial \langle \mathbf{U} \rangle \partial \langle \mathbf{U} \rangle}\right] = -\left[\frac{\partial \{ \mathbf{P} \}}{\partial \langle \mathbf{U} \rangle}\right] \quad \text{as} \quad \{ \mathbf{P} \} = \left\{ \frac{\partial \mathbf{W}}{\partial \langle \mathbf{U} \rangle} \right\}$$

In linear analysis, these terms are not included.

- III. **PRESTRESS.** This is nonlinearity in the form of the global geometric stiffness matrix due to global PRESTRESS and large global displacements.

$$\left[\frac{\partial^2 \langle \mathbf{d} \rangle}{\partial \langle \mathbf{U} \rangle \partial \langle \mathbf{U} \rangle} \{ \mathbf{f} \} \right]$$

where  $\{ \mathbf{f} \} = \left\{ \int_{\Omega} [\mathbf{B}]^T [\mathbf{D}] [\mathbf{B}] d\Omega \right\} \langle \mathbf{d} \rangle + \left\{ \int_{\Omega} [\mathbf{B}]^T \{ \sigma \}_i d\Omega \right\} - \left\{ \int_{\Omega} [\mathbf{B}]^T [\mathbf{D}] \{ \varepsilon \}_i d\Omega \right\} - \left\{ \int_{\Omega} [\mathbf{N}]^T \{ \mathbf{b} \} d\Omega \right\}$

Geometric stiffening or destiffening is due to element stress, prestress and prestrain. There is a contribution to the geometric (or differential) stiffness matrix from the fact that an element would have internal stresses and forces. The stiffness of the structure is dependent upon the current magnitude and nature of the internal force actions within the structural element that is dependent upon the current deflected configuration. A tensile load within a structural element increases the stiffness (increasing its natural frequency) as it tends to return the element to its undeflected shape whilst a compressive load decreases the stiffness (decreasing its natural frequency) as it tends to amplify the deflected shape. Hence the high bending stiffness in prestressed cables where an unstressed cable will have negligible bending stiffness. Likewise is the reduction in stiffness in a compressed column. Also, the gradual prestressing of a structural element such as a thin plate that is restrained from longitudinal contraction and subject to bending causing the neutral surface to stretch and generate significant tensile stresses, which serve to stiffen the plate in bending due to the geometric stiffness. Of course, if the plate is not restrained, there will simply be longitudinal contraction and no in plane stress will be generated, a linear analysis is then often sufficient. Clearly, this longitudinal contraction when there are no restraints or the generation of in plane forces due to transverse bending when there are restraints, is only observed in a nonlinear analysis, not a linear one. Hence, if there is an element prestress  $\{ \sigma_i \}$  or if the deflections  $\{ \mathbf{d} \}$  or  $\{ \mathbf{U} \}$  is sufficiently large to make the change in element stress  $\{ \sigma_n \}$  prominent in affecting the stiffness as the analysis progresses, the geometric (or differential) stiffness matrix should be accounted for. In linear analysis, these terms are not included unless special techniques such as P- $\Delta$  analyses are performed.

- IV. **LOCAL TO GLOBAL TRANSFORMATION MATRIX.** This is the nonlinearity of the transformation matrix  $[\mathbf{T}]$  with respect to deflections  $\{ \mathbf{U} \}$ . If the deflections (U) are large, then it is appropriate to account for the variation of the  $[\mathbf{T}]$  matrix with  $\{ \mathbf{U} \}$ . Even if the elemental strains are small (which can be the case if the finite element mesh is very fine), if the global deflections  $\{ \mathbf{U} \}$  are large, it is prudent to employ a nonlinear solution scheme.

$$[T] = \left[ \frac{\partial \{d\}}{\partial \{U\}} \right]$$

In linear analysis  $[T]$  is constant and is based on the initial undeflected configuration, i.e.  $[T^A]$ . In geometrically nonlinear analysis, equilibrium and compatibility is satisfied in the deformed configuration whilst in geometrically linear analysis, equilibrium and compatibility is satisfied in the undeformed configuration. Further, the force transformation matrix is not the transpose of the displacement transformation matrix in geometrically nonlinear analysis whilst it is in linear analysis. Thus, since displacements are directly proportional to loads in linear analysis, results from different load cases can be superimposed, whilst that cannot be done for nonlinear analysis. Accounting for the nonlinearity of  $[T]$  is significant for large displacements and rotations in the case of cables, arches and thin plates. Consider a thin plate subjected to transverse loads. Shell elements are based on classical bending theory, which assumes that the transverse loads on a flat panel are resisted by bending alone. As a thin shell has little bending resistance a linear analysis would then predict a very large displacement, much larger than the limit of displacement/thickness ratios (often quoted from 0.3 to 1.0) for which the classical theory applies. In reality, once some deformation has occurred a thin shell can resist loads by membrane tension, which is very stiff compared with bending. Hence when we talk of small displacements for linear analysis to be valid, it should be quoted in view of the thickness of the element, not the absolute displacement magnitude. This is a geometric nonlinear effect where the **load path** and **nature of deformation and stress field** literally changes with deflections, an effect that cannot be predicted by linear analysis. This does not occur with curved panels such as cylinders under internal pressure, where the transverse load is carried by hoop stresses, in which case a linear analysis may be sufficient.

### 2.1.5.2 Material Nonlinearity

In nonlinear material finite elements, the stress-strain relationships is nonlinear i.e.  $[D]$  would be a function of  $\{\varepsilon\}$ .

$$\left[ \int_{\Omega} [B]^T [D] [B] d\Omega \right]$$

In linear analysis, the stress-strain relationship is linear.

### 2.1.5.3 Contact and Boundary Conditions Nonlinearity

Nonlinear analysis is also able to change the boundary conditions as the analysis progresses. Contact can be simulated where two or more parts of the structure collide, slide and separate.

### 2.1.6 GL, ML and GNL, MNL Dynamic Finite Element Elemental and Global Formulation

Dynamic analysis formulations differ from static analysis by the fact that in general they require two additional matrices in the mass  $[M]$  and the damping  $[C]$  matrices. Assumed element interpolation functions now define the element mass, damping and stiffness matrices, i.e. employing the constitutive law. The dynamic global equilibrium equations are assembled (equilibrium law) from element contributions transformed (compatibility law) as appropriate. The general global dynamic equilibrium equations for nonlinear analyses are

$$[M]\delta\{\ddot{U}\} + [C_T]\delta\{\dot{U}\} + [K_T]\delta\{U\} = \delta\{P(t)\}$$

Since there can be prominent variations in the stiffness (and damping) matrices, the equilibrium equations is only valid for small time steps at a time. Hence, either an implicit or explicit time stepping algorithm must be employed to solve these equations for the unknowns, i.e. the global nodal displacement vector  $\{U\}$ . Finally, the element stress recovery is performed based on the nodal displacement vector and the assumed interpolation function.

## 2.2 Static Analysis Concepts

### 2.2.1 Overview of Methods of Structural Static Analyses

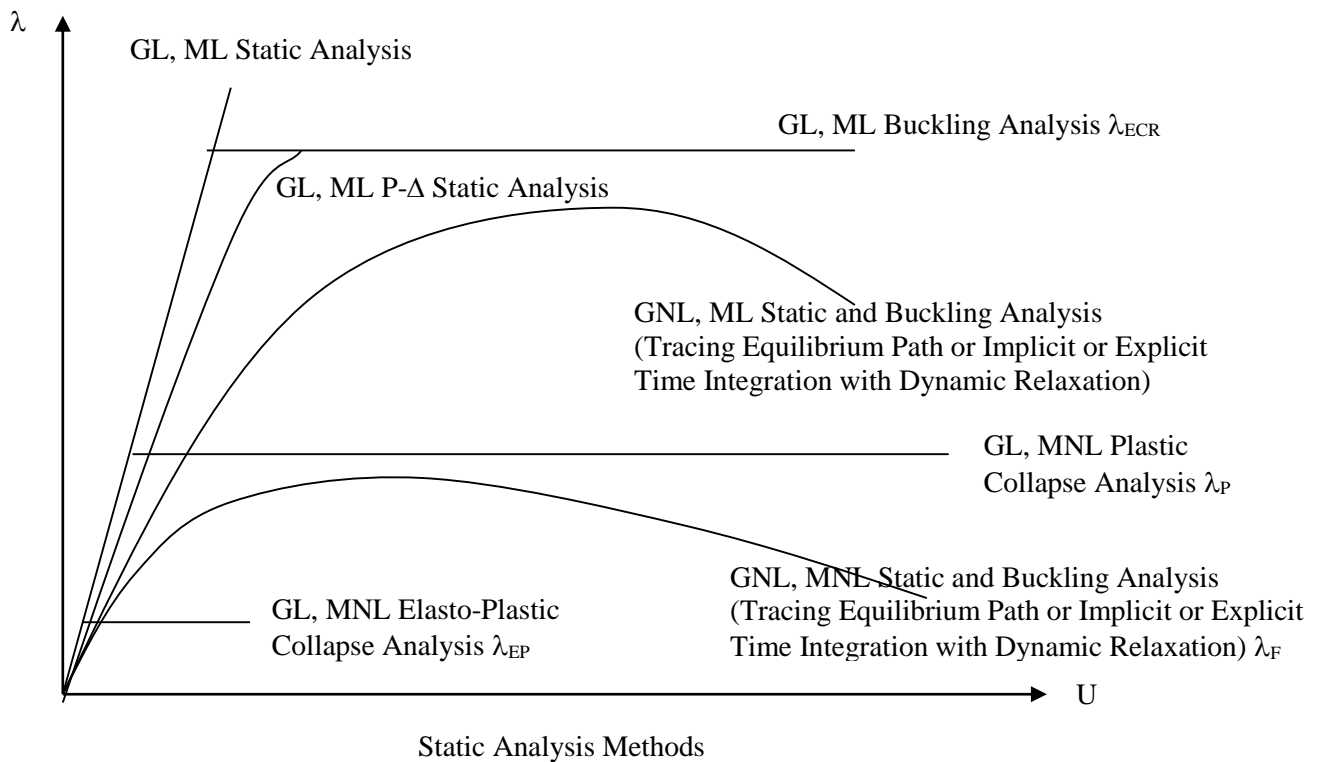
Methods of structural static analysis may or may not incorporate nonlinearity in the form of geometric nonlinearity and/or material nonlinearity.

#### 1. Geometrically linear (GL) analysis

- 1.1 **ML Static analysis** (the implicit direct stiffness method)
- 1.2 **ML P- $\Delta$  Static analysis** (the implicit direct stiffness method)
- 1.3 **ML Buckling** (linear elastic instability) **analysis** (the implicit linear eigenvalue analysis)
- 1.4 **MNL Plastic collapse analysis** (the implicit linear simplex programming)
- 1.5 **MNL Elasto-plastic collapse analysis**

#### 2. Geometrically nonlinear (GNL) analysis

- 2.1 **ML/MNL Static and buckling analysis** (the implicit tracing the equilibrium path method, the implicit time integration method employing dynamic relaxation or the explicit time integration method employing dynamic relaxation)



GL: Geometrically Linear  
 GNL: Geometrically Nonlinear  
 ML: Materially Linear  
 MNL: Materially Nonlinear

## 2.3 Dynamic Analysis Concepts

### 2.3.1 Overview of Methods of Structural Dynamic Analyses

#### 2.3.1.1 Modal Analyses

The modal properties of linear systems can be ascertained by either one of the following methods: -

- (i) **GL, ML Real modal (eigenvalue) analysis** SOL 103 to establish the modal frequencies, real modal mass (and modal stiffness) and the real mode shapes
- (ii) **GL, ML Complex modal (eigenvalue) analysis** SOL 107 to establish the modal frequencies, modal damping, complex modal mass (and complex modal stiffness) and the complex mode shapes
- (iii) **GL, ML Time domain implicit** (SOL 109, SOL 112 or SOL 129) **or explicit** (LS-DYNA) **impulse analysis** to excite the modes of interest. The duration of the impulse must be sufficiently long ( $t_d/T_1 > \sim 0.4$ ) to excite the first fundamental mode, which is usually of concern. This would result in a response that includes the first fundamental mode and most likely higher modes as well. The first fundamental mode is readily ascertained from inspection of the response time history curve at any node. Higher natural frequencies can also be ascertained by performing an FFT on the response curve.

#### 2.3.1.2 Forced Response Analyses

The methods of calculating forced dynamic response in MSC.NASTRAN are particularly of concern. Dynamic forced response analyses can be performed in the frequency or the time domain.

It is important to understand the components of the result solved for by NASTRAN from the different forced response solution schemes. In general, there are two components of response, i.e.

- (i) the starting transient, and
- (ii) the steady-state response

The excitations that contribute to the above components of response are

- (i) the initial conditions, contributing to the starting transient
- (ii) the steady-state force, contributing to both the starting transient and the steady-state response

<b>MSC.NASTRAN Forced Response Analysis</b>			
Forced Response Analysis	Initial Conditions	Starting Transient Response	Steady State Response
Modal Frequency	No	No	Yes
Direct Frequency	No	No	Yes
Modal Transient	No	Yes	Yes
Direct Transient	Yes	Yes	Yes

Methods of calculating the forced response generally depend on the nature of the excitation function. Dynamic analysis can be performed in either the time domain or the frequency domain. Time domain dynamic analyses include both transient and steady-state response, whilst frequency domain dynamic analysis only computes the steady-state response. The types of excitations and the corresponding solution methods are: -

- (i) **GL, ML Deterministic periodic harmonic long duration** excitations; The starting transient is insignificant compared to the steady-state response. Forced response (steady-state) is performed in the frequency domain using SOL 108 or SOL 111. Damping estimates ARE crucial.

- (ii) **GL, ML Deterministic periodic non-harmonic long duration** excitations; The starting transient is insignificant compared to the steady-state response. A periodic (of period T) function that is not necessarily harmonic can be expressed as a summation of an infinite number of sine and cosine terms, i.e. a Fourier Series. Forced responses (steady-state) are performed in the frequency domain using SOL 108 or SOL 111 with these individual harmonics (with the correct amplitudes and phase differences) as the excitations. The total steady-state response is thus the summation of the responses of the individual harmonics. Damping estimates ARE crucial.
- (iii) **GL/GNL, ML/MNL Deterministic non-periodic short duration impulse (a.k.a. blast)** excitations with subsequent **wave propagation**; The starting transient is significant as is the steady-state response. Sources of excitation include the *start up of rotating machines* (not the continuous functioning) being brought to speed passing through various frequencies, but not sustaining any as to cause steady-state conditions. Other sources include sudden impulse (force applied is the rate of change of momentum of relatively small mass compared to mass of structure) or blast excitations. Forced response (starting transient and steady-state) is performed in the time domain using SOL 109, SOL 112 or SOL 129. Material properties that are not only nonlinear with the level of load but also the rate of loading (strain-rate) may have to be incorporated in these sudden impulse analyses. Damping estimates ARE NOT crucial.
- (iv) **GL, ML Random stationary (and ergodic) long duration** excitations; This is the random equivalent of the deterministic periodic (harmonic or non-harmonic) long duration excitation. The starting transient is insignificant compared to the steady-state response. Forced response (steady-state) is performed in the frequency domain using random vibration analysis (with Fast Fourier Transforms FFT) utilizing SOL 108 or SOL 111. Damping estimates ARE crucial. Forced response in the time domain using deterministic methods may not be appropriate as they will be too computationally expensive due to the long duration of the excitation and the maximum response will be governed by steady-state conditions, not by the starting transient response.
- (v) **GL/GNL, ML/MNL Random non-stationary short duration impulse** excitations; This is the random equivalent of the deterministic non-periodic short duration impulse excitations. The starting transient is significant as is the steady-state response. Earthquake signals can be said to fall in this category. Forced responses (starting transient and steady-state) are performed in the time domain using SOL 109, SOL 112 or SOL 129 with a set of deterministic transient excitations generated from the non-stationary random excitations and the results enveloped. Alternatively, forced response (starting transient and steady-state) is performed crudely in the time domain using response (shock) spectrum analysis. Damping estimates ARE still quite crucial. Steady-state forced response in the frequency domain may not be appropriate since the duration of excitation may not be long enough for the response of the structure to reach steady-state conditions.
- (vi) **GNL, MNL Projectile (a.k.a. impact)** excitations with subsequent **wave propagation**; Forced response (starting transient and steady-state) can only be performed in the time domain using an explicit (implicit would be too expensive because of the high nonlinearity) nonlinear time integration scheme. Sudden impulse analyses involve the specification of an initial velocity to the impacting particle placed very close to the impacted structure. The particle will travel at this constant initial velocity (since no other forces, retarding or accelerating) until impacting the structure whereby a certain percentage of the mass of the structure and the mass of the particle will interact to cause a change of momentum, i.e. an impulse. Material properties that are not only nonlinear with the level of load but also the rate of loading (strain-rate) will have to be incorporated in these sudden impact analyses. Damping estimates ARE NOT crucial.
- (vii) **GNL, MNL Brittle snap or redundancy check**; These include the analysis of sudden fracture of structural members from the static equilibrium configuration such as the sudden snapping of a prestressed structural cable, and evaluates the redundancy available within the structure. Forced

response (starting transient and steady-state) can only be performed in the time domain using an explicit (implicit would be too expensive because of the high nonlinearity) nonlinear time integration scheme. This analysis always involves a two-stage procedure. The first stage involves a static solution by a linear static method or a nonlinear static method (either Newton's tracing the equilibrium path SOL 106, an implicit dynamic relaxation by SOL 129 or an explicit dynamic relaxation method LS-DYNA) in order to obtain the deflected configuration and the stiffness of the structure in the deflected configuration  $K_T$  by the prestress (prestressing of structural members such as cables contribute greatly to a large change in stiffness within the static solution and hence will require a nonlinear static method) and gravity. The second stage involves a restart into a nonlinear transient dynamic solution scheme with no additional dynamic excitation but with a change in the structure (in the deletion of a member that fails in brittle fashion simulating a redundancy check) or a change in boundary condition (to simulate the effect of the loss of a support or anchor attached to a prestressed cable etc.). An example would be the gradual prestressing of structural cable elements within a suspension bridge or a cable prestressed tower until a static solution (by SOL 106, implicit SOL 129 or explicit LS-DYNA) is achieved. The cables can be prestressed using a gradual temperature load case (or a gradual enforced displacement on the cable anchorage points) plus gravitational loads until the correct level of prestress is achieved (by SOL 106, implicit SOL 129 or explicit LS-DYNA). Then with a restart into an explicit transient dynamic scheme of LS-DYNA, the boundary condition supporting the cable is released or a cable element is deleted, causing the structure to experience an out-of-balance of forces and hence vibrate to a new static equilibrium configuration. Damping estimates ARE NOT crucial.

### 2.3.2 Nature of Trial Solution in Harmonic Frequency Vibrations

Complementary Function (Starting Transient)		
SDOF	Modal MDOF	Direct MDOF
$u(t) = Ge^{\lambda t}$ $G = G_1 + iG_2$ $\lambda = \alpha + i\omega$	N/A	N/A

Particular Integral Function		
SDOF	Modal MDOF	Direct MDOF
$u(t) = F(\omega)e^{i\omega t}$ $F(\omega) = F_1(\omega) + iF_2(\omega)$	$\{u(t)\} = [\Phi]\{\xi(\omega)\}e^{i\omega t}$ $\{\xi(\omega)\} = \{\xi_1(\omega)\} + i\{\xi_2(\omega)\}$	$\{u(t)\} = \{F(\omega)\}e^{i\omega t}$ $\{F(\omega)\} = \{F_1(\omega)\} + i\{F_2(\omega)\}$

## 2.4 Static and Dynamic Analyses Sequences

A dynamic analysis is always performed about the static equilibrium position. That is to say, the structure should be in static equilibrium before dynamic loads are applied. To obtain the total response, a few approaches may be used.

**In the first approach, valid for both LINEAR AND NONLINEAR TIME DOMAIN solutions,** the static response must be added to the dynamic response if the dynamic analysis is performed about the initial undeflected (by the static loads) state with only the dynamic loads applied, hence causing the dynamic response to be measured relative to the static equilibrium position. This is because if the response is taken to be measured from this static equilibrium position, it can be shown that the static loads do not feature in the dynamic equation of motion. This enables the exclusion of static loads in the dynamic analysis. **However, since the dynamic response is measured from the static equilibrium position, the total response = the dynamic response + the static response to static loads.**

**In the second approach, valid for both LINEAR AND NONLINEAR TIME DOMAIN solutions,** if the dynamic analysis is performed with the deflected static shape as initial input and the static loads maintained throughout the dynamic excitations, the total or absolute response (static and dynamic) is obtained straight away from the dynamic analysis. **Hence total response = dynamic response (which already includes the static response to static loads).**

**In the third approach, valid for LINEAR FREQUENCY DOMAIN solutions,** not only that the static response has to be added separately, but also the mean of the dynamic excitation has also got to be added separately as a static response. This is because for both deterministic periodic excitations and random PSD excitations the mean of the dynamically applied force is not included in the dynamic excitations. **Hence the total response = static response to mean of dynamic excitation + dynamic response + static response to static loads.**

Analyses Sequences			
	Static Analysis	Dynamic Analysis	Remark
GL Modal Analysis	None	GL modal analysis with $[K_E^A]$	Modal analysis about static equilibrium position. Performed if both static and dynamic displacements are small.
	GNL (SOL 106, implicit relaxation SOL 129 or explicit relaxation LS-DYNA) analysis to establish $[K_T^A]$ at position of static equilibrium A. Approximate $[K_T^A]$ can be obtained by repetitive P-Δ static analysis.	GL modal analysis with $[K_T^A]$	Modal analysis about static equilibrium position. Performed if static displacements are large and dynamic displacements are small such as in the analysis of cable vibrations.
GL Buckling Analysis	None	GL buckling analysis with $[K_E^A]$ and hence $[K_G^{KEA}]$	Buckling analysis about static equilibrium position. Performed if both static and buckling displacements are small.
	GNL (SOL 106, implicit relaxation SOL 129 or explicit relaxation LS-DYNA) analysis to establish $[K_T^A]$ at position of static equilibrium A. Approximate $[K_T^A]$ can be obtained by repetitive P-Δ static analysis.	GL buckling analysis with $[K_T^A]$ and hence $[K_G^{KTA}]$	Buckling analysis about static equilibrium position. Performed if static displacements are large and buckling displacements are small such as in the analysis of systems with prestress.

<b>GL Forced Frequency Response</b>	None	GL frequency response analysis (no static loads, only frequency dependent loads)	Forced frequency response analysis about static equilibrium position. Performed if both static and dynamic displacements are small. The dynamic response is measured from the static equilibrium position. Hence, to ascertain the total response, the static response to static loads and static response to the mean of the dynamic excitations must be superposed.
	GNL (SOL 106, implicit relaxation SOL 129 or explicit relaxation LS-DYNA) analysis to establish $[K_T^A]$ at position of static equilibrium A. Approximate $[K_T^A]$ can be obtained by repetitive P- $\Delta$ static analysis.	GL frequency response analysis with $[K_T^A]$ (no static loads, only frequency dependent loads)	Forced frequency response analysis about static equilibrium position. Performed if static displacements are large and dynamic displacements are small. The dynamic response is measured from the static equilibrium position. Hence, to ascertain the total response, the static response to static loads and static response to the mean of the dynamic excitations must be superposed.
<b>GL Forced Transient Response</b>	None	GL transient response analysis (no static loads, only transient loads)	Forced transient response analysis about static equilibrium position. Performed if both static and dynamic displacements are small. The dynamic response is measured from the static equilibrium position. Hence, to ascertain the total response, the static response to static loads must be superposed.
	GNL (SOL 106, implicit relaxation SOL 129 or explicit relaxation LS-DYNA) analysis to establish $[K_T^A]$ at position of static equilibrium A. Approximate $[K_T^A]$ can be obtained by repetitive P- $\Delta$ static analysis.	GL transient response analysis with $[K_T^A]$ (no static loads, only transient loads)	Forced transient response analysis about static equilibrium position. Performed if static displacements are large and dynamic displacements are small. The dynamic response is measured from the static equilibrium position. Hence, to ascertain the total response, the static response to static loads must be superposed.
	GNL (SOL 106, implicit relaxation SOL 129 or explicit relaxation LS-DYNA) analysis to establish $[K_T^A]$ at position of static equilibrium A and the converged static displacements. Approximate $[K_T^A]$ and the converged static displacements can also be obtained by repetitive P- $\Delta$ static analysis.	GL transient response analysis with $[K_T^A]$ and initial dynamic displacements as the converged static displacements (with constant with time equivalent dynamic static loads, and the transient loads)	Forced transient response analysis about initial undeflected by static loads position i.e. the absolute response. Performed if static displacements are large and dynamic displacements are small. The response is the absolute response, i.e. includes both the static and dynamic response.

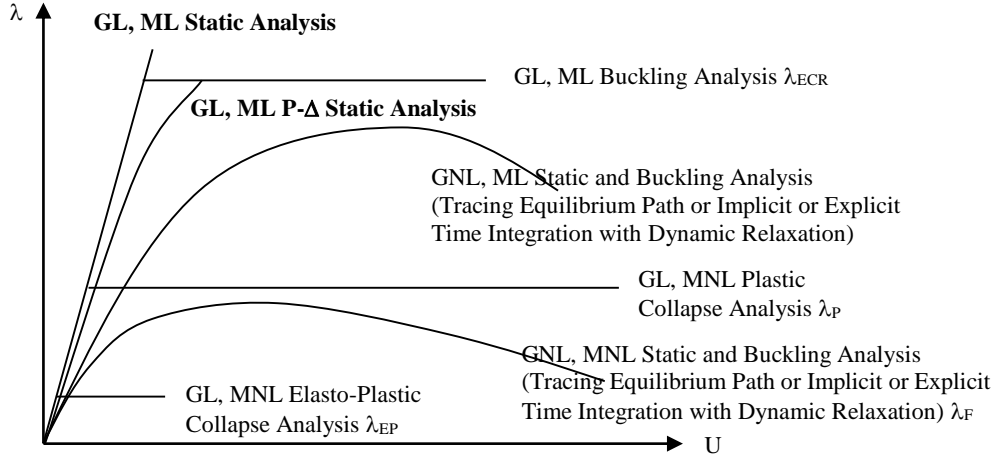
<b>GNL Forced Transient Response</b>	None	GNL transient response analysis (no equivalent static loads, only transient loads)	Forced transient response analysis about static equilibrium position. Performed if static displacements are small and dynamic displacements are large. The dynamic response is measured from the static equilibrium position. Hence, to ascertain the total response, the static response to static loads must be superposed.
	None	GNL transient response analysis with constant with time equivalent dynamic static loads, and the transient loads)	This should not be performed. The structure eventually vibrates about its static equilibrium position, albeit in a while. However, by applying the static loads together with the dynamic loads can cause dynamic amplification that is unrealistic. The static loads should not cause any dynamic effects (if that happens, nonlinear materials in the model may yield prematurely), because by its very definition, the static loads are static i.e. applied over an infinitely long duration. Instead, the static loads should be applied by SOL 106, implicit relaxation SOL 129 or explicit relaxation, then only dynamic analysis be performed.
	GNL (SOL 106, implicit relaxation SOL 129 or explicit relaxation LS-DYNA) analysis to establish $[K_T^A]$ at position of static equilibrium A and the converged static displacements. Approximate $[K_T^A]$ and the converged static displacements can also be obtained by repetitive P- $\Delta$ static analysis.	GNL transient response analysis with $[K_T^A]$ and initial dynamic displacements as the converged static displacements with (with constant with time equivalent dynamic static loads, and the transient loads)	Forced transient response analysis about initial undeflected by static loads position i.e. the absolute response. Performed if both static and dynamic displacements are large. The response is the absolute response, i.e. includes both the static and dynamic response.

Note that when restarting a transient analysis from a nonlinear static analysis (SOL 106, implicit relaxation SOL 129 or explicit relaxation LS-DYNA), the static loads which have been applied must be maintained throughout the transient phase in order to preserve the correct stiffness and the correct static equilibrium at the deflected static equilibrium position. Hence, when a transient phase dynamic analysis follows a dynamic relaxation analysis, it is prudent to define two curves for the static loads or prescribed motions, one ramped from zero to the static value in the dynamic relaxation phase and the other maintained at the same static throughout the transient dynamic analysis phase. Transient analysis is usually performed after a static solution has been achieved either by SOL 106, implicit relaxation SOL 129 or explicit relaxation LS-DYNA. The only benefit of performing dynamic relaxation prior to a transient analysis is that the structure would reach its static equilibrium position quicker before the transient phase takes place. In dynamic relaxation, the damping applied very large, in the order of about 5% of critical, whereas in the transient phase, the structure is very much under-damped. But even if the transient analysis were to be performed without dynamic relaxation, the structure would eventually vibrate about its static equilibrium position, albeit in a while as long as the static gravitational loads are applied. Hence of course, if dynamic relaxation is employed, after the dynamic relaxation phase, the static loads should be maintained throughout the transient dynamic analysis phase. It is however, theoretically incorrect to vibrate the structure from an unstressed position as in reality, the structure would be in its static equilibrium position before being subjected to transient dynamic vibration. In practice however, it can be argued that a dynamic analysis can be done without a static solution if negligible change in stiffness occurs from the static deflections (valid if static deflections are small), of course so long as it is clear that the total response must then be the addition of the static response and the dynamic response, both performed separately from the initial undeflected configuration.

### 3 METHODS OF STATIC ANALYSES

#### 3.1 GL, ML Static Analysis by The Implicit Direct Stiffness Method

##### 3.1.1 Mathematical Formulation of Analysis



We have shown that the nodal static equilibrium equations can be written as a set of linear simultaneous equations

$$\{P\} = [K_E^A] \{U\} + [T^A]^T \left\{ \int_{\Omega} [B^A]^T \{\sigma\}_i d\Omega \right\} - [T^A]^T \left\{ \int_{\Omega} [B^A]^T [D^A] \{\epsilon\}_i d\Omega \right\} - [T^A]^T \left\{ \int_{\Omega} [N]^T \{b\} d\Omega \right\}$$

where  $[K_E^A] = [T^A]^T [k_E^A] [T^A] = [T^A]^T \left[ \int_{\Omega} [B^A]^T [D^A] [B^A] d\Omega \right] [T^A]$

Geometrically linear stiffness response represents only a tangential approximation to the fundamental path at the initial unloaded state. Hence, the results are valid in a range of small displacements and loading. Tangential accuracy of linear analysis depends upon the magnitude of deflection, the component forces and the applied loading. The geometrically linear equilibrium equations are solved for the unknown displacements  $\{U\}$ .

$$\text{Linear static } [K_E^A] \{U\} = \{P\} + \{\text{Fixed End Forces}\}$$

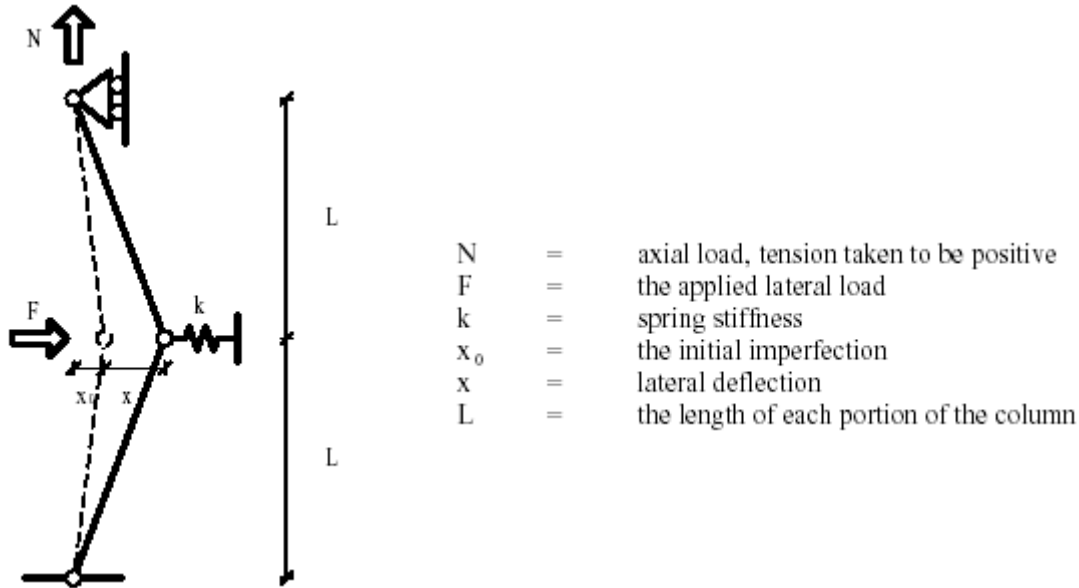
$$\text{Linear static P - Delta } [K_T^A] \{U\} = \{P\} + \{\text{Fixed End Forces}\}$$

The linear static analysis is based on only the instantaneous stiffness matrix  $[K_E]$  at the initial undeflected stage  $[K_E^A]$ . The linear static P- $\Delta$  analysis is based on the instantaneous and geometric (or differential) stiffness at the initial undeflected stage i.e. taking in to account the initial prestress and initial external load on the stiffness of the structure. The linear equations are solved simultaneously by decomposing  $[K]$  to triangular matrices, and then performing forward-backward substitution to obtain  $\{U\}$ . This is called the LU-decomposition method of solving linear simultaneous equations.

$$\begin{aligned} [K] \{U\} &= \{P\} + \{\text{Fixed End Forces}\} \\ [L] \{U\} &= \{P\} + \{\text{Fixed End Forces}\} \\ \text{Forward Pass } [L] \{y\} &= \{P\} + \{\text{Fixed End Forces}\} && \text{for } \{y\} \\ \text{Backward Pass } [U] \{U\} &= \{y\} && \text{for } \{U\} \end{aligned}$$

### 3.1.2 Concepts of Geometric Stiffness or P-Δ (K<sub>G</sub><sup>A</sup> From K<sub>E</sub><sup>A</sup>) Analysis <sup>1</sup>

The **geometric stiffness or P-Δ concept** will be illustrated for a simple system. A parameter that describes the prominence of the geometric stiffness **for a particular system and level of loading** will then be presented.



Let us assume that **deflections are small (hence geometrically linear analysis)** hence the rotation of the column segments can be described and any change in height can be neglected. Lateral equilibrium at the central pin shows that

$$F = kx + \frac{2N}{L}(x + x_0)$$

Note that the spring force depends only on the deflection  $x$ , while the lateral force generated by the component of  $N$  depends on the deflection plus the initial imperfection,  $x + x_0$ . Rearranging so that we have the form Stiffness x Displacement = Applied Force, we get

$$kx + \frac{2N}{L}x = F - \frac{2N}{L}x_0$$

and hence the deflection

$$x = \frac{F - \frac{2N}{L}x_0}{k + \frac{2N}{L}} \quad \text{i.e.} \quad x = \frac{\frac{F}{k} - \frac{2N}{kL}x_0}{\left(1 + \frac{2N}{kL}\right)}$$

Geometric Stiffness  $2N/L$

We can see that the effect of the force  $N$  acting on this system can be seen as being like an additional stiffness term  $2N/L$ , i.e. the geometric (aka differential) stiffness. The effect of the axial force is equivalent to an additional stiffness of value  $2N / L$  acting laterally at the pin location. If the force is tensile (i.e. positive) then the geometric stiffness will act to increase the overall stiffness of the system. The effects on the system tend to be beneficial, the lateral deflection and hence the restraining force in the spring are reduced. Some practical examples where this type of stiffness is important are in the strings of musical instruments where the tension is adjusted to give the required natural frequency, in the blades of jet engines where the vibration characteristics are improved and the root bending

<sup>1</sup> DALLARD, PAT. *Buckling – An Approach Based on Geometric Stiffness and Eigen Analysis*. Ove Arup & Partners International Ltd., London, June 1998.

moments reduced by the tension stiffening arising from rotation and in the antisymmetric response of unbraced cable trusses and cable nets where the ‘real’ (i.e. instantaneous, not geometric) stiffness may be negligible. On the other hand, if it is compressive then the term will be negative and the system stiffness will decrease. The effects on the system tend to be detrimental, the lateral deflection and hence the restraining force in the spring are increased. To reiterate, if N is compressive then the geometric stiffness is negative and x (the deflection) will be greater than it would be otherwise. If x is greater then the force in the spring will be greater. If we were designing that spring then we would need a stronger one than we first suspected. Therefore **the effect of negative geometric stiffness (also known as the P-Δ effect)** can be significant in design in some circumstances.

The question is, when will this **negative geometric stiffness** effect be significant and when can we ignore it? One good answer to this question is to examine the dimensionless parameter  $\lambda_{cr}$  (also known as the critical linear elastic buckling load factor of a system).

$$\lambda_{cr} = \frac{N_{cr}}{N}$$

$\lambda_{cr}$  indicates the level of significance of the **negative geometric stiffness (P-Δ effects)** in a structure. Finding the value of  $\lambda_{cr}$  is effectively a linearized buckling analysis (SOL 105). Note that  $\lambda_{cr}$  refers to the critical linear elastic buckling load factor and not to the slenderness parameter associated with member elements such as columns and beams, which is also normally referred to by  $\lambda$ . In this simple pin jointed system example however, the buckling factor can easily be derived by considering the condition at which the axial compression is so great that the lateral stiffness of the system is zero.

$$k + \frac{2N_{cr}}{L} = 0 \quad \text{i.e.} \quad N_{cr} = - \frac{kL}{2}$$

The  $\lambda_{cr}$  expression is **independent of the lateral load and the initial lateral imperfections**. Hence, **in the absence of geometric stiffness considerations**, there would be an abrupt bifurcation in the behavior of the system at the critical load. It is the deflection expression, presented hereafter, that the effects of the geometric stiffness considerations are seen as causing progressive amplification to lateral loads and initial lateral imperfections as the compressive load is increased until the critical load. Expressing the deflection expression in terms of  $N_{cr}$

$$x = \frac{\frac{F}{k} + \frac{N}{N_{cr}} x_0}{\left(1 - \frac{N}{N_{cr}}\right)}$$

Expressing the deflection equation again, but now in terms of  $\lambda_{cr}$  and the deflection without geometric stiffness considerations (i.e.  $N = 0$ )

$$x_{N=0} = \frac{F}{k}$$

we have thus the deflection expression a function of  $\lambda_{cr}$ , the initial imperfection  $x_0$  and  $x_{N=0}$

$$x = \frac{1}{\left(1 - \frac{1}{\lambda_{cr}}\right)} x_{N=0} + \frac{\frac{1}{\lambda_{cr}}}{\left(1 - \frac{1}{\lambda_{cr}}\right)} x_0 \quad \dots\dots\dots \text{Deflection Expression}$$

This expression consists of two terms, the first being the **amplified lateral response to lateral load when there is the geometric stiffness consideration** and the second being the **amplified (addition to the) lateral response to an initial imperfection when there is the geometric stiffness consideration**. We say ‘addition to the’ lateral response for the second term because the deflection x is measured relative to the initial imperfection and not from the initial undeflected configuration. If there were no geometric stiffness consideration, there would be an abrupt bifurcation in the behavior of the system at the critical load  $N_{cr}$ . The effect of the geometric stiffness consideration are seen as causing progressive amplification to the lateral loads and initial lateral imperfections as the compressive load is increased until the critical load. **It has the effect of amplifying the lateral deflection and**

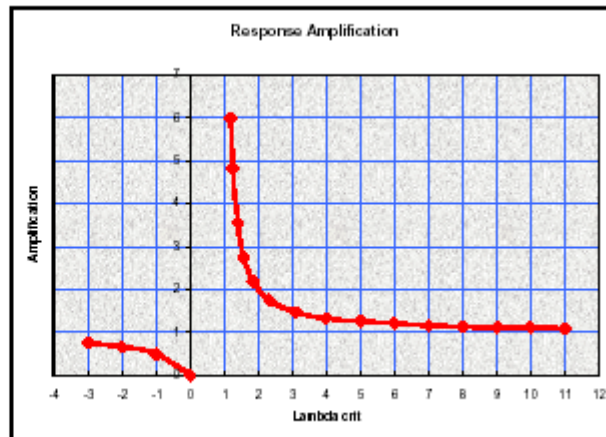
hence the spring force, or more generally, the forces in the elements resisting the lateral load. This is the P-Δ effect. The effects are apparent in practice. With the geometric stiffness consideration (and the existence of lateral loads and/or initial lateral imperfections), when a slender element is subject to axial compression, it tends to gradually bend before reaching the point of elastic instability. With the geometric stiffness consideration (and the existence of lateral loads and/or initial lateral imperfections), if a beam is subject to major axis bending, there is a tendency for the beam to twist and bend about its minor axis before lateral torsional buckling eventually occurs.

We shall investigate the amplified lateral displacement to lateral loads when there is the geometric stiffness consideration, which was shown to be

$$\frac{1}{\left(1 - \frac{1}{\lambda_{cr}}\right)} x_{N=0}$$

The definition of  $\lambda_{cr}$  is handy because it means that if  $\lambda_{cr}$  is a positive number greater than 1, then you have a structure that is stable, but that the structural response will be amplified by negative geometric stiffness effects. If  $0 < \lambda_{cr} < 1$ , then the system is unstable. And if  $\lambda_{cr}$  is negative then the structural response will be attenuated by positive geometric effects. Here are some values of  $\lambda_{cr}$  and their corresponding amplification values.

$\lambda_{crit}$	Amplification
$\infty$	1
20	1.05
10	1.11
5	1.25
2	2
1.25	5
1	$\infty$
-2	0.66



We can see that when  $\lambda_{cr} > 10$  the effects of negative geometric stiffness (P-Δ effects) are so small as to be insignificant to an engineering level of accuracy (accurate within 10%), whereas as they approach 1 they are very significant indeed. This then is the test that we were looking for. We can use the value of  $\lambda_{cr}$  to decide whether we need to take further account of negative geometric stiffness in our design and analysis. Generally,

If  $\lambda_{cr} > 10$  then P-Δ effects are insignificant and can be neglected – Perform linear analysis

If  $4 < \lambda_{cr} < 10$ , P-Δ effects (i.e. the geometric stiffness) should be incorporated – Perform P-Δ analysis

If  $\lambda_{cr} < 4$ , a second order nonlinear analysis should be undertaken – Perform GNL SOL 106 analysis

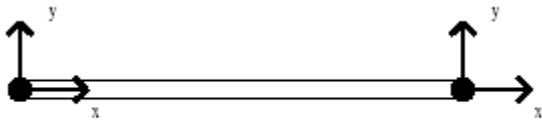
If  $\lambda_{cr}$  is 1 or less (but still positive) then amplification is infinite and some significant changes must be made to the design! It would be a mistake to be too scared of low  $\lambda_{cr}$  values. A very ordinary column in a building can have a  $\lambda_{cr}$  of  $< 1.6$ , and quite ordinary bracing systems for office buildings can have a  $\lambda_{cr}$  of  $< 4$ . But conversely it is not something that we can ignore and if response calculations are intended, a GNL SOL 106 must be performed.

The amplified (addition to the) lateral displacement to an initial imperfection when there is the geometric stiffness consideration was shown to be

$$\frac{1}{\left(1 - \frac{1}{\lambda_{cr}}\right)} x_0$$

When  $\lambda_{cr}$  is large the response will be small, when  $\lambda_{cr}$  is small, but  $>1$  the response will be large, and when  $\lambda_{cr} = 1$  the response becomes infinite, in a similar way to the amplified lateral displacement to lateral loads due to the geometric stiffness consideration.

The geometric stiffness equation for a 2D bar element is presented. Assume the bar has an axial force  $N$  (tension +) and length  $L$ , and use the local directions shown in the following diagram.



$$\begin{bmatrix} f_{x_1} \\ f_{y_1} \\ f_{x_2} \\ f_{y_2} \end{bmatrix} = \begin{bmatrix} 0 & 0 & 0 & 0 \\ 0 & N/L & 0 & -N/L \\ 0 & 0 & 0 & 0 \\ 0 & -N/L & 0 & N/L \end{bmatrix} \begin{bmatrix} x_1 \\ y_1 \\ x_2 \\ y_2 \end{bmatrix}$$

The active terms relate the geometric stiffening forces to the products of member forces and deflections. The terms in the instantaneous stiffness matrix  $K_E$  depend on the Young's modulus and Poisson's ratio of the material, and the geometry of the element (the geometry of a beam element, for example, would include both the cross sectional properties and the length of the element). In contrast, the terms in the geometric stiffness matrix  $K_G$  depend (linearly) on the forces in the element and the element geometry. The variation of the  $K_G$  matrix with element forces means that any analysis using a  $K_G$  matrix needs to be carried out in two stages. In the first stage the problem is solved ignoring the effects of geometric stiffening, establishing a set of element forces. These element forces are used in the second stage to construct the  $K_G$  matrix. An important consequence of the variation of the  $K_G$  matrix with element forces is that the  $K_G$  matrix for one load case will differ from that for another. Hence while we can always refer to the instantaneous stiffness matrix as  $K_E$ , we need to identify the geometric stiffness matrix by reference to the load case  $m$  for which it was derived, say  $K_{Gm}$ . The  $K_G$  matrix is symmetric with connectivity similar to the  $K_E$  matrix.

**In conclusion, the P- $\Delta$  effect is the reduction of lateral stiffness when the element is subjected to axial compression such that there is an amplified lateral response to lateral loads and an amplified (addition to the) lateral response to initial lateral imperfections (and subsequently the response of the elements providing lateral restraint) according to**

$$x = \frac{1}{1 - \frac{1}{\lambda_{cr}}} x_{N=0} + \frac{\frac{1}{\lambda_{cr}}}{1 - \frac{1}{\lambda_{cr}}} x_0 \quad \text{i.e.} \quad x = \frac{\lambda_{cr}}{\lambda_{cr} - 1} x_{N=0} + \frac{1}{\lambda_{cr} - 1} x_0$$

**We have said that the deflection  $x$  is measured relative to the initial imperfection  $x_0$ . If instead we present the deflection relative to the initial undeflected configuration, then we need to add  $x_0$ . Hence**

$$\begin{aligned}
 x + x_0 &= \frac{\lambda_{cr}}{\lambda_{cr} - 1} x_{N=0} + \frac{1}{\lambda_{cr} - 1} x_0 + x_0 = \frac{\lambda_{cr}}{\lambda_{cr} - 1} x_{N=0} + \frac{1}{\lambda_{cr} - 1} x_0 + \frac{\lambda_{cr} - 1}{\lambda_{cr} - 1} x_0 = \frac{\lambda_{cr}}{\lambda_{cr} - 1} x_{N=0} + \frac{\lambda_{cr}}{\lambda_{cr} - 1} x_0 \\
 x + x_0 &= \frac{\lambda_{cr}}{\lambda_{cr} - 1} (x_{N=0} + x_0)
 \end{aligned}$$

**Thus the deflection (measured from the initial undeflected configuration) to lateral loads and initial lateral imperfections is amplified by  $\lambda_{cr} / (\lambda_{cr} - 1)$ . This is a very important formula and can be applied approximately to all other general cases.**

To reiterate this rather important point, the above amplification  $\lambda_{cr} / (\lambda_{cr} - 1)$  was derived for a pin jointed system. It can be shown that the same amplification results for the deflection and stress effects on other general systems. For example, a strut with an initial imperfection  $x_0$  would have a transverse deflection distribution according to  $x_0 \sin(\pi x/L)$ . With an axial load  $N$ , the transverse deflection would be  $x_0 \sin(\pi x/L) [\lambda_{cr} / (\lambda_{cr} - 1)]$  where the buckling load is the Euler load, i.e.  $\pi^2 EI/L^2$ . It follows that the bending moment distribution would be  $N x_0 \sin(\pi x/L) [\lambda_{cr} / (\lambda_{cr} - 1)]$ . For another example, a beam with a UDL would have a central deflection of  $5\omega L^4/384EI$  and bending moment of  $\omega L^2/8$ . A good approximation to the central deflection of the beam-column with an axial load of  $N$  is  $(5\omega L^4/384EI) [\lambda_{cr} / (\lambda_{cr} - 1)]$  where the buckling load is the Euler load, i.e.  $\pi^2 EI/L^2$ . It follows that the central bending moment is approximately  $(\omega L^2/8) [\lambda_{cr} / (\lambda_{cr} - 1)]$ .

**Generally, for response computations**

**If  $\lambda_{cr} > 10$  then P- $\Delta$  effects are insignificant and can be neglected – Perform linear analysis**

**If  $4 < \lambda_{cr} < 10$ , P- $\Delta$  effects (i.e. the geometric stiffness) should be incorporated – Perform P- $\Delta$  analysis**

**If  $\lambda_{cr} < 4$ , a second order nonlinear analysis should be undertaken – Perform GNL SOL 106 analysis**

**Note that  $\lambda_{cr}$  is obtained from a linearized buckling analysis (SOL 105).**

The above proceedings described P- $\Delta$  analysis as a procedure by which the lateral stiffness is altered when a member is subject to an axial force, hence causing more lateral deflection and thus a greater bending moment in the member. An analogous way of looking at this is to consider an axial strut also subject to a lateral force. The lateral force causes a lateral deflection,  $\Delta$ . On application of the axial force  $P$ , a bending moment equal to  $P\Delta$  will be induced in the member.

### 3.1.3 Performing P-Δ (K<sub>G</sub><sup>A</sup> From K<sub>E</sub><sup>A</sup>) Linear Static Analysis – Direct Approach

The governing equation is

$$[\mathbf{K}_T^A]\{\mathbf{U}\} = \{\mathbf{P}\} + \{\text{Fixed End Forces}\} + \{\text{Initial Imperfections}\}$$

This equation is directly analogous to the equilibrium equation derived for the simple pin jointed system above.

$$F = kx + \frac{2N}{L}(x + x_0)$$

The initial imperfections are functions of the geometric stiffness, hence

$$[\mathbf{K}_E^A + \mathbf{K}_G^A]\{\mathbf{U}\} = \{\mathbf{P}\} + \{\text{Fixed End Forces}\} - [\mathbf{K}_G^A]\{\mathbf{U}_0\}$$

Note that  $\{\mathbf{U}_0\}$  is a vector of initial imperfections. Because  $\{\mathbf{U}_0\}$  is difficult and unintuitive to define, the modal approach presented in **Section 3.1.4** should be employed to perform the P-Δ analysis.

To perform a P-Δ analysis, first the value of  $\lambda_{cr}$  is established to decide whether and how account is made of the negative geometric stiffness.

If  $\lambda_{cr} > 10$  then P-Δ effects are unlikely to be significant and can be neglected

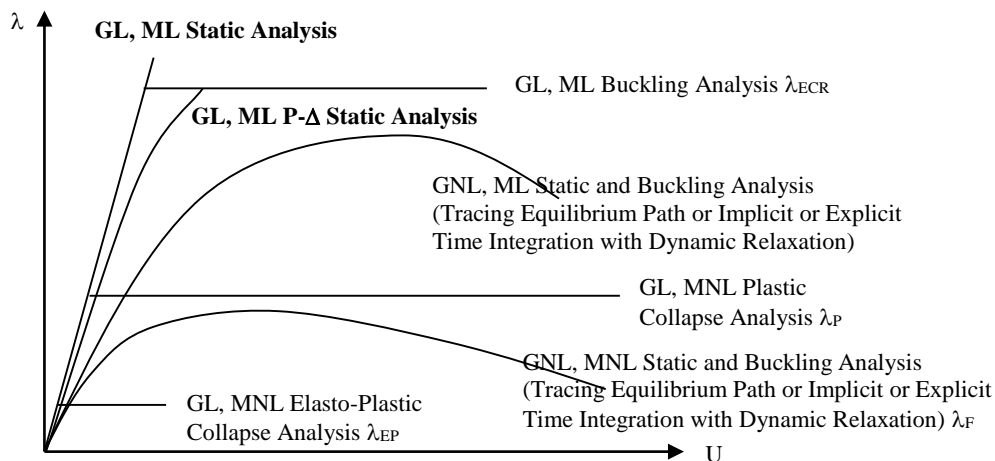
If  $4 < \lambda_{cr} < 10$ , P-Δ effects (i.e. the geometric stiffness) should be incorporated

If  $\lambda_{cr} < 4$ , a second order nonlinear analysis (GNL analysis SOL 106) should be undertaken

Hence, **only if  $\lambda_{cr} > 4$  can we employ the P-Δ method for response computations**. Any less, and a SOL 106 must be undertaken. To perform the P-Δ analysis, two linear static analyses are required. First, a linear static analysis is performed with the (ultimate limit state) loads  $m$  upon the instantaneous stiffness  $\mathbf{K}_E^A$  to assess the distribution of axial forces in the structure. These axial forces are used to generate the geometric stiffness matrix for that load case  $m$ ,  $\mathbf{K}_{Gm}^A$  which is combined with  $\mathbf{K}_E^A$  to form the tangent stiffness matrix  $\mathbf{K}_{Tm}^A$ . A second linear analysis is then performed with the (ultimate limit state) loads upon the tangent stiffness  $\mathbf{K}_{Tm}^A$  to generate the P-Δ response.

$$\{\mathbf{U}_m\} = [\mathbf{K}_E^A + \mathbf{K}_{Gm}^A]^{-1} \{ \{\mathbf{P}_m\} + \{\text{Fixed End Forces}\}_m - [\mathbf{K}_{Gm}^A]\{\mathbf{U}_0\} \}$$

Note that when we are doing an ultimate limit state design, as we generally are, the axial forces that cause the P-Δ amplification need to be ultimate axial forces, otherwise we will underestimate the amplification. For this reason the loading on the structure needs to be the ultimate loading. And the results will be ultimate forces. You can't apply characteristic loads, run the P-Δ analysis, and then factor the loads and responses up, because the **amplification effect is nonlinear, as observed on the P-Δ curve below, i.e. if the initial compressive loads  $m$  were higher, then the geometric stiffness will be larger and the response will be greater**. Of course, the initial loads  $m$  should be too great as to cause  $\lambda_{cr}$  to be less than 4. The down side of this is that each P-Δ case has to be run as an individual analysis and **you can't combine P-Δ results** in the conventional way, though you can of course envelope them.



**The P-Δ method can be used to evaluate the fundamental buckling load factor.** If the loads  $m$  were made too high, the geometric stiffness may become greater than the instantaneous stiffness, and the equations cannot be solved. Linear elastic buckling would have occurred. This means that we could in theory gradually increase the load  $m$ , run the P-Δ analysis involving the two passes each time, until the equations cannot be solved. The load at this stage is the lowest elastic buckling load. Performing this traces the above P-Δ equilibrium path. Note that the line is curved, but not flat at the onset of buckling as it is not a nonlinear method. Response calculations near the buckling load **may not be** accurate as  $\lambda_{cr}$  would be less than 4. It is much faster (and far more efficient in design) to evaluate the buckling load factor by performing an eigenvalue analysis (SOL 105). Moreover, the buckling mode shape will be clearly visible.

**The P-Δ method may NOT be accurate in evaluating the deflection response just before the onset of the fundamental buckling mode.**

$$[K_E^A + K_G^A]\{U\} = \{P_{cr}\} + \{\text{Fixed End Forces}\} - [K_G^A]\{U_0\}$$

P-Δ analysis is only accurate when  $\lambda$  is large, i.e.  $\lambda > 4$ . Hence, if the loads  $p_0$  were scaled to just below  $\lambda p_0$ , and a P-Δ analysis undertaken, the displacement response may be inaccurate because now the load factor on  $\lambda p_0$  is very close to unity. A nonlinear static and buckling analysis SOL 106 is recommended.

### 3.1.4 Performing P-Δ (K<sub>G</sub><sup>A</sup> From K<sub>E</sub><sup>A</sup>) Linear Static Analysis – Modal Approach; And Hence P-Δ Based Buckling<sup>2</sup>

#### 3.1.4.1 Objectives

Finding the P-Δ response by solving the P-Δ equation directly is presented in **Section 3.1.3**. While this method certainly works, a more intuitive modal approach may be desirable. The advantages of the modal approach are that

- (i) it helps to determine the most critical load combination to maximize the P-Δ effects
- (ii) it also allows for the imperfections (modeled to be proportional to the mode shape) to be incorporated to maximize the response and hence determine the elastic buckling capacity based on a P-Δ approach as is consistent with the BS 5950 code based Perry-Robertson method.

The basis of the modal approach is the ability of the buckling mode shapes to orthogonalize the P-Δ static equilibrium equation into a set of uncoupled modal equilibrium equations, which can be solved independently for the modal responses. These modal responses can then be transformed into the physical coordinates in order to obtain the physical response. In doing so, of course there will be a certain degree of modal truncation. To obtain the same answer as that of the direct approach (without imperfections), **ALL** the modes (equal to the number of DOFs) need to be employed. Since it is difficult (and unnecessary) to determine which modes really contribute to the static response, we **shall employ the direct approach anyway**. But with the addition here, that we include the response due to the imperfections as well. The imperfections are assumed to be proportional to the mode shape. In fact, the imperfections that really need to be incorporated are that of only the lower modes ( $\lambda_{cr} < 10$ ). Thus, the modal approach here is not intended as an alternative to the direct approach, but simply as an addition to incorporate the **(modal) imperfections for a P-Δ based buckling capacity prediction in line with the code based Perry-Robertson method** and also to aid the selection of the critical load case.

#### 3.1.4.2 Mathematical Formulation

A linear static analysis is first performed with load case m upon the instantaneous stiffness K<sub>E</sub><sup>A</sup> in order to generate the geometric stiffness matrix for the particular load case K<sub>Gm</sub>. The eigenvalue problem is

$$K\Phi_m + \Lambda_m K_{gm}\Phi_m = 0$$

- $\Lambda_m$  = a diagonal matrix of eigenvalues corresponding to the critical load factors  $\lambda_{cm}$  for loadcase m
- $\Phi_m$  = a matrix the columns of which are the modeshape vectors corresponding to loadcase m

Note that the eigenvalue problem has to be associated with a particular load case m as the geometric stiffness matrix is dependent upon the particular load case. The eigenvalue problem is solved for the critical load factors and associated mode shapes.

Solving the eigenvalue problem does not however produce a physical response. For this we consider the static equilibrium equation.

$$Kx_m + K_{gm}(x_m + x_o) = f_m$$

- $x_m$  = deflection vector in loadcase m
- $x_o$  = vector of initial imperfections
- $K$  = the normal stiffness matrix
- $K_{gm}$  = the geometry stiffness matrix for loadcase m
- $f_m$  = the external load vector in loadcase m

<sup>2</sup> DALLARD, PAT. *Buckling – An Approach Based on Geometric Stiffness and Eigen Analysis*. Ove Arup & Partners International Ltd., London, June 1998.

Note that the initial imperfections is really just an additional load and is probably more illustrated if the associated terms were brought onto the RHS of the equation as  $-K_{Gm}x_0$ . This equation can be solved directly as performed in **Section 3.1.3**. But this provides little insight into the buckled mode and hence the critical loading and pattern of imperfection that should be considered in design. As mentioned, the following eigenvalue approach is much more insightful in determining the response (deflections and forces). Representing the deflections as the summation of the responses in the individual modes

$$x_m = \Phi_m q_m$$

and the initial imperfections as the summation of imperfections in the individual modes (**hence assuming that the shape of the imperfections is the same as the shape of the buckled mode shapes**)

$$x_o = \Phi_m q_{mo}$$

$$\begin{aligned} q_m &= \text{vector of nondimensional modal responses} \\ q_{mo} &= \text{vector of nondimensional modal imperfections} \end{aligned}$$

On substitution,

$$K\Phi_m q_m + K_{gm}\Phi_m(q_m + q_{mo}) = f_m$$

Premultiplying by the transpose of the mode shape matrix, rightly treating the imperfections as additional loads

$$\Phi_m^T K \Phi_m q_m + \Phi_m^T K_{gm} \Phi_m q_m = \Phi_m^T f_m - \Phi_m^T K_{gm} \Phi_m q_{mo}$$

Both  $K_E$  and  $K_{Gm}$  will be diagonalized to give the modal stiffness and modal geometric stiffness

$$[\Phi_m^T K \Phi_m] = [K_m]$$

$$[\Phi_m^T K_{gm} \Phi_m] = [K_{gm}]$$

This is now a set of independent equations. Consider the  $i^{\text{th}}$  equation as typical

$$(k_i + k_{gi})q_i = \Phi_i^T f - k_{gi}q_{oi}$$

Hence, the modal response

$$q_i = \frac{\Phi_i^T f - k_{gi}q_{oi}}{(k_i + k_{gi})}$$

Separating the force and imperfection terms

$$q_i = \frac{1}{(1 + \frac{k_{gi}}{k_i})} \frac{\Phi_i^T f}{k_i} - \frac{\frac{k_{gi}}{k_i}}{(1 + \frac{k_{gi}}{k_i})} q_{oi}$$

The relationship between the modal stiffness, the modal geometric stiffness and the critical load factor  $\lambda_{cri}$  is

$$k_i + \lambda_{cri} k_{gi} = 0$$

Also, from the modal response expression, the modal response ignoring the geometric stiffening effects is seen to be the modal load  $\{\phi_i\}^T \{f\}$  divided by the modal stiffness

$$q'_i = \frac{\Phi_i^T f}{k_i}$$

Hence, the modal response expression can be rewritten as

$$q_i = \frac{1}{\left(1 - \frac{1}{\lambda_{cri}}\right)} q'_i + \frac{\frac{1}{\lambda_{cri}}}{\left(1 - \frac{1}{\lambda_{cri}}\right)} q_{oi} \quad \dots\dots\dots \text{Modal Deflection Expression}$$

This modal deflection expression is analogous to the deflection expression derived in **Section 3.1.2** for the simple pin-jointed column. Again, **when there is geometric stiffness considerations, there is an amplified modal response to modal loads and an amplified (addition to the) modal response to initial modal imperfections (and subsequently the response of the elements providing restraint to the modal response).**

A consequence of the modal nature of equation of the modal deflection expression is that the overall response amplifier is difficult to predict. The amplifier  $1/(1-1/\lambda_{cri})$  corresponding to the lowest buckling mode only applies to that part of the loading which contributes to the modal force  $\{\phi_1\}^T\{f\}$ , different amplifiers apply to the other components of load. Hence it is unlikely that the total response will be amplified by  $1/(1-1/\lambda_{cri})$ . To illustrate this consider a simple pin ended column subject to axial load and distributed lateral load. The  $1/(1-1/\lambda_{cri})$  amplifier would apply overall if the lateral load distribution followed the sinusoidal shape of the first buckling mode. This pattern of loading would result in zero modal forces in all modes except the first. If the lateral load distribution was uniform, say, it would generate modal forces in all odd numbered modes, each of which would have a different modal amplifier, and would result in a different overall amplifier.

In theory, the physical P-Δ response can finally be obtained from

$$x_m = \Phi_m q_m$$

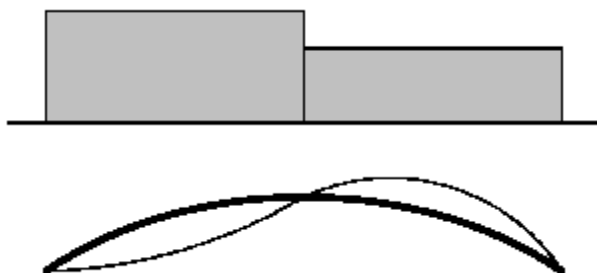
And by employing **ALL** the modes, the exact same response as that from the direct approach (without imperfections) will be obtained. But that is not the purpose of our exercise here. We are going to employ the direct approach anyway, this exercise is simply to aid the selection of the critical load case and for the modelling of the (modal) imperfections.

### 3.1.4.3 Critical Load Case Considerations

The loading used to design a structure prone to buckling must be selected with care. This is done in order to obtain the lowest possible load factor. Greater understanding of what loading may be critical can be gained from the modal deflection equation. It is useful to consider the loading on a structure as consisting of two parts applied simultaneously

- (a) loading which determines the value of the amplifier (via  $\lambda_{cri}$ ) but does not contribute to the linear modal response,  $q_i'$
- (b) loading which determines the value of the linear modal response  $q_i'$  (via  $\{\phi_i\}^T\{f\}$ ) but does not affect the amplifier (via  $\lambda_{cri}$ )

In a column, the axial load determines the value of the amplifier but does not contribute to the linear bending, while the lateral load determines the linear bending but does not affect the amplifier. Consider an arch prone to sway buckling and subject to asymmetric loading



Divide the loading into symmetric funicular and antisymmetric non-funicular components.



The funicular loading determines the axial force in the arch and hence the amplifier, but does not contribute to the linear bending. The antisymmetric loading determines the linear bending but does not affect the amplifier.

In the design of buckling sensitive structures, consideration needs to be given to how these two types of loading vary against each other. **The greatest overall response is likely to occur when the product of the linear response and the amplification factor is maximized.**

### 3.1.4.4 Modelling (Modal) Imperfections

Imperfections corresponding to a particular mode shape cause response in that mode shape and not in any other. The modal response (in modal coordinates) due to imperfections is  $1/(\lambda_{crit}-1)$  times the magnitude of the modal imperfection,  $q_{0i}$ . Thus in physical coordinates, the modal response due to imperfections will be  $(1/(\lambda_{crit}-1))q_{0i}\{\phi\}_i$ . Hence, the additional element forces due to imperfections can be calculated in a post-processing operation, using the additional modal responses due to imperfections simply to scale the modal element forces. It is usually sufficient to consider imperfections mode by mode, rather than combined. The value of  $q_{0i}$  should be selected to cover the effects of all imperfections, including residual stresses and tolerance.

Now, from the theoretical derivation of the Perry-Robertson buckling capacity formula, the **theoretical Perry imperfection factor**  $\eta$  is obtained

$$\eta = \frac{Ax_0}{Z} = \frac{x_0 y}{r^2} = \frac{x_0}{r} \frac{y}{r} = \frac{x_0}{L} \frac{L}{r} \frac{y}{r}$$

where  $x_0$  is the initial imperfection. The Perry factor  $\eta$  is the **imperfection factor** which is dependent upon the **initial eccentricity**,  $x_0$  and also the **cross sectional properties**. But BS 5950-Part 1:2000 goes a step further and requires an increase in the Perry factor due to residual stresses from rolling and welding. It thus states that the Perry factor should be

$$\eta = \frac{a}{1000} \frac{(L_e - L_o)}{r_y} \quad a = \text{Robertson constant}$$

$a$  = the Robertson constant as defined in 5950

Strut Curve (From BS 5950)	$a$
(a)	2.0
(b)	3.5
(c)	5.5
(d)	8.0

The Robertson constant,  $a$  divided by 1000, i.e.  $a/1000$  is equivalent to  $(x_0/L)(y/r)$  and includes the initial imperfection, the section shape and also residual stresses. On equivalence of the two expressions for the Perry factor, an equivalent initial imperfection  $x_0$  (or rather  $q_{0i}$  here) can be obtained as

$$q_{0i} = \frac{x_0}{x_g} \quad \text{where } x_0 = \frac{r_y}{y} \frac{a}{1000} L_d$$

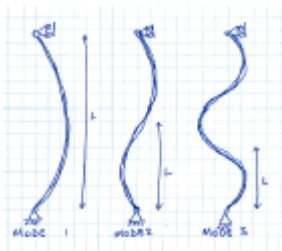
The value of the initial imperfection  $x_0$  is purposely derived to be perfectly consistent with the BS 5950-Part 1:2000 Perry-Robertson formula. We can get values for  $x_0$  that depend on the strut curve (Table 23 in BS 5950-Part 1:2000), the length of the buckled waveform  $L_d$ , and a single geometric property ( $r_y/y$ ) of the section that is buckling. The table below shows some appropriate values of  $x_0$  to use in common cases.

Most significant section type involved in the buckling	Max Thickness	$X_0$ (Initial imperfection)	
		Strong axis Buckling	Weak axis buckling
Hot finished CHS ( $r_y/y < 0.60$ )		$L_d / 720$	
Hot finished RHS or SHS ( $r_y/y < 0.84$ both axes)		$L_d / 600$	$L_d / 600$
Cold Formed CHS ( $r_y/y < 0.60$ )		$L_d / 260$	
Cold Formed RHS or SHS ( $r_y/y < 0.84$ both axes)		$L_d / 220$	$L_d / 220$
UB (rolled I section with $r_y/y < 0.84$ in the strong axis and 0.48 in the weak axis)	< 40mm > 40mm	$L_d / 600$ $L_d / 340$	$L_d / 600$ $L_d / 380$
UC (rolled I section with $r_y/y < 0.86$ in the strong axis and 0.52 in the weak axis)	< 40mm > 40mm	$L_d / 330$ $L_d / 210$	$L_d / 350$ $L_d / 240$
Welded I or H section (with $r_y/y < 0.9$ in the strong axis and 0.55 in the weak axis)	< 40mm > 40mm	$L_d / 320$ $L_d / 320$	$L_d / 330$ $L_d / 230$
Welded Box section (with $r_y/y < 0.8$ in the strong axis and 0.75 in the weak axis)	< 40mm > 40mm	$L_d / 360$ $L_d / 230$	$L_d / 380$ $L_d / 240$
Round bar	< 40mm > 40mm	$L_d / 570$ $L_d / 360$	
Square or Flat bar	< 40mm > 40mm	$L_d / 500$ $L_d / 320$	$L_d / 500$ $L_d / 320$
Generally strut curve (c) and $r_y/y = 1$		$L_d / 180$	

These values apply for the situations in the table. We have used values of  $r_y/y$  that are conservative for each of the particular ranges of section type. If your structure doesn't conform to one of the ones listed then you need to derive a value of  $x_0$  for your particular structure using the equation for  $x_0$ . Don't forget that  $r_y/y$  can never be greater than 1 for a symmetrical section. The values of  $x_0$  that are given by the equation and shown in the table are derived for flexural buckling, that is buckled modes that are controlled by bending of some element or elements. When the buckling is controlled by axial extension of, for instance, a bracing system, or by shear deflections, then there is no direct method of calculating a correlation to BS 5950-Part 1:2000. In these 'shear buckling' situations it seems prudent to use a value of  $x_0 = L_d/250$ .

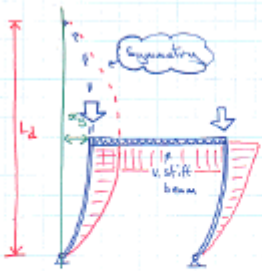
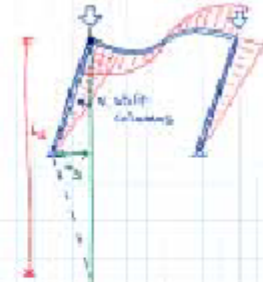
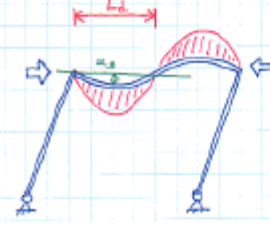
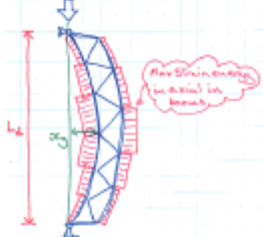
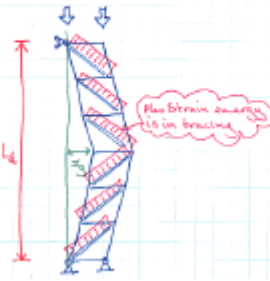
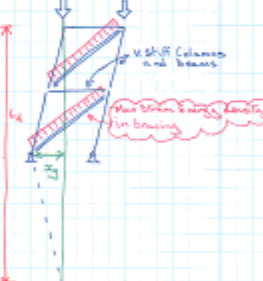
Mind you, don't get too hung up on the detail of these calculations; BS 5950-Part 1:2000 says that we can ignore these effects if they contribute less than 10% of the moment in a section. By implication it is pointless to try to evaluate these effects to very high degree of accuracy. Also, the odds of the steel fabricator building the structure with an initial imperfection that exactly resembles one of the buckled mode shapes that GSA has calculated are pretty small.

We still need to define the length of the waveform  $L_d$  and the deflection assumed by the solution code for the eigenvector at the middle of the waveform  $x_g$  usually 1.0 for MAX normalization. In the case of the Euler strut, in mode 1, the length of the buckled waveform is equal to the length of the strut. In mode 2,  $L$  is equal to half the length of the strut, and in mode 3,  $L$  is equal to one third of the length of the strut.



In the general case however, it may be more complicated.

<p><b>Example 1</b></p> <p>It follows from the definition of <math>L_d</math> in section 11 that, for the case of a pin ended strut, <math>L_d</math> is equal to the length and <math>x_g</math> is equal to the total deflection at the centre:</p>	<p><b>Example 2</b></p> <p>The second mode has half the effective length of the first mode. <math>x_g</math> is still equal to the deflection from the at rest position.</p>
<p><b>Example 3</b></p> <p>When the strut has ends fixed against rotation, <math>L_d</math> is equal to <math>L/2</math>, as we would expect. Notice that <math>x_g</math> now has to be measured relative to the deflection of the points of contra flexure, but that it is numerically equal to the <math>x_g</math> in Example 2 above.</p>	<p><b>Example 4</b></p> <p>This is a simple extension of the principle demonstrated in 3. <math>L_d</math> and <math>x_g</math> provide the mathematical relationship between our calculation and the simple strut in BS5950.</p>
<p><b>Example 5</b></p> <p>The simple cantilever case is an old friend from Euler buckling.</p>	<p><b>Example 6</b></p> <p>This strut has three intermediate restraints. In this mode they are acting as full restraints and the strut is buckling between them.</p>
<p><b>Example 7</b></p> <p>The strut shown in example 6 might also have an overall mode of buckling. In this case the GSA results will show an axial force in the restraints.</p>	<p><b>Example 8</b></p> <p>This strut has a less regular arrangement of restraints. The critical span is most likely to be the one that has the highest strain energy density.</p>

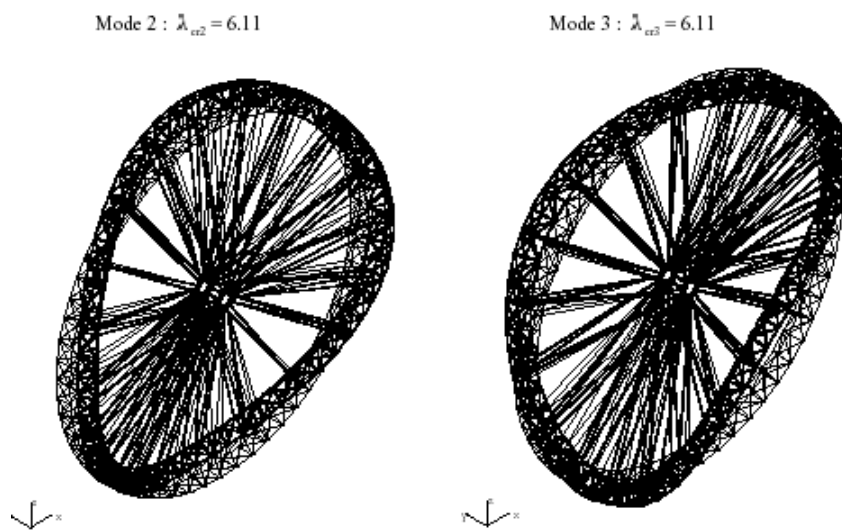
<p><b>Example 9</b></p> <p>Where the buckling of a portal frame is controlled by leg stiffness we can think of it as being similar to an upside down cantilevered column.</p> 	<p><b>Example 10</b></p> <p>If it is the stiffness of the beam that is controlling the behaviour then it acts as a rotational restraint to the head of the column.</p> 
<p><b>Example 11</b></p> <p>Here it is the beam that is buckling under a horizontal load. The sway happens because the columns follow the beams.</p> 	<p><b>Example 12</b></p> <p>This truss is behaving like a simple strut in flexural buckling. Theoretically obvious but, I suspect, rather rare in real life.</p> 
<p><b>Example 13</b></p> <p>Trusses are often prone to some variety of shear buckling, where it is the extension of the diagonals that is the primary mode of buckling.</p> <p>(This would be accompanied by secondary bending in the booms of course but I have omitted that 'for clarity'.)</p> 	<p><b>Example 14</b></p> <p>Bracing systems tend towards shear buckling too.</p> <p>(But don't be tempted to try and do without the notional horizontal load calc for the overall stability of buildings. We don't know enough to make a meaningful correlation.)</p> 

For real structures, when we look at a real buckling mode the first thing that we need to establish is which member, or members, is it that is a) causing the buckling and b) being affected by the buckling. When we say that a member, or members, is 'causing the buckling' what we mean is that we are assuming that the structure has been built with an imperfection in that member, or members (that mimics the shape of the buckled mode shape). In the case of the simple strut in example 1 this means that the strut is initially bowed. In the case of the bracing in example 14 this means that the bracing members were too long. When we say that a member is 'affected by' the buckling we mean that moments or forces are induced in them, under the normal structural loads, as a result of the imperfection that the structure was built with. Luckily, our definition of a buckling mode leads to the situation where the two sets of members (a) and (b) above are generally coincident. A member that the analysis code identifies as having a high curvature (or extension) becomes the one that has a curvature (or extension) as its initial imperfection. And it is no coincidence that a member with high curvature (or extension) in the buckled mode is a member that has a high moment (or axial force) in the force results for that mode. Let us call these members the primary buckling members for the mode. Spotting the primary buckling members for any given mode is made easier by looking for the maximum 'total strain energy density' in the structure in that mode. The total strain energy density is a value that the analysis code calculates, and will display, either as a diagram, or as a contoured value. It is, roughly speaking, defined as moment  $\times$  curvature (or axial force  $\times$  axial extension) divided by member area to give an energy density per meter along the beam. Since the total strain energy density is the product of the two variables that we are most interested in when we want to find the sets of members (a) and (b) above, it gives us a powerful graphical tool for highlighting which the primary buckling members are.

The resultant forces from each buckled mode can then be combined with the other ultimate forces in the structure (from the P- $\Delta$  analyses) to give sets of design forces for the final stress check. **Note that each set of resultant buckling forces occurs because the structure was (we assume) built with a specific initial imperfection shape that corresponded to the buckled mode shape. Therefore we do not need to combine forces from one mode with forces from another since the structure cannot be built into both shapes at the same time.**

The sign of  $q_{0i}$  should be taken so as to maximize the total response in terms of section utilization. Usually imperfections in the lowest buckling modes ( $\lambda_{cr} < 10$ ) will cause the greatest additional response. Several such modes may need to be considered, each maximizing the utilization of particular sections.

It is sometimes necessary to consider the effect of combining modal imperfections. The following plots show two mode shapes of the Millennium Wheel. The rim buckles under the compression induced by the prestress in the spokes. The load factors for the two modes are virtually identical, as are the mode shapes, except they are rotated such that the position of nodes and antinodes are swapped.



It would be incorrect only to consider imperfections in each mode separately, as this would suggest that the strength requirement for the rim varies around the circumference. A more general imperfection of the required magnitude can be obtained by combining the imperfections due to  $\sin\alpha \cdot q_{02}$  and  $\cos\alpha \cdot q_{03}$ . The same amplifier applies to this combined imperfection, resulting in the same maximum response, except that the maximum can occur anywhere around the rim. This supports intuition, the rim strength should be constant around the circumference. Another such example is a long beam on elastic foundations, which has a numerous modes of very similar shape and load factor. Again, an analysis using a generalized imperfection, based on combined modal imperfections, would demonstrate that, away from the ends, the beam strength needs to be constant. Such paired or multiple modes arise because structure and loading have a high degree of symmetry. The Millennium Wheel has cyclic symmetry and the beam on elastic foundations has longitudinal repetition.

### 3.1.4.5 Design

It is quite normal to analyze structures assuming they remain linear elastic but then to check the member forces against plastic capacities. Provided the system is not prone to buckling, partial plasticity causes redistribution of the forces within the structure but it does not change the overall loading. To be strictly conservative when using linear buckling analysis, the member forces would need to be limited to the **elastic capacities**, reduced to allow for the effects of residual stresses. Codes of practice may allow for this by making the magnitude of the strut imperfection depend on whether the member is to be checked elastically or plastically. A similar allowance can be made in the proposed method by increasing the magnitude of the design imperfections.

The simplified overall buckling check in BS 5950-Part 1:2000 Clause 4.8.3.3 does not amplify the applied moments. While this is not conservative, it is usually argued that the effect is small. The more exact approach does include moment amplification, as does the proposed method.

#### **3.1.4.6 Limitations**

The proposed first order analysis method will not be appropriate if the shape of the structure changes significantly under the applied loading. The classic example would be very shallow arches that flatten under load and are prone to snap through buckling. The axial force in the arch would be significantly underestimated if calculated on the basis of the initial geometry, it needs to be calculated based on the reduced curvature of the flattened, loaded arch. The significance of the effect could be assessed by considering the change in geometry arising from limiting elastic strain in the arch.

### 3.1.4.7 Methodology

Thus, to perform a linearized elastic buckling analysis, the following procedure is undertaken for **each** ultimate state load combination.

- (a) **P-Δ:** Apply ultimate limit state load case combination onto the structure (hence the load factors will be factors upon the ultimate limit state effects). Perform a P-Δ analysis; note two passes required.
- (b) **Eigenvalue:** Perform the linear eigenvalue buckling analysis (two passes required) to obtain the lowest buckling factor. If  $\lambda_{cr1} > 10$ , then a linear static analysis (no P-Δ effects) may be sufficient.
- (c) **Modify load case combination to maximize the amplification terms (by minimizing  $\lambda_{cr}$  i.e. by maximizing the geometric stiffness):** Modify the load case combination in order to obtain an even lower buckling factor by maximizing the geometric stiffness matrix. From observation of the critical buckling mode shape, the loading that contributes to the geometric stiffness can be identified. This should be maximized to increase the geometric stiffness, and hence obtain the lowest buckling load factor. For example, for an arch this would mean identifying the load case combination causing the maximum arch compression and for a column, the maximum axial compression. Again, of course, the two passes (linear static on  $K_E^A$  and eigenvalue on  $K_E^A$  and  $K_G^A$ ) must be performed for the eigenvalue analysis. Hence the lowest ( $\lambda_{cr1} < 10$ ) buckling load factors and associated mode shapes are obtained.

$$q_i = \left( \frac{1}{1 - \frac{1}{\lambda_{cr1}}} \right) q'_i + \left( \frac{\frac{1}{\lambda_{cr1}}}{1 - \frac{1}{\lambda_{cr1}}} \right) q_{oi}$$

Amplification terms

- (d) **Modify load case combination to maximize linear response of critical mode:** Modify the load case combination seeking to maximize the product of the linear response, dependant on the modal force  $\{\phi_1\}^T \{f\}$ .

$$q'_i = \frac{\phi_i^T f}{k_i}$$

- (e) **Iteration:** Repeat steps 1-4 until the smallest buckling load factors and largest P-Δ response obtained.
- (f) **Incorporate modal imperfection responses:** Calculate the modal imperfection responses as

$$\frac{\frac{1}{\lambda_{cr1}}}{1 - \frac{1}{\lambda_{cr1}}} q_{oi} = \frac{x_0}{x_g} \text{ where } x_0 = \frac{r_y}{y} \frac{a}{1000} L_d = \frac{L_d}{\text{some constant}}$$

$$\therefore q_{oi} = \frac{L_d}{x_g \cdot \text{some constant}}$$

for every significant mode, i.e. all modes that give rise to significant forces in the structure. This usually means the modes with  $\lambda_{cr}$  of less than 10.

- (g) **Total physical response:** The total physical response will be the summation of the P-Δ case and the modal imperfection responses (of the significant modes with  $\lambda_{cr} < 10$ ) in physical coordinates.

$$\text{Total response} = \text{P-}\Delta \text{ response} \pm 1/(\lambda_{cr1}-1)q_{01} \times \{\phi\}_1$$

$$\text{Total response} = \text{P-}\Delta \text{ response} \pm 1/(\lambda_{cr2}-1)q_{02} \times \{\phi\}_2$$

...

$$\text{Total response} = \text{P-}\Delta \text{ response} \pm 1/(\lambda_{crn}-1)q_{0n} \times \{\phi\}_n$$

...

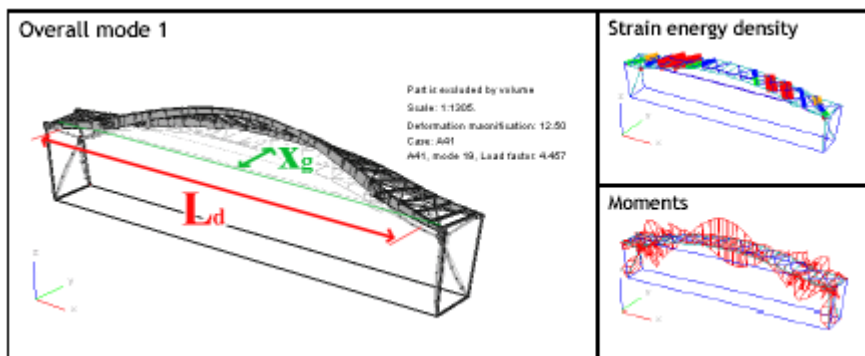
... etc ... until  $\lambda_{cr} \sim 10$

We do not need to combine forces from one mode with forces from another since the structure cannot be built into both shapes at the same time. Envelope the results, hence incorporating the imperfections in all the modes up to  $\lambda_{cr} \sim 10$ .

- (h) **Design:** Perform local linear *elastic* (not ULS plastic) capacity checks on the enveloped response. This then becomes analogous to the code based Perry-Robertson element buckling check applied to global modes.

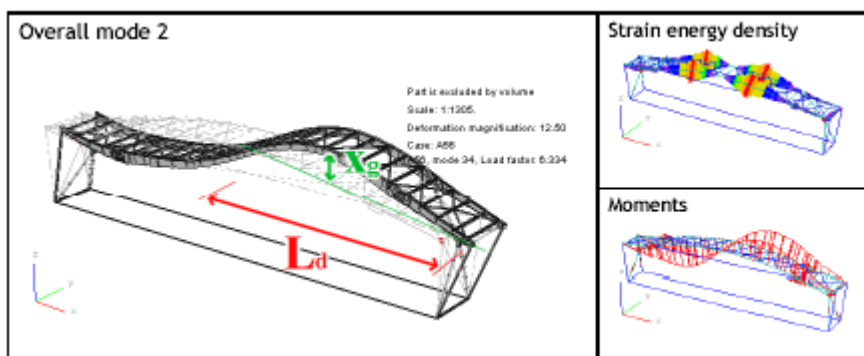
Let us look at a real example. The Core Terminal Building roof at Terminal 5, Heathrow, London is not only a very fine piece of structural engineering and a good example to look at. The model includes 2 rafters and a single pair of support structures. This frame spans the width of the terminal building and will be repeated 11 times to cover the length.

The first overall buckling mode looks, at first sight, to be major axis buckling of the rafters (which are prestressed into compression as well as having an arched shape). It looks as though one goes up and the other goes down, with each behaving rather like the strut in example 1. However, examination of the strain energy density diagram reveals that it is the bracing in the roof plane that is the primary buckling member set, rather like example 13. The y direction sway and the major axis moments in the rafters are secondary effects. The value of  $L_d$  has therefore been taken as the distance between the centres of rotation of the two ends of the roof plane horizontal truss (as observed from the deflected shape diagram when viewed from above). And  $x_g$  has been taken as the horizontal deflection of the centre of the truss relative to its two ends (as defined by those centres of rotation).



The forces predicted by mode 1 are those that result from the bracing being installed with incorrect lengths. They tend to be axial forces in the bracing, but there are moments induced in the rafters as well.

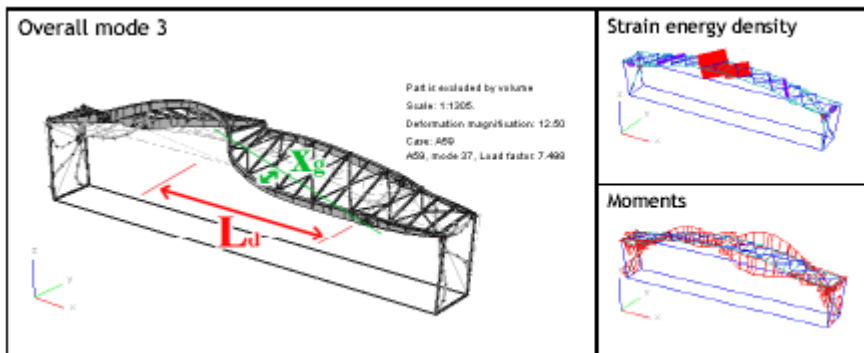
The second overall mode could also have been deceptive. The primary buckling members are clearly the main rafters but what is causing the buckling? One might imagine that the structure was swaying in the east west direction because of the heavy vertical loads on the legs, as in examples 9 or 10. However a simplified model showed that the  $\lambda_{crit}$  for that behaviour should be in the region of 40 rather than the value of 6 that the full model predicts. It turns out that a simple model based on the action displayed in example 11 is a much closer match to the behaviour of the full model. The rafter itself behaves rather like the strut in example 2, or indeed the beam in example 11. Therefore the appropriate value of  $L_d$  is measured from the end, to the point of contra flexure in the centre. And  $x_g$  is taken as the vertical deflection of the rafter  $\frac{1}{4}$  point (this is to avoid an overestimate of  $x_g$  that might result if the east west movement were included).



The forces predicted by mode 2 are caused by incorrect curvature of the rafters. The primary effect is moment in the rafters themselves, but there are also significant axial forces induced in the support structures.

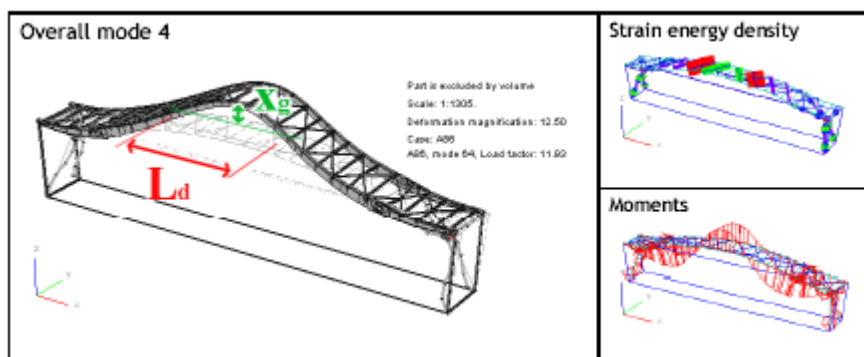
The third mode is rather like the first in that the primary buckling members are in the roof bracing. In this case the action is a little more complex structurally. The centre bay of bracing diagonals has been omitted for visual reasons.

This means that imperfections in the length of adjacent bracing diagonals have a significant effect, and shear of this central bay forms the third mode. Again  $L_d$  is taken between points of rotation of the roof plane truss and  $x_g$  has been measured horizontally.



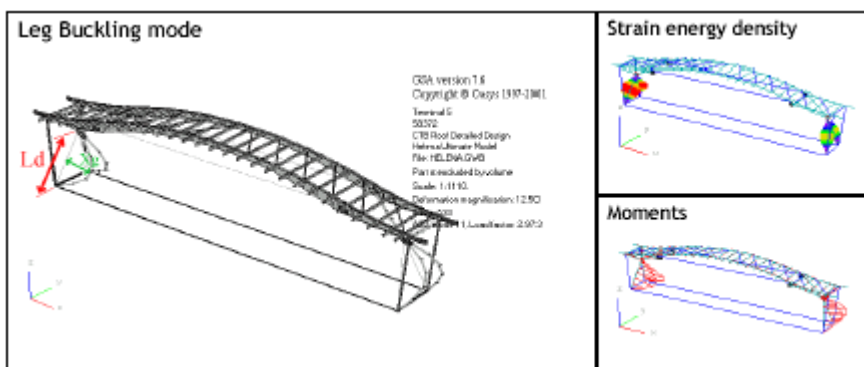
The forces predicted by mode 3 arise because of imperfect bracing lengths. The primary effect is axial in the bracing, but this mode also causes some rather inconvenient lateral moments in the CHSs of the support structures.

The fourth mode illustrates the need to keep our eyes open. The strain energy density diagram would lead us to think that the primary buckling members were the roof plane bracing, like in modes 1 and 3. But the deflected shape, and the bending moment diagram do not fit with this hypothesis. A simplified model confirmed that a straight rafter in compression would buckle in a very similar shape at a similar  $\lambda_{crit}$ . Therefore we conclude that the mode is very like example 3.  $L_d$  is the length of the centre portion of rafter between the points of contra flexure.  $x_g$  is measured vertically, relative to the vertical deflection of the points of contra flexure.



In common with mode 2, the forces predicted by mode 4 are caused by incorrect curvature of the rafters. The primary effect is moment in the rafters themselves, but there are also significant axial forces induced in the support structures.

In addition to these overall modes there are plenty of modes that show buckling of only one part of the structure. In the case shown below it is the legs that are buckling. If you wanted to, you could use results from this analysis to check the capacity of the leg CHSs themselves. It would be just as valid, however, and probably much quicker, to use the code of practice for these sections. In this case  $L_d$  and  $x_g$  would be just what you would expect from looking at example 1, and so are the forces.



### 3.1.5 MSC.NASTRAN Decks

#### 3.1.5.1 GL, ML Static Analysis

```

$ EXECUTIVE CONTROL SECTION
SOL 101
$ CASE CONTROL SECTION
DISPLACEMENT(<PRINT,PUNCH,PLOT>) = ALL/<Grid Set ID>
SPCFORCES(<PRINT,PUNCH,PLOT>) = ALL/<Grid Set ID>
OLOAD(<PRINT,PUNCH,PLOT>) = ALL/<Grid Set ID>
ELSTRESS(<PRINT,PUNCH,PLOT>) = ALL/<Element Set ID>
ELFORCE(<PRINT,PUNCH,PLOT>) = ALL/<Element Set ID>
STRAIN(<PRINT,PUNCH,PLOT>) = ALL/<Element Set ID>
ESE(<PRINT,PUNCH,PLOT>) = ALL/<Element Set ID>
LOAD = < ID of FORCEi, MOMENTi, PLOADi, GRAV, LOAD, SPCD Cards in Bulk Data >
TEMP(LOAD) = < ID of TEMP, TEMPRB, TEMPP1 Cards in Bulk Data >
DEFORM = < ID of DEFORM Cards in Bulk Data >
SPC = < ID of SPC Cards in Bulk Data >
    
```

The DISPLACEMENT request outputs the displacement vector

D I S P L A C E M E N T   V E C T O R							
POINT ID.	TYPE	T1	T2	T3	R1	R2	R3
1	G	.0	.0	.0	.0	.0	.0
2	G	.0	.0	.0	.0	.0	.0
3	G	7.578219E-03	-2.504843E-02	.0	.0	.0	.0
4	G	-2.421781E-03	-2.495156E-02	.0	.0	.0	.0

Displacements expressed in the global coordinate system

G for grid point, S for scalar point

The OLOAD request outputs the applied loads vector

L O A D   V E C T O R							
POINT ID.	TYPE	T1	T2	T3	R1	R2	R3
4	G	.0	-1.000000E+03	.0	.0	.0	.0

Applied loads and moments expressed in the global coordinate system

The applied loads are reported at the grid points, and include implicitly defined loads such as pressure or gravity.

### 3.1.5.1.1 Applied Loads

**FORCE** or **MOMENT** is used to apply a concentrated force or moment at a grid in either the basic or a user-defined coordinate system.

\$ BULK DATA									
FORCE	SID	Grid ID	CID	Scale Factor	N1	N2	N3		
MOMENT	SID	Grid ID	CID	Scale Factor	N1	N2	N3		

To apply a concentrated force or moment at a grid point in or about a vector defined by two arbitrary grid points, **FORCE1** or **MOMENT1** is used. To apply a concentrated force at a grid point in or about a vector defined by the cross product of two vectors defined by four grid points, **FORCE2** or **MOMENT2** is used.

To define a linearly varying element load on CBAR, CBEAM and CELBOW elements, the **PLOAD1** card is used.

\$ BULK DATA									
PLOAD1	SID	EID	TYPE	SCALE	X1	P1	X2	P2	

- TYPE refers to direction and coordinate system  
basic coordinate system FX, FY, FZ, MX, MY, MZ  
element coordinate system FXE, FYE, FZE, MXE, MYE, MZE
- SCALE refers to either LE which means that the values of Xi are based on actual length of element or FR which means that the values of Xi are based on fractional distances with the length of element normalized to 1.0
- X1, X2 the distances from end A, bounding the region where the load is applied
- P1, P2 the load factors at positions X1, X2

To apply a uniform **normal** pressure load on CQUAD4, CTRIA3 or CSHEAR surfaces defined by three or four grids on one or many shell elements, the **PLOAD** card is used. The direction of the pressure is based on the right hand rule and the ordering sequence of the grids.

\$ BULK DATA									
PLOAD	SID	Pressure	G1	G2	G3	G4			

To apply uniform **normal** pressure load on CQUAD4, CTRIA3 or CSHEAR using element ids, the **PLOAD2** card is used. The direction of the pressure is based on the right hand rule and the element grid definition order.

\$ BULK DATA									
PLOAD2	SID	Pressure	EID1	EID2	THRU	EID77	EID89	EID97	

To apply a **linearly** varying **not necessarily normal** pressure load (such as hydrostatic pressure) on a surface of **any** two or three-dimensional elements, the **PLOAD4** card is used.

Note that point loads and moments on 1D elements are independent of the geometry of the element. Pressure loads (applied in stress units) on 2D and 3D elements are dependent upon the dimensions of the loaded face of the element. Line edge loads (applied in stress units) on 2D elements are dependent upon the thickness and the dimension of the loaded edge.

To apply acceleration forces on elements (such as force due to gravitational or centripetal acceleration), the **GRAV** card is used. The GRAV card is used to simulate a load resulting from the inertia of the component of system. Gravity may be one example. Another example may be the acceleration induced in a car component when the car accelerates. The inertia of the component will resist the acceleration and hence produce a force in the same way as it resists gravitational acceleration. Likewise, a centrifugal acceleration load allows rotating systems to be evaluated statically.

\$ BULK DATA									
GRAV	SID	CID	Scale Factor	N1	N2	N3	MB		

The force due to acceleration is calculated by multiplying the mass matrix with the acceleration specified. To specify a gravitational acceleration of  $9.81 \text{ m/s}^2$ , with the scale factor equaling 1.0,  $N3 = -9.81$ , with the vertical direction being the global Z direction. The mass definition is defined by the density on a material entry.

The GRAV card cannot have the same ID as other static load types. Hence, a load combination must be specified using the LOAD bulk data entry with the ID equal to that specified by the LOAD card in the Case Control Section. The LOAD bulk data entry can be used to combine FORCEi, MOMENTi, PLOADi, GRAV, and SPCD cards.

\$ BULK DATA									
LOAD	SID	Overall Scale Factor	S1	L1	S2	L2	S3	L3	
	S4	L4	...etc...						

### 3.1.5.1.2 Enforced Displacement

There are two methods available for specifying an enforced displacement at a component. The first method is to enter the value of the enforced displacement directly on an SPC entry. The alternate method to enforce a displacement at a component is to use the SPCD Bulk Data entry. The SPCD entry is actually a force, not a constraint, but it is used in conjunction with an SPC entry to enforce the displacement. When you use an SPCD entry, internal forces are computed that are applied to the structure to produce the desired enforced displacements.

To specify a static enforced displacement at grid points, the **SPCD** card may be used.

\$ BULK DATA									
SPCD	SID	G1	C1	D1	G2	C2	D2		

Grid points with an enforced displacement using the SPCD entry must also appear on an SPC or an SPC1 Bulk Data entry. The SPCD method of enforcing a nonzero constraint is more efficient than using an SPC entry alone when you are using multiple subcases that specify different constraint conditions. Note also that when you use an SPCD entry, the displacement values entered on the SPC entry are ignored-only the SPCD values are used.

### 3.1.5.1.3 Lack-of-Fit

To specify a lack-of-fit or vice versa on line elements, the **DEFORM** card can be used.

\$ BULK DATA									
DEFORM	SID	EID	D1	EID2	D2	EID3	D3		

A positive deformation D1 refers to elongation and a negative D1 refers to a contraction (lack-of-fit). When using the DEFORM entry, you must remember that in general you are not enforcing a strain or an actual extensional length to the element. What you are doing is applying a force to the element that produces the specified extension if the element is free to expand without internal forces being generated. This computed force is added to the other forces in the model. Since most elements in your model are not free to expand, the extension value you specify may not be achieved.

### 3.1.5.1.4 Prestressed Member

The prestress is an element (such as a prestressed cable) can be modeled using temperature loads. The axial force generated from applying the temperature load on a line element that is totally fixed at its nodes can be calculated as follows,

$$f_{axial} = EA\delta/L$$

$$f_{axial} = EA\varepsilon_{strain}L/L$$

$$f_{axial} = EA\varepsilon_{strain}$$

where  $\varepsilon_{strain} = \alpha \Delta T$ ,  $\alpha$  is the coefficient of thermal expansion (per °C) and  $\Delta T$  is the change in temperature in °C. Note that the loads induced by the temperature are independent of the length of the element, L.

However, it must be realized that the force calculated above is based on a fixed end line element. In reality and in the numerical model, the ends will in general not be fixed. Hence the element will contract with tensile temperature loading causing the force to decrease. Thus the specified  $\Delta T$  will have to correspond to a force which is greater than the intended final prestress. Hence an iterative procedure is required (hence the need to perform the analysis repeatedly) until the required prestress is achieved in the final deflected configuration.

### 3.1.5.1.5 Thermal Expansion or Contraction

Thermal expansion and contraction is a structural rather than a thermal solution i.e. it is the analysis of stress and displacement due to thermal effects that is being considered, not the temperature at a point in the structure, which requires a heat transfer analysis. In fact, a heat transfer analysis can actually be used to generate the temperature profile and distribution and these results can in turn be applied as temperature loads in a thermal stress analysis.

The input data required for analyzing thermal expansion is the coefficient of thermal expansion and the temperature distribution in model. The temperature data and the thermal expansion coefficients (in the material entry cards) are used internally to calculate equivalent forces and moments acting at grid points. Temperatures can be specified at grid point using **TEMP** cards, or at elements using **TEMPRB** (line elements) or **TEMPP1** (shell elements). Average temperature specified directly for an element will take precedence over the temperature interpolated from the elements connected grid points. Solid elements get their temperature only by interpolation from connected grid points. Temperature load is calculated for a fixed ended member as

$$f_{axial} = EA\varepsilon_{strain}$$

where  $\varepsilon_{strain} = \alpha \Delta T$ ,  $\alpha$  is the coefficient of thermal expansion (per °C) and  $\Delta T$  is the change in temperature in °C

This equivalent nodal load is only attained if the element is constrained from expanding and contracting. Note that the loads induced by the temperature are **independent of the length** of the element, L. However, if the elements is not constrained from expanding and contracting, then there will be a lateral deflection of  $f_{axial}/k = f_{axial}/(EA/L) = EA\varepsilon_{strain}/(EA/L) = \varepsilon_{strain}L$  which clearly is **dependent upon the length** of the element, L. Temperature loads are defined as follows.

<b>\$ CASE CONTROL SECTION</b>									
TEMP (INIT) = < ID of TEMP, TEMPD, TEMPP1, TEMPRB, TEMPF or TEMPAX Bulk Data Say 99 >									
TEMP (LOAD) = < ID of TEMP, TEMPD, TEMPP1, TEMPRB, TEMPF or TEMPAX Bulk Data Say 1 >									
<b>\$ BULK DATA</b>									
TEMPD	ID Say 99	Temperature 0.0							
TEMPD	ID Say 1	Temperature 0.0							
TEMPRB	ID Say 1	EID1	TA	TB					
	EID2	THRU	EID100	EID200	THRU	EID300			

TEMPD is to define temperatures at all grid points not given a temperature. It is good practice to define these and the initial nodal temperatures. TA and TB are the variations of temperature  $\Delta T$  **from the reference temperature** defined by TEMP (INIT).

Note also that SUBCOM **cannot** be used conventionally to combine temperature load cases. The following procedure is required. SUBCOM 3 combines the mechanical loads of load cases 1 and 2, but not their temperature loads. Temperature loads must thus be specified separately calling a separate TEMPi bulk data entry card, which can be made to combine the temperature loads of the load cases 1 and 2.

<b>\$ CASE CONTROL SECTION</b>									
SUBCOM 3									
SUBSEQ = 1.0, 0.5 \$ 1.0 x subcase 1 + 0.5 subcase 2									
TEMP (LOAD) = < ID of TEMP, TEMPD, TEMPP1, TEMPRB, TEMPF or TEMPAX Bulk Data >									

### 3.1.5.1.6 Linear Contact Definition with MPC Equations for SOL 101

Contact definitions (normal to contacting surfaces, no sliding friction) can be made within a linear static analysis (albeit using an iterative method). RBE2 elements can be defined between adjacent grids of surfaces, then a linear static analysis performed, then the RBE2s in tension deleted (as a contact cannot sustain tension), further linear static analyses performed and further RBE2 elements deleted until there are no RBE2 elements in tension within the contact interface. Although this method works, it is extremely cumbersome, as every load case will have a different contact distribution. This process can be automated far more elegantly using MPC equations in SOL 101. It uses an iterative constraint type approach. The constraints are applied to grid points or SPOINTS. The constraint ensures that:

1. The displacement (UR) cannot be negative. This is to ensure that there is no penetration. Therefore, the chosen degree-of-freedom must be perpendicular to the contact surface and positive in the opening direction.

2. The force of constraint (QR) cannot be negative. This is to ensure that there is no tension.

The constraints are satisfied by an iterative technique that is built into SOL 101. The iterative process starts with a random vector. This random vector assumes certain grids to be in contact and other grids to be in an open state. A solution is obtained when all the gap constraints are satisfied, i.e., there's no penetration and no tension forces. If a limit cycle (return to a previous state) is detected during the iterations, a new random start vector is tried. This approach provides an alternate method to the use of GAP elements in SOL 106. Some experiments have shown that the cost of analysis will be about the same. The advantage is that you do not have to learn how to calculate the GAP stiffness nor how to control SOL 106. Multiple load conditions are allowed, and each will be solved separately. If the constraint is between a finite element model and a fixed boundary, then arrange to have one of the degrees-of-freedom at the boundary grid points represent motion perpendicular to the boundary. A positive displacement represents motion away from the boundary. If, on the other hand, the constraint represents relative motion between two bodies, MPC equations are needed to define a relative motion degree-of-freedom, which is then constrained to have a non-negative displacement. Consider the following contact interface between two faces of the FE model



The MPC for each and every pair of grids is defined as

$$S = U_{G2} - U_{G1} + S_0$$

where S is the relative motion DOF,  $U_{G2} - U_{G1}$  arranged such that a positive value indicates opening of the contact and  $S_0$  representing the initial gap opening, zero if the model interface gap is zero. The MPC is rearranged

$$S - U_{G2} + U_{G1} - S_0 = 0$$

for the definition of the card.

To model a fixed contact interface between a surface of the FE model and a fixed boundary, simply omit  $U_{G1}$  to represent a fixed boundary.

§ CASE CONTROL SECTION									
MPCFORCES (<PRINT, PUNCH, PLOT>) = ALL									
MPC = < ID of MPC Cards in Bulk Data, Say 1 >									
§ BULK DATA									
PARAM, CDITER, < Number of Iterations Allowed For Convergence >									
PARAM, CDPRT, YES (Requests printing of constraint violations during iterations)									
MPC	1 (MPC ID)	S (Relative Motion SPOINT ID)	0 (SPOINT Component)	1.0	G2 (G2 ID)	U (G2 Component)	-1.0		
		G1 (G1 ID)	U (G1 Component)	1.0	S <sub>0</sub> (Initial Gap SPOINT ID)	0 (SPOINT Component)	-1.0		
SUPPORT	S (Relative Motion SPOINT ID)	0 (SPOINT Component)							

SPOINT	S (Relative Motion SPOINT ID)	S <sub>0</sub> (Initial Gap SPOINT ID)							
--------	----------------------------------	---	--	--	--	--	--	--	--

PARAM, CDPRT requests the printing of constraint violations (in terms of UR for negative displacements denoting overlap and QR denoting negative forces of constraints) during the iterations. The output is as follows.

```

0
0
    POINT      QRI      VALUE      POINT      VALUE      POINT      VALUE
COLUMN        1
5 T2 -2.37141E-02
*** END ITERATION      3, CHANGES      1
*** END ITERATION      4, CHANGES      0
*** USER INFORMATION MESSAGE 9097 (CSTRDISP)
*** CONSTRAINED DISPLACEMENT ITERATIONS CONVERGED      LOAD CASE =      1
    
```

Negative force in constraint

At the end of the third iteration, 1 change still required

No more iteration required, QR and UR satisfied after 4 iterations. i.e. after 4 static analyses.

The number of changes (to the constraints) required at the end of each iteration is denoted by CHANGES and gradually will reduce until zero. At this stage, the contact interface is defined for the particular load case and all the linear GAP constraints satisfy both QR and UR. It must be checked that the CHANGES reduce to **ZERO**, otherwise the solution has not converged! PARAM, CDITER should be increased until convergence is achieved. NASTRAN will adopt the results of the final iteration irrespective of whether the solution has converged or not! Once convergence has been achieved, it is illustrative to find out the pairs of grids (or rather the SPOINT defining their relative motion) that are *SHUT*. i.e. in contact. This is indicated as follows.

```

0
0
    POINT      SHUT      VALUE      POINT      VALUE      POINT      VALUE      POINT      VALUE
COLUMN        1
51 S 1.00000E+00
    
```

Relative motion SPOINT ID and 1.0E+0 indicating the contact is *SHUT*, i.e. in contact.

Finally, the intention would be to find out the value of the constraint forces. This is best found from MPCFORCES (PRINT) from the G TYPE Grid output. S TYPE SPOINT forces also correspond.

```

FORCES OF MULTIPOINT CONSTRAINT
POINT ID.  TYPE  T1      T2      T3      R1      R2      R3
12         G    0.0      9.166666E+00  0.0      0.0      0.0      0.0
51         S   -9.166666E+00
101        S    9.166666E+00
    
```

Relative motion SPOINT force.

Initial gap SPOINT force.

Force on one of the grids (note G TYPE) of the contact grid pair. One grid will show a positive value, and the other a negative value. If the FE surface contacts a fixed boundary, then there will only be one grid MFC (G TYPE) output.

The same values are also presented in the SPCFORCES output (only for SPOINTS), somewhat redundantly.

```

FORCES OF SINGLE-POINT CONSTRAINT
POINT ID.  TYPE  T1      T2      T3      R1      R2      R3
11         G    0.0      2.083333E+01  0.0      0.0      0.0      1.250000E+03
51         S    9.166666E+00
101        S   -9.166666E+00
    
```

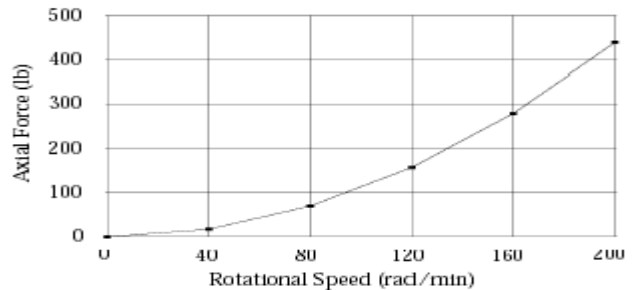
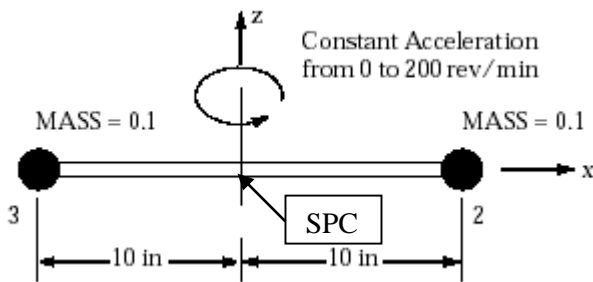
Relative motion SPOINT force.

Initial gap SPOINT force.

Also note that large non-zero values for EPSILON and strain energy for the SUPORT degree of freedom can be safely ignored, as we are not performing inertia relief analysis.

**3.1.5.1.7 Modelling Centrifugal Force in SOL 101– Modelling Steady State Static Equilibrium Conditions**

Centrifugal force is applied onto systems assumed to be in a steady-state, equivalent to static equilibrium. For instance, the forces acting on a car spinning in a test track at a certain velocity and/or acceleration can be ascertained using linear static analysis with centrifugal force as the system is in static equilibrium. Likewise the forces in components rotating in a rotating drum can be ascertained. The six rigid-body boundary conditions must of course still be applied onto the static system. The **RFORCE** entry is used to apply the force due to **rotational velocity** and/or **acceleration**. On the RFORCE entry, the components of a spin vector used internally to compute centrifugal forces are input. Each component of the spin vector is multiplied by the same scale factor. For instance consider the two rotating masses shown below. The masses are accelerated at constant angular acceleration of 20 rev/sec<sup>2</sup> from 0 to 200 rev/min. The goal is to determine the CBAR axial force as a function of angular velocity.



From graph, note that **centrifugal forces are not linear** with angular velocity, but proportional to  $\omega^2$ . Hence, using a SUBCOM command to scale the subcases with RFORCE entries can lead to misleading results if abused.

The force of a single rotating part out-of-balance is

$$F(t) = F_0 \sin(\Omega t)$$

where the amplitude is

$$\begin{aligned}
 F_0 &= m.e. \frac{4\pi^2}{3600} .n^2 \\
 &= m.e.4\pi^2 .f_B^2 \\
 &= m.e.\Omega^2
 \end{aligned}$$

where

- $F_0$  = centrifugal force (N)
- $m$  = mass of the rotating part (unbalanced fraction) (kg)
- $e$  = eccentricity of the unbalanced mass fraction (m)
- $n$  = rate of rotation (speed of revolution of the unbalanced mass expressed in rev per minute) (r.p.m.)
- $f_B$  = operating frequency ( $f_B = n/60$ ) (Hz)
- $\Omega$  = angular velocity of the rotating part ( $=2\pi f_B$ ) (rad/s)

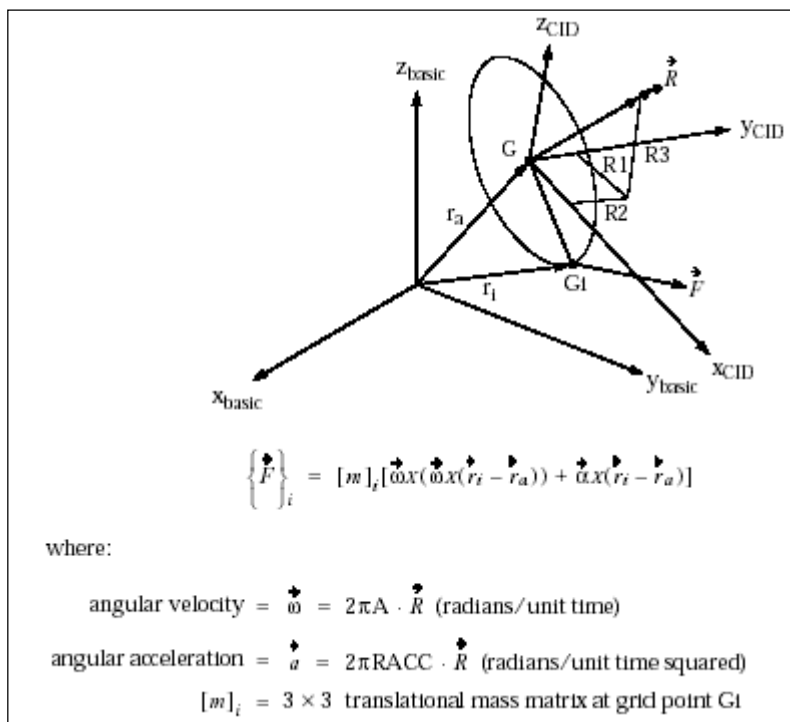
Another interesting note is that the model really does not rotate; it is actually fixed at the center. If the constraints permitted the model to rotate, the run would fail. RFORCE is called by the LOAD case control command.

\$ BULK DATA									
RFORCE	SID	Grid ID	CID	Velocity Scale Factor A = ...rev/s	R1	R2	R3	METHOD	
	Acceleration Scale Factor RACC = 20rev/s <sup>2</sup>								

Method=1 yields correct results only when there is no coupling in the mass matrix. This occurs when the lumped mass option is used with or without the ZOFFS option (see the CQUAD4 entry for a description of ZOFFS). Method=2 yields correct results for lumped or consistent mass matrix only if the ZOFFS option is not used. The acceleration terms due to the mass offset (X1, X2, X3) on the CONM2 entry are not computed with method=2. The possible combinations are

	No Offset	Offset
Lumped	Method=1 or Method=2	Method=1
Coupled	Method=2	Neither

In addition, for problems with elements that have edge grid points (CQUAD8, CTRIA6, CTRIA6, CHEXA, CPENTA, and CTETRA), correct centrifugal loads are produced only if the parameter PARAM, COUPMASS, x (where x is greater than 1), is included and Method 2 is used.



### 3.1.5.2 GL, ML P- $\Delta$ ( $K_G^A$ From $K_E^A$ ) Static Analysis

In order to perform a P- $\Delta$  static analysis, the geometric stiffness matrix must be calculated. However, because the geometric stiffness matrix is dependent upon the state of element stresses (or the forces in the elements), it is necessary to perform a static analysis without the geometric stiffness as a first pass, and then only perform another static analyses incorporating the geometric stiffness matrix. The following procedure can be adopted.

#### Phase 1

Perform static analysis (with loads that cause the greatest negative or positive geometric stiffness) based on  $[K_E^A]$  but include the `segyroa.v2001` alter prior to the Case Control Section in order to compute the geometric stiffness matrix  $[K_G^A]$  (and output into a `.pch` file) based on the generated element loads from the  $[K_E^A]$  static analysis.

#### Phase 2

Perform static analysis with a general loading function based on  $[K_E^A] + [K_G^A]$  by including the `k2gg = ktjj` statement in the Case Control Section and the outputted `.pch` file which contains the `ktjj` matrix in the Bulk Data. The responses at this stage represent the P- $\Delta$  ( $K_G^A$  From  $K_E^A$ ) static response to the general loading function.

The method is valid when **only the prestress is judged to affect the geometric stiffness** such as in the compressive preload of building columns due to gravitational loads and the prestressing of extremely taut cables that sag very little under gravity but not in systems such as suspension bridges. Where lateral loads are large enough to affect the geometry of the system with prestress, then a repetitive P- $\Delta$ , SOL 106, implicit dynamic relaxation SOL 129 or explicit dynamic relaxation must be employed. But in single P- $\Delta$  analysis, because cables do not have much elastic bending stiffness, the initial static preload subcase should only include the prestress and not gravity as including gravity is the same as solving two linear static problems of stiffness  $K_E^A$  with preload and gravity as the applied loads respectively. Clearly, in the gravity case, it is nonsensical as the cables do in reality have differential stiffness (from the prestress) to resist the gravitational force. Prestress in one direction (i.e. along the axis of cable) will cause a differential stiffness in the orthogonal direction. Gravity acts in the orthogonal direction and hence cannot be accounted for in the calculation of the prestress in this single P- $\Delta$  analysis. To quantitatively decide if gravity need not be considered in contributing to the differential stiffness of the cables, a static P- $\Delta$  analysis should be carried out, the first subcase being a SOL 101 with only the prestress as applied loads and the second subcase a P- $\Delta$  SOL 101 (i.e. utilizing the induced prestress from the first subcase to form a geometric stiffness matrix) with both the gravity and prestress included as applied loads. If the difference in the cable element forces between subcases 1 and 2 is negligible, then gravity has little influence in affecting the geometric stiffness. If there is a major difference in the cable element force, then clearly, gravity will affect the geometric stiffness and as such, a repetitive P- $\Delta$ , SOL 106, implicit dynamic relaxation or explicit dynamic relaxation must be used to converge to the true  $K_T$ . Likewise, in the single P- $\Delta$  analysis of multi-storey buildings, gravity (and only gravity) acts in axis of columns to generate prestress, and the differential stiffness is computed for the orthogonal direction reducing resistance to lateral wind forces, applied in the second subcase with gravity too.

The `segyroa.v2001` alter computes the differential stiffness due to the prestress and also the follower force. The follower force is calculated and incorporated by the use of `PARAM, FOLLOWK, YES`. We know how the prestress affects the differential stiffness, namely a tensile prestress causing an increase in stiffness. The effect of the follower force on the stiffness is different. For example, for a cylinder under external pressure critical buckling load may be over-estimated (even though the mode shapes are similar) in a SOL 105 and the natural frequencies in vibration may be under-estimated (even though the mode shapes are similar) in a SOL 103 in the absence of follower stiffness. To the contrary, this observations are reversed in case of centrifugal loads. Centrifugal forces as a constant (static) load are applied by a Bulk Data `RFORCE` to any elements that have masses. The follower stiffness due to centrifugal load has the effect of lowering stiffness (although the centrifugal load tensioning effect increases stiffness), consequently lowering natural frequencies (even though the mode shapes are similar) in a SOL 103 and lowering the buckling loads (even though the mode shapes are similar) in a SOL 105. This effect increases as the RPM increases, and it becomes significant when the RPM is over 1000.

### 3.1.5.3 GL, ML P- $\Delta$ ( $K_G^A$ From Exact or Approximate $K_T^A$ ) Static Analysis

To obtain  $K_T^A$ , to be theoretically exact, a GNL SOL 106 (or implicit dynamic relaxation SOL 129 or explicit dynamic relaxation LS-DYNA) with prestress (as temperature loads say) and gravity must be undertaken. Alternatively, an approximation to  $K_T^A$  can be obtained by repetitive P- $\Delta$  static analyses with the prestress (as temperature loads say) and gravity applied. The procedure to obtain this approximate  $K_T^A$  will be presented. Note that the approximate  $K_T^A$  will be the summation of the elastic stiffness  $K_E$  at the undeflected (by the prestress and gravity) state but  $K_G$  at the deflected (by the prestress and gravity) state. Hence if  $K_E$  changes considerably during the application of the prestress, a full SOL 106 (or implicit dynamic relaxation SOL 129 or explicit dynamic relaxation LS-DYNA), which converges to the  $K_E$  and  $K_G$  at the deflected (by the prestress and gravity) state should be employed. Hence for the modelling of a suspension bridge where there is a great change in geometry (known in the bridge industry as **form-finding**, so-called because it is necessary to find the form or shape of the catenary suspension cables), it may be prudent to employ SOL 106 (or implicit dynamic relaxation SOL 129 or explicit dynamic relaxation LS-DYNA), but for a high tension low sag cable on say a tower with prestressed cables, the repetitive P- $\Delta$  static analysis may be adequate. The repetitive P- $\Delta$  analysis basically involves a number of iterations of linear static analyses to obtain an approximate  $K_T^A$ . Note again that A refers to the initial undeflected (by the collapsing load) state, but deflected by the prestress and gravity. To perform the repetitive P- $\Delta$  analysis, a static analysis is performed based on  $K_E^A$  with temperature loads and gravity to generate forces in the structural elements, which in turn provides input for the computation of  $K_{G_i}^{AKT_m}$  where m is the iterations. Repetitive static analysis is performed with the prestress and gravity updating the stiffness matrix  $K_E^A + K_{G_i}^{AKT_{m-1}} + K_{G_i}^{AKT_m}$  until convergence of displacements is obtained. The tangent stiffness at this stage is the approximate converged tangent stiffness matrix  $K_T^A = K_E^A + K_{G_i}^{AKT}$ . The converged displacements represent the approximate P- $\Delta$  ( $K_G^A$  From Approximate  $K_T^A$ ) static response to the initial prestress loads. The converged geometric stiffness at this stage would be that based upon the approximate tangent stiffness matrix  $K_T^A$ , i.e.  $K_{G_i}^{AKT}$ .

#### Phase 1

Perform static analysis (with prestress and gravity) based on  $[K_E^A]$  but include the segyroa.v2001 alter prior to the Case Control Section in order to compute the geometric stiffness matrix  $[K_G^A]_1$  (and output into a .pch file) based on the generated element loads from the  $[K_E^A]$  static analysis.

#### Phase 2

Perform static analysis (with prestress and gravity) based on  $[K_E^A] + [K_G^A]_1$  by including the k2gg = ktjj statement in the Case Control Section, the outputted .pch file which contains the ktjj matrix in the Bulk Data and the segyroa.v2001 alter prior to the Case Control Section to compute the  $[K_G^A]_2$  (and output into the .pch file overwriting previous data) based on the generated element loads from the  $[K_E^A] + [K_G^A]_1$  static analysis.

#### Phase 3

Repeatedly perform the Phase 2 static analysis (with prestress and gravity) based on  $[K_E^A] + [K_G^A]_i$  for  $i = 2$  to  $n$  where  $n$  represents the number of iterations required for the change in deflections between analyses to become negligible. This would signify that the change in the  $[K_G^A]$  matrix become negligible and the correct  $[K_G^A]$  is attained. The deflections and the other responses at this stage represent the P- $\Delta$  ( $K_G^A$  From Approximate  $K_T^A$ ) static response to the prestress and gravity. The stiffness of the structure is  $K_T^A$ .

#### Phase 4

The P- $\Delta$  response to a general loading function can now be ascertained by performing a P- $\Delta$  static analysis with the converged tangent stiffness of the structure,  $K_T^A$ . The responses at this stage represent the P- $\Delta$  ( $K_G^A$  From Approximate  $K_T^A$ ) response to the general loading function.

### 3.1.6 Hand Methods Verification

#### 3.1.6.1 Static Displacements by the Unit Load Method of the Virtual Work Principle

$P \Delta = f \delta$  expresses virtual work i.e. external work = internal work

$P' \Delta = f' \delta$  expresses the load method where

$P'$  = virtual external action, specified usually as unity for the unit load method

$\Delta$  = real external kinematic, the item to be found

$f'$  = virtual internal action, due to the virtual external actions  $P'$

$\delta$  = real internal kinematic, due to the real external actions on the structure

$1' \Delta = f_1' \delta$  expresses the unit load method

$1' \Delta_1 = f_1' \delta_1$  represents the unit load method with the real external actions also unity i.e. both the virtual external actions and real external actions are unity

$\Delta_1$  = external real kinematic due to unit external real action

$$= f_1' \delta_1$$

$$= \int (M_1)_v \left( \frac{M_1}{EI} ds \right)_R + \int (P_1)_v \left( \frac{P_1}{EA} ds \right)_R \text{ or } (P_1)_v \left( \frac{P_1 L}{EA} \right)_R + \int (T_1)_v \left( \frac{T_1}{GK_t} ds \right)_R + \int (V_1)_v \left( \frac{V_1 Q}{GIb} ds \right)_R$$

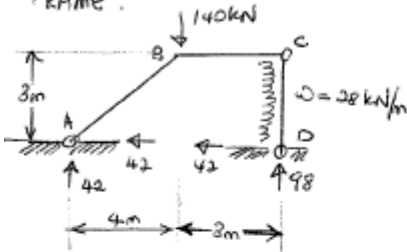
$$+ (P_{1spring})_v \left( \frac{P_{1spring}}{k_{spring}} \right)_R + (M_{1spring})_v \left( \frac{M_{1spring}}{k_{rotational\ spring}} \right)_R + (T_{1spring})_v \left( \frac{T_{1spring}}{k_{torsional\ spring}} \right)_R$$

$$= \int M_1 \frac{M_1}{EI} ds + \int P_1 \frac{P_1}{EA} ds \text{ or } P_1 \frac{P_1 L}{EA} + \int T_1 \frac{T_1}{GK_t} ds + \int V_1 \frac{V_1 Q}{GIb} ds + P_{1sp} \frac{P_{1sp}}{k_{sp}} + M_{1sp} \frac{M_{1sp}}{k_{rot\ sp}} + T_{1sp} \frac{T_{1sp}}{k_{tor\ sp}}$$

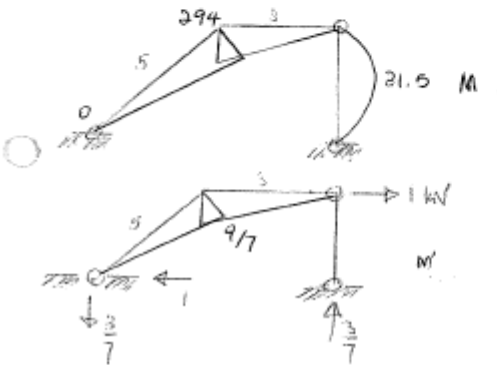
The integrals can be evaluated using classical calculus integration methods, product integrals or using the numerical Simpson's Rule  $I = h/3[f_0+4f_1+f_2]$ . Simpson's Rule is exact for the multiplication of continuous functions up to and including cubic variations. Non-continuous piecewise functions should be split at the discontinuities and integrated in sections.

VIRTUAL FORCE

FRAME:



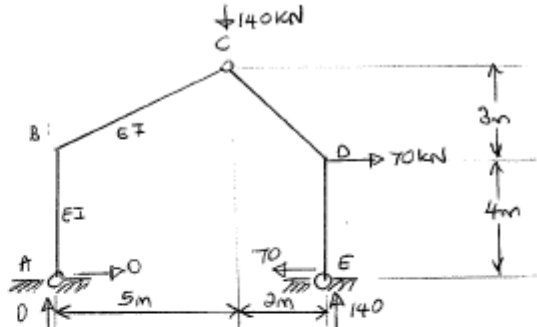
Given  $EI = 42 \times 10^3 \text{ kNm}^2$ , find horizontal deflection at C,  $u_c$  considering bending effects only.



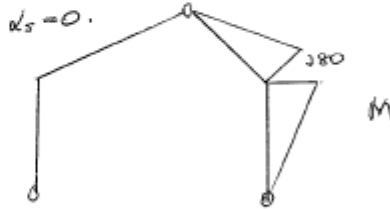
$$VW: 1u_c = \int M_v M_r \frac{ds}{EI}$$

$$u_c = \left\{ \frac{1}{3}(5)\left(\frac{9}{7}\right)(294) + \frac{1}{3}(7)\left(\frac{9}{7}\right)(294) \right\} \frac{1}{EI}$$

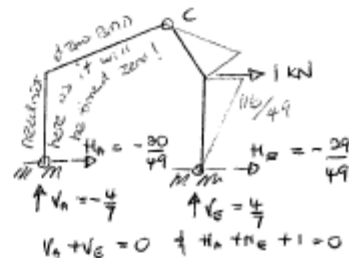
$$u_c = \frac{1008}{EI} = 24 \text{ mm (in direction shown)}$$



Spread of eaves? (ANS:  $\frac{1216.9}{EI}$  apart)



With unit load at D to the right



Cutting at C and considering LHS:

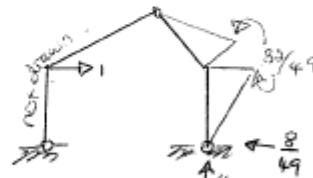
$$V_A(5) - H_A(7) = 0$$

And  $\sum \mathcal{M}_A: V_E(7) = (1)(4) \Rightarrow V_E = \frac{4}{7}$

$$VW: 1 \cdot \delta = \int M_v M_r \frac{ds}{EI} = \frac{1}{EI} \left\{ \frac{1}{3}(4)\left(\frac{116}{49}\right)(280) + \frac{1}{3}(\sqrt{13})(280)\left(\frac{116}{49}\right) \right\}$$

$$= \frac{1680.465}{EI}$$

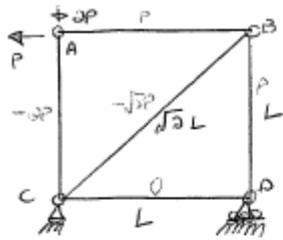
With unit load to the right at E,



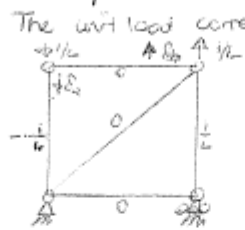
$$VW: 1 \cdot \delta = \frac{1}{EI} \left\{ \frac{1}{3}(4)(280)\left(\frac{32}{49}\right) + \frac{1}{3}(\sqrt{13})(280)\left(\frac{32}{49}\right) \right\}$$

$$= \frac{463.576}{EI}$$

$$\text{Spread of eaves} = \frac{EI}{(1680.465 - 463.576)} = \frac{1216.9}{EI}$$



Find the angle of rotation of AB and the change in distance between joints A & D.



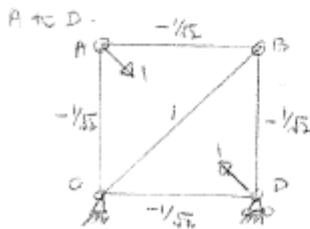
The unit load corresponding to a rotation is a unit couple.  
 Thus external work  
 $W_{ext} = \frac{1}{L} \delta_a + \frac{1}{L} \delta_b = \frac{1}{L} (\delta_a + \delta_b)$   
 Angle of rotation  $\theta_{ab} = \frac{\delta_a + \delta_b}{L}$   
 Thus  $W_{ext} = 1 \cdot \theta_{ab}$

Thus the application of a unit couple in the form of the 2 forces will enable us to find the angle of rotation.

$$VW: 1 \cdot \theta_{ab} = \sum P_i \frac{\delta_i}{EA} = \frac{1}{L} \left( \frac{PL}{EA} \right) + \left( -\frac{1}{L} \right) \left( \frac{-2PL}{EA} \right) = \frac{3P}{EA}$$

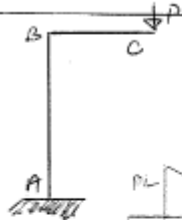
The  $\theta_{ab}$  meaning rotation counter-clockwise as defined by the two forces at A & B.

Now to find the relative change in distance between A & D the corresponding unit load consists of 2 equal & opposite unit forces acting along the line from A to D.

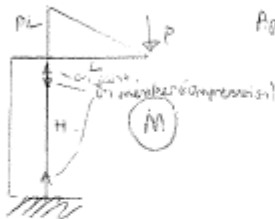


$$1 \cdot \delta_{ad} = \sum P_i \frac{\delta_i}{EA} = \left( -\frac{1}{\sqrt{2}} \right) \left( -\frac{1}{\sqrt{2}} \right) \frac{L}{EA} + \left( -\frac{1}{\sqrt{2}} \right) \left( \frac{1}{\sqrt{2}} \right) \frac{L}{EA} + \left( -\frac{1}{\sqrt{2}} \right) \left( \frac{1}{\sqrt{2}} \right) \frac{L}{EA} + \left( -\frac{1}{\sqrt{2}} \right) \left( -\frac{1}{\sqrt{2}} \right) \frac{L}{EA} = -2 \frac{PL}{EA}$$

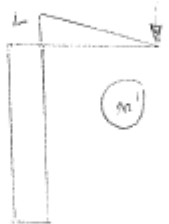
in which a minus sign indicates that the distance between A & D has increased (ie relative translation opposite to the sense of the unit loads).



Given flexural rigidity EI and axial rigidity EA, find vertical deflection at C.



Applying unit vertical load at C



$$VW: 1 \cdot \delta_v = \int N' \frac{N}{EA} dx + \sum P_i \frac{\delta_i}{EA}$$

$$= \left\{ \frac{1}{3} L (PL)(L) + PL(L) \right\} + \left\{ (1) \frac{PL}{EA} \right\}$$

$$\delta_v = \frac{PL^2(L+3H)}{3EI} + \frac{PL}{EA}$$

When numerical values substituted, we find the last term, representing the effects of axial deformations, is extremely small compared to the first term, and the term usually neglected as with unit.



STATICAL INDETERMINACY,  $\alpha_s$

① TRUSSES

(i)  $\alpha_s = m + r - 2j$

$m$  = no. of members  
 $r$  = no. of external reactions  
 $j$  = no. of 'joints' or other vertices

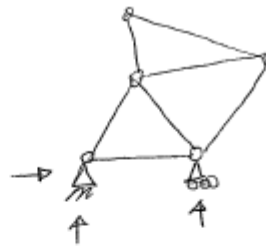
Note:  $m + r$  = unknowns

$2j$  = knowns; also to maintain statical determinacy ( $\alpha_s = 0$ ) add one joint to every 2 members added.

(ii) For fully triangulated trusses:

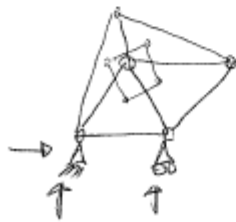
$\alpha_s = c + r - 3$

$c$  = no. of circuits obtained by inserting a point inside each triangle & connecting adjacent points.  
 $r$  = no. of external reactions



$\alpha_s = m + r - 2j$   
 $= 7 + 3 - 2(5)$   
 $= 0$

○



$\alpha_s = c + r - 3$   
 $= 1 + 3 - 3$   
 $= 1$

- TO FORM CIRCUITS
- ① PUT DOT IN EACH TRIANGLE
  - ② JOIN ADJACENT POINTS ONLY
  - ③ CIRCUITS MAY CLASH

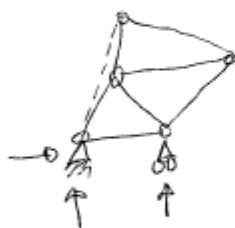
(iii) For partially triangulated trusses

$\alpha_s = c + r - 3 - m_i$

$c$  = no. of circuits obtained by inserting a point inside each triangle & connecting adjacent points

$r$  = no. of external reactions

$m_i$  = no. of members inserted to triangulate truss (Always have to triangulate partially triangulated truss)



$\alpha_s = c + r - 3 - m_i$   
 $= 1 + 3 - 3 - 1$   
 $= 0$  (agrees with method (i) above)

Note: consider no. of circuits after triangulating the truss as above. But we must always triangulate a truss even if we do not produce any circuits in that way-

Eg:



$\alpha_s = c + r - 3 - m_i$   
 $c = 0$   
 $r = 5$   
 $m_i = 1$   
 $\alpha_s = 0 + 5 - 3 - 1$   
 $= 1$

② FRAMES (INCLUDING BEAMS)

(i)  $\alpha_s = (3m+r) - 3j - P_i$  (Valid for all types of frames)

$m$  = no. of members

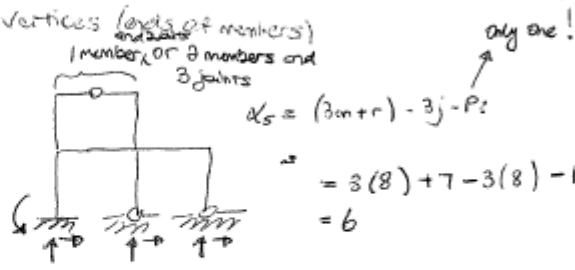
$r$  = no. of external reactions

$j$  = no. of "joints" or other vertices (ends of members) and bars

$P_i$  = no. of internal releases.

NOTE:  $3m+r$  = no. of unknowns.

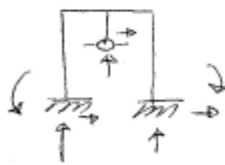
$3j+P_i$  = no. of knowns.



(ii) One story portal frame

$\alpha_s$  = no. of unknowns - knowns (including internal releases)

$\alpha_s = 8 - 3 = 5$  (known equilibrium reactions)



(iii) Also for any frames (single story or much more)

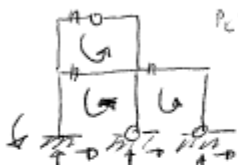
$\alpha_s = 3C - P_i$

$C$  = no. of cuts or loops or trees resulting from cuts

$P_i$  = total no. of releases, external & internal

3 loops or 3 cuts (3 trees)

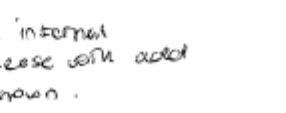
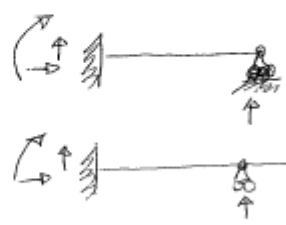
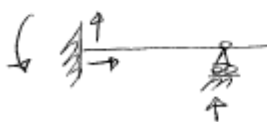
$\alpha_s = 3(3) - 3$   
 $= 6$  (as above)



③ BEAMS

(i)  $\alpha_s = (3m+r) - 3j - P_i$  { as above }

(ii)  $\alpha_s = \text{unknowns} - \text{knowns (including internal releases)}$

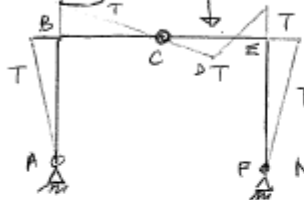


an internal release will add a known.

3 joints!

THE ART OF STRUCTURAL ANALYSIS BY DR. JESSE SLADE @ IMPERIAL

We know that there is a general coherence between the shapes of the bending moment diagram and the deflections, with hogging curvature wherever the bending moment is drawn above. Say for the 3-pinned portal frame,

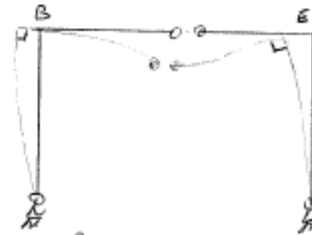


indicating sides of tension on BMD, therefore the outer side of curvature. Next, we study restraint of supports. A & F allow only rotation (no horizontal or vertical movement). No rotation allowed if fixed support. Nodes B and C and E may move horizontally or vertically or rotate but is restrained axially. So B and E is restrained vertically and horizontal displacement of B, C, E must be consistent. Members connected at a hinge (D) can take up different slopes on either side.

Considering separate halves:



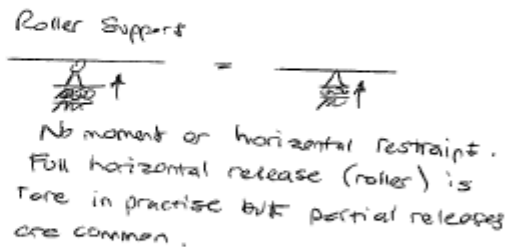
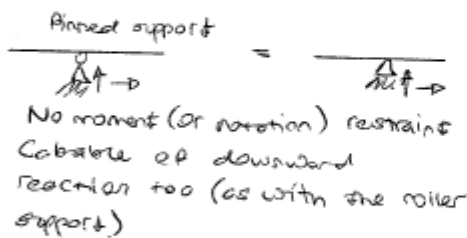
For continuity C on both sides must meet, though one side is higher than the other. Thus rotate. Allow B, and E to move horizontally allowing some rotation on both parts sufficiently for C to meet.



- side of tension
- supports restraint
- member restraints only nodes

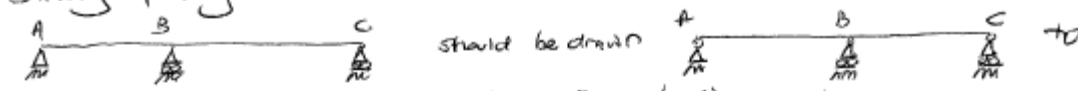
The horizontal deflection at the top of the frame, which has been caused by a load with a vertical component only, is called the sway of the frame. It always arises in a frame type structure when either the loading is applied unsymmetrical or the structure itself is unsymmetrical.

SUPPORT CONDITIONS

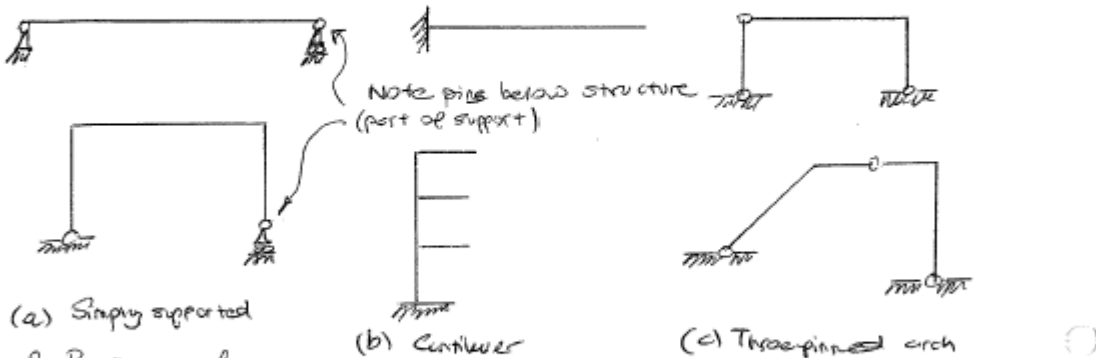


- $d_s$
- TRUSS → use  $1+r-3j$
  - BEAMS → unknowns-knowns (including internal releases) or reduction method
  - FRAMES → crestory portal frames (use unknowns-knowns); or use reduction method (reduce to simply supported, cantilever, i.e. cuts = 3, or 3 pinned-arch)
  - COMBINATION OF FRAMES + TRUSS → analyse frame without tie(s) then add to  $d_s$ .

Strictly speaking



Basic ( $k_s=0$ ) statically determinate structures are the simply supported, cantilever and three-pinned arch.



(a) Simply supported

(b) Cantilever

(c) Three-pinned arch

3 Basic forms of statically determinate structures.

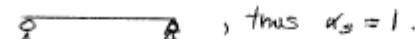
Reduction method (of obtaining  $k_s$  for beams and frames)

Fixed cantilever

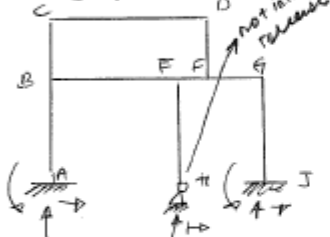


thus  $d_s = 1$ .

Note, the degree of statical indeterminacy is a property of the structure, not the loading. Or it can be reduced to a simply supported beam by introducing one moment release



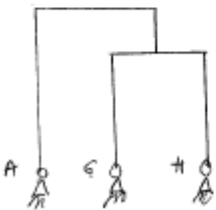
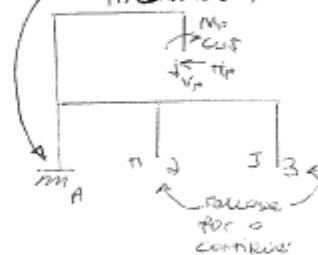
Two bay two storey



Using formulae  
 $k_s = 3(9) + 8 - 3(9) - 0 = 8$

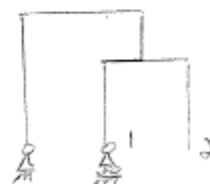
or by reduction  
 (release 2 at H and 3 at J at C ± (=3) top storey)  
 $k_s = 2 + 3 + 3 = 8$

For cantilever, one side must be totally fixed (encasté)

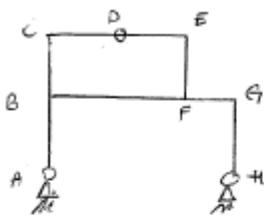


Using formulae  
 $k_s = 3(7) + 6 - 3(8) - 0 = 3$

or by reduction  
 (release one at G and 2 at H; note that we can't release 2 at G for a cantilever because A is not encasté; thus we must reduce to simply supported structure)  
 $d_s = 2 + 1 = 3$

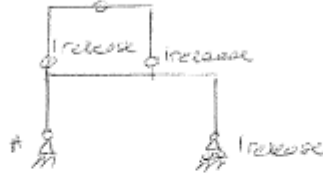


$d_s = 2 + 1 = 3$

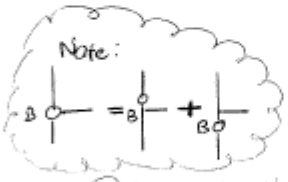
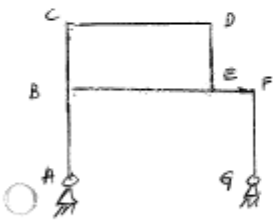


$$d_s = 3(7) + 4 - 3(7) - 1 = 3$$

⊖ by reduction: No cuts possible as we can't produce cantilevers. Reduced to a simply supported structure and a 3 pinned arch.



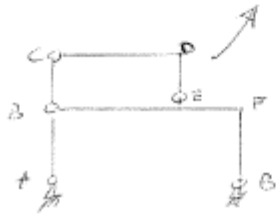
$$d_s = 3 \text{ releases} + 0 \text{ cuts} = 3$$



⊖ by reduction

$$d_s = 3(7) + 4 - 3(7) - 0 = 4$$

⊖ is not 3 releases but only 2 because if we release 2 end member moments, the third automatically becomes zero and so we can place hinge right in between all three.



Reduced to 2 3 pinned arches

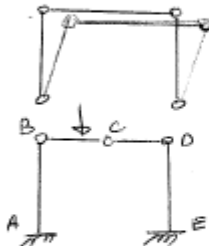
$$d_s = 4 \text{ releases} + 0 \text{ cuts} = 4$$

(i.e. release at C, D at B, and 1 at F)

Note: If there are less than 3 external restraints, no matter how many internal restraints the structure will fail, i.e. mechanism



Mechanism (no horizontal restraint)



Mechanism (no sway restraint)  
 $d_s = -1$

Mechanism (beam will collapse)  
 $d_s = 0$   
Pseudo-mechanism.

Consider  

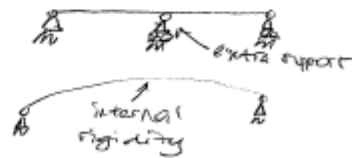
 is equilibrium.  
 Release any 2 moments, thus third becomes zero. If we release one then  

 If we release 2 then  

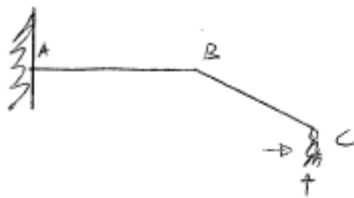
 = 0 = 0

Indeterminacy may be a result of

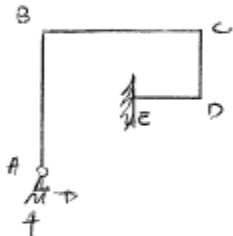
- (i) additional external reactions
- (ii) internal rigidity
- (iii) the addition of members



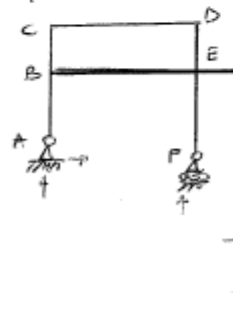
Note: triangulate truss to avoid a collapse (mechanism) even though  $d_s = m+r-j=0$ .  
 eg. triangulate that!



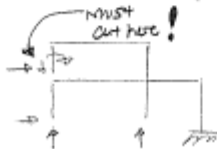
$d_s = 3(2) + 5 - 3(3) - 0 = 2$   
 (do not use  $d_s = 3n - r$  unknowns - knowns because not a beam or a single story portal frame)  
 (or) by reducing to a cantilever, we release 2 (vertical and horizontal reactions at C)  
 $d_s = 2 \text{ releases for cantilever} = 2$



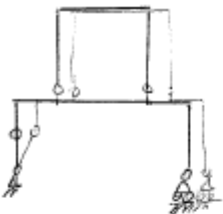
$d_s = 3(4) + 5 - 3(5) - 0 = 2$   
 (or) by reducing 2 restraints of A for a cantilever (for cantilever one side must be fixed exactly)  
 $d_s = 2 \text{ releases} = 2$



$d_s = 3(8) + 6 - 3(8) - 0 = 6$   
 (or) by reducing the entire structure to cantilever  
 - release 2 at A, one at F and cut CB just before B (=3)



$d_s = 3 \text{ releases} + 1 \text{ cut} = 3 + 3 = 6$

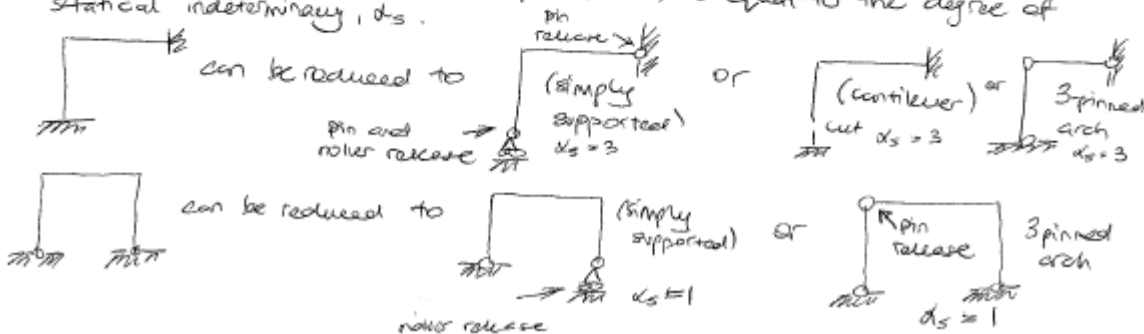


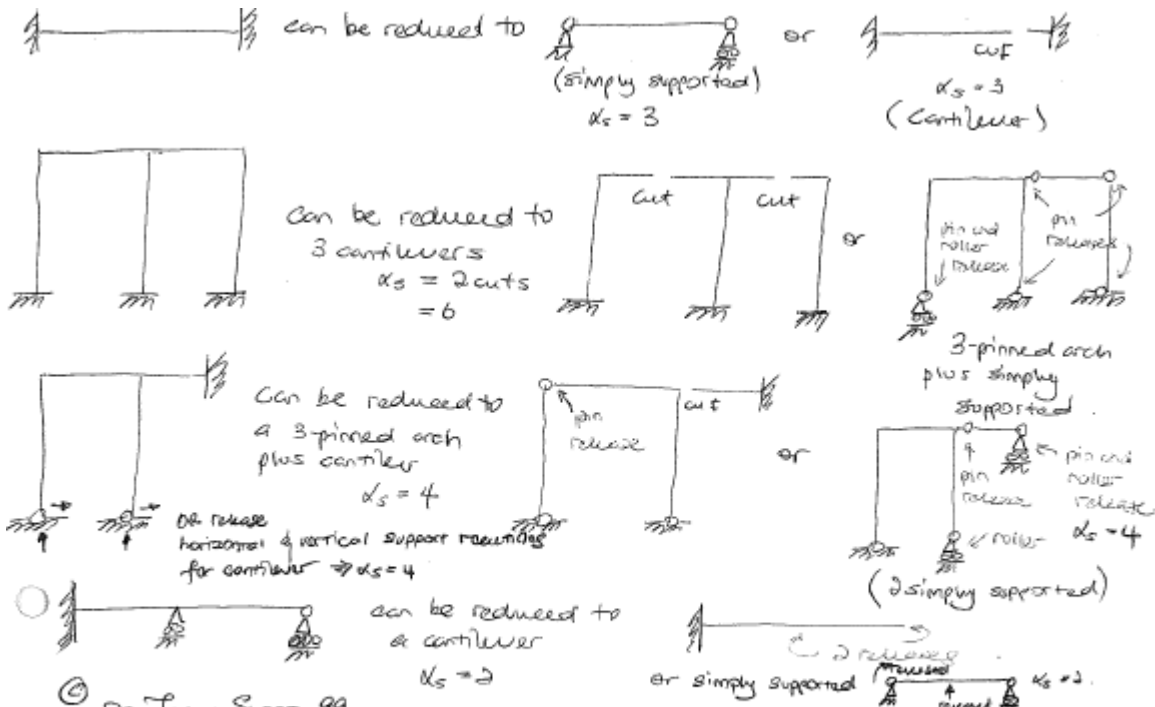
$d_s = 3(8) + 3 - 3(8) - 3 = 0$   
 But lower portion is a mechanism.

Reduction of structure

- this method is most appropriate for rigid-jointed frames. Releases include a pin, rollers or even a complete cutting (each cut introduces 2 releases in a plane frame, 6 in space frame).

- the number of releases required to produce a chosen primary structure (i.e. simply supported, cantilever, three-pin-arched) is equal to the degree of static indeterminacy,  $d_s$ .





DR. JESSE SLIDE 99

EXAM

A note on compatibility for  $k_s > 1$ . Take  $k_s = 2$  for simplicity

Compatibility equation:  $f_{10} + x_1 f_{11} + x_2 f_{12} = 0$

Note that all first subscripts are 1 i.e. the virtual BMD is  $M_1$ , because we want deflection in the '1' direction. Only then can they be summed for zero for compatibility.  $f_{10}$  is deflection in '1' direction for released structure;  $f_{11}$  is deflection in '1' direction due to unit force in '1' direction;  $f_{12}$  is deflection in '1' direction due to unit force in '2' direction

$$f_{20} + x_1 f_{21} + x_2 f_{22} = 0$$

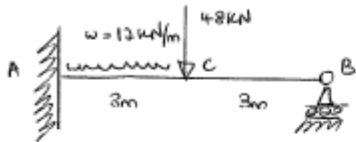
All three first subscripts are 2 denoting virtual BMD is  $M_2$ .

$$f_{nk} = \int \frac{m_n m_k}{EI} \text{ with } m_n \text{ virtual and } m_k \text{ real, } \frac{m_k}{EI} \text{ real curvature}$$

$f_{10}$  is deflection of released structure in '1' direction;  $f_{11}$  is deflection in '1' direction due to unit load in '1' direction;  $f_{12}$  is deflection in '1' direction due to unit load in '2' direction.

All three terms must be in the same direction (and hence first subscript is common for a common virtual BMD) for compatibility to be applicable. Finally  $x_1, x_2$  applied as scale factors.  $x_1$  is applied to  $f_{11}$  and  $f_{21}$  (second subscript common) because  $x_1$  is scale factor for  $M_1$ , i.e. real unit load in '1' direction. Likewise  $x_2$  is applied to  $f_{12}$  and  $f_{22}$  as  $x_2$  is scale factor for  $M_2$ , i.e. real unit load in '2' direction.

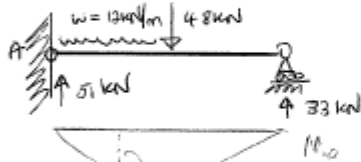
© DR. JESSE STADE.  
 FLEXIBILITY METHOD (INCORPORATING VIRTUAL WORK) IN STRUCTURAL ANALYSIS



Given  $EI_{AB}$  is constant, draw BMD.

SOLUTION:  $\alpha_s = 1$ .

(a) Form primary structure by inserting a moment release at A. Draw BMD,  $M_0$ .



$$M_{C,0} = (51)(1.5) - \frac{12(1.5)^2}{2} = 63.75 \text{ kNm}$$

(b) Reinsert redundant force (or moment) as an external load (or moment) onto the primary structure with all other externally applied loads removed. Assume direction of the moment or force. But note, instead of reinserting the value of the redundant as an unknown  $M_{redundant}$  in order to utilise virtual work in the flexibility analysis, we let  $M_{redundant} = 1X_1$  where 1 is a unit moment (or force) and  $X_1$  is a scale factor. Draw BMD,  $M_1$ , for the unit moment.



(c) Write an equation of compatibility involving the redundant force (or moment)

$$(\text{Rotation at A for } M_0) + (\text{Rotation at A for } M_1)X_1 = 0$$

(d) Use virtual work to find the deflections (or rotations) in the compatibility equation.

$$\int M_0 \frac{M_1}{EI} ds + \left( \int M_1 \frac{M_1}{EI} ds \right) X_1 = 0$$

as  $M_1$  is the BMD for a virtual unit moment and the position the rotation is intended.

$$\int M_0 \frac{M_1}{EI} ds = \frac{1}{EI} \left\{ \frac{1}{6}(3)(1)(0 + 2 \times (-63)) + \frac{1}{6}(3)(0.5)(2 \times (-63) + (-99)) + \frac{1}{3}(3)(0.5)(-99) \right\}$$

$\leftarrow$  TRIANGLE X PARABOLA (4,9)  $\rightarrow$

$$= -\frac{168.75}{EI}$$

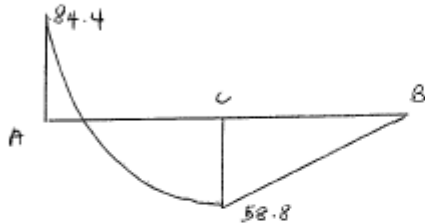
$$\int M_1 \frac{M_1}{EI} ds = \frac{1}{EI} \left\{ \frac{1}{3}(6)(1)(1) \right\} = \frac{2}{EI}$$

$$\therefore -\frac{168.75}{EI} + \frac{2}{EI} X_1 = 0 \Rightarrow X_1 = 84.37$$

Thus value of <sup>the external reaction</sup> <sub>A</sub> moment at A in the direction assumed is 83.37 kNm.

The +ve sign indicates assumed direction of unit moment in  $M_1$  is correct.

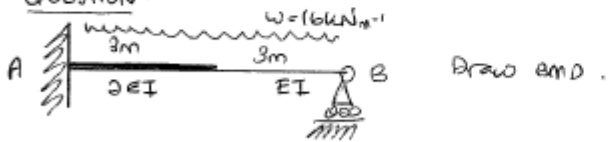
Thus BMD of original structure can be drawn as all reactions are known.



This final BMD can also be obtained from  $M = M_0 + M_1 X_1$  i.e.

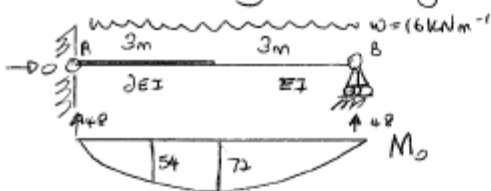
evaluate at critical points using values drawn on  $M_0$  and  $M_1$ .

QUESTION:

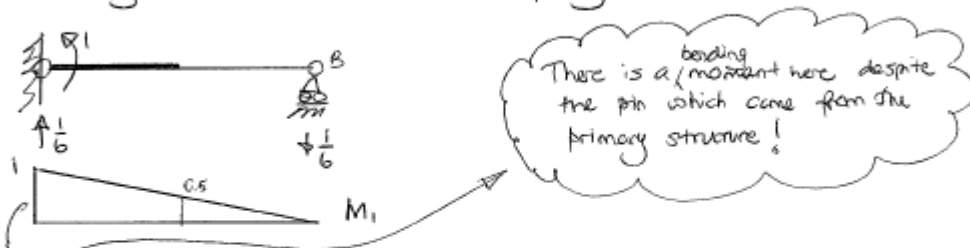


SOLUTION:  $\alpha_s = 1$

Form a primary structure by inserting a moment release at A.



Inserting a unit moment at A on the primary structure



The equation of compatibility gives

$$f_{10} + f_{11} X_1 = 0$$

$$\int M_1 M_0 \frac{ds}{EI} + \left( \int M_1 M_1 \frac{ds}{EI} \right) X_1 = 0$$

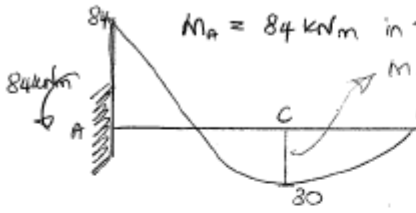
$$\int M_1 M_0 \frac{ds}{EI} = \frac{1}{2EI} \left[ \frac{1}{6} (3) (1) (0 + 2x - 54) + \frac{1}{6} (3) (0.5) (2x - 54 + 72) \right] + \frac{1}{EI} \left[ \frac{1}{6} (3) (0.5) (-72) + 2x - 54 \right] = -\frac{94.5}{EI}$$

trapezium x parabola

$$\int M_1 M_1 \frac{ds}{EI} = \frac{1}{2EI} \left[ \frac{1}{6} (3) (1) (2 + 0.5) + \frac{1}{6} (3) (0.5) (1 + 1) \right] + \frac{1}{EI} \left[ \frac{1}{6} (3) (0.5) (0.5) \right] = \frac{1.125}{EI}$$

Remember to separate this too  $\rightarrow$  MISTAKE AT 15

$$\Rightarrow -\frac{94.5}{EI} + \frac{1.135}{EI} X_1 = 0 \Rightarrow X_1 = 84$$

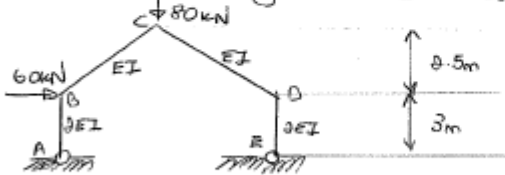


$M_A = 84 \text{ kNm}$  in the direction assumed by the unit moment.

$$M = m_0 + X_1 M_1 = -72 + (0.5)(84) = -30$$

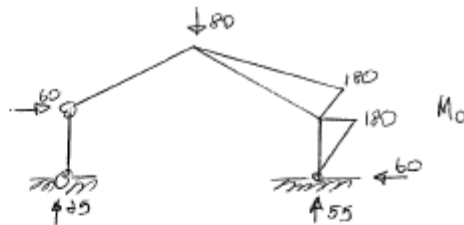
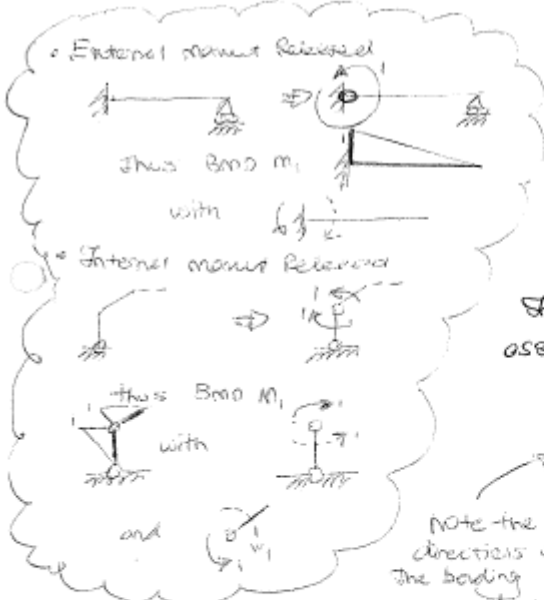
Note that it is entirely different (reaction magnitude) from the primary structure. But BMD can easily be obtained from  $M = M_0 + X_1 M_1$ . Or just resolve reactions again with the known indeterminate (or redundant) reaction.

FRAME: Draw BMD given  $EI_{AB} = EI_{DE} = 2EI$  &  $EI_{BC} = EI_{CD} = EI$ .

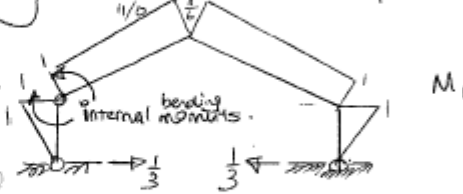


SOLUTION:  $X_5 = 4 - 3 = 1$

Form primary structure by inserting a moment release at B. Here we release an internal redundant force (or moment).



Shows a unit internal bending moment of B assuming a moment inside to be positive (doesn't really matter)



Note the directions of the bending moments here!

$$\therefore \int M_1 M_0 \frac{ds}{EI} = \frac{1}{EI} \left[ \frac{1}{6} (6.5) (180) \left( \frac{1}{6} + 2(1) \right) \right] + \frac{1}{2EI} \left[ \frac{1}{3} (3) (1) (180) \right]$$

$$= \frac{837.5}{EI}$$

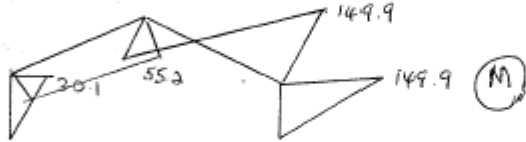
Note! (Trapezium x triangle)  $\Rightarrow$  times the side of the trapezium with the longer side of triangle.

$$\int M_1 M_1 \frac{ds}{EI} = 2 \times \left\{ \frac{1}{EI} \left[ \frac{1}{6} (6.5) \left( \frac{1}{6} \right) \left( 2 \times \frac{1}{6} + 1 \right) + \frac{1}{6} (6.5) (1) \left( \frac{1}{6} + 2(1) \right) \right] + \frac{1}{2EI} \left[ \frac{1}{3} (3) (1) (1) \right] \right\} = \frac{27.84}{EI}$$

$$\int \frac{1}{EI} M_1 M_0 ds + X_1 \int \frac{1}{EI} M_1 M_1 ds = 0$$

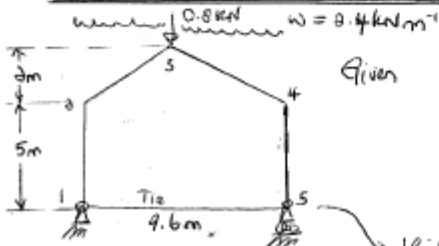
$$\frac{1}{EI} (837.5) + \frac{1}{EI} (27.84) X_1 = 0 \Rightarrow X_1 = -30.08$$

$$M = M_0 + X_1 M_1 \Rightarrow \begin{cases} M_3 = (0) + (-1) \times (-30.08) = 30.1 \text{ kNm} \\ M_0 = (0) + \left(-\frac{11}{6}\right) \times (-30.08) = 55.1 \text{ kNm} \\ M_6 = (-180) + (-1) \times (-30.08) = -149.9 \text{ kNm} \end{cases}$$



Note: Choice of redundants: For indeterminate beams & rigid-jointed frames, it is generally a good technique to insert hinges.

FLEXIBILITY ANALYSIS OF A TIED-PORTAL FRAME (Fundamentals of structural analysis w.J. Spenser)

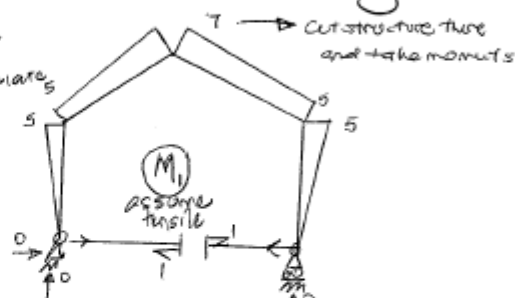
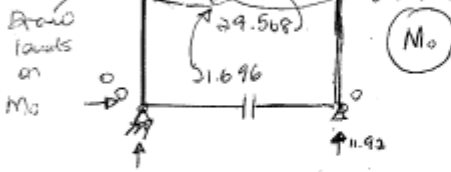


Given: Column and rafters DO NOT forget to change to kN & m!  
 $I = 100 \times 10^6 \text{ mm}^4 = 100 \times 10^{-6} \text{ m}^4$   
 $E = 200 \text{ kN/mm}^2 = 200 \times 10^6 \text{ kN/m}^2$   
 Tie:  $A = 100 \text{ mm}^2 = 100 \times 10^{-6} \text{ m}^2$   
 $E = 200 \text{ kN/mm}^2 = 200 \times 10^6 \text{ kN/m}^2$

Solution:  $d_s = 1$  (imagine the 3 pins same way up)  
 $d_s = 3m + r - 3j - p = 3(5) + 3 - 3(5) - 2 = 1$  Without tie  $d_s = 0$ .   
 If it connects two members, can think of it as a release. But use best method and use best method.

Note that the tie might be necessary when poor soil conditions or one side trees of the site prevent the development of a lateral restraint at one footing.   
 Simply supported frame as add 1 to  $d_s$ .

Cut the tie for a released structure. need not solve.   
 Cut at apex & calculate b. moment.



$$f_{10} = \int M_0 \frac{M_1}{EI} ds + \sum P_i \frac{P_i L}{EA} = \left\{ \frac{1}{6} (5.2) (5) (0 + 2x - 21.696) + \frac{1}{6} (5.2) (7) (2x - 21.696 + -29.568) \right\}$$

$$\times 2 \frac{1}{EI} + (1) \frac{(0)L}{EA} = -63.07 \text{ mm}$$

$$f_{11} = \int M_1 \frac{M_1}{EI} ds + \sum P_i \frac{P_i L}{EA} = \left\{ \frac{1}{3} (5) (5) (5) + \frac{1}{6} (5.2) (5) (2x + 7) + \frac{1}{6} (5.2) (7) (5 + 2x + 7) \right\}$$

$$\times 2 \frac{1}{EI} + (1) \frac{(9.6)L}{EA} = 23.54 \text{ mm}$$

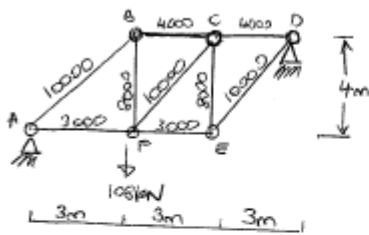
$$X_1 = \frac{63.07}{23.54} = 2.68 \text{ kN}$$

Final BMD



STATICALLY INDETERMINATE TROSS USING FLEXIBILITY.

For the pin-jointed frame find the member forces.

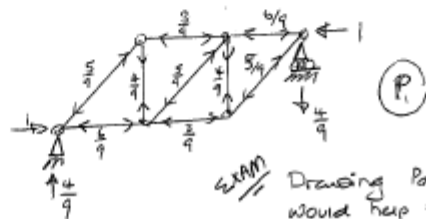
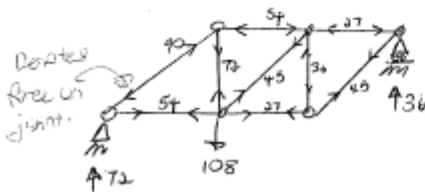


The numbers on the members are their areas  $A$  and  $E = 200 \text{ kN/mm}^2$ .

Solution:  $d_s = m+r-j = 9+4-2(6) = 1$

Insert roller at D so form the primary structure. Thus all the member forces can be obtained by the method of joints after finding external reactions from equilibrium. These forces  $P_0$  are tabled below.

Then, a unit force is applied at D on the primary structure and  $P_1$  set of forces is obtained.



**EXAM**  
Drawing  $P_0$  &  $P_1$  diagram would help tremendously. Draw forces with correct directions on joints. Then fill up  $P_0$  &  $P_1$  according to appropriate sign convention.

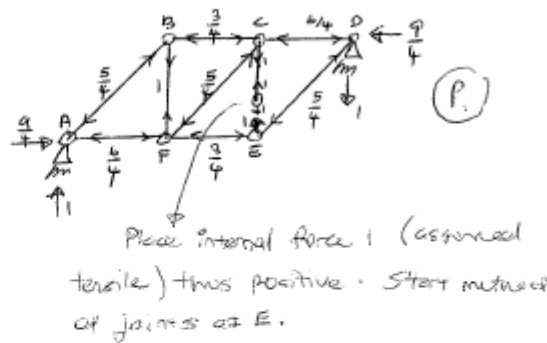
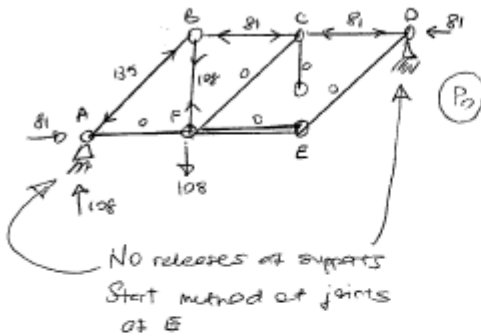
$$f_{i0} + X_1 f_{i1} = 0$$

$$\sum P_i \frac{P_{0i}}{EA} + X_1 \sum P_i \frac{P_{1i}}{EA} = 0$$

	$\frac{L}{A}$	$P_0$	$P_1$	$P_0 \frac{L}{A}$	$P_1 \frac{L}{A}$	$P = P_0 + X_1 P_1$
AB	0.5	-40	-0.56	25.0	0.154	-93.4
BC	0.75	-54	-0.33	13.5	0.083	-56.0
CD	0.75	-27	-0.67	13.5	0.333	-31.1
DE	0.5	45	-0.56	-12.5	0.154	41.6
EF	1.0	27	-0.33	-9.0	0.111	24.9
AF	1.0	54	-0.67	-36.0	0.444	49.9
BF	0.5	72	0.44	16.0	0.099	74.7
CF	0.5	45	-0.56	-12.5	0.154	41.6
CE	0.5	-36	0.44	-8.0	0.099	-33.3
$\Sigma$				-10.0	1.633	

$\Rightarrow -10.0 + X_1 (1.633) = 0 \Rightarrow X_1 = 6.12$

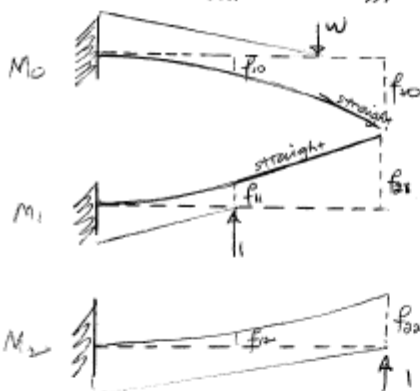
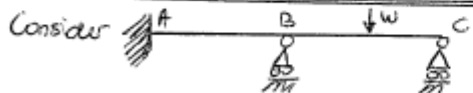
But it must be realised that the choice of the release was inefficient. We should instead release an internal force  $\Rightarrow$  i.e. disconnect a member.



The same answers result but computation of

$$\sum P_i P_0 \frac{L}{EA} + X_1 \sum P_i P_1 \frac{L}{EA} = 0 \text{ is greatly simplified.}$$

Understanding flexibility for  $\alpha_s = 2$  (Alternative solution elsewhere; consider moments release).



This is the chosen primary structure (a cantilever)

At the direction and position of released actions there is a displacement,  $f_{10}$  &  $f_{20}$ .

$f_{10} = \int \frac{M_1 M_0}{EI}$  i.e. the vertical deflection at point B (point 1). By the method of virtual forces, we apply a unit load at position we want the deflection. This corresponds to  $M_1$ . Similarly  $f_{20} = \int \frac{M_2 M_0}{EI}$

$f_{11} = \int \frac{M_1 M_1}{EI}$  i.e. apply a unit virtual load at B. But here it will be the same diagram  $M_1$ . Similarly for  $f_{22} = \int \frac{M_2 M_2}{EI}$ .

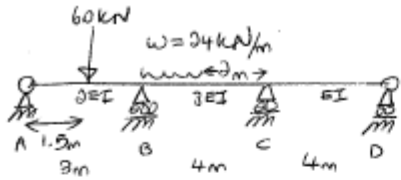
Now  $f_{12} = \int \frac{M_2 M_1}{EI}$ .  $M_1$  refers to the real BMD. Thus real curvature term  $(\frac{M_1}{EI})$ . To get deflection at point C (point 2) due to  $M_1$ , we apply a unit virtual load at point 2. This corresponds to  $M_2$ .

Similarly  $f_{21} = \int \frac{M_1 M_2}{EI}$  i.e. deflection at point 1 due to real  $M_2$ .

The virtual bmd will now be  $M_1$ .

From compatibility,  $f_{10} + X_1 f_{11} + X_2 f_{12} = 0$  } Principle of superposition.  
 $f_{20} + X_1 f_{21} + X_2 f_{22} = 0$

where  $X_1$  and  $X_2$  are scale factors to satisfy compatibility.



Draw BMD. For beams use  
 $\alpha_s = \text{unknowns} - \text{knowns}$   
 with knowns being increased by one with each inner pin. Pins at extremes are irrelevant.

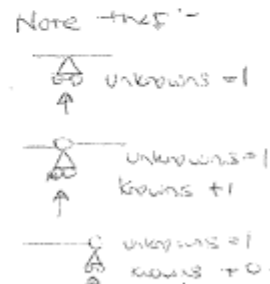
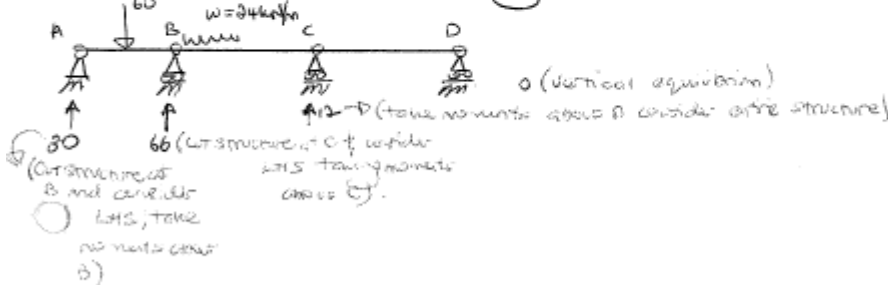
SOLUTION:

$$\alpha_s = 5 - 3 = 2 \text{ (unknowns - knowns)}$$

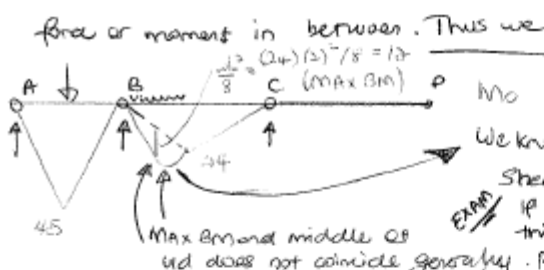
$$\alpha_s = 3m + (-3j - P_i) = 3(3) + 7 - 3(4) - 2 = 2$$

This is because we can cut inner pin to reveal no BMD and take moments considering structure.

Form primary structure by inserting moment releases at B and C. One half at structure.

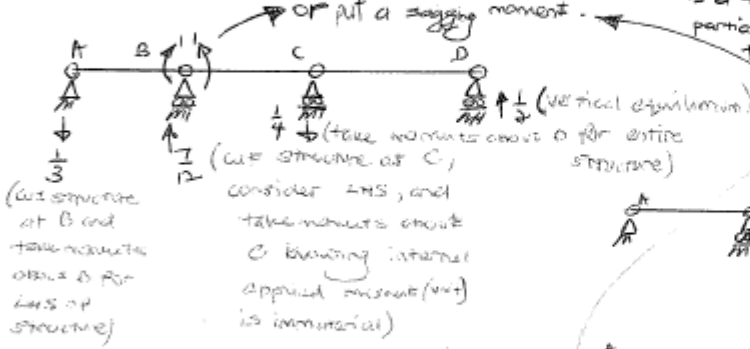


Now we need to draw  $M_0$ . Bending moment at hinges are 0. This is no bending moment between C and D as the extremes are zero bending moment and no external force or moment in between. Thus we need not actually know  $V_0 = 0 \text{ kN}$ .

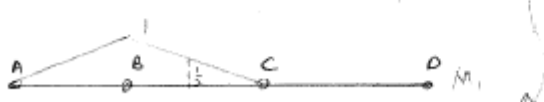


EXCELLENT METHOD! VITAL!  
 (Full PARABOLA EQUATION USED IN PRODUCT INTEGRALS)  
 We know that there is a max (or min) because Shear Force Diagram cross zero.

Apply unit internal moments at B (for  $M_1$ ) and C (for  $M_2$ ) in turn on primary structure



If this is a maximum/minimum point, then use this breaking up method utilising  $\frac{d^2y}{dx^2}$  and full parabola equation or standard integral tables. If there is a turning point we cannot use one partial parabola equation just one, we need to break up portions and apply 0 times. If no max/min point then use partial parabola equation.



COULD USE SIMPSONS RULE BY PROP HOBBS METHOD!

Actually as with  $M_1$ , we need not find reactions at supports cause all we need is the BMD which is zero at all pins except where internal unit moment is applied.

$$f_{10} + X_1 f_{11} + X_2 f_{12} = 0 \dots \dots \dots (1)$$

$$f_{20} + X_1 f_{21} + X_2 f_{22} = 0 \dots \dots \dots (2)$$

(1) :  $\int_0^L \frac{M_1 M_0}{EI} + X_1 \int_0^L \frac{M_1 M_1}{EI} + X_2 \int_0^L \frac{M_1 M_2}{EI} = 0$

*equilateral triangle and right-angled triangle.*

*full parabola and trapezium equation (3,4)*

$$f_{10} = \int_0^L \frac{M_1 M_0}{EI} = \left[ \frac{1}{2EI} \left( \frac{1}{4} (3)(4)(-1) \right) + \left\{ \frac{1}{3EI} \left( \frac{1}{3} (2)(4) \left( 1 + \frac{1}{2} \right) \right) + \frac{1}{3EI} \left( \frac{1}{4} (4)(-2)(1) \right) \right\} \right] = \frac{-28.875}{EI}$$

*l.u.l. = 8*

$$f_{11} = \left[ \frac{1}{3EI} \left( \frac{1}{3} (3)(1)(1) \right) + \frac{1}{3EI} \left( \frac{1}{3} (4)(1)(1) \right) \right] = \frac{0.944}{EI}$$

*\* Differing EI*  
*\* DO NOT forget -ve sign when multiplying M. (product integrals)*

$$f_{12} = f_{21} = \frac{1}{3EI} \left( \frac{1}{6} (4)(1)(1) \right) = \frac{0.222}{EI} \text{ (or } \frac{2}{9EI} \text{)}$$

*\*  $f_{10} = \int \frac{M_1 M_0}{EI} ds$*   
 *$f_{11} = \int \frac{M_1 M_1}{EI} ds$*   
*Subscript on f follows M diagram!*  
*(thus  $f_{12} = f_{21}$ )*

$$f_{20} = \frac{1}{3EI} \left( \frac{1}{3} (2)(4) \left( \frac{2}{3} \right) \right) + \frac{1}{3EI} \left( \frac{1}{4} (4)(1)(-2) \right) = \frac{-28}{3EI}$$

*It is half not one (mistake by JS)*  
*length is 4m not 3m (mistake by JS)*

$$f_{22} = \frac{1}{3EI} \left( \frac{1}{3} (4)(1)(1) \right) + \frac{1}{EI} \left( \frac{1}{3} (4)(1)(1) \right) = \frac{16}{9EI}$$

*flexibility matrix*

$$\begin{pmatrix} f_{10} \\ f_{20} \end{pmatrix} + \begin{pmatrix} f_{11} & f_{12} \\ f_{21} & f_{22} \end{pmatrix} \begin{pmatrix} X_1 \\ X_2 \end{pmatrix} = \begin{pmatrix} 0 \\ 0 \end{pmatrix}$$

$$\frac{1}{EI} \begin{pmatrix} -28.875 \\ -\frac{28}{3} \end{pmatrix} + \frac{1}{EI} \begin{pmatrix} 0.944 & \frac{2}{9} \\ \frac{2}{9} & \frac{16}{9} \end{pmatrix} \begin{pmatrix} X_1 \\ X_2 \end{pmatrix} = \begin{pmatrix} 0 \\ 0 \end{pmatrix}$$

*put inverse before this term.*

$$\begin{pmatrix} X_1 \\ X_2 \end{pmatrix} = \frac{1}{1.028} \begin{pmatrix} \frac{16}{9} & -\frac{2}{9} \\ -\frac{2}{9} & 0.944 \end{pmatrix} \begin{pmatrix} 28.875 \\ \frac{28}{3} \end{pmatrix} = \begin{pmatrix} 30.24 \\ 1.47 \end{pmatrix} \text{ (ANS)}$$

$X_1$  and  $X_2$  are values of  $M_B$  and  $M_C$  (on the real indeterminate structure) in directions assumed by unit load/moment/bending moment.

$M_B = 30.24 \text{ kNm}$  tension in upper surface } THEY TENSION ON UPPER SURFACE.  
 $M_C = 1.47 \text{ kNm}$  tension in upper surface }  is a pair of internal bending moments.

Also deducible from  $M = M_0 + \sum M_i X_i$

Here  $M = M_0 + M_1 X_1 + M_2 X_2$   
 (Draw S.M.D for the indeterminate structure from this).

Left moment belongs to left member and right moment to right member. This happens (i.e. tension at top) just because of the way we define these internal bending moments.

Dr. Jesse Chaffin

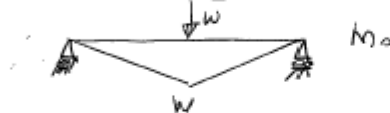
Evidence Suggesting Possible Use of Differing Release Sets for  $M_1, M_2$

Consider



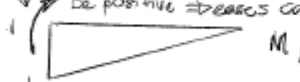
(different from that  
chosen for  $M_0$ )  
But release sets  
for  $M_1$  and  $M_2$   
still the same.

Release  $M_0$  and  $V_0$  for simply supported structure.



Conventional

note choose direction of  
unit load/moment such that  $M_1, M_2$  will  
be positive stresses calculations



$$f_{10} = \frac{1}{4}(4)(1)(w) = w$$

$$f_{20} = \frac{1}{3}(4)(1)(w) = \frac{4w}{3}$$

$$f_{11} = \frac{1}{3}(4)(1)(1) = \frac{4}{3}$$

$$f_{21} = \frac{1}{3}(4)(1)(1) = \frac{4}{3}$$

$$f_{12} = \frac{1}{7}(4)(1)(1) = \frac{4}{7}$$

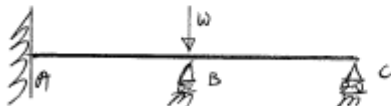
$$\begin{pmatrix} f_{10} \\ f_{20} \end{pmatrix} + \begin{pmatrix} f_{11} & f_{12} \\ f_{21} & f_{22} \end{pmatrix} \begin{pmatrix} X_1 \\ X_2 \end{pmatrix} = \begin{pmatrix} 0 \\ 0 \end{pmatrix}$$

$$\begin{pmatrix} \frac{4}{3} & 1 \\ 1 & \frac{4}{3} \end{pmatrix} \begin{pmatrix} X_1 \\ X_2 \end{pmatrix} = \begin{pmatrix} -w \\ -\frac{4w}{3} \end{pmatrix}$$

$$\begin{pmatrix} X_1 \\ X_2 \end{pmatrix} = \frac{1}{\frac{7}{9}} \begin{pmatrix} \frac{4}{3} & -1 \\ -1 & \frac{4}{3} \end{pmatrix} \begin{pmatrix} -w \\ -\frac{4w}{3} \end{pmatrix}$$

$$\begin{pmatrix} X_1 \\ X_2 \end{pmatrix} = \begin{pmatrix} 0w \\ -1w \end{pmatrix}$$

$$M = M_0 + X_1 M_1 + X_2 M_2$$



Should have known in  
the first phase.

Doing

Release  $V_0, V_c$



$$f_{10} = \frac{1}{4}(4)(4)(w) = 4w$$

$$f_{20} = \frac{1}{6}(2)(2)(w) = \frac{2w}{3}$$

$$f_{11} = \frac{1}{3}(4)(4)(4) = \frac{64}{3}$$

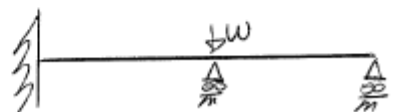
$$f_{21} = \frac{1}{3}(2)(2)(2) = \frac{4}{3}$$

$$f_{12} = \frac{1}{6}(2)(2)(2+2+4) = \frac{40}{6}$$

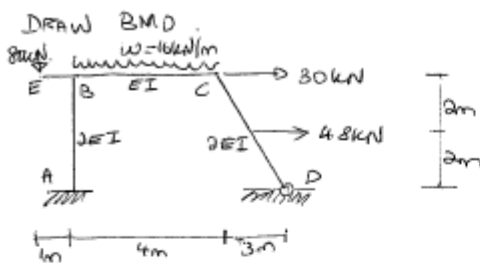
$$\begin{pmatrix} 4w \\ \frac{2w}{3} \end{pmatrix} + \begin{pmatrix} \frac{64}{3} & \frac{40}{6} \\ \frac{40}{6} & \frac{4}{3} \end{pmatrix} \begin{pmatrix} X_1 \\ X_2 \end{pmatrix} = \begin{pmatrix} 0 \\ 0 \end{pmatrix}$$

$$\begin{pmatrix} X_1 \\ X_2 \end{pmatrix} = \frac{1}{\frac{112}{9}} \begin{pmatrix} \frac{64}{3} & -\frac{40}{6} \\ -\frac{40}{6} & \frac{4}{3} \end{pmatrix} \begin{pmatrix} -4w \\ -\frac{2w}{3} \end{pmatrix}$$

$$\begin{pmatrix} X_1 \\ X_2 \end{pmatrix} = \begin{pmatrix} -\frac{1}{2}w \\ 1w \end{pmatrix}; M = M_0 + X_1 M_1 + X_2 M_2$$



Again - Suggested true. In fact actually  
true, can be proven (through 3D vectors)



Cut B: R.H.S:  $V_D(7) - H_D(4) + (4E)(2) - \frac{16(4)^2}{2} = 0$

Cut C: R.H.S:  $(4E)(2) + V_D(3) - H_D(2) = 0$

$$\left(\frac{4H_D - 96}{3}\right)(3) - 4H_D = 32$$

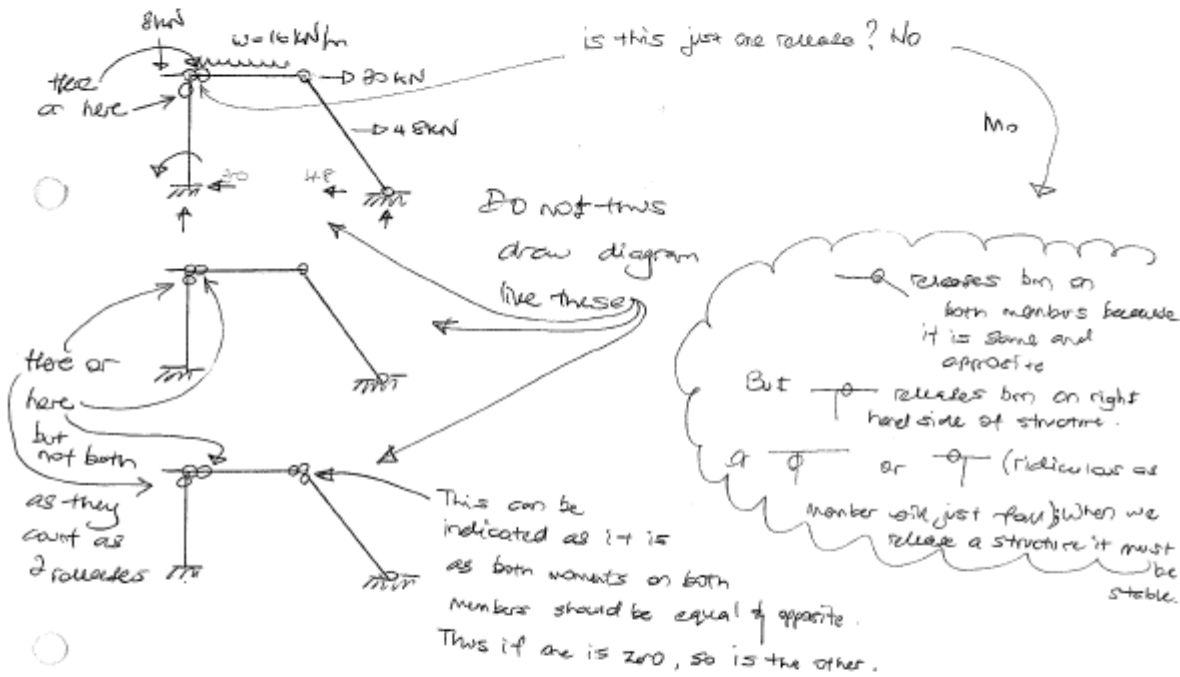
$$\frac{28}{3}H_D - 224 - 4H_D = 32$$

$$\frac{16}{3}H_D = 256$$

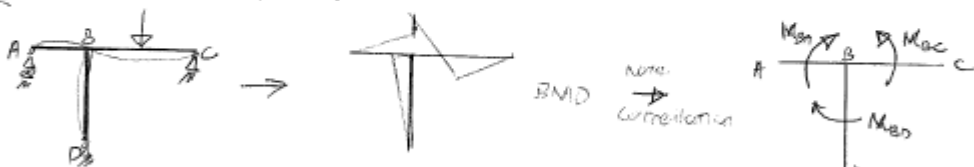
$$H_D = 48$$

$$d_s = 3m + r - 3j - p_i = 3(4) + 5 - 3(5) - 0 = 2$$

Form primary structure by inserting moment release at B and C.

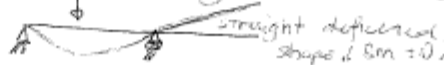


⊥ bending moment here at the joint will be a result of the 3 members  $\Rightarrow 0$ .



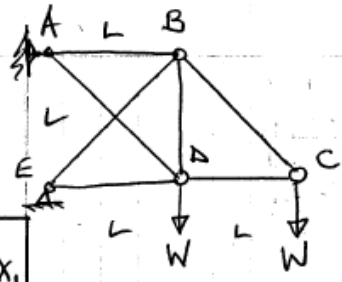
Note: BMD becomes zero at points of contra flexure (equal brium at joint) cause no stresses at change of curvature.

Note: If a part of structure remains straight after loading, thus no bending moment there



Signs carry through.

Member	Member properties	Forces in Released structure	Forces in Released Str. "Unit due to Displacement"	Calculate $f_{i0}$	Calculate $f_{i1}$	When $X_1$ found, calc $X_1 P_1$	Hence final forces
Member	$L/AE$	$P_0$	$P_1$	Contributions to $P_i P_0 L/AE$	Contributions to $P_i^2 L/AE$	$P_i X_1$	$P = P_0 + P_i X_1$
AB	1	3W	$-\frac{1}{\sqrt{2}}$	$-3/\sqrt{2}$	$\frac{1}{2}$	-W	2W
BC	$\sqrt{2}$	$\sqrt{2}W$	0	0	0	0	$\sqrt{2}W$
CD	1	-W	0	0	0	0	-W
DE	1	-W	$-\frac{1}{\sqrt{2}}$	$\frac{1}{\sqrt{2}}$	$\frac{1}{2}$	-W	-2W
AD	$\sqrt{2}$	0	Assumeel tensile	0	$\sqrt{2}$	$\sqrt{2}W$	$\sqrt{2}W$
BE	$\sqrt{2}$	$-2\sqrt{2}W$	1	-4	$\sqrt{2}$	$\sqrt{2}W$	$-\sqrt{2}W$
BD	1	W	$-\frac{1}{\sqrt{2}}$	$-\frac{1}{\sqrt{2}}$	$\frac{1}{2}$	-W	0



FLEXIBILITY ANALYSIS OF A TRUSS  
( $\delta_3 = 1$ )  
RELEASE: AD

Times  $L/AE$

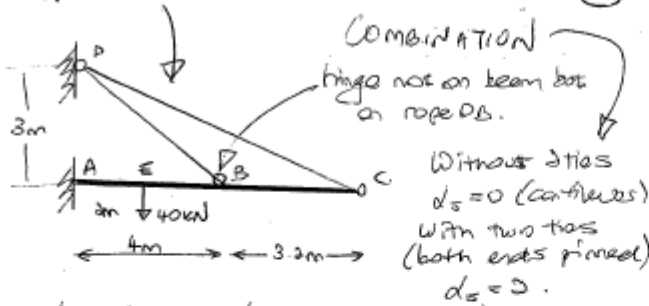
$\sum$

Units $WL/AE$	Units $L/AE$
$-4 - 3/\sqrt{2}$	$\frac{3}{2} + 2\sqrt{2}$
ie $f_{i0}$	$f_{i1}$

Solve  $(f_{i0}) + (f_{i1}) X_1 = 0$   
 $(-4 - \frac{3}{\sqrt{2}}) + (\frac{3}{2} + 2\sqrt{2}) X_1 = 0$   
 ie  $X_1 = \sqrt{2}W$

M

Given Cables are allowed to carry tensile forces only. Given

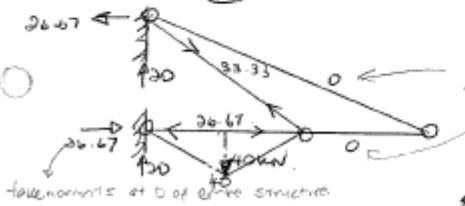


	Area (m <sup>2</sup> )
BA	7.5 x 10 <sup>-3</sup>
CD	2.6 x 10 <sup>-3</sup>
ABC	20.0 x 10 <sup>-3</sup>

Without ties  $d_s = 0$  (conflexes)  
 With two ties (both ends pinned)  $d_s = 2$   
 $I_{ABC} = 1 \times 10^{-3} \text{ m}^4$   
 $E \text{ for all} = 200 \times 10^6 \text{ kN/m}^2$

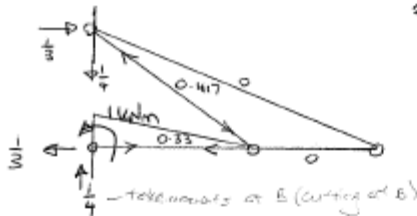
$d_s = 5 - 3 = 2$  (unknowns - knowns)  $\rightarrow$  cutting at C finite cause end of member  
 $\rightarrow$  hinge B is not on beam; cut out and consider LHS of beam; NO.

Form primary structure by inserting hinge at A and B. ~~Maybe releasing the ties would be better.~~



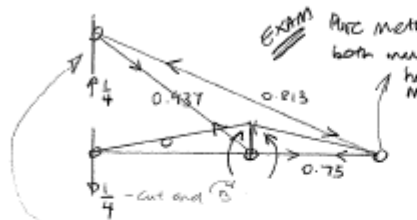
$P_0$  and  $M_0$   
 Consider joint C (instead of joints)

Get bending moments in beam by normal procedures. Get axial forces by the method joints.



EXAM Method of joints is applicable but the member force would be zero at combinations!  
 $P_1$  and  $M_1$

Even though the cables are allowed to carry tensile forces only, in the virtual system, it is



EXAM Pure method of joints give both numbers zero, but here there is member too. Thus  $P_2/M_2$  not zero. Solve simultaneously at pure truss joint, or from  $(33.33)(5)$   $\rightarrow$   $0.875$  from the x component.

$$f_{00} = \int M_0 \frac{M_0}{EI} + \sum P_0 \frac{P_0 L}{EA}$$

$$= \frac{1}{EI} \left( \frac{1}{4} (4) (40) (-1) \right) + \frac{1}{EA_{BD}} (-0.417)$$

$$= \frac{1}{EI} (33.33)(5) + \frac{1}{EA_{BD}} ((0.33)(-36.67)(4))$$

$$f_{10} = \int M_1 \frac{M_1}{EI} + \sum P_1 \frac{P_1}{EA} = \frac{1}{EI} \left( \frac{1}{3} (4) (1) (1) \right) + \frac{1}{EA_{BD}} ((0.937)(33.33)(5))$$

$$f_{11} = \int M_1 \frac{M_1}{EI} + \sum P_1 \frac{P_1}{EA} = \frac{1}{EI} \left( \frac{1}{3} (4) (1) (1) + \frac{1}{3} (3.2) (1) (1) \right) + \frac{1}{EA_{BD}} ((0.937)(0.937)(5))$$

$$f_{20} = \int M_2 \frac{M_2}{EI} + \sum P_2 \frac{P_2}{EA} = \frac{1}{EI} \left( \frac{1}{6} (4) (1) (1) \right) + \frac{1}{EA_{BD}} ((0.937)(-0.417)(5))$$

$$\frac{10^3}{E} \begin{pmatrix} -40 & -11.03 \\ -40 & +20.83 \end{pmatrix} + \frac{10^3}{E} \begin{pmatrix} (1.33+0.14) & (0.67-0.26) \\ (0.67-0.26) & (2.4+2.66) \end{pmatrix} \begin{pmatrix} X_1 \\ X_2 \end{pmatrix} = \begin{pmatrix} 0 \\ 0 \end{pmatrix}$$

$$\begin{pmatrix} X_1 \\ X_2 \end{pmatrix} = \begin{pmatrix} 34.43 \\ 0.99 \end{pmatrix}$$

Axial forces in the cables BD and CD can be found from

$$P = P_0 + X_1 P_1 + X_2 P_2$$

$$P_{BD} = (33.33) + (34.43)(-0.417) + (0.99)(0.9375)$$

$$= 19.91 \text{ kN}$$

$$P_{CD} = (0) + (0)(34.43) + (-0.8125)(0.99)$$

$$= -0.81 \text{ kN (compression)}$$

Since CD cannot carry compression, it would become inactive under given loading. Thus structure reduced to cantilever AC and supported by single cable BD. Thus  $\alpha_2 = 1$ . Insert single moment release at A.  $M_1/P_1$  and  $M_0/P_0$  happens to be the same as before.

$$\left[ \int M_1 \frac{M_0}{EI} dx + \sum P_1 P_0 \frac{L}{EA} \right] + \left[ \int N_1 \frac{N_0}{EI} dx + \sum P_1 P_1 \frac{L}{EA} \right] X_1 = (0)$$

$$X_1 = 34.71$$

$$M = M_0 + M_1 X_1 \quad \text{and} \quad P = P_0 + P_1 X_1$$

$$M_A = 0 + (1)(34.71) = 34.7 \text{ kNm (tension on top)}$$

because of direction of unit moment is correctly assumed

$$M_B = 0 \text{ kNm}$$

$$P_{BD} = (33.33) + (-0.417)(34.71)$$

$$= 18.86 \text{ kN (tension)}$$

$$P_{CD} = 0 \text{ kN}$$

PRODUCT INTEGRALS

Important note is that LHS of  $m(x)$  must correspond to LHS of  $M(x)$  & vice versa.

$M(x)$ REAL	$m(x)$ VIRTUAL (ONLY)	FOUR TYPES	MUST BE EQUILATERAL	
	$b$	$b$	$b$	$b > d$ or $d > b$
	Lab	$\frac{1}{2} Lab$	$\frac{1}{2} Lab$	$\frac{1}{2} La(b+d)$
	$\frac{1}{2} Lab$	$\frac{1}{3} Lab$	$\frac{1}{4} Lab$	$\frac{1}{6} La(2b+d)$
Follows orientation		Reversed		
	$\frac{1}{2} Lab$	$\frac{1}{6} Lab$	$\frac{1}{4} Lab$	$\frac{1}{6} La(b+2d)$
Follows orientation				
	$\frac{1}{2} Lab$	$\frac{1}{4} Lab$	$\frac{1}{3} Lab$	$\frac{1}{4} La(b+d)$
* MUST BE EQUILATERAL				
	$\frac{2}{3} Lab$	$\frac{1}{3} Lab$	$\frac{3}{12} Lab$	$\frac{1}{3} La(b+d)$
	$\frac{1}{2} Lb(a+c)$	$\frac{2}{3}$ side of trapezium with greater triangle side. $\frac{1}{6} Lb(2a+c)$	$\frac{1}{4} Lb(a+c)$	$\frac{1}{6} La(2b+d) + \frac{1}{6} Lc(b+2d)$
$a > c$ or $c > a$				
	$\frac{1}{3} Lab$	$\frac{1}{4} Lab$	$\frac{7}{48} Lab$	$\frac{1}{12} La(3b+d)$
Follows orientation				
	$\frac{1}{3} Lab$	$\frac{1}{12} Lab$	$\frac{7}{48} Lab$	$\frac{1}{12} La(b+3d)$
Follows orientation				
	$\frac{1}{6} Lb(a+4c+e)$	$\frac{1}{6} Lb(a+2c)$	$\frac{1}{24} Lb(a+10c+e)$	$\frac{1}{6} Lb(a+2c) + \frac{1}{6} Ld(2c+e)$
* a or e can be 0. no turning point between a & e! MUST		a is the side with the greater triangle length.		

\* = restrictions; others simply left times left & right times right respecting sign.

$$\int_0^L M(x)m(x)dx$$

DLS/REH Nov 97

Trapezoidal diagrams don't regardless of orientation, i.e. a could be bigger or smaller than c and b could be smaller or bigger than d. But as always a must correspond to b & c to d.

### 3.1.6.3 Bending Moments, Shear Force, and Displacements of Structural Elements by the Stiffness Method

The flexural stiffness relations for a beam element gives the relationships between the actions shear force & bending moment and the kinematics displacements and rotations.

<b>Beam With Both Ends Fixed</b>		
	<b>Same End of Beam</b>	<b>Opposite End of Beam</b>
<b>Bending Moment / Rotation</b>	4EI/L	2EI/L
<b>Shear Force / Translation</b>	12EI/L <sup>3</sup>	-12EI/L <sup>3</sup>
<b>Bending Moment / Translation or Shear Force / Rotation</b>	±6EI/L <sup>2</sup>	
<b>Beam With One End Fixed And The Other Pinned</b>		
	<b>Same End of Beam</b>	<b>Opposite End of Beam</b>
<b>Bending Moment / Rotation</b>	3EI/L	0
<b>Shear Force / Translation</b>	3EI/L <sup>3</sup>	-3EI/L <sup>3</sup>
<b>Bending Moment / Translation or Shear Force / Rotation</b>	±3EI/L <sup>2</sup> but no force (hence stiffness) generated by rotation of pinned end and no moments generated at pinned end due to other kinematics	
<b>Beam With Both Ends Pinned</b>		
	<b>Same End of Beam</b>	<b>Opposite End of Beam</b>
<b>Bending Moment / Rotation</b>	0	0
<b>Shear Force / Translation</b>	0	0
<b>Bending Moment / Translation or Shear Force / Rotation</b>	0	

The force-displacement relationship of the Timoshenko beam is as follows. For the Euler-Bernoulli beam,  $\beta$  is zero.

$$\begin{Bmatrix} F_1 \\ M_1 \\ F_2 \\ M_2 \end{Bmatrix} = \frac{EI}{L^3(1+\beta)} \begin{bmatrix} 12 & 6L & -12 & 6L \\ 6L & (4+\beta)L^2 & -6L & (2-\beta)L^2 \\ -12 & -6L & 12 & -6L \\ 6L & (2-\beta)L^2 & -6L & (4+\beta)L^2 \end{bmatrix} \begin{Bmatrix} \delta_1 \\ \theta_1 \\ \delta_2 \\ \theta_2 \end{Bmatrix} \quad \beta = \frac{12EI}{GAL^2}$$

### 3.1.6.4 Bending Moments and Shear Force of Structures of Low Kinematic Indeterminacies by Moment Distribution

Fixed end forces due to distributed loading is  $-/+wL^2/8$  and that due to a mid point load is  $-/+PL/8$ . The drop-down due to distributed loading is  $wL^2/8$  and that due to a point load is  $PL/4$ . The distribution factors summary is as follows

Location	Distribution Factor
Kinematic DOF	Stiffness Ratio
Kinematic Fixity	Nothing
Pinned End	1
Cantilever	1:0

The analysis of a structure with kinematic indeterminacy  $\alpha_k = 1$  is exact, and those with  $\alpha_k > 1$  is iterative. The kinematic indeterminacies are reduced by

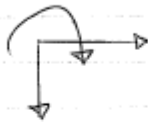
- (a) changing moment/rotational stiffness of pinned end beam to  $3EI/L$  from  $4EI/L$ , hence eliminating the pinned ended kinematic
- (b) employing symmetry and anti-symmetry of structure and loading as follows
  - (i) axis of symmetry through a joint and symmetric loading  
 $\phi_{\text{centre}} = 0$ , hence analyze half structure with equivalent central rotational fixity
  - (ii) axis of symmetry through a joint and anti-symmetric loading  
 $BM_{\text{center}} = 0$ , hence analyze half structure with equivalent central pinned end
  - (iii) axis of symmetry through a member and symmetric loading  
analyze half structure with the stiffness of middle member of  $2EI/L$
  - (iv) axis of symmetry through a member and anti-symmetric loading  
analyze half structure with the stiffness of middle member of  $6EI/L$

Hence, the analysis of pinned ended two-span continuous beams and propped cantilever is exact.

Beam and External Load	Effects	Bending Deflection
Simply supported beam uniformly loaded $w$	$M_{\text{mid}} = wL^2/8$	$\delta = 5wL^4 / (384EI)$
Simply supported beam mid-span point load $P$	$M_{\text{mid}} = PL/4$	$\delta = PL^3 / (48EI)$
Cantilever uniformly loaded $w$	$M_{\text{fixed-end}} = wL^2/2$	$\delta = wL^4 / (8EI)$
Cantilever free-end point load $P$	$M_{\text{free-end}} = PL$	$\delta = PL^3 / (3EI)$
Fixed-ended beam (both sides) uniformly loaded $w$	$M_{\text{fixed-end}} = wL^2/12$ $M_{\text{mid}} = wL^2/24$	$\delta = wL^4 / (384EI)$
Fixed-ended beam (both sides) mid-span point load $P$	$M_{\text{fixed-end}} = PL/8$ $M_{\text{mid}} = PL/8$	$\delta = PL^3 / (192EI)$
Propped cantilever uniformly loaded $w$	$M_{\text{fixed-end}} = wL^2/8$ $M_{\text{sag}} = 9wL^2/128$	$\delta_{\text{sag}} = wL^4 / (185EI)$
Propped cantilever mid-span point load $P$	$M_{\text{fixed-end}} = 3PL/16$ $M_{\text{sag}} = 5PL/32$	$\delta_{\text{sag}} = 0.00932PL^3/EI$

MOMENT DISTRIBUTION: AN ENGINEER'S PERSPECTIVE

SIGN CONVENTION



STIFFNESS OF FIXED ENDED BEAM

Stiffness	FIXED Same end of beam	FIXED Opposite end of beam
$\frac{\text{Moment}}{\text{rotation}}$	$\frac{4EI}{L}$	$\frac{2EI}{L}$
$\frac{\text{force}}{\text{displacement}}$	$\frac{12EI}{L^3}$	$-\frac{12EI}{L^3}$

Force/rotation and moment/displacement stiffnesses are all  $6EI/L^2$  or  $-6EI/L^2$  and can be obtained from equilibrium.

STIFFNESS OF FIXED-PINNED ENDED BEAM

Stiffness	FIXED Same end of beam	PINNED Opposite end of beam
$\frac{\text{moment}}{\text{rotation}}$	$\frac{3EI}{L}$	0
$\frac{\text{force}}{\text{displacement}}$	$\frac{3EI}{L^3}$	$-\frac{3EI}{L^3}$

Force/rotation and moment/displacement stiffnesses are all  $3EI/L^2$  or  $-3EI/L^2$  and can be obtained from equilibrium. Obviously moment at pinned end is zero.

STIFFNESS OF PINNED-PINNED ENDED BEAM

No stiffness at all, i.e. no rotational nor transverse stiffness, only axial.

FIXED END FORCES

Distributed loading  $= \frac{WL^2}{12}$

Point load  $= \frac{PL}{8}$

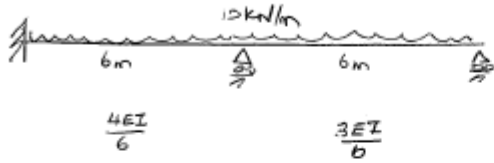
DROP DOWN

Distributed loading  $\frac{WL^2}{8}$

Point load  $\frac{PL}{4}$

Moment Distribution

(A) Propped beam



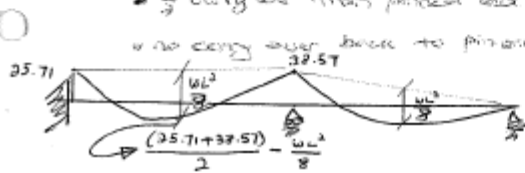
$k_k = 2$   
 Reduced to  $k_k = 1$  by putting stiffness of propped beam as  $\frac{3EI}{L}$ .

	$\frac{4}{7}$	$\frac{3}{7}$	1
-30	30	-30	30
		-15	-30
4.29	8.57	6.43	
-35.71	38.57	-38.57	0

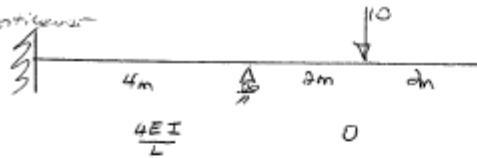
df  
 form  $(\pm \frac{WL^2}{12})$   
 bal  
 bal  
 bal  
 +ve convention  
 distribution factors only of kinematic degrees of indeterminacy (kinematic degrees of freedom)  
 Propped: 1  
 Cantilever: 1:0

$\frac{1}{3}$  carry over from propped end balances end and for all of there is a form

no carry over back to propped.



(B) Cantilever



	1	0
		-30
30	0	0
10	30	-30

df  
 not  $\frac{WL}{8}$  form but  $2(10)$ ; note sign as if form  
 bal

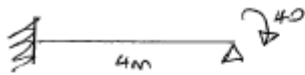
zero stiffness of cantilever

df: 1:0

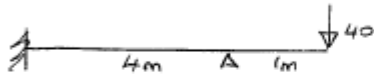
not form at cantilever but force times lever arm, however note the sign as if form.



Ⓒ Externally Applied Moment



Modified DO = fictitious cantilever - stub



$\frac{4EI}{4}$		0
1	0	0
0	40	0
0	40	-40

df.  
 $f_{em} = \text{force} \times \text{lever arm}$ ; note sign as if  $f_{em}$ .  
 bar



Ⓓ Symmetry

(a) Axis of symmetry through a joint

- Symmetric Loading —  $\theta_j = 0$ , hence analyse with equivalent rotational fixity half the structure.
- Anti-symmetric Loading —  $M_j = 0$ , hence analyse with pin end at joint half the structure.

(b) Axis of symmetry through a member

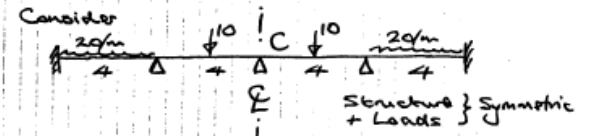
- Symmetric Loading — Stiffness of mid-member is  $\frac{2EI}{L}$  and analyse half the structure; Account for  $f_{em}$  of this mid member but of course no carry over to the imaginary half.
- Anti-symmetric Loading — Stiffness of mid-member is  $\frac{EI}{L}$  and analyse half the structure; Account for  $f_{em}$  of this mid member but of course no carry over to the imaginary half.

Ⓔ Distribution Factors

- (i) Kinematic Degree of Freedom: Stiffness ratios
- (ii) Kinematic fixity: Nothing
- (iii) Pinned end: 1
- (iv) Cantilever: 1:0

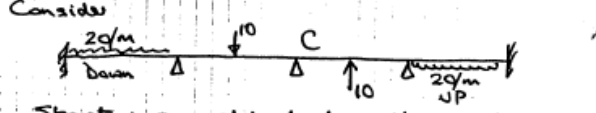
**M.D Symmetry & Antisymmetry**  
 (References used for non-swept structures)

**A** Axis of symmetry through a joint:  
 These are easy.

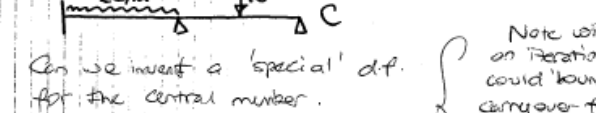


At C, clearly  $\theta_C = 0$  by symmetry, so analyse (with equivalent fixity at C) just half the structure

**A#** Antisymmetry, with axis thro' a joint



Structure symmetric, loads antisymmetric. In this case, at C the fixed b.m. = 0, so analyse half the structure with a pin at C; or

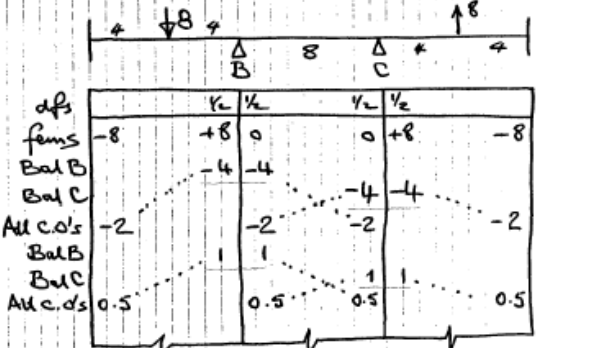


Can we invent a 'special' d.f. for the central number. Note within an iteration we could bounce the carryover from B back to B with a sign change. Some kind of 'mirror' effect.

**Antisymmetry**

**C1** Standard M.D 'hides' the antisymmetry in the table

**C2** With delayed c.o., we retain a visible antisymmetry, but get slow convergence - as in this illustration

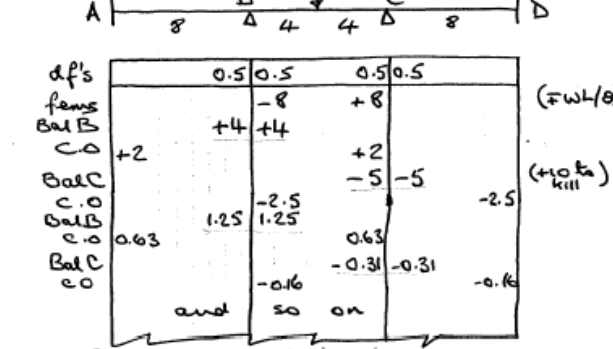


Note in any iteration  $\Delta\theta_B = \Delta\theta_C$

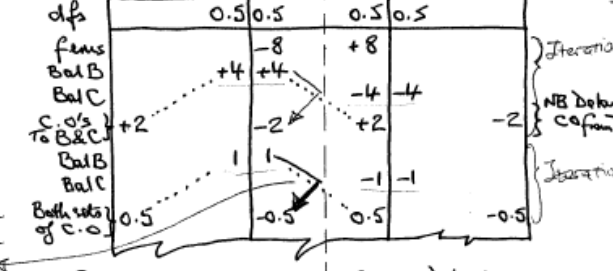
- Balance only joints that can be rotated.
- Joint rotations - moment distribution without sway
- Joint translations - moment distribution with sway
- Sway is merely a descriptive word for the translation displacements of the joints.

**M.D: Symmetry**

**B1** Standard M.D. Note lack of symmetry in table.

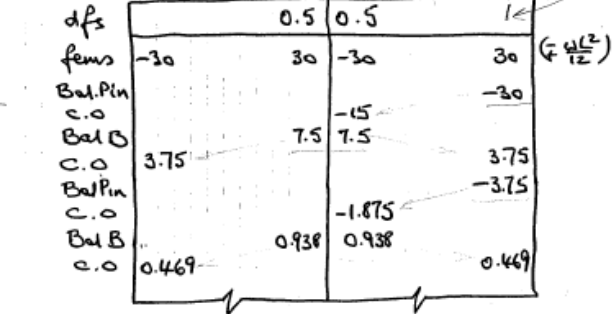
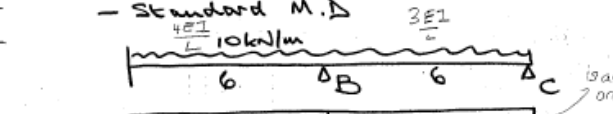


Balance only joints that can be rotated. Standard M.D. with DELAYED carry overs NB. ILLUSTRATION ONLY: DO NOT DO THIS!

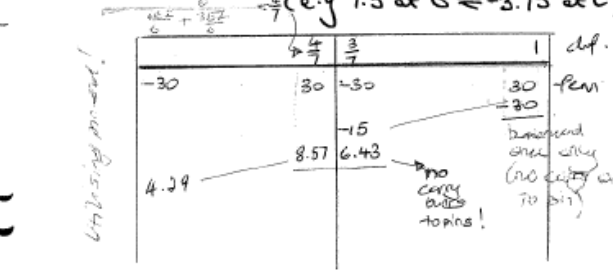


Retains symmetry (good) but slow progress (bad). Note  $\Delta\theta_B = -\Delta\theta_C$  at each iteration! Can we condense the 3 steps per iteration into one? Yes!

**D] Pin-ended member**

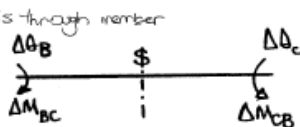


Notice how standard M.D sends moments to the pin by carrying over, only to get rid of them again. In any iteration, then,  $\Delta\theta_C = -\Delta\theta_B/2$



MOMENT DISTRIBUTION - SPECIAL CASES

① Symmetry



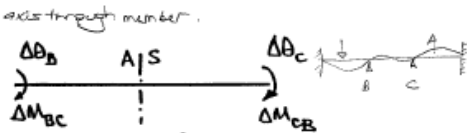
In a delayed carry over calc.,  $\Delta\theta_B = -\Delta\theta_C$  and  $\Delta M_{BC} = -\Delta M_{CB}$  from symmetry and sign convention.

By matrix (2A), at B Look at previous diagram increment for balance B plus subsequent c.o. from C

$$\Delta M_{BC} = \frac{4EI}{L} \Delta\theta_B + \frac{2EI}{L} \Delta\theta_C = \frac{4EI}{L} \Delta\theta_B - \frac{2EI}{L} \Delta\theta_B$$

$$\therefore \Delta M_{BC} = \frac{2EI}{L} \Delta\theta_B \quad \text{and} \quad \Delta M_{CB} = \frac{2EI}{L} \Delta\theta_B$$

② Anti-symmetry

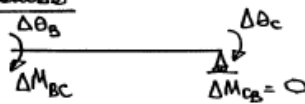


In a delayed c.o. calc  $\Delta\theta_B = \Delta\theta_C$  and  $\Delta M_{BC} = \Delta M_{CB}$  using stiffness sign conv. By (2A), at B

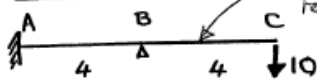
$$\Delta M_{BC} = \frac{4EI}{L} \Delta\theta_B + \frac{2EI}{L} \Delta\theta_C = \frac{4EI}{L} \Delta\theta_B + \frac{2EI}{L} \Delta\theta_B$$

$$\therefore \Delta M_{BC} = \frac{6EI}{L} \Delta\theta_B \quad \text{and} \quad \Delta M_{CB} = \frac{6EI}{L} \Delta\theta_B$$

③ Pin-ended member



M.D. for cantilevers & ext. applied moments  
Ex: CANTILEVER



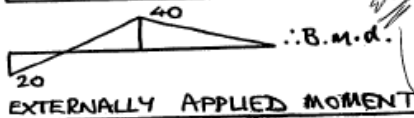
f.e.m.s: clearly  $M_{BC} = -40$

dist. factors: take care! Imagine a rotation  $\Delta\theta_B$ . This generates  $\Delta M_{BA}$ , of course, but does not cause a moment  $\Delta M_{BC}$ , still less  $\Delta M_{CB}$ , as the cantilever has no rot. stiffness at B. Hence d.f.'s are

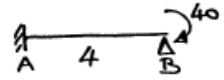
$$\frac{AB}{BC} = \frac{4EI}{L} : 0$$

Hence table:

A	B	C	ie 1 : 0
	1 0 no c.o.		d.f.s
	+40	-40	f.e.m.s
+20			Bal. B
+20	+40	-40	c.o. (not BC)
		0	CANTILEVER



EXTERNALLY APPLIED MOMENT



Procedure: imagine the moment applied via a fictitious stub cantilever and proceed as above i.e. we analyse the second structure instead. (This avoids worrying about a sign change)

By matrix (2A),  $\Delta M_{CB} = \frac{4EI}{L} \Delta\theta_C + \frac{2EI}{L} \Delta\theta_B = 0$  (pin)

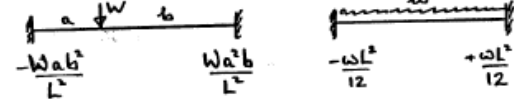
i.e.  $\Delta\theta_C = -\Delta\theta_B / 2$  (rearranging)  
 $\therefore \Delta M_{BC} = \frac{4EI}{L} \Delta\theta_B + \frac{2EI}{L} \Delta\theta_C$   
 $= \frac{4EI}{L} \Delta\theta_B - \frac{EI}{L} \Delta\theta_B = \frac{3EI}{L} \Delta\theta_B$

Thus  $\frac{\Delta M_{BC}}{\Delta\theta_B} = \frac{3EI}{L}$

④ Summary Case

Case	Stiffness	c.o. factor
Standard	$4EI/L$	$1/2$
Symmetric	$2EI/L$	0
Antisym.	$6EI/L$	0
Pin-end	$3EI/L$	0 to the pin-end $1/2$ from the pin-end

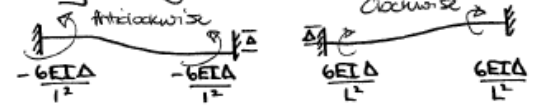
Fixed end moments



S.S.B.M.:-  $Wab/L$

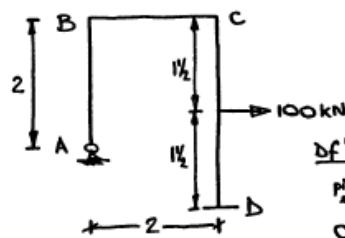
$$\frac{wL^2}{8}$$

Sway (Knowing actual movements of supports)



MOMENT DISTRIBUTION

2ND SWAY EXAMPLE



$EI = 10 \times 10^3$  AB, BC  
 $EI = 20 \times 10^3$  CD  
 KN-M<sup>2</sup>

D.f.'s B AB:BC  
 pin end  $\frac{3EI}{L} : \frac{4EI}{L} = \frac{3}{4}$

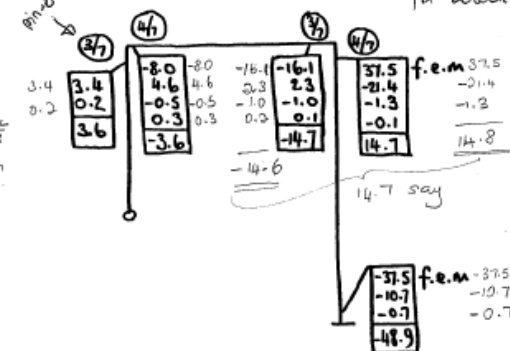
C BC:CD  
 $\frac{4EI}{L} : \frac{4EI}{L} = 20 : 20$

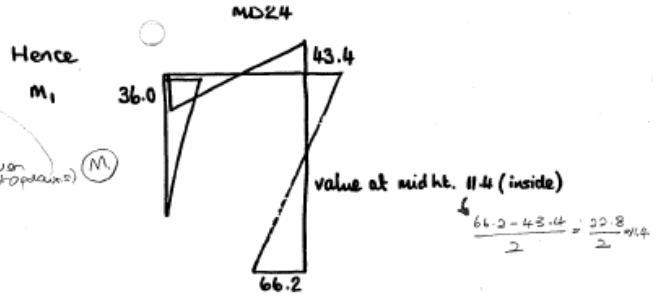
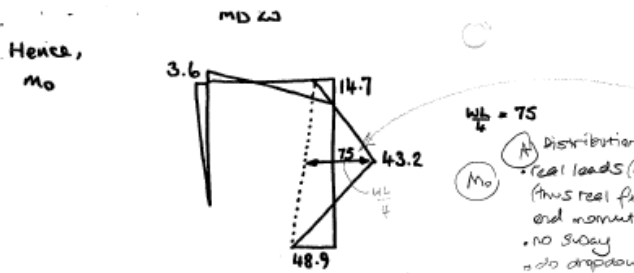
$= \frac{3}{4} : \frac{4}{4}$

FIRST DISTRIBUTION (NO-SWAY)

f.e.m.s  $M_{CB} = 37.5$   
 $M_{BC} = -37.5$  ( $\pm WL/B$ )

Distribution factors always for bending stiffness.





**SECOND DISTRIBUTION (SWAY)**  
Obtain bmd for an arbitrary  $\delta$ , eg one which gives f.e.m's in AB of -100 [NB: Load f.e.m's not put in this calculation]

So if  $-100 = \left[ \frac{6EI\delta}{L^2} \right]_{AB}$ , then  $\delta = \frac{20}{3} \times 10^{-3} \text{ m}$ .

and f.e.m's in CD =  $\left[ \frac{6EI\delta}{L^2} \right]_{CD} = -88.9$

i.e. different f.e.m's as col. lengths and stiffnesses are different - but  $\delta$  is the same for both as AB doesn't stretch. Distribution factors as before.

**EQUILIBRIUM**: true bmd =  $M = M_0 + X_1 M_1$  } Real eq'm Applied loads } system

Arbitrary displ. system - one possibility:-



$\delta_B = 2\theta = 3\phi = \delta_C$  } kinematics  
ie  $\theta = 3\phi/2$

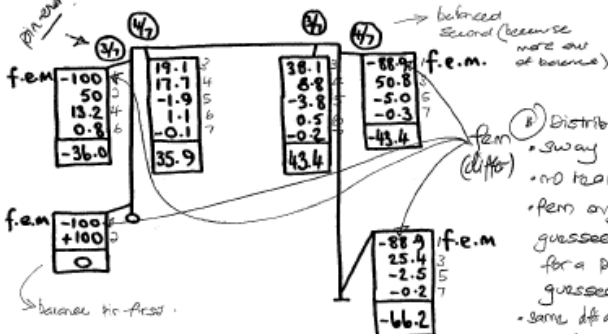
V.W. Eqn External 100kN force acts on original structure. distance moved.  
Ext. V.W =  $100 \times \frac{3\phi}{2}$

Use convention = Int. V.W = 0 +  $\left[ \theta (36.0X, -3.6) \right]_{at A}$  } tens. inside  
+  $\left[ \phi (43.4X, -14.7) \right]_{at C}$  } tens. outside  
+  $\left[ \phi (66.2X, +48.9) \right]_{at D}$  } tens. inside

$150\phi = \phi [163.6X + 28.8]$

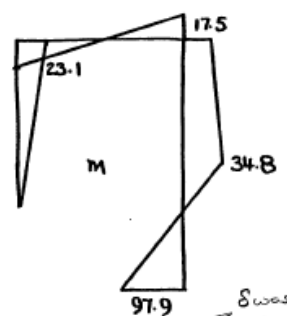
or  $X_1 = 121.2 / 163.6 = 0.741$

- (C)  $M = M_0 + X_1 M_1$  (do dropdowns)
- Find  $X_1$  from virtual work and draw
- Final BMD  $M = M_0 + X_1 M_1$
- (D) Final sway  $\Delta = X_1 \delta$



- (B) Distribution  $M_1$ 
  - sway
  - no real loads
  - f.e.m's from guessed f.e.m for a particular guessed  $\delta$ , sway.
  - same d.f.s as in  $M_0$  distribution.

Hence final bmd,  $M = M_0 + X_1 M_1$



Final sway,  $\Delta = X_1 \delta$   
=  $0.741 \times \frac{20}{3} \times 10^{-3} \text{ m}$   
=  $4.95 \text{ mm}$

**Moment Distribution**

1. Distribution Factors
2. Fixed End Moments
3. Balance a joint at a time (i.e. times negative of distribution factors) and draw line below.
4. Carry-over

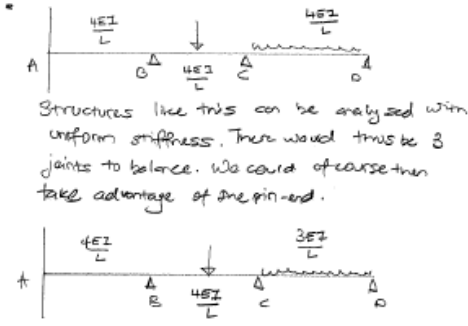
(A) - Symmetric axis through joint + symmetric structure  
 A1 Symmetric loading -  $\theta_2 = 0$  (with equivalent fixity and analyse half structure)  
 A2 Anti-symmetric -  $M_2 = 0$  (pin at centre joint and analyse half structure)

(B) - Symmetric axis through member + symmetric structure  
 B1 Symmetric loading - stiffness of half member is  $\frac{2EI}{L}$ . Analyse half of structure. (no c.o.g) for middle structure taken into account.  
 B2 Anti-symmetric loading - stiffness of half member is  $\frac{6EI}{L}$ . Analyse half of structure. (no. c.o.g.)

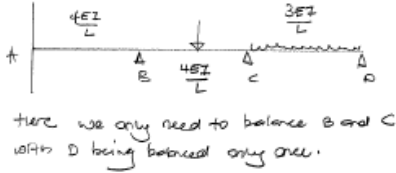
(D) Corner - 0 stiffness (i.e. 0 d.p.)  
 fixed end moments probable? Not actually fixed (simple supports but take end moment but stiffness sign conventions) same reaction.

(E) Externally applied moment - fictitious end concept to avoid forgetting sign change.

(C) - Pin-ended member - stiffness is  $\frac{3EI}{L}$  & c.o.  $\perp$  from pin end (still have to balance pin but only once because to carry over to pin.)

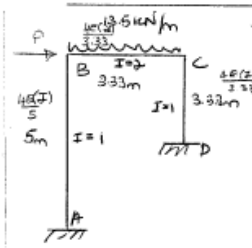


Structures like this can be analyzed with uniform stiffness. There would thus be 3 joints to balance. We could of course then take advantage of the pin-end.



Stiffness coefficients for columns can be taken as zero, thus getting rid of the 3 kinematics at the free end.

**DETERMINATION OF PROPPING FORCE**



Propping force P required to prevent sway.

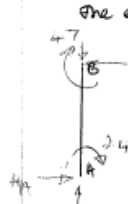
Since no 3 member joint, table will do.

	B		C		
A	1	2	3	4	D
1	0.25	0.75	0.67	0.33	0
2					
3					
4					
5					
6					
7					
8					
9					
10					
11					
12					
13					
14					
15					
16					
17					
18					
19					
20					
21					
22					
23					
24					
25					
26					
27					
28					
29					
30					
31					
32					
33					
34					
35					
36					
37					
38					
39					
40					
41					
42					
43					
44					
45					
46					
47					
48					
49					
50					
51					
52					
53					
54					
55					
56					
57					
58					
59					
60					
61					
62					
63					
64					
65					
66					
67					
68					
69					
70					
71					
72					
73					
74					
75					
76					
77					
78					
79					
80					
81					
82					
83					
84					
85					
86					
87					
88					
89					
90					
91					
92					
93					
94					
95					
96					
97					
98					
99					
100					

Only one distribution before being able to find P.

dp.  $fem = \frac{wL^2}{12}$   
Should take at least 2dp.

To obtain P, we obtain the reactions (horizontal) at B and C by considering the equilibrium of the 2 vertical members. Then consider the equilibrium (horizontal) of BC.

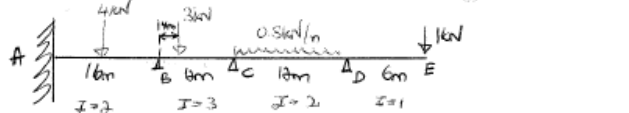


$$H_A = \frac{M_{AB} + M_{BA}}{L_{AB}} = \frac{2.4 + 4.8}{5} = 1.44 \text{ kN}$$

$$H_C = \frac{M_{CB} + M_{BC}}{L_{BC}} = \frac{-6.5 - 3.4}{3.33} = -2.97 \text{ kN}$$

Finally,  $P + H_A + H_C = 0$   
 $P = -1.44 + 2.97 = 1.53 \text{ kN (Ans)}$

**SETTLEMENT OF SUPPORTS MATHE (LOTTES, COVIC, KONG)**



EXTRA: Member DE has stiffness zero (ie no resistance to rotation). Thus bending moment at D is known and constant. That is, once equilibrium at D is assured there is no need for variation in the moment there and D can be treated as pinned! Thus CD has stiffness  $\frac{3EI}{12}$ . We could also take CD's stiffness as  $\frac{4EI}{12}$  but we would have 3 joints to keep on balancing.

	B		C		
A	1	2	3	4	D
1	0.33	0.67	0.67	0.33	1
2					
3					
4					
5					
6					
7					
8					
9					
10					
11					
12					
13					
14					
15					
16					
17					
18					
19					
20					
21					
22					
23					
24					
25					
26					
27					
28					
29					
30					
31					
32					
33					
34					
35					
36					
37					
38					
39					
40					
41					
42					
43					
44					
45					
46					
47					
48					
49					
50					
51					
52					
53					
54					
55					
56					
57					
58					
59					
60					
61					
62					
63					
64					
65					
66					
67					
68					
69					
70					
71					
72					
73					
74					
75					
76					
77					
78					
79					
80					
81					
82					
83					
84					
85					
86					
87					
88					
89					
90					
91					
92					
93					
94					
95					
96					
97					
98					
99					
100					

Write this! (note sign)

Balance D first.  $\rightarrow$  just kept!

Distribution factors only consider moment stiffnesses. No shear even in sway analysis

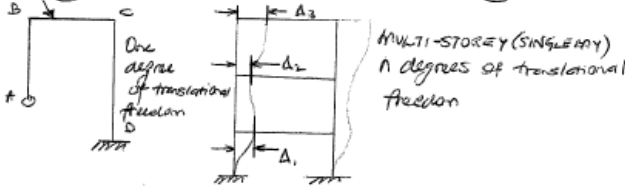
Now, during loading of the structure, supports may settle by small amounts. Since the reactive forces are most unlikely to be equal, the settlement of the various supports will differ, causing relative movement of the ends of a particular span. If the relative movement (or the overall movement for all supports as this will give relative movements) can be estimated, their effects can be included in the general analysis by increasing the apparent fixed end moments caused by the loads at the first stage of the distribution process. If the right of element settles,  $M = -\frac{6EI}{L^2}\Delta$  and if left of element settles then  $M = \frac{6EI}{L^2}\Delta$ . It is necessary therefore to know the modulus of elasticity E and the actual values of the settlement at area I before solution can be achieved.

The relative clockwise sinkage of AB:BC:CD is 1:1:2. For clockwise sinkage we use  $M = -\frac{6EI}{L^2}\Delta$ .

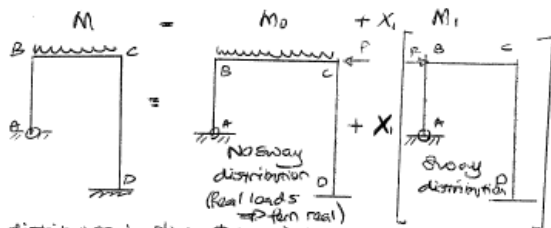
	B		C		
A	1	2	3	4	D
1	0.33	0.67	0.67	0.33	1
2					
3					
4					
5					
6					
7					
8					
9					
10					
11					
12					
13					
14					
15					
16					
17					
18					
19					
20					
21					
22					
23					
24					
25					
26					
27					
28					
29					
30					
31					
32					
33					
34					
35					
36					
37					
38					
39					
40					
41					
42					
43					
44					
45					
46					
47					
48					
49					
50					
51					
52					
53					

FRAMES IN WHICH SWAY OCCUR (i.e. NO LATERAL RESTRAINT)

Wanted that should relative movement of the ends of members occur, a knowledge of the numerical value of that movement was needed before analysis can be completed. In many frames, loading will imply some sideways movement which is unknown beforehand, and cannot be guessed since an error would mean some departure from the obvious equations of equilibrium. Only the case of a symmetrical structure with symmetrical vertical loading would not exhibit sway. This frame below will move to the right.



Solution of ABCD involves



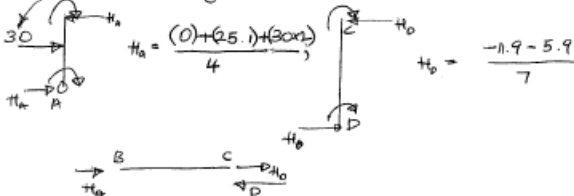
The distribution in which the existence of a propping force P, of unknown magnitude, prevents horizontal movement of the beam BC. Real loads apply and thus fixed-end-moments. The application of moment distribution method implies no translational movement exists and the use of the sway equation (i.e. method outlined earlier to obtain P) allows calculation of P & Xi. In the simple case of no lateral load as above  $P = Xi, F = Xi$  obtained.

	A	B	C	D	
	1	0.6	0.4	0.47	0.53
	441	441		144	144
	-441				
	0.0	-133	-88		-44
(kNm)	0	103	-103	-88	88
					115

ferm due to sway balance on ACB

③  $M = M_0 + X_1 M_1$ ; TO find  $X_1$  (This differs from @IC)

Look at equilibrium of no-sway and sway distribution diagrams for P and F respectively. Do not forget +ve's.

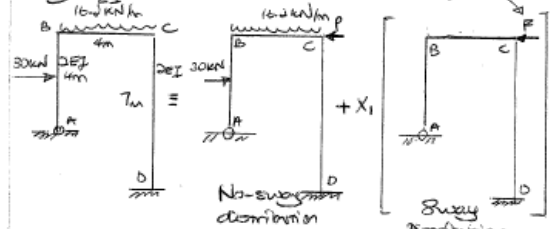


$P = H_D + H_A = 18.73$  KN in direction assumed.

Now for F,  $F = H_D + H_A = \frac{88+115}{7} + \frac{0+103}{4} = 54.75$  KN

Now for  $X_1$ , it must be such that  $P + X_1 F = 0 \Rightarrow X_1 = -\frac{18.73}{54.75} = -0.342$

This method is exactly the same as the method shown in this notes (Hobbs @ Imperial) only that the finding of  $X_1$  differs. Here the carry-over, Kory method is illustrated. Consider



$M_0 + X_1 M_1$   
 • real loads (then real)  
 • no-sway  
 • no real load  
 • then arbitrary from guess but  $M_{0C}$  must correspond to similar sway  $\delta$ .

①  $M_0$  distribution (Same as @IC)

	1	0.6	0.4	0.47	0.53	df
	-15	+15	-31.6	21.6		ferm ( $\frac{wL^2}{12}$ )
	15		7.5	-0.5		( $= \frac{wL}{8}$ )
						balance A (prod)
(kNm)	0.0	25.1	-25.1	11.9	-11.9	-5.9

②  $M_1$  distribution (same as @IC)  
 Arbitrary  $\delta$  that causes sway +441 kNm at A  
 $M_{AB} = -\frac{6(EI)}{L^2} \delta \Rightarrow \delta = \frac{588}{EI}$   
 $\Rightarrow M_{DC} = -\frac{6(EI)}{L^2} \delta + 144$  kNm

(continued)

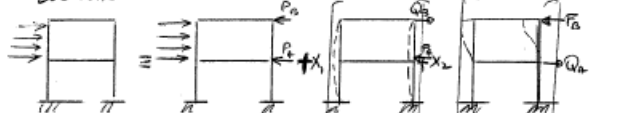
Thus final BMO obtainable from  $M = M_0 + X_1 M_1$

	A	B	C	D	
No-sway moments	0.0	25.1	-25.1	11.9	-11.9
$-0.342 \times X_1$ (sway moments)	0.0	-85.1	85.1	80.0	-80.0
Required solution ( $M = M_0 + X_1 M_1$ )	0.0	-10.0	10.0	41.9	-41.9

④ Sway  
 $\Delta = X_1 \delta = (-0.342) \left( -\frac{588}{EI} \right) = + \frac{201.096}{EI}$  (in direction assumed)

FRAMES WITH TWO OR MORE MODES OF SWAY

If the frame has 2 degrees of freedom, as in a 2-storey single-bay frame or in a single storey frame, the procedure is similar, but it must be realised that the no-sway distribution using the applied loads will imply in general the existence of two propping forces, the effect of which may only be determined by simultaneous equations.

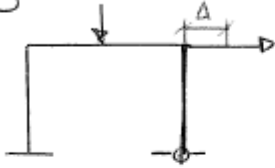


Separate independent sway modes indicated by dotted lines.  $P_a + F_a X_1 - Q_a X_2 = 0$  &  $P_b - Q_b X_1 + F_b X_2 = 0$   
 Similar procedure for frames with n degrees of freedom, where no. of distributions is (n+1) with n simultaneous equations.

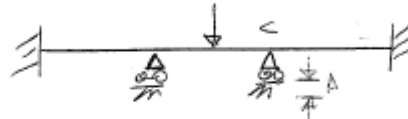
MD for SWAY cases (PROP. TOURS @FC)

'Sway' - active degrees of freedom include one (or more) translations.

Typically for one translation

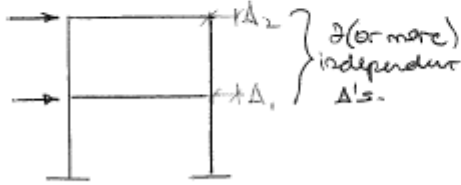


This frame sways

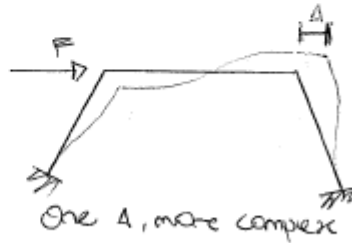


or (say) C settles a distance Δ.

More complex cases



2 (or more) independent Δ's.



One Δ, more complex

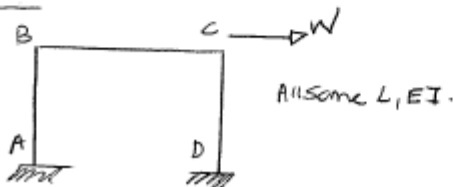
So for one simple sway degree of freedom... Kinematics.  
a 3 stage process (relies on superposition):

- 1) Make a standard MD analysis for the applied loads, ignoring any chance of sway; pursue right through to a BMD, say  $M_0$ .
- 2) Ignore the applied loads and make MD analysis of fixed end moments caused by an arbitrary sway,  $\delta$ . Again pursue through to a second BMD  $M_1$ .
- 3) Real BMD  $M$  is given by  $M_0$  plus a scaled version (factor  $X_1$ ) of  $M_1$ .

ie.  $M = M_0 + X_1 M_1$ , where  $X_1$  is found from equilibrium. (such as virtual work or summing column shears (Leaves, Costie, Kong) to match the applied loads).

Vector by-product:  $A = X_1 \delta$ . This is much faster than unit load method at sway this point of the game.

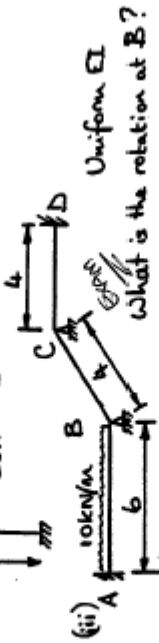
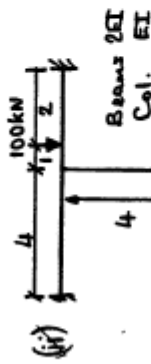
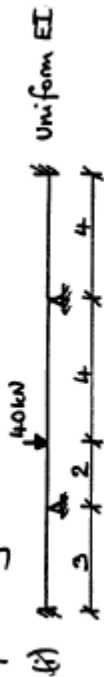
Example 1



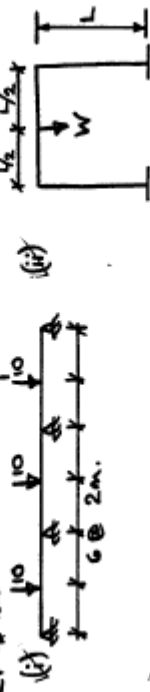


2C STRUCTURES - MOMENT DISTRIBUTION

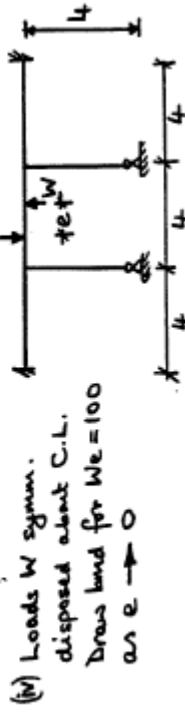
1. Draw the bending moment diagrams for the following structures.



2. Draw the b.m.d's for these structures.

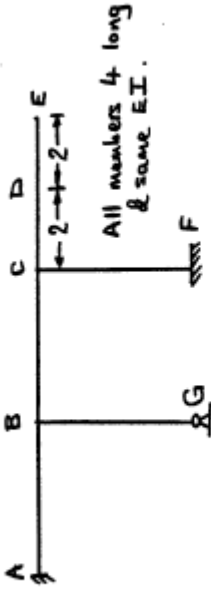


(iii) as (ii) except column bases pinned.

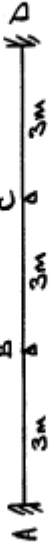


M.D SHEET page 2.

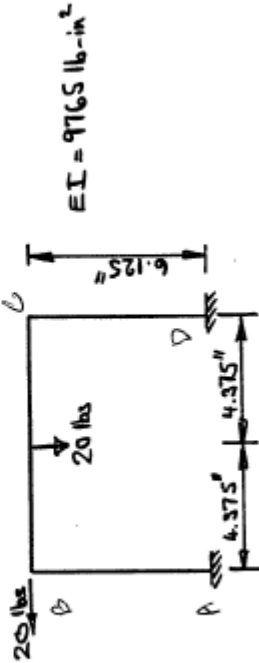
3 Draw the b.m. diagrams for this structure if  
(i) it carries 20 kN at D  
(ii) it carries a clockwise moment of 40 kN-m at B



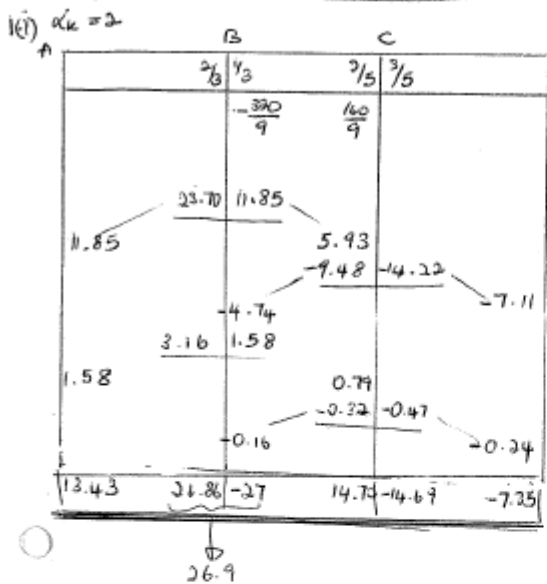
4 Draw the b.m.d for the beam ABCD when the support B sinks 10 mm.  
 $E = 207 \text{ kN/mm}^2$   $I = 8.0 \times 10^7 \text{ mm}^4$



(ii) Draw the b.m.d for this frame. What is the horizontal defn. of B? Use M.D.  
Hint The 1st distib. is symm. } and the 'special'  
The 2nd distib. is antisymm. } d.f's can be used.



MOMENT DISTRIBUTION MATE @ IMPERIAL COLLEGE.

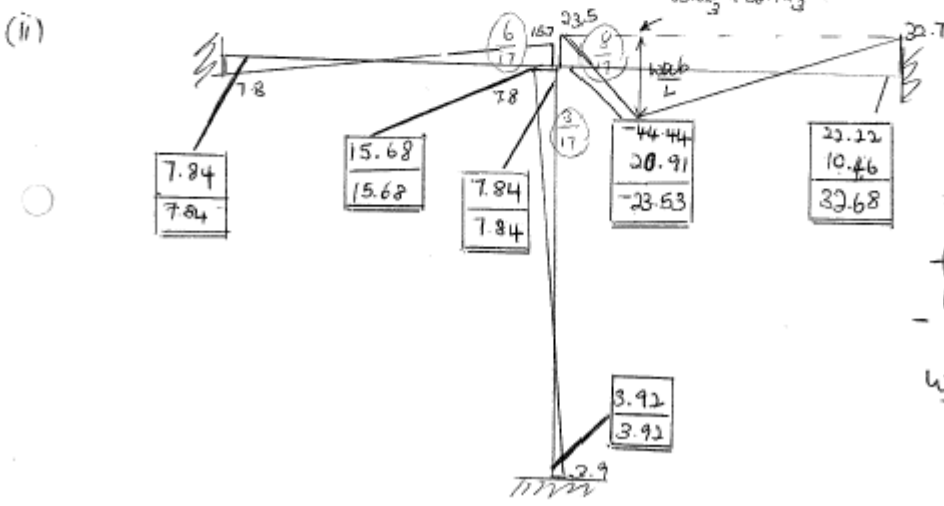
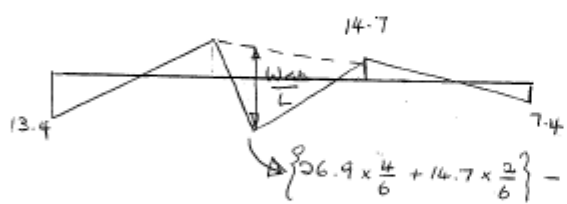


d.f.

$$\text{fem.} - \frac{Wab^2}{L^2} = \frac{(40)(2)(4)^2}{6^2} = -\frac{320}{9}$$

$$\text{and } + \frac{Wa^2b}{L^2} = \frac{(40)(2)^2(4)}{6^2} = \frac{160}{9}$$

taking s.d.p. Do not forget -ve signs when carrying over!



$$\frac{4(3EI)}{3} + \frac{4(3EI)}{4} + \frac{4(3EI)}{4}$$

$$= \frac{8}{17}$$

fem

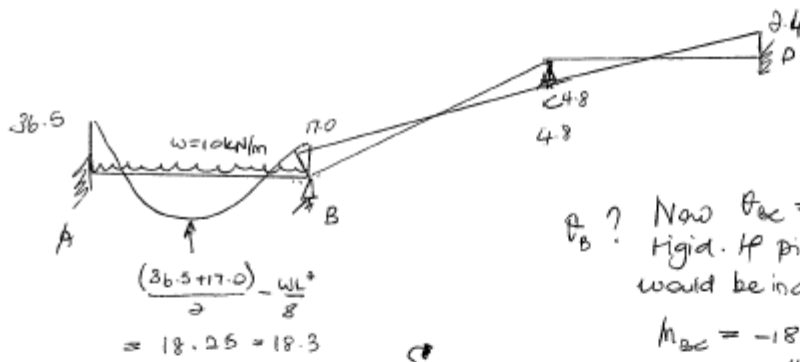
$$-\frac{Wab^2}{L^2} = -44.44$$

$$\frac{Wa^2b}{L^2} = 22.22$$

(ii)

	$\frac{2}{5}$	$\frac{3}{5}$	$\frac{1}{2}$	$\frac{1}{2}$	
-30	30	-18			
-6	-12		-9	4.5	
		3.25			2.25
-0.45	-0.9	1.35	-0.68	0.34	
		0.17	0.34	0.34	0.17
-36.45	17.1	-16.93	-4.54	4.54	2.42

d.f.  
 $fem = \frac{wL^2}{12} = 30$



$$\frac{(36.5 + 17.0) \cdot wL^2}{8} = 18.25 = 18.3$$

2(i) Symmetric of pin-ended.

$\theta_B$ ? Now  $\theta_{ac} = \theta_{ca}$  as joint is rigid. If pin-jointed, rotation would be independent.

$$M_{ac} = -18 - 1.35 = -19.35$$

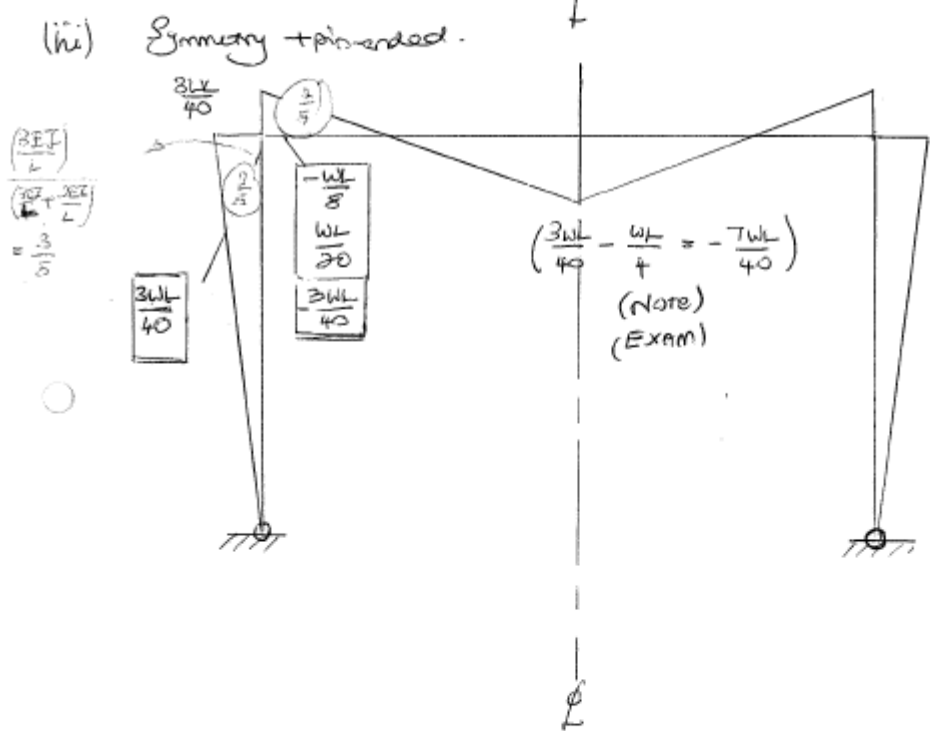
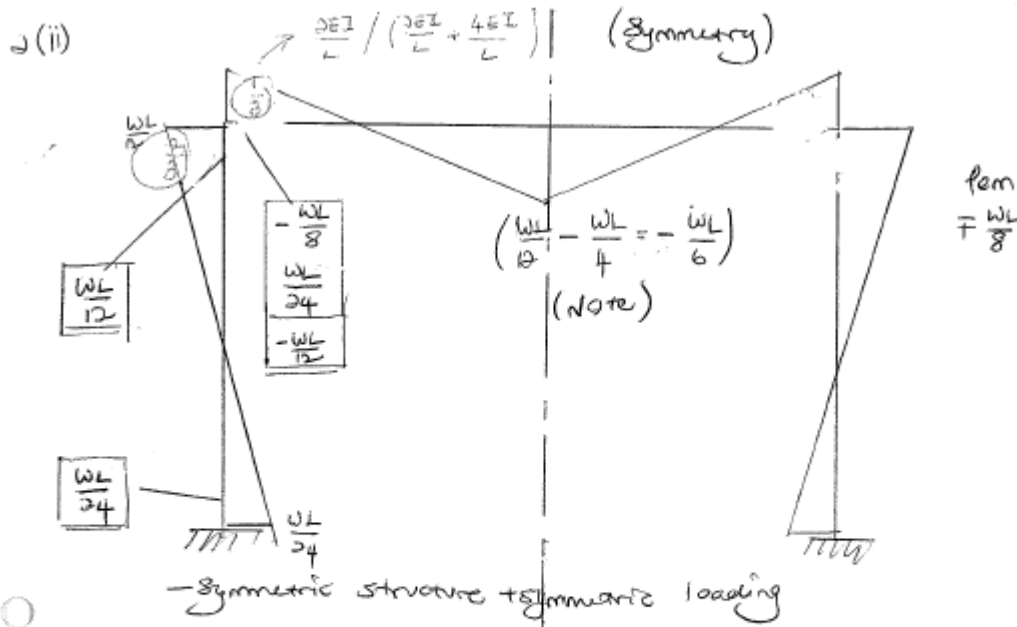
$$M_{ac} = \frac{4EI}{L} \theta_{ac}$$

$$\theta_B = \theta_{ac} = \frac{-19.35(4)}{4EI} = \frac{-19.4}{EI} \text{ (ANS)}$$

	$\frac{3EI}{4}$	$\frac{3EI}{4}$		
1	$\frac{5}{5}$	$\frac{2}{5}$		
-5	+5	-5		
5		2.5		
		-1.5	-1.0	0 c.o.
0	6	-6		

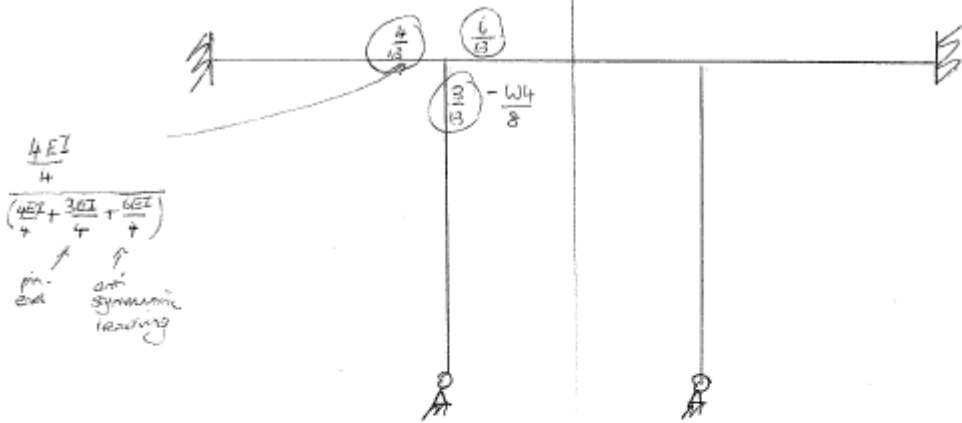
d.f.  $\theta_B$   
 $fem = \frac{wL}{8}$   
 $M_{eff} = -12.09 = -12.9$   
 $\theta_B = \theta_{eff} = \frac{-12.9(6)}{4EI} = -19.35/EI = -19.4 \text{ (ANS)}$



- Symmetric structure + symmetric loading
- Pin-ended.

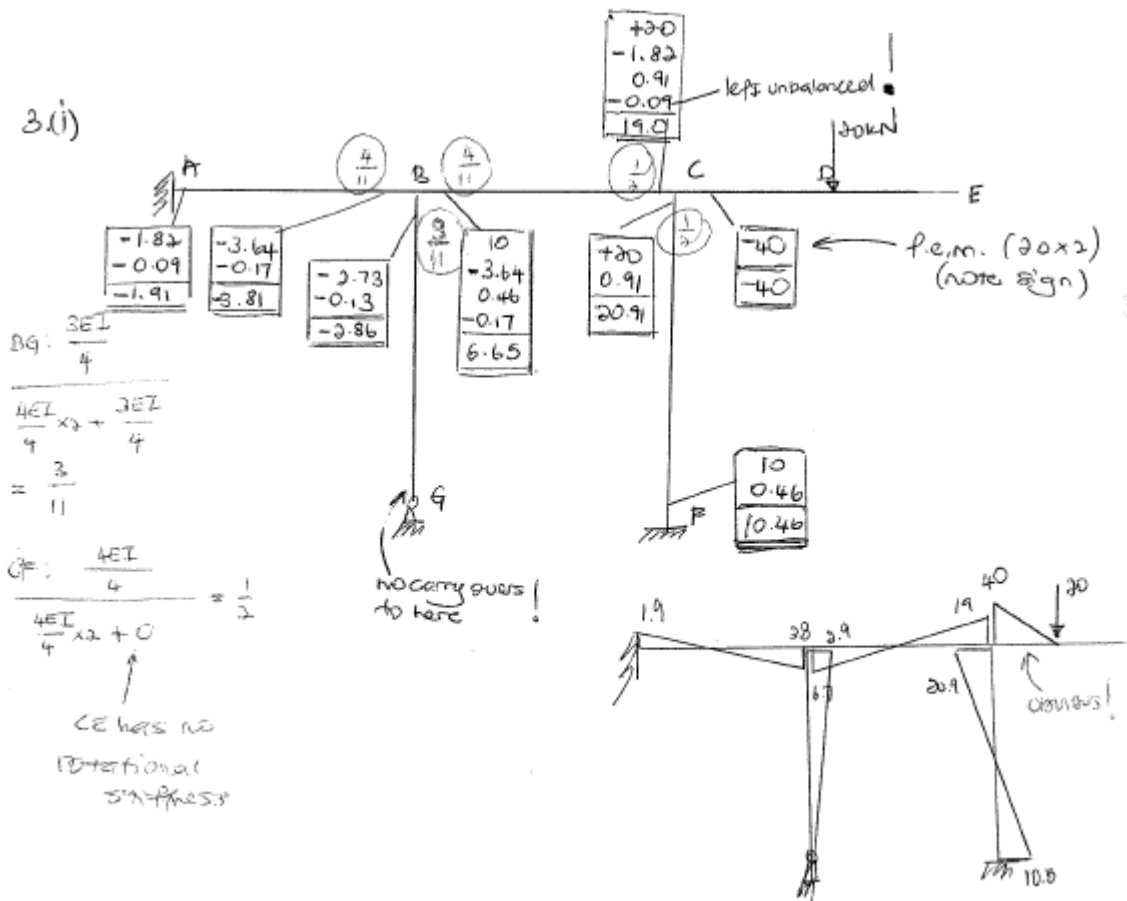
No sway in these questions as both loading + structure is symmetric

(iv)

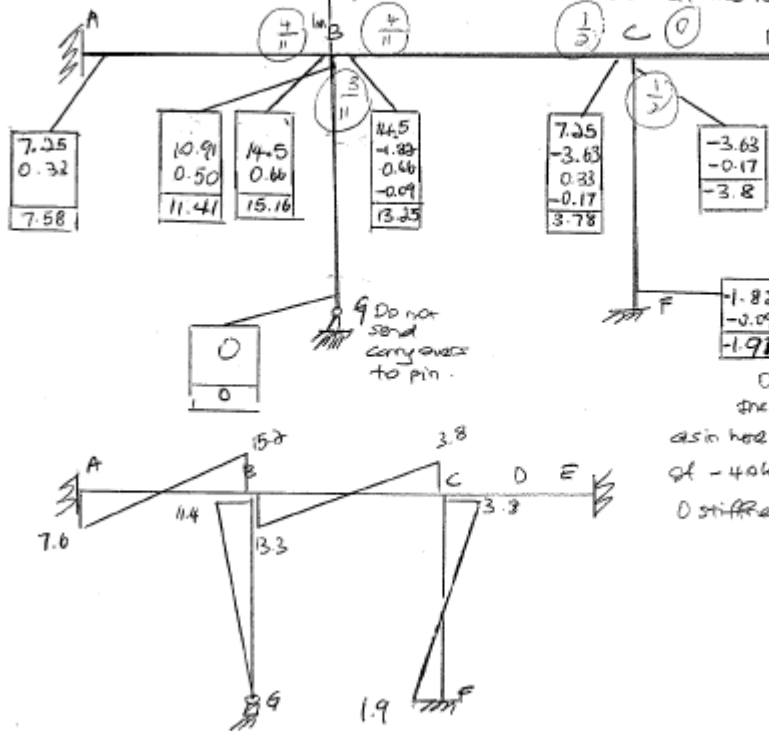


- symmetric structure, anti-symmetric loading  
- pin-end

3(i)

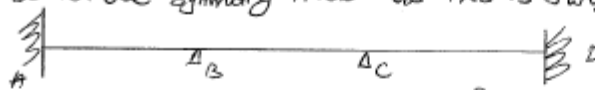


(ii) ... a clockwise moment of 40 kNm at B means <sup>40 kNm</sup> at a artificial in cantilever where stiffness is zero. Note that the reaction at B would then be -40 kNm.

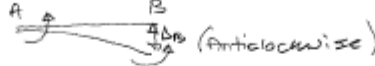


Also note that this number is not placed anywhere on the moment distribution table. If it was a cantilever (real) with a force on it, then we would put it on the nod. table on the cantilever joint towards the cantilever. But in moment case as in here we make a mental note of -40 kNm and distribute (ofcourse 0 stiffness => 0 df. at cantilever fixed)

4. (i) Do not use symmetry tricks as this is sway structure.



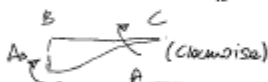
Support B sinks 10mm,



$$M_{AB} = M_{BA} = -\frac{6EI}{L^2} \Delta_B = -\frac{6EI}{3^2} (\Delta_B) = -\frac{6(207)(8 \times 10^7)}{(3000)^2} (10) \text{ All in kNm}$$

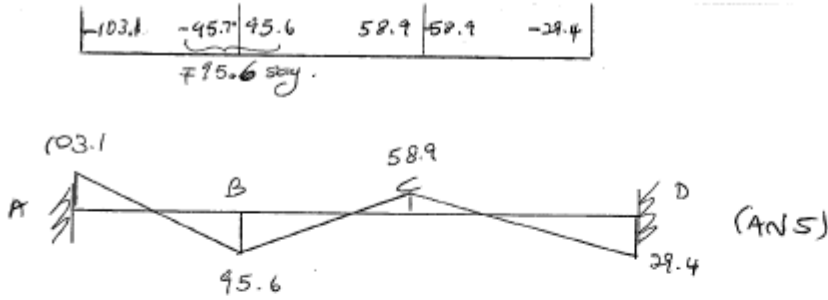
$$= -110400 \text{ kNm} = -110.4 \text{ kNm}$$

$$M_{BC} = M_{CB} = \frac{6EI}{L^2} \Delta_B = \frac{6(207)(8 \times 10^7)}{(3000)^2} (10) = 110.4 \text{ kNm}$$



	B	C	D
0.5	0.5	0.5	0.5
-110.4	-110.4	110.4	110.4
		-55.2	-55.2
	-37.6		
	13.8	13.8	
6.9		6.9	
		-3.45	-3.45
	-1.73		-1.73
0.44	0.87	0.87	
		0.44	
		-0.22	-0.22
	-0.11		-0.11

df.  
f.m (due to sway settlement)  
Balance C (as it is more an or balance).



4.(ii) Sway (Horizontal)

(a) First distribution (with real loads)  $M_0$  → Symmetric

$\frac{4EI}{6 \cdot 125}$	$\frac{6EI}{8 \cdot 75}$		
0.74	0.26		
	$-\frac{20(8.75)}{8} = -21.88$		
8.10	16.19	5.69	
8.10	16.19	-16.19	+16.19
			-8.10

d.f. fem. • Symmetric first distribution (no sway) even though 20 lbs at B is balanced by propping force probably. • 20 lbs does not contribute to term. (it contributes to external virtual work)

(b) Second distribution (without real loads)  $M_1$

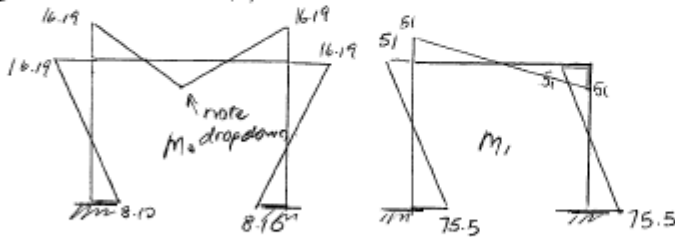
Assume  $\delta$  such that  $M_{AB} = M_{BA} = -\frac{6EI}{(6 \cdot 125)^2} \delta = 100$  i.e.  $\delta$  to right horizontally (virtual work)

Obviously  $M_{AC} = M_{CA} = M_{AD} = M_{DA} = 100$

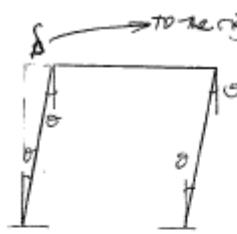
$\frac{4EI}{6 \cdot 125}$	$\frac{6EI}{8 \cdot 75}$		
0.49	0.51		
100	100		
-24.5	-49	-51	
75.5	51	-51	-51
			51
			75.5

d.f. fem. • asymmetric

(c)  $M = M_0 + X_1 M_1$



note the asymmetric graph



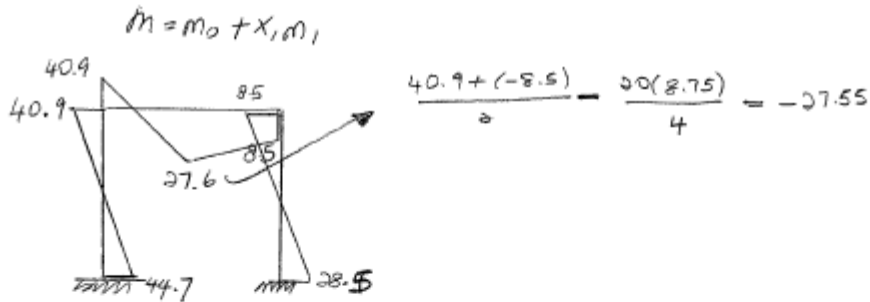
to the right as assumed earlier in  $M = -\frac{6EI\delta}{L^2}$

VW: Ext. Work = Internal Work.

$$\begin{aligned} \text{Internal Work} &= \theta \overset{\text{tensile outside}}{(-8.10 - x_1, 75.5)} + \theta \overset{\text{tensile inside}}{(-16.19 - x_1, 51)} \\ &\quad + \theta \overset{\text{tensile outside}}{(16.19 - x_1, 51)} + \theta \overset{\text{tensile inside}}{(8.10 - x_1, 75.5)} \\ &= \theta(-253 x_1) \end{aligned}$$

External Work =  $-20 \times \theta(6.125)$  (vertical force does not contribute)

$$\begin{aligned} \text{VW:} \quad -20 \times 6.125 &= -253 x_1 \\ x_1 &= 0.4842 \end{aligned}$$



d

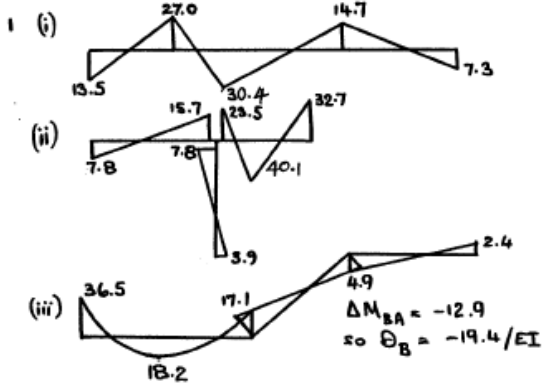
Deflection of B,  $\Delta_B = X_1 \delta = 0.4842 \times \delta = 0.4842 \times \frac{100 \times (6.125)^3}{6(9765)}$

$$= -0.031 \text{ inches.}$$

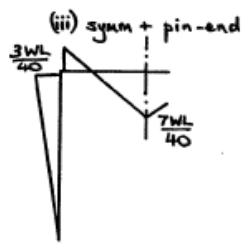
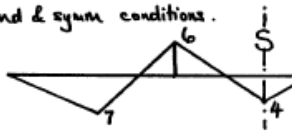
Thus deflection 0.031 inches to the left (i.e. opposite to original  $\delta$  assumption).

(3)

2C M.D. : ANSWERS



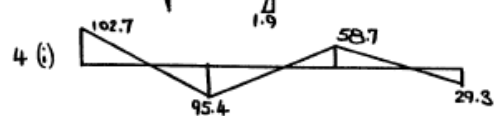
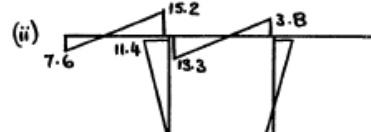
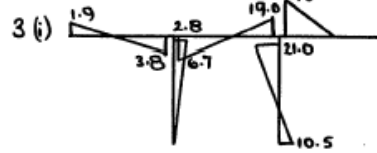
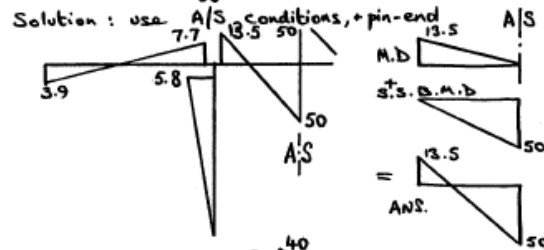
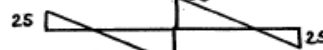
2 (i) pin-end & symm conditions.



(4)

ANSWERS CONT'D.

2 (iv) F.e. b.m.d as limiting case of 2 point loads:



(ii) This is the lab expt. again. Leading moments are 44.6, 40.9, 27.6, 8.5, 28.4 lb-in  
Defln. is 0.031"

EXAM  
 Recognize sway if there is translational kinematic.

Use moment distribution to obtain the bending moment diagram for the non-uniform beam shown in Fig. Q.4. (18 marks)

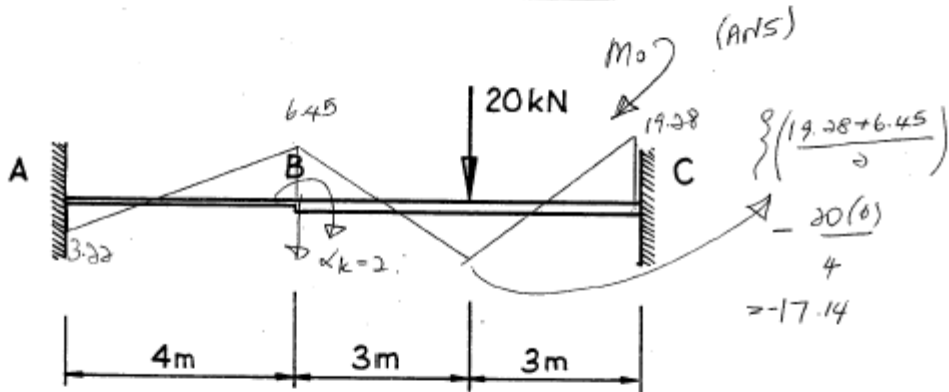
What is the deflection at B? (2 marks)

EI: AB  $16 \text{ MNm}^2$   
 BC  $32 \text{ MNm}^2$   
 $\frac{4(16 \times 10^3)}{4}$        $\frac{4(32 \times 10^3)}{6}$

First distribution (no sway)

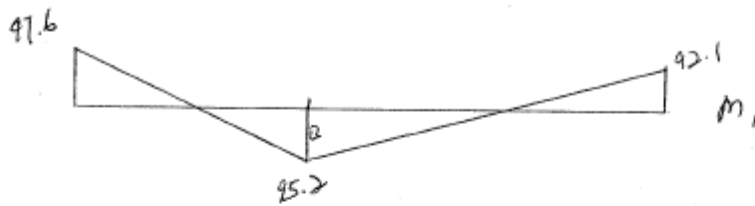
	0.43	0.57	
3.23	6.45	-15 8.55	115 4.28
3.23	6.45	-6.45	19.28

d.f.  
 fem ( $\frac{WL}{8}$ )



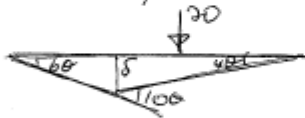
Sway.  
 Notice here we are not given deflection but need to find it. So not settlement method by frame sway analysis.  
 For  $M_{AB} = M_{BA} = -100 = -\frac{6(16 \times 10^3)}{4^2} \delta \Rightarrow \delta = 0.01666 \text{ m}$  ( $\delta$  downwards)  
 $\Rightarrow M_{BC} = M_{CB} = \frac{6(32 \times 10^3)}{6^2} \delta = 88.89 \text{ kNm}$ .  
 Fig. Q.4

	0.43	0.57	d.f.
-100	-100	88.89	88.89 fem
2.89	4.78	6.33	3.17
-97.61	-95.22	95.22	92.06



$$M = M_0 + X_1 M_1$$

To obtain  $X_1$ ,



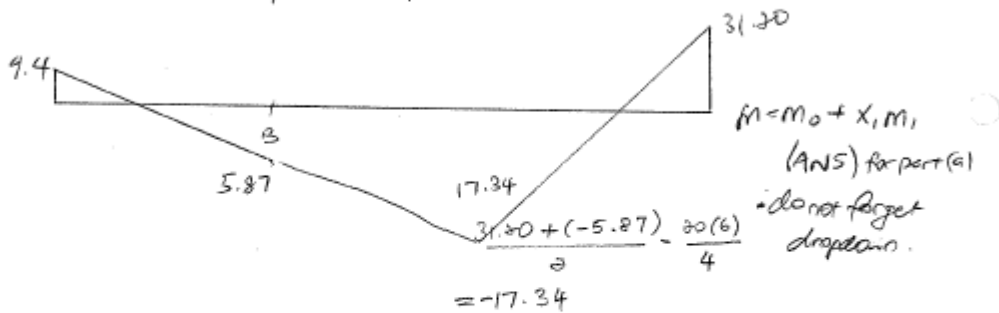
$$\begin{aligned} \text{Internal Work} &= 60(-3.22 + X_1 97.6) + 40(19.28 + X_1 92.1) \\ &\quad + 100(-6.45 + X_1 95.2) \leftarrow \text{Remember.} \\ &= 0(-6.7 + 1906X_1) \end{aligned}$$

$$\text{External work} = 20(3 \times 40) = -2400$$

VW: External Work = Internal Work

$$-6.7 + 1906X_1 = 2400$$

$$X_1 = 0.1294 \text{ (ANS)}$$



(b)

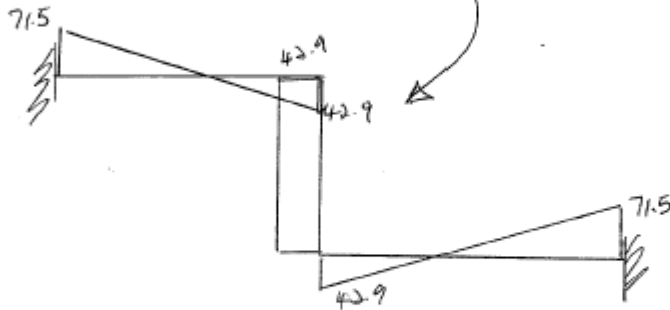
$$\begin{aligned} \text{Actual vertical deflection of B, } \Delta_B &= X_1 \delta_B = 0.1294 \times 0.01666666 \\ &= 2.1566 \times 10^{-3} \text{ m} \\ &= 2.16 \text{ mm (ANS)} \end{aligned}$$



0.7	1.4	0.1	1.1	-0.4	
		-0.3	-0.7		-0.2
-71.5	42.9	42.9	-42.9	42.9	71.5

Carry-over

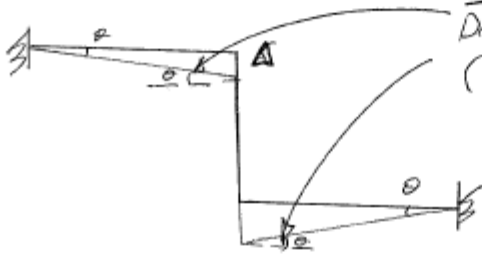
7 42.9  
 take because ...



c)  $M = m_0 + X_1 m_1$

To obtain  $X_1$ ,

EXAM! Imp!  
 DO NOT FORGET  
 (Consider all joints)

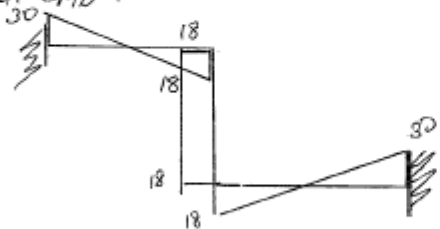


VW: Internal Work = External Work

$$\left\{ \theta(71.5x_1) + \theta(71.5x_1) \right\} + \theta(42.9x_1) + \theta(42.9x_1) = 16 \times \theta \times 6$$

$x_1 = 0.420$

Final BMD



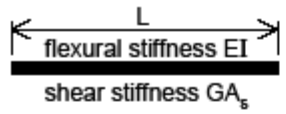
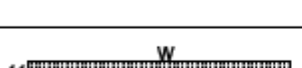
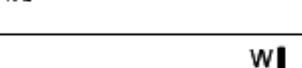
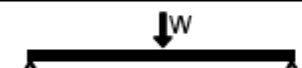
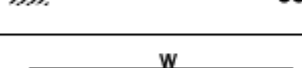
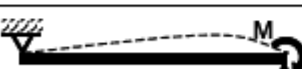
(ANS)

Deflection of B,  $\delta_B = X_1 \times \Delta_0 = 0.42 \times 0.03 = 0.0126m$   
 $= 12.6mm$  (ANS).

3.1.6.5 Summary of Deflections and Effects

Hand calculations

Effect of shear deformations on bending moments, shear forces and displacements

	Flexural		Shear		
	End deflection	End slope and rotation of cross-section	End deflection	End slope	End rotation of cross-section
	$\frac{ML^2}{2EI}$	$\frac{ML}{EI}$	0	0	0
	$\frac{WL^3}{3EI}$	$\frac{WL^2}{2EI}$	$\frac{WL}{GA_s}$	$\frac{W}{GA_s}$	0
	$\frac{wL^4}{8EI}$	$\frac{wL^3}{6EI}$	$\frac{wL^2}{2GA_s}$	$\frac{wL}{GA_s}$	0
	$\frac{WL^3}{12EI}$	0	$\frac{WL}{GA_s}$	$\frac{W}{GA_s}$	0
	Mid-span deflection	End slope and rotation of cross-section	Mid-span deflection	End slope	End rotation of cross-section
	$\frac{WL^3}{48EI}$	$\frac{WL^2}{16EI}$	$\frac{WL}{4GA_s}$	$\frac{W}{2GA_s}$	0
	$\frac{5wL^4}{384EI}$	$\frac{wL^3}{24EI}$	$\frac{wL^2}{8GA_s}$	$\frac{wL}{2GA_s}$	0
	$\frac{ML^2}{8EI}$	$\frac{ML}{2EI}$	0	0	0
	$\frac{ML^2}{16EI}$	L	$\frac{ML}{6EI}$	0	$\frac{-M}{LGA_s}$
		R	$\frac{ML}{3EI}$		
	$\frac{ML^2}{32EI}$	L	0	$\frac{9M}{32(1+3k)GA_s}$	$\frac{3M}{2(1+3k)LGA_s}$
$M_0 = \frac{M(1-6k)}{2(1+3k)}$ ; $k = \frac{EI}{L^2GA_s}$		R	$\frac{ML}{4EI}$		$\frac{3M}{4(1+3k)LGA_s}$

Support moments and displacements can be calculated by hand using the formulae given. Consider, for example, a propped cantilever loaded with a uniformly distributed load. If the beam were simply supported, the end rotation would be  $\frac{wL^3}{24EI}$ . If the cross-section is supported in such a way that it cannot rotate at the support, the end rotation from the end moment,  $M_0$ , must be such as to counteract this end rotation. Therefore  $M_0 \left( \frac{L}{3EI} + \frac{1}{LGA_s} \right) = \frac{wL^3}{24EI}$ , giving

$$M_0 = \frac{\frac{wL^3}{24EI}}{\frac{L}{3EI} + \frac{1}{LGA_s}} = \frac{wL^2}{8(1+3k)}, \text{ where } k = \frac{EI}{L^2GA_s}, \text{ which tends to } \frac{wL^2}{8} \text{ as shear deformations}$$

become insignificant. The mid-span deflection is given by,  $\frac{5wL^4}{384EI} + \frac{wL^2}{8GA_s} - \frac{M_0L^2}{16EI}$ , equal to

$$\frac{wL^4}{192EI} + \frac{wL^2}{128GA_s} \left( \frac{19+48k}{1+3k} \right), \text{ which tends to } \frac{wL^4}{192EI} \text{ as shear deformations become insignificant.}$$

Note that the slope of the beam at the support,  $\frac{wL^3}{24EI} + \frac{wL}{GA_s} - \frac{M_0L}{3EI}$ , is not zero but equals

$$\frac{wL}{8GA_s} \left( \frac{5+12k}{1+3k} \right).$$

CANTILEVERS	
LOADING	
MOMENT	$M_x = \frac{Wx^2}{2a}$ $M_{max} = \frac{Wa}{2}$
SHEAR	$R_A = W$
DEFLECTION	$d_C = \frac{Wa^3}{8EI}$ $d_{max} = \frac{Wa^3}{8EI} \left(1 + \frac{4b}{3a}\right)$
LOADING	
MOMENT	$M_{max} = W\left(a + \frac{b}{2}\right)$ $M_x = \frac{Wx^3}{3a^2}$ $M_A = \frac{Wa}{3}$
SHEAR	$R_A = W$
DEFLECTION	$d_C = \frac{Wa^3}{15EI}$ $d_{max} = \frac{Wa^3}{15EI} \left(1 + \frac{5b}{4a}\right)$
LOADING	
MOMENT	$M_{max} = W\left(a + \frac{b}{2}\right)$ $M_x = \frac{Wx^3}{3a^2}$ $M_A = \frac{Wa}{3}$
SHEAR	$R_A = W$
DEFLECTION	$d_{max} = \frac{W}{24EI} x$ $(8a^4 + 8a^2b + 12ab^2 + 3b^3 + 12a^2c + 12abc + 4b^2c)$

		CANTILEVERS	
LOADING			
	MOMENT		
		$M_x = \frac{Wa}{3} \left[ \left(\frac{x}{a}\right)^3 - \frac{3x}{a} + 2 \right]$	$M_{max} = W \left( a + \frac{2b}{3} \right)$
	SHEAR		
$R_A = W$		$R_A = W$	
DEFLECTION			
	$d_c = \frac{11Wa^3}{60EI}$ $d_{max} = \frac{11Wa^3}{60EI} \left( 1 + \frac{15b}{11a} \right)$	$d_{max} = \frac{W(20a^3 + 50a^2b + 40ab^2 + 11b^3)}{60EI}$	
LOADING			
	MOMENT		
		$M_x = P \cdot x$ $M_{max} = P \cdot a$	$M_{max} = M_x = M_c$
	SHEAR		<p style="text-align: center;">No shears</p>
$R_A = P$			
DEFLECTION			
	$d_c = \frac{Pa^3}{3EI}$ $d_{max} = \frac{Pa^3}{3EI} \left( 1 + \frac{3b}{2a} \right)$	$d_c = \frac{M \cdot a^2}{2EI}$ $d_{max} = \frac{M \cdot a^2}{2EI} \left( 1 + \frac{2b}{a} \right)$	

N.B. For anti-clockwise moments the deflection is upwards.

SIMPLY SUPPORTED BEAMS	
LOADING	
MOMENT	$M_x = \frac{Wx}{2} \left(1 - \frac{x}{L}\right)$ $M_{max} = \frac{WL}{8}$
SHEAR	$R_A = R_B = \frac{W}{2}$
DEFLECTION	$d_{max} = \frac{5}{384} \cdot \frac{WL^3}{EI}$
LOADING	
MOMENT	$M_{max} = \frac{Wa}{4}$
SHEAR	$R_A = R_B = \frac{W}{2}$
DEFLECTION	$d_{max} = \frac{Wa(3L^2 - 2a^2)}{96EI}$
LOADING	
MOMENT	$M_{max} = \frac{W}{b} \left( \frac{x_1^2 - a^2}{2} \right)$ <p>when <math>x_1 = a + \frac{Rab}{W}</math></p>
SHEAR	$R_A = \frac{W}{L} \left( \frac{b}{2} + c \right)$ $R_B = \frac{W}{L} \left( \frac{b}{2} + a \right)$
DEFLECTION	<p>When <math>a = c</math></p> $d_{max} = \frac{W}{384EI} (8L^3 - 4Lb^2 + b^3)$
LOADING	
MOMENT	$M_{max} = \frac{Wa}{2} \left(1 - \frac{a}{2L}\right)^2$ <p>when <math>x_1 = a \left(1 - \frac{a}{2L}\right)</math></p>
SHEAR	$R_A = W \left(1 - \frac{a}{2L}\right)$ $R_B = \frac{Wa}{2L}$
DEFLECTION	<p>When <math>x &lt; a</math>,</p> $d = \frac{WL^4}{24aEI} [m^4 - 2n(2-n)m^2 + n^2(2-n)^2m]$ <p>When <math>x &gt; a</math>,</p> $d = \frac{WL^4}{24aEI} n^2 [2m^3 - 6m^2 + m(4+n^2) - n^2]$ <p>where <math>m = x/L</math> and <math>n = a/L</math></p>

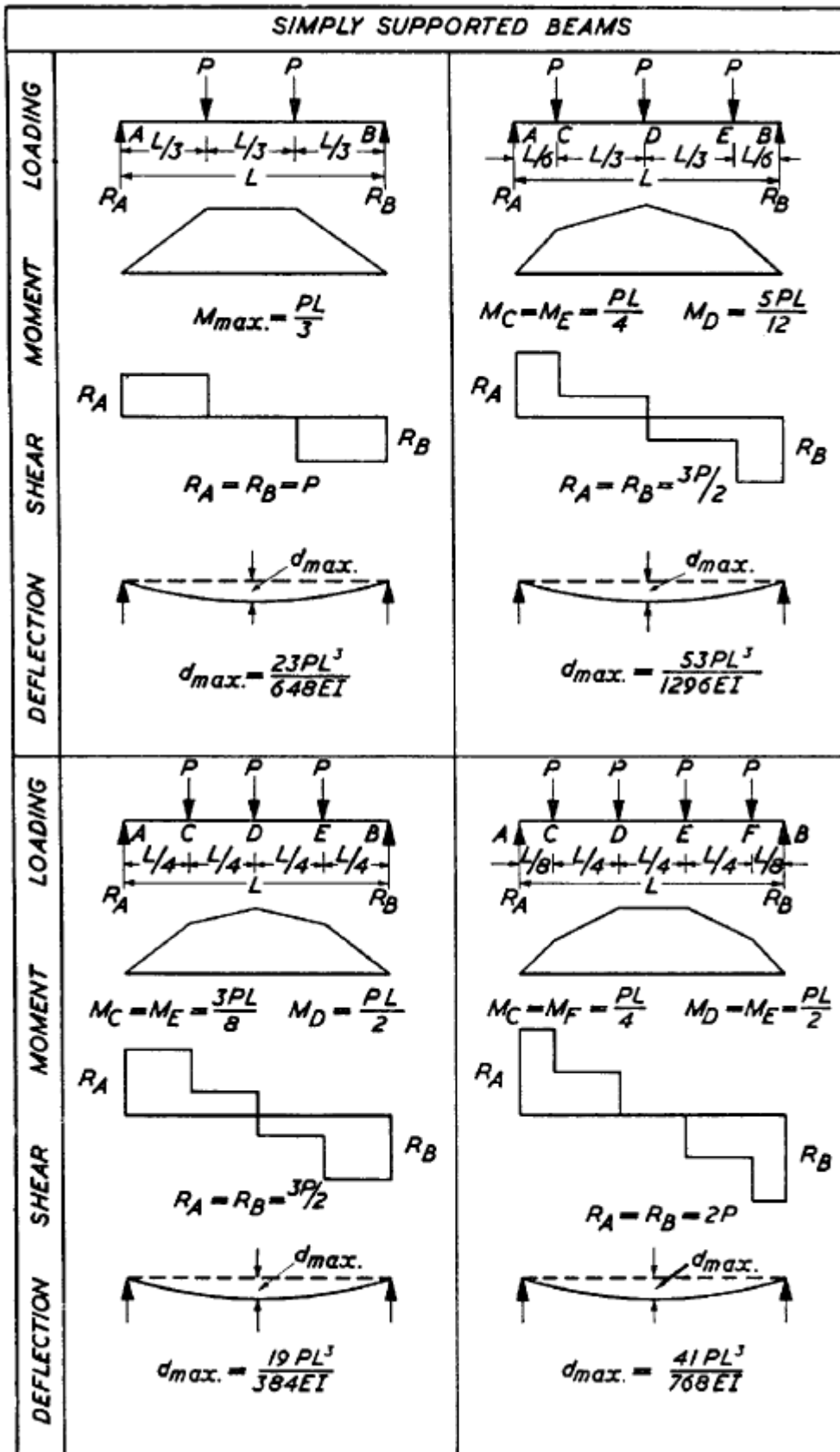
SIMPLY SUPPORTED BEAMS	
LOADING	
MOMENT	$M_x = \frac{Wx}{3} \left( 1 - \frac{x^2}{L^2} \right)$ $M_{max.} = 0.128WL$ <p>when <math>x_1 = 0.5774L</math></p>
SHEAR	$R_A = W/3$ $R_B = 2W/3$
DEFLECTION	$d_{max.} = \frac{0.01304WL^3}{EI}$ <p>when <math>x = 0.5193L</math></p>
LOADING	
MOMENT	$M_x = Wx \left( \frac{1}{2} - \frac{x}{L} + \frac{2x^2}{3L^2} \right)$ $M_{max.} = WL/12$
SHEAR	$R_A = R_B = W/2$
DEFLECTION	$d_{max.} = \frac{3WL^3}{320EI}$
LOADING	
MOMENT	$M_{max.} = \frac{W}{4} \left( L - \frac{b}{3} \right)$
SHEAR	$R_A = R_B = W/2$
DEFLECTION	$d_{max.} = \frac{W}{480EI} (8L^3 + 7aL^2 - 4a^2L - 4a^3)$

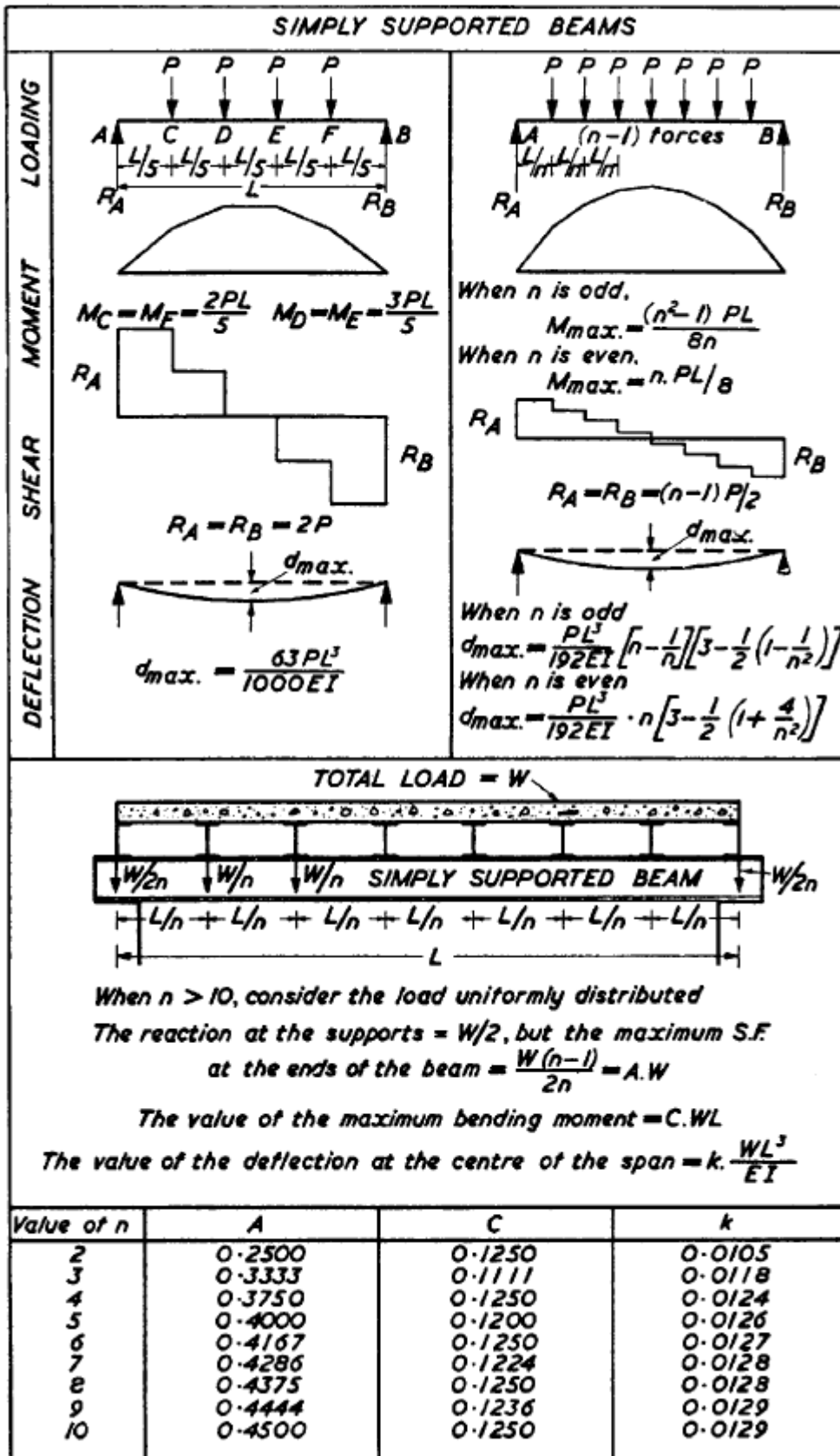
SIMPLY SUPPORTED BEAMS	
LOADING	
MOMENT	<p style="text-align: center;"><math>M_{max.} = \frac{Wa}{6}</math></p>
SHEAR	<p style="text-align: center;"><math>R_A = R_B = W/2</math></p>
DEFLECTION	<p style="text-align: center;"><math>d_{max.} = \frac{Wa}{240EI} (18a^2 + 20ab + 5b^2)</math></p>
LOADING	
MOMENT	<p style="text-align: center;"><math>m = a/L</math></p> <p style="text-align: center;"><math>M_{max.} = \frac{Wa}{3} (1 - m + \frac{2m}{3} \sqrt{\frac{m}{3}})</math></p> <p style="text-align: center;">when <math>x = a(1 - \sqrt{\frac{m}{3}})</math></p>
SHEAR	<p style="text-align: center;"><math>R_A = W(1 - \frac{m}{3})</math></p> <p style="text-align: center;"><math>R_B = \frac{Wm}{3}</math></p>
DEFLECTION	<p style="text-align: center;">—</p>
LOADING	
MOMENT	<p style="text-align: center;"><math>M_{max.} = \frac{Wa}{3}</math></p>
SHEAR	<p style="text-align: center;"><math>R_A = R_B = W/2</math></p>
DEFLECTION	<p style="text-align: center;"><math>d_{max.} = \frac{Wa}{120EI} (16a^2 + 20ab + 5b^2)</math></p>
LOADING	
MOMENT	<p style="text-align: center;"><math>M_{max.} = \frac{2Wa}{3} (1 - \frac{2m}{3})^{3/2}</math></p> <p style="text-align: center;">when <math>x = a\sqrt{1 - \frac{2m}{3}}</math></p>
SHEAR	<p style="text-align: center;"><math>R_A = W(1 - \frac{2m}{3})</math></p> <p style="text-align: center;"><math>R_B = \frac{2Wm}{3}</math></p>
DEFLECTION	<p style="text-align: center;">—</p>

SIMPLY SUPPORTED BEAMS	
LOADING	
MOMENT	$M_x = \frac{Wx}{3} \left( 1 - \frac{x^2}{L^2} \right)$ $M_{max.} = 0.128WL$ <p>when <math>x_1 = 0.5774L</math></p>
SHEAR	$R_A = W/3$ $R_B = 2W/3$
DEFLECTION	$d_{max.} = \frac{0.01304WL^3}{EI}$ <p>when <math>x = 0.5193L</math></p>
LOADING	
MOMENT	$M_{max.} = \frac{W}{4} \left( L - \frac{b}{3} \right)$
SHEAR	$R_A = R_B = W/2$
DEFLECTION	$d_{max.} = \frac{W}{480EI} (8L^3 + 7aL^2 - 4a^2L - 4a^3)$
LOADING	
MOMENT	$M_x = Wx \left( \frac{1}{2} - \frac{x}{L} + \frac{2x^2}{3L^2} \right)$ $M_{max.} = WL/12$
SHEAR	$R_A = R_B = \frac{W}{2}$
DEFLECTION	$d_{max.} = \frac{3WL^3}{320EI}$

SIMPLY SUPPORTED BEAMS	
LOADING	
MOMENT	$M_{max.} = \frac{Wa}{6}$
SHEAR	$R_A = R_B = W/2$
DEFLECTION	$d_{max.} = \frac{Wa}{240EI} (18a^2 + 20ab + 5b^2)$
LOADING	
MOMENT	$M_{max.} = \frac{Wa}{3} \left( 1 - m + \frac{2m}{3} \sqrt{\frac{m}{3}} \right)$ <p>when <math>x = a \left( 1 - \sqrt{\frac{m}{3}} \right)</math></p>
SHEAR	$R_A = W \left( 1 - \frac{m}{3} \right)$ $R_B = \frac{Wm}{3}$
DEFLECTION	<p>—</p>
LOADING	
MOMENT	$M_{max.} = \frac{Wa}{3}$
SHEAR	$R_A = R_B = W/2$
DEFLECTION	$d_{max.} = \frac{Wa}{120EI} (16a^2 + 20ab + 5b^2)$
LOADING	
MOMENT	$M_{max.} = \frac{2Wa}{3} \left( 1 - \frac{2m}{3} \right)^{3/2}$ <p>when <math>x = a \sqrt{1 - \frac{2m}{3}}</math></p>
SHEAR	$R_A = W \left( 1 - \frac{2m}{3} \right)$ $R_B = \frac{2Wm}{3}$
DEFLECTION	<p>—</p>

SIMPLY SUPPORTED BEAMS	
LOADING	
MOMENT	$M_{max.} = \frac{PL}{4}$
SHEAR	$R_A = R_B = \frac{P}{2}$
DEFLECTION	$d_{max.} = \frac{PL^3}{48EI}$
LOADING	
MOMENT	$M_{max.} = Pa$
SHEAR	$R_A = R_B = P$
DEFLECTION	$d_{max.} = \frac{PL^3}{6EI} \left[ \frac{3a}{4L} - \left(\frac{a}{L}\right)^3 \right]$
LOADING	
MOMENT	$M_{max.} = \frac{Pab}{L}$
SHEAR	$R_A = \frac{Pb}{L} \quad R_B = \frac{Pa}{L}$
DEFLECTION	<p><i>d<sub>max.</sub> always occurs within 0.074L of the centre of the beam. When <math>b \geq a</math>,</i></p> $d_{centre} = \frac{PL^3}{48EI} \left[ \frac{3a}{L} - 4\left(\frac{a}{L}\right)^3 \right]$ <p><i>This value is always within 2.5% of the maximum value.</i></p>
LOADING	
MOMENT	$M_C = \frac{Pa(b+2c)}{L}$ $M_D = \frac{Pc(b+2a)}{L}$
SHEAR	$R_A = \frac{P(b+2c)}{L}$ $R_B = \frac{P(b+2a)}{L}$
DEFLECTION	<p><i>For central deflection add the values for each P derived from the formula in the adjacent diagram.</i></p>

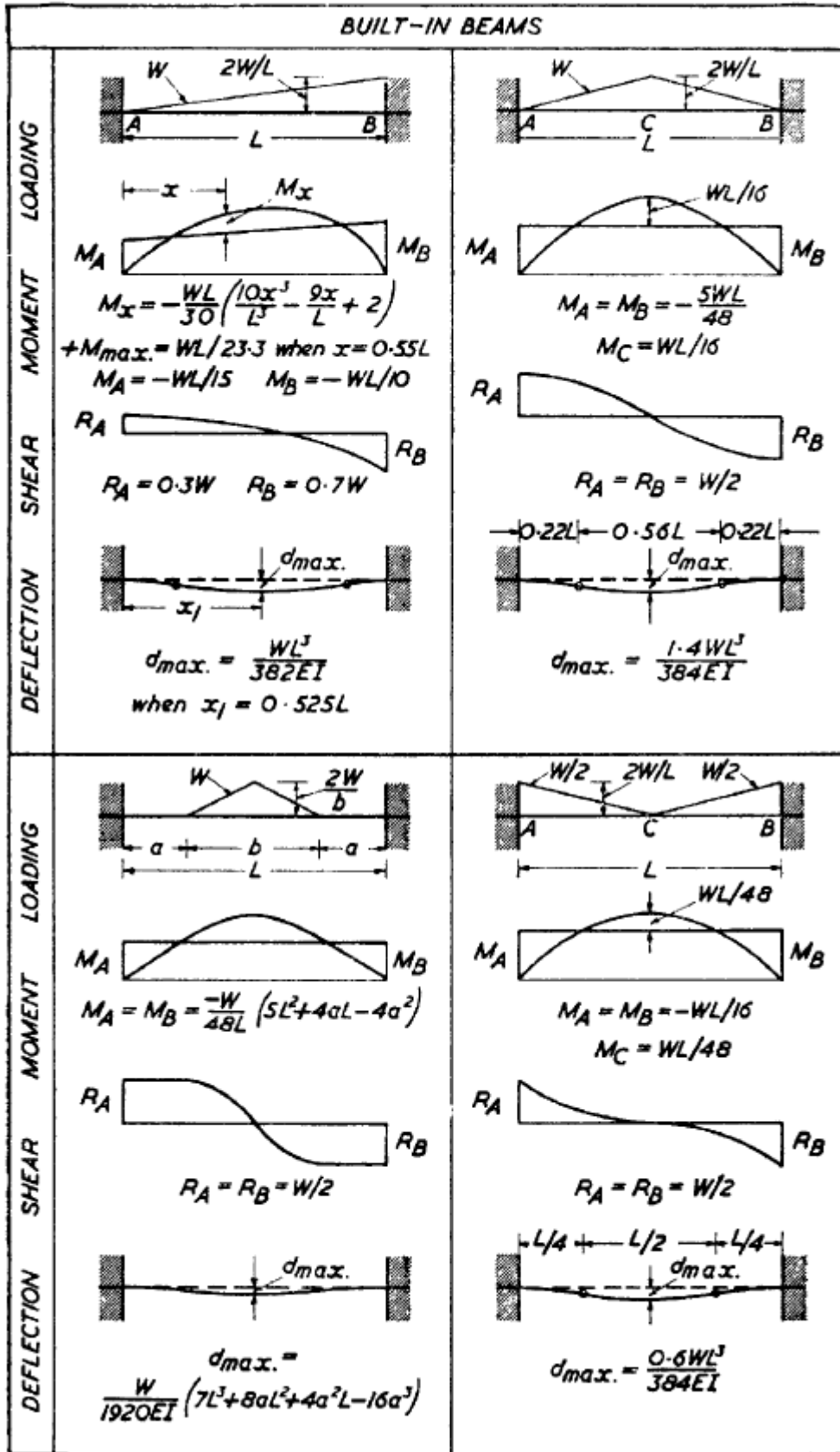




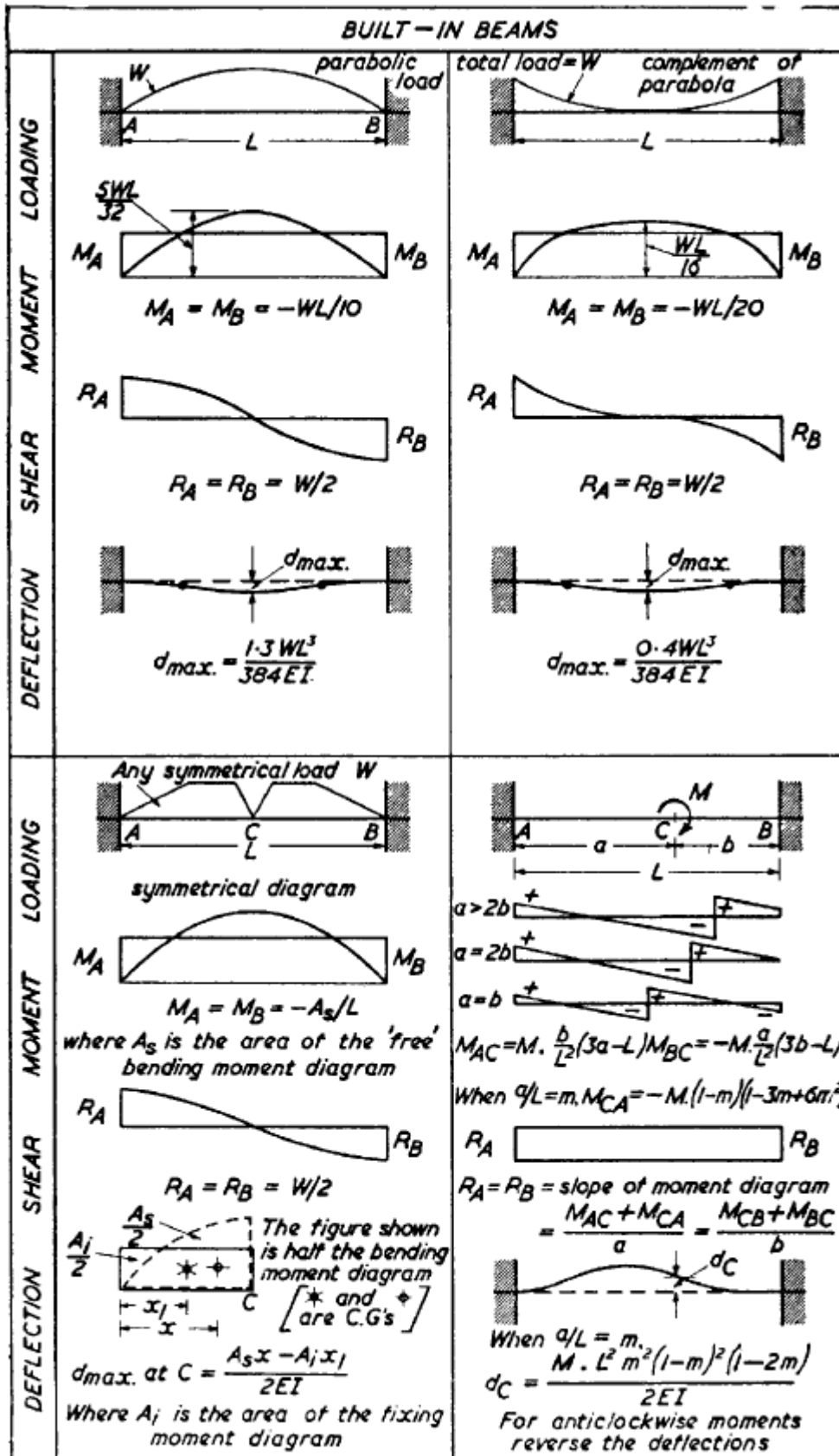
SIMPLY SUPPORTED BEAMS	
LOADING	
MOMENT	<p> <math>M_{CA} = M \cdot a/L</math>   <math>M_{CB} = M \cdot b/L</math> </p>
SHEAR	<p> <math>R_A = R_B = M/L</math> </p>
DEFLECTION	<p> <math>d_C = \frac{M \cdot ab}{3EI} \left( \frac{a}{L} - \frac{b}{L} \right)</math> </p> <p>As shown <math>a &gt; b</math>.</p> <p>For anti-clockwise moments the deflections are reversed.</p>
LOADING	
MOMENT	<p> <math>M_A = M_B</math>  <math>M_A &gt; M_B</math>  <math>M_A &gt; -M_B</math> </p> <p>(<math>M_B</math> anti-clockwise)  <math>-M_B</math> </p>
SHEAR	<p> <math>R_A = -R_B = \frac{M_A - M_B}{L}</math> </p>
DEFLECTION	<p>When <math>M_A = M_B</math>.</p> <p> <math>d_{max} = -\frac{ML^2}{8EI}</math> </p>
LOADING	<p>2nd degree parabola. <math>W</math></p>
MOMENT	<p> <math>M_x = \frac{WL}{2} (m^4 - 2m^3 + m)</math>  <math>M_{max} = \frac{5WL}{32}</math> </p>
SHEAR	<p> <math>R_A = R_B = W/2</math> </p>
DEFLECTION	<p> <math>d_{max} = \frac{6 \cdot 1WL^3}{384EI}</math> </p>
LOADING	<p>Complement of parabola. Total load = <math>W</math></p>
MOMENT	<p> <math>M_x = \frac{WL}{2} (m - 3m^2 + 4m^3 - 2m^4)</math>  <math>M_{max} = \frac{WL}{16}</math> </p>
SHEAR	<p> <math>R_A = R_B = W/2</math> </p>
DEFLECTION	<p> <math>d_{max} = \frac{2 \cdot 8WL^3}{384EI}</math> </p>

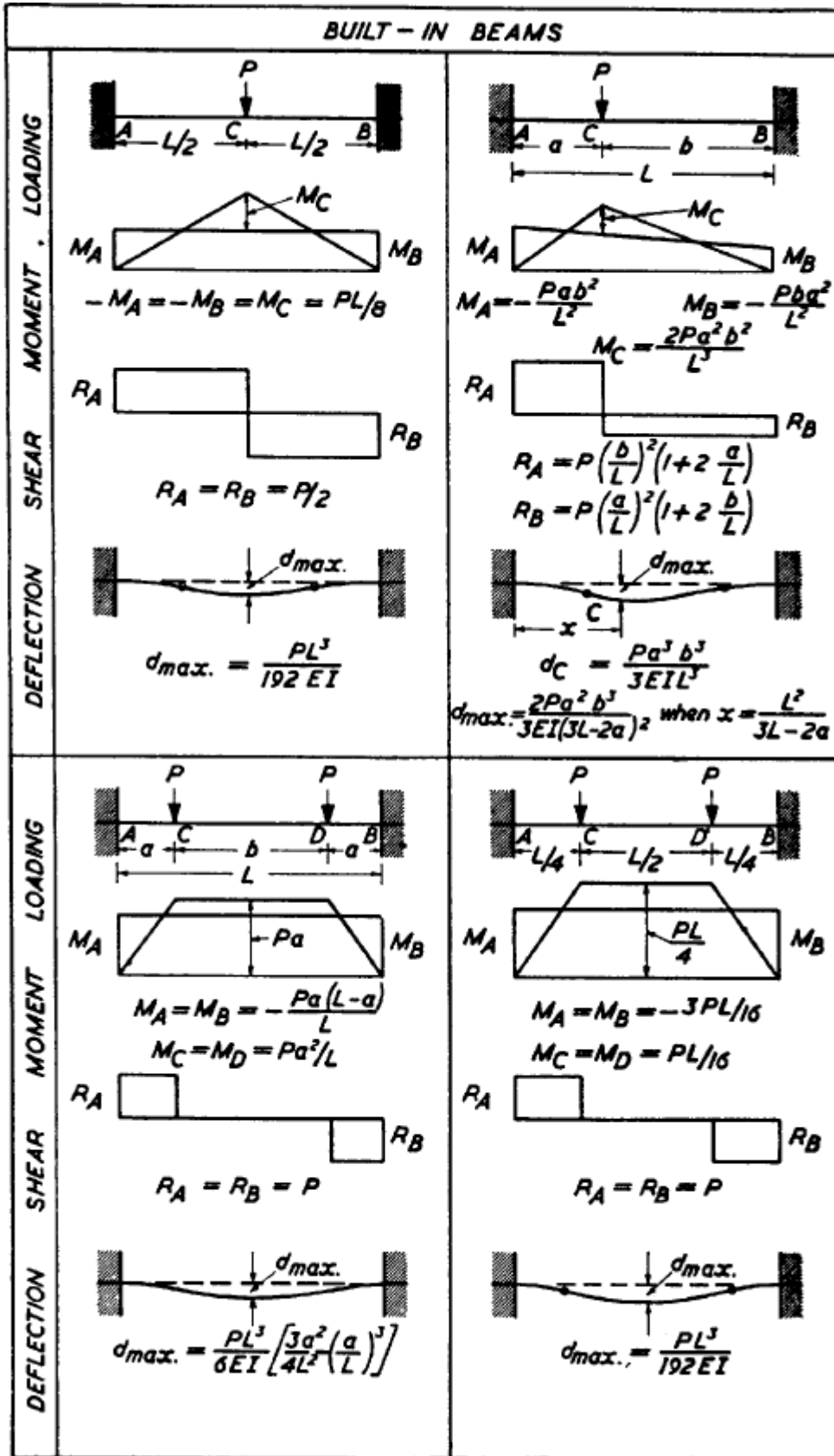
SIMPLY SUPPORTED BEAMS		
LOADING		
MOMENT	$M_A = M_B = -\frac{wN^2}{2} \quad M_D = \frac{wL^2}{8} + M_A$	$M_A = M_B = -\frac{wN^2}{2}$
SHEAR	$R_A = R_B = w\left(N + \frac{L}{2}\right)$	$R_A = R_B = wN$
DEFLECTION	$d_C = d_E = \frac{wL^3 N}{24EI} (3n^3 + 6n^2 - 1)$ $d_D = \frac{wL^4}{384EI} (5 - 24n^2)$ <p>Where <math>n = N/L</math></p>	$d_C = d_E = \frac{wLN^3}{8EI} \left(2 + \frac{N}{L}\right)$ $d_D = -\frac{wL^2 N^2}{16EI}$
LOADING		
MOMENT	$M_A = -\frac{wN^2}{2}$	$M_A = -\frac{wN^2}{2}$
SHEAR	$R_A = \frac{w(N+L)^2}{2L} \quad R_B = \frac{w(L+N)(L-N)}{2L}$ <p><math>m = x/L \quad n = N/L</math></p>	$R_A = \frac{wN(2L+N)}{2L} \quad R_B = \frac{wN^2}{2L}$
DEFLECTION	$d_C = \frac{wL^3 N}{24EI} (3n^3 + 4n^2 - 1)$ $d_x = \frac{wL^4}{24EI} [m^4 - 2m^3(1-n^2) + m(1-2n^2)]$ $d_D = -\frac{wL^3 Q}{24EI} (2n^2 - 1)$	$d_C = \frac{wLN^3}{24EI} \left(4 + 3\frac{N}{L}\right)$ $d_D = -\frac{0.032wL^2 N^2}{EI}$ $d_E = \frac{wLN^2 Q}{12EI}$

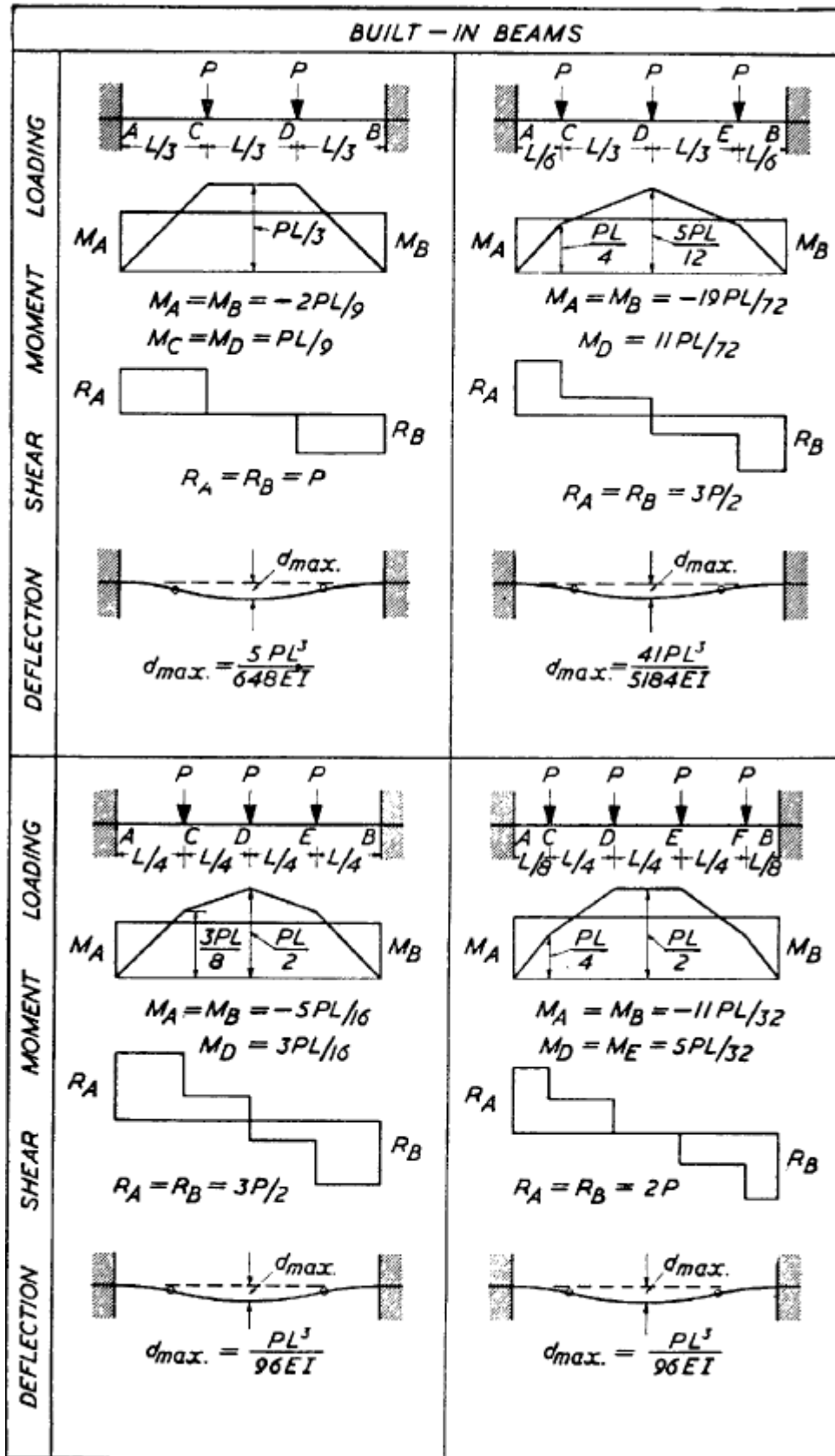
		BUILT-IN BEAMS	
DEFLECTION	SHEAR		
	MOMENT	$M_A = M_B = -\frac{WL}{12}$ $M_C = \frac{WL}{24}$	$M_A = M_B = -\frac{Wa}{12L}(3L-2a)$
	LOADING	$R_A = R_B = W/2$	$R_A = R_B = W/2$
		$d_{max} = \frac{WL^3}{384EI}$	$d_{max} = \frac{Wa^2}{48EI}(L-a)$
DEFLECTION	SHEAR		
	MOMENT	$M_A = -\frac{W}{12L^2b} [e^3(4L-3e) - c^3(4L-3c)]$ $M_B = -\frac{W}{12L^2b} [d^3(4L-3d) - a^3(4L-3a)]$	$M_A = -\frac{WL}{12} \cdot m(3m^2 - 8m + 6)$ $M_B = -\frac{WL}{12} \cdot m^2(4-3m) + M_{max} = \frac{WL}{12} m^2 \left( -\frac{3}{2}m^2 + 6m^4 - 6m^2 - 6m^2 + 15m - 8 \right)$ <p style="text-align: center;">When <math>x = \frac{a}{2}(m^2 - 2m^2 + 2)</math></p>
	LOADING	<p>When <math>r</math> is the simple support reaction</p> $R_A = r_A + \frac{M_A - M_B}{L} \quad R_B = r_B + \frac{M_B - M_A}{L}$	$R_A = \frac{W(m^2 - 2m^2 + 2)}{2} \quad R_B = \frac{W \cdot m^2(2-m)}{2m}$
		<p>When <math>a = c</math>, <math>d_{max} = \frac{W}{384EI}(L^3 + 2L^2a + 4La^2 - 8a^3)</math></p>	<p>When <math>a = L/2</math> and <math>x_1 = 0.445L</math></p> $d_{max} = \frac{WL^3}{333EI}$ $d_C = \frac{WL^3}{384EI}$

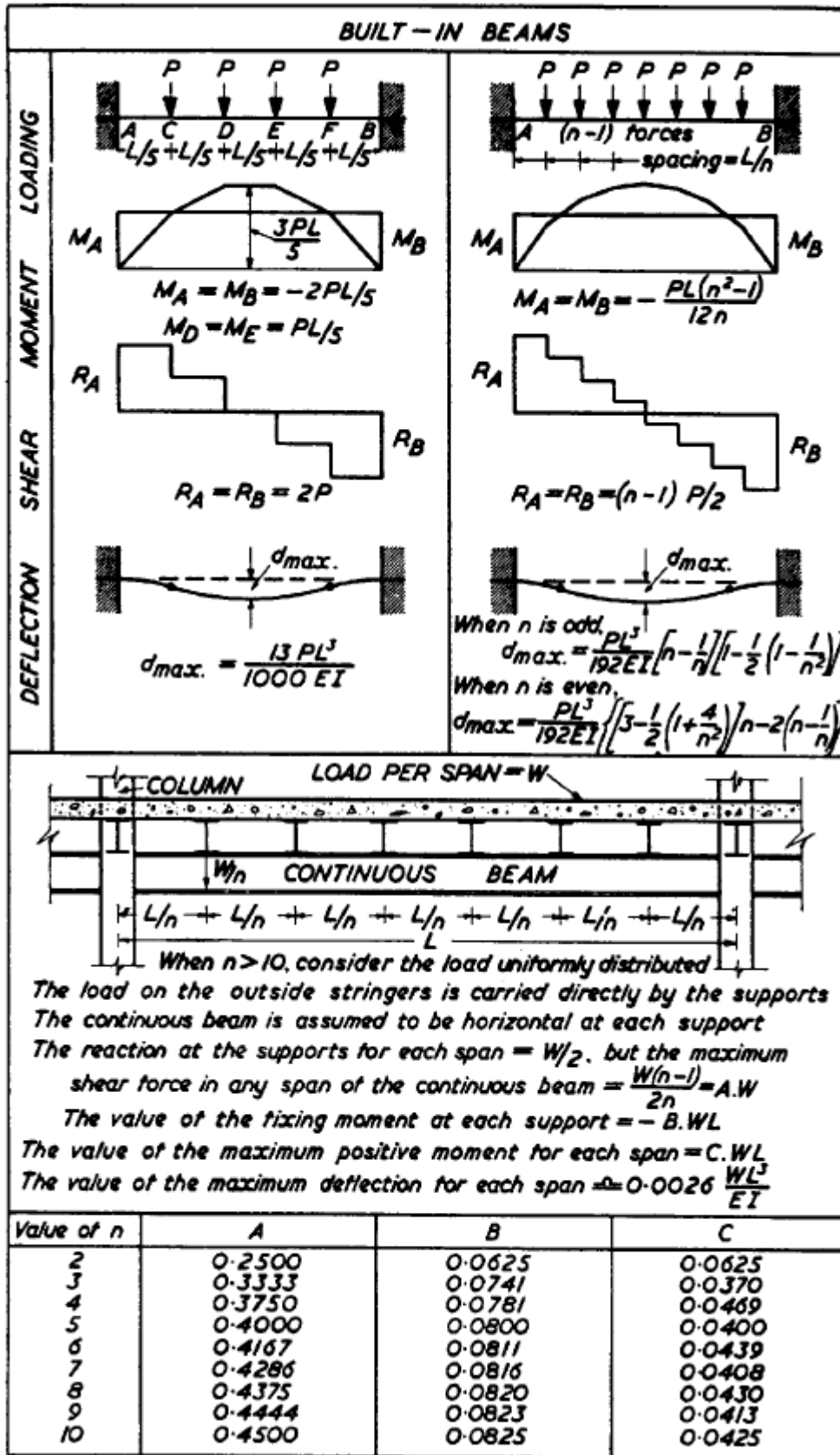


		BUILT-IN BEAMS	
DEFLECTION			
	MOMENT		
	SHEAR	$M_A = M_B = -\frac{Wa}{12L}(2L-a)$	$M_A = -\frac{Wa}{30L^2}(3a^2+10bL)$ $M_B = -\frac{Wa^2}{30L^2}(5L-3a)$
	LOADING	$R_A = R_B = W/2$	<i>In AC.</i> $M_x = R_B \cdot x + M_B - \frac{2W(x-b)^2}{6ab}$ <i>In CB.</i> $M_x = R_B \cdot x + M_B$
DEFLECTION			
	MOMENT	$R_A = R_B = W/2$	$R_A = \frac{W}{10L^2}(10L^3-5La^2+2a^3)$ $R_B = \frac{Wa^2}{10L^2}(5L-2a)$
	SHEAR	$d_{max.} = \frac{Wa^2}{480EI}(5L-4a)$	
	LOADING		
DEFLECTION			
	MOMENT	$M_A = M_B = -\frac{Wa}{12L}(4L-3a)$	$M_A = -\frac{Wa}{15L^2}(10L^2-15aL+6a^2)$ $M_B = -\frac{Wa^2}{10L^2}(5L-4a)$
	SHEAR	$R_A = R_B = W/2$	$R_A = \frac{W}{10L^2}(10L^3-15La^2+8a^3)$ $R_B = \frac{Wa^2}{10L^2}(15L-8a)$
	LOADING	$d_{max.} = \frac{Wa^2}{480EI}(15L-16a)$	

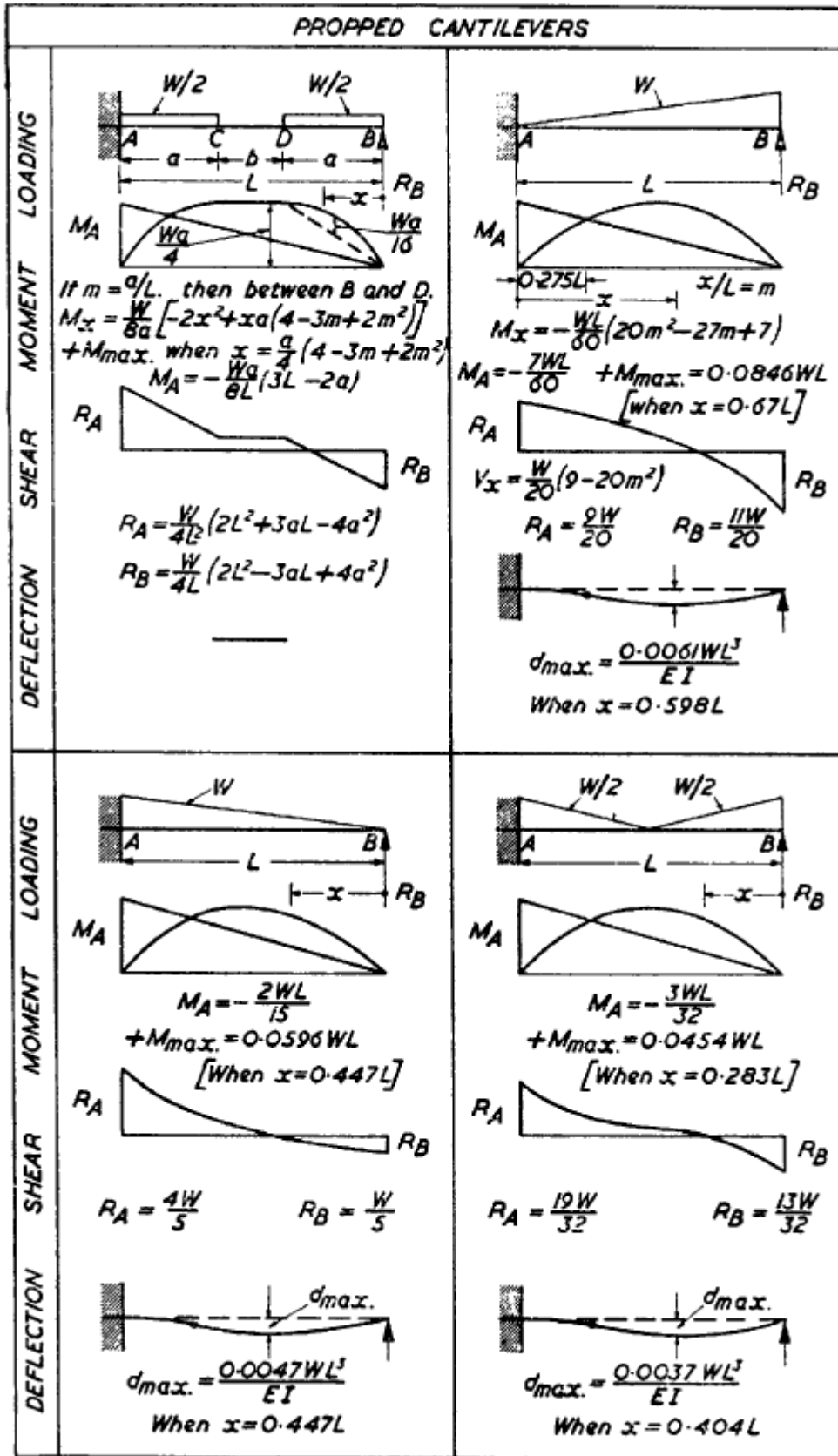


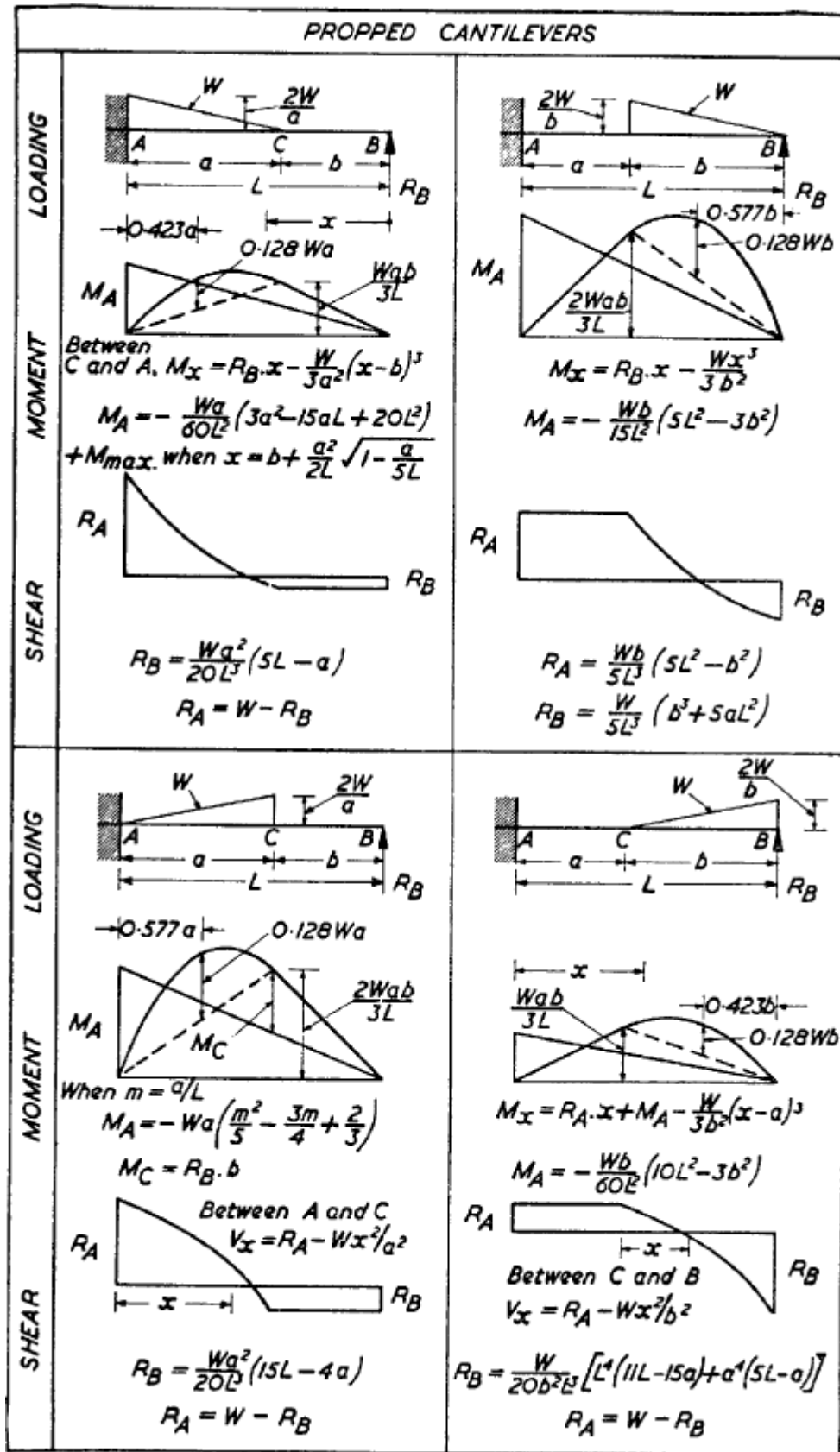






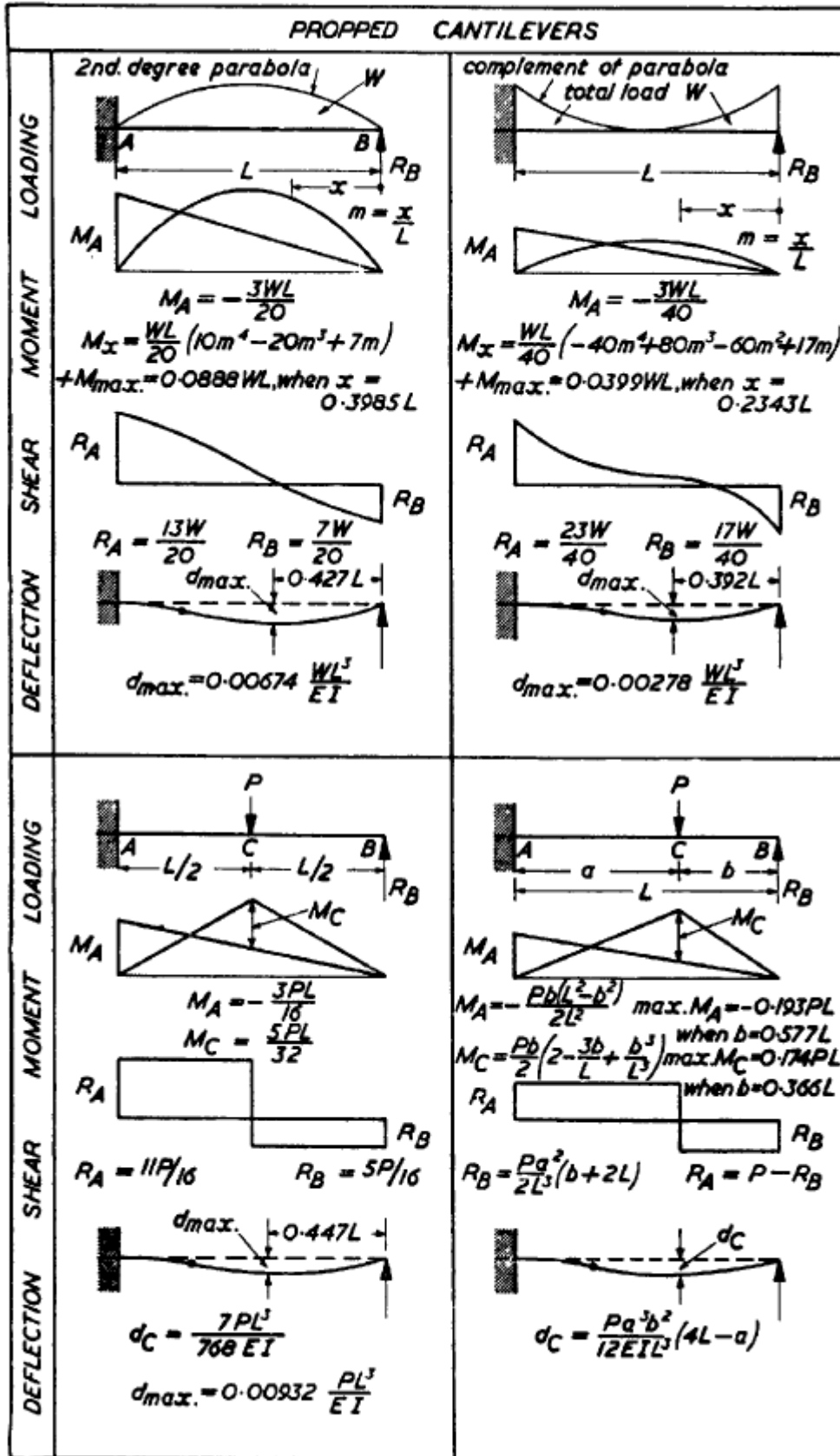
PROPPED CANTILEVERS	
MOMENT · LOADING	<p> <math>M_A = -\frac{WL}{8}</math>    <math>M_C = \frac{9WL}{128}</math> </p>
SHEAR	<p> <math>R_A = \frac{5W}{8}</math>    <math>R_B = \frac{3W}{8}</math> </p>
DEFLECTION	<p> <math>d = \frac{WL^3}{48EI} (m - 3m^3 + 2m^4)</math>  <math>d_{max.} = \frac{WL^3}{185EI}</math> </p>
MOMENT · LOADING	<p> <math>M_A = -\frac{Wa}{8}(2-n)^2</math> where <math>a/L=n</math>  <math>+M_{max.} = \frac{Wa}{8L} \left[ \frac{[8-n^2(4-n)]^2}{16} + 4-n(4-n) \right]</math> </p>
SHEAR	<p> <math>R_A = \frac{W}{8} [8-n^2(4-n)]</math>  <math>R_B = \frac{Wn^2}{8} (4-n)</math> </p>
DEFLECTION	<p> <math>d_C = \frac{Wa^3}{48EI} (6-12n+7n^2-n^3)</math> </p>
MOMENT · LOADING	<p> <math>M_A = -\frac{Wb}{8}(2-n^2)</math>    <math>M_C = \frac{Wb}{8}(6n-n^3-4)</math> </p>
SHEAR	<p> <math>R_A = \frac{Wn}{8} (6-n^2)</math>  <math>R_B = \frac{W}{8} (n^3-6n+8)</math> </p>
DEFLECTION	<p> <math>d_B = \frac{Wb^3}{48EI} (6-12n+7n^2-n^3)</math> </p>
MOMENT · LOADING	<p> <math>M_A = -\frac{W}{8L^2b} (d^2-c^2)(2L^2-c^2-d^2)</math> </p>
SHEAR	<p> <math>R_A = r_A + \frac{MA}{L}</math>    <math>R_B = r_B - \frac{MA}{L}</math> </p>
DEFLECTION	<p>Where <math>r_A</math> and <math>r_B</math> are the simple support reactions for the beam (<math>M_A</math> being considered positive)</p>

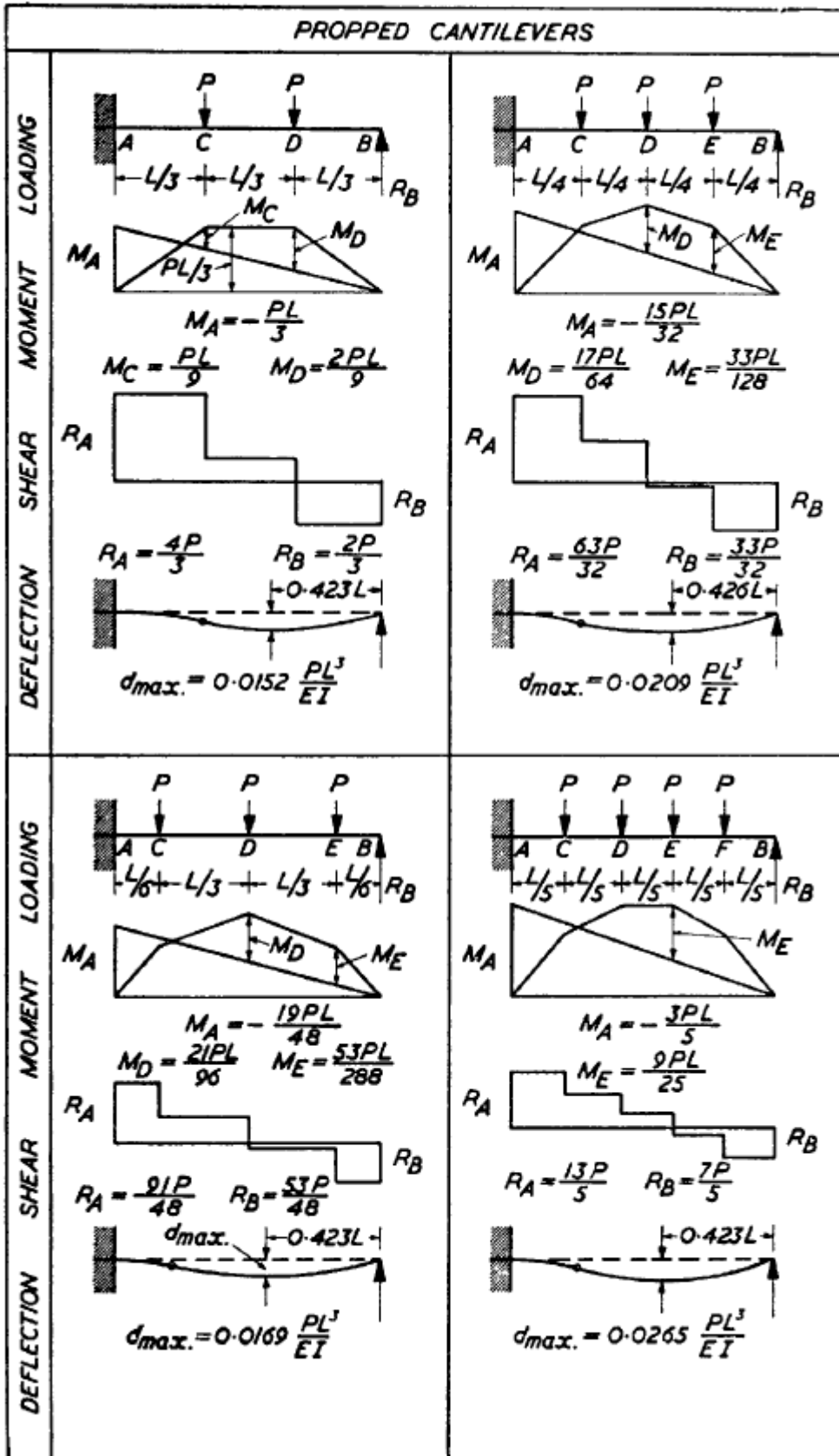




PROPPED CANTILEVERS	
LOADING	
MOMENT	<p> <math>M_B = -\frac{wL^2}{2}</math>    <math>M_A = -\frac{w}{8}(L^2 - 2a^2)</math>  <math>+M_{max} = \frac{wL^2}{128}(36p^4 - 28p^2 + 9)</math>                      when <math>x/L = \frac{5}{8} - \frac{3p^2}{4}</math> </p>
SHEAR	<p> <math>R_A = wL\left(\frac{5}{8} - \frac{3p^2}{4}\right)</math>  <math>R_B = wL\left(\frac{3p^2}{4} + p + \frac{3}{8}\right)</math> </p>
DEFLECTION	<p> <math>d_D = \frac{wL^4}{48EI} [(8p^3 + 6p^2 - 1)(p+q) - 2p^3]</math>  <math>d_x = \frac{wL^4}{48EI} [2n^4 + (6p^2 - 5)n^3 - (6p^2 - 3)n^2]</math>  <math>d_{max} \text{ when } x/L = \frac{1}{18} [15 - 18p^2 + \sqrt{324p^4 - 156p^2 + 33}]</math> </p>
LOADING	
MOMENT	<p> <math>M_B = -2M_A = -Pa</math>  <math>p = a/L</math>  <math>q = b/L</math> </p>
SHEAR	<p> <math>R_A = -\frac{3Pp}{2}</math>  <math>R_B = P\left(1 + \frac{3p}{2}\right)</math> </p>
DEFLECTION	<p> <math>d_D = \frac{PL^3p}{12EI} (4p^2 + 6pq + 3p + 3q)</math>  <math>-d_{max} = -\frac{PL^3p}{27EI}</math> </p>
LOADING	
MOMENT	<p> <math>M_B = -2M_A = -\frac{wq^2}{2}</math>  <math>p = a/L</math>  <math>q = b/L</math> </p>
SHEAR	<p> <math>R_A = -\frac{3wap}{4}</math>  <math>R_B = wa\left(1 + \frac{3p}{4}\right)</math> </p>
DEFLECTION	<p> <math>d_D = \frac{wL^4}{48EI} [p^2(8p+6)q + 6p^3(p+1)]</math>  <math>-d_{max} = -\frac{wL^4p^2}{54EI}</math> </p>
LOADING	
MOMENT	<p> <math>M_B = -2M_A = -M</math> </p>
SHEAR	<p> <math>R_A = -R_B = -\frac{3M}{2L}</math> </p>
DEFLECTION	<p> <math>d_D = \frac{M}{4EI} [L(a+b) + a^2(2 + \frac{4b}{a})]</math>  <math>-d_{max} = -\frac{ML^2}{27EI}</math> </p>

		PROPPED CANTILEVERS	
LOADING			
		$n = a/L \quad q = x/a$	
MOMENT			
	$M_A = -\frac{Wa}{8L}(2L-a)$	$M_A = -\frac{Wa}{8L}(4L-3a)$	
SHEAR			
	$R_A = \frac{W}{8L^2}(4L^2 + 2aL - a^2)$ $R_B = W - R_A$	$R_A = \frac{W}{8L^2}(4L^2 + 4aL - 3a^2)$ $R_B = W - R_A$	
LOADING			
MOMENT			
	$M_A = -\frac{5WL}{32}$ $+M_{max} = 0.0948WL$	$M_A = \frac{W}{32L}(5L^2 + 4aL - 4a^2)$	
SHEAR			
	$R_A = \frac{21W}{32} \quad R_B = \frac{11W}{32}$	$R_A = \frac{W}{32L^2}(21L^2 + 4aL - 4a^2)$ $R_B = W - R_A$	
DEFLECTION			
	$d_{max} = 0.00727 \frac{WL^3}{EI}$		



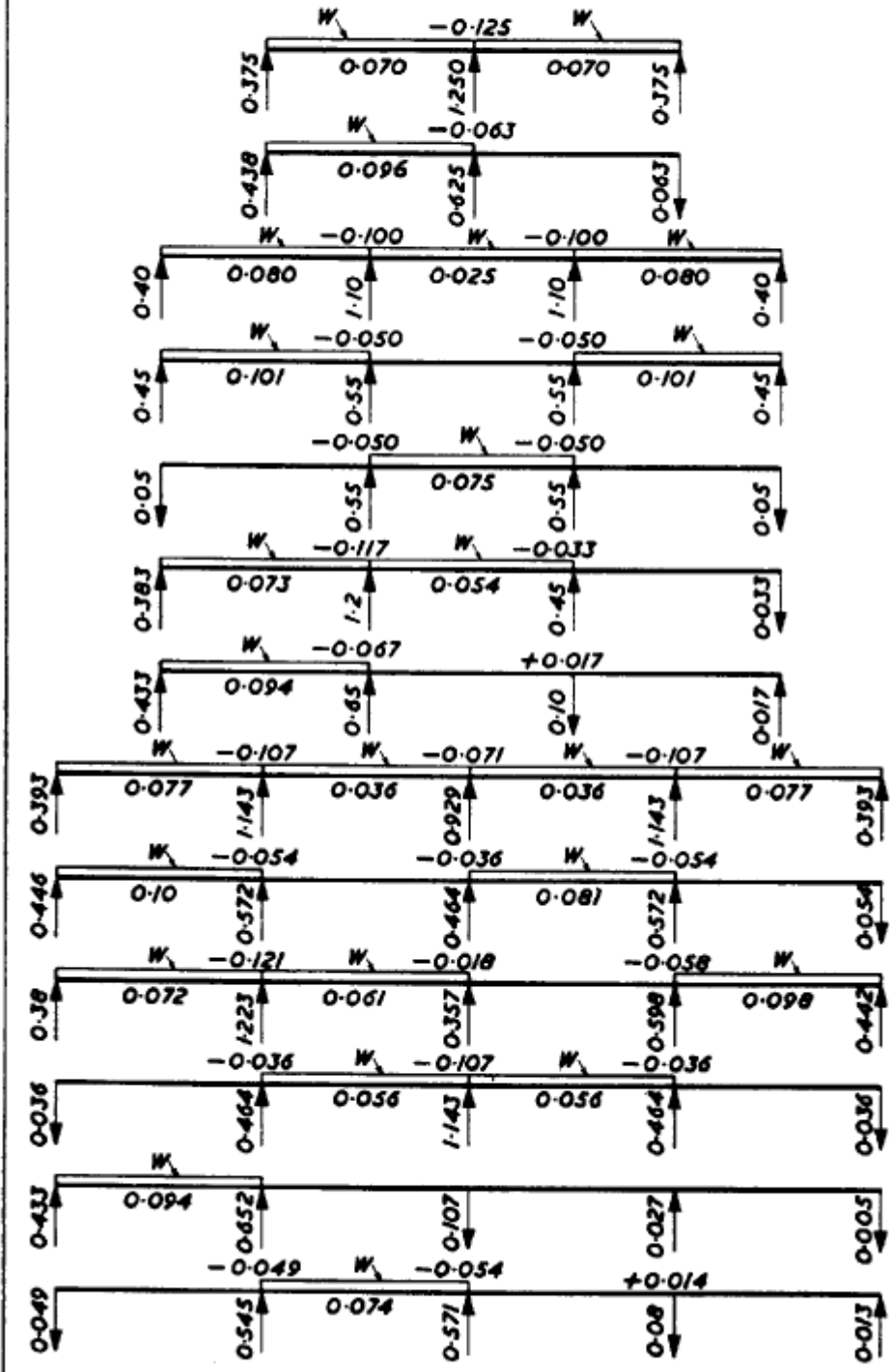


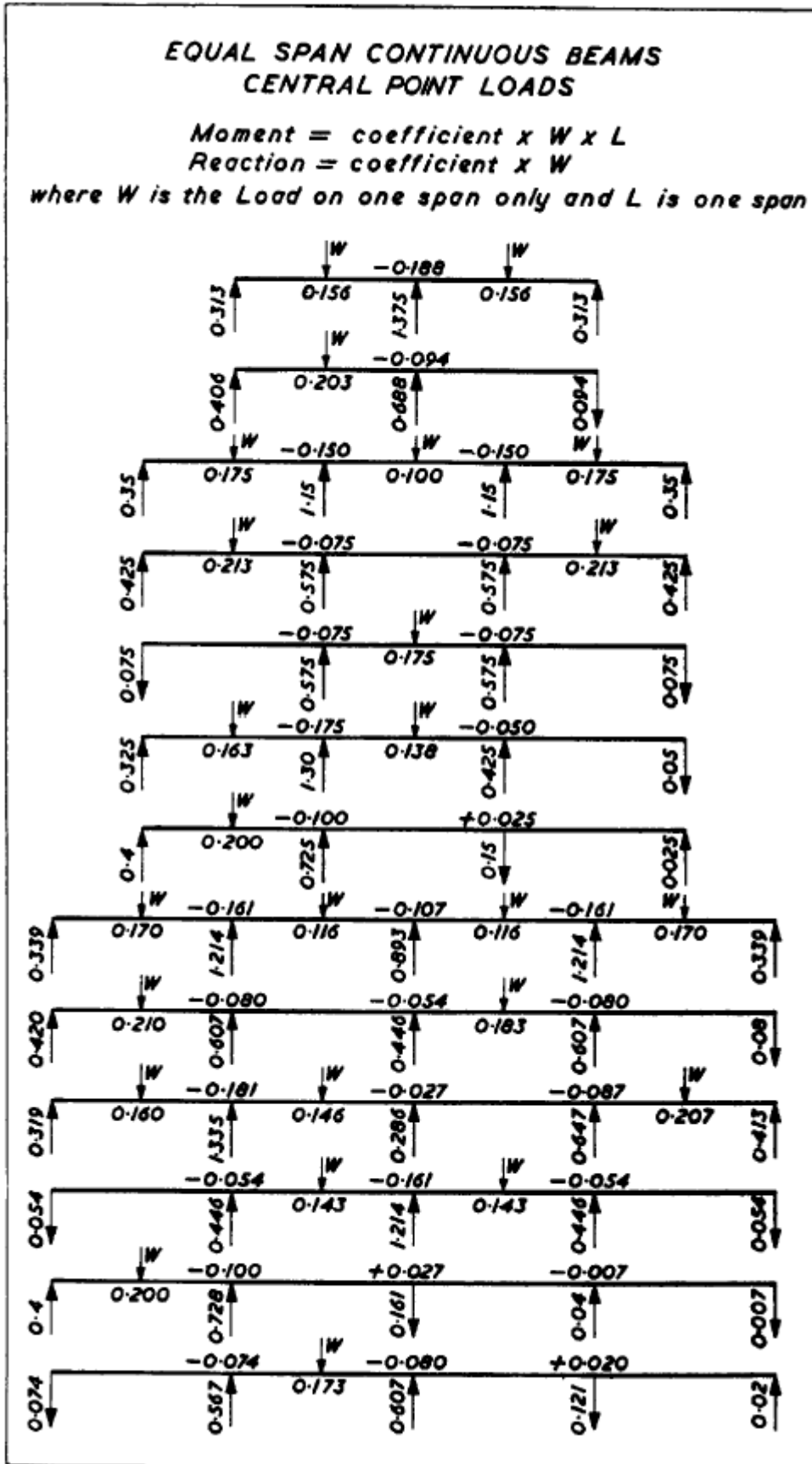
PROPPED CANTILEVERS	
LOADING	
MOMENT	$M_A = -\frac{33PL}{64}$ $M_E = \frac{157PL}{512}$
SHEAR	$R_A = \frac{161P}{64} \quad R_B = \frac{95P}{64}$
DEFLECTION	$d_{max} = 0.0221 \frac{PL^3}{EI}$
LOADING	
MOMENT	$M_A = -\frac{PL(n^2-1)}{8n}$
SHEAR	$R_A = \frac{P}{8n}(5n^2-4n-1)$ $R_B = \frac{P}{8n}(3n^2-4n+1)$
DEFLECTION	<p>when <math>n</math> is large, <math>d_{max} \approx \frac{nPL^3}{185EI}</math></p>
LOADING	<p>Any symmetrical load <math>W</math></p>
MOMENT	<p>If <math>A_S = \text{Area of free B.M. Diagram}</math></p> $M_A = \frac{3A_S}{2L}$
SHEAR	$R_A = \frac{W}{2} + \frac{M_A}{L} \quad R_B = \frac{W}{2} - \frac{M_A}{L}$
DEFLECTION	<p><math>d_{max}</math> occurs at point corresponding to <math>X</math> on B.M. diagram, the area <math>R</math> being equal to the area <math>Q</math></p> $d_{max} = \frac{\text{Area } SXx}{EI}$
LOADING	<p><math>a/L = n</math></p>
MOMENT	<p>① <math>a=L</math> <math>M_A = -M/2</math> <math>M_{CB} = +M</math></p> <p>② <math>a &gt; 0.423L</math> <math>M_{CA} = +M</math></p> <p>③ <math>a = 0.423L</math></p> <p>④ <math>a &lt; 0.423L</math></p>
SHEAR	$M_A = \frac{M}{2}(2-6n+3n^2)$ $M_{CA} = \frac{M}{2}(2-6n+9n^2-3n^3)$ $M_{CB} = \frac{3Mn}{2}(2-3n+n^2)$
DEFLECTION	$-R_A = R_B = \frac{M+M_A}{L}$ <p>In Case 1, <math>R = 3M/2L</math> Case 3, <math>R = M/L</math></p>

**EQUAL SPAN CONTINUOUS BEAMS  
UNIFORMLY DISTRIBUTED LOADS**

Moment = coefficient  $\times W \times L$   
Reaction = coefficient  $\times W$

where  $W$  is the U.D.L. on one span only and  $L$  is one span



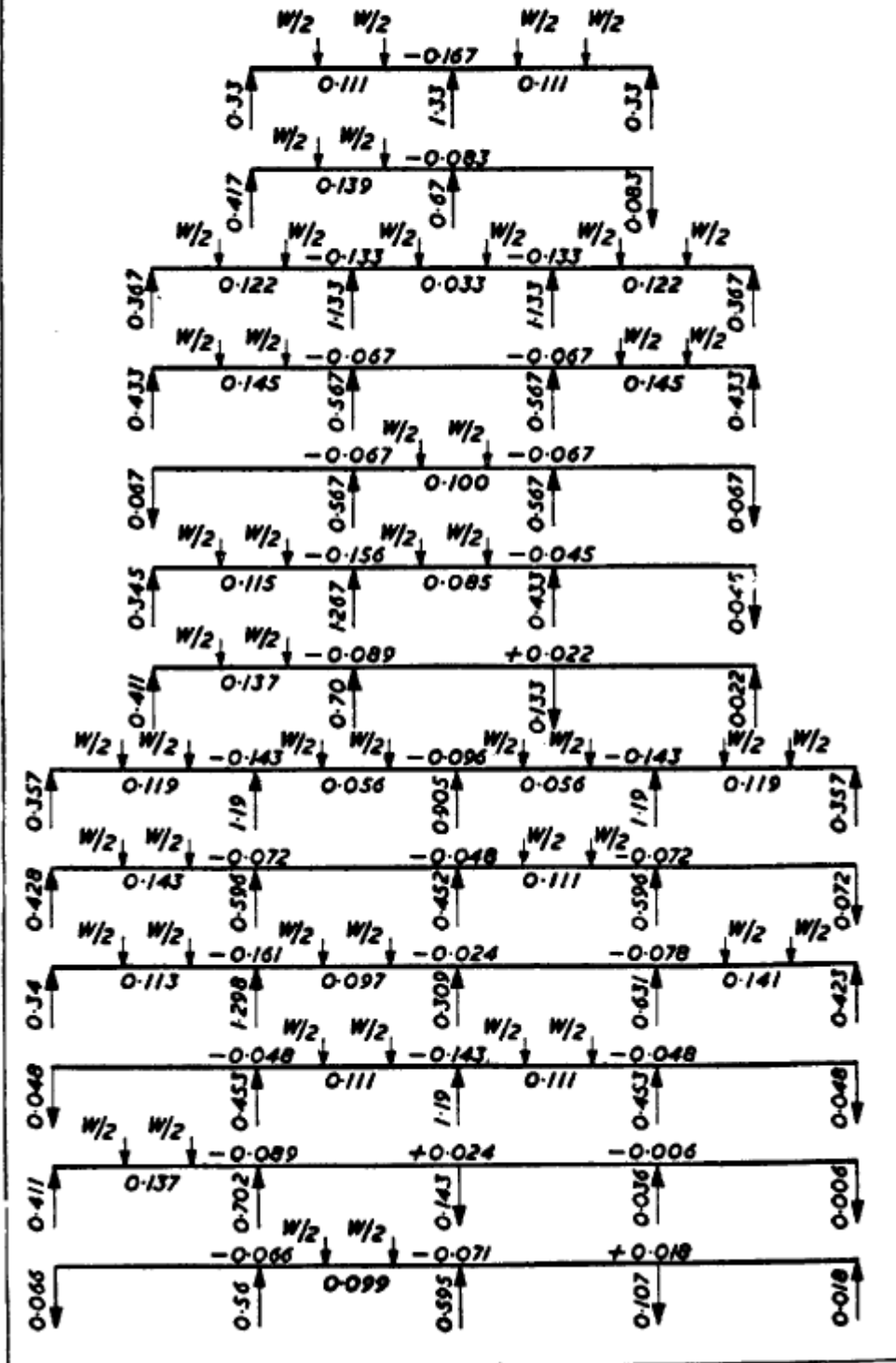


### EQUAL SPAN CONTINUOUS BEAMS POINT LOADS AT THIRD POINTS OF SPANS

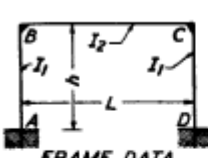
Moment = coefficient  $\times W \times L$

Reaction = coefficient  $\times W$

where  $W$  is the total load on one span only &  $L$  is one span



**Frame I**



**FRAME DATA**

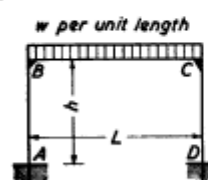
Coefficients:

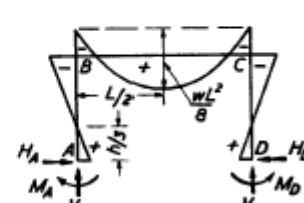
$$k = \frac{I_2 \cdot h}{I_1 \cdot L}$$

$$N_1 = k + 2 \quad N_2 = 6k + 1$$

---

w per unit length



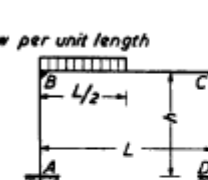


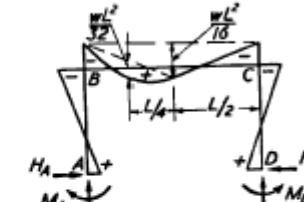
$$M_A = M_D = \frac{wL^2}{12N_1} \quad M_B = M_C = -\frac{wL^2}{6N_1} = -2M_A$$

$$M_{max} = \frac{wL^2}{8} + M_B \quad V_A = V_D = \frac{wL}{2} \quad H_A = H_D = \frac{3M_A}{h}$$


---

w per unit length



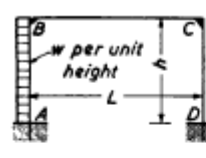
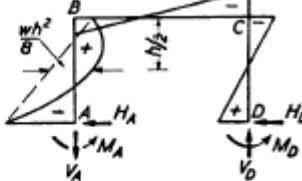


$$M_A = \frac{wL^2}{8} \left[ \frac{1}{3N_1} - \frac{1}{8N_2} \right] \quad M_B = -\frac{wL^2}{8} \left[ \frac{2}{3N_1} + \frac{1}{8N_2} \right]$$

$$M_D = \frac{wL^2}{8} \left[ \frac{1}{3N_1} + \frac{1}{8N_2} \right] \quad M_C = -\frac{wL^2}{8} \left[ \frac{2}{3N_1} - \frac{1}{8N_2} \right]$$

$$V_D = \frac{wL}{8} \left[ 1 - \frac{1}{4N_2} \right] \quad V_A = \frac{wL}{2} - V_D \quad H_A = H_D = \frac{wL^2}{8hN_1}$$

Extract: 'Kleinogel, Rahmenformeln' 11. Auflage Berlin—Verlag von Wilhelm Ernst & Sohn.

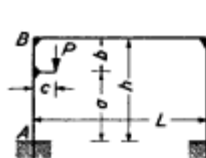
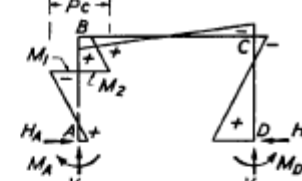



$$M_A = \frac{wh^2}{4} \left[ -\frac{k+3}{6N_1} - \frac{4k+1}{N_2} \right] \quad M_B = \frac{wh^2}{4} \left[ -\frac{k}{6N_1} + \frac{2k}{N_2} \right]$$

$$M_D = \frac{wh^2}{4} \left[ -\frac{k+3}{6N_1} + \frac{4k+1}{N_2} \right] \quad M_C = \frac{wh^2}{4} \left[ -\frac{k}{6N_1} - \frac{2k}{N_2} \right]$$

$$H_D = \frac{wh(2k+3)}{8N_1} \quad H_A = -(wh - H_D) \quad V_A = -V_D = -\frac{wh^2k}{LN_2}$$


---

Constants:  $a_1 = \frac{a}{h} \quad b_1 = \frac{b}{h}$

$$X_1 = \frac{Pc}{2N_1} [1 + 2b_1k - 3b_1^2(k+1)] \quad X_2 = \frac{Pcka_1(3a_1 - 2)}{2N_1}$$

$$X_3 = \frac{3Pcka_1}{N_2}$$

$$M_A = +X_1 - \left( \frac{Pc}{2} - X_3 \right) \quad M_B = +X_2 + X_3$$

$$M_D = +X_1 + \left( \frac{Pc}{2} - X_3 \right) \quad M_C = +X_2 - X_3$$

$$H_A = H_D = \frac{Pc}{2h} + \frac{X_1 - X_2}{h} \quad V_D = \frac{2X_3}{L} \quad V_A = P - V_D$$

$$M_1 = M_A - H_A a \quad M_2 = M_B + H_D b$$

Extract: 'Kleinogel, Rahmenformeln' 11. Auflage Berlin—Verlag von Wilhelm Ernst & Sohn.

$$\text{Constants: } a_1 = \frac{a}{h} \quad b_1 = \frac{b}{h}$$

$$X_1 = \frac{Pc}{2N_1} [1 + 2b_1k - 3b_1^2(k+1)] \quad X_2 = \frac{Pcka_1(3a_1-2)}{2N_1}$$

$$M_A = M_D = \frac{Pc}{N_1} [1 + 2b_1k - 3b_1^2(k+1)] - 2X_1$$

$$M_B = M_C = \frac{Pcka_1(3a_1-2)}{N_1} = 2X_2$$

$$V_A = V_D = P \quad H_A = H_D = \frac{Pc + M_A - M_B}{h}$$

$$M_1 = M_A - H_A a \quad M_2 = M_B + H_D b$$

---

$$\text{Constants: } a_1 = \frac{a}{h} \quad X_1 = \frac{3Paa_1k}{N_2}$$

$$M_A = -Pa + X_1 \quad M_B = X_1$$

$$M_D = +Pa - X_1 \quad M_C = -X_1$$

$$V_A = -V_D = -\frac{2X_1}{L} \quad H_A = -H_D = -P$$

Extract: 'Kleinogel, Rahmenformeln' 11. Auflage Berlin—Verlag von Wilhelm Ernst & Sohn.

$$M_A = M_D = +\frac{PL}{8N_1} \quad M_B = M_C = -2M_A$$

$$V_A = V_D = \frac{P}{2} \quad H_A = H_D = \frac{3M_A}{h}$$

$$M_A = -\frac{Ph}{2} \cdot \frac{3k+1}{N_2} \quad M_B = +\frac{Ph}{2} \cdot \frac{3k}{N_2}$$

$$M_D = +\frac{Ph}{2} \cdot \frac{3k+1}{N_2} \quad M_C = -\frac{Ph}{2} \cdot \frac{3k}{N_2}$$

$$H_A = -H_D = -\frac{P}{2} \quad V_A = -V_D = -\frac{2M_B}{L}$$

$$\text{Constants: } a_1 = a/L \quad b_1 = b/L$$

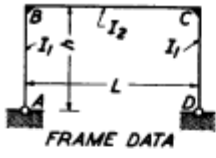
$$M_A = +\frac{Pab}{L} \left[ \frac{1}{2N_1} \frac{b_1 - a_1}{2N_2} \right] \quad M_B = -\frac{Pab}{L} \left[ \frac{1}{N_1} + \frac{b_1 - a_1}{2N_2} \right]$$

$$M_D = +\frac{Pab}{L} \left[ \frac{1}{2N_1} + \frac{b_1 - a_1}{2N_2} \right] \quad M_C = -\frac{Pab}{L} \left[ \frac{1}{N_1} - \frac{b_1 - a_1}{2N_2} \right]$$

$$V_A = Pb_1 \left[ 1 + \frac{a_1(b_1 - a_1)}{N_2} \right] \quad V_D = P - V_A \quad H_A = H_D = \frac{3Pab}{2LhN_1}$$

Extract: 'Kleinogel, Rahmenformeln' 11. Auflage Berlin—Verlag von Wilhelm Ernst & Sohn.

**Frame II**



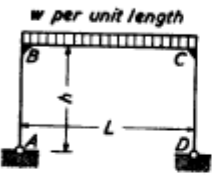
FRAME DATA

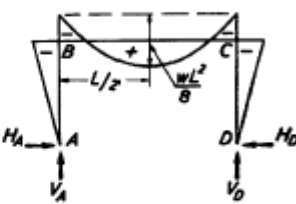
Coefficients:

$$k = \frac{I_2}{I_1} \cdot \frac{h}{L}$$

$$N = 2k + 3$$

---





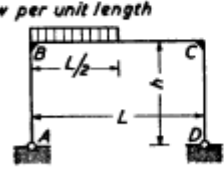
$$M_B = M_C = -\frac{wL^2}{4N}$$

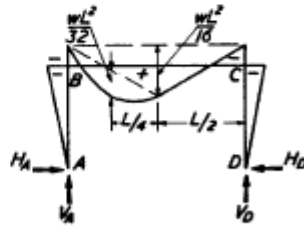
$$M_{max} = \frac{wL^2}{8} + M_B$$

$$V_A = V_D = \frac{wL}{2}$$

$$H_A = H_D = -\frac{M_B}{h}$$


---

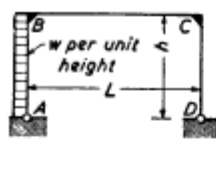


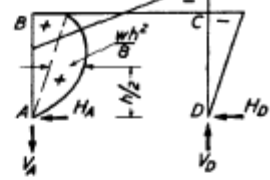


$$M_B = M_C = -\frac{wL^2}{8N}$$

$$V_A = \frac{3wL}{8} \quad V_D = \frac{wL}{8} \quad H_A = H_D = -\frac{M_B}{h}$$

Extract: 'Kleinogel, Rahmenformeln' 11. Auflage Berlin—Verlag von Wilhelm Ernst & Sohn.



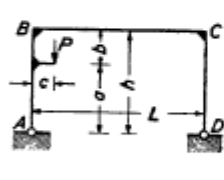


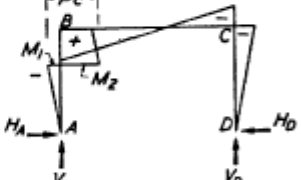
$$M_B = \frac{wh^2}{4} \left[ -\frac{k}{2N} + 1 \right] \quad H_D = -\frac{M_C}{h}$$

$$M_C = \frac{wh^2}{4} \left[ -\frac{k}{2N} - 1 \right] \quad H_A = -(wh - H_D)$$

$$V_A = -V_D = -\frac{wh^2}{2L}$$


---





Constant:  $a_1 = \frac{a}{h}$

$$M_B = \frac{Pc}{2} \left[ \frac{(3a_1^2 - 1)k}{N} + 1 \right] \quad H_A = H_D = -\frac{M_C}{h}$$

$$M_C = \frac{Pc}{2} \left[ \frac{(3a_1^2 - 1)k}{N} - 1 \right]$$

$$V_D = \frac{Pc}{L} \quad V_A = P - V_D$$

$$M_1 = -H_A a \quad M_2 = Pc - H_A a$$

Extract: 'Kleinogel, Rahmenformeln' 11. Auflage Berlin—Verlag von Wilhelm Ernst & Sohn.

Constant:  $a_1 = \frac{a}{h}$

$$M_B = M_C = \frac{Pc(3a_1^2 - 1)k}{N}$$

$$H_A = H_D = \frac{Pc - M_B}{h} \quad V_A = V_D = P$$

$$M_1 = -H_A a \quad M_2 = Pc - H_A a$$


---


$$M_B = -M_C = Pa \quad H_A = H_D = P$$

$$V_A = -V_D = -\frac{2Pa}{L}$$

Moment at loads =  $\pm Pa$

Extract: 'Kleinogel, Rahmenformeln' 11. Auflage Berlin—Verlag von Wilhelm Ernst & Sohn.

$$M_B = M_C = -\frac{3PL}{8N} \quad V_A = V_D = \frac{P}{2} \quad H_A = H_D = -\frac{1M_B}{h}$$


---


$$M_B = -M_C = \frac{Ph}{2}$$

$$V_A = -V_D = -\frac{Ph}{L} \quad H_A = -H_D = -\frac{P}{2}$$

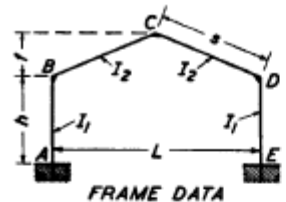

---


$$M_B = M_C = -\frac{Pab}{L} \cdot \frac{3}{2N}$$

$$V_A = \frac{Pb}{L} \quad V_D = \frac{Pa}{L} \quad H_A = H_D = -\frac{M_B}{h}$$

Extract: 'Kleinogel, Rahmenformeln' 11. Auflage Berlin—Verlag von Wilhelm Ernst & Sohn.

**Frame III**



**FRAME DATA**

Coefficients:

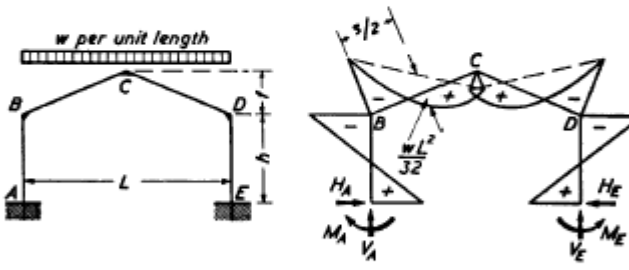
$$k = \frac{I_2}{I_1} \cdot \frac{h}{s} \quad \phi = \frac{f}{h}$$

$$m = 1 + \phi \quad B = 3k + 2 \quad C = 1 + 2m$$

$$K_1 = 2(k + 1 + m + m^2) \quad K_2 = 2(k + \phi^2)$$

$$R = \phi C - k \quad N_1 = K_1 K_2 - R^2 \quad N_2 = 3k + B$$


---



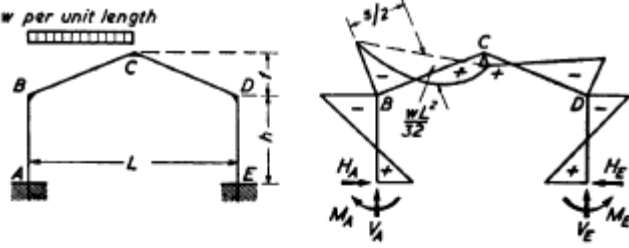
$$M_A = M_E = \frac{wL^2}{16} \cdot \frac{k(8 + 15\phi) + \phi(6 - \phi)}{N_1}$$

$$M_B = M_D = -\frac{wL^2}{16} \cdot \frac{k(16 + 15\phi) + \phi^2}{N_1}$$

$$M_C = \frac{wL^2}{8} - \phi M_A + m M_B$$

$$V_A = V_E = \frac{wL}{2} \quad H_A = H_E = \frac{M_A - M_B}{h}$$

Extract: 'Kleinogel, Rahmenformeln' 11. Auflage Berlin—Verlag von Wilhelm Ernst & Sohn.



**Constants:**

$$*X_1 = \frac{wL^2}{32} \cdot \frac{k(8 + 15\phi) + \phi(6 - \phi)}{N_1}$$

$$*X_2 = \frac{wL^2}{32} \cdot \frac{k(16 + 15\phi) + \phi^2}{N_1} \quad X_3 = \frac{wL^2}{32N_2}$$

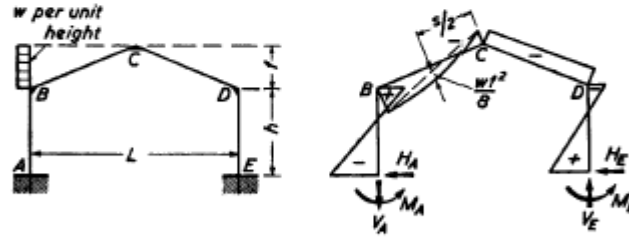
$$M_A = +X_1 - X_3 \quad M_B = -X_2 - X_3 \quad M_E = +X_1 + X_3 \quad M_D = -X_2 + X_3$$

$$*M_C = \frac{wL^2}{16} - \phi X_1 - m X_2$$

$$V_E = \frac{wL}{8} - \frac{2X_3}{L} \quad V_A = \frac{wL}{2} - V_E \quad H_A = H_E = \frac{X_1 + X_3}{h}$$

\* Note that  $X_1$ ,  $-X_1$  and  $M_C$  are respectively half the values of  $M_A$  ( $=M_E$ ),  $M_B$  ( $=M_D$ ) and  $M_C$  from the previous set of formulæ where the whole span was loaded.

---



**Constants:**

$$X_1 = \frac{wf^2}{8} \cdot \frac{k(9\phi + 4) + \phi(6 + \phi)}{N_1}$$

$$X_2 = \frac{wf^2}{8} \cdot \frac{k(8 + 9\phi) - \phi^2}{N_1} \quad X_3 = \frac{wf^2}{8} \cdot \frac{4B + \phi}{N_2}$$

$$M_A = -X_1 - X_3 \quad M_B = +X_2 + \left(\frac{wf}{2} - X_3\right)$$

$$M_E = -X_1 + X_3 \quad M_D = +X_2 - \left(\frac{wf}{2} - X_3\right)$$

$$M_C = -\frac{wf^2}{4} + \phi X_1 + m X_2$$

$$V_A = -V_E = -\frac{wf(2 + \phi)}{2L} + \frac{2X_3}{L} \quad H_E = \frac{wf}{2} - \frac{X_1 + X_3}{h} \quad H_A = -(wf - H_E)$$

Constants:  $X_1 = \frac{wh^2}{8} \cdot \frac{k(k+6) + k\phi(15+16\phi) + 6\phi^2}{N_1}$   
 $X_2 = \frac{wh^2k(9\phi + 8\phi^2 - k)}{8N_1}$      $X_3 = \frac{wh^2(2k+1)}{2N_2}$   
 $M_A = -X_1 - X_3$      $M_B = +X_2 + \left(\frac{wh^2}{4} - X_3\right)$   
 $M_E = -X_1 + X_3$      $M_D = +X_2 - \left(\frac{wh^2}{4} - X_3\right)$   
 $M_C = -\frac{wh\phi}{4} + \phi X_1 + mX_2$   
 $V_A = -V_E = -\frac{wh^2}{2L} + \frac{2X_3}{L}$      $H_E = \frac{wh}{4} - \frac{X_1 + X_2}{h}$      $H_A = -(wh - H_E)$

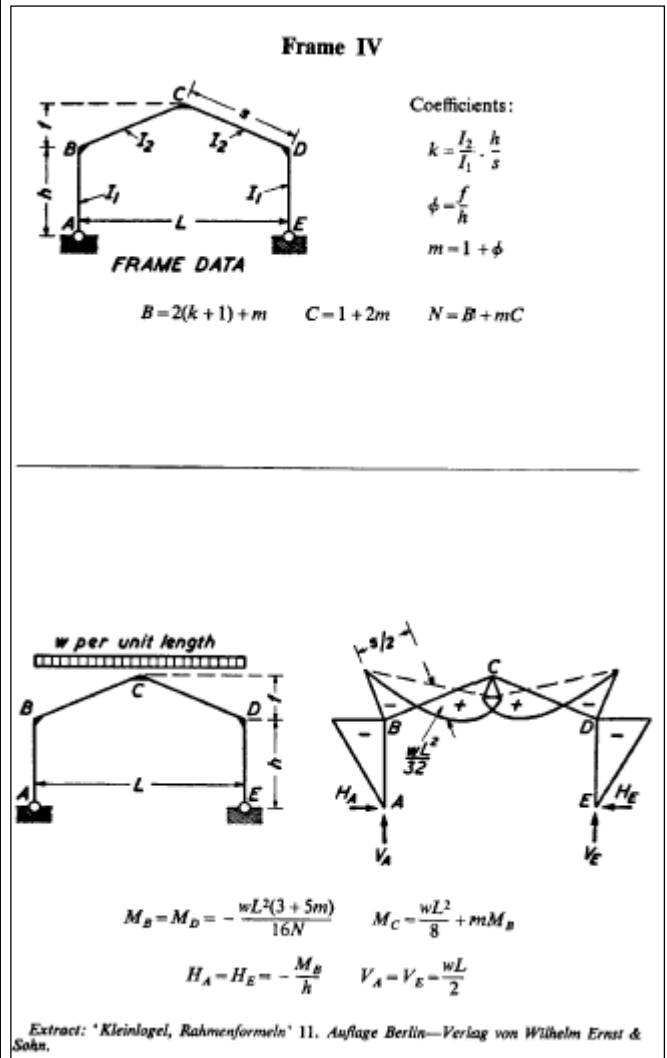
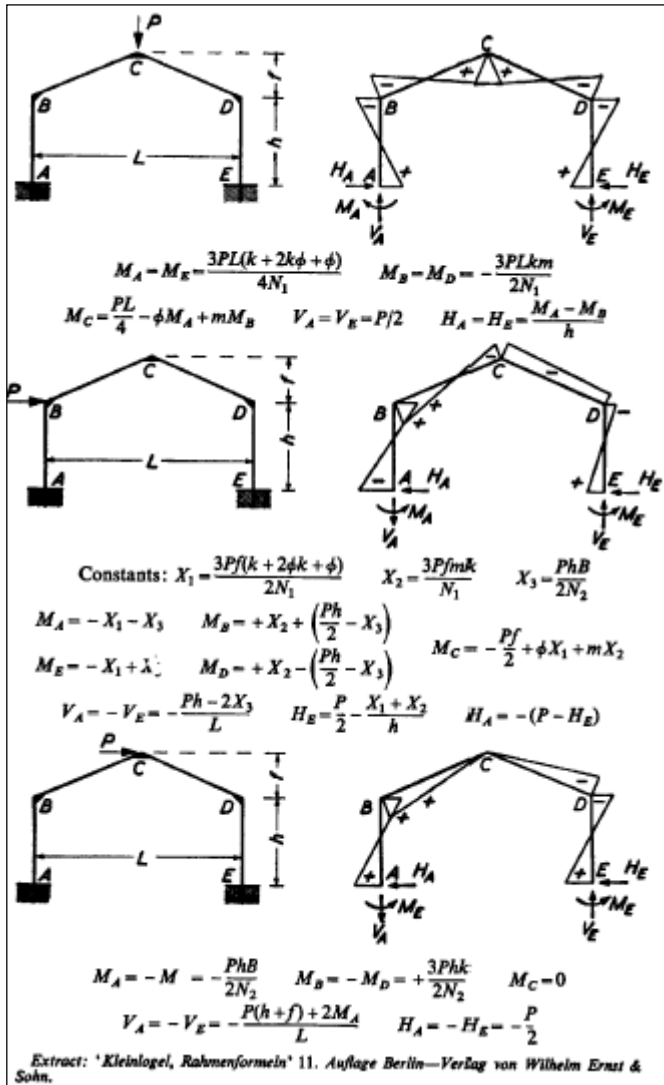
Constants:  $a_1 = \frac{a}{h}$      $b_1 = \frac{b}{h}$   
 $Y_1 = Pc[2\phi^2 - (1 - 3b_1^2)k]$      $Y_2 = Pc[\phi C - (3a_1^2 - 1)k]$   
 $X_1 = \frac{Y_1K_1 - Y_2R}{2N_1}$      $X_2 = \frac{Y_2K_2 - Y_1R}{2N_1}$      $X_3 = \frac{Pc}{2} \cdot \frac{B - 3(a_1 - b_1)k}{N_2}$   
 $M_A = -X_1 - X_3$      $M_B = +X_2 + \left(\frac{Pc}{2} - X_3\right)$   
 $M_E = -X_1 + X_3$      $M_D = +X_2 - \left(\frac{Pc}{2} - X_3\right)$      $M_C = -\frac{\phi Pc}{2} + \phi X_1 + mX_2$   
 $M_1 = M_A - H_A a$      $M_2 = M_B + H_E b$   
 $V_E = \frac{Pc - 2X_3}{L}$      $V_A = P - V_E$      $H_A = H_E = \frac{Pc}{2h} - \frac{X_1 + X_2}{h}$

Extract: 'Kleinogel, Rahmenformeln' 11. Auflage Berlin—Verlag von Wilhelm Ernst & Sohn.

Constants:  $a_1 = \frac{a}{h}$      $b_1 = \frac{b}{h}$   
 $Y_1 = Pc[2\phi^2 - (1 - 3b_1^2)k]$   
 $Y_2 = Pc[\phi C + (3a_1^2 - 1)k]$   
 $M_A - M_E = \frac{Y_2R - Y_1K_1}{N_1}$      $M_B - M_D = \frac{Y_2K_2 - Y_1R}{N_1}$   
 $M_C = -\phi(Pc + M_A) + mM_B$   
 $V_A - V_D = P$      $H_A = H_E = \frac{Pc + M_A - M_B}{h}$   
 $M_1 = M_A - H_A a$      $M_2 = M_B + H_E b$

Constant:  $X_1 = \frac{Pa(B + 3b_1k)}{N_2}$   
 $M_A = -M_E = -X_1$      $M_B = -M_D = Pa - X_1$      $M_C = 0$   
 $V_A = -V_E = -2\left[\frac{Pa - X_1}{L}\right]$      $H_A = -H_E = -P$

Extract: 'Kleinogel, Rahmenformeln' 11. Auflage Berlin—Verlag von Wilhelm Ernst & Sohn.



*w per unit length*

$$M_B - M_D = -\frac{wL^2(3+5m)}{32N} \quad M_C = \frac{wL^2}{16} + mM_B$$

$$H_A - H_E = -\frac{M_B}{h} \quad V_A = \frac{3wL}{8} \quad V_E = \frac{wL}{8}$$


---

*w per unit height*

Constant:  $X = \frac{wf^2(C+m)}{8N}$

$$M_B = +X + \frac{wfh}{2} \quad M_C = -\frac{wf^2}{4} + mX$$

$$M_D = +X - \frac{wfh}{2} \quad V_A = -V_E = -\frac{wfh(1+m)}{2L}$$

$$H_A = -\frac{X}{h} - \frac{wf}{2} \quad H_E = -\frac{X}{h} + \frac{wf}{2}$$

Extract: 'Kleinogel, Rahmenformeln' 11. Auflage Berlin—Verlag von Wilhelm Ernst & Sohn.

$$M_D = -\frac{wh^2}{8} \cdot \frac{2(B+C)+k}{N} \quad M_B = \frac{wh^2}{2} + M_D$$

$$M_C = \frac{wh^2}{4} + mM_D$$

$$V_A = -V_E = -\frac{wh^2}{2L} \quad H_E = -\frac{M_D}{h} \quad H_A = -(wh - H_E)$$


---

Constants:  $a_1 = \frac{a}{h} \quad X = \frac{Pc}{2} \cdot \frac{B+C-k(3a_1^2-1)}{N}$

$$M_B = Pc - X \quad M_D = -X \quad M_C = \frac{Pc}{2} - mX$$

$$M_1 = -a_1X \quad M_2 = Pc - a_1X$$

$$V_E = \frac{Pc}{L} \quad V_A = P - V_E \quad H_A = H_E = \frac{X}{h}$$

Extract: 'Kleinogel, Rahmenformeln' 11. Auflage Berlin—Verlag von Wilhelm Ernst & Sohn.

Constant:  $a_1 = \frac{a}{h}$

$$M_B - M_D = Pc \cdot \frac{\phi C + k(3a^2 - 1)}{N} \quad M_C = -\phi Pc + mM_B$$

$$H_A - H_E = \frac{Pc - M_B}{h} \quad V_A - V_E = P$$

$$M_1 = -a_1(Pc - M_B) \quad M_2 = (1 - a_1)Pc + a_1 M_B$$


---


$$M_B = -M_D = Pa \quad M_C = 0$$

$$H_A = -H_E = -P \quad V_A = -V_E = -\frac{2Pa}{L}$$

Moment at loads =  $\pm Pa$

Extract: 'Kleinogel, Rahmenformeln' 11. Auflage Berlin—Verlag von Wilhelm Ernst & Sohn.

$$M_B - M_D = -\frac{PL}{4} \cdot \frac{C}{N} \quad M_C = +\frac{PL}{4} \cdot \frac{B}{N}$$

$$V_A - V_E = \frac{P}{2} \quad H_A - H_E = -\frac{M_B}{h}$$


---


$$M_D = -\frac{Ph(B+C)}{2N} \quad M_B = Ph + M_D \quad M_C = \frac{Ph}{2} + mM_D$$

$$V_A = -V_E = -\frac{Ph}{L} \quad H_E = -\frac{M_D}{h} \quad H_A = -(P - H_E)$$


---


$$M_B = -M_D = +\frac{Ph}{2} \quad M_C = 0 \quad V_A = -V_E = -\frac{Phm}{L} \quad H_A = -H_E = -\frac{P}{2}$$

Extract: 'Kleinogel, Rahmenformeln' 11. Auflage Berlin—Verlag von Wilhelm Ernst & Sohn.

### 3.1.6.6 Member Buckling Check Using The P-Δ Method To Incorporate Imperfections, Residual Stresses

#### 3.1.6.6.1 GL, ML (P-Δ Based) Perry-Robertson Buckling of Column (Primary Stress is Only Axial) Elements With Imperfections and Residual Stresses

Euler buckling considers only the axial stresses with no provisions for bending stresses. Hence, it is only valid for perfectly straight columns. Perry-Robertson on the other hand includes the decrease in capacity due to initial imperfections of the column. It is based upon finding the mean axial stress that will cause **the onset of yielding** of extreme fibers due to the combined effects of both axial stresses and longitudinal bending stresses. Hence Perry-Robertson implicitly includes yielding of the column at low slenderness ratios. It can be shown starting from the basic equation for the onset of outer fiber yielding (utilizing the amplification factor derived in **Section 3.1.2**, hence the reason it is called buckling by the P-Δ method)

$$\frac{P_{PR}}{A} + \frac{M}{Z} \left( \frac{1}{1 - P_{PR}/P_E} \right) = \sigma_y \quad \text{i.e.} \quad \sigma_{PR} + \frac{Px_0}{Z} \left( \frac{1}{1 - P_{PR}/P_E} \right) = \sigma_y$$

that the Perry-Robertson buckling capacity stress is

$$\sigma_{PR} = \frac{\sigma_y + (1 + \eta)\sigma_E}{2} - \sqrt{\left[ \frac{\sigma_y + (1 + \eta)\sigma_E}{2} \right]^2 - \sigma_y\sigma_E} \quad \text{where the Perry factor, } \eta = \frac{Ax_0}{Z} = \frac{x_0 y}{r^2} = \frac{x_0}{r} \frac{y}{r}$$

The Perry factor  $\eta$  above is the **theoretical imperfection factor** which is dependent upon the **initial eccentricity**,  $x_0$  and also the **cross sectional properties**. But BS 5950-Part 1:2000 goes a step further and requires an increase in the Perry factor due to residual stresses from rolling and welding. It thus states that the Perry factor should be

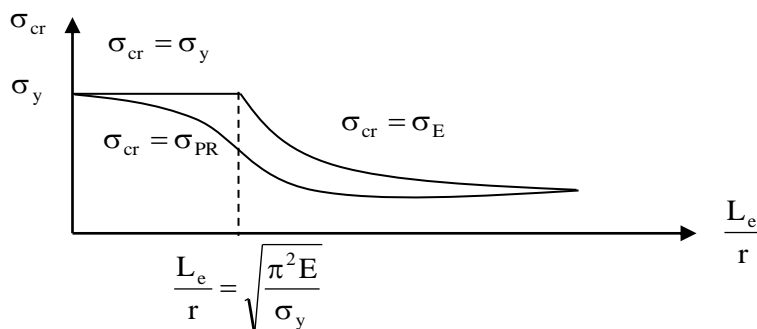
$$\eta = \frac{a}{1000} \frac{(L_e - L_o)}{r_y} \quad a = \text{Robertson constant}$$

$a$  = the Robertson constant as defined in 5950

Strut Curve (From BS 5950)	$a$
(a)	2.0
(b)	3.5
(c)	5.5
(d)	8.0

The Robertson constant,  $a$  divided by 1000, i.e.  $a/1000$  is equivalent to  $(x_0/L)(y/r)$  and includes the initial imperfection, the section shape and also residual stresses. The  $L_o$  plateau is introduced so that for a very low slenderness, the strut reaches its full yield capacity. As an aside, note that although the radius of gyration of an area has no physical meaning, we can consider it to be the distance (from the reference axis) at which the entire area could be concentrated and still have the same moment of inertia as the original area.

Note that  $\sigma_{PR}$  approaches  $\sigma_E$  for large slenderness ratios i.e. for very slender columns; This means that the sensitivity of slender columns to imperfections is less than that of stocky columns.



The capacity to buckling should be checked **about both the major and minor axes**. The slenderness is a function of the cross section and the boundary conditions, hence the critical buckling capacity may occur about either the major or minor axes. The critical load capacity is

$$P_{PR} = \sigma_{PR} A$$

Column Buckling Check BS 5950-Part 1:2000	cl. 4.7.4
Allocation of strut curve = f (section type, max thickness, axis of buckling)	Table 23
Compressive strength, $p_c$ , smaller of $p_{c_{xx}} = f(p_y, \lambda_{xx})$ and $p_{c_{yy}} = f(p_y, \lambda_{yy})$ (N/mm <sup>2</sup> )	Table 24
Slenderness, $\lambda_{xx} = L_{E_{xx}} / r_{xx}$ and $\lambda_{yy} = L_{E_{yy}} / r_{yy}$	
Effective length, $L_{E_{xx}}$ and $L_{E_{yy}}$	Table 22
Ensure $F/(A p_c) < 1$ for Class 1, 2 and 3 sections	cl. 4.7.4

Note that for **welded** I, H or box sections,  $p_c$  should be obtained from Table 24 or calculated using a  $p_y$  value **lessened by 20 N/mm<sup>2</sup>**. A fundamental parameter is the effective length,  $L_E$ .

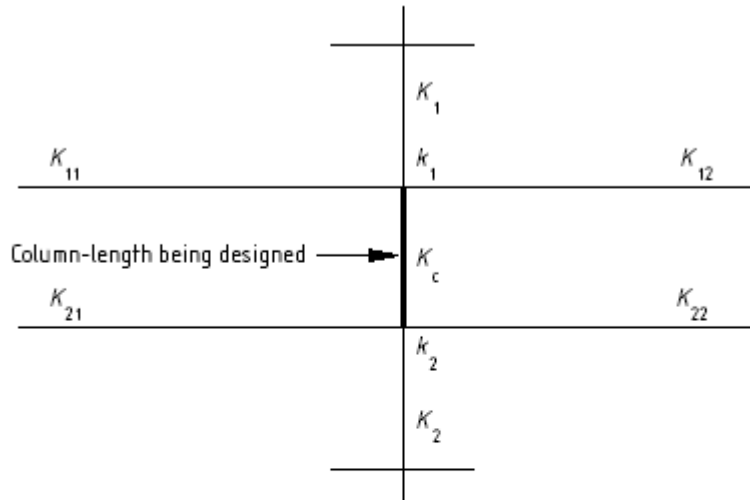
**Table 22 — Nominal effective length  $L_E$  for a compression member<sup>a</sup>**

a) non-sway mode			
Restraint (in the plane under consideration) by other parts of the structure		$L_E$	
Effectively held in position at both ends	Effectively restrained in direction at both ends	0.7L	
	Partially restrained in direction at both ends	0.85L	
	Restrained in direction at one end	0.85L	
	Not restrained in direction at either end	1.0L	
b) sway mode			
One end	Other end	$L_E$	
Effectively held in position and restrained in direction	Not held in position	Effectively restrained in direction	1.2L
		Partially restrained in direction	1.5L
		Not restrained in direction	2.0L

<sup>a</sup> Excluding angle, channel or T-section struts designed in accordance with 4.7.10.

model	example	factor
		1.0
		0.85
		2.0
		0.7
		1.0

Another method used to determine  $L_E$  in buildings given in BS 5950-Part 1:2000 is based on the adjacent member stiffnesses to determine coefficient  $k_1$  and  $k_2$  from which design charts are used to determine  $L_E$  for sway and non-sway frames (the latter only employed if the alternative amplified sway method is not used).



Distribution factors:

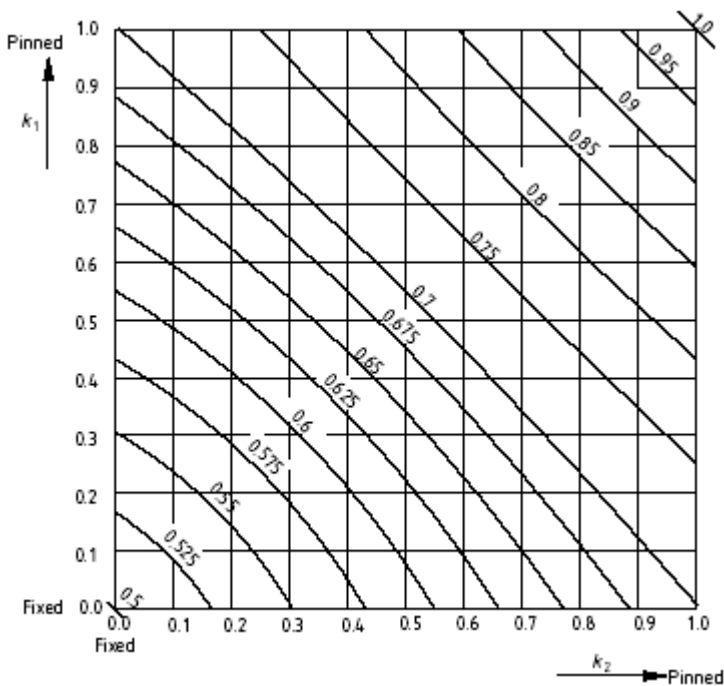
$$k_1 = \frac{K_c + K_1}{K_c + K_1 + K_{11} + K_{12}}$$

$$k_2 = \frac{K_c + K_2}{K_c + K_2 + K_{21} + K_{22}}$$

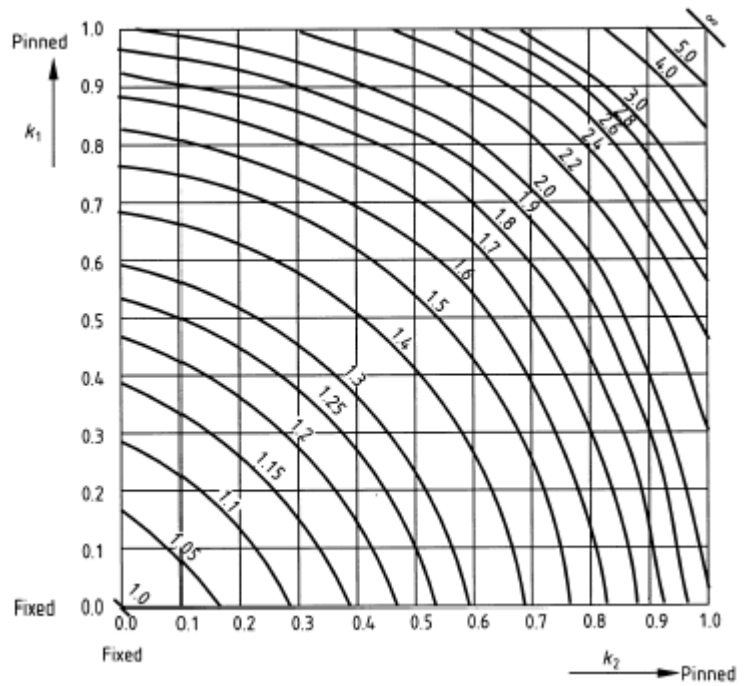
where

$K_1$  and  $K_2$  are the values of  $K_c$  for the adjacent column-lengths;

$K_{11}$ ,  $K_{12}$ ,  $K_{21}$  and  $K_{22}$  are the values of  $K_b$  for the adjacent beams.



Non-Sway



Sway

The choice of strut curve is defined by Table 23 as follows.

**Table 23 — Allocation of strut curve**

Type of section	Maximum thickness (see note 1)	Axis of buckling	
		x-x	y-y
Hot-finished structural hollow section		a)	a)
Cold-formed structural hollow section		c)	c)
Rolled I-section	≤ 40 mm	a)	b)
	> 40 mm	b)	c)
Rolled H-section	≤ 40 mm	b)	c)
	> 40 mm	c)	d)
Welded I or H-section (see note 2 and 4.7.5)	≤ 40 mm	b)	c)
	> 40 mm	b)	d)
Rolled I-section with welded flange cover plates with 0.25 < U/B < 0.8 as shown in Figure 14a)	≤ 40 mm	a)	b)
	> 40 mm	b)	c)
Rolled H-section with welded flange cover plates with 0.25 < U/B < 0.8 as shown in Figure 14a)	≤ 40 mm	b)	c)
	> 40 mm	c)	d)
Rolled I or H-section with welded flange cover plates with U/B ≥ 0.8 as shown in Figure 14b)	≤ 40 mm	b)	a)
	> 40 mm	c)	b)
Rolled I or H-section with welded flange cover plates with U/B ≤ 0.25 as shown in Figure 14c)	≤ 40 mm	b)	c)
	> 40 mm	b)	d)
Welded box section (see note 3 and 4.7.5)	≤ 40 mm	b)	b)
	> 40 mm	c)	c)
Round, square or flat bar	≤ 40 mm	b)	b)
	> 40 mm	c)	c)
Rolled angle, channel or T-section		Any axis: c)	
Two rolled sections laced, battened or back-to-back			
Compound rolled sections			
NOTE 1 For thicknesses between 40 mm and 50 mm the value of $p_c$ may be taken as the average of the values for thicknesses up to 40 mm and over 40 mm for the relevant value of $p_y$ .			
NOTE 2 For welded I or H-sections with their flanges thermally cut by machine without subsequent edge grinding or machining, for buckling about the y-y axis, strut curve b) may be used for flanges up to 40 mm thick and strut curve c) for flanges over 40 mm thick.			
NOTE 3 The category "welded box section" includes any box section fabricated from plates or rolled sections, provided that all of the longitudinal welds are near the corners of the cross-section. Box sections with longitudinal stiffeners are NOT included in this category.			

The  $p_c$  of Table 24 can be calculated as

$$p_c = \frac{p_E p_y}{\phi + (\phi^2 - p_E p_y)^{0.5}}$$

where

$$\phi = \frac{p_y + (\eta + 1)p_E}{2}$$

$$p_E = (\pi^2 E / \lambda^2)$$

and the Perry factor,  $\eta$

$$\eta = a(\lambda - \lambda_0) / 1\,000 \text{ but } \eta \geq 0$$

in which the limiting slenderness  $\lambda_0$  is

$$0.2(\pi^2 E / p_y)^{0.5}$$

and the Robertson constant,  $a$  is defined as follows

$a$  = the Robertson constant as defined in 5950

Strut Curve (From BS 5950)	$a$
(a)	2.0
(b)	3.5
(c)	5.5
(d)	8.0

Table 23 — Compressive strength  $p_c$  (N/mm<sup>2</sup>) (continued)

3) Values of  $p_c$  (N/mm<sup>2</sup>) with  $l \leq 100$  for stress curve 3

l	Steel grade and design strength $p_y$ (N/mm <sup>2</sup> )															
	S 275								S 460							
	275	295	355	390	460	510	550	590	460	510	550	590	660	725	785	845
10	275	295	355	390	460	510	550	590	590	660	725	785	845	910	975	
20	275	295	355	390	460	510	550	590	590	660	725	785	845	910	975	
30	275	295	355	390	460	510	550	590	590	660	725	785	845	910	975	
40	275	295	355	390	460	510	550	590	590	660	725	785	845	910	975	
50	275	295	355	390	460	510	550	590	590	660	725	785	845	910	975	
60	275	295	355	390	460	510	550	590	590	660	725	785	845	910	975	
70	275	295	355	390	460	510	550	590	590	660	725	785	845	910	975	
80	275	295	355	390	460	510	550	590	590	660	725	785	845	910	975	
90	275	295	355	390	460	510	550	590	590	660	725	785	845	910	975	
100	275	295	355	390	460	510	550	590	590	660	725	785	845	910	975	

Table 24 — Compressive strength  $p_c$  (N/mm<sup>2</sup>) (continued)

3) Values of  $p_c$  (N/mm<sup>2</sup>) with  $l \geq 110$  for stress curve 3

l	Steel grade and design strength $p_y$ (N/mm <sup>2</sup> )															
	S 275								S 460							
	275	295	355	390	460	510	550	590	460	510	550	590	660	725	785	845
110	275	295	355	390	460	510	550	590	590	660	725	785	845	910	975	
120	275	295	355	390	460	510	550	590	590	660	725	785	845	910	975	
130	275	295	355	390	460	510	550	590	590	660	725	785	845	910	975	
140	275	295	355	390	460	510	550	590	590	660	725	785	845	910	975	
150	275	295	355	390	460	510	550	590	590	660	725	785	845	910	975	
160	275	295	355	390	460	510	550	590	590	660	725	785	845	910	975	
170	275	295	355	390	460	510	550	590	590	660	725	785	845	910	975	
180	275	295	355	390	460	510	550	590	590	660	725	785	845	910	975	
190	275	295	355	390	460	510	550	590	590	660	725	785	845	910	975	
200	275	295	355	390	460	510	550	590	590	660	725	785	845	910	975	

Table 23 — Compressive strength  $p_c$  (N/mm<sup>2</sup>) (continued)

3) Values of  $p_c$  (N/mm<sup>2</sup>) with  $l \leq 110$  for stress curve 3

l	Steel grade and design strength $p_y$ (N/mm <sup>2</sup> )															
	S 275								S 460							
	275	295	355	390	460	510	550	590	460	510	550	590	660	725	785	845
110	275	295	355	390	460	510	550	590	590	660	725	785	845	910	975	
120	275	295	355	390	460	510	550	590	590	660	725	785	845	910	975	
130	275	295	355	390	460	510	550	590	590	660	725	785	845	910	975	
140	275	295	355	390	460	510	550	590	590	660	725	785	845	910	975	
150	275	295	355	390	460	510	550	590	590	660	725	785	845	910	975	
160	275	295	355	390	460	510	550	590	590	660	725	785	845	910	975	
170	275	295	355	390	460	510	550	590	590	660	725	785	845	910	975	
180	275	295	355	390	460	510	550	590	590	660	725	785	845	910	975	
190	275	295	355	390	460	510	550	590	590	660	725	785	845	910	975	
200	275	295	355	390	460	510	550	590	590	660	725	785	845	910	975	

Table 24 — Compressive strength  $p_c$  (N/mm<sup>2</sup>) (continued)

3) Values of  $p_c$  (N/mm<sup>2</sup>) with  $l \geq 110$  for stress curve 3

l	Steel grade and design strength $p_y$ (N/mm <sup>2</sup> )															
	S 275								S 460							
	275	295	355	390	460	510	550	590	460	510	550	590	660	725	785	845
110	275	295	355	390	460	510	550	590	590	660	725	785	845	910	975	
120	275	295	355	390	460	510	550	590	590	660	725	785	845	910	975	
130	275	295	355	390	460	510	550	590	590	660	725	785	845	910	975	
140	275	295	355	390	460	510	550	590	590	660	725	785	845	910	975	
150	275	295	355	390	460	510	550	590	590	660	725	785	845	910	975	
160	275	295	355	390	460	510	550	590	590	660	725	785	845	910	975	
170	275	295	355	390	460	510	550	590	590	660	725	785	845	910	975	
180	275	295	355	390	460	510	550	590	590	660	725	785	845	910	975	
190	275	295	355	390	460	510	550	590	590	660	725	785	845	910	975	
200	275	295	355	390	460	510	550	590	590	660	725	785	845	910	975	



### 3.1.6.6.2 GL, ML (P-Δ Based) Secant Buckling of Column (Primary Stress is Axial) Elements With Eccentric Loading, Initial Imperfections and Residual Stresses

The Secant buckling stress for an eccentrically (with eccentricity  $e$ ) loaded column is as follows. It is based upon finding the mean axial stress that will cause **the onset of** yielding of extreme fibers due to the combined effects of both axial stresses and longitudinal bending stresses, the latter of which is primarily a result of the eccentricity of the axial load. The initial imperfections and residual stresses can also be added to the loading eccentricity,  $e$  for an equivalent eccentricity,  $e$ .

$$\sigma_{\text{SECANT}} = \frac{\sigma_y}{1 + \frac{ec}{r^2} \sec\left(\frac{L_e}{2r} \sqrt{\frac{\sigma_{\text{SECANT}}}{E}}\right)}$$

The equation is an implicit formula, and hence iteration is required to solve for  $\sigma_{\text{SECANT}}$ . Note that the radius of gyration,  $r$  is the minor axis radius of gyration. Also,  $c$  denotes the distance from the neutral axis to the extreme fibre on the concave or compression side of the bent column. The term  $ec/r^2$  is called the **eccentric ratio**, a value which is often calibrated to physical tests. In fact, it is the same as the Perry factor,  $\eta$  had there been no eccentricity of the loading. Typical conventional design of structural steel columns employs a value of 0.25 for  $ec/r^2$ .

**3.1.6.6.3 GL, ML (P-Δ Based) Lateral-Torsional Buckling of Beam (Primary Stress is Only Bending) Elements With Imperfections and Residual Stresses**

A critical parameter is the effective length,  $L_E$  and is defined in clauses cl. 4.3.5.1 to cl. 4.3.5.5 for

- simple beams without intermediate lateral restraints (Table 13),**
- simple beams with intermediate lateral restraints ( $1.0L_{LT}$  normal loads or  $1.2L_{LT}$  destabilizing loads),**
- beams with double curvature bending,**
- cantilever beams without intermediate lateral restraints (Table 14),**
- cantilever beams with intermediate lateral restraints ( $1.0L$  normal loads or Table 14 destabilizing loads).**

Note that  $L_{LT}$  is the segment length between restraints, and the span length is  $L$ . Note that the destabilizing loading condition should be taken where a load is applied to the top flange of a beam or a cantilever, and both the load and the flange are free to deflect laterally (and possibly rotationally also) relative to the centroid of the cross-section.

<b>Lateral Torsional Buckling Moment Capacity, <math>M_b / m_{LT}</math> BS 5950-Part 1:2000</b>	cl.4.3
<b>Critical slenderness about minor axis <math>\lambda_{yy} = L_{Ey}/r_y</math></b>	
Effective length, $L_{Ey}$	cl. 4.3.5.1 to cl 4.3.5.5
Radius of gyration about the minor axis, $r_y$	
<b>Effective critical axis slenderness <math>\lambda_{LT} = uv\lambda(\beta_w)^{0.5}</math></b>	
Buckling parameter, $u$ For rolled equal flange I-, H- or channel section, $u = 0.9$ conservatively	cl. 4.3.6.8
Torsional index, $x$ For rolled equal flange I-, H- or channel section, $x = D/T$ conservatively	cl. 4.3.6.8
Slenderness factor, $v = f(\lambda/x, \text{flange ratio } \eta)$ For equal flange I-, H- or channel $v = 1/(1+0.05(\lambda/x)^2)^{1/4}$	cl. 4.3.6.7 Table 19
$\beta_w = 1.0$ for Class 1 plastic and Class 2 compact sections	cl. 4.3.6.9
<b>Lateral torsional buckling moment capacity, <math>M_b/m</math></b>	
Buckling resistance moment, $M_b = p_b S_x$ for Class 1 and Class 2 sections Buckling resistance moment, $M_b = p_b Z_x$ for Class 3 sections Buckling resistance moment, $M_b = p_b Z_{eff}$ for Class 4 sections	cl. 4.3.6.4
Bending strength, $p_b = f(p_y, \lambda_{LT})$	cl. 4.3.6.5 Table 16 or Table 17
Equivalent uniform moment factor, $m_{LT}$	cl. 4.3.6.6 Table 18
<b>Ensure LTB moment capacity <math>M_b/m_{LT} &gt;</math> applied design moment <math>M_d</math></b>	

Lateral torsional buckling cannot occur in beams loaded in their weaker principal plane; under the action of increasing load they will collapse simply by plastic action and excessive in-plane deformation. Hence, the check need only be made for bending about the major axis.

Lateral torsional buckling cannot occur for sections which are double symmetric such as a SHS, this being accounted for by the fact that  $\lambda_{LT}$  becomes zero when  $I_{xx} = I_{yy}$ .

The equivalent uniform moment factor,  $m_{LT}$  is used when the bending moment is not uniform across the length of the beam. A value of 1.0 is obviously conservative. For the destabilizing loading condition  $m_{LT}$  should be taken as 1.0.

The LTB bending resistance given by Table 16 or Table 17 is derived from

$$p_b = \frac{p_E p_y}{\phi_{LT} + (\phi_{LT}^2 - p_E p_y)^{0.5}}$$

where

$$p_E = (\pi^2 E / \lambda_{LT}^2)$$

$$\phi_{LT} = \frac{p_y + (\eta_{LT} + 1)p_E}{2}$$

where the Perry factor  $\eta_{LT}$

a) for rolled sections:

$$\eta_{LT} = \alpha_{LT}(\lambda_{LT} - \lambda_{L0})/1\,000 \quad \text{but} \quad \eta_{LT} \geq 0$$

b) for welded sections:

$$\text{— if } \lambda_{LT} \leq \lambda_{L0}: \quad \eta_{LT} = 0$$

$$\text{— if } \lambda_{L0} < \lambda_{LT} < 2\lambda_{L0}: \quad \eta_{LT} = 2\alpha_{LT}(\lambda_{LT} - \lambda_{L0})/1\,000$$

$$\text{— if } 2\lambda_{L0} \leq \lambda_{LT} \leq 3\lambda_{L0}: \quad \eta_{LT} = 2\alpha_{LT}\lambda_{L0}/1\,000$$

$$\text{— if } \lambda_{LT} > 3\lambda_{L0}: \quad \eta_{LT} = \alpha_{LT}(\lambda_{LT} - \lambda_{L0})/1\,000$$

and where the Robertson constant  $\alpha_{LT}$  should be taken as 7.0 and the limiting equivalent slenderness,  $\lambda_{L0}$  is  $0.4(\pi^2 E / p_y)^{0.5}$

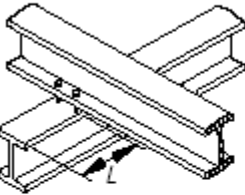
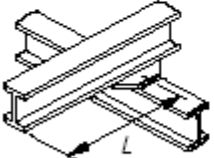
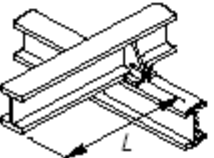
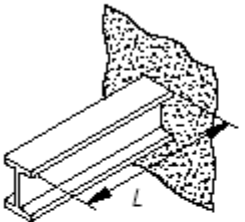
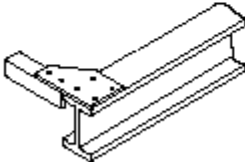
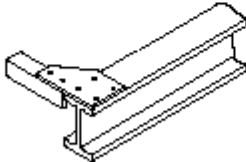
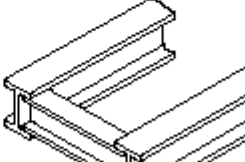
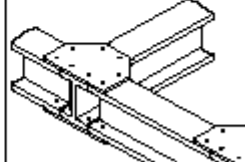
**Restraints** may be deemed to provide adequate stiffness and strength if capable of resisting a lateral force of at least **2.5%** of the maximum **factored** force in the compression flange.

**Table 13 — Effective length  $L_E$  for beams without intermediate restraint**

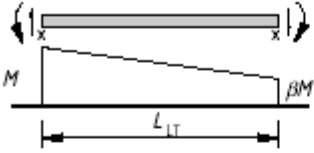
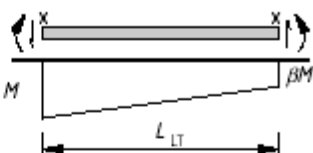
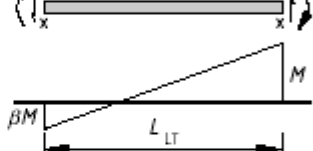
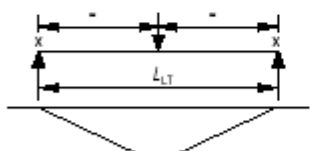
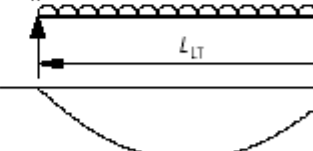
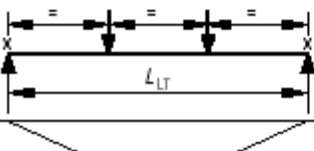
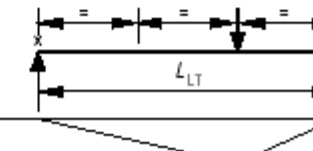
Conditions of restraint at supports		Loading condition	
		Normal	Destabilizing
Compression flange laterally restrained.	Both flanges fully restrained against rotation on plan.	$0.7L_{LT}$	$0.85L_{LT}$
Nominal torsional restraint against rotation about longitudinal axis, as given in 4.2.2.	Compression flange fully restrained against rotation on plan.	$0.75L_{LT}$	$0.9L_{LT}$
	Both flanges partially restrained against rotation on plan.	$0.8L_{LT}$	$0.95L_{LT}$
	Compression flange partially restrained against rotation on plan.	$0.85L_{LT}$	$1.0L_{LT}$
	Both flanges free to rotate on plan.	$1.0L_{LT}$	$1.2L_{LT}$
Compression flange laterally unrestrained.	Partial torsional restraint against rotation about longitudinal axis provided by connection of bottom flange to supports.	$1.0L_{LT} + 2D$	$1.2L_{LT} + 2D$
Both flanges free to rotate on plan.	Partial torsional restraint against rotation about longitudinal axis provided only by pressure of bottom flange onto supports.	$1.2L_{LT} + 2D$	$1.4L_{LT} + 2D$

*D* is the overall depth of the beam.

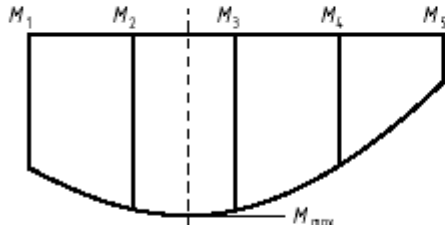
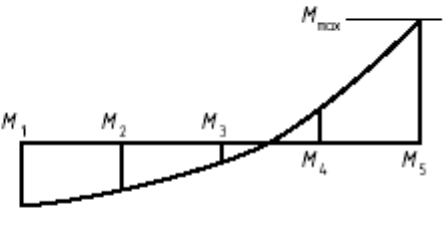
**Table 14 — Effective length  $L_E$  for cantilevers without intermediate restraint**

Restraint conditions		Loading conditions	
At support	At tip	Normal	Destabilizing
a) Continuous, with lateral restraint to top flange 	1) Free 2) Lateral restraint to top flange 3) Torsional restraint 4) Lateral and torsional restraint	3.0L 2.7L 2.4L 2.1L	7.5L 7.5L 4.5L 3.6L
b) Continuous, with partial torsional restraint 	1) Free 2) Lateral restraint to top flange 3) Torsional restraint 4) Lateral and torsional restraint	2.0L 1.8L 1.6L 1.4L	5.0L 5.0L 3.0L 2.4L
c) Continuous, with lateral and torsional restraint 	1) Free 2) Lateral restraint to top flange 3) Torsional restraint 4) Lateral and torsional restraint	1.0L 0.9L 0.8L 0.7L	2.5L 2.5L 1.5L 1.2L
d) Restrained laterally, torsionally and against rotation on plan 	1) Free 2) Lateral restraint to top flange 3) Torsional restraint 4) Lateral and torsional restraint	0.8L 0.7L 0.6L 0.5L	1.4L 1.4L 0.6L 0.5L
<b>Tip restraint conditions</b>			
1) Free  (not braced on plan)	2) Lateral restraint to top flange  (braced on plan in at least one bay)	3) Torsional restraint  (not braced on plan)	4) Lateral and torsional restraint  (braced on plan in at least one bay)

**Table 18 — Equivalent uniform moment factor  $m_{LT}$  for lateral-torsional buckling**  
(continued overleaf)

Segments with end moments only (values of $m_{LT}$ from the formula for the general case)		$\beta$	$m_{LT}$
$\beta$ positive		1.0	1.00
		0.9	0.96
		0.8	0.92
		0.7	0.88
		0.6	0.84
		0.5	0.80
		0.4	0.76
		0.3	0.72
		0.2	0.68
		0.1	0.64
$\times$ Lateral restraint		0.0	0.60
$\beta$ negative		-0.1	0.56
		-0.2	0.52
		-0.3	0.48
		-0.4	0.46
		-0.5	0.44
		-0.6	0.44
		-0.7	0.44
		-0.8	0.44
		-0.9	0.44
		-1.0	0.44
<b>Specific cases (no intermediate lateral restraint)</b>			
		$m_{LT} = 0.850$	
		$m_{LT} = 0.925$	
		$m_{LT} = 0.925$	
		$m_{LT} = 0.744$	

**Table 18 — Equivalent uniform moment factor  $m_{LT}$  for lateral-torsional buckling** (continued)

General case (segments between intermediate lateral restraints)	
	
For beams: $m_{LT} = 0.2 + \frac{0.15M_2 + 0.5M_3 + 0.15M_4}{M_{max}}$	but $m_{LT} \geq 0.44$
All moments are taken as positive. The moments $M_2$ and $M_4$ are the values at the quarter points, the moment $M_3$ is the value at mid-length and $M_{max}$ is the maximum moment in the segment.	
For cantilevers without intermediate lateral restraint: $m_{LT} = 1.00$ .	

### 3.1.6.6.4 GL, ML (P-Δ Based) Buckling of Beam-Column Elements (Primary Stress is Axial and Bending) With Imperfections and Residual Stresses

#### Simplified Approach (cl. 4.8.3.3.1)

For **Perry-Robertson flexural buckling** about the major or minor axes with **additional primary moments** about the major and minor axes, the following expression must be satisfied

$$\frac{F_c}{P_c} + \frac{m_x M_x}{P_y Z_x} + \frac{m_y M_y}{P_y Z_y} \leq 1$$

Although unconservatively no amplification of major axis moment considered, conservatively the minor axis elastic capacity is used.

Note that  $P_c$  is the Perry-Robertson flexural buckling capacity and is the smaller of  $P_{cx}$  and  $P_{cy}$ . The major axis flexural buckling factor,  $m_x$  and the minor axis flexural buckling factor,  $m_y$  are obtained from Table 26 (cl. 4.8.3.3.4).

For **lateral torsional buckling** with **Perry-Robertson flexural buckling about minor axis** and **additional primary moment about minor axis**, the following expression must also be satisfied.

$$\frac{F_c}{P_{cy}} + \frac{m_{LT} M_{LT}}{M_b} + \frac{m_y M_y}{P_y Z_y} \leq 1$$

Although unconservatively no amplification of minor axis moment considered, conservatively the minor axis elastic capacity is used.

Note that  $P_{cy}$  is the minor axis Perry-Robertson flexural buckling capacity.  $M_{LT}$  is the applied major axis moment.  $M_y$  is the applied minor axis moment.  $M_b / m_{LT}$  is the lateral torsional buckling capacity.

#### More Exact Approach for I- or H- Sections with Equal Flanges (cl. 4.8.3.3.2)

For **Perry-Robertson flexural buckling** about the major with **additional primary moments** about the major or minor axes, the following expression must be satisfied

$$\frac{F_c}{P_{cx}} + \frac{m_x M_x}{M_{cx}} \left( 1 + 0.5 \frac{F_c}{P_{cx}} \right) + 0.5 \frac{m_{yx} M_y}{M_{cy}} \leq 1$$

where  $m_{yx}$  is obtained from Table 26 (cl. 4.8.3.3.4). The major axis flexural buckling factor,  $m_x$  is also obtained from Table 26 (cl. 4.8.3.3.4). Note that  $P_{cx}$  is the major axis Perry-Robertson flexural buckling capacity.  $M_x$  and  $M_y$  are the major and minor axes applied moments.  $M_{cx}$  and  $M_{cy}$  are the major and minor axes plastic moment capacities.

For **lateral torsional buckling (of course about minor axis)** with **Perry-Robertson flexural buckling about minor axis** and **additional primary moment about minor axis**, the following expression must also be satisfied.

$$\frac{F_c}{P_{cy}} + \frac{m_{LT} M_{LT}}{M_b} + \frac{m_y M_y}{M_{cy}} \left( 1 + \frac{F_c}{P_{cy}} \right) \leq 1$$

For an **interactive buckling**, the following expression must also be satisfied.

$$\frac{m_x M_x (1 + 0.5(F_c/P_{cx}))}{M_{cx} (1 - F_c/P_{cx})} + \frac{m_y M_y (1 + F_c/P_{cy})}{M_{cy} (1 - F_c/P_{cy})} \leq 1$$

Similar more exact equations exist for CHS, RHS and box sections with equal flanges in cl. 4.8.3.3.3.

**Table 26 — Equivalent uniform moment factor  $m$  for flexural buckling**

Segments with end moments only (values of $m$ from the formula for the general case)		$\beta$	$m$
$\beta$ positive		1.0	1.00
		0.9	0.96
		0.8	0.92
		0.7	0.88
		0.6	0.84
		0.5	0.80
		0.4	0.76
		0.3	0.72
		0.2	0.68
		0.1	0.64
		0.0	0.60
		-0.1	0.58
		-0.2	0.56
		-0.3	0.54
		-0.4	0.52
		-0.5	0.50
$\beta$ negative		-0.6	0.48
		-0.7	0.46
		-0.8	0.44
		-0.9	0.42
		-1.0	0.40

Segments between intermediate lateral restraints	
Specific cases	General case
$m = 0.2 + \frac{0.1M_2 + 0.6M_3 + 0.1M_4}{M_{max}} \text{ but } m \geq \frac{0.8M_{24}}{M_{max}}$	
<p>The moments <math>M_2</math> and <math>M_4</math> are the values at the quarter points and the moment <math>M_3</math> is the value at mid-length.</p>	
<p>If <math>M_2</math>, <math>M_3</math> and <math>M_4</math> all lie on the same side of the axis, their values are all taken as positive. If they lie both sides of the axis, the side leading to the larger value of <math>m</math> is taken as the positive side.</p>	
<p>The values of <math>M_{max}</math> and <math>M_{24}</math> are always taken as positive. <math>M_{max}</math> is the maximum moment in the segment and <math>M_{24}</math> is the maximum moment in the central half of the segment.</p>	

### 3.1.6.7 Overall Portal Frame and Multi-Storey Building P-Δ Analysis Using The Amplified Sway Method

Sufficient lateral stability must be provided to prevent instability. Sufficient strength must be provided to take the increased forces (P-Δ effects) as a result of the slenderness.

To investigate the susceptibility of a structure to P-Δ effects, the elastic buckling load factor is calculated. Methods based on BS 5950-Part 1:2000 for calculating  $\lambda_{cr}$  is given in **Section 3.2.5.2.2**.

Then assuming  $4 < \lambda_{cr} < 10$ , the P-Δ effects should be taken into account for the **real horizontal loads (wind)** according to the amplified sway method. Had  $\lambda_{cr}$  been greater than 10, then the building is considered **non-sway** and amplification effects,  $m$  on lateral forces need not be considered. For portal frames, if under the Notional Horizontal Forces (NHF) of the gravity load combination, the horizontal deflections at the tops of the column are less than height/1000, P-Δ effects need not be considered. Had  $\lambda_{cr}$  been less than 4, then a full nonlinear static analysis must be undertaken to account for the P-Δ effect.

The amplified sway factor for the real horizontal loads (wind) (in perfect accordance with theory presented in **Section 3.1.2**) is (cl. 2.4.2.7)

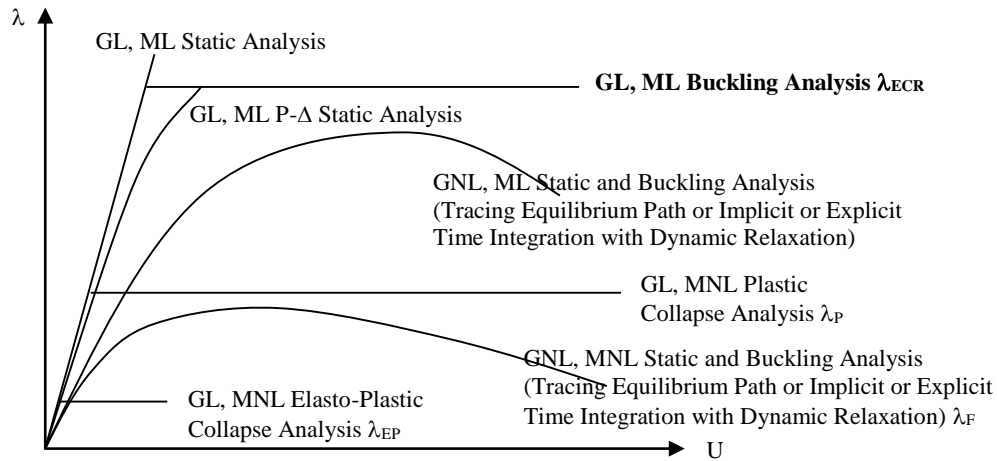
$$m = \frac{\lambda_{cr}}{\lambda_{cr} - 1}$$

For clad structures with the stiffening effect of masonry infill wall panels or diaphragms of profiled steel sheeting the amplified sway factor is decreased to

$$m = \frac{\lambda_{cr}}{1.15\lambda_{cr} - 1.5} \quad \text{but} \quad m > 1.0$$

## 3.2 GL, ML Buckling Analysis by The Implicit Linearized Eigenvalue Analysis

### 3.2.1 Linearization of Tangent Stiffness Matrix and Formulating The Linear Eigenvalue Problem



This section describes a simple and practical method of allowing for the effects of overall buckling of the structure. While the method can be applied to the buckling of single members, this is more easily dealt with using conventional codified methods. Where conventional codified methods falls short, is when the boundary conditions of the structural members (which determines the all important buckling effective length) is not intuitive.

Linear elastic buckling analysis is the prediction of the critical loads (and their associated buckling mode shapes) when the structure is at the point of elastic instability. This instability occurs when the tangent stiffness matrix becomes singular as a result of the increase in the negative stiffness contribution of the geometric (differential) stiffness.

At collapse, the structure has buckled (experienced elastic instability) but has no fully plastic hinges i.e. no considerations of material nonlinearity have been taken into account. Hence this method of analysis is only valid if firstly, the structure remains materially linear elastic throughout until the application of the critical load causes an elastic instability. Secondly, it is a geometrically linear method of analysis. Hence the deflections must be small enough for the stiffnesses to be based upon the initial undeflected (by the collapsing load factor) geometry.

Let us denote the initial undeflected (by the collapsing load factor) configuration by A. In the ( $\mathbf{K}_G^A$  From  $\mathbf{K}_E^A$ ) elastic buckling analysis, at collapse, the elastic stiffness matrix at the initial undeflected (by the collapsing load factor) configuration is balanced by the geometric (differential) stiffness due to the load factor.

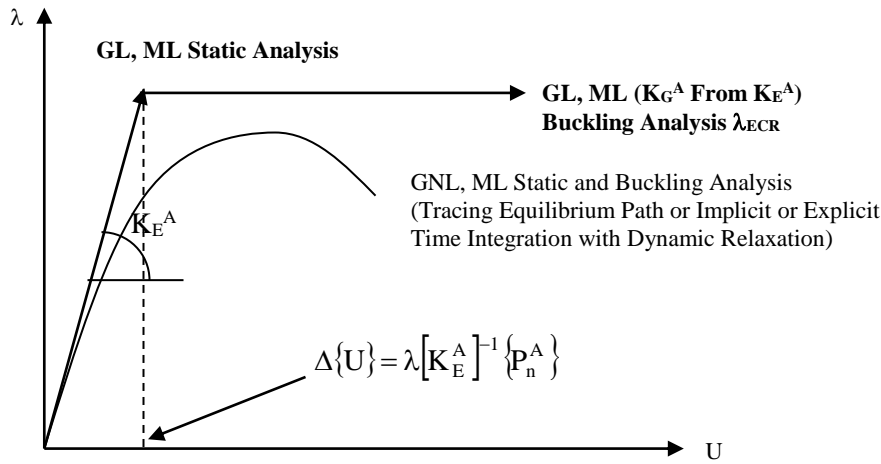
$$[\mathbf{K}_E^A] + \lambda[\mathbf{K}_G^{AKE}] \{\phi\} = \{0\}$$

$\mathbf{K}_G^{AKE}$  represents the geometric stiffness matrix which was calculated based on the *small* displacements obtained by solving the system (with the collapsing load) with stiffness  $\mathbf{K}_E^A$ . Hence, a static analysis is first performed (a first pass) based on  $\mathbf{K}_E^A$  with an applied external load (which is a fraction of the critical buckling load so that the buckling load factor will be more than 1) to generate forces in the structural elements, which in turn provides input for the computation of  $\mathbf{K}_G^{AKE}$ . Then, a buckling analysis is performed effectively finding the instances when factored by  $\lambda$ ,  $\mathbf{K}_G^{AKE}$  balances  $\mathbf{K}_E^A$ . Hence, since both the elastic stiffness matrix  $\mathbf{K}_E^A$  and the geometric stiffness matrix  $\mathbf{K}_G^{AKE}$  are based upon the initial undeflected (by the collapsing load factor) configuration A, the method is only valid if deflections are small enough for there to be **negligible change in  $\mathbf{K}_E^A$  and the geometric stiffness matrix varies linearly with the load factor such that it can be expressed as  $\lambda\mathbf{K}_G^{AKE}$  until elastic instability has been attained.** The inherent assumption that the geometric stiffness matrix varies linearly with the load factor  $\lambda\mathbf{K}_G^{AKE}$  enables any external load to be applied in the first pass since  $\mathbf{K}_G^{AKE}$  will be scaled accordingly. Hence, any initial load (less than the collapse load so that  $\lambda < 1$ ) may be applied and the corresponding load factor  $\lambda$  will be obtained such that the collapse load  $\lambda P_{initial}$  or rather expressed as  $\lambda P_n^A$  will be the same. The value  $\lambda$  are the scale

factor by which the applied load  $P_n^A$  is multiplied to produce the critical buckling load  $P_{cr}$ . The magnitude of the applied load  $P_n^A$  is arbitrary for arriving at the correct  $P_{cr}$ . As an example, if  $P_n^A$  is increased by a factor of 10, then the calculated value of  $\lambda$  is reduced by a factor of 10; in other words, their resulting product  $P_{cr}$  remains the same. This is because the differential stiffness of the finite elements are linear functions of the axial load  $F_x$  and the geometry  $l$  of the element (as shown below for the CBAR element) and for linear analyses, the axial load increases linearly with the applied loads  $P_n^A$ .

$$[k_d]_l = \begin{bmatrix} \frac{6F_{x_l}}{5l_l} & \frac{-F_{x_l}}{10} & \frac{-6F_{x_l}}{5l_l} & \frac{-F_{x_l}}{10} \\ \frac{-F_{x_l}}{10} & \frac{2l_l F_{x_l}}{15} & \frac{F_{x_l}}{10} & \frac{-l_l F_{x_l}}{30} \\ \frac{-6F_{x_l}}{5l_l} & \frac{F_{x_l}}{10} & \frac{6F_{x_l}}{5l_l} & \frac{F_{x_l}}{10} \\ \frac{-F_{x_l}}{10} & \frac{-l_l F_{x_l}}{30} & \frac{F_{x_l}}{10} & \frac{2l_l F_{x_l}}{15} \end{bmatrix}$$

Clearly, assuming that deflections are indeed small, the method is only valid for the first buckling mode as subsequent deflections will certainly be too large. To illustrate the assumption, this linearized buckling analysis basically traces the following equilibrium path.



That is to say, the structure follows the equilibrium path governed by the **constant** stiffness  $K_E^A$  until suddenly it loses all its stiffness (in a direction dissimilar to that of the critical load) and buckles when  $\lambda K_G^{AKE}$  matches  $K_E^A$ . This is valid if  $K_E^A$  is assumed not to vary with the  $\{U\}$  and if the component forces  $\{f\}$  are approximately linear in terms of the load factor  $\lambda$  such that the geometric stiffness matrix varies linearly with the load factor allowing it to be expressed as  $\lambda K_G^{AKE}$  until elastic instability has been attained, both of which are quite valid as long as the tangential increment of displacement due to  $\lambda$  is small. This can be estimated from

$$\Delta\{U\} = \lambda [K_E^A]^{-1} \{P_n^A\} \longleftarrow \text{Hence, the forces at linear buckling are the load factor times the linear static displacement.}$$

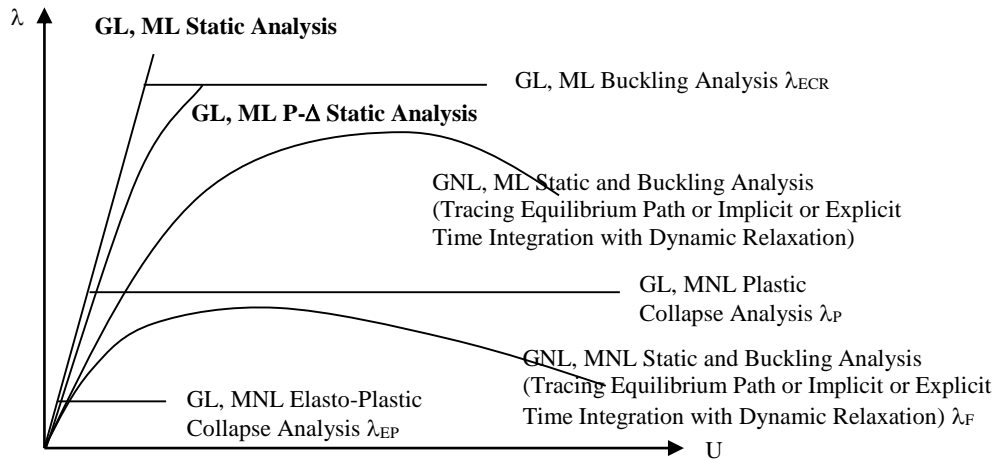
where  $\Delta\{U\}$  is the tangential increment of displacement due to  $\lambda$ . From the expression above, clearly the same elastic buckling displacement (and force) response will be obtained irrespective of the initial loads applied as  $\lambda$  will be obtained to scale the responses accordingly. Hence, in this approach, the response at buckling is insensitive to the initial loads applied. Conversely, calculating the displacement response from a P- $\Delta$  static analysis, we will find that the initial loads applied do affect the response at buckling. The P- $\Delta$  response is obtained from

$$\{U_m\} = [K_E^A + K_{Gm}^A]^{-1} \{ \{P_m\} + \{Fixed\ End\ Forces\}_m - [K_{Gm}^A] \{U_0\} \}$$

where  $K_G^A$  which depends on the initial loads is obtained from a first pass

$$\{U_m\} = [K_E^A]^{-1} \{ \{P_m\} + \{Fixed\ End\ Forces\}_m \}$$

The slightly nonlinear P-Δ path traced is shown below.



Of course, P-Δ response calculations become inaccurate when the initial load  $\{P_m\}$  applied is very high such that had a linearized buckling analysis been performed, the elastic buckling load factor  $\lambda_{ECR}$  would be less than 4.

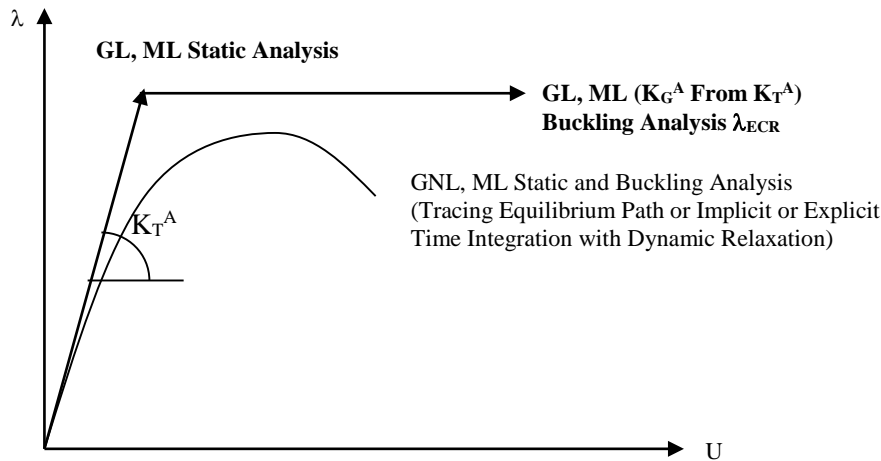
Both the buckling load factor scaled response and the P-Δ response is not ideal. In reality of course, the gradual application of the load would cause a gradual reduction of stiffness (as the differential stiffness gradually becomes more negative) until buckling occurs as depicted on the smoothed curve above. This path can be traced by performing a nonlinear static and buckling analysis (MSC.NASTRAN SOL 106) and is the recommended approach to determining the response (displacement and element forces) at buckling.

The above ( $K_G^A$  From  $K_E^A$ ) may prove inadequate in many instances such as when there is prestress in the elements even before the application of the collapsing load factor. In this case, the ( $K_G^A$  From  $K_T^A$ ) elastic buckling analysis is performed where at collapse, the tangent stiffness matrix at the initial undeflected (by the collapsing load factor, but includes the stiffness contribution of prestressed members) stage A configuration is balanced by the geometric (differential) stiffness due to the load factor.

$$[K_T^A] + \lambda[K_{Gn}^{AKT}] \{\phi\} = \{0\}$$

$K_{Gn}^{AKT}$  represents the geometric stiffness matrix which was calculated based on the *small* displacements obtained by solving the system with a linear static analysis (with the collapsing load) with stiffness  $K_T^A$ . To obtain  $K_T^A$ , to be theoretically exact, a GNL SOL 106 (or implicit dynamic relaxation SOL 129 or explicit dynamic relaxation LS-DYNA) with prestress (as temperature loads say) and gravity must be undertaken. Alternatively, an approximation to  $K_T^A$  can be obtained by repetitive P-Δ static analyses with the prestress (as temperature loads say) and gravity applied. The procedure to obtain this approximate  $K_T^A$  will be presented. Note that the approximate  $K_T^A$  will be the summation of the elastic stiffness  $K_E$  at the undeflected (by the prestress and gravity) state but  $K_G$  at the deflected (by the prestress and gravity) state. Hence if  $K_E$  changes considerably during the application of the prestress and gravity, a full SOL 106 (or implicit dynamic relaxation SOL 129 or explicit dynamic relaxation LS-DYNA), which converges to the  $K_E$  and  $K_G$  at the deflected (by the prestress and gravity) state should be employed. Hence for the modelling of a suspension bridge where there is a great change in geometry, it may be prudent to employ SOL 106 (or implicit dynamic relaxation SOL 129 or explicit dynamic relaxation LS-DYNA), but for a high tension low sag cable on say a tower with prestressed cables, the repetitive P-Δ static analysis may be adequate. The repetitive P-Δ analysis basically involves a number of iterations of linear static analyses to obtain an approximate  $K_T^A$ . Note again that A refers to the initial undeflected (by the collapsing load) state, but deflected by the prestress and gravity. To perform the repetitive P-Δ analysis, a static analysis is performed based on  $K_E^A$  with temperature loads and gravity

to generate forces in the structural elements, which in turn provides input for the computation of  $K_{Gi}^{AKT_m}$  where  $m$  is the iterations. Repetitive static analysis is performed with the prestress and gravity updating the stiffness matrix  $K_E^A + K_{Gi}^{AKT_{m-1}} + K_{Gi}^{AKT_m}$  until convergence of displacements is obtained. The tangent stiffness at this stage is the approximate converged tangent stiffness matrix  $K_T^A = K_E^A + K_{Gi}^{AKT}$ . The converged displacements represent the approximate P- $\Delta$  ( $K_G^A$  From Approximate  $K_T^A$ ) static response to the initial prestress loads and gravity. The converged geometric stiffness at this stage would be that based upon the approximate tangent stiffness matrix  $K_T^A$ , i.e.  $K_{Gi}^{AKT}$ . Irrespective of the method of obtaining  $K_T^A$ , whether by SOL 106 (or implicit dynamic relaxation SOL 129 or explicit dynamic relaxation LS-DYNA) or repetitive P- $\Delta$ , another static analysis is performed on  $K_T^A$ , this time with the collapsing applied external loads (which is a fraction of the critical buckling load so that the buckling load factor will be more than 1). This generates  $K_{Gn}^{AKT}$ . Then, a buckling analysis is performed, effectively finding the instances when factored by  $\lambda$ ,  $K_{Gn}^{AKT}$  balances  $K_T^A$ . Hence, since both the tangent stiffness matrix  $K_T^A$  and the geometric stiffness matrix  $K_{Gn}^{AKT}$  are based upon the initial undeflected (by the collapsing load factor) configuration A, the method is only valid if deflections are small enough for there to be **negligible change in  $K_T^A$  and the geometric stiffness matrix varies linearly with the load factor such that it can be expressed as  $\lambda K_{Gn}^{AKT}$  until elastic instability has been attained.** The inherent assumption that the geometric stiffness matrix varies linearly with the load factor  $\lambda K_{Gn}^{AKT}$  enables any external load to be applied in the first pass since  $K_{Gn}^{AKT}$  will be scaled accordingly. However, in any FE model, even an extremely linear one, the geometric stiffness matrix does not actually vary perfectly linear with the load factor, hence choosing a different external load value as a first pass will result in minor discrepancies in the load factor. Clearly, assuming that deflections are indeed small, the method is only valid for the first buckling mode as subsequent deflections will certainly be too large. To illustrate the assumption, this linearized buckling analysis basically traces the following equilibrium path.



That is to say, the structure follows the equilibrium path governed by the **constant** stiffness  $K_T^A$  until suddenly it loses all its stiffness (in a direction dissimilar to that of the critical load) and buckles when  $\lambda K_{Gn}^{AKT}$  matches  $K_T^A$ . This is valid if  $K_T^A$  is assumed not to vary with the  $\{U\}$  and if the component forces  $\{f\}_n$  are approximately linear in terms of the load factor  $\lambda$  such that the geometric stiffness matrix varies linearly with the load factor allowing it to be expressed as  $\lambda K_{Gn}^{AKT}$  until elastic instability has been attained, both of which are quite valid as long as the tangential increment of displacement due to  $\lambda$  is small. This can be estimated from

$$\Delta\{U\} = \lambda [K_T^A]^{-1} \{P_n^A\}$$

where  $\Delta\{U\}$  is the tangential increment of displacement due to  $\lambda$ . In reality of course, the gradual application of the load would cause a gradual reduction of stiffness (as the differential stiffness gradually becomes more negative) until buckling occurs as depicted on the smoothed curve above. This path can be traced by performing a nonlinear static and buckling analysis (MSC.NASTRAN SOL 106).

Buckling analyses based on  $K_T^A$  is used in instances where there is prestressing and gravity before the application of the critical buckling loads, for instance in the buckling of **suspension bridge piers** or **cable prestressed towers**. A static solution based upon  $K_T^A$  (incorporating the prestress and gravity) which is obtained exactly by SOL 106

(or implicit dynamic relaxation SOL 129 or explicit dynamic relaxation) or approximately by repetitive P- $\Delta$  analysis (the latter may be valid for low sag high tension cable problems where  $K_E$  does not change much due to the prestress and gravity) must be first obtained. Then, the buckling load is applied to generate the geometric stiffness matrix (for that buckling load) and an eigenvalue analysis is performed.

The nonlinear (in that it is dependent upon  $\{U\}$ ) tangent stiffness matrix is restated as follows.

$$[K_T] = [K_E] + [K_G]$$

$$\text{where } [K_E] = [T]^T [[k_E]] [T]$$

$$\text{for which } [k_E] = \int_{\Omega} [B]^T [D] [B] d\Omega$$

$$\text{and } [K_G] = [T]^T [[k_G]] [T] + \left[ \frac{\partial^2 \langle d \rangle}{\partial \{U\} \partial \langle U \rangle} \{f\} \right]$$

$$\text{for which } [k_G] = \int_{\Omega} \left[ \frac{\partial^2 \langle \varepsilon \rangle}{\partial \{d\} \partial \langle d \rangle} \{ \{ \sigma \}_n + \{ \sigma \}_i - [D] \{ \varepsilon \}_i \} \right] d\Omega - \left[ \frac{\partial^2 W_i}{\partial \{d\} \partial \langle d \rangle} \right] - \lambda \left[ \frac{\partial^2 W_n}{\partial \{d\} \partial \langle d \rangle} \right]$$

$$\text{and } \{ \sigma \}_n = [D] [B] \{ d \}$$

$$\text{and } \{ f \} = \left[ \int_{\Omega} [B]^T [D] [B] d\Omega \right] \{ d \} + \left\{ \int_{\Omega} [B]^T \{ \sigma \}_i d\Omega \right\} - \left\{ \int_{\Omega} [B]^T [D] \{ \varepsilon \}_i d\Omega \right\} - \left\{ \int_{\Omega} [N]^T \{ b \} d\Omega \right\}$$

As stated, we have omitted the second order variation of work due to the external nodal loadings  $\{P\}$  from the above tangent stiffness matrix expression, i.e.

$$- \left[ \frac{\partial^2 W}{\partial \{U\} \partial \langle U \rangle} \right] = - \left[ \frac{\partial \{P\}}{\partial \langle U \rangle} \right] \quad \text{as} \quad \{P\} = \left\{ \frac{\partial W}{\partial \{U\}} \right\}$$

This is because, as mentioned, the externally applied loads at the nodes are in commercial codes always work-conjugate with the nodal DOFs  $\{U\}$ , failing which the above term must be incorporated. The second order variation of work due to loads applied on the finite elements is obviously still taken into account.

$[K_T]$  is inherently nonlinearly dependent upon  $\lambda$  and  $\{U\}$ . The buckling problem **can be expressed as a linear eigenvalue problem if  $[K_T]$  is assumed not to vary with the  $\{U\}$  and if the component forces  $\{f\}$  are approximately linear in terms of the load factor  $\lambda$** . The objective is to linearize the eigenvalue problem around the initial equilibrium state A. The first order change in  $[K_T]$  for state A

$$[K_T] = [K_T^A] + \Delta [K_T] = [K_T^A] + \Delta [K_E] + \Delta [K_G]$$

$$\Delta [K_E] = \Delta [T]^T [k_E^A] [T^A] + [T^A]^T [k_E^A] \Delta [T]$$

$$\Delta [K_G] = \left[ \frac{\partial^2 \langle d \rangle}{\partial \{U\} \partial \langle U \rangle} \right]^A \Delta \{f\} - \Delta \lambda \left[ \frac{\partial^2 W_n}{\partial \{U\} \partial \langle U \rangle} \right]^A + \left[ \Delta \frac{\partial^2 \langle d \rangle}{\partial \{U\} \partial \langle U \rangle} \right]^A \{f^A\} - \Delta \left[ \frac{\partial^2 W_i}{\partial \{U\} \partial \langle U \rangle} \right] - \lambda^A \Delta \left[ \frac{\partial^2 W_n}{\partial \{d\} \partial \langle d \rangle} \right]$$

Although the above can be used directly for formulating a linear eigenvalue problem, the influence of a change of geometry on  $[K_T]$  is normally ignored, and hence  $\Delta [K_E]$  and the last 3 components of  $\Delta [K_G]$  are ignored. The linearized buckling (eigenvalue) problem is thus expressed as

$$\begin{aligned} [K_T] \{\phi\} &= \{0\} \\ ([K_T^A] + \lambda [K_{Gn}^A]) \{\phi\} &= \{0\} \end{aligned}$$

The nontrivial solution is obtained by solving for the eigenvalue  $\lambda$  in the expression

$$\begin{aligned} \text{DET}([K_T]) &= 0, \text{ the corresponding } \{\phi\} \text{ being the eigenvector or the buckling mode shape} \\ \text{DET}([K_T^A] + \lambda[K_{Gn}^A]) &= 0 \\ [K_T^A] &= [K_E^A] + [K_G^A] \\ &= [T^A]^T [k_E^A] [T^A] + [T^A]^T \left[ \frac{\partial^2 \langle \varepsilon \rangle}{\partial \{d\} \partial \langle d \rangle} \right]^A \{ \{\sigma_n^A\} + \{\sigma_i^A\} - [D] \{\varepsilon_i^A\} \} - \frac{\partial^2 W_i}{\partial \{d\} \partial \langle d \rangle} \Big|_A [T^A] + \left[ \frac{\partial^2 \langle d \rangle}{\partial \{U\} \partial \langle U \rangle} \right]^A \{f_i^A\} \\ [K_{Gn}^A] &= \left[ \frac{\partial^2 \langle \varepsilon \rangle}{\partial \{d\} \partial \langle d \rangle} \right]^A \{ \sigma_n^A \} - \left[ \frac{\partial^2 W_n}{\partial \{d\} \partial \langle d \rangle} \right]^A + \left[ \frac{\partial^2 \langle d \rangle}{\partial \{U\} \partial \langle U \rangle} \right]^A \{f_n^A\} \end{aligned}$$

where

$$\begin{aligned} \{f_i^A\} &= \left\{ \int_{\Omega} [B]^T \{\sigma\}_i d\Omega \right\} - \left\{ \int_{\Omega} [B]^T [D] \{\varepsilon\}_i d\Omega \right\} \\ \{f_n^A\} &= \left\{ \int_{\Omega} [B^A]^T [D^A] [B^A] d\Omega \right\} \{d_n^A\} - \left\{ \int_{\Omega} [N]^T \{b\}_n d\Omega \right\} \end{aligned}$$

The displacements are estimated from the following equation

$$\Delta\{U\} = \lambda [K_T^A]^{-1} \{P_n^A\}$$

where  $\Delta\{U\}$  is the tangential increment of displacement due to  $\lambda$ .

The physical meaning of the  $[K_T^A]$  matrix is that it represents the tangent stiffness matrix at the initial undeflected configuration with the effect of the prestress and the initial second order work variation included. In the linearized buckling analysis, a load factor is found which causes the tangent stiffness to become zero by a term which multiplies this load factor to the nominal part of the geometric (or differential) stiffness based on the initial undeflected configuration. The nominal part refers to the additional element force  $\{f_n\}$  and additional work  $W_n$  terms, not the prestress  $\{f_i\}$ . Hence, it is assumed that in the application of the load factor that both the nominal internal forces  $\{f_n^A\}$  and the nominal second order work term vary linearly with the load factor. These factored nominal internal force and factored nominal second order work terms are based on values at the initial state A. Also it is assumed that the transformation matrix  $[T]$  is constant at  $[T^A]$ . Thus it can be concluded that the linearized buckling analysis is only valid when the deflections  $\{U\}$  are small i.e. to predict buckling along the trivial fundamental path or along a path close to the trivial path.

A buckling point in the response of a discrete structural system is either a bifurcation point or a limit point. Accordingly, it corresponds to an equilibrium state for which the tangent stiffness matrix  $[K_T]$  becomes singular, indicating the presence of an infinitesimally adjacent equilibrium state at the same level of loading. Linearized buckling analysis is based on the initial undeflected geometry, i.e. (A) = initial state to determine  $[K_T^A]$ .  $[K_T^A]$  is thus the tangential value of  $[K_T]$  at the initial undeflected shape (A). There is no point in choosing another state (A) to find  $[K_T^A]$ , as we then might as well perform nonlinear buckling analysis.

Linear buckling analysis tends to provide good approximations to the critical load when the critical point is a bifurcation point. But linear buckling analysis can overestimate the critical load when the critical point is a limit point and if the buckling occurs at significant incremental deflection  $\Delta\{U\}$  from state (A) as the change in  $[K_T]$  due to the change in  $\{U\}$  is ignored. This value of  $\Delta\{U\}$  is estimated using the equation stated above in order to make a judgment. Higher critical modes in linear buckling analysis are inaccurate if the first mode is a limit point due to subsequent larger deflections. Hence, linear buckling analysis is most suitable for detecting bifurcation points along trivial (or almost trivial) fundamental paths, in which case state (A) can be the initial state, and for detecting critical points which are close to the known equilibrium state (A).

### 3.2.2 Problem Reduction and Trial Modes in Linear Buckling Analysis

The number of degrees of freedom  $n$  of the linear eigenvalue problem can be reduced to  $m$  as an approximation.

The linear eigenvalue problem of size  $n$  is expressed as

$$\left( \left[ \mathbf{K}_T^A \right] + \Delta\lambda \left[ \mathbf{K}_{Gn}^A \right] \right) \{\Phi\} = \{0\}$$

for which the exact eigenvalue  $\Delta\lambda$  is obtained from

$$\det \left( \left[ \mathbf{K}_T^A \right] + \Delta\lambda \left[ \mathbf{K}_{Gn}^A \right] \right) = 0$$

and  $\{\Phi\}$  being the corresponding buckling modes shape or eigenvector

However, an approximate solution is obtained by approximating the exact buckling mode  $\{\Phi\}$

as a linear combination of  $m$  pre - defined modes in

$$[\Phi_t] = [\{\Phi_{t1}\} + \{\Phi_{t2}\} + \{\Phi_{t3}\} + \dots + \{\Phi_{tm}\}]$$

using  $m$  unknown modal parameters  $\{\phi\}$ ,  $m < n$

$$\{\Phi\} = [\Phi_t] \{\phi\}$$

Hence,

$$\left( \left[ \mathbf{K}_T^A \right] + \Delta\lambda \left[ \mathbf{K}_{Gn}^A \right] \right) [\Phi_t] \{\phi\} = \{0\}$$

Pr emultiplying by  $[\Phi_t]^T$ , the reduced linear eigenvalue problem of size  $m$  ( $m < n$ ) is expressed as

$$\left( \left[ \mathbf{k}_T^A \right] + \Delta\lambda \left[ \mathbf{k}_{Gn}^A \right] \right) \{\phi\} = \{0\} \quad \text{where} \quad \left[ \mathbf{k}_T^A \right] = [\Phi_t]^T \left[ \mathbf{K}_T^A \right] [\Phi_t] \quad \text{and} \quad \left[ \mathbf{k}_{Gn}^A \right] = [\Phi_t]^T \left[ \mathbf{K}_{Gn}^A \right] [\Phi_t]$$

for which the approximate eigenvalue  $\Delta\lambda$  is obtained from

$$\det \left( \left[ \mathbf{k}_T^A \right] + \Delta\lambda \left[ \mathbf{k}_{Gn}^A \right] \right) = 0 \quad \text{and} \quad \{\phi\} \text{ being the corresponding buckling modes shape or eigenvector}$$

Naturally, the solution would be exact in this  $m$  size eigenvalue problem if the exact mode shape can be modelled by  $[\Phi_t]$ . This can be done if  $m = n$ , i.e. if the number of independent modes of deformation equal the number of degrees of freedom. This would be equivalent to solving the original eigenvalue problem.

In the special case that the trial mode is to be approximated straight away such that the trial mode matrix  $[\Phi_t]$  reduces to a single column vector  $\{\Phi_t\}$ , then

$$\{\Phi\} = \{\Phi_t\} \{\phi\}$$

for which the approximate eigenvalue  $\Delta\lambda$  is obtained from

$$\Delta\lambda = - \frac{\mathbf{k}_T^A}{\mathbf{k}_{Gn}^A} = - \frac{\{\Phi_t\}^T \left[ \mathbf{K}_T^A \right] \{\Phi_t\}}{\{\Phi_t\}^T \left[ \mathbf{K}_{Gn}^A \right] \{\Phi_t\}}$$

and  $\{\Phi_t\}$  being the corresponding buckling modes shape or eigenvector

A good approximate mode shape for uniform shear frames based on Rayleigh's is  $\{\Phi_t\} = \left[ \mathbf{K}_T^A \right]^{-1} \{\mathbf{P}_n\}$

where  $\{\mathbf{P}_n\}$  is the vertical loads applied horizontally.

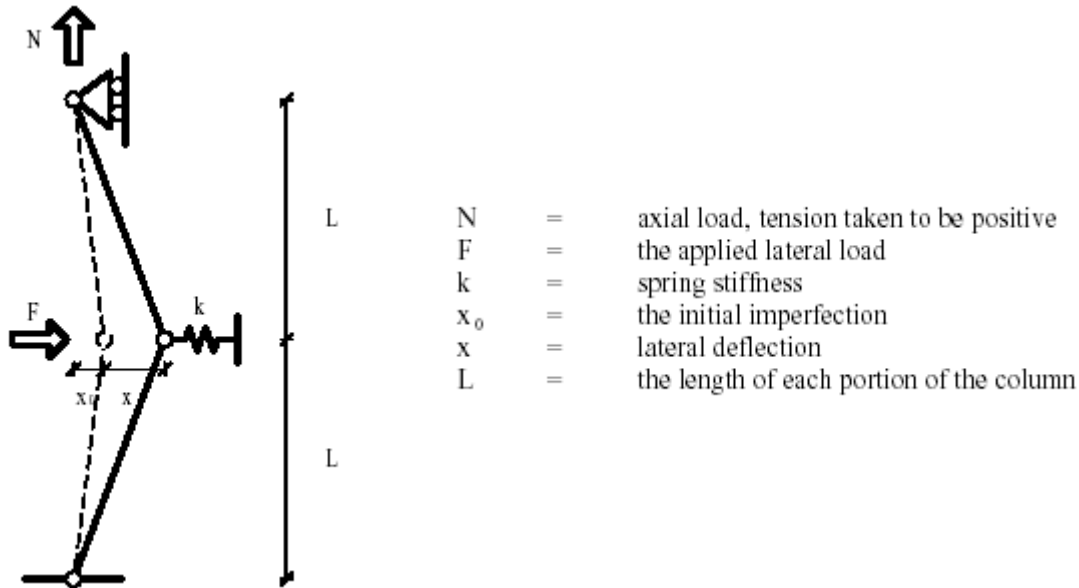
Naturally, the solution would be exact if  $\{\Phi_t\}$  is the exact mode shape. This is ensured if

$$\left[ \mathbf{K}_T^A \right] \{\Phi_t\} = \lambda \left[ \mathbf{K}_{Gn}^A \right] \{\Phi_t\} \quad \text{i.e.} \quad \left[ \mathbf{K}_T^A \right] \{\Phi_t\} \propto \left[ \mathbf{K}_{Gn}^A \right] \{\Phi_t\}$$

The trial mode matrix  $[\Phi_t]$  for the problem reduction in linear buckling analysis is a multi modal matrix. The trial mode method assumes just one mode shape  $\{\Phi_t\}$  whilst the problem reduction method assumes a linear combination of mode shapes,  $[\Phi_t] = [\{\Phi_{t1}\} + \{\Phi_{t2}\} + \{\Phi_{t3}\} + \dots + \{\Phi_{tm}\}]$ . Hence the problem reduction method is more accurate evidently. Hence, the problem reduction method will yield a lower estimate of  $\Delta\lambda$  than the trial mode shape method. The nonlinear eigenvalue problem will of course yield the lowest exact value of  $\Delta\lambda$ .

### 3.2.3 Concepts of Linearized ( $K_G^A$ From $K_E^A$ ) Buckling Analysis

The concept of GL, ML buckling analysis will be illustrated for a simple system.



Let us assume that **deflections are small (hence geometrically linear analysis)** hence the rotation of the column segments can be described and any change in height can be neglected. Lateral equilibrium at the central pin shows that

$$F = kx + \frac{2N}{L}(x + x_0)$$

Rearranging so that we have the form Stiffness x Displacement = Applied Force, we get

$$kx + \frac{2N}{L}x = F - \frac{2N}{L}x_0$$

and hence the deflection

$$x = \frac{F - \frac{2N}{L}x_0}{k + \frac{2N}{L}}$$

Geometric Stiffness  $2N/L$

We can see that the effect of the force  $N$  acting on this system can be seen as being like an additional stiffness term  $2N/L$ , i.e. the geometric (aka differential) stiffness. The effect of the axial force is equivalent to an additional stiffness of value  $2N/L$  acting laterally at the pin location. If the force is tensile (i.e. positive) then the geometric stiffness will act to increase the overall stiffness of the system. On the other hand, if it is compressive then the term will be negative and the system stiffness will decrease. Consider the condition at which the axial compression in our simple pin jointed system is so great that the lateral stiffness of the system is zero.

$$k + \frac{2N_{cr}}{L} = 0 \quad \text{i.e.} \quad N_{cr} = -\frac{kL}{2}$$

At this critical load, buckling occurs. And the critical linear elastic buckling load factor  $\lambda_{cr}$  of the system is

$$\lambda_{cr} = \frac{N_{cr}}{N}$$

**It cannot be emphasized enough that, the buckling load factor is independent of the initial lateral imperfections, the lateral load and material strength.**

This linear buckling critical load factor is **independent of the applied lateral force  $F$  and the initial lateral imperfection**. Of course, the amplified displacement response is dependent upon  $F$  and the initial imperfection. The buckling factor is also **independent of the material strength** as it depends on the stiffness instead.

### 3.2.4 MSC.NASTRAN Decks

#### 3.2.4.1 GL, ML ( $K_G^A$ From $K_E^A$ ) Buckling Analysis

```

$ EXECUTIVE CONTROL SECTION
SOL 105

$ CASE CONTROL SECTION
DISPLACEMENT(<PRINT,PUNCH,PLOT>) = ALL/<Grid Set ID> $ Plots the buckled shapes
SPCFORCES(<PRINT,PUNCH,PLOT>) = ALL/<Grid Set ID>
OLOAD(<PRINT,PUNCH,PLOT>) = ALL/<Grid Set ID>
ELSTRESS(<PRINT,PUNCH,PLOT>) = ALL/<Element Set ID>
ELFORCE(<PRINT,PUNCH,PLOT>) = ALL/<Element Set ID>
STRAIN(<PRINT,PUNCH,PLOT>) = ALL/<Element Set ID>
ESE(<PRINT,PUNCH,PLOT>) = ALL/<Element Set ID>
$
SUBCASE 1
LABEL = Static Load Case With Buckling Load
LOAD = < ID of FORCEi, MOMENTi, PLOADi, GRAV, LOAD, SPCD Cards in Bulk Data >
TEMP(LOAD) = < ID of TEMP, TEMPRB, TEMPP1 Cards in Bulk Data >
DEFORM = < ID of DEFORM Cards in Bulk Data >
SPC = < ID of SPC Cards in Bulk Data >
$
SUBCASE 2
LABEL = Buckling Case
STATSUB(BUCKLING) = < Static Subcase Number >
SPC = < ID of SPC Cards in Bulk Data >
METHOD = < ID in EIGRL or EIGB >
    
```

For medium to large models, the Lanczos method is the recommended eigenvalue extraction method. Furthermore, the Lanczos method takes full advantage of sparse matrix methods that can substantially increase computational speed and reduce disk space usage. For overall robustness, the Lanczos method is the recommended method.

\$ BULK DATA									
EIGRL	ID	Lower Eigenvalue	Upper Eigenvalue	Number of Roots					

Unlike dynamic modal analysis, linear buckling analysis produces eigenvalues that can be either positive or negative. Note that these negative roots are legitimate both from a physical and a mathematical standpoint. In general, this situation only occurs if the applied buckling load is in the opposite direction of the buckling load, that is to say a buckled shape with the same magnitude of eigenvalue can be produced if the applied loading was reversed in direction. Hence, if on the EIGRL card, only the upper eigenvalue range is specified, NASTRAN will attempt to extract all eigenvectors below that value, including all the negative eigenvalues. Thus if we are only interested in the fundamental mode, it is necessary to also specify the number of roots.

REAL MODE NO.	EIGENVALUES EXTRACTION ORDER	EIGENVALUE	RADIANS	CYCLES	GENERALIZED MASS	GENERALIZED STIFFNESS
1	1	2.183456E-01	4.672747E-01	7.436907E-02	1.749877E+02	3.820780E+01
2	2	-2.183456E-01	4.672747E-01	7.436907E-02	-1.749877E+02	3.820780E+01

Buckling load factor.  $\lambda$

The enhanced inverse power method (SINV) can be a good choice if the model is too large to fit into memory, only a few modes are needed, and you have a reasonable idea of your eigenvalue range of interest. It is useful for models

in which only the lowest few modes are desired. This method is also useful as a backup method to verify the accuracy of other methods.

\$ BULK DATA									
EIGB	ID	SINV	Lower Eigenvalue	Upper Frequency					

At least two subcases are necessary, the first being the static subcase that is used in the second subcase to generate the differential stiffness matrix from the internal element loads and then solve the eigenvalue problem. The differential stiffness is supported by CONROD, CROD, CTUBE, CBAR (for both Euler and lateral torsional buckling), CBEAM, CBEND, CQUAD4, CQUAD8, CTRIA3, CTRIA6, CSHEAR, CHEXA, CPENTA and CTETRA. The contribution to the differential stiffness from the follower force effect is not included. Offsets should not be used in beam, plate, or shell elements for buckling analysis. For 3-D buckling problems, the use of PARAM, K6ROT is recommended for CQUAD4 and CTRIA3 elements. A value of 100 is recommended. Note that each subcase may have a different boundary condition.

Although the element stresses, forces and strains for each buckled mode may be output, it is meaningless as they are based upon the eigenvectors that have been scaled arbitrarily. These values **DO NOT INDICATE RESPONSE**. To obtain the response (displacement and element forces) at buckling, the response from a linear static analysis of the initial applied loads, and scaled by the critical load factor can be used.

$$\Delta\{U\} = \lambda [K_E^A]^{-1} \{P_n^A\}$$

Of course though, the element strain energy density distribution (ESE request), although have likewise meaningless magnitudes (again due to arbitrary scaling of eigenvectors), is an important design tool which shows elements which work the most in causing that buckled mode shape. Stiffening elements with a high ESE would increase the buckling load factor.

The number of buckled modes obtained will be limited to the number of DOFs in the finite element model. The mesh should be fine enough to represent the buckled shape. CBAR elements have cubic polynomial transverse interpolation functions (shape functions). But unlike in a static analysis where the cubic deflection over a beam element can be mapped, in a buckling analysis the deflected shape is provided only by the deflections at the nodes. Hence the beam element must be refined. Also note that the buckled mode shape of a beam member is not cubic polynomial anyway. One dimensional elements such as CBAR elements (in a fine mesh as they may be) do not model the local buckling of members. The local buckling of a tube or pipe (i.e. the crippling of the thin wall) in compression must be modeled with a fine mesh of shells. A coarse mesh may predict an unconservative larger fundamental buckling load factor as the local mode cannot be captured. It is thus important to anticipate the buckling mode, or alternatively, continuous refinement be made. Buckling is a state of loss of stiffness, an unstable state, i.e. failure. If the local crippling buckling mode is more critical than the overall beam buckling mode, it is imperative that shell elements are used as line elements will give an unconservative result. Buckling generally requires a fine mesh. If the buckled shape is jagged, it is a clear indication that the mesh is not fine enough. There must be several elements per wavelength, usually 4 (or 8, 16, 32 etc...other numbers even 5 tend to be inferior) elements per half sine wavelength.

Local buckling can also be checked using hand calculations based upon the physical boundary conditions and thickness on a relevant panel to estimate the buckling stress and comparison with the stress from a linear static SOL 101 analysis to evaluate if the component would buckle under that load.

Linear buckling analysis assumed the deflections to be small and the elements stresses elastic. For structures that exhibit nonlinear material or large deflection deformations, the linear buckling load obtained from Solution 105 may be different than the actual buckling load. For structures with significant nonlinearities, it is recommended that a nonlinear buckling analysis using SOL 106 be performed.

The preliminary scheme stage buckling analysis of the Centre Pompidou, Metz timber roof is presented.

### Centre Pompidou Timber Roof Scheme Design Linear Buckling Analysis

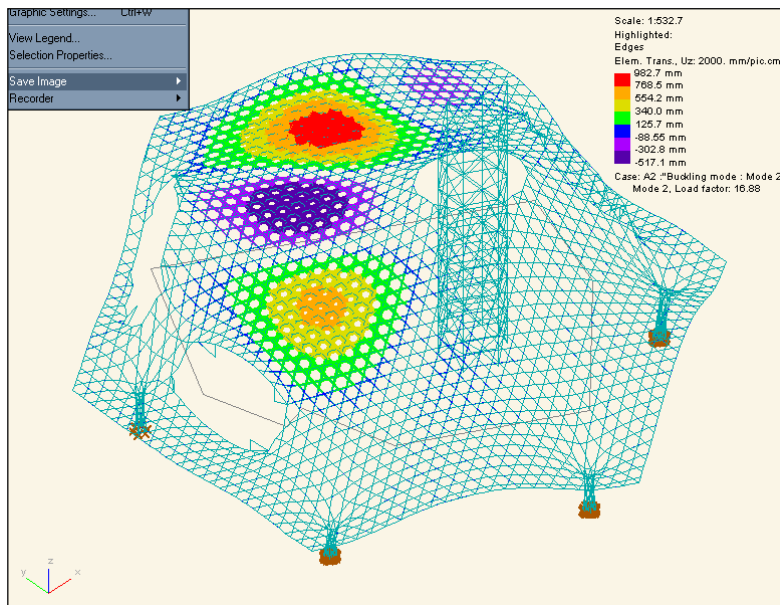
#### Linearized Buckling Due To Self-Weight (Applied Vertical Resultant 9547kN)

The applied load consists of timber planks (6097kN), intermediate packs (1039kN) and roof covering (2411kN). The linearized buckling problem is

$$[[\mathbf{K}_E^A] + \lambda[\mathbf{K}_G^{AKE}]]\{\phi\} = \{0\}$$

The instantaneous and geometric stiffnesses are based on the unfactored 5<sup>th</sup> percentile stiffness values ( $E = 12\text{GPa}$ ;  $G = 0.4\text{GPa}$ ) for the timber material, hence conservative as far as buckling analysis is concerned. The geometric stiffness is a function of the internal forces. For example, for a straight column subject to axial compression  $F$ , the geometric stiffness is simply  $F/L$ . The critical load case which causes the greatest compression and hence the greatest geometric stiffness is sought.

The lowest buckled mode shape (which could be replicated in reality) due to self-weight is presented. The load factor is **16.9**. Note that there was another mode with a load factor of  $-14.75$ , this indicating an upward gravity, which is implausible, hence ignored.

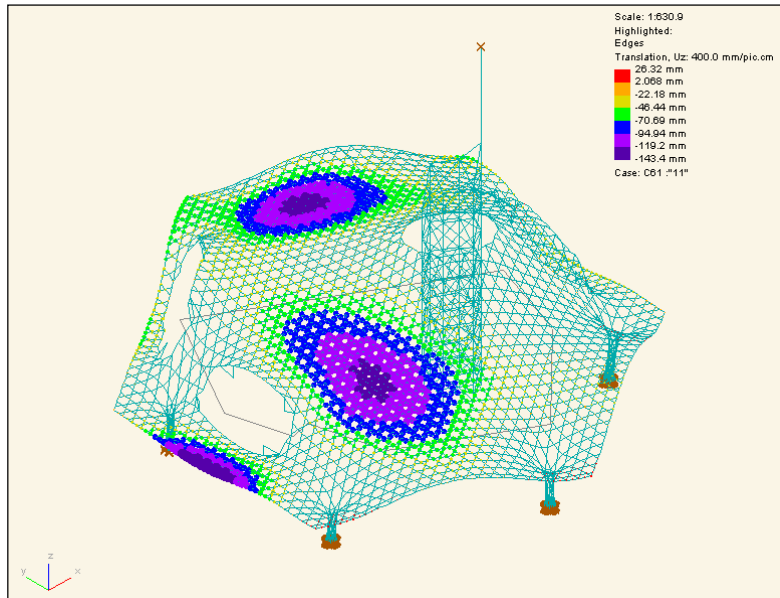


Hence the first global buckling load factor to unfactored self-weight = **16.9**. From plot, buckled mode shape shows primarily vertical displacement, as the normalization is 1000 mm and the vertical displacement reach up to 982.7 mm.

The **static** displacement at the onset of buckling can be estimated by the following projection

$$\Delta\{U\} = \lambda[\mathbf{K}_E^A]^{-1}\{P_n^A\}$$

This can be used to ascertain whether geometrically nonlinear effects or material nonlinearity for that matter, affects the estimation of the buckling load and the **static** displacement at the onset of buckling. The following is the **static displacement** from the unfactored self-weight load case.

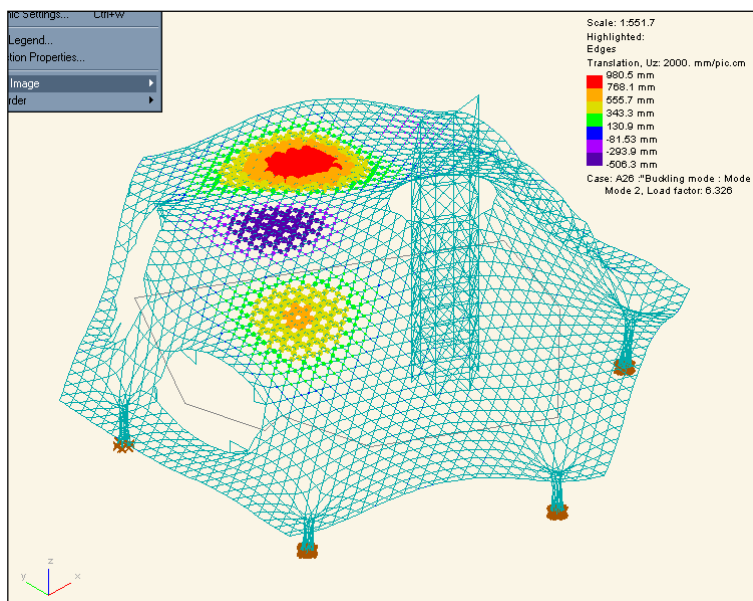


The predicted max **static** displacement from the unfactored self-weight case at onset of buckling is  
 $16.9 \times 143\text{mm} = 2414\text{mm}$

Note that this is the max displacement, not the average. A geometrically nonlinear buckling analysis is required to predict a more accurate buckling load.

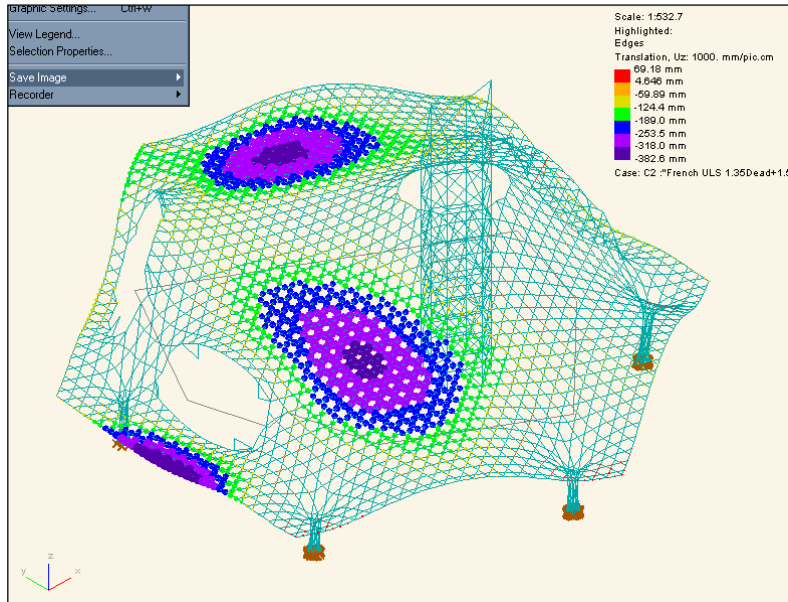
**Linearized Buckling Due To ULS Load Case A**  
**(Max Downward Symmetrical Load 1.35Dead+1.5Snow With Applied Vertical Resultant 22530kN)**

The factor of safety on buckling to the ULS load case is of interest. The first realistic mode shape is presented. The load factor is **6.33**.



As a check, from a linear projection of the self-weight case, since the distribution of load is similar, the load factor from this ULS case should be  $9547 / 22530 * 16.9 = 7.15$ , not too dissimilar to the above prediction.

The following is the **static** displacement from this ULS load case.

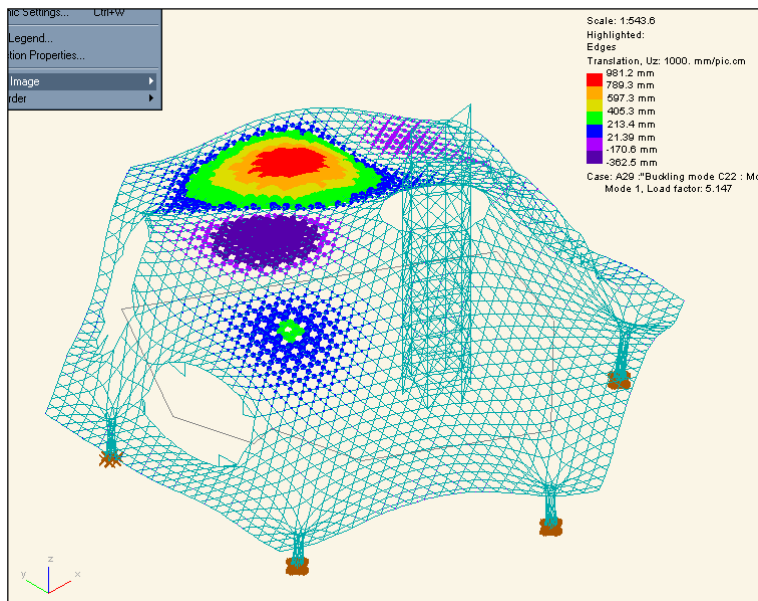


Hence, at the onset of buckling from the ULS case, from the above projection, the max **static** displacement is  $6.33 \times 382\text{mm} = 2418\text{mm}$

This is a 2.4m deflection in a span of 40m, i.e. span/depth of 16.5. The effect of this on the accuracy of the linear buckling load factor estimate needs to be quantified using a geometrically nonlinear buckling analysis solver.

**Linearized Buckling Due To ULS Load Case B  
(Asymmetrical Load 1.35Dead+1.35Wind North+1.35Snow With Applied Vertical Resultant 21280kN)**

The North Wind load case refers to an asymmetric wind load case such that the windward direction experiences a downward pressure and the leeward direction experiences an upward pressure. The first realistic mode shape is presented. The load factor is **5.15**.



**Conclusion**

The critical self-weight linearized buckling load factor is **16.9**. Since the value is greater than 10.0, the effect of P- $\Delta$  in increasing the effects on the structure and reducing the load factor due to self-weight is negligible. The critical ULS linearized buckling load factor is **5.15**. Since the value is less than 10.0, the effect of P- $\Delta$  in increasing the effects on the structure and reducing the load factor due to the ULS load case is not negligible. However the risk of catastrophic buckling instability is low.

### Assumptions

The following should be borne in mind when considering results.

1. Material linear and elastic until buckling.
2. Geometrically linear; Elastic stiffness  $K_E^A$  constant until onset of buckling and based on initial undeformed geometry; Valid if deflections small (for negligible change in  $K_E^A$ ) until onset on buckling and no prestress (whether compressive which is unfavourable or tensile which is favourable) in structure. Check magnitude of  $\Delta\{U\}$  to be small and ensure no prestress in system.
3. Geometrically linear; Geometric stiffness  $K_G^{KEA}$  based on  $K_E^A$ ; Valid if deflections small (for negligible change in  $K_E^A$  and  $K_G^{KEA}$ ) until onset on buckling. Check magnitude of  $\Delta\{U\}$  to be small.

### 3.2.4.2 GL, ML ( $K_G^A$ From Exact or Approximate $K_T^A$ ) Buckling Analysis

The above subcase definitions will solve the following eigenvalue problem.

$$[[K_E^A] + \lambda[K_G^{AKE}]]\{\phi\} = \{0\}$$

$K_G^{AKE}$  represents the geometric stiffness matrix which was calculated based on displacements obtained by solving the system with stiffness  $K_E^A$ . This may prove inadequate in many instances such as when there is prestress in the elements. The linearized buckling problem as described in the theory section is sought as

$$[[K_T^A] + \lambda[K_{G_i}^{AKT}]]\{\phi\} = \{0\}$$

$K_G^{AKT}$  represents the geometric stiffness matrix which was calculated based on displacements obtained by solving the system with stiffness  $K_T^A$ .

To obtain  $K_T^A$ , to be theoretically exact, a GNL SOL 106 (or implicit dynamic relaxation SOL 129 or explicit dynamic relaxation LS-DYNA) with prestress (as temperature loads say) and gravity must be undertaken. Alternatively, an approximation to  $K_T^A$  can be obtained by repetitive P- $\Delta$  static analyses with the prestress (as temperature loads say) and gravity applied. The procedure to obtain this approximate  $K_T^A$  will be presented. Note that the approximate  $K_T^A$  will be the summation of the elastic stiffness  $K_E$  at the undeflected (by the prestress and gravity) state but  $K_G$  at the deflected (by the prestress and gravity) state. Hence if  $K_E$  changes considerably during the application of the prestress, a full SOL 106 (or implicit dynamic relaxation SOL 129 or explicit dynamic relaxation LS-DYNA), which converges to the  $K_E$  and  $K_G$  at the deflected (by the prestress and gravity) state should be employed. Hence for the modelling of a suspension bridge where there is a great change in geometry (known in the bridge industry as **form-finding**, so-called because it is necessary to find the form or shape of the catenary suspension cables), it may be prudent to employ SOL 106 (or implicit dynamic relaxation SOL 129 or explicit dynamic relaxation LS-DYNA), but for a high tension low sag cable on say a tower with prestressed cables, the repetitive P- $\Delta$  static analysis may be adequate. The repetitive P- $\Delta$  analysis basically involves a number of iterations of linear static analyses to obtain an approximate  $K_T^A$ . Note again that A refers to the initial undeflected (by the collapsing load) state, but deflected by the prestress and gravity. To perform the repetitive P- $\Delta$  analysis, a static analysis is performed based on  $K_E^A$  with temperature loads and gravity to generate forces in the structural elements, which in turn provides input for the computation of  $K_{G_i}^{AKT_m}$  where m is the iterations. Repetitive static analysis is performed with the prestress and gravity updating the stiffness matrix  $K_E^A + K_{G_i}^{AKT_{m-1}} + K_{G_i}^{AKT_m}$  until convergence of displacements is obtained. The tangent stiffness at this stage is the approximate converged tangent stiffness matrix  $K_T^A = K_E^A + K_{G_i}^{AKT}$ . The converged displacements represent the approximate P- $\Delta$  ( $K_G^A$  From Approximate  $K_T^A$ ) static response to the initial prestress loads. The converged geometric stiffness at this stage would be that based upon the approximate tangent stiffness matrix  $K_T^A$ , i.e.  $K_{G_i}^{AKT}$ .

#### Phase 1

Perform static analysis (with prestress and gravity) based on  $[K_E^A]$  but include the segyroa.v2001 alter prior to the Case Control Section in order to compute the geometric stiffness matrix  $[K_G^A]_1$  (and output into a .pch file) based on the generated element loads from the  $[K_E^A]$  static analysis.

#### Phase 2

Perform static analysis (with prestress and gravity) based on  $[K_E^A] + [K_G^A]_1$  by including the k2gg = ktjj statement in the Case Control Section, the outputted .pch file which contains the ktjj matrix in the Bulk Data and the segyroa.v2001 alter prior to the Case Control Section to compute the  $[K_G^A]_2$  (and output into the .pch file overwriting previous data) based on the generated element loads from the  $[K_E^A] + [K_G^A]_1$  static analysis.

#### Phase 3

Repeatedly perform the Phase 2 static analysis (with prestress and gravity) based on  $[K_E^A] + [K_G^A]_i$  for  $i = 2$  to  $n$  where  $n$  represents the number of iterations required for the change in deflections between analyses to become

negligible. This would signify that the change in the  $[K_G^A]$  matrix become negligible and the correct  $[K_G^A]$  is attained. The deflections and the other responses at this stage represent the P- $\Delta$  ( $K_G^A$  From Approximate  $K_T^A$ ) static response to the prestress and gravity. The stiffness of the structure is  $K_T^A$ .

#### Phase 4

Linearized buckling analysis is now performed with the stiffness of the structure at  $K_T^A$  and with a general buckling load. A SOL 105 is undertaken with the Case Control Section described as follows. It includes one more static analysis with the collapsing buckling load (a fraction of the critical load so that the load factor is more than 1) in order to generate the  $K_{Gn}^{AKT}$  matrix. Then a buckling analysis is performed.

<p><b>\$ CASE CONTROL SECTION</b></p> <p><b>SUBCASE 1</b>          LABEL = P-<math>\Delta</math> (<math>K_G^A</math> From Approximate <math>K_T^A</math>) Static Load Case With Buckling Load          k2gg = ktjj          LOAD = &lt; ID of FORCEi, MOMENTi, PLOADi, GRAV, LOAD, SPCD Cards in Bulk Data &gt;          TEMP(LOAD) = &lt; ID of TEMP, TEMPRB, TEMPP1 Cards in Bulk Data &gt;          DEFORM = &lt; ID of DEFORM Cards in Bulk Data &gt;          SPC = &lt; ID of SPC Cards in Bulk Data &gt;</p> <p><b>SUBCASE 2</b>          LABEL = Buckling Case          k2gg = ktjj          SPC = &lt; ID of SPC Cards in Bulk Data &gt;          METHOD = &lt; ID in EIGRL &gt;</p>
<p><b>\$ BULK DATA</b></p> <p>Include '...pch file containing ktjj'</p>

The responses at this stage represent the ( $K_G^A$  From Approximate  $K_T^A$ ) linear buckling response.

We have thus introduced so far 4 methods of getting the  $K_T^A$  matrix, namely full SOL 106, an implicit dynamic relaxation SOL 129, an explicit dynamic relaxation LS-DYNA or a repetitive P- $\Delta$  static analysis, all with the prestress and other loads. Once the  $K_T^A$  matrix is obtained, all that is required is to perform a linear static analysis with the buckling loads in order to generate a  $K_G^A$  (clearly from  $K_T^A$ ) matrix. Now the linearized buckling problem can be solved as the linear eigenvalue problem  $[K_T^A + \lambda K_G^A]\{\phi\}=\{0\}$ . Another approximate procedure can also be employed in order to generate the  $K_T^A$  matrix.

<p><b>\$ CASE CONTROL SECTION</b></p> <p><b>SUBCASE 1</b>          LABEL = Static Preload Load Case          LOAD = &lt; ID of FORCEi, MOMENTi, PLOADi, GRAV, LOAD, SPCD Cards in Bulk Data &gt;          TEMP(LOAD) = &lt; ID of TEMP, TEMPRB, TEMPP1 Cards in Bulk Data &gt;          DEFORM = &lt; ID of DEFORM Cards in Bulk Data &gt;</p> <p><b>SUBCASE 2</b>          LABEL = Static Load Case With Buckling Load          LOAD = &lt; ID of FORCEi, MOMENTi, PLOADi, GRAV, LOAD, SPCD Cards in Bulk Data &gt;          TEMP(LOAD) = &lt; ID of TEMP, TEMPRB, TEMPP1 Cards in Bulk Data &gt;          DEFORM = &lt; ID of DEFORM Cards in Bulk Data &gt;</p> <p><b>SUBCASE 3</b>          LABEL = Buckling Case          STATSUB(PRELOAD) = 1          STATSUB(BUCKLING) = 2          METHOD = &lt; ID in EIGRL &gt;</p>
--

The method is valid when **only the prestress is judged to affect the geometric stiffness** such as in the compressive preload of building columns due to gravitational loads and the prestressing of extremely taut cables that sag very little under gravity but not in systems such as suspension bridges. Where lateral loads are large enough to affect the geometry of the system with prestress, then a repetitive P-Δ, SOL 106, implicit dynamic relaxation SOL 129 or explicit dynamic relaxation must be employed. But in single P-Δ analysis, because cables do not have much elastic bending stiffness, the initial static preload subcase should only include the prestress and not gravity as including gravity is the same as solving two linear static problems of stiffness  $K_E^A$  with preload and gravity as the applied loads respectively. Clearly, in the gravity case, it is nonsensical as the cables do in reality have differential stiffness (from the prestress) to resist the gravitational force. Prestress in one direction (i.e. along the axis of cable) will cause a differential stiffness in the orthogonal direction. Gravity acts in the orthogonal direction and hence cannot be accounted for in the calculation of the prestress in this single P-Δ analysis. To quantitatively decide if gravity need not be considered in contributing to the differential stiffness of the cables, a static P-Δ analysis should be carried out, the first subcase being a SOL 101 with only the prestress as applied loads and the second subcase a P-Δ SOL 101 (i.e. utilizing the induced prestress from the first subcase to form a geometric stiffness matrix) with both the gravity and prestress included as applied loads. If the difference in the cable element forces between subcases 1 and 2 is negligible, then gravity has little influence in affecting the geometric stiffness. If there is a major difference in the cable element force, then clearly, gravity will affect the geometric stiffness and as such, a repetitive P-Δ, SOL 106, implicit dynamic relaxation or explicit dynamic relaxation must be used to converge to the true  $K_T$ . Likewise, in the single P-Δ analysis of multi-storey buildings, gravity (and only gravity) acts in axis of columns to generate prestress, and the differential stiffness is computed for the orthogonal direction reducing resistance to lateral wind forces, applied in the second subcase with gravity too.

The STATSUB(PRELOAD) computes the differential stiffness due to the prestress and also the follower force. The follower force is calculated and incorporated by the use of PARAM, FOLLOWK, YES. We know how the prestress affects the differential stiffness, namely a tensile prestress causing an increase in stiffness. The effect of the follower force on the stiffness is different. For example, for a cylinder under external pressure critical buckling load may be over-estimated (even though the mode shapes are similar) in a SOL 105 and the natural frequencies in vibration may be under-estimated (even though the mode shapes are similar) in a SOL 103 in the absence of follower stiffness. To the contrary, these observations are reversed in case of centrifugal loads. Centrifugal forces as a constant (static) load are applied by a Bulk Data RFORCE to any elements that have masses. The follower stiffness due to centrifugal load has the effect of lowering stiffness (although the centrifugal load tensioning effect increases stiffness), consequently lowering natural frequencies (even though the mode shapes are similar) in a SOL 103 and lowering the buckling loads (even though the mode shapes are similar) in a SOL 105. This effect increases as the RPM increases, and it becomes significant when the RPM is over 1000.

Another important observation is that the preload cannot buckle the structure. The basic eigenvalue problem was expressed as

$$[K + \lambda K^d] \{\phi\} = \{0\}$$

where  $\lambda$  is an eigenvalue which is a multiplier to the applied load to attain a critical buckling load. If there exists constant preloads other than the buckling load in question, the above equation should include additional differential stiffness, i.e.

$$[K + K_{preload}^d + \lambda K_{buckle}] \{\phi\} = \{0\}$$

in which differential stiffness is distinguished for constant preload and variable buckling load. Notice that **no eigenvalue solutions are meaningful if the preload makes the structure buckle**, i.e.

$$[K + K_{preload}^d]$$

should be positive definite.

### 3.2.5 Hand Methods Verification

#### 3.2.5.1 Member or Local ( $K_G^A$ From $K_E^A$ ) Buckling

##### 3.2.5.1.1 GL, ML Euler Buckling of Column Elements (Primary Stress is Only Axial)

The Euler equation for the critical elastic buckling load for an **elastic, isotropic** and **straight** column is

$$P_E = \frac{\pi^2 EI}{L_E^2}$$

The Euler load estimate is perfectly analogous to the SOL 105 buckling load estimate.

where  $L_E$  is the effective length (distance between the points of contraflexure) depending on the boundary conditions.

Boundary Conditions	Effective Length, $L_E$	
	Non-Sway	Sway
Pinned-Pinned	1.0L (Truss)	
Pinned-Rigid	0.699L	2.0L
Rigid-Rigid	0.5L	1.0L

The Euler equation is of course only valid for columns that are sufficiently long enough to experience linear elastic instability before yielding. Hence it is better to work in terms of axial stresses as the yield stress is clearly defined. The critical Euler stress is

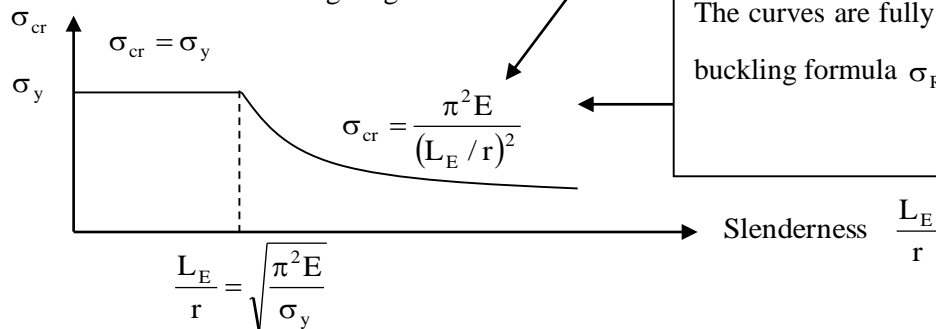
$$\sigma_E = \frac{\pi^2 E}{(L_E / r)^2} \quad \text{where} \quad r = \sqrt{\frac{I}{A}}$$

and is only valid if

$$\frac{L_E}{r} > \sqrt{\frac{\pi^2 E}{\sigma_y}}$$

It cannot be emphasized enough that, the theoretical buckling load factor is independent of the initial lateral imperfections, the lateral load and material strength.

This is all illustrated in the following diagram.



The curves are fully described by the **Rankine** buckling formula  $\sigma_{\text{RANKINE}} = \frac{\sigma_y}{1 + \frac{\sigma_y}{\pi^2 E} \left(\frac{L_e}{r}\right)^2}$

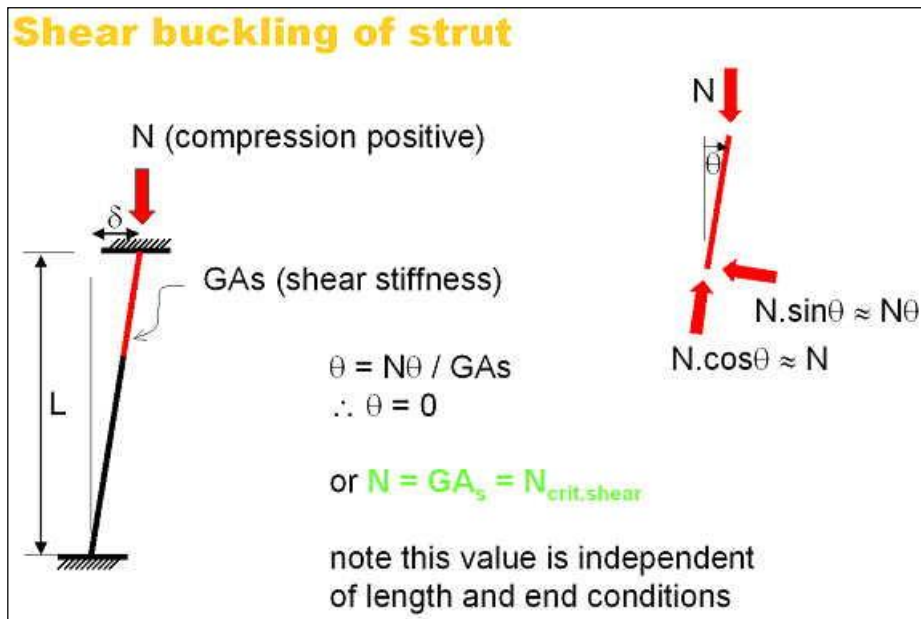
The buckling stress capacity depends on the stiffness of the element and the boundary conditions, both of which is accounted for in the slenderness parameter  $L_E/r$ . For low slenderness, the beam fails by yielding, and for high slenderness, it fails by buckling. This slenderness parameter should be checked for **both the major axis and the minor axis** as the boundary conditions may differ. The capacity corresponding to the greater slenderness is clearly critical. The critical load capacity is

$$P_E = \sigma_E A$$

The Euler buckling load presented hitherto is actually the **flexural** Euler buckling load

$$P_E = \sigma_E A = \frac{\pi^2 EA}{(L_E / r)^2}$$

There is also the much smaller possibility of **shear** buckling. When buckling occurs, shear forces act on the section. These give rise to additional **shear deformations** that reduce the force that the member can take in compression before it becomes unstable and buckles.



The critical load for **combined flexural and shear buckling** is given by

$$1/N_{crit} = 1/N_{crit, flexural} + 1/N_{crit, shear}$$

Hence, the critical force is reduced approximately by the factor  $1/[1+N_{crit}/GA_s]$ , where  $N_{crit}$  is the critical force in the absence of **shear deformation**.

On top of **Euler flexural and shear buckling**, columns are also subject to **torsional buckling** and **flexural-torsional buckling**. These occur when the ratio of torsional to flexural stiffness is very much reduced.

### 3.2.5.1.2 GL, ML Lateral-Torsional Buckling of Beam Elements (Primary Stress is Only Bending)

From classical mechanics, it can be shown that the lateral torsional buckling capacity for an **elastic, isotropic** beam with a **uniform** bending moment diagram is

$$M_{LTB} = \frac{\pi}{L_E} \sqrt{EI_{MINOR} GJ} \sqrt{1 + \frac{\pi^2 EI_w}{L_E^2 GJ}}$$

**The LTB load estimate is perfectly analogous to the SOL 105 buckling load estimate.**

$I_w = \text{warping stiffness} = I_{MINOR} \frac{h^2}{4}$  for an I - section

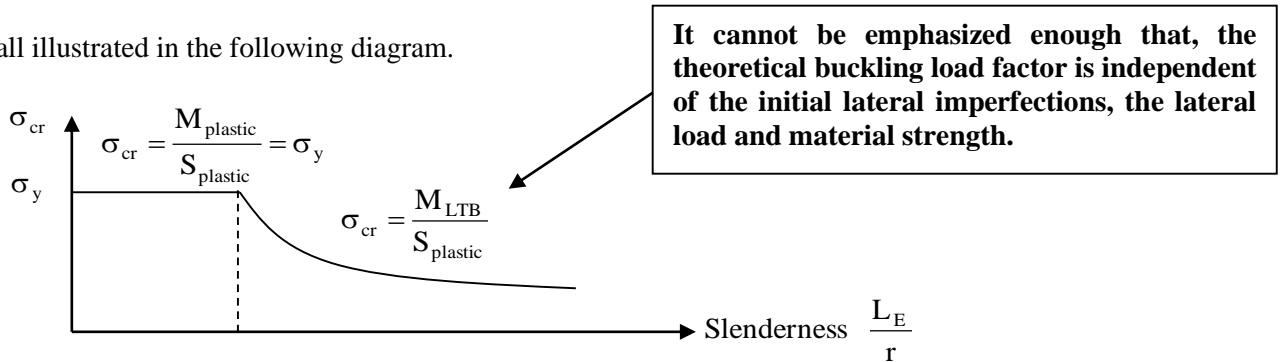
The lateral-torsional buckling of a beam is governed by both the minor axis elastic second moment of area,  $I_{MINOR}$  and also the torsional constant,  $J$ . Contrast with the Euler buckling which depended upon only the minor axis elastic second moment of area,  $I_{MINOR}$ .

The  $\pi$  is replaced with another value depending on the bending moment diagram; 4.24 for a triangular BMD due to a central point load; 3.53 for a uniform uniformly distributed load BMD.

However, beams are subject to plastic failure (attainment of plastic moment capacity) at low slenderness and to lateral torsional buckling at higher slenderness. The plastic moment capacity is

$$M_{plastic} = S_{plastic} \sigma_y$$

This is all illustrated in the following diagram.



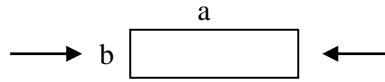
The buckling stress capacity depends on the stiffness of the element and the boundary conditions, both of which is accounted for in the slenderness parameter ( $L_E/r$ ). For low slenderness, the beam fails by yielding, and for high slenderness, it fails by lateral torsional buckling.

Lateral torsional buckling cannot occur in beams loaded in their weaker principal plane; under the action of increasing load they will collapse simply by plastic action and excessive in-plane deformation. Hence, the check need only be made for bending about the major axis.

### 3.2.5.1.3 GL, ML Euler Buckling of Plate Elements

Theoretical solution for the **Euler buckling of a plate (panel)** of thickness  $t$ , width of  $b$  and the two loaded edges **simply supported** is

$$\sigma_E = \frac{k\pi^2 E}{12(1-\nu^2)(b/t)^2}$$



where  $k$  is dependent upon the boundary conditions of the two non-loaded edges and also on the ratio of  $a/b$ , where  $a$  is the length of the panel. The table below presents the minimum values of  $k$  for different boundary conditions of the unloaded edge, with the **loaded edge simply supported**.

Unloaded Edge Condition	$k$
Both fixed	6.970
One fixed, one simply supported	5.420
Both simply supported	4.000
One fixed, one free	1.280
One simply supported, one free	0.425

Unlike columns, plates do not collapse when the critical buckling load is achieved. Constraints due to the two-dimensional nature of the plates allow plates to resist increasing loads beyond buckling. Hence the nonlinear post-buckling analysis is more important for plates.

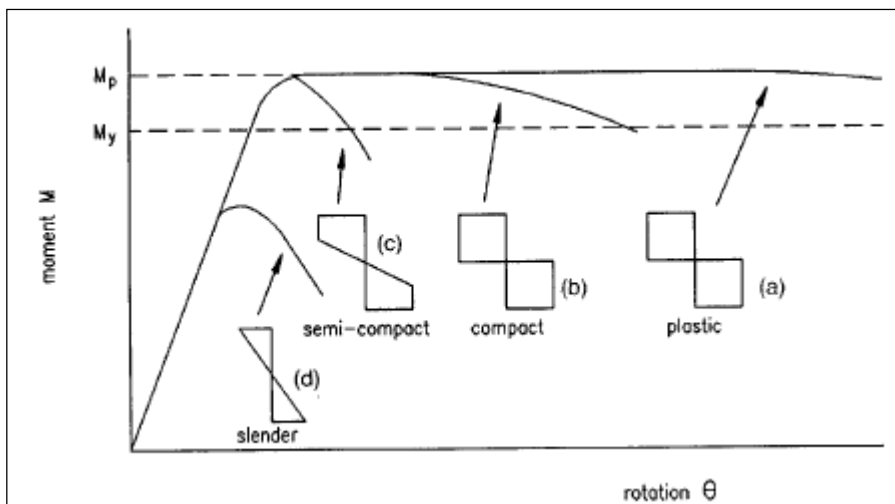
In **BS 5950-Part 1:2000**, cross-sections are classified to determine whether local buckling influences their capacity, without calculating their local buckling resistance. The classification of each element of a cross-section subject to compression (due to a bending moment or an axial force) should be based on its width-to-thickness ratio. The section classes are as follows.

**Class 1 Plastic:** Sections with plastic hinge rotation capacity. The **full plastic modulus S** may be used in design.

**Class 2 Compact:** Sections with plastic moment capacity. The **full plastic modulus S** may be used in design.

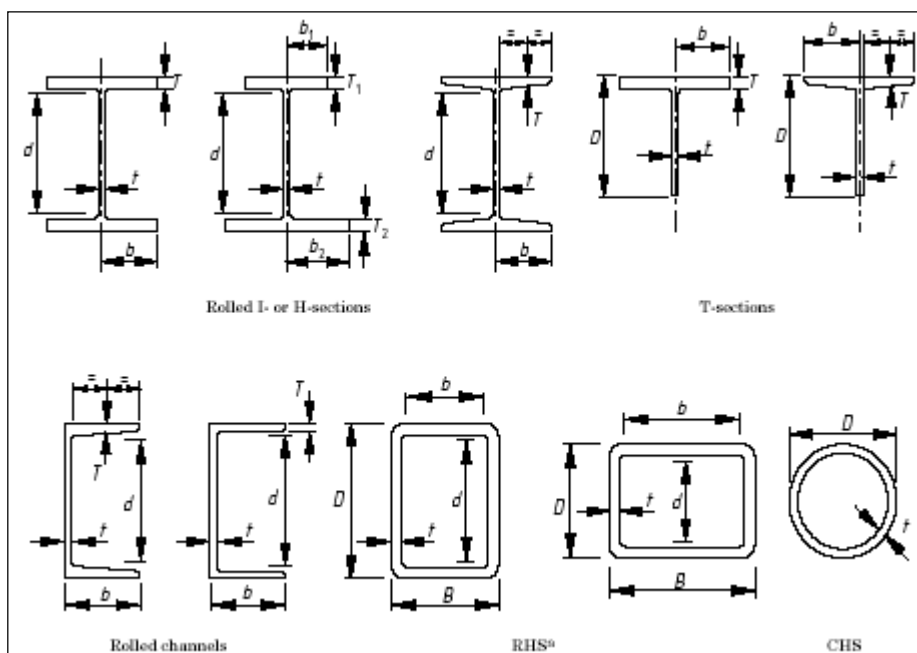
**Class 3 Semi-Compact:** Sections in which the stress at the extreme compression fibre can reach the design strength, but the plastic moment capacity cannot be developed. Elastic design methods must be adopted, i.e. the **full elastic modulus Z** must be used in design.

**Class 4 Slender:** Sections in which it is necessary to make explicit allowance for the effects of local buckling. BS 5950-Part 1:2000 gives approximate methods using **an effective area for Z** calculation in cl. 3.6.



Section Classification BS 5950-Part 1:2000	cl. 3.5
Design strength of steel, $p_y = f(\text{steel Grade, thickness}) \text{ (N/mm}^2\text{)}$	Table 9
For Class 1, 2, 3, the outstand element of rolled compression flange $b/T$ (half of the width of flange divided by the flange thickness) must be $< 9\epsilon, 10\epsilon, 15\epsilon$	Table 11 or Table 12
For Class 1, 2, 3, the internal element of compression flange $b/T$ (width of attached plate on flange divided by thickness of attached plate) must be $< 28\epsilon, 32\epsilon, 40\epsilon$	Table 11 or Table 12
For Class 1, 2, 3, the outstand element of welded compression flange $b/T$ (width of the outstand portion of attached plate on flange divided by the thickness of the attached plate) must be $< 8\epsilon, 9\epsilon, 13\epsilon$	Table 11 or Table 12
For Class 1, 2, 3, an angle or the outstand of an angle connected onto another component $b/t$ and $d/t$ must be $< 9\epsilon, 10\epsilon, 15\epsilon$	Table 11 or Table 12
For Class 1, 2, 3, the stem of a T- section $D/t$ must be $< 8\epsilon, 9\epsilon, 18\epsilon$	Table 11 or Table 12
For Class 1, 2, 3, the web of I-, H- or Box section $d/t$ must be $< 80\epsilon, 100\epsilon, 120\epsilon$	Table 11 or Table 12
For Class 1, 2, 3, the web of a channel section $d/t$ must be $< 40\epsilon, 40\epsilon, 40\epsilon$	Table 11 or Table 12
For Class 1, 2, 3, CHS must have $D/t < 40\epsilon^2, 50\epsilon^2, 140\epsilon^2$	Table 11 or Table 12
For Class 1, 2, 3, RHS must have $b/t < 28\epsilon, 32\epsilon, 40\epsilon$ and $d/t < 64\epsilon, 80\epsilon, 120\epsilon$	Table 11 or Table 12
Note that $\epsilon = (275/p_y)^{0.5}$ .	

Note the much tighter criteria (**about 9ε, 10ε, 15ε**) for local sections which are not constrained such as the outstand of a flange, an angle or the stem of T- section. Note the fairly relaxed criteria (**about 40ε, 40ε, 40ε**) for partially constrained sections such as the web of a channel. And note the very relaxed criteria (**about 80ε, 100ε, 120ε**) for constrained sections such as the web of a I-, H- or Box section.



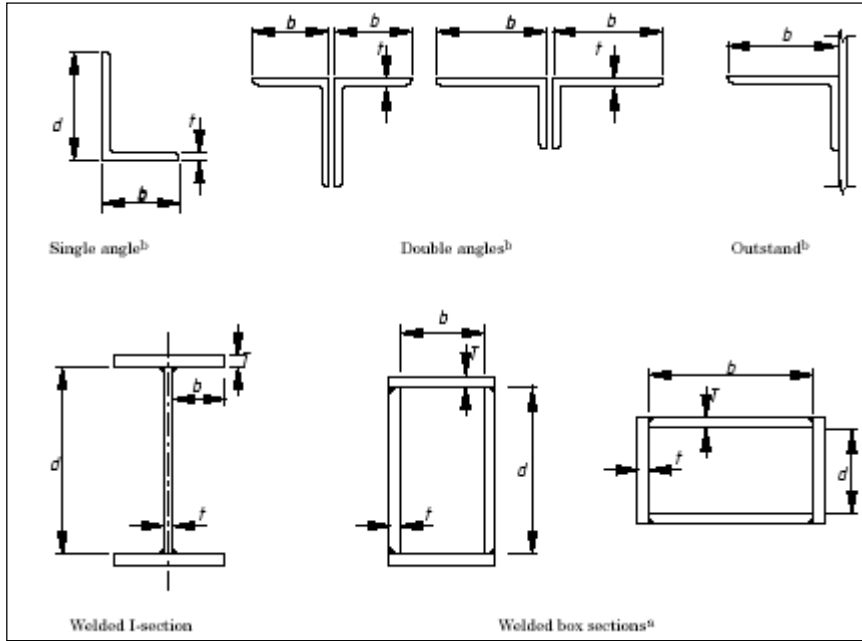


**Table 11 — Limiting width-to-thickness ratios for sections other than CHS and RHS**

Compression element		Ratio <sup>a</sup>	Limiting value <sup>b</sup>		
			Class 1 plastic	Class 2 compact	Class 3 semi-compact
Outstand element of compression flange	Rolled section	$b/T$	$9\epsilon$	$10\epsilon$	$15\epsilon$
	Welded section	$b/T$	$8\epsilon$	$9\epsilon$	$13\epsilon$
Internal element of compression flange	Compression due to bending	$b/T$	$28\epsilon$	$32\epsilon$	$40\epsilon$
	Axial compression	$b/T$	Not applicable		
Web of an I-, H- or box section <sup>c</sup>	Neutral axis at mid-depth	$d/t$	$80\epsilon$	$100\epsilon$	$120\epsilon$
	Generally <sup>d</sup>	If $r_1$ is negative:		$\frac{100\epsilon}{1+r_1}$	$\frac{120\epsilon}{1+2r_2}$ but $\geq 40\epsilon$
		If $r_1$ is positive:	$d/t$	$\frac{80\epsilon}{1+r_1}$ but $\geq 40\epsilon$	
	Axial compression <sup>d</sup>	$d/t$	Not applicable		
Web of a channel	$d/t$	$40\epsilon$	$40\epsilon$	$40\epsilon$	
Angle, compression due to bending (Both criteria should be satisfied)		$b/t$	$9\epsilon$	$10\epsilon$	$15\epsilon$
		$d/t$	$9\epsilon$	$10\epsilon$	$15\epsilon$
Single angle, or double angles with the components separated, axial compression (All three criteria should be satisfied)		$b/t$	Not applicable		$15\epsilon$
		$d/t$ $(b+d)/t$	Not applicable		$15\epsilon$ $24\epsilon$
Outstand leg of an angle in contact back-to-back in a double angle member	$b/t$	$9\epsilon$	$10\epsilon$	$15\epsilon$	
Outstand leg of an angle with its back in continuous contact with another component					
Stem of a T-section, rolled or cut from a rolled I- or H-section	$D/t$	$8\epsilon$	$9\epsilon$	$18\epsilon$	

<sup>a</sup> Dimensions  $b$ ,  $D$ ,  $d$ ,  $T$  and  $t$  are defined in Figure 5. For a box section  $b$  and  $T$  are flange dimensions and  $d$  and  $t$  are web dimensions, where the distinction between webs and flanges depends upon whether the box section is bent about its major axis or its minor axis, see 3.5.1.

<sup>b</sup> The parameter  $\epsilon = (275/p_y)^{0.5}$ .

<sup>c</sup> For the web of a hybrid section  $\epsilon$  should be based on the design strength  $p_y$  of the flanges.

<sup>d</sup> The stress ratios  $r_1$  and  $r_2$  are defined in 3.5.5.

**Table 12 — Limiting width-to-thickness ratios for CHS and RHS**

Compression element		Ratio <sup>a</sup>	Limiting value <sup>b</sup>			
			Class 1 plastic	Class 2 compact	Class 3 semi-compact	
CHS	Compression due to bending	$D/t$	$40\epsilon^2$	$50\epsilon^2$	$140\epsilon^2$	
	Axial compression	$D/t$	Not applicable		$80\epsilon^2$	
HF RHS	Flange	Compression due to bending	$b/t$	$28\epsilon$ but $\leq 80\epsilon - d/t$	$32\epsilon$ but $\leq 62\epsilon - 0.5d/t$	$40\epsilon$
		Axial compression	$b/t$	Not applicable		
	Web	Neutral axis at mid-depth	$d/t$	$64\epsilon$	$80\epsilon$	$120\epsilon$
		Generally <sup>cd</sup>	$d/t$	$\frac{64\epsilon}{1 + 0.6r_1}$ but $\geq 40\epsilon$	$\frac{80\epsilon}{1 + r_1}$ but $\geq 40\epsilon$	$\frac{120\epsilon}{1 + 2r_2}$ but $\geq 40\epsilon$
		Axial compression <sup>d</sup>	$d/t$	Not applicable		
CF RHS	Flange	Compression due to bending	$b/t$	$26\epsilon$ but $\leq 72\epsilon - d/t$	$28\epsilon$ but $\leq 54\epsilon - 0.5d/t$	$35\epsilon$
		Axial compression <sup>d</sup>	$b/t$	Not applicable		
	Web	Neutral axis at mid-depth	$d/t$	$56\epsilon$	$70\epsilon$	$105\epsilon$
		Generally <sup>cd</sup>	$d/t$	$\frac{56\epsilon}{1 + 0.6r_1}$ but $\geq 35\epsilon$	$\frac{70\epsilon}{1 + r_1}$ but $\geq 35\epsilon$	$\frac{105\epsilon}{1 + 2r_2}$ but $\geq 35\epsilon$
		Axial compression <sup>d</sup>	$d/t$	Not applicable		
Abbreviations CF Cold formed; CHS Circular hollow section — including welded tube; HF Hot finished; RHS Rectangular hollow section — including square hollow section.						
<sup>a</sup> For an RHS, the dimensions $b$ and $d$ should be taken as follows: — for HF RHS to BS EN 10210: $b = B - 3t$ ; $d = D - 3t$ — for CF RHS to BS EN 10219: $b = B - 5t$ ; $d = D - 5t$ and $B$ , $D$ and $t$ are defined in Figure 5. For an RHS subject to bending $B$ and $b$ are always flange dimensions and $D$ and $d$ are always web dimensions, but the definition of which sides of the RHS are webs and which are flanges changes according to the axis of bending, see 3.5.1.						
<sup>b</sup> The parameter $\epsilon = (275/p_y)^{0.5}$ .						
<sup>c</sup> For RHS subject to moments about both axes see H.3.						
<sup>d</sup> The stress ratios $r_1$ and $r_2$ are defined in 3.5.5.						

#### 3.2.5.1.4 Web Shear Buckling

<b>Web Shear Buckling BS 5950-Part 1:2000</b>	cl. 4.4.5
Ensure $d/t < 62\varepsilon$ for welded sections or $70\varepsilon$ for rolled sections to avoid web shear buckling	

Additional considerations to moment capacity must be made according to cl. 4.4.4.2 if web is subject to shear buckling.

### 3.2.5.2 Overall System ( $K_G^A$ From $K_E^A$ ) Buckling

#### 3.2.5.2.1 Linear Elastic Buckling Based on Energy Principles

##### ENERGY METHODS IN THE STABILITY ANALYSIS OF SYSTEMS

	Perfect	Imperfect
Stable symmetric bifurcation	1	5
Unstable symmetric bifurcation	2	6
Asymmetric bifurcation	3	7
Limit load instability	4	8

- (A) Obtain total potential energy function  $V = U - P\Delta$
- (B) Obtain equilibrium path(s) by solving for  $\frac{\partial V}{\partial \theta} = 0$ .
- (i) Systems 1, 2, 3 give two solutions of equilibrium paths, i.e. one for  $\theta$  i.e.  $\theta = 0$  and one for  $P$  in terms of  $\theta$ ; hence two equilibrium paths:-  
 $\theta = 0, P = \text{anything}$   
 $P = f(\theta) \Rightarrow$  usually can plot  $P$  vs  $\theta$  already to recognise the type of perfect bifurcation system and determine critical point.
- (ii) System 4 gives one solution of  $P$  in terms of  $\theta$ ; hence one equilibrium path:-  
 $P = f(\theta)$
- (iii) Systems 5, 6, 7, 8 give one solution of  $P$  in terms of  $\theta$  and  $\epsilon$ .  
 $P = f(\theta, \epsilon)$

(C) Investigate the stability of each of the obtained equilibrium paths.

Replace each equilibrium path separately into  $\frac{\partial^2 V}{\partial \theta^2}$ .

$\frac{\partial^2 V}{\partial \theta^2} > 0$  defines regions of stability on the equilibrium path concerned.

$\frac{\partial^2 V}{\partial \theta^2} < 0$  defines regions of instability on the equilibrium path concerned.

(D) Identify the critical point (i.e. boundary between stability and instability).

The critical point is either the bifurcation point or the limit point.

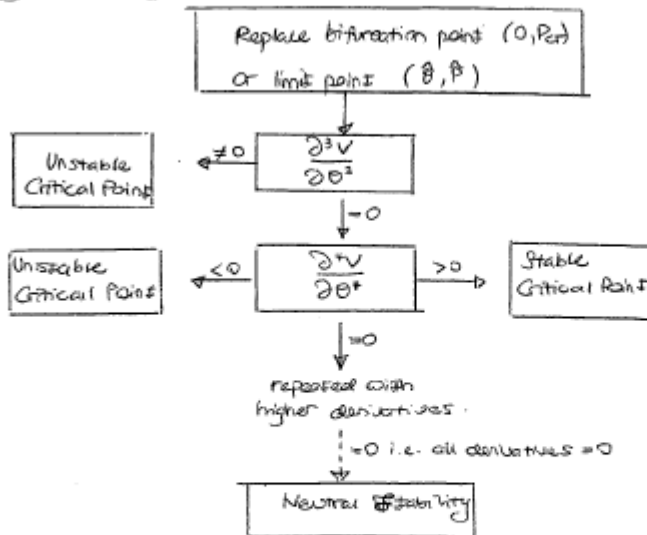
	Perfect	Imperfect
Stable symmetric bifurcation	Bifurcation Point	—
Unstable symmetric bifurcation	Bifurcation Point	Limit Point
Asymmetric bifurcation	Bifurcation Point	Limit Point
Limit load instability	Limit Point	Limit Point

(i) Systems 1, 2, 3 yield the bifurcation point  $(0, P_{cr})$  which can be obtained by inspection of the  $P$  vs  $\theta$  graph; To confirm the point  $(0, P_{cr})$  must satisfy  $\frac{\partial^2 V}{\partial \theta^2} = 0$ .

(ii) Systems 4, 6, 7, 8 have limit points which is obtained by finding the turning point of the equilibrium path:-

Hence,  $\frac{dP}{d\theta} = 0 \Rightarrow$  solve for  $\hat{\theta} \Rightarrow \hat{P}$  obtained  $\Rightarrow (\hat{\theta}, \hat{P})$  defines limit point.

(E) Investigate stability of the critical point (bifurcation point or limit point)



(F) Optional: Imperfection Sensitivity Analysis for systems 6, 7, 8

We have already the

limit point  $(\hat{\theta}, \hat{P})$

however,  $\hat{P}$  is actually in terms of  $\epsilon$ , the imperfection.

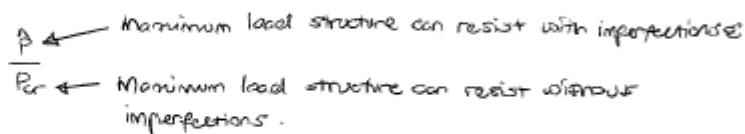
$$\hat{P} = p(\epsilon) \text{ not } \theta \text{ at all.}$$

$$\Rightarrow \frac{\hat{P}}{P_{cr}} = f(\epsilon)$$

A plot of  $\frac{\hat{P}}{P_{cr}}$  vs  $\epsilon$  gives the imperfection sensitivity diagram.

The imperfection sensitivity diagram shows the degree of reduction of failure loads from  $P_{cr}$  (of the perfect case) with increasing imperfections  $\epsilon$ .

The smaller the ratio  $\frac{\hat{P}}{P_{cr}}$ , the greater the sensitivity of the system to imperfections  $\epsilon$ .



Note that for system 6,

$$\frac{\hat{P}}{P_{cr}} \approx 1 - a\epsilon^{2/3} \text{ where } a \text{ depends on the system in question.}$$

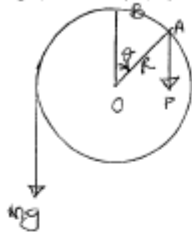


Note that equilibrium diagrams plot  $P$  versus  $\theta$  whilst imperfection sensitivity diagrams plot  $\frac{\hat{P}}{P_{cr}}$  versus  $\epsilon$ .

ENERGY METHODS IN STABILITY ANALYSIS OF SYSTEMS :

TO OBTAIN THE TOTAL POTENTIAL ENERGY FUNCTION  $V = U - P\Delta$ . Work done by load P.  
Gained potential energy

(A) Bucket in a well pulled through a pulley.



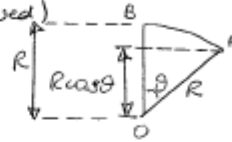
$$U = mg (\text{curve } AB)$$

$$= mgR\theta \quad ; \theta \text{ in radians}$$

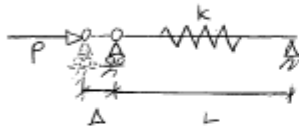
$$P\Delta = P (\text{vertical distance moved})$$

$$= PR(1 - \cos\theta)$$

$$V = mgR\theta - PR(1 - \cos\theta) \quad ; \theta \text{ in radians}$$



(B) Straight linear spring

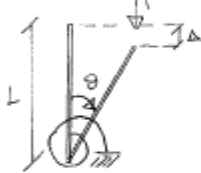


$$U = \frac{1}{2} k \Delta^2$$

$$P\Delta = P\Delta$$

$$V = \frac{1}{2} k \Delta^2 - P\Delta$$

(C) Rotational Linear Spring

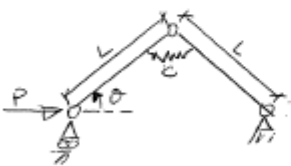


$$U = \frac{1}{2} k \theta^2$$

$$P\Delta = PL(1 - \cos\theta)$$

$$V = \frac{1}{2} k \theta^2 - PL(1 - \cos\theta)$$

(D)



$$U = \frac{1}{2} c \theta^2 \quad \leftarrow \text{note because initially } \theta = 0; \text{ hence total rotation is } \theta$$

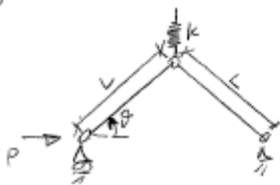
Initially (when  $\theta = 0$ ):

$$P\Delta = P(2L - 2L\cos\theta)$$

$$= 2LP(1 - \cos\theta)$$

$$V = \frac{1}{2} c \theta^2 - 2LP(1 - \cos\theta)$$

(E)



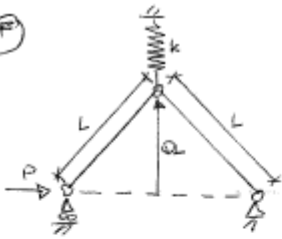
$$U = \frac{1}{2} k (L\sin\theta)^2 \quad \leftarrow \text{note because initially } \theta = 0; \text{ hence total contraction of spring is } L\sin\theta$$

$$P\Delta = P(2L - 2L\cos\theta)$$

$$= 2PL(1 - \cos\theta)$$

$$V = \frac{1}{2} k (L\sin\theta)^2 - 2PL(1 - \cos\theta)$$

8


 Note  $QL$  definition instead of  $\theta$ .

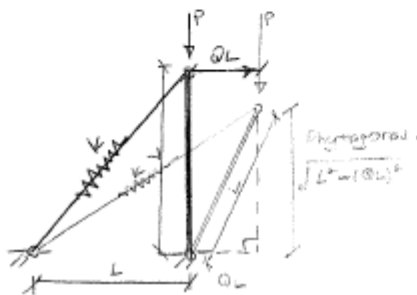
$$u = \frac{1}{2} k (QL)^2 \quad \leftarrow \text{note initially } QL=0 \text{ hence contraction of spring is } QL.$$

$$\text{By Pythagoras, base width} = 2 \cdot \sqrt{L^2 - (QL)^2}$$

$$\begin{aligned} P\Delta &= (2L - 2\sqrt{L^2 - Q^2L^2})P \\ &= 2PL(1 - \sqrt{1 - Q^2}) \end{aligned}$$

$$V = \frac{1}{2} k Q^2 L^2 - 2PL(1 - \sqrt{1 - Q^2})$$

9


 Initially  $QL=0$ .

$$\begin{aligned} P\Delta &= P \left\{ L - (\sqrt{L^2 - (QL)^2}) \right\} \\ &= PL(1 - \sqrt{1 - Q^2}) \end{aligned}$$

To find extension of spring, need to know initial and final lengths.

$$\text{Initial length} = \sqrt{L^2 + L^2} = L\sqrt{2}$$

$$\begin{aligned} \text{Final length} &= \sqrt{(L+QL)^2 + (\sqrt{L^2 - (QL)^2})^2} \\ &= \sqrt{L^2(1+Q)^2 + L^2 - Q^2L^2} \\ &= L\sqrt{1+Q^2+2Q+1-Q^2} \\ &= L\sqrt{2(1+Q)} \end{aligned}$$

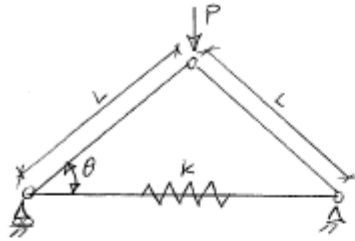
$$\begin{aligned} \text{Extension} &= L\sqrt{2(1+Q)} - L\sqrt{2} \\ &= \sqrt{2}L(\sqrt{1+Q} - 1) \end{aligned}$$

$$\begin{aligned} u &= \frac{1}{2} k (\text{extension})^2 \\ &= \frac{1}{2} k (2)L^2 (\sqrt{1+Q} - 1)^2 \\ &= kL^2 [\sqrt{1+Q} - 1]^2 \end{aligned}$$

$$V = kL^2 [\sqrt{1+Q} - 1]^2 - PL(1 - \sqrt{1 - Q^2})$$

(H)

Given initially  $\theta = \alpha$



Initially,



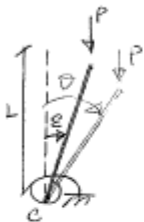
$$U = \frac{1}{2} k (2L \cos \theta - 2L \cos \alpha)^2$$

$$= 2kL^2 (\cos \theta - \cos \alpha)^2$$

$$P\Delta = P(L \sin \alpha - L \sin \theta)$$

$$V = 2kL^2 (\cos \theta - \cos \alpha)^2 - PL(\sin \alpha - \sin \theta)$$

(I)

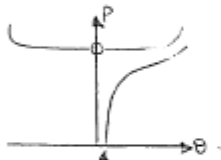


$$U = \frac{1}{2} c (\theta - \epsilon)^2$$

$$P\Delta = P(L \cos \epsilon - L \cos \theta) \text{ or } P\Delta = P(L - L \cos \theta)$$

Work done by load depends on where it is measured from. It is easier to measure from vertical position, i.e.  $\theta = 0$ .

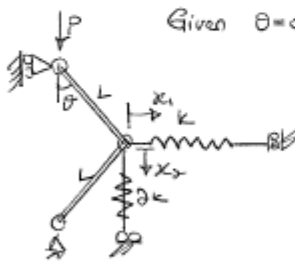
When differentiated, same result obtained anyway.



$\theta = 0$  imperfection at  $P = 0$

(J)

Given  $\theta = 0$  initially.



$$P\Delta = P(2L - 2L \cos \theta)$$

$$= 2PL(1 - \cos \theta)$$

$$U = \frac{1}{2} k x_1^2 + \frac{1}{2} k x_2^2$$

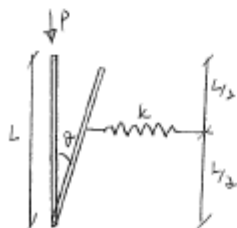
$$x_1 = L \sin \theta$$

$$x_2 = L - L \cos \theta$$

Not  $2L - 2L \cos \theta$  of course.

$$V = \frac{1}{2} k (L \sin \theta)^2 + \frac{1}{2} k (L - L \cos \theta)^2 - 2PL(1 - \cos \theta)$$

(K)



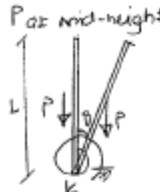
$$P\Delta = P(L - L \cos \theta)$$

$$U = \frac{1}{2} k \left( \frac{L}{2} \sin \theta \right)^2$$

$$V = \frac{1}{2} k \left( \frac{L}{2} \sin \theta \right)^2 - PL(1 - \cos \theta)$$

Note  $\frac{L}{2}$  not  $L$  because need horizontal distance at elevation of spring.

(L)  $P$  at mid-height

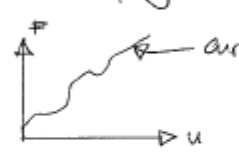


$$\Delta = P \left( \frac{1}{3} - \frac{1}{3} \cos \theta \right)$$

$$U = \frac{1}{3} k \theta^2$$

$$V = \frac{1}{3} k \theta^2 - P \frac{1}{3} (1 - \cos \theta)$$

(M) Non-linear spring



curve defined by  $F = f(u)$   
 Slope of curve = stiffness  $k = \frac{F}{u} = \frac{f(u)}{u}$   
 Strain energy  $U = \int_0^u F du$

If say given force in spring is  $F = ku \left( 1 + \frac{u}{a} \right)$ , then

$$U = \int_0^u \underbrace{ku \left( 1 + \frac{u}{a} \right)}_{\text{put force expression, not stiffness}} du$$

In the special case that the spring is linear,  
 $F = ku$  where  $k$  is the stiffness.

$$U = \int_0^u ku du$$

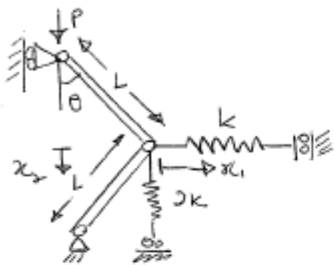
$$= \frac{ku^2}{2} \text{ as expected.}$$

LINK MODELS

Method:

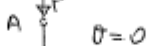
- (i) Check initial (unloaded) geometry of system.
- (ii) Find out (determine) the ranges of the degree-of freedom.
- (iii) Solve it.

Example 1

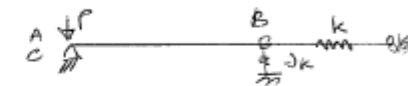


Find the critical load  $P^c$ , and the stability of the equilibrium paths of the system. The springs are unstressed when  $\theta = 0$ .

(i) Check initial system (i.e.  $\theta = 0$ )



(ii)  $\theta = 90^\circ$



(ii) We can say that  $0 \leq |\theta| \leq \frac{\pi}{2}$

(iii) Solve the system ( $\theta \neq 0$ )

Total potential energy:

$$V = U - P\Delta$$

↑ Strain energy for the springs
 ↑ Work done by load.

$$U = \frac{1}{2} k (x_1)^2 + \frac{1}{2} (2k) (x_2)^2$$

$$x_1 = L \sin \theta$$

$$x_2 = L - L \cos \theta = L(1 - \cos \theta)$$

Not  $2L - 2L \cos \theta$

$$\therefore U = \frac{1}{2} k L^2 \sin^2 \theta + k L^2 (1 - \cos \theta)^2$$

$$\begin{aligned} \text{Work done by } P &= P\Delta = P(L - L \cos \theta) \quad (2) \\ &= 2PL(1 - \cos \theta) \end{aligned}$$

$$\therefore V = \frac{1}{2} k L^2 \sin^2 \theta + k L^2 (1 - \cos \theta)^2 - 2PL(1 - \cos \theta) \quad \text{Total Potential Energy}$$

Determine  $P^c$  and stability.

Equilibrium is defined by  $\frac{\partial V}{\partial \theta} = 0$ .

$$kL^2 [\sin \theta \cos \theta + 2(1 - \cos \theta) \sin \theta] - 2PL \sin \theta = 0$$

Factorise:  $\leftarrow$  good!

$$\sin \theta [kL^2 (\cos \theta + 2(1 - \cos \theta)) - 2PL] = 0$$

One solution:  $\sin \theta = 0$

$\theta = 0, \pi, 2\pi$  (however physical solution only 0)

i.e. as  $|\theta| \leq \pi/2$  we can say that the only physical solution is  $\theta = 0$ .  
The other solution is to make the term in brackets vanish.

$$KL^2[2 - \cos\theta] - 2PL = 0$$

$$P = \frac{KL}{2}[2 - \cos\theta] \quad (\text{second solution}).$$

Check stability

First derivative of  $V$ ,

$$\frac{\partial V}{\partial \theta} = KL^2 \left[ 2\sin\theta - \frac{1}{2}\sin 2\theta \right] - 2PL\sin\theta$$

Differentiating again,

$$\frac{\partial^2 V}{\partial \theta^2} = KL^2 [2\cos\theta - \cos 2\theta] - 2PL\cos\theta$$

(i)  $\theta = 0$

$$\text{For stability } \frac{\partial^2 V}{\partial \theta^2} > 0$$

$$KL^2(1) - 2PL > 0$$

$$P < \frac{KL}{2}$$

System is stable for  $\theta = 0, P < \frac{KL}{2}$  but unstable for  $\theta = 0, P > \frac{KL}{2}$ .

(ii)  $P = \frac{KL}{2}[2 - \cos\theta]$

$$\text{For stability: } \frac{\partial^2 V}{\partial \theta^2} > 0$$

$$KL^2 [2\cos\theta - \cos 2\theta] - KL^2 (2 - \cos\theta)\cos\theta > 0$$

$$[\cos 2\theta = \cos^2\theta - \sin^2\theta]$$

$$KL^2 \sin^2\theta > 0$$

Now for  $|\theta| > 0, \sin^2\theta > 0$

hence  $\frac{\partial^2 V}{\partial \theta^2} > 0$  for  $|\theta| > 0$

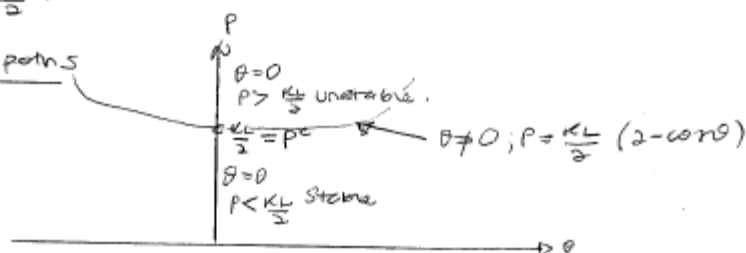
$\Rightarrow$  stable for non-trivial values of  $\theta$ .

Find  $P^c$

From checking stability we find  $P < \frac{KL}{2}$  the system is stable and unstable for  $P > \frac{KL}{2}$ . Thus something special about  $\frac{KL}{2}$ , which is that  $\frac{\partial^2 V}{\partial \theta^2}$  vanishes. And this defines our critical load  $P^c$ .

$$\therefore P^c = \frac{KL}{2}$$

Plot equilibrium paths



check stability for  $P=P_c, \theta=0$

We see that for this point,  $\frac{\partial^2 V}{\partial \theta^2}$  vanishes, so we must use higher derivatives to check stability, i.e. 3rd derivative.

$$\frac{\partial^3 V}{\partial \theta^3} = kL^2 [2\sin 2\theta - 2\sin \theta] + 2PL \sin \theta$$

When  $\theta=0$ :  $\frac{\partial^3 V}{\partial \theta^3} = 0 \therefore$  look at 4<sup>th</sup> derivative.

$$\frac{\partial^4 V}{\partial \theta^4} = kL^2 (4\cos 2\theta - 2\cos \theta) + 2PL \cos \theta$$

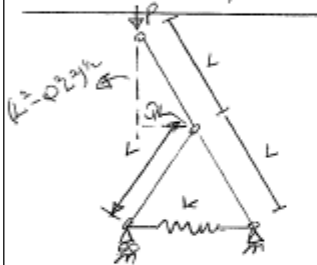
For  $\theta=0$ :  $\frac{\partial^4 V}{\partial \theta^4} = kL^2 (4-2) + 2PL > 0$  for stability

$$P=P_c = kL/2$$

$$\frac{\partial^4 V}{\partial \theta^4} = 2kL^2 + kL^2 = 3kL^2 > 0 \therefore P=P_c \text{ is stable.}$$

Therefore we have a stable symmetric system.

### Worked Example 2

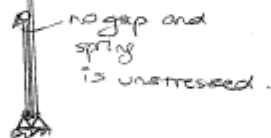


Degree of freedom is  $Q$ .

Draw initial and final system.

(i) Initial  $Q=0$

(ii) Final  $Q: Q=1$



Range of  $Q$  is

$$0 \leq |Q| \leq 1$$

Note:

Total potential energy

$$V = U - PA$$

Strain energy in spring:  $U = \frac{1}{2} kx^2$  note

By similar triangles  $x = 2QL$

$$U = \frac{1}{2} k(4Q^2 L^2) = 2kL^2 Q^2$$

$$\begin{aligned} 2L - 2(L^2 - Q^2 L^2)^{1/2} \\ = 2L - 2L(1 - Q^2)^{1/2} \\ = 2(L - L(1 - Q^2)^{1/2}) \end{aligned}$$

Work done: Drop in P's position:  $2(L - L\sqrt{1 - Q^2}) = \Delta = 2L(1 - \sqrt{1 - Q^2})$

$$V = U - PA$$

$$= 2kL^2 Q^2 - 2PL(1 - \sqrt{1 - Q^2})$$

Equilibrium:  $\frac{\partial V}{\partial Q} = 0$  ← differentiate wrt  $Q$ !

$$4kL^2 Q - 2PL \left( -\frac{1}{2} (-2Q) (1 - Q^2)^{-1/2} \right) = 0$$

$$4kL^2 Q = \frac{2PLQ}{\sqrt{1 - Q^2}}$$

Equilibrium paths:  $\sqrt{1 - Q^2}$

(i)  $Q=0$  is one solution (by inspection).

(ii)  $P = 2KL\sqrt{1-Q^2}$  is the second solution.

Stability of equilibrium paths

$$\frac{\partial^2 V}{\partial Q^2} > 0 \text{ for stability}$$

$$\frac{\partial^2 V}{\partial Q^2} = 4KL^2 - 2PL \left[ (1-Q^2)^{-3/2} + Q^2 (1-Q^2)^{-5/2} \right] > 0$$

(i)  $Q=0$

$$4KL^2 - 2PL > 0$$

$P < 2KL$  is stable,  $P > 2KL$  is unstable.

$\therefore$  When  $P = 2KL \Rightarrow \frac{\partial^2 V}{\partial Q^2} = 0 \Rightarrow P = P^c = 2KL$  (Critical Load).

(ii)  $P = 2KL\sqrt{1-Q^2}$

$$\frac{\partial^2 V}{\partial Q^2} > 0 \text{ for stability}$$

$$\frac{\partial^2 V}{\partial Q^2} = 4KL^2 - 4KL^2 \left[ 1 + \frac{Q^2}{1-Q^2} \right] > 0$$

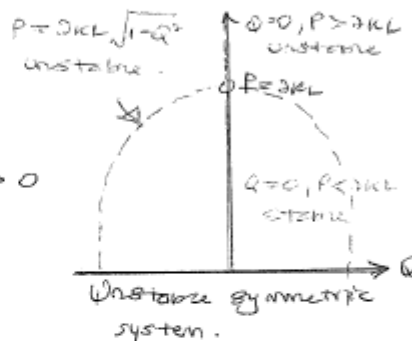
$$4KL^2 \left\{ 1 - 1 - \frac{Q^2}{1-Q^2} \right\} > 0$$

$$-4KL^2 \left( \frac{Q^2}{1-Q^2} \right) > 0$$

So for our physical range of  $Q$ , the term  $\frac{Q^2}{1-Q^2} > 0$ .

$$\therefore \frac{\partial^2 V}{\partial Q^2} = -4KL^2 \text{ (+ve term)}$$

$\therefore \frac{\partial^2 V}{\partial Q^2} < 0$  Hence system unstable for all physical values of  $Q$ .



Stability of the critical point: ( $P = P^c = 2KL, Q = 0$ )

We know that here:

$$\frac{\partial^2 V}{\partial Q^2} = 0, \text{ so we check higher derivatives of } V.$$

Third derivative:

$$\frac{\partial^3 V}{\partial Q^3} = -2PL \left[ 3Q(1-Q^2)^{-3/2} + 3Q^3(1-Q^2)^{-5/2} \right]$$

for  $Q=0, \frac{\partial^3 V}{\partial Q^3} = 0 \Rightarrow$  look at 4<sup>th</sup> derivative.

Fourth derivative:

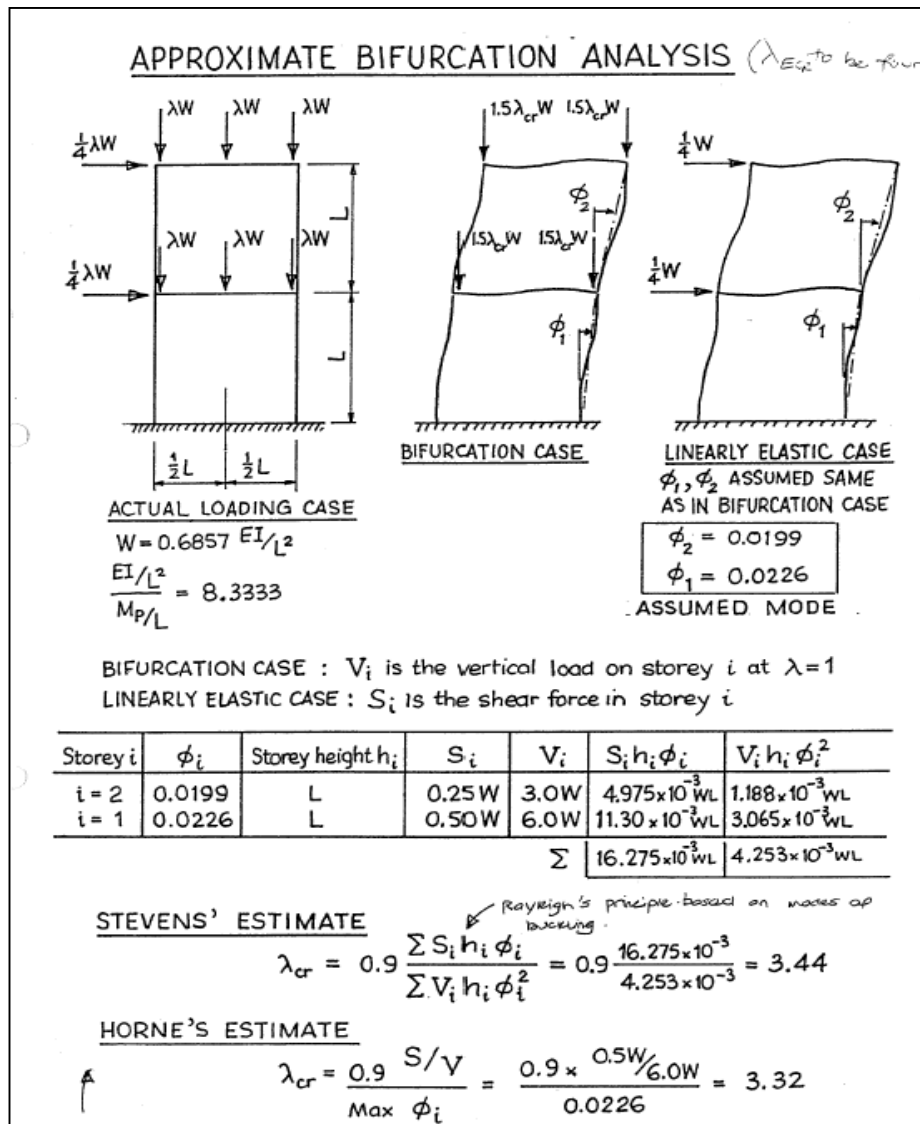
$$\frac{\partial^4 V}{\partial Q^4} = -6PL \left[ (1-Q^2)^{-3/2} + 6Q^2(1-Q^2)^{-5/2} + 5Q^4(1-Q^2)^{-7/2} \right]$$

for  $Q=0 \Rightarrow \frac{\partial^4 V}{\partial Q^4} = -6PL$

Hence  $P = P^c = 2KL: \frac{\partial^4 V}{\partial Q^4} = -12KL^2 < 0 \Rightarrow$  unstable.

### 3.2.5.2.2 GL, ML Approximate Bifurcation (Linear Buckling) Analysis of Multi-Story Frames

The approximate bifurcation analysis of multi-story frames estimates an approximate elastic critical load,  $\lambda_{Ecr}$ .



BS 5950-Part 1:2000 (cl. 2.4.2.6) gives a method for calculating  $\lambda_{cr}$  for simple (symmetric in plan) multi-storey buildings (excluding single-storey frames with moment-resisting joints and other multi-storey frames in which sloping members have moment-resisting connections) based on the deflection due to the **Notional Horizontal Forces of 0.5% of the factored vertical (1.4 dead + 1.6 live) load or 1.0% of the factored vertical (1.4 dead) load, whichever the greater** applied at the same level.

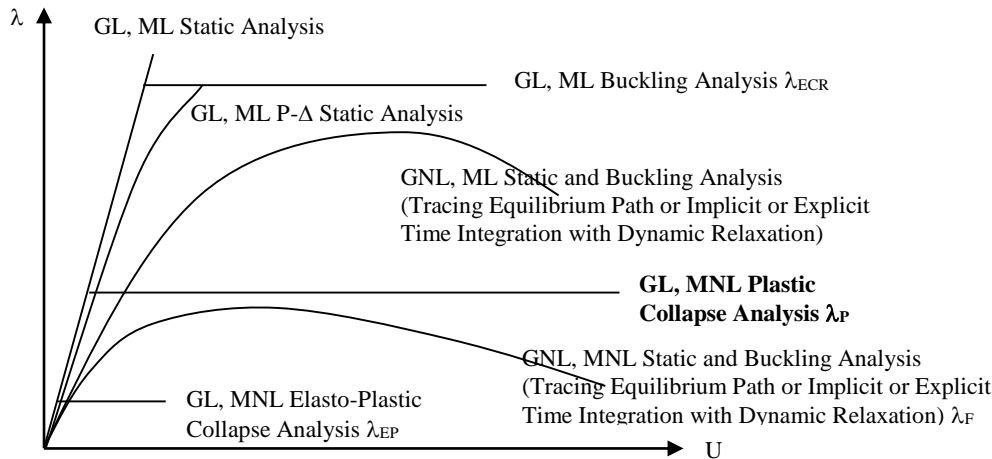
$$\lambda_{cr} = \frac{1}{200} \frac{h}{\delta}$$

where  $h/\delta$  is the value of the storey height divided by the deflection over that storey (deflection at top of storey relative to deflection at bottom of storey) for any storey in the building. The smallest value considering every storey should be used. This equation is based on a shear mode buckling and gives very good agreement with more detailed analysis. Lower buildings tend to be governed by shear buckling whilst taller buildings are governed by the flexural buckling mode. If the mode is flexural, the above simple equation is likely to underestimate (conservative)  $\lambda_{cr}$ . The stability systems for steel buildings are often braced cores. It can be shown that if the stress in the diagonals is greater than 57MPa, however stiff the columns and beams,  $\lambda_{cr}$  will be less than 10.

### 3.3 GL, MNL Plastic Collapse Analysis by the Implicit Linear Simplex Programming

#### 3.3.1 Mathematical Formulation of Analysis

Great structural engineering failures since time immemorial can be attributed to a lack of redundancy. A plastic collapse analysis is a brilliant method of finding out the amount of redundancy that a structure had to a load.



Plastic collapse analysis is performed if material non-linearity (yielding and subsequent formation of plastic hinges) is thought to be more significant than elastic buckling instability in causing the failure of the structure. The structure has not buckled (experienced elastic instability) but has  $\alpha + 1$  fully plastic hinges, i.e. a mechanism.

In order to use plastic collapse analysis methods, the beams and columns must be ductile, i.e. must be able to deform sufficiently to form plastic hinges. Ductility in beams improved by having less than 4% steel reinforcement, having shear links to confine concrete in three dimensions, having a little compression steel, too much of which will reduce ductility. Ductility in columns improved by having shear links to confine concrete in three dimensions to avoid the propagation of micro-cracks.

The Uniqueness Theorem states that the smallest critical plastic collapse load factor is attained if the 3 following condition are achieved: -

- I. Equilibrium condition: The bending moment distribution must be in equilibrium with the external applied loads
- II. Yield condition: The bending moment must nowhere exceed the plastic moment capacity of the section
- III. Mechanism condition: There must be sufficient plastic hinges to form a mechanism.

The Upper Bound Mechanism Method of Plastic Limit Analysis to find  $\lambda_P$  uses the equilibrium conditions and postulates many collapse mechanisms, finding the critical combination by minimizing  $\lambda_P$ . If the postulated collapse mechanisms subsumes the critical one, then the collapse bending moment diagram will show that no part of the structure does the moment exceed the plastic moment capacity, i.e. the yield condition would have been met.



The proposed plastic collapse analysis is a geometrically linear method. Often, P-Δ effects (reduction in lateral bending stiffness of axially loaded columns) need to be accounted for. We could approximately incorporate geometric non-linearity to find an approximate  $\lambda_F$  by employing Wood's adaptation of the Merchant-Rankine empirical formula based on an estimate of the critical elastic load factor,  $\lambda_E$ . Note also that should the axial forces be large in certain elements, the value of the plastic moment capacity  $M_P$  would decrease in accordance with the M-N diagram.

The analysis is performed as follows

- (i) Select critical sections C or C\* (i.e. whether simple frame or multi-bay multi-storey frame), identify degree of static indeterminacy  $\alpha$  or  $\alpha^*$  (i.e. whether simple frame or multi-bay multi-storey frame), and establish the sign convention for positive bending moments and rotations.

Select critical sections C i.e. potential plastic hinge locations

- fixed supports
- joints between members
  - between two members without applied moment, only one possible critical section at the joint, i.e. at the weaker member
  - between two members with applied moment, two possible critical sections
  - at a 3 or more member joint, all the member ends must be included as possible critical sections
- under concentrated loads
- under uniform loads
- at changes of member detailing, i.e. discontinuity in  $M_p$  and plastic hinge occurs in weaker section

Degree of static indeterminacy for plane frames = 3 (number of windows) – releases r

Degree of static indeterminacy for space frames = 6 (number of windows) – releases r

Degree of static indeterminacy for grillages = 3 (number of windows – 1) – releases r

Hyperstatic	Isostatic
Statically indeterminate, $\alpha > 0$	Statically determinate, $\alpha = 0$
Many stress paths from any point to root	Only one stress paths from any point to root
One or more mesh or closed loop	No mesh or closed loop

Bending moments and rotations are defined as positive if they cause tension or extension at the side with the dotted lines. For multi-storey multi-bay buildings, the dotted line is drawn under beams and on the right of columns by convention.

- (ii) Formulate the equilibrium law equations

Draw bending diagrams (employing sign convention) on released structure for: -

- (a) Releases  $p_1, p_2, p_3 \dots$   
 (b) External load parameter  $\lambda$

$$\underline{m}_C = [\underline{B} \quad \underline{b}_0] \begin{bmatrix} p_\alpha \\ \lambda \end{bmatrix}$$

$$\begin{bmatrix} m_1 \\ \cdot \\ \cdot \\ m_C \end{bmatrix} = \begin{bmatrix} B & \cdot & \cdot & \cdot & b_0 \\ \cdot & \cdot & \cdot & \cdot & \cdot \\ \cdot & \cdot & \cdot & \cdot & \cdot \\ \cdot & \cdot & \cdot & B & b_0 \end{bmatrix} \begin{bmatrix} p_1 \\ \cdot \\ \cdot \\ p_\alpha \\ \lambda \end{bmatrix} = \begin{bmatrix} B & \cdot & \cdot & \cdot \\ \cdot & \cdot & \cdot & \cdot \\ \cdot & \cdot & \cdot & \cdot \\ \cdot & \cdot & \cdot & B \end{bmatrix} \begin{bmatrix} p_1 \\ \cdot \\ \cdot \\ p_\alpha \end{bmatrix} + \lambda \begin{bmatrix} b_0 \\ \cdot \\ \cdot \\ b_0 \end{bmatrix}$$

(iii) Formulate the mesh kinematic linear program for the plastic limit analysis

$$\text{minimise } \lambda = \underline{M}_P^T \dot{\underline{\theta}}_{*2C} \quad \text{subject to} \quad \begin{bmatrix} \underline{b}_0^T - \underline{b}_0^T \\ \underline{B}^T - \underline{B}^T \end{bmatrix} \dot{\underline{\theta}}_* = \begin{bmatrix} 1 \\ 0 \end{bmatrix}$$

$$\text{positivity condition } \dot{\underline{\theta}}_* \geq 0$$

- (iv) Solve the linear program using the Simplex method
- (v) Determine the uniqueness of the collapse mechanism
- (vi) Determine the uniqueness of the bending moment diagram at collapse
- (vii) Establish the bending moment distribution at collapse from the equilibrium equations
- (viii) Establish the actual elastic and plastic deformations (i.e. rotations and displacements)

$$[\mathbf{B}_a]^T \{\theta_{Pa}\} = -[\mathbf{B}]^T [\mathbf{f}] \{\mathbf{m}\}$$

$[\mathbf{B}_a]$  = mesh matrix associated with active plastic hinges  
 $\{\theta_{Pa}\}$  = active plastic hinges vector  
 $[\mathbf{B}]$  = complete mesh matrix  
 $[\mathbf{f}]$  = flexibility matrix  
 $\{\mathbf{m}\}$  = bending moment at collapse vector

$$\{\mathbf{d}\} = [\mathbf{B}_0]^T \{\{\theta_E\} + \{\theta_{Pa}\}\}$$

$$= [\mathbf{B}_0]^T \{\{[\mathbf{f}]\{\mathbf{m}\} + \{\theta_{Pa}\}\}$$

$\{\mathbf{d}\}$  = displacement vector  
 $[\mathbf{B}_0]$  = matrix equilibrating a unit load without compatibility considerations at each and every station where the deflection is sought

(ix) Employ the approximate bifurcation analysis for simple frames or other methods to find an approximate  $\lambda_{ECR}$

$$\text{Steven's Estimate} \quad \lambda_{ECR} = 0.9 \frac{\sum S_i h_i \phi_i}{\sum V_i h_i \phi_i^2}$$

$$\text{Horne's Estimate} \quad \lambda_{ECR} = 0.9 \frac{S/V}{\text{Max } \phi_i}$$

(x) Employ Wood's adaptation of the Merchant-Rankine empirical formula to find an approximate  $\lambda_F$ . This effectively accounts for the P- $\Delta$  ( $K_G^A$  From  $K_E^A$ ) effect from the linear elastic buckling load, which is based on the initial undeflected geometry.

$$\frac{\lambda_F}{\lambda_P} = \frac{1}{0.9 + \frac{\lambda_P}{\lambda_{ECR}}} \quad \text{for} \quad 4 \leq \frac{\lambda_{ECR}}{\lambda_P} \leq 10$$

$$\frac{\lambda_F}{\lambda_P} = 1 \quad \text{for} \quad \frac{\lambda_{ECR}}{\lambda_P} \geq 10 \text{ i.e. assume no geometric nonlinearity effect beyond ratio of 10}$$

Note that in conceptually well designed structures,  $\lambda_{ECR} \gg \lambda_P$  such that  $\lambda_F \sim \lambda_P$  (Merchant-Rankine). Also,  $\lambda_E \ll \lambda_P$  so that the structure deforms considerably in plasticity before failure.

### 3.3.2 Mathematical Proof

Equilibrium law equations

$$\underline{m} = \begin{bmatrix} \underline{B} & \underline{B}_0 \end{bmatrix} \begin{bmatrix} \underline{p} \\ \underline{\lambda} \end{bmatrix}$$

$$\begin{bmatrix} m_1 \\ \cdot \\ \cdot \\ m_c \end{bmatrix} = \begin{bmatrix} \underline{B} & \cdot & \cdot & \cdot & \underline{B}_0 & \cdot & \cdot \\ \cdot & \cdot & \cdot & \cdot & \cdot & \cdot & \cdot \\ \cdot & \cdot & \cdot & \cdot & \cdot & \cdot & \cdot \\ \cdot & \cdot & \cdot & \underline{B} & \cdot & \cdot & \underline{B}_0 \end{bmatrix} \begin{bmatrix} p_1 \\ \cdot \\ \cdot \\ p_\alpha \\ \lambda_1 \\ \cdot \\ \lambda_{total} \end{bmatrix}$$

Incorporating the single parameter loading  $\lambda$ , the equilibrium law equations become

$$\underline{m} = \begin{bmatrix} \underline{B} & \underline{b}_0 \end{bmatrix} \begin{bmatrix} \underline{p} \\ \underline{\lambda} \end{bmatrix} = \underline{B}\underline{p} + \lambda\underline{b}_0$$

$$\begin{bmatrix} m_1 \\ \cdot \\ \cdot \\ m_c \end{bmatrix} = \begin{bmatrix} \underline{B} & \cdot & \cdot & \cdot & \underline{b}_0 \\ \cdot & \cdot & \cdot & \cdot & \cdot \\ \cdot & \cdot & \cdot & \cdot & \cdot \\ \cdot & \cdot & \cdot & \underline{B} & \underline{b}_0 \end{bmatrix} \begin{bmatrix} p_1 \\ \cdot \\ \cdot \\ p_\alpha \\ \lambda \end{bmatrix} = \begin{bmatrix} \underline{B} & \cdot & \cdot & \cdot \\ \cdot & \cdot & \cdot & \cdot \\ \cdot & \cdot & \cdot & \underline{B} \end{bmatrix} \begin{bmatrix} p_1 \\ \cdot \\ \cdot \\ p_\alpha \end{bmatrix} + \lambda \begin{bmatrix} b_0 \\ \cdot \\ \cdot \\ b_0 \end{bmatrix}$$

Kinematic law equations by the static-kinematic duality law

$$\begin{bmatrix} \dot{\underline{v}} \\ \dot{\underline{\delta}} \end{bmatrix} = \begin{bmatrix} \underline{B}^T \\ \underline{B}_0^T \end{bmatrix} \dot{\underline{q}}$$

$$\begin{bmatrix} \dot{v}_1 \\ \cdot \\ \cdot \\ \dot{v}_\alpha \\ \dot{\delta}_1 \\ \cdot \\ \dot{\delta}_{total} \end{bmatrix} = \begin{bmatrix} \underline{B}^T & \cdot & \cdot & \cdot \\ \cdot & \cdot & \cdot & \cdot \\ \cdot & \cdot & \cdot & \cdot \\ \cdot & \cdot & \cdot & \underline{B}^T \\ \underline{B}_0^T & \cdot & \cdot & \cdot \\ \cdot & \cdot & \cdot & \cdot \\ \cdot & \cdot & \cdot & \underline{B}_0^T \end{bmatrix} \begin{bmatrix} \dot{\theta}_1 \\ \cdot \\ \cdot \\ \dot{\theta}_c \end{bmatrix}$$

Incorporating the single parameter loading  $\lambda$ , the kinematic law equations become

$$\begin{bmatrix} \dot{\underline{v}} \\ \dot{\underline{W}}_{\lambda=1} \end{bmatrix} = \begin{bmatrix} \underline{B}^T \\ \underline{b}_0^T \end{bmatrix} \dot{\underline{\theta}}$$

$$\begin{bmatrix} \dot{v}_1 \\ \cdot \\ \cdot \\ \dot{v}_\alpha \\ \dot{\underline{W}}_{\lambda=1} \end{bmatrix} = \begin{bmatrix} B^T & \cdot & \cdot & \cdot & \cdot \\ \cdot & \cdot & \cdot & \cdot & \cdot \\ \cdot & \cdot & \cdot & \cdot & \cdot \\ \cdot & \cdot & \cdot & B^T & \cdot \\ \underline{b}_0^T & \cdot & \cdot & \underline{b}_0^T & \cdot \end{bmatrix} \begin{bmatrix} \dot{\theta}_1 \\ \cdot \\ \cdot \\ \dot{\theta}_C \\ \cdot \end{bmatrix}$$

Mechanism compatibility law

$$[0] = [B^T] \dot{\underline{\theta}}$$

$$\begin{bmatrix} 0 \\ \cdot \\ \cdot \\ 0 \end{bmatrix} = \begin{bmatrix} B^T & \cdot & \cdot & \cdot \\ \cdot & \cdot & \cdot & \cdot \\ \cdot & \cdot & \cdot & \cdot \\ \cdot & \cdot & \cdot & B^T \end{bmatrix} \begin{bmatrix} \dot{\theta}_1 \\ \cdot \\ \cdot \\ \dot{\theta}_C \end{bmatrix}$$

Rate of Work

$$\begin{aligned} \dot{W} &= \underline{\lambda}^T \dot{\underline{\theta}} \\ \dot{W} &= \underline{\lambda}^T [\underline{B}_0^T \dot{\underline{\theta}}] \text{ from the kinematic law} \\ \dot{W} &= [\underline{\lambda}^T \underline{B}_0^T] \dot{\underline{\theta}} \\ \dot{W} &= [\underline{B}_0 \underline{\lambda}]^T \dot{\underline{\theta}} \\ \dot{W} &= [\underline{b}_0 \underline{\lambda}]^T \dot{\underline{\theta}} \\ \dot{W} &= \underline{\lambda} \underline{b}_0^T \dot{\underline{\theta}} \\ \text{at unit load factor, } \dot{W}_{\lambda=1} &= \underline{b}_0^T \dot{\underline{\theta}} \end{aligned}$$

Rate of Energy Dissipation

$$\dot{D} = \underline{M}_P^T \dot{\underline{\theta}}_*, \quad \dot{\underline{\theta}}_* \geq 0$$

$$\dot{D} = \begin{bmatrix} M_P^{+1} & \cdot & \cdot & M_P^{+C} \\ \cdot & \cdot & \cdot & \cdot \\ \cdot & \cdot & \cdot & \cdot \\ \cdot & \cdot & \cdot & \cdot \end{bmatrix} \begin{bmatrix} \dot{\theta}_*^{+1} \\ \cdot \\ \cdot \\ \dot{\theta}_*^{+C} \\ \cdot \\ \dot{\theta}_*^{-1} \\ \cdot \\ \cdot \\ \dot{\theta}_*^{-C} \end{bmatrix}, \quad \dot{\underline{\theta}}_* \geq 0$$



Rewriting, the mesh kinematic linear program for plastic limit analysis is

$$\text{minimise } \lambda = \begin{bmatrix} M_P^{+1} & \dots & M_P^{+C} & M_P^{-1} & \dots & M_P^{-C} \end{bmatrix} \begin{bmatrix} \dot{\theta}_*^{+1} \\ \cdot \\ \cdot \\ \dot{\theta}_*^{+C} \\ \dot{\theta}_*^{-1} \\ \cdot \\ \cdot \\ \dot{\theta}_*^{-C} \end{bmatrix}$$

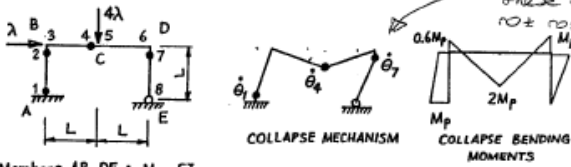
$$\text{subject to } \begin{bmatrix} \mathbf{b}_0^T & \dots & \mathbf{b}_0^{TC} & -\mathbf{b}_0^T & \dots & -\mathbf{b}_0^{TC} \\ \mathbf{B}^T & \dots & \mathbf{B}_C^T & -\mathbf{B}^T & \dots & -\mathbf{B}_C^T \\ \cdot & \cdot & \cdot & \cdot & \cdot & \cdot \\ \cdot & \cdot & \cdot & \cdot & \cdot & \cdot \\ \mathbf{B}_\alpha^T & \dots & \mathbf{B}_{\alpha,C}^T & -\mathbf{B}_\alpha^T & \dots & -\mathbf{B}_{\alpha,C}^T \end{bmatrix} \begin{bmatrix} \dot{\theta}_*^{+1} \\ \cdot \\ \cdot \\ \dot{\theta}_*^{+C} \\ \dot{\theta}_*^{-1} \\ \cdot \\ \cdot \\ \dot{\theta}_*^{-C} \end{bmatrix} = \begin{bmatrix} 1 \\ 0 \\ 0 \\ 0 \\ 0 \\ 0 \end{bmatrix}$$

(1 equation for the normalisation condition with 2C terms, and  $\alpha$  equations for mechanism compatibility with 2C terms)

positivity condition  $\underline{\dot{\theta}_*^+} \geq \underline{0}, \underline{\dot{\theta}_*^-} \geq \underline{0}$

### 3.3.3 Displacements and Rotations at Collapse

#### DISPLACEMENTS and DEFORMATIONS at COLLAPSE



Members AB, DE :  $M_p, EI$   
Members BC, CD :  $2M_p, 2.5 EI$

COLLAPSE LOAD FACTOR  $1.4 M_p/L$

The above information is obtained from plastic limit analysis



From the self-equilibrating diagrams of bending moments

$$\underline{B}^T = \begin{bmatrix} 1 & 1/2 & 1/2 & 0 & 0 & -1/2 & -1/2 & 0 \\ 0 & 1 & 1 & 1 & 1 & 1 & 1 & 0 \end{bmatrix} \quad \bullet \text{ denotes plastic hinge}$$

From the flexibility matrix of the unassembled elements

$$\underline{f} = \frac{L}{30EI} \begin{bmatrix} 5 \begin{bmatrix} 2 & 1 \\ 1 & 2 \end{bmatrix} & & & & & & & \\ & 2 \begin{bmatrix} 2 & 1 \\ 1 & 2 \end{bmatrix} & & & & & & \\ & & 2 \begin{bmatrix} 2 & 1 \\ 1 & 2 \end{bmatrix} & & & & & \\ & & & 2 \begin{bmatrix} 2 & 1 \\ 1 & 2 \end{bmatrix} & & & & \\ & & & & 5 \begin{bmatrix} 2 & 1 \\ 1 & 2 \end{bmatrix} & & & \end{bmatrix}$$

Then the compatibility conditions become :

$$\begin{bmatrix} 1 & 0 & -1/2 \\ 0 & 1 & 1 \end{bmatrix} \begin{bmatrix} \theta_{P1} \\ \theta_{P4} \\ \theta_{P7} \end{bmatrix} = \frac{M_p L}{30EI} \begin{bmatrix} 12.7 \\ 6.6 \end{bmatrix}$$

where the signs of the  $\theta_{P_i}$  must correspond with the bending moments  $m_i$  at the member ends  $i$ . Thus

$$\theta_{P1} \leq 0, \quad \theta_{P4} \geq 0, \quad \theta_{P7} \leq 0$$

At collapse, the last plastic hinge to form will have  $\theta_P = 0$

Try  $\theta_{P1} = 0$  Then the compatibility equations give

$$\theta_{P7} = -25.4 \frac{M_p L}{30EI}, \quad \theta_{P4} = 32 \frac{M_p L}{30EI}$$

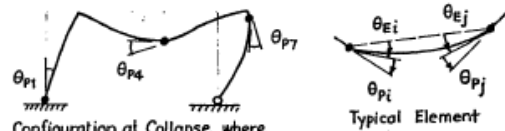
The sense of each  $\theta_P$  is correct and the solution is valid

More generally, if the sense of any  $\theta_P$  is not correct, further trials must be made in which each  $\theta_{P_i}$  is set to zero in turn.

From the bending moments at collapse

$$\underline{m}^T = M_p [-1 \ -0.6 \ -0.6 \ 2 \ 2 \ -1 \ -1 \ 0]$$

Elastoplastic Compatibility of Collapse Configuration  
PLASTIC HINGE ROTATIONS



Configuration at Collapse where at least one of  $\theta_{P1}, \theta_{P4}, \theta_{P7}$  must be zero

$$\underline{v} = \underline{B}^T (\underline{\theta}_E + \underline{\theta}_P) = \underline{0}$$

and since  $\underline{\theta}_E = \underline{f} \underline{m}$

it follows that

$$\underline{B}^T \underline{\theta}_P = -\underline{B}^T \underline{f} \underline{m}$$

a system of  $\alpha$  equations in  $(\alpha+1)$  variables  $\theta_{P_i}$

For the example above

$$(\underline{f} \underline{m})^T = \frac{M_p L}{30EI} [-13 \ -11 \ 1.6 \ 6.8 \ 6.0 \ 0 \ -10 \ -5]$$

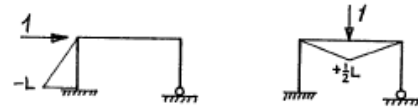
$$\underline{B}^T \underline{f} \underline{m} = \frac{M_p L}{30EI} \begin{bmatrix} -12.7 \\ -6.6 \end{bmatrix}$$

#### ELASTOPLASTIC DISPLACEMENTS

Let  $\delta_1$  and  $\delta_2$  be the horizontal displacement at B and the vertical displacement at C respectively. Then

$$\underline{\delta} = \underline{B}_0^T (\underline{\theta}_E + \underline{\theta}_P) = \underline{B}_0^T (\underline{f} \underline{m} + \underline{\theta}_P)$$

where matrix  $\underline{B}_0$  equilibrates a unit load at each of the stations where  $\delta_1$  and  $\delta_2$  are to be found.



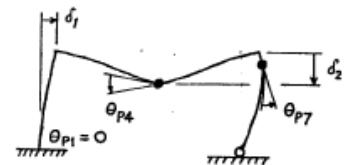
$$\underline{B}_0^T = L \begin{bmatrix} -1 & 0 & 0 & 0 & 0 & 0 & 0 & 0 \\ 0 & 0 & 0 & 1/2 & 1/2 & 0 & 0 & 0 \end{bmatrix} \quad \bullet \text{ denotes ACTIVE plastic hinge}$$

Then, calculating  $\underline{B}_0^T \underline{f} \underline{m}$  from  $\underline{f} \underline{m}$  given above,

$$\begin{bmatrix} \delta_1 \\ \delta_2 \end{bmatrix} = \frac{M_p L^2}{30EI} \begin{bmatrix} 13 \\ 6.4 \end{bmatrix} + L \begin{bmatrix} 0 & 0 \\ 1/2 & 0 \end{bmatrix} \begin{bmatrix} 32 \\ -25.4 \end{bmatrix} \frac{M_p L}{30EI}$$

$$\delta_1 = 13 \frac{M_p L^2}{30EI}$$

$$\delta_2 = 22.4 \frac{M_p L^2}{30EI}$$

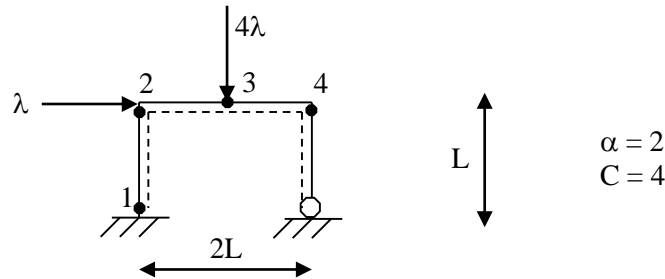


### 3.3.4 Plastic Limit Analysis of Simple Framed Structures

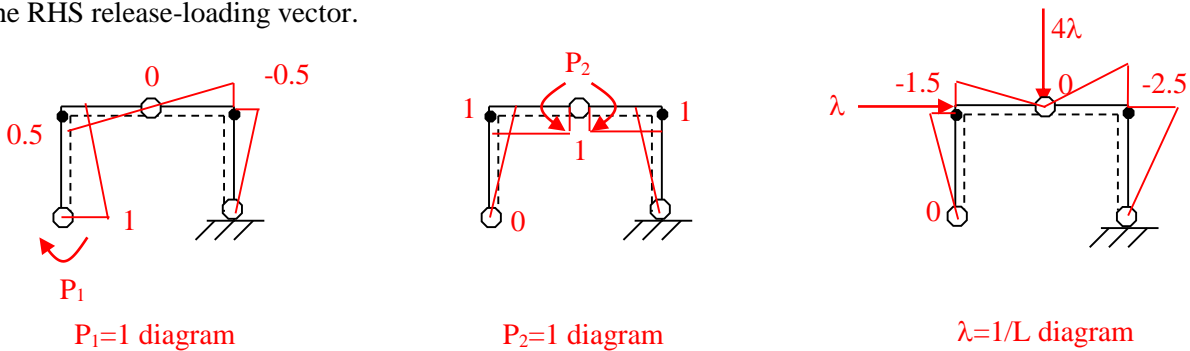
#### 3.3.4.1 Portal Frame

Given simple frame with beam  $2M_P$  and columns  $M_P$  subject to vertical  $4\lambda$  and horizontal  $1\lambda$  loading as shown. The plastic collapse load factor is required.

Select critical sections C (shown by the blackened circles), identify the degree of static indeterminacy  $\alpha$ , and establish the sign convention for positive bending moments and rotations. For bending moments, tension is positive and for rotations, extension is positive.



Draw bending diagrams (employing sign convention) on released structure for releases  $p_1$ ,  $p_2$  and external loads defined by single parameter loading  $\lambda$ . We only need a load-equilibrating BMD (that not necessarily satisfies compatibility) for the external load whilst the BMD for the releases should satisfy compatibility. The flexural analysis for the releases  $p_1$  and  $p_2$  does not include the external loads, whilst that of  $\lambda$  naturally does. One solution would be to release two rotational freedoms at 1 and 3 such that a **three-pinned-arch** is formed. The releases of an internal action would necessitate the use of a bi-external action to define the p-action diagram. For instance, the releases of an internal bending moment would require the use of a bi-external moment to define the p-BMD. Formulate the equilibrium law equations. Leave the  $\underline{b}_0$  matrix vector numerical, hence placing the variables  $\lambda$ ,  $L$  etc in the RHS release-loading vector.



$$\underline{m}_c = [\underline{B} \quad \underline{b}_0] \begin{bmatrix} p_\alpha \\ \lambda \end{bmatrix} \quad \begin{bmatrix} m_1 \\ m_2 \\ m_3 \\ m_4 \end{bmatrix} = \begin{bmatrix} 1 & 0 & 0 \\ \frac{1}{2} & 1 & -\frac{3}{2} \\ 0 & 1 & 0 \\ -\frac{1}{2} & 1 & -\frac{5}{2} \end{bmatrix} \begin{bmatrix} p_1 \\ p_2 \\ \lambda L \end{bmatrix}$$

Formulate the mesh kinematic linear program for the plastic limit analysis of the frame. Leave  $\underline{M}_P^T$  numerical. All  $\underline{M}_P^T$  values are positive and are repeated in the latter half of the row vector.

$$\text{minimise } \lambda = \underline{M}_P^T \dot{\underline{\theta}}_{*2C} \quad \text{subject to} \quad \begin{bmatrix} \underline{b}_0^T - \underline{b}_0^T \\ \underline{B}^T - \underline{B}^T \end{bmatrix} \dot{\underline{\theta}}_* = \begin{bmatrix} 1 \\ 0 \end{bmatrix}$$

positivity condition  $\dot{\underline{\theta}}_* \geq 0$

$$\text{minimise } z = [1 \quad 1 \quad 2 \quad 1 \quad 1 \quad 1 \quad 2 \quad 1] \begin{bmatrix} \dot{\theta}_*^{+1} \\ \dot{\theta}_*^{+2} \\ \dot{\theta}_*^{+3} \\ \dot{\theta}_*^{+4} \\ \dot{\theta}_*^{-1} \\ \dot{\theta}_*^{-2} \\ \dot{\theta}_*^{-3} \\ \dot{\theta}_*^{-4} \end{bmatrix} \text{ subject to } \begin{bmatrix} 0 & -\frac{3}{2} & 0 & -\frac{5}{2} & 0 & \frac{3}{2} & 0 & \frac{5}{2} \\ 1 & \frac{1}{2} & 0 & -\frac{1}{2} & -1 & -\frac{1}{2} & 0 & \frac{1}{2} \\ 0 & 1 & 1 & 1 & 0 & -1 & -1 & -1 \end{bmatrix} \begin{bmatrix} \dot{\theta}_*^{+1} \\ \dot{\theta}_*^{+2} \\ \dot{\theta}_*^{+3} \\ \dot{\theta}_*^{+4} \\ \dot{\theta}_*^{-1} \\ \dot{\theta}_*^{-2} \\ \dot{\theta}_*^{-3} \\ \dot{\theta}_*^{-4} \end{bmatrix} = \begin{bmatrix} 1 \\ 0 \\ 0 \end{bmatrix}$$

positivity condition  $\dot{\theta}_* \geq 0$  and note that  $\lambda_{\text{MIN}} = z_{\text{MIN}} \frac{M_P}{L}$  since  $\underline{M}_P^T$  and  $\underline{b}_0$  were left numerical.

Alternatively, numerical values could have been used for  $M_P$  and  $L$ , in which case  $\lambda_{\text{MIN}} = z_{\text{MIN}}$ . Set up and solve the linear programme (LP) in a Simplex Solver.

**PLASTIC MOMENT OF RESISTANCE, MP**

1            1            2            1            1            1            2            1

**KINEMATIC MATRIX**

0	-1.5	0	-2.5	0	1.5	0	2.5
1	0.5	0	-0.5	-1	-0.5	0	0.5
0	1	1	1	0	-1	-1	-1

**VARIABLES,  $\theta$**

0	0	0.4	0	0.2	0	0	0.4
---	---	-----	---	-----	---	---	-----

Cells to change

Target cell to minimize

**OBJECTIVE FUNCTION TERMS (= MP x  $\theta$ )**

0	0	0.8	0	0.2	0	0	0.4
---	---	-----	---	-----	---	---	-----

SUM 1.4

**CONSTRAINT FUNCTION TERMS (= KINEMATIC MATRIX x  $\theta$ )**

0	0	0	0	0	0	0	1
0	0	0	0	-0.2	0	0	0.2
0	0	0.4	0	0	0	0	-0.4

SUM 1  
0  
0

Also include positivity condition

Constraints

The changed cells in red represent the solution. The Sensitivity Report will also be produced by the solver.

**Microsoft Excel 9.0 Sensitivity Report**  
**Worksheet: [simplex - plastic collapse analysis.xls]Sheet1**  
**Report Created: 26/05/2003 17:02:57**

Adjustable Cells

Cell	Name	Final Value	Reduced Cost	Objective Coefficient	Allowable Increase	Allowable Decrease
\$A\$10	VARIABLES, $\theta$	0	2	1	1E+30	2
\$B\$10		0	1.6	1	1E+30	1.6
\$C\$10		0.4	0	2	4	1
\$D\$10		0	2	1	1E+30	2

\$E\$10	0.2	0	1	0.5	2
\$F\$10	0	0.4	1	1E+30	0.4
\$G\$10	0	4	2	1E+30	4
\$H\$10	0.4	0	10.666666667		2

Constraints

Cell	Name	Final Value	Shadow Price	Constraint R.H. Side	Allowable Increase	Allowable Decrease
\$J\$16	SUM	1	1.4	1	1E+30	1
\$J\$18	SUM	0	2	0	1E+30	0.4
\$J\$17	SUM	0	-1	0	0.2	1E+30

Constraints

Cell	Name	Cell Value	Formula	Status	Slack
\$J\$16	SUM		1\$J\$16=1	Binding	0
\$J\$18	SUM		0\$J\$18=0	Not Binding	0
\$J\$17	SUM		0\$J\$17=0	Binding	0

We shall interpret the results and the Sensitivity Report.

- (a) The collapse load factor  $\lambda_{MIN}$  and plastic hinge angular velocities  $\theta$  at collapse

$$\lambda_{MIN} = z_{MIN} M_P / L = 1.4 M_P / L \text{ (take } M_P = 1 \text{ and } \lambda = 1 \text{ if they have been included numerically)}$$

$\theta_*^{+1}$	$\theta_*^{+2}$	$\theta_*^{+3}$	$\theta_*^{+4}$	$\theta_*^{-1}$	$\theta_*^{-2}$	$\theta_*^{-3}$	$\theta_*^{-4}$
0	0	0.4	0	0.2	0	0	0.4

- (b) Current basic variables, potential basic variables (but as of the final tableau still non-basic) and non-basic variables recognition

Current basic variables (participating or non-participating plastic hinges) could be zero (non-participating) as well as have a non-zero (participating) value. Hence, current basic variables (i.e. variables in the basis in the final tableau) are recognized by the fact that they: -

- (i) have finite (zero inclusive) allowable increase in cost coefficient  $M_{Pj}$

*Note that current basic variables can have zero or non-zero final values. Current basic variables will definitely have zero reduced cost values.*

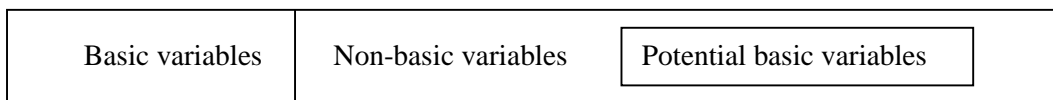
Non-basic variables include all variables that are not basic variables. Non-basic variables are recognized by the fact that they: -

- (i) have infinite allowable increase in cost coefficient  $M_{Pj}$ ,

*Note that non-basic variables will definitely have zero final values. Non-basic variables can have reduced cost values of zero or non-zero.*

Potential basic variables (but as of the final tableau still non-basic) are recognized by the fact that they: -

- (i) are non-basic variables, hence contain all recognition conditions of non-basic variables as above, AND  
 (ii) have zero reduced cost



(c) Reduced costs

The reduced costs are the objective function coefficients in the optimal tableau. For each variable  $x_j$  (or  $\theta_j$ ), the reduced cost gives the increase in the target cell ( $z$ ) for a unit change in the variable  $x_j$  (or  $\theta_j$ ). Hence, if we take a non-basic (which is not a potential basic variable) angular velocity  $\theta_*$  and increase it by a unit, this would cause  $\lambda$  to increase by the reduced cost and hence  $\lambda$  would no longer be optimal.

$$\text{Reduced cost } \bar{C}_j = \frac{\partial z}{\partial \theta_*^j}$$

The reduced cost values associated with the basic variables (plastic hinge velocities) must be zero. However, if any reduced cost is zero for a non-basic variable, there can be an alternate collapse mechanism having the same load factor because this non-basic variable could be brought into the basis to form another collapse mechanism without increasing the plastic collapse load factor.

(d) Allowable increase and allowable decrease

The allowable increase is the amount by which the objective function coefficient  $c_j$  ( $M_{Pj}$ ) in the original tableau may increase before the value of  $x_j$  (or  $\theta_j$ ) in the optimal solution is changed. For a non-basic variable,  $c_j$  ( $M_{Pj}$ ) can vary between  $\min c_j$  and  $+\infty$  before the  $x_j$  (or  $\theta_j$ ) value is changed. Basic variables on the other hand have finite (zero inclusive) allowable increase values for its corresponding coefficients.

(e) Shadow prices (a.k.a. Lagrange multipliers or dual variables)

There is a shadow price associated with each constraint. The shadow price measures the change in the objective function  $z$  due to a unit change in the RHS of the constraints  $b_i$ . But then, in this context of plastic limit analysis, the RHS of the constraints are either 0 or 1.

$$\text{Shadow price } \Pi_i = \frac{\partial z}{\partial b_i}$$

The shadow price corresponding to the normalization constraint is the collapse load factor as obtained earlier. More importantly, the shadow prices associated with the mechanism compatibility constraints are the indeterminate forces from which the bending moment distribution at collapse can be ascertained. There is an indeterminate  $p$  force value for every mechanism compatibility constraint. It is crucial that the  $p$  value is associated with its corresponding constraint. Hence the manner in which the constraints are inserted into the Excel Solver tool determines the manner in which the  $p$  values are outputted. Note the cell name column in the constraints table for clarification. *Here  $\lambda = 1.4M_P / L$ ,  $p_1 = -1M_P$  and  $p_2 = 2M_P$ .*

(f) Uniqueness of collapse mechanism

The existence of a potential basic variable (but as of the final tableau still non-basic) confirms the non-uniqueness of the collapse mechanism. Other potential collapse mechanisms involve the activation of these potential basic variables (but non-basic as of the final tableau). The true collapse mechanism will involve some form of addition of all these potential plastic collapse mechanisms, i.e.  $M_{\text{TRUE}} = \alpha_1 M_1 + \alpha_2 M_2 + \alpha_3 M_3 + \dots$ . The existence of non-uniqueness in the collapse mechanism usually occurs when there are two concentrated loads of equal magnitudes acting on a beam and so causing two potential partial collapse mechanisms with the true collapse mechanism being the addition of the two, i.e. a complete collapse mechanism.

(g) Uniqueness of bending moment diagram (BMD) at collapse

The uniqueness of the BMD can be tested on a potential collapse mechanism or even the true collapse mechanism. The uniqueness of the collapse mechanism and the uniqueness of the BMD are independent properties. A collapse mechanism has a unique BMD if and only if it is a complete collapse mechanism, i.e. it has  $\alpha+1$  active participating (non-zero) angular velocities of plastic hinges. Note that some basic variables are zero and they cannot be included as one of the  $\alpha+1$  active participating hinges. The uniqueness of the BMD comes from the fact that having  $\alpha+1$  known  $M_P$  locations will allow  $\alpha+1$  equations in the equilibrium law define uniquely the values of  $\lambda$ ,  $p_1$ ,  $p_2 \dots p_\alpha$ . However, if there are not  $\alpha+1$  active plastic hinges (and hence no unique BMD as the structure is statically indeterminate at collapse), then any BMD that satisfies equilibrium

will be on the safe side and can be accepted for design. Hence we could just use the shadow price values (of  $\lambda$ ,  $p_1$ ,  $p_2 \dots p_\alpha$ ) off Excel in the equilibrium equations for a BMD.

(h) Bending moment distribution at collapse

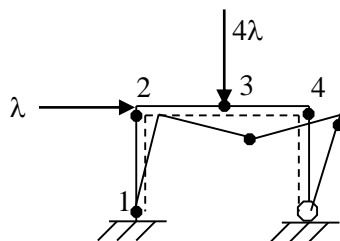
$$\underline{m}_c = [\underline{B} \quad \underline{b}_0] \begin{bmatrix} p_\alpha \\ \lambda \end{bmatrix}$$

$$\begin{bmatrix} m_1 \\ m_2 \\ m_3 \\ m_4 \end{bmatrix} = \begin{bmatrix} 1 & 0 & 0 \\ \frac{1}{2} & 1 & -\frac{3}{2} \\ 0 & 1 & 0 \\ -\frac{1}{2} & 1 & -\frac{5}{2} \end{bmatrix} \begin{bmatrix} p_1 \\ p_2 \\ \lambda L \end{bmatrix} = \begin{bmatrix} 1 & 0 & 0 \\ \frac{1}{2} & 1 & -\frac{3}{2} \\ 0 & 1 & 0 \\ -\frac{1}{2} & 1 & -\frac{5}{2} \end{bmatrix} \begin{bmatrix} -1M_p \\ 2M_p \\ 1.4 \frac{M_p}{L} L \end{bmatrix} = \begin{bmatrix} -1.0M_p \\ -0.6M_p \\ 2.0M_p \\ -1.0M_p \end{bmatrix}$$

Check that the bending moment everywhere is less than the particular plastic moment of resistance of the member. If so, we have correctly chosen the critical sections C that will produce the smallest value of  $\lambda$ . And hence the Yield Condition is met and  $\lambda$  is the unique collapse load factor according to the Uniqueness Theorem.

To reiterate the above results for ease of understanding, we make the following observations in this order: -

- I. The critical plastic load factor is  $\lambda_p = 1.4 M_p / L$  shown in the **target cell to minimize** and again in the Shadow Price of the Sensitivity Report.
- II. Identify the basic variables, i.e. the locations that a plastic hinge forms to form the collapse mechanism. This is identified in the Sensitivity Report on variables with a **Finite (zero included) Allowable Increase**. Here, they are  $\theta_3$ ,  $\theta_1$  and  $\theta_4$ , the latter two of which are negative. This means that they rotate such as to cause compression on the positive sign convention side. Usually (but not necessarily) the basic variables will be non-zero.



The value of the Allowable Increase is the amount by which the objective function coefficient i.e. the  $M_p$  value corresponding to the basic variable can increase before the solution (i.e. values of the angular velocity  $\theta_j$ ) changes. This is useful to **force another (maybe less catastrophic) collapse mechanism**. To do this the structural engineer would have to increase the  $M_p$  value at section 3 by  $4M_p$ , or at section 1 by  $0.5M_p$  or at section 4 by  $0.67M_p$ . **Clearly, if say the engineer does not want the column to collapse (that being catastrophic), he would have to increase the  $M_p$  of the column at section 1 to a little over  $1.5M_p$ .** If that were done, in this case, sections 2, 3, and 4 would then form the mechanism, i.e. a less catastrophic beam mechanism.

- III. Next, we look for the **existence of an alternate collapse mechanism**. For each variable  $\theta_j$ , the reduced cost gives the increase in the target cell ( $z$ ) for a unit change in the variable  $\theta_j$ . Thus the reduced cost of all the basic variables, i.e. the plastic hinges must be zero for the optimal conditions (i.e. minimum  $\lambda$ ). Thus, if any reduced cost is zero for a non-basic variable (infinite Allowable Increase), there can be an alternate collapse mechanism having the same load factor because this non-basic variable could be brought into the basis to form another collapse mechanism without increasing the plastic collapse load factor. **Here there is not any alternate collapse mechanism since all the variables with infinite Allowable Increase have non-zero Reduced Costs.**

IV. Finally we draw the BMD at collapse.

$$\underline{m}_C = [\underline{B} \quad \underline{b}_0] \begin{bmatrix} \underline{p}_\alpha \\ \lambda \end{bmatrix}$$

$$\begin{bmatrix} m_1 \\ m_2 \\ m_3 \\ m_4 \end{bmatrix} = \begin{bmatrix} 1 & 0 & 0 \\ \frac{1}{2} & 1 & -\frac{3}{2} \\ 0 & 1 & 0 \\ -\frac{1}{2} & 1 & -\frac{5}{2} \end{bmatrix} \begin{bmatrix} p_1 \\ p_2 \\ \lambda L \end{bmatrix} = \begin{bmatrix} 1 & 0 & 0 \\ \frac{1}{2} & 1 & -\frac{3}{2} \\ 0 & 1 & 0 \\ -\frac{1}{2} & 1 & -\frac{5}{2} \end{bmatrix} \begin{bmatrix} -1M_P \\ 2M_P \\ 1.4 \frac{M_P}{L} L \end{bmatrix} = \begin{bmatrix} -1.0M_P \\ -0.6M_P \\ 2.0M_P \\ -1.0M_P \end{bmatrix}$$

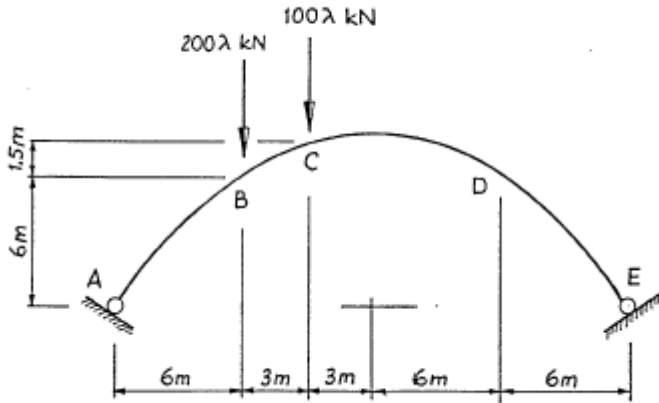
Check that the bending moment everywhere is less than the particular plastic moment of resistance of the member. If so, we have correctly chosen the critical sections C that will produce the smallest value of  $\lambda$ . And hence the Yield Condition is met and  $\lambda$  is the unique collapse load factor according to the Uniqueness Theorem. If the yield condition were not met, we would have reduced the estimate of critical plastic collapse factor as follows.

$$\lambda_{\text{Reduced}} = \lambda_P \frac{M_{\text{Exceeding}}}{M_P}$$

And we would say that the true critical collapse load factor lies between

$$\lambda_{\text{Reduced}} < \lambda_{\text{true}} < \lambda_P$$

3.3.4.2 Parabolic Arch

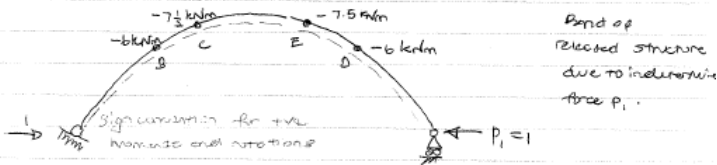


Given  $M_p = 590 \text{ kNm}$

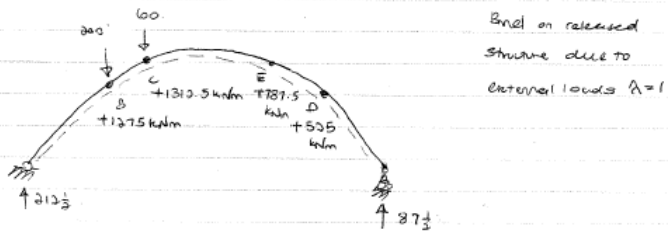
$$\{M_c\} = [C] \{P_0\} \quad \{P_0\} = \lambda \{P\}$$

$\alpha = 1$ ,  $C = A$  i.e. B, C, D, E

Choose 2D released horizontal supports.



Bend of released structure due to inelastic force  $P_1$ .



Bend on released structure due to external loads  $\lambda = 1$

$$\begin{Bmatrix} M_B \\ M_C \\ M_D \\ M_E \end{Bmatrix} = \begin{bmatrix} -6 & 1275 \\ -7.5 & 1312.5 \\ -6 & 525 \\ -7.5 & 787.5 \end{bmatrix} \begin{Bmatrix} P_1 \\ \lambda \end{Bmatrix}$$

Mesh kinematic linear programme

$$\min \lambda = \{M_p\}^T \{P_0\}$$

$$\text{subject to } \begin{bmatrix} +\{C\}^T & -\{I\}^T \\ [B]^T & -[A]^T \end{bmatrix} \{P_0\} \leq \{1\}$$

$$\text{and } \dot{\theta}_x \geq 0$$

$$\min \lambda = [590 \ 590 \ 590 \ 590 \mid 590 \ 590 \ 590 \ 590] \begin{Bmatrix} \theta_c^+ \\ \theta_c^- \\ \theta_d^+ \\ \theta_d^- \end{Bmatrix}$$

$$\text{subject to } \begin{bmatrix} 1275 & 1312.5 & 525 & 787.5 & -1275 & -1312.5 & -525 & -787.5 \\ -6 & -7.5 & -6 & -7.5 & 6 & 7.5 & 6 & 7.5 \end{bmatrix} \begin{Bmatrix} \theta_c^+ \\ \theta_c^- \\ \theta_d^+ \\ \theta_d^- \end{Bmatrix} = \begin{Bmatrix} 1 \\ 0 \end{Bmatrix}$$

$$\text{and } \dot{\theta}_x \geq 0$$

Say  $\theta_c^+$  and  $\theta_c^-$  are the basic variables.

$$1312.5 \theta_c^+ - 525 \theta_c^- = 1$$

$$\text{and } -7.5 \theta_c^+ + 6 \theta_c^- = 0$$

$$\therefore \theta_c^+ = 0.8 \theta_c^-$$

$$\therefore \theta_c^- = 1.9048 \times 10^{-3}$$

$$\theta_c^+ = 1.5239 \times 10^{-3}$$

hence  $\lambda = 590 (\theta_c^+ + \theta_c^-) = 2.023$  need not change any signs

An alternate approach: from the equilibrium equations

$$M_C = 590 = -7.5 P_1 + 1312.5 \lambda$$

$$M_D = -590 = -6 P_1 + 525 \lambda$$

Sign  
miss  
matter!

$$\text{solving simultaneously, } P_1 = \frac{-525\lambda - 590}{-6}$$

$$590 = 1.25(525\lambda - 590) + 1312.5\lambda$$

$$\lambda = 2.023$$

$$\therefore P_1 = 275 \frac{1}{3}$$

Check yield condition,

$$M_B = -6 P_1 + 1275 \lambda = 927.325 \text{ kNm} > M_p$$

$$M_E = -7.5 P_1 + 787.5 \lambda = -471.3875 \text{ kNm} < M_p$$

Yield condition not satisfied, lower  $\lambda$  estimate

$$\lambda = 2.023 \times \frac{590}{927.325} = 1.287$$

$$1.287 \leq \lambda \leq 2.023 \quad \leftarrow \text{upper bound estimate}$$

• the location of span hinges at D & E is an assumption, hence  $\lambda$  is overestimated.

• the large axial force in the arch may have some effect on  $M_p$ , i.e. reduces  $M_p$  as arch like column.

### 3.3.4.3 Displacements and Rotations at Collapse

The four-element plane frame of Figure Q.4(a) has member-end points numbered 1,2,3,4,5,6,7,8. It has a fixed base at member-end 1 and a pinned base at member-end 8. Plastic limit analysis identifies the collapse mechanism of Figure Q.4(b) and the associated bending moment distribution of Figure Q.4(c). The flexural rigidity and the plastic moment of resistance are  $EI$  and  $M_p$  for the columns and  $2.5EI$  and  $2M_p$  for the beam.

If  $f$  is the flexibility matrix of the unassembled elements of the frame and  $m$  is the vector of collapse bending moments, the matrix product  $fm$  may be taken to be:

$$fm = \left[ -\frac{1}{3}, -\frac{1}{3}, \frac{4}{45}, \frac{11}{45}, \frac{1}{3}, 0, -\frac{1}{3}, -\frac{1}{6} \right]^T \frac{M_p L}{EI}$$

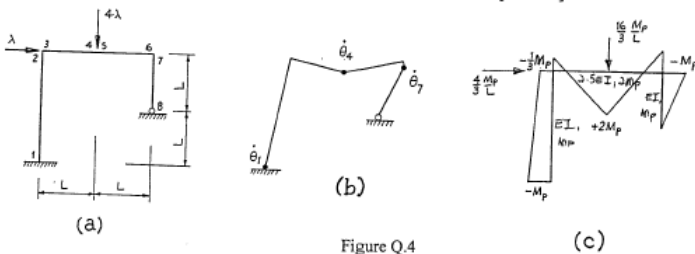
From this information, determine the last plastic hinge to form and calculate the plastic hinge rotations that have accumulated during loading up to incipient collapse. [10 marks]

Calculate, at incipient collapse, the vertical displacement at the midspan point of the beam (member-end points 4 and 5). [6 marks]

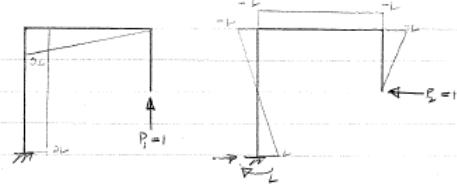
A systematic approach to the calculation of the plastic hinge rotations  $\theta^a$  at collapse would require the solution of the relations

$$B^T N^a \theta^a = -B^T f m, \quad \theta^a \geq 0$$

where  $B$  is a suitable mesh matrix and superscript  $a$  involves the activated plastic hinges only. Explain how spreadsheets such as Microsoft Excel and Corel Quattro Pro provide a ready solution of such relations. [4 marks]



$$[B_a]^T \theta^a = -[B]^T [f] m$$



$$[B]^T = \begin{bmatrix} 2L & 2L & 2L & L & L & 0 & 0 & 0 \\ L & -L & -L & -L & -L & -L & -L & 0 \end{bmatrix} \begin{matrix} P \\ P \end{matrix}$$

$$-[B]^T [f] m = -\frac{M_p L^2}{EI} \begin{bmatrix} -2 & 2 \\ 4 & 5 \end{bmatrix}$$

Given  $\theta_4, \theta_7$  and  $\theta_7$  are active do not forget minus sign!

$$\begin{bmatrix} 2L & L & 0 \\ L & -L & -L \end{bmatrix} \begin{bmatrix} \theta_4 \\ \theta_7 \\ \theta_7 \end{bmatrix} = -\frac{M_p L^2}{EI} \begin{bmatrix} -2 & 2 \\ 4 & 5 \end{bmatrix}$$

The rotations must correspond to limit  $\{m\}$ . Hence  $\theta_4 \leq 0, \theta_7 \geq 0, \theta_7 \leq 0$ .

Try  $\theta_7 = 0$  as last hinge to form, then

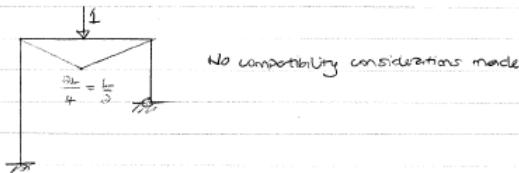
$$L\theta_4 = +2 \frac{M_p L^2}{EI} \quad \therefore \theta_4 = +2 \frac{M_p L}{EI} \quad (\text{sign ok})$$

$$\text{and } -\theta_4 - \theta_7 = \frac{19}{45} \frac{M_p L^2}{EI} \quad \therefore \theta_7 = -2 \frac{M_p L}{EI} \quad (\text{sign ok})$$

Hence, since signs ok the rotations to incipient collapse are  $\theta_1 = 0$  (last hinge to form);  $\theta_4 = 2 \frac{M_p L}{EI}$ ;  $\theta_7 = -2 \frac{M_p L}{EI}$ .

$$\{d\} = [B_a]^T \{ \theta^a \} + \{ \theta_p \}$$

$$= [B_a]^T \{ [f] m \} + \{ \theta_p \}$$



$$\therefore [B_a]^T = \begin{bmatrix} 1 & 2 & 3 & 4 & 5 & 6 & 7 & 8 \\ 0 & 0 & 0 & \frac{1}{2} & \frac{1}{2} & 0 & 0 & 0 \end{bmatrix}$$

$$\{ \theta_p \}^T = \begin{bmatrix} 0 & 0 & 0 & 2 \frac{M_p L}{45 EI} & 0 & 0 & -2 \frac{M_p L}{15 EI} & 0 \end{bmatrix}$$

$$\{ [f] m \}^T = \begin{bmatrix} -\frac{1}{3}, -\frac{1}{3}, \frac{4}{45}, \frac{11}{45}, \frac{1}{3}, 0, -\frac{1}{3}, -\frac{1}{6} \end{bmatrix} \frac{M_p L}{EI}$$

$$\therefore \{d\} = \frac{1}{2} \left\{ 2 \frac{M_p L}{45} + \frac{11}{45} \right\} \frac{M_p L}{EI} + \frac{1}{2} \left\{ 0 + \frac{1}{3} \right\} \frac{M_p L}{EI}$$

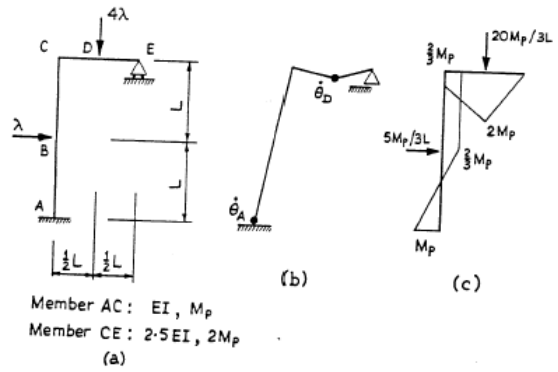
$$= \frac{56}{45} \frac{M_p L^2}{EI}$$

$$[B_a]^T \theta^a = -[B]^T [f] m$$

$$\{d\} = [B_a]^T \{ [f] m \} + \{ \theta_p \}$$

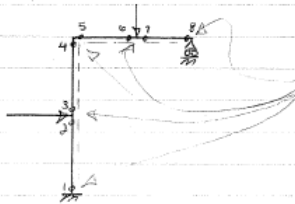
The plastic limit analysis of the plane frame shown in Figure Q.4(a) produces the collapse mechanism of Figure Q.4(b) and the collapse bending moment distribution of Figure Q.4(c).

- ✓ Determine which of the two plastic hinges participating in the collapse mechanism forms at incipient collapse, and calculate the plastic deformation (rotation) that would then have developed in the other plastic hinge. [13 marks]
- ✓ Calculate the horizontal displacement at C of the elastoplastic structure at incipient plastic collapse. [7 marks]



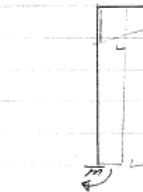
Elastoplastic compatibility  $\{v\} = [e]^T \{\theta_e\} + \{\theta_p\} = \{0\}$   
Elastic constitutive law  $\{\theta_e\} = [f]\{m\}$   
 $[B]^T \{\theta_p\} = -[e]^T [f] \{m\}$   
 $[B_0]^T \{\theta_{p0}\} = -[B]^T [f] \{m\}$

$$\{[f]\{m\}\}^T = \frac{M_p L}{6EI} \langle -\frac{4}{3} \frac{1}{3} \frac{2}{3} \frac{2}{3} \frac{14}{15} \frac{4}{5} \frac{2}{5} \rangle$$



Notice for the purposes of finding rotations and deflections we must pick critical section on either side - load or edge because of the need to establish the sign convention.

$$\{m\}^T = \langle -1 \frac{2}{3} \frac{2}{3} \frac{2}{3} \frac{14}{15} \frac{4}{5} \frac{2}{5} \rangle M_p \leftarrow \text{remember to include sign}$$



$$[B]^T = \begin{bmatrix} 1 & 2 & 3 & 4 & 5 & 6 & 7 & 8 \\ 1 & 1 & 1 & 1 & 1 & \frac{1}{2} & \frac{1}{2} & 0 \end{bmatrix} L$$

$$\therefore -[B]^T \{[f]\{m\}\} = -\frac{M_p L^2}{6EI} \begin{bmatrix} \frac{48}{15} \end{bmatrix}$$

$$[B_0]^T \{\theta_{p0}\} = -[B]^T \{[f]\{m\}\}$$

Given  $\theta_1$  and  $\theta_6$  (or  $\theta_7$ ) activated.

$$L \begin{bmatrix} 1 & \frac{1}{2} \end{bmatrix} \begin{Bmatrix} \theta_1 \\ \theta_6 \end{Bmatrix} = -\frac{M_p L^2}{6EI} \begin{bmatrix} 68 \\ 15 \end{bmatrix}$$

Require  $\theta_1 \leq 0$  and  $\theta_6 \geq 0$  from  $S_m$  i.e. the rotation and bending moment at collapse must be of the same sense.

Try  $\theta_6 = 0, \theta_1 = -\frac{68}{15} \frac{M_p L}{6EI}$  ( $\leq 0$  hence ok)

These rotations at incipient collapse:

$\theta_6 = 0$  (last hinge to form before collapse)

$\theta_1 = -\frac{34}{45} \frac{M_p L}{EI}$

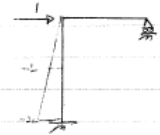
$\{d\} = [B_0]^T \{\theta_{p0}\} + \{\theta_p\}$

$[B_0]^T = \begin{bmatrix} -2 & -1 & -1 & 0 & 0 & 0 & 0 & 0 \\ 1 & 2 & 3 & 4 & 5 & 6 & 7 & 8 \end{bmatrix} L$

$\{d\} = -2L \left\{ -\frac{4}{3} \frac{M_p L}{6EI} - \frac{34}{45} \frac{M_p L}{EI} \right\} - L \left\{ \frac{1}{3} \frac{M_p L}{6EI} + 0 \right\}$

$-L \left\{ \frac{2M_p L}{6EI} + 0 \right\}$

$= \frac{17}{30} \frac{M_p L^2}{EI}$



$$[f] = \begin{bmatrix} \frac{2}{3} & 1 \\ 1 & 2 \\ \frac{2}{3} & 1 \\ \frac{1}{3} & 2 \end{bmatrix} \frac{L}{6EI}$$

b)

### 3.3.5 Plastic Limit Analysis of Rectangular Multi-Storey Multi-Bay Frames with Improved Data Generation

- (a) Select critical sections inclusive of articulation  $C^*$ , identify the degree of static indeterminacy with articulation ignored  $\alpha^*$ , and establish the sign convention for positive bending moments and rotations  
Critical sections inclusive of articulation  $C^*$  are identified.

$\alpha$  for plane frames with articulation = 3 (number of windows or cells) – releases  $r$

$\alpha^*$  for plane frames with articulation ignored = 3 (number of windows or cells)

Bending moments and rotations are defined as positive if they cause tension or extension at the side with the dotted lines. For multi-storey multi-bay buildings, the dotted line is drawn under beams and on the right of columns by convention.

- (b) Formulate the equilibrium law equations

$$\underline{m}_{C^*} = [\underline{B} \quad \underline{b}_0] \begin{bmatrix} p \\ \lambda \end{bmatrix}$$

- (i) 3 self equilibrating BMDs (due to shear, bending and axial actions) for each cell (sign convention applies)  
Note that  $C^*$  is the number of critical sections inclusive of those originally articulated and  $\alpha^*$  is the degree of static indeterminacy with all articulation ignored. The articulation positions will thus also be regarded and denoted as critical sections. Hence, each cell will contribute 3 indeterminate forces and hence 3 columns in the  $\underline{B}$  matrix. Fill in the  $\underline{B}$  matrix column-by-column with the bending moment values of the 3 normalized cell self-equilibrating BMDs at the critical section positions of  $C^*$ .

- (ii) 1 load equilibrating BMD for the load factor  $\lambda$  (sign convention applies)  
Vertical loads are transferred through simply supported beams, and hence  $M_{MAX} = PL/4$  if central load.  
Horizontal loads are transferred through cantilever action and multiple loads on the same column have their independent BMDs superimposed upon each other.

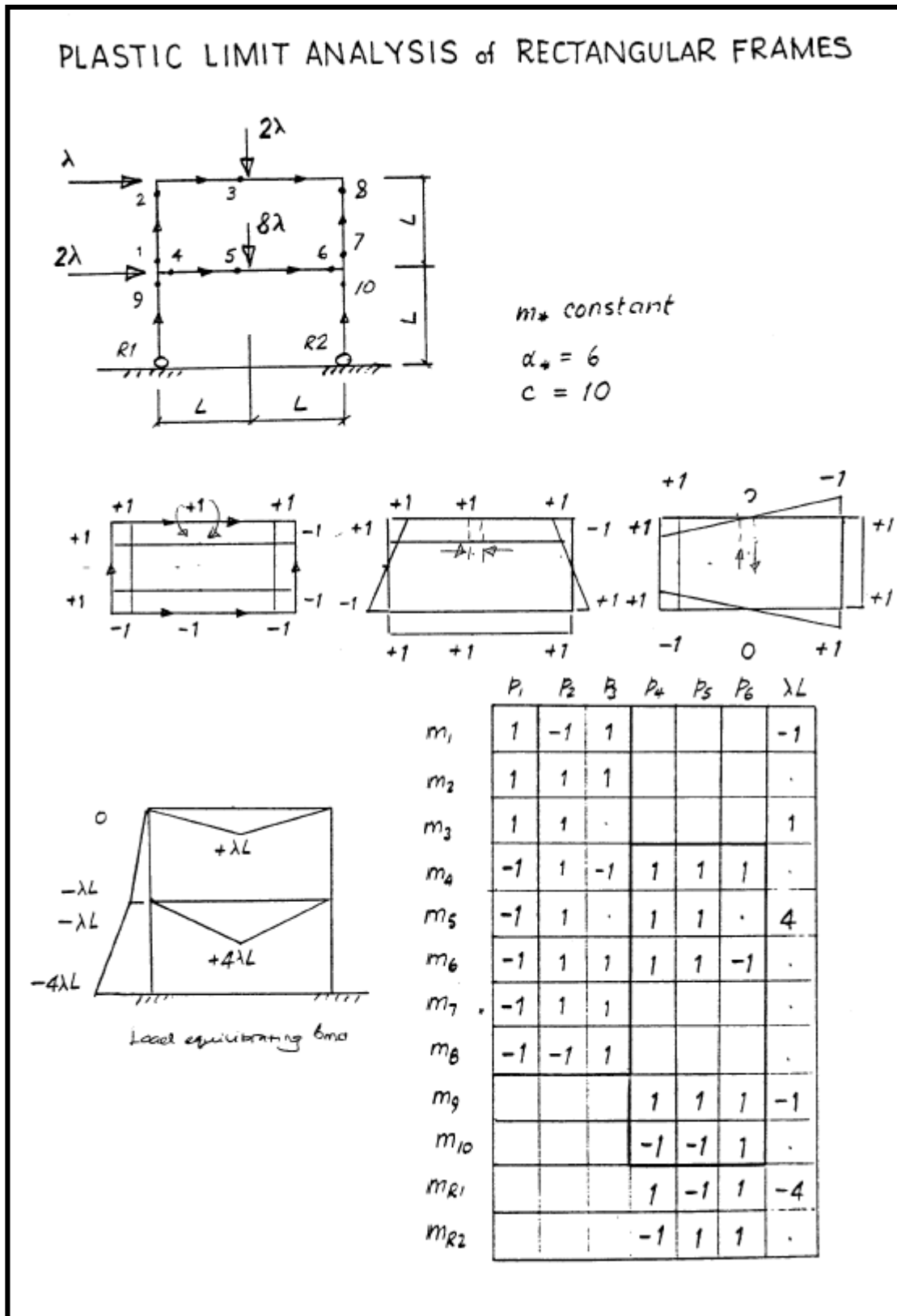
- (c) Formulate the mesh kinematic linear program for the plastic limit analysis of the frame and solve the LP  
Set the  $M_P$  value of the real articulation (hinges) to zero in the  $\underline{M}_P^T$  matrix.

$$\text{minimise } \lambda = \underline{M}_P^T \dot{\underline{\theta}}_{*2C^*} \quad \text{subject to} \quad \begin{bmatrix} \underline{b}_0^T & -\underline{b}_0^T \\ \underline{B}^T & -\underline{B}^T \end{bmatrix} \dot{\underline{\theta}}_* = \begin{bmatrix} 1 \\ 0 \end{bmatrix}$$

$$\text{positivity condition } \dot{\underline{\theta}}_* \geq \underline{0}$$

Solve the LP and perform sensitivity analysis as before.

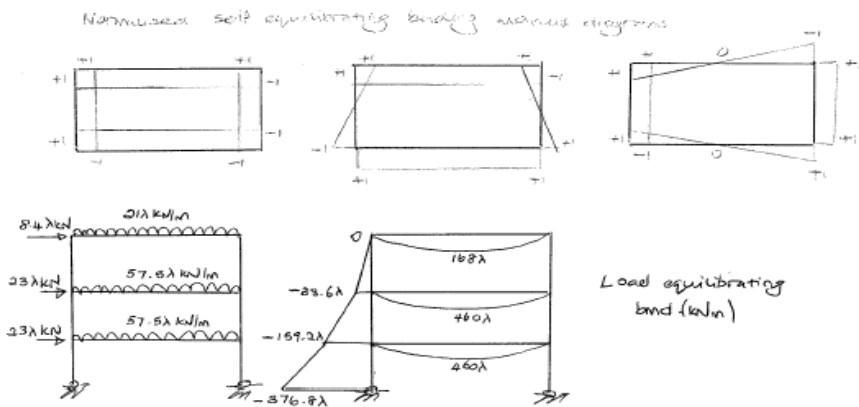
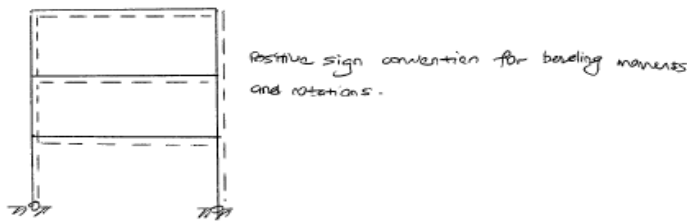
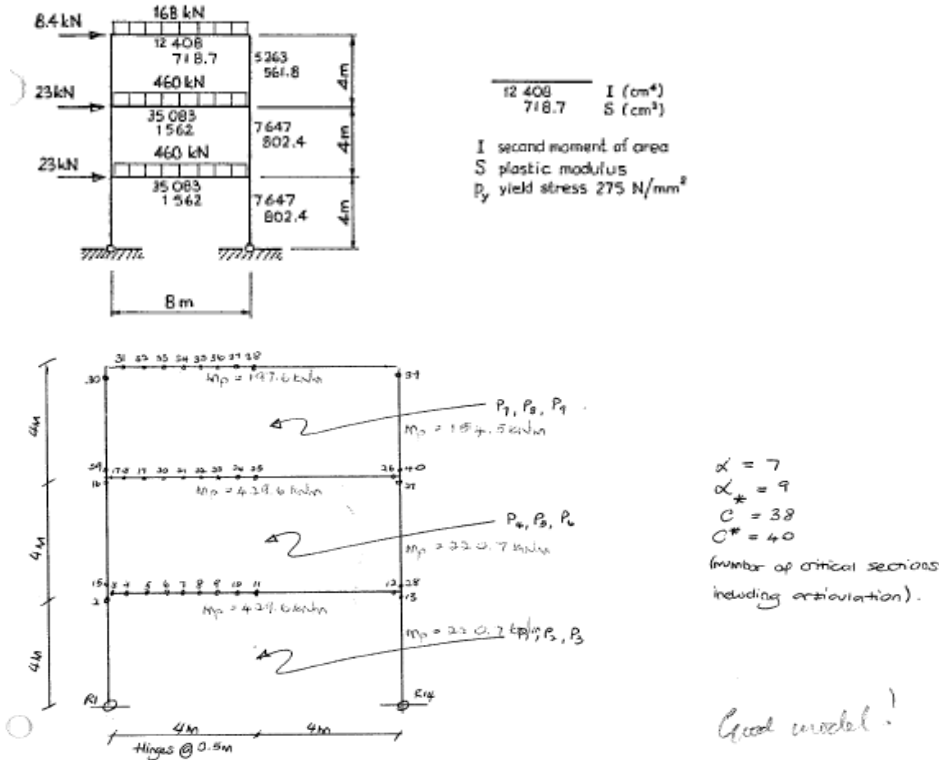
3.3.5.1 Two Storey Frame With Concentrated Loading





### 3.3.5.2 Three Storey Frame With Distributed Load

An unbraced and rigid-jointed frame fabricated from S275 steel with pinned bases is shown. An investigation of the possibility of elasto-plastic instability is to be carried out to establish what load factor, applied to the given load would be required to cause such a failure.



The equilibrium equations are

	P <sub>1</sub>	P <sub>2</sub>	P <sub>3</sub>	P <sub>4</sub>	P <sub>5</sub>	P <sub>6</sub>	P <sub>7</sub>	P <sub>8</sub>	P <sub>9</sub>	λ			P <sub>1</sub>	P <sub>2</sub>	P <sub>3</sub>	P <sub>4</sub>	P <sub>5</sub>	P <sub>6</sub>	P <sub>7</sub>	P <sub>8</sub>	P <sub>9</sub>	λ	
m <sub>21</sub>	1	-1	1							-377		m <sub>21</sub>				1	1	0.50	-1	1	-0.50	345	
m <sub>2</sub>	1	1	1							-159		m <sub>22</sub>				1	1	0.38	-1	1	-0.38	395.3	
m <sub>3</sub>	1	1	1	-1	1	-1				0		m <sub>23</sub>				1	1	0.2	-1	1	-0.2	431.3	
m <sub>4</sub>	1	1	0.88	-1	1	-0.88				107.8		m <sub>24</sub>				1	1	0.13	-1	1	-0.13	452.8	
m <sub>5</sub>	1	1	0.75	-1	1	-0.75				201.3		m <sub>25</sub>				1	1	0	-1	1	0	460	
m <sub>6</sub>	1	1	0.63	-1	1	-0.63				280.3		m <sub>26</sub>				1	1	-1	-1	1	1		
m <sub>7</sub>	1	1	0.50	-1	1	-0.50				345		m <sub>27</sub>				-1	-1	1					
m <sub>8</sub>	1	1	0.38	-1	1	-0.38				395.3		m <sub>28</sub>				-1	1	1					
m <sub>9</sub>	1	1	0.2	-1	1	-0.2				431.3		m <sub>29</sub>								1	-1	1	-33.6
m <sub>10</sub>	1	1	0.13	-1	1	-0.13				452.8		m <sub>30</sub>								1	1	1	0
m <sub>11</sub>	1	1	0	-1	1	0				460		m <sub>31</sub>								1	1	0.88	39.38
m <sub>12</sub>	1	1	-1	-1		1						m <sub>32</sub>								1	1	0.75	73.5
m <sub>13</sub>	-1	-1	1									m <sub>33</sub>								1	1	0.63	102.4
m <sub>14</sub>	-1	1	1									m <sub>34</sub>								1	1	0.50	126
m <sub>15</sub>				1	-1	1				-159		m <sub>35</sub>								1	1	0.38	144.4
m <sub>16</sub>				1	1	1				-33.6		m <sub>36</sub>								1	1	0.2	157.5
m <sub>17</sub>				1	1	1	-1	1	-1	0		m <sub>37</sub>								1	1	0.13	165.4
m <sub>18</sub>				1	1	0.88	-1	1	-0.88	107.8		m <sub>38</sub>								1	1	0	168
m <sub>19</sub>				1	1	0.75	-1	1	-0.75	201.3		m <sub>39</sub>								-1	-1	1	
m <sub>20</sub>				1	1	0.63	-1	1	-0.63	280.3		m <sub>40</sub>								-1	1	1	

And the Sensitivity Report,

Microsoft Excel 8.0 Sensitivity Report

Cell	Name	Final Value	Reduced Cost	Objective Coefficient	Allowable Increase	Allowable Decrease
+0 <sub>1</sub>	Variables	0	0	0	1E+30	0
+0 <sub>2</sub>		0 111.9050742		220.7	1E+30	111.9050742
+0 <sub>3</sub>		0 541.5050742		429.6	1E+30	541.5050742
+0 <sub>4</sub>		0 398.8463394		429.6	1E+30	398.8463394
+0 <sub>5</sub>		0 277.9545603		429.6	1E+30	277.9545603
+0 <sub>6</sub>		0 178.8297368		429.6	1E+30	178.8297368
+0 <sub>7</sub>		0 101.4718691		429.6	1E+30	101.4718691
+0 <sub>8</sub>		0 45.88095704		429.6	1E+30	45.88095704
+0 <sub>9</sub>		0 20.29437382		429.6	1E+30	20.29437382
+0 <sub>10</sub>		0.001738488	0	429.6	9.819422468	17.45459448
+0 <sub>11</sub>		0 9.709955017		429.6	1E+30	9.709955017
+0 <sub>12</sub>		0	650.3	429.6	1E+30	650.3
+0 <sub>13</sub>		0.001738488	0	220.7	13.3632925	17.45459448
+0 <sub>14</sub>		0	0	0	1E+30	0
+0 <sub>15</sub>		0.000977899	0	220.7	11.31897968	15.05914144
+0 <sub>16</sub>		0 251.2135906		220.7	1E+30	251.2135906
+0 <sub>17</sub>		0 592.9939631		429.6	1E+30	592.9939631
+0 <sub>18</sub>		0 442.9796727		429.6	1E+30	442.9796727
+0 <sub>19</sub>		0 314.732338		429.6	1E+30	314.732338
+0 <sub>20</sub>		0 208.2519591		429.6	1E+30	208.2519591
+0 <sub>21</sub>		0 123.5385358		429.6	1E+30	123.5385358
+0 <sub>22</sub>		0 60.59206815		429.6	1E+30	60.59206815
+0 <sub>23</sub>		0 24.70770715		429.6	1E+30	24.70770715
+0 <sub>24</sub>		2.94878E-20	0	429.6	2.648699394	12.16104049
+0 <sub>25</sub>		0 2.354399461		429.6	1E+30	2.354399461
+0 <sub>26</sub>		0	804.8	429.6	1E+30	804.8
+0 <sub>27</sub>		2.76486E-19	0	220.7	16.4577743	12.16104049
+0 <sub>28</sub>		0 441.4		220.7	1E+30	441.4
+0 <sub>29</sub>		0 21.61962753		154.5	1E+30	21.61962753
+0 <sub>30</sub>		0 279.7417346		154.5	1E+30	279.7417346
+0 <sub>31</sub>		0 265.0478454		197.6	1E+30	265.0478454
+0 <sub>32</sub>		0 215.2036269		197.6	1E+30	215.2036269
+0 <sub>33</sub>		0 173.3090793		197.6	1E+30	173.3090793
+0 <sub>34</sub>		0 139.3642024		197.6	1E+30	139.3642024
+0 <sub>35</sub>		0 113.3689962		197.6	1E+30	113.3689962
+0 <sub>36</sub>		0 96.05491753		197.6	1E+30	96.05491753
+0 <sub>37</sub>		0 85.22759632		197.6	1E+30	85.22759632
+0 <sub>38</sub>		0 83.08140253		197.6	1E+30	83.08140253
+0 <sub>39</sub>		-1.6369E-36	0	154.5	29.25826542	83.08140253
+0 <sub>40</sub>		0 309		154.5	1E+30	309
-0 <sub>1</sub>		0.000977899	0	0	23.75696444	0
-0 <sub>2</sub>		0 329.4949258		220.7	1E+30	329.4949258
-0 <sub>3</sub>		0 317.6949258		429.6	1E+30	317.6949258
-0 <sub>4</sub>		0 460.3536606		429.6	1E+30	460.3536606

-0 <sub>5</sub>		0 581.2454397		429.6	1E+30	581.2454397
-0 <sub>6</sub>		0 680.3702632		429.6	1E+30	680.3702632
-0 <sub>7</sub>		0 757.7281309		429.6	1E+30	757.7281309
-0 <sub>8</sub>		0 813.319043		429.6	1E+30	813.319043
-0 <sub>9</sub>		0 838.9056262		429.6	1E+30	838.9056262
-0 <sub>10</sub>		0 859.2		429.6	1E+30	859.2
-0 <sub>11</sub>		0 849.490045		429.6	1E+30	849.490045
-0 <sub>12</sub>		0 208.9		429.6	1E+30	208.9
-0 <sub>13</sub>		0 441.4		220.7	1E+30	441.4
-0 <sub>14</sub>		0.000977899	0	0	23.75696444	0
-0 <sub>15</sub>		0 441.4		220.7	1E+30	441.4
-0 <sub>16</sub>		0 190.1864094		220.7	1E+30	190.1864094
-0 <sub>17</sub>		0 266.2060369		429.6	1E+30	266.2060369
-0 <sub>18</sub>		0 416.2203273		429.6	1E+30	416.2203273
-0 <sub>19</sub>		0 544.467662		429.6	1E+30	544.467662
-0 <sub>20</sub>		0 650.9480409		429.6	1E+30	650.9480409
-0 <sub>21</sub>		0 735.6614642		429.6	1E+30	735.6614642
-0 <sub>22</sub>		0 798.6079319		429.6	1E+30	798.6079319
-0 <sub>23</sub>		0 834.4922928		429.6	1E+30	834.4922928
-0 <sub>24</sub>		0 859.2		429.6	1E+30	859.2
-0 <sub>25</sub>		0 856.8456005		429.6	1E+30	856.8456005
-0 <sub>26</sub>		0 54.4		429.6	1E+30	54.4
-0 <sub>27</sub>		0 441.4		220.7	1E+30	441.4
-0 <sub>28</sub>		0.000760588	0	220.7	53.83473292	73.99006396
-0 <sub>29</sub>		0 287.3803725		154.5	1E+30	287.3803725
-0 <sub>30</sub>		0 29.25826542		154.5	1E+30	29.25826542
-0 <sub>31</sub>		0 130.1521546		197.6	1E+30	130.1521546
-0 <sub>32</sub>		0 179.9963731		197.6	1E+30	179.9963731
-0 <sub>33</sub>		0 221.8909207		197.6	1E+30	221.8909207
-0 <sub>34</sub>		0 255.8357976		197.6	1E+30	255.8357976
-0 <sub>35</sub>		0 281.8310038		197.6	1E+30	281.8310038
-0 <sub>36</sub>		0 299.1450825		197.6	1E+30	299.1450825
-0 <sub>37</sub>		0 309.9724037		197.6	1E+30	309.9724037
-0 <sub>38</sub>		0 312.1185975		197.6	1E+30	312.1185975
-0 <sub>39</sub>		0 309		154.5	1E+30	309
-0 <sub>40</sub>		2.94878E-20	0	154.5	16.4577743	21.18959515

Constraints

Cell	Name	Final Value	Shadow Price	Constraint R.H. Side	Allowable Increase	Allowable Decrease
\$CC\$20	Constraint	1	1.514223005	1	1E+30	1
\$CC\$21	Constraint	6.50521E-19	174.9296141	0	0.003096934	0.005307856
\$CC\$22	Constraint	6.50521E-19	-110.35	0	0.001955799	1E+30
\$CC\$23	Constraint	8.67362E-19	285.2796141	0	0.003096934	0.005307856
\$CC\$24	Constraint	-5.42101E-19	120.5321512	0	0	0.001692334
\$CC\$25	Constraint	-1.0842E-19	-220.7	0	0	1E+30
\$CC\$26	Constraint	-1.0842E-19	120.5321512	0	0.001730745	0.001692334
\$CC\$27	Constraint	0 14.62913271	0	0	0	0.001006644
\$CC\$28	Constraint	0	-154.5	0	0	1E+30
\$CC\$29	Constraint	-3.31738E-20	14.62913271	0	0	0.001006644

The collapse load factor  $\lambda_{Pmin}$  is 1.514

The basic variables as of the final tableau are those with finite allowable increase in the cost coefficient  $M_p$

$+\theta_{10}$	<u>0.001738488</u>	$+\theta_{39}$	0
$+\theta_{13}$	<u>0.001738488</u>	$-\theta_1$	0.000977899
$+\theta_{15}$	0.000977899	$-\theta_{14}$	0.000977899
$+\theta_{24}$	0	$-\theta_{28}$	0.000760588
$+\theta_{27}$	0	$-\theta_{40}$	0

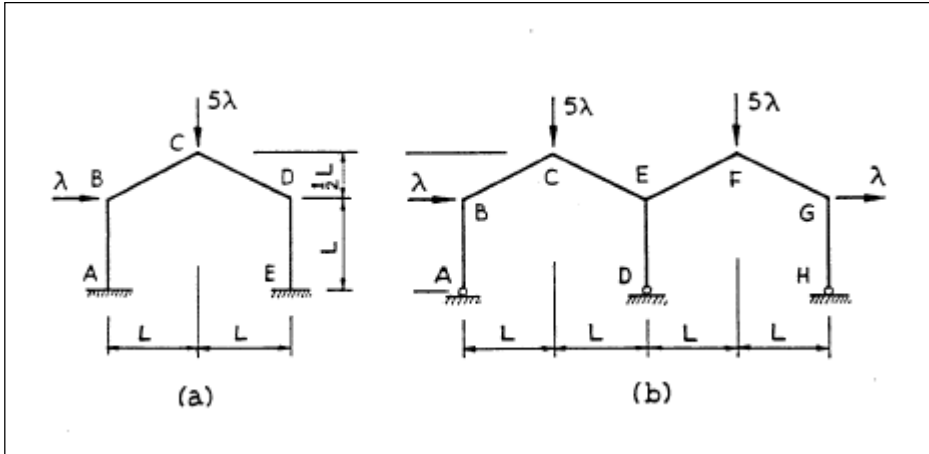
Conversely, a non-basic variable is one with an infinite allowable increase in the cost coefficient  $M_p$ . Amongst these, a potential basic variable is one with also a zero reduced cost. Here there is not any. Hence, there cannot be an alternate collapse mechanism, and the one predicted is unique.

A unique bending moment distribution is obtainable if and only if there are  $\alpha^*+1$  active participating hinges. Here,  $\alpha^*+1 = 10$ , and the number of active participating hinges is 6 from above. Hence, the exact bending moment distribution at collapse is not unique and is indeterminate.

Plastic collapse load factor,  $\lambda_P =$

1.51

3.3.5.3 Multi-Bay Portal Frame



Self-equilibrating loads of repetitive cells

Bridge moments  
Vertical reaction  
Horizontal reaction

- \* No signs on the self-equilibrating loads.
- \* Divide the arbitrarily chosen reaction by L in order to normalise the self-equilibrating loads and make them independent of L.
- \* release bending, shear, axial at apex and apply indeterminate force on released structure: here, think imagine cut at apex.

Sign convention for structure to be analysed and the critical sections  $C^*$  &  $x^*$

Moments and reactions are positive if they cause tension on the closed side:  
 $C = 5$ ;  $C^* = 5$ ;  $x = 3$ ;  $x^* = 3$ .

Local equilibrating load for  $\lambda = 1$

The loads due to the indeterminate actions are close on the released structure as in the frame structure method: however the external load load is close on the full structure (which is the same structure as that where we still use the released structure) has any load in equilibrium with these external loads is valid, usually we employ shape associated beams and vertical columns.

Equilibrium equations

If self-equilibrating load side of tension means the sign convention of the analysed structure, then positive contribution used. Note: it is important to check critical section positions exactly, as here if  $\theta$  had been defined in the column, the  $M_0$  value of  $P_1$  would be -1 instead of 3.

$$\{M_{ex}\} = [B] \{P_{ex}\} \lambda$$

$$\begin{bmatrix} M_A \\ M_B \\ M_C \\ M_D \\ M_E \end{bmatrix} = \begin{bmatrix} 1 & 1 & 3 & -1 \\ 1 & 1 & 1 & 0 \\ 1 & 0 & 0 & 3 \\ 1 & -1 & 1 & 0 \\ -1 & 1 & -3 & 0 \end{bmatrix} \begin{bmatrix} P_1 \\ P_2 \\ P_3 \\ \lambda L \end{bmatrix}$$

don't forget L in this case

Given A, C, D, E are plastic hinges in the assumed mechanism. However the sense of the rotations must still be assumed. The better the assumption, the closer the estimate of  $\lambda$  to the true  $\lambda_c$ . Of course, if the exact actual mechanism was guessed, then the estimate  $\lambda = \lambda_c$ . To perform the mechanism method, we could either:

- (a) Formulate the mesh linear programme for the mechanism method of plastic limit analysis and solve for certain  $\theta$  assuming a collapse mechanism; all  $\theta$  values obtained will be positive as there are both  $\theta^+$  and  $\theta^-$ . However for every critical section, only one of  $\theta^+$  or  $\theta^-$  can be used, the choice dependent upon the chosen guessed failure mechanism noting that the sign of the  $M_p$  values do matter and should correspond to the assumed failure mechanism.
- (b) Solve the equilibrium equations for a certain assumed failure mechanism.

Here, we employ the latter method.

$$M_A = -M_p = P_1 + P_2 + 3P_3 - \lambda L \quad (1)$$

$$M_C = M_p = P_1 + 2.5\lambda L \quad (2)$$

Assumed failure mechanism

$$M_D = -M_p = P_1 - P_2 + P_3 \quad (3)$$

$$M_E = -M_p = -P_1 + P_2 - 3P_3 \quad (4)$$

Solving these simultaneously,

$$(3) + (4) : -2M_p = -2P_3 \quad \therefore P_3 = M_p$$

$$(1) : -4M_p = P_1 + P_2 - \lambda L \quad (5)$$

$$(2) - (5) : 5M_p = -P_1 + 3.5\lambda L \quad (6)$$

$$(6) - (3) : 6M_p = -P_1 + 3.5\lambda L - M_p$$

$$7M_p = -P_1 + 3.5\lambda L \quad (7)$$

$$(5) + (7) : 8M_p = 6\lambda L \quad \therefore \lambda = 4M_p / 3L \quad (8)$$

$$(8) \text{ into } (7) : P_1 = -2/3 M_p$$

$$\text{into } (3) : P_2 = -1/3 M_p$$

Hence check yield conditions,

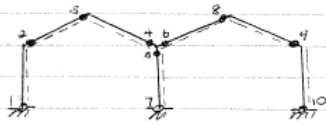
$$M_B = P_1 + P_2 + P_3 = -5/3 M_p \quad \therefore \text{yield condition not reversed}$$

Lower bound  $M_0 = \frac{4M_p}{3L} \cdot \frac{M_p}{5/3 M_p} = \frac{4}{5} M_p / L$

$$\frac{4M_p}{3L} \leq \lambda_c \leq \frac{4M_p}{3L}$$

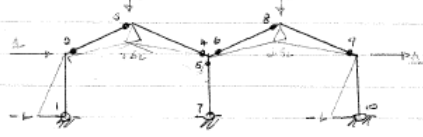
lower bound estimate      upper bound estimate

Sign convention for structure to be analysed and the critical section  $c^* \neq \alpha^*$ .



$C = 7, C^* = 10$   
 $\alpha = 3, \alpha^* = 6$   
 Transformed variables are always  $\Rightarrow$  the nonrotated variables

Load equilibrating load for  $\lambda = 1$



sliding supported beams and continuous columns irrespective of boundary conditions.

Equilibrium equations

$$\{m_{\alpha}\} = [ [B] \{b_{\alpha}\} ] \left\{ \begin{matrix} P_{\alpha} \\ \lambda \end{matrix} \right\}$$

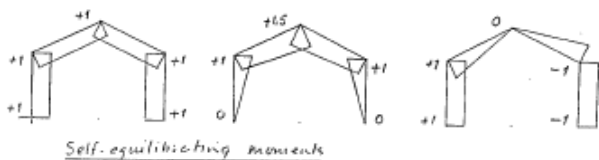
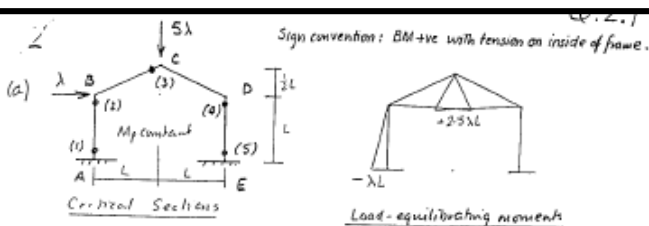
$$\begin{bmatrix} m_1 \\ m_2 \\ m_3 \\ m_4 \\ m_5 \\ m_6 \\ m_7 \\ m_8 \\ m_9 \\ m_{10} \end{bmatrix} = \begin{bmatrix} 1 & 1 & 3 & & & & & & & & -1 \\ & 1 & 1 & & & & & & & & 0 \\ & 1 & 0 & 0 & & & & & & & 2.5 \\ & 1 & -1 & 1 & & & & & & & 0 \\ -1 & 1 & -1 & 1 & 1 & 1 & 0 & & & & \\ & & & & 1 & 1 & 1 & 0 & & & \\ -1 & 1 & -3 & 1 & 1 & 3 & 0 & & & & \\ & & & & 1 & 0 & 0 & 2.5 & & & \\ & & & & & & 1 & -1 & 1 & 0 & \\ & & & & & & & -1 & 1 & -3 & -1 \end{bmatrix} \begin{bmatrix} P_1 \\ P_2 \\ P_3 \\ P_4 \\ P_5 \\ P_6 \\ \lambda L \\ \lambda L \\ \lambda L \\ \lambda L \end{bmatrix}$$

Do not forget sign in  $\lambda L$  column!  
 Do not forget to put the signs in the load equilibrating load for  $\lambda = 1$ .

Sections 3 and 7 are same

By member cells, have contribution from multiple cells

To account for the articulation, the  $m_p$  of the column bases at 1, 7, 10 are set to zero in the linear programme for plastic limit analysis (freehoism method).



Equilibrium Equations for critical sections

$$\begin{bmatrix} m_1 \\ m_2 \\ m_3 \\ m_4 \\ m_5 \end{bmatrix} = \begin{bmatrix} 1 & 0 & 1 & -1 \\ 1 & 1 & 1 & 0 \\ 1 & 1.5 & 0 & 2.5 \\ 1 & 1 & -1 & 0 \\ 1 & 0 & -1 & 0 \end{bmatrix} \begin{bmatrix} P_1 \\ P_2 \\ P_3 \\ \lambda L \end{bmatrix} = \begin{bmatrix} -M_p \\ M_p \\ +M_p \\ -M_p \\ +M_p \end{bmatrix}$$

(b) With hinges at A, C, D, E

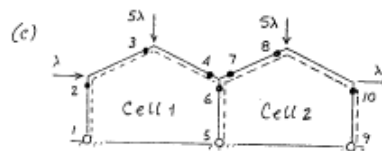
$m_1$  gives  $P_1 + P_3 = -M_p + \lambda L \therefore m_5$  gives  $P_1 - P_3 = M_p \quad P_1 = \frac{1}{2} \lambda L$   
 $m_4$  gives  $P_2 = P_3 - M_p = -2M_p$   
 $m_3$  gives  $2.5 \lambda L = -P_1 - 1.5 P_2 + M_p = -\frac{1}{2} \lambda L + 4M_p$   
 $3 \lambda L = 4M_p \quad \lambda L = \frac{4}{3} M_p$

Q.2.1

From (a)  $P_1 = \frac{2}{3} M_p \quad P_2 = -2 M_p \quad P_3 = -\frac{1}{3} M_p$   
 Check the yield condition at section 2

$$m_2 = P_1 + P_2 + P_3 = +\frac{2}{3} M_p - 2 M_p - \frac{1}{3} M_p = -\frac{5}{3} M_p \quad \text{CONTRAVENES YIELD COND.}$$

Lower bound  $\lambda_2 \quad \lambda_2 L = \frac{4}{3} M_p / \frac{5}{3} = \frac{4}{5} M_p$

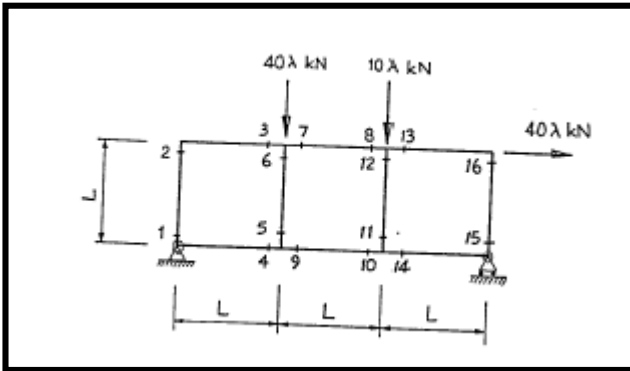


Equilibrium Equations

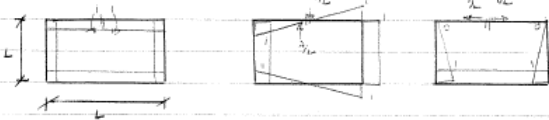
$$\begin{bmatrix} m_1 \\ m_2 \\ m_3 \\ m_4 \\ m_5 \\ m_6 \\ m_7 \\ m_8 \\ m_9 \\ m_{10} \end{bmatrix} = \begin{bmatrix} 1 & 0 & 1 & & & & & & & & 0 \\ 1 & 1 & 1 & & & & & & & & 0 \\ 1 & 1.5 & 0 & & & & & & & & 2.5 \\ 1 & 1 & -1 & & & & & & & & 0 \\ -1 & 0 & 1 & 1 & 0 & 1 & -1 & & & & \\ -1 & -1 & 1 & 1 & 1 & 1 & 0 & & & & \\ & & & 1 & 1 & 1 & 0 & & & & \\ & & & 1 & 1.5 & 0 & 2.5 & & & & \\ & & & -1 & 0 & 1 & -1 & & & & \\ & & & -1 & -1 & 1 & 0 & & & & \end{bmatrix} \begin{bmatrix} P_1 \\ P_2 \\ P_3 \\ P_4 \\ P_5 \\ P_6 \\ \lambda L \\ \lambda L \end{bmatrix}$$

The equilibrium conditions at the column bases  $m_1 = m_2 = m_3 = 0$  are not satisfied in the above. They can be imposed "a posteriori" by setting  $M_p = 0$  at each column base in the linear program for plastic limit analysis.

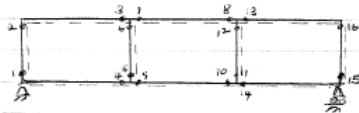
3.3.5.4 Vierendeel Truss



Self equilibrating loads of repetitive cells



Sign convention for structure to be analysed and the critical sections \$C^\*\$ & \$\alpha^\*\$.



$C = 15$   
 $\alpha = m + r - 2j$  (if pinned joints)  
 $\alpha = 3m + r - 3j - P_c$  (if rigid joints)  
 $= 3(10) + 3 - 3(9) - 0$   
 $= 9$   
 $\alpha^* = 9$

Load equilibrating load for \$R=1\$ not asked for here.

$\{M_{c^*}\} = [RB] \{b_k\} \{P_{c^*}\}$

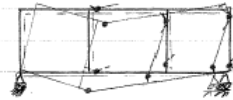
$$\begin{bmatrix} M_1 \\ M_2 \\ M_3 \\ M_4 \\ M_5 \\ M_6 \\ M_7 \\ M_8 \\ M_9 \\ M_{10} \\ M_{11} \\ M_{12} \\ M_{13} \\ M_{14} \\ M_{15} \end{bmatrix} = \begin{bmatrix} 1 & 1 & 1 & 0 & 0 & 0 & 0 & 0 & 0 & 0 & 0 & 0 & 0 & 0 & 0 \\ 1 & 1 & 0 & 0 & 0 & 0 & 0 & 0 & 0 & 0 & 0 & 0 & 0 & 0 & 0 \\ 1 & -1 & 0 & 0 & 0 & 0 & 0 & 0 & 0 & 0 & 0 & 0 & 0 & 0 & 0 \\ -1 & 1 & -1 & 0 & 0 & 0 & 0 & 0 & 0 & 0 & 0 & 0 & 0 & 0 & 0 \\ -1 & 1 & -1 & 0 & 0 & 0 & 0 & 0 & 0 & 0 & 0 & 0 & 0 & 0 & 0 \\ 0 & 0 & 0 & 1 & 1 & 1 & 0 & 0 & 0 & 0 & 0 & 0 & 0 & 0 & 0 \\ 0 & 0 & 0 & 1 & 1 & 0 & 0 & 0 & 0 & 0 & 0 & 0 & 0 & 0 & 0 \\ 0 & 0 & 0 & 1 & 1 & 0 & 0 & 0 & 0 & 0 & 0 & 0 & 0 & 0 & 0 \\ 0 & 0 & 0 & 1 & -1 & 0 & 0 & 0 & 0 & 0 & 0 & 0 & 0 & 0 & 0 \\ 0 & 0 & 0 & -1 & -1 & -1 & 0 & 0 & 0 & 0 & 0 & 0 & 0 & 0 & 0 \\ 0 & 0 & 0 & -1 & -1 & -1 & 0 & 0 & 0 & 0 & 0 & 0 & 0 & 0 & 0 \\ 0 & 0 & 0 & -1 & 1 & -1 & 1 & 1 & 1 & 0 & 0 & 0 & 0 & 0 & 0 \\ 0 & 0 & 0 & -1 & 1 & 0 & 1 & 1 & 0 & 0 & 0 & 0 & 0 & 0 & 0 \\ 0 & 0 & 0 & -1 & 1 & 0 & 1 & 1 & 0 & 0 & 0 & 0 & 0 & 0 & 0 \\ 0 & 0 & 0 & -1 & 1 & 0 & 1 & 1 & 0 & 0 & 0 & 0 & 0 & 0 & 0 \\ 0 & 0 & 0 & -1 & 1 & 0 & 1 & 1 & 0 & 0 & 0 & 0 & 0 & 0 & 0 \\ 0 & 0 & 0 & -1 & 1 & 0 & 1 & 1 & 0 & 0 & 0 & 0 & 0 & 0 & 0 \end{bmatrix} \begin{bmatrix} P_1 \\ P_2 \\ P_3 \\ P_4 \\ P_5 \\ P_6 \\ P_7 \\ P_8 \\ P_9 \\ \lambda L \end{bmatrix}$$

(i) Basic variables

Basic variables have a finite value of allowable increase in the objective function coefficient. The allowable increase is the means by which the objective function coefficient \$c\_j\$ (\$M\_{P\_j}\$) may increase before the value of \$c\_j\$ in the optimal solution is changed. Hence, here the basic variables are the angular velocities of

$PH(1), PH(2), PH(3), PH(7), PH(9), PH(12), PH(13), PH(16), PH(-11), PH(-5)$

(ii) Collapse mechanism and uniqueness



Look of the final value shown to obtain the optimal active non-zero velocities

The collapse mechanism is unique because it has no potential basic variables i.e. basic variables (infinite allowable increase) with

zero reduced cost. For each variable \$c\_j\$ the reduced cost gives the increase in the target cell \$z\$ for a unit change in the variable \$c\_j\$. Hence, if a nonbasic variable has a zero reduced cost, that variable could also be brought into the basis without increasing the value of the objective function (\$z\$), suggesting an alternate collapse mechanism.

(iii) Shadow prices

There are \$\alpha^\*\$ shadow prices. The first correspondingly to the mechanism normalisation is the load factor at collapse \$\lambda\_c\$. The other 9, corresponding to the mechanism compatibility are the 9 values \$P\_i, i=1\$ to 9 that control the bending moment distribution at collapse.

$\{M_{c^*}\} = [RB] \{b_k\} \{P_{c^*}\}$

(iv) Uniqueness of load

A collapse mechanism has a unique load only if it is a complete collapse mechanism, i.e. it has \$\alpha^\*\$ active participating (non-zero) angular velocities of plastic hinges. Here \$\alpha^\* = 10\$. From the final value column, of the \$\alpha^\* = 10\$ basic variables, 4 are zero. The mechanism is thus not complete and the load is indeterminate at collapse. Hence the load is not unique.

(v)  $\lambda_c = 0.10588 \frac{kN}{L}$ . For \$\lambda\_c = 1.8 \uparrow L = 4, M\_p = \frac{1.8 \times 4}{0.10588} = 68 \text{ kNm}\$

Microsoft Excel 8.0 Sensitivity Report  
Worksheet: [Vierendeel Frame.xls]Sheet2  
Report Created: 24/03/00 11:32:46

Cell	Name	Final Value	Reduced Cost	Objective Coefficient	Allowable Increase	Allowable Decrease
SAHS3	PH(1)	0	0	1	0.764705882	0.235294118
SAHS4	PH(2)	0	0	1	0.235294118	0.764705882
SAHS5	PH(3)	0	0	1	0.764705882	0.235294118
SAHS6	PH(4)	0	0.235294118	1	1E+30	0.235294118
SAHS7	PH(5)	0	1.235294118	1	1E+30	1.235294118
SAHS8	PH(6)	0	1	1	1E+30	1
SAHS9	PH(7)	0.017647059	0	1	0.8	0.9
SAHS10	PH(8)	0	1	1	1E+30	1
SAHS11	PH(9)	0.017647059	0	1	0.8	0.9
SAHS12	PH(10)	0	1.470588235	1	1E+30	1.470588235
SAHS13	PH(11)	0	2	1	1E+30	2
SAHS14	PH(12)	0.017647059	0	1	0.8	0.9
SAHS15	PH(13)	0	0	1	0.529411765	0.470588235
SAHS16	PH(14)	0	0.470588235	1	1E+30	0.470588235
SAHS17	PH(15)	0	2	1	1E+30	2
SAHS18	PH(16)	0.017647059	0	1	0.8	1.142857143
SAHS19	PH(-1)	0	2	1	1E+30	2
SAHS20	PH(-2)	0	2	1	1E+30	2
SAHS21	PH(-3)	0	2	1	1E+30	2
SAHS22	PH(-4)	0	1.764705882	1	1E+30	1.764705882
SAHS23	PH(-5)	0	0.764705882	1	1E+30	0.764705882
SAHS24	PH(-6)	0	1	1	1E+30	1
SAHS25	PH(-7)	0	2	1	1E+30	2
SAHS26	PH(-8)	0	1	1	1E+30	1
SAHS27	PH(-9)	0	2	1	1E+30	2
SAHS28	PH(-10)	0	0.529411765	1	1E+30	0.529411765
SAHS29	PH(-11)	0.017647059	0	1	0.8	0.9
SAHS30	PH(-12)	0	2	1	1E+30	2
SAHS31	PH(-13)	0	2	1	1E+30	2
SAHS32	PH(-14)	0	1.529411765	1	1E+30	1.529411765
SAHS33	PH(-15)	0.017647059	0	1	0.8	1.142857143
SAHS34	PH(-16)	0	2	1	1E+30	2

Cell	Name	Final Value	Shadow Price	Constraint R.H. Side	Allowable Increase	Allowable Decrease
SAJS5	normalisation	1	0.105882353	1	1E+30	1
SAJS6	compatibility (1)	0	2.058823529	0	1E+30	0
SAJS7	compatibility (2)	0	-1.058823529	0	0	0
SAJS8	compatibility (3)	0	0	0	0	0
SAJS9	compatibility (4)	0	1.441176471	0	0.1	0
SAJS10	compatibility (5)	0	-0.941176471	0	0.054545455	0.1
SAJS11	compatibility (7)	0	0.5	0	0	0.035294118
SAJS12	compatibility (8)	0	-0.058823529	0	0.1	0
SAJS13	compatibility (9)	0	0.058823529	0	0.054545455	0.1
SAJS14	compatibility (9)	0	1	0	1E+30	0

### 3.3.6 Hand Methods Verification

#### 3.3.6.1 Plastic Collapse Analysis by Solving Equilibrium Equations

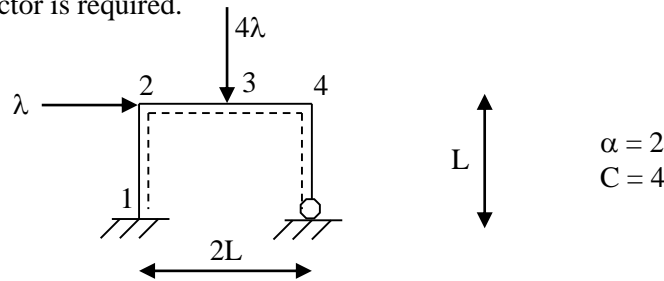
The linear programming simplex method described above performs the plastic collapse analysis meeting the fundamental theoretical requirements as follows

- (i) The equilibrium equation is employed, hence satisfying the equilibrium condition
- (ii) Many different collapse mechanisms is postulated, hence satisfying the mechanism condition, and a linear solving algorithm is used to find the smallest  $\lambda$
- (iii) The yield condition is automatically met since  $\lambda$  is minimized assuming that the chosen critical sections contains the critical mechanism.

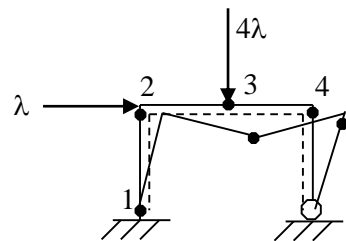
The hand method of plastic collapse analysis for simple structures of low degrees of static indeterminacies and a small number of critical sections is as follows

- (i) The equilibrium equation is employed, hence satisfying the equilibrium condition
- (ii) A collapse mechanism is postulated i.e. values and signs of the assumed bending moments  $M_P$  is put into the bending moment at collapse  $\{m\}$  vector, hence satisfying the mechanism condition, and  $\lambda$  is solved for.
- (iii) Then  $\{m\}$  is computed and it is ensured that at no point of the structure, the bending moment is greater than the local  $M_P$  value, hence satisfying the yield condition. Hence, naturally the smallest  $\lambda$  is found.

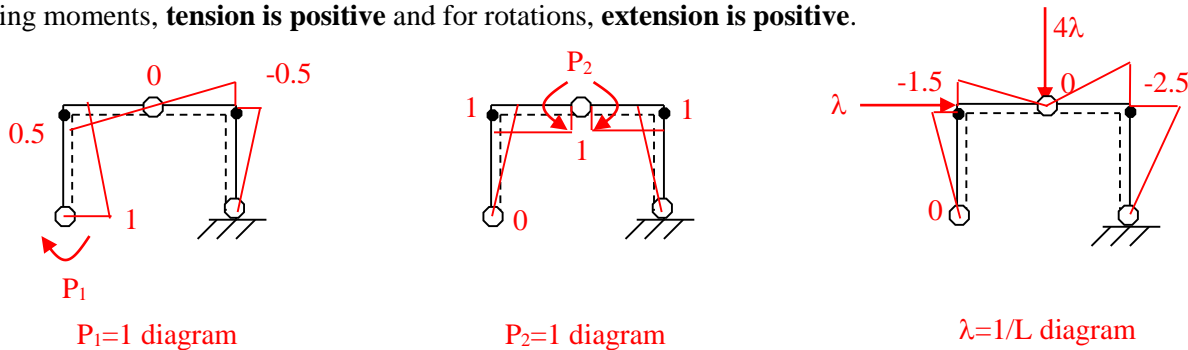
Given simple frame with beam  $2M_P$  and columns  $M_P$  subject to vertical  $4\lambda$  and horizontal  $1\lambda$  loading as shown. The plastic collapse load factor is required.



Appreciate that to form a mechanism we need  $\alpha + 1$  plastic hinges. Postulate **Mechanism Condition** with hinges at 1, 3 and 4.



Formulate the equilibrium conditions noting the sign convention for positive **bending moments** and **rotations**. For bending moments, **tension is positive** and for rotations, **extension is positive**.



The **Equilibrium Conditions** are then

$$\underline{m}_c = [\underline{B} \quad \underline{b}_0] \begin{bmatrix} \underline{p}_\alpha \\ \lambda \end{bmatrix} = \begin{bmatrix} -M_p \\ M_2 \\ 2M_p \\ -M_p \end{bmatrix} = \begin{bmatrix} 1 & 0 & 0 \\ \frac{1}{2} & 1 & -\frac{3}{2} \\ 0 & 1 & 0 \\ -\frac{1}{2} & 1 & -\frac{5}{2} \end{bmatrix} \begin{bmatrix} p_1 \\ p_2 \\ \lambda L \end{bmatrix}$$

Sign convention for extension positive

Sign convention for tension positive

Solve the equations simultaneously.

- (1):  $p_1 = -M_p$
- (3):  $p_2 = 2M_p$
- (4):  $-M_p = -0.5(-M_p) + 2M_p - 2.5\lambda L$   
 thus,  $\lambda = 1.4M_p/L$
- (2):  $M_2 = 0.5(-M_p) + 2M_p - 1.5(1.4M_p/L)L$   
 $= -0.6M_p$

Check that everywhere  $M \leq M_p$ . Here, OK. Thus **Yield Condition** met. Since mechanism condition, equilibrium condition and yield condition attained, the **Uniqueness Theorem** achieved.

Note that we only need a load-equilibrating BMD (that not necessarily satisfies compatibility) for the external load whilst the BMD for the releases should satisfy compatibility. Let us try a different load-equilibrating diagram that **DOES NOT** satisfy compatibility, say pinned beams and cantilever columns. Postulate the same mechanism.

$$\begin{bmatrix} M_p \\ M_2 \\ 2M_p \\ -M_p \end{bmatrix} = \begin{bmatrix} 1 & 0 & -1 \\ 0.5 & 1 & 0 \\ 0 & 1 & 2 \\ -0.5 & 1 & 0 \end{bmatrix} \begin{bmatrix} p_1 \\ p_2 \\ \lambda L \end{bmatrix}$$

Solving these equations simultaneously will again result in  $\lambda = 1.4M_p/L$ . But now,  $p_1 = 0.4M_p$  and  $p_2 = -0.8M_p$ . The values of  $p_1$  and  $p_2$  are no longer physically meaningful. Before it used to be the values of the indeterminate forces, now it is meaningless because of the non-compatible load-equilibrating BMD.

An **example design** of a portal frame with **haunches** is presented.

<b>ARUP</b>	Calculation sheet			
Job Title		Member/Location		
SINGLE STOREY PORTAL FRAME		Dwg. Ref.		
		Made by SR	Date 11 04 04	Chd.

**BRIEF**  
 30m span ; 6m centres  
 6° pitch of roof ; 6m to underside of haunch  
 foundations 450mm below FFL ; pinned base

**LOADING**  
 dead = 0.2 kPa  
 services = 0.1 kPa  
 imposed = 0.6 kPa  
 w/s load per unit area = 1.4(0.2+0.1) + 1.6(0.6) = 1.38 kPa  
 w/s load on frame, w = 6m x 1.38 kPa = 8.28 kN/m

**PLASTIC ANALYSIS**

(a) Number of possible hinge locations,  $C = 5$  as shown above encircled.  
 (b) Postulate a collapse mechanism with  $x+1 = 1+1 = 2$  hinges

Note positive sign convention for extension

(c) Release  $x$  unknowns such that statically determinate and present  $P_{max}$  and loading  $\lambda$  diagrams, noting positive sign convention for tension

(d) Formulate equilibrium equations and solve the problem

$$M_c = \begin{bmatrix} B & b \end{bmatrix} \begin{bmatrix} P_x \\ \lambda \end{bmatrix}$$

<h1 style="margin: 0;">ARUP</h1>	Calculation sheet	Job No.	Sheet No.	Rev.
		Member/Location		
Job Title		Drg. Ref.		
		Made by	Date	Chd.

$$\begin{bmatrix} M_1 \\ -M_{PR} \\ +M_{PR} \\ M_4 \\ M_5 \end{bmatrix} = \begin{bmatrix} 0.89 & -680.4 \\ 1.0 & -462.8 \\ 1.0 & 0.0 \\ 1.0 & -462.8 \\ 0.89 & -680.4 \end{bmatrix} \begin{bmatrix} P_1 \\ \lambda \end{bmatrix}$$

← Utilize equations (2) and (3) here!

Solving simultaneously

(2):  $-M_{PR} = P_1 - 462.8\lambda \therefore P_1 = 462.8\lambda - M_{PR}$

(2) → (3):  $M_{PR} = 462.8\lambda - M_{PR} - 0.0\lambda$

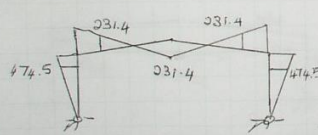
$\therefore M_{PR} = 231.4\lambda$

and  $P_1 = 231.4\lambda$

Choose  $\lambda = 1$

$M_{PR} = 231.4 \text{ kNm}$   
 $P_1 = 231.4 \text{ kNm}$   
 $\therefore M_1 = -474.5 \text{ kNm}$   
 $M_4 = -231.4 \text{ kNm}$   
 $M_5 = -474.5 \text{ kNm}$

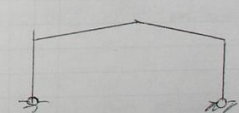
Hence bending moment, shear force and axial force diagram at plastic collapse is presented.



BMD



SFD



AFD

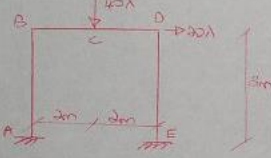
Calculate from statics knowing BMD @ collapse

### 3.3.6.2 Plastic Collapse Analysis by Virtual Work (Hobbs)

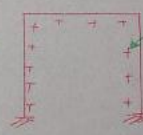
VIRTUAL DISPLACEMENTS TO FIND SMALLEST  $\lambda$  AND DRAW BMD FOR STATICALLY INDETERMINATE STRUCTURES AT COLLAPSE (GIVEN  $M_p$ ). (HOBBS)

1. Test various collapse mechanisms and obtain smallest  $\lambda$  by applying virtual displacements  $\sum Pd' = \sum M_p \theta_p'$ . In theory should consider the sign convention for  $M_p$  and  $\theta_p$ , although in most instances they work out nicely.
2. The collapse mechanism is the mechanism which yields the smallest  $\lambda$ , i.e. critical value. For this mechanism, an assumed bmd is drawn with  $M_p$ 's on the obvious tension sides of the collapse mechanism. Denote unknown bending moments with a variable  $M_x, M_y$ , etc. drawn on either side. We refer to this as the original governing collapse mechanism.
3. Obtain the unknown  $M_x, M_y$ , etc. by applying virtual displacements on the structure. Choose mechanisms that yield equations with only one unknown. Note sign conventions. The sign for  $\theta$  comes from this new collapse mechanism involving  $M_x$  or  $M_y$  but sign of the moment values comes from the original governing collapse mechanism.
4. Complete bmd obtained. If  $M_x$  or  $M_y$  turns out -ve, then opposite to that originally assumed in the original governing collapse mechanism. Hence bmd for  $\lambda > 0$  at collapse drawn.
5. If any  $M > M_p$  then the original governing collapse mechanism is invalid, i.e. not the critical one.

**Example:** Given  $M_p = 42$

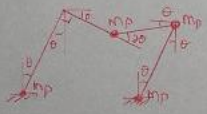


Adapt convention for B and M:



Means +ve  $\theta$  or  $M$  produces tension inside.

(a) Critical  $\lambda$



External work = Internal work

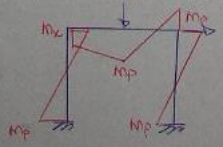
$$(40\lambda)(2\theta) + (20\lambda)(2\theta) = (-M_p)(-\theta) + (M_p)(\theta) + (-M_p)(-\theta)$$

$$\therefore \lambda = 1.8$$

Signs always work out at this stage

Sign convention always applied when we compare internal work.

(b) Incomplete bmd for the original governing collapse mechanism.

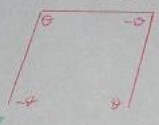


$M_p$  down outside of tension according to original governing collapse mechanism.

$M_x$  arbitrarily set.

Actually these values and signs of  $M_x$  correspond to the equation

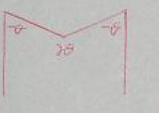
(c) Obtain unknowns by performing virtual displacements on the unknowns.  
 Choose say the following new collapse mechanism



Virtual work (virtual displacements):  
 External work = Internal work  
 $(20x)(\theta) = (-M_p)(-\theta) + M_x(\theta) + (-M_p)(-\theta) + (M_p)(\theta)$   
 With  $M_p = +10$ ,  $M_x = -18$   
 Sign convention for  $M_x$  comes from the original governing collapse mechanism.

Sign convention for rotation comes from this new collapse mechanism

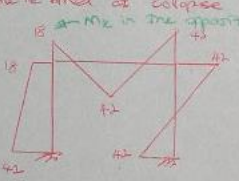
Or choose the following new collapse mechanism:



Virtual displacements:  
 External work = Internal work  
 $(40x)(\theta) = M_x(-\theta) + (M_p)(\theta) + (-M_p)(\theta)$   
 $M_x = -18$  again  
 of governing collapse mechanism

External work of new mechanism

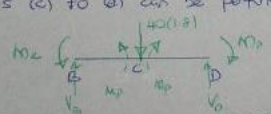
(d) Compute limit of collapse



$M_x$  in the opposite sense to that originally assumed because  $M_x$  yielded as -ve.

(e) Check all  $M \leq M_p$ . Ok. If not then step (c) was carried out incorrectly. This also means that if too many collapse mechanisms identified in step (c) just choose the most intuitively recognized possible one, then go through all the steps to (e). If  $M$  indeed  $\leq M_p$  everywhere then the assumed collapse mechanism is indeed the most critical.

Steps (c) to (d) can be performed alternatively by equilibrium,



Bottom lines to denote internal moments. (Note orientations, tension at bottom)

First: Take overall equilibrium for  $V_D$  (normalised moments)  
 $\sum B: M_x - (40)(1.8)(2) + 4V_D - M_p = 0$

Second: Take moment equilibrium for help beam as we know an internal moment of  $M_p$   
 $\sum C: -M_p - M_p + 2V_D = 0 \Rightarrow V_D = M_p$

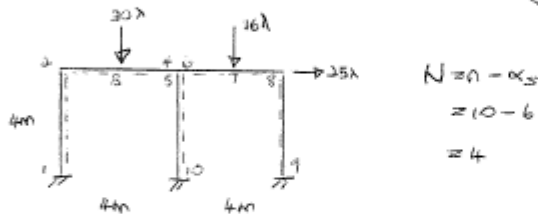
Solve simultaneously:  $\frac{-M_x + (40)(1.8)(2) + M_p}{4} = M_p$       $M_x = 18 \text{ kNm}$   
 (orientation assumed correctly)

### 3.3.6.3 Plastic Collapse Analysis by Virtual Work (Chryssanthopoulos)

#### KINEMATIC COLLAPSE ANALYSIS (CHRYSANTHOPOULOS)

ASSUMES :-  $\nu = 1 \Rightarrow$  concentrated plastic hinge  
 • change in  $\epsilon$  and  $k$  zero in real mechanism and  $\epsilon = k = 0$  in virtual mechanism. Hence internal energy dissipation only at plastic hinges.

(A) Compute  $N = n - \alpha_s$  and adopt sign convention marking the  $n$  hinge positions.



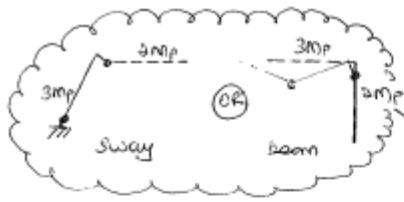
(B) Independent Equilibrium Equations (by Virtual mechanisms) and Kinematic Collapse Analysis (by Real mechanisms) for the Independent Elementary Mechanisms.

Independent Equilibrium Equation :- Employ sign convention for  $\theta$  but none for  $M$  as  $M_1, M_2, M_3$  etc unknown.

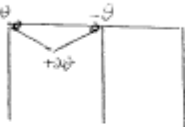
Kinematic Collapse Analysis :- Employ sign convention for both  $\theta$  and  $M$  but they always tend to produce positive internal work terms.

Obtain  $\lambda$  for each mechanism.  $\lambda = \infty$  for joint mechanism unless there is an externally applied load at that particular joint.

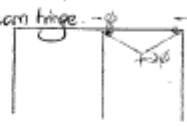
At two member joints, always take hinges to form in lower  $M_p$  member even if beam mechanism with corner hinge or sway with beam hinge.



(A) Beam



(B) Beam



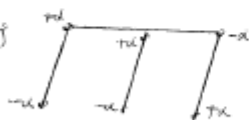
Equilibrium:  $(30\lambda)(2\theta) = -\theta M_3 + 2\theta M_2 - \theta M_4 \dots (1)$

Collapse Analysis:  $60\lambda = 4M_p$  (given  $M_p = 30kN/m$ )  
 $\lambda = 2$

Equilibrium:  $36\lambda(2\phi) = -\phi M_6 + 2\phi M_7 - \phi M_8 \dots (2)$

Collapse Analysis:  $72\lambda\phi = 4\phi M_p$   
 $\lambda = 1.67$

(C) Sway



Equilibrium:  $25\lambda(4\epsilon) = -\epsilon M_1 + \epsilon M_2 + \epsilon M_3 - \epsilon M_4 - \epsilon M_5 + \epsilon M_6 \dots (3)$

Collapse Analysis:  $100\lambda\epsilon = 6\epsilon M_p$   
 $\lambda = 1.8$

(D) Joint

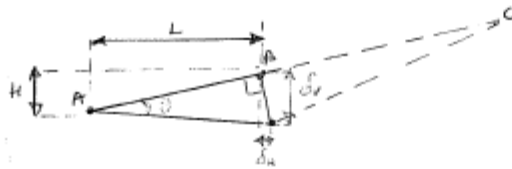


Equilibrium:  $0 = -\phi M_4 - \phi M_5 + \phi M_6 \dots (4)$

Collapse Analysis:  $\lambda = \infty$

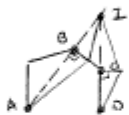
③ Combination of Elementary Collapse Mechanisms for Lower  $\lambda_u$ .

- Combine mechanisms such that internal energy dissipation is minimized external work done is minimized so that  $\lambda_u$  is as low as possible.
- Minimize internal energy by:-
  - (i) If hinge at a 2 member joint, then choose rotation at lower  $M_p$  member.
  - (ii) If hinge at a joint with 3 or more members, employ joint rotation to minimize  $\sum M_p \theta$  at that joint.
- Two methods of combination, i.e. geometrically or numerically, both equivalent.
- Employ numerical combination if the members are inclined and it is very difficult to fashion geometrically, although it is possible geometrically. Actually both methods are parallel except when members are inclined and we need to use the instantaneous centre of rotation, in which case numerically is faster. Basically  $\left\{ \begin{array}{l} \text{Numerical} \rightarrow \text{geometrical representation} \rightarrow \text{if we know elementary mechanisms} \\ \text{straight geometrical} \rightarrow \text{if we don't know elementary mechanisms} \end{array} \right.$
- In using instantaneous centre of rotation:-
  - (i) Obtain distances to I from hinges and between hinges.
  - (ii) Obtain rotations of hinges
  - (iii) Obtain internal work or energy dissipation.
  - (iv) Use mnemonic rule to obtain distances in the direction of externally applied loads.



horizontal deflection due to  $\theta \rightarrow \delta_H = H\theta$   $\leftarrow$  vertical projection of AB  
 Vertical deflection due to  $\theta \rightarrow \delta_V = L\theta$   $\leftarrow$  horizontal projection of AB

(V) Rotation at the middle hinge is the summation of the rotations of the edges.



$\theta_B = \theta_1 + \theta_2$   
 $\theta_C = \theta_2 + \theta_0$  just like beams



(d) Choose  $\psi = \phi = \alpha$  and combine ② + ③ + ④

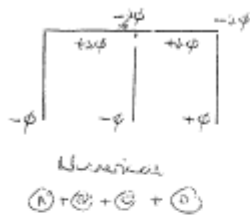


Numerical  
 ② + ③ + ④

Geometrical  
 Obtain external work distances from elementary mech. All positive terms.

Collapse analysis:  $36\lambda(2\phi) + 25\lambda(4\phi) = 4M_p\phi$  (given  $M_p = 80kNm$ ).  
 $\lambda = 1.57$

(b) Choose  $\theta = \phi = \alpha$  and combine (A) + (B) + (C) + (D)



collapse analysis:  $(80\lambda)(2\phi) + (3+\lambda)(2\phi) + (25\lambda)(4\phi) = 11 M_p \phi$

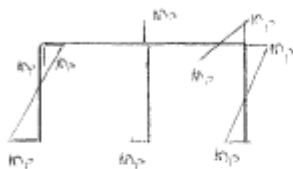
All positive terms!

Obtain external work done from notations of elementary mechanism, not the combined mechanism! Actually just add all the external work terms from the elementary mechanisms used to Hence methods of mechanism combination:-  
 form this (a) Numerical addition then conversion to geometrical representation; Done if the independent elementary mechanisms were considered as above.  
 Combined mechanism!

(b) Geometrical only; Usually done if the independent elementary mechanisms were not to be considered explicitly, but straight to the combined mechanism. In this case the instantaneous centre of rotation.

(c) Static check for mechanism with lowest  $\lambda_u$ .

Need to draw complete bending moment diagram for structure (statically indeterminate) of collapse.  $M$  comes from governing collapse mechanism whereas  $\theta$  comes from elementary mechanisms.  
 (a) Try  $\lambda = 1.57$  mechanism:-



Partial BMD (M based on assumed governing collapse mechanism; i.e. directly associated with the signs of  $\theta$  of the assumed governing collapse mechanism; if  $+\theta$ ,  $M_p$  on side of dashed line and if  $-\theta$ ,  $M_p$  on opposite side of dashed line).

$M_3 \geq M_5 \geq M_6$  unknown.

if  $\theta$  is then  $M_3$  also +ve and vice versa.  $\Rightarrow$  within governing collapse mechanism.

Equilibrium equation (1)

$$(30\lambda)(2\theta) = -\theta(M_p) + 2\theta M_3 - \theta(M_p)$$

with  $\lambda = 1.57, M_p = 30$

$\Rightarrow M_3 = 47.1 \text{ kNm}$

Like wise  $M_5 = 7 \text{ kNm}$  and  $M_6 = 37 \text{ kNm}$   
 Yield condition not satisfied

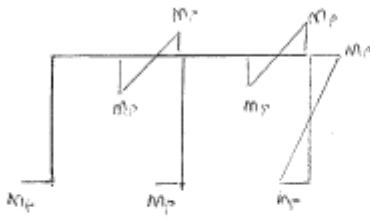
as  $M_2 > M_p$

$\lambda_u = 1.57$		$\lambda_u = 1$
$ M_1  = M_p$		$ M_1  = 19.1$
$ M_2  = M_p$		$ M_2  = 19.1$
$ M_3  = 47.1$	$\Rightarrow * \frac{82}{47.1} \Rightarrow$	$ M_3  = 80$
$ M_4  \dots$		$ M_4  \dots$
$ M_{10}  \dots$		$ M_{10}  \dots$
		$\dots = 19.1$

$$1 \leq \lambda_c \leq 1.57$$

Scaled based on  $M_3$  not  $M_6$  as  $M_3$  greater than  $M_6$ .

(b) Try  $\lambda = 1.422$



$M_2, M_5, M_6$  ?  
(Partial bond)

$$(1): 60\lambda\theta = -\theta M_2 + 2\theta M_P - \theta(-M_P)$$

$$M_2 = 4.68 \text{ kNm}$$

$$(2): 72\lambda\phi = -\phi(M_6) + 2\phi M_P - \phi(-M_P)$$

$$M_6 = -12.384 \text{ kNm}$$

$$(4): 0 = -\psi(M_P) - \psi M_5 + \psi(-12.384)$$

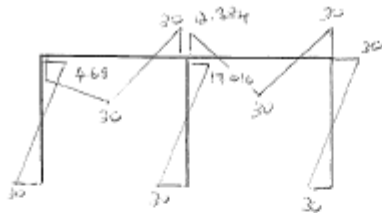
$$M_5 = 17.616 \text{ kNm}$$

Static check successful, yield condition satisfied, uniqueness theorem met.

$$|M| \leq M_P$$

$$1.422 \leq \lambda_c \leq 1.422$$

$$\lambda_c = 1.422$$



(Complete bond @ collapse)

(E) Required  $M_P$  for  $a\lambda_c$

If  $\lambda_c$  was to be increased to  $a\lambda_c$ , then required  $M_P$  is

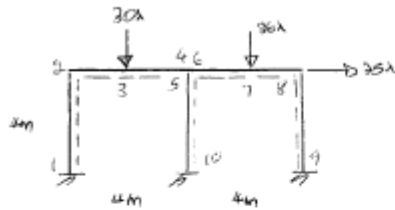
$$= \left( \frac{a\lambda_c}{\lambda_c} \right) (M_P)$$

$$= a (M_P)$$

$$= a (30)$$

KINEMATIC COLLAPSE ANALYSIS (EXAM ORIENTED BARE ESSENTIALS)

Given  $M_p = 30 \text{ kNm}$  throughout.

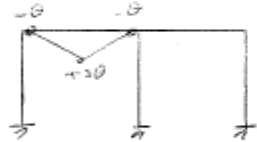


$$N = n - \alpha_5$$

$$= 10 - 6$$

$$= 4$$

(A) Beam

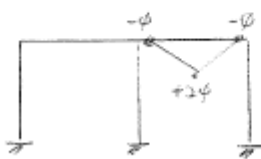


$$30\lambda(2\theta) = -\theta M_2 + 2\theta M_3 - \theta M_4 \quad \text{--- (1)}$$

$60\lambda\theta = 4M_p\theta$  ← ignore signs or rather sign is complementary to each other.

$$\lambda = 2$$

(B) Beam

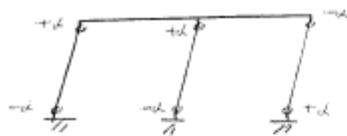


$$30\lambda(2\phi) = -\phi M_6 + 2\phi M_7 - \phi M_8 \quad \text{--- (2)}$$

$$72\lambda\phi = 4M_p\phi$$

$$\lambda = 1.67$$

(C) Sway

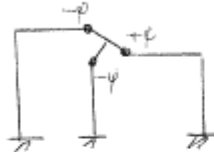


$$25\lambda(4\alpha) = -\alpha M_1 + \alpha M_2 + \alpha M_5 - \alpha M_{10} - \alpha M_8 + \alpha M_9 \quad \text{--- (3)}$$

$$100\lambda\alpha = 6M_p\alpha$$

$$\lambda = 1.8$$

(D) Joint

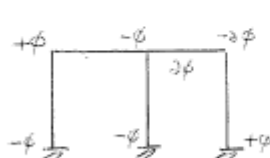


$$0 = -\psi M_4 - \psi M_5 + \psi M_6 \quad \text{--- (4)}$$

$$\lambda = \infty$$

(E) Combined Mechanism 1

Choose to rid certain hinges (using of higher  $M_p$ ).  
Choose  $\phi = \psi = \alpha$  and combine (A) + (C) + (D)



Direct addition of corresponding rotations in the elementary mechanisms.

$$36\lambda(2\phi) + 25\lambda(4\phi) = 9M_p\phi$$

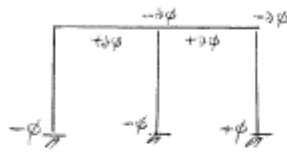
$$\lambda = 1.57$$

External work is combined mechanism directly from the external terms in the relevant independent elementary equilibrium equations.

Internal work of the combined mechanism. Ignore sign or rather sign always become positive.

**(F) Combined mechanism 3.**

Choose  $\theta = \psi = \phi = \alpha$  and combine (A) + (B) + (C) + (D)



$$(20\lambda)(2\phi) + (36\lambda)(2\phi) + (25\lambda)(4\phi) = 11m_p\phi$$

$$\lambda = 1.432$$

**Static Check for Mechanism Combined 1:**

Need  $M_3, M_5, M_6 = -$

$$(1): 30\lambda(2\theta) = -\theta(M_p) + 2\theta(M_3) - \theta(-M_p)$$

Unknown parameter

With  $\lambda = 1.57$  and  $m_p = 30$

$$\Rightarrow m_3 = 47.1 \text{ kNm (yield condition not satisfied)}$$

$$(3): 100\lambda\alpha = -\alpha(-M_p) + \alpha M_p + \alpha M_5 - \alpha(-M_p) - \alpha(-M_p) + \alpha M_p$$

With  $\lambda = 1.57$  and  $m_p = 30$

$$\Rightarrow m_5 = 7 \text{ kNm}$$

directly

$$(4): 0 = -\psi(-M_p) - \psi(7) + \psi(M_6)$$

With  $\lambda = 1.57$  and  $m_p = 30$

$$\Rightarrow m_6 = -23 \text{ kNm}$$

Since static check failed, scale linearly:

$$\lambda = 1.57$$

$$m_1 = m_4 = m_8 = m_{10} = -30$$

$$m_2 = m_7 = m_9 = 30$$

$$m_3 = 47.1, m_5 = 7, m_6 = -23$$

$$\Rightarrow * \frac{30}{47.1} \Rightarrow$$

$$\lambda_4 = 1$$

$$m_1 = m_4 = m_8 = m_{10} = -19.1$$

$$m_2 = m_7 = m_9 = 19.1$$

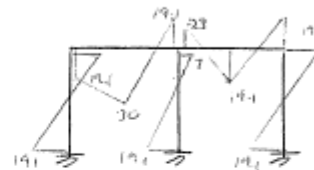
$$m_3 = 30, m_5 = 4.5, m_6 = -14.6$$

$$\text{hence, } 1 \leq \lambda_c \leq 1.57$$

Based on the rotation signs of the combined mechanism.

For instance @ joint 1, rotation is  $-\psi$  i.e. minus,

thus  $m_1 = -19.1$  and drawn opposite to dotted side.



**Static Check for Mechanism Combined 2:**

Need  $M_3, M_6, M_5$

$$(1): 60\lambda\theta = -\theta M_3 + 2\theta M_6 - \theta(-M_p)$$

$$M_3 = 4.68 \text{ kNm}$$

$$(2): 72\lambda\phi = -\phi M_6 + 2\phi M_5 - \phi(-M_p)$$

$$M_6 = -12.384 \text{ kNm}$$

$$(4): 0 = -\psi(-M_p) - \psi M_5 + \psi(-12.384)$$

$$M_5 = 17.616 \text{ kNm}$$

Static Check successful since

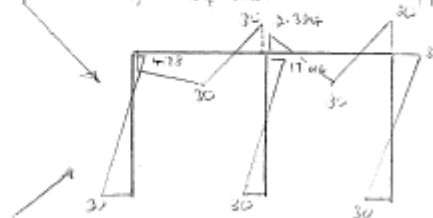
$|M| \leq m_p$  and thus

$$\lambda_c = 1.432$$

Based on the rotation signs of the combined mech.

For instance @ joint 1, rotation is  $-\phi$  i.e. minus,

thus  $m_1 = -19.1$  and drawn on opposite to dotted side.



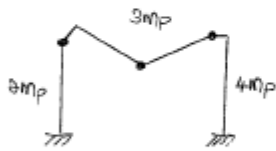
$M_6$  has been calculated as  $-12.384$ ; hence drawn on opposite to dotted side.

## SURVIVAL KIT

### (A) Kinematic Collapse Analysis of Independent Elementary Mechanisms with 2-Member Joints.

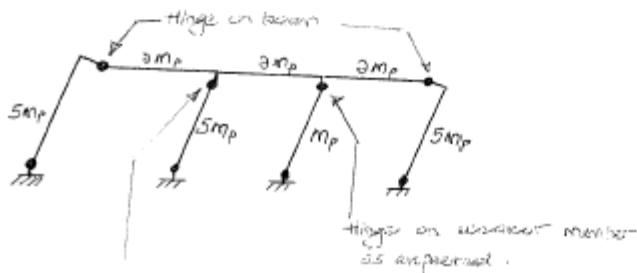
At 2 member joints, ALWAYS place hinge at lower Mp member. At 3+ member joints, this need not be done because shall be considered separately by the joint mechanism.

(a) Beam with hinge on column.



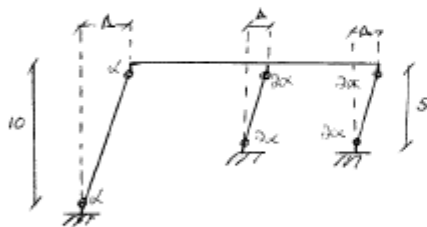
Rare in practice as column usually has higher  $M_p$ .

(b) Slab with hinge on beam



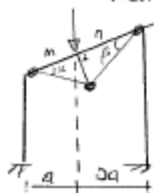
hinge on column even though stronger member. At 3+ member joints, joint mechanism considered independently.

### (B) Multiple Length Columns



$$A = 10x$$

### (C) Inclined Members

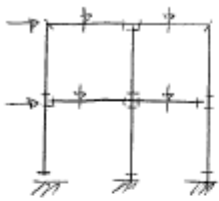


Note the direction (perpendicular) to which beam mechanism forms.

•  $a\alpha = 2a\beta$  is true and can be proven by finding inclined distances  $m = \frac{a}{\cos\alpha}$  and  $n = \frac{2a}{\cos\beta}$ .

• also, the plastic work gives  $\delta_v = a\alpha$  and  $\delta_v = 2a\beta$

④  $N = n - d_s$



$n = 22$   
 $d_s = 4 \times 3 = 12$

$N = 22 - 12 = 10$

- o 4 beam mechanisms
- o 4 joint mechanisms (a joint mechanism occurs at every joint with 3 or more members).
- o 2 sway mechanisms



n contribution of a 2 member joint is 1, but  
 n contribution of a 3 or more member joint is 3 or more as appropriate.

⑤ REITERATION OF METHODS OF COMBINATION OF MECHANISMS

(a) Numerical addition then geometrical representation

- use when we know all the independent elementary mechanisms

$N = n - d_s$

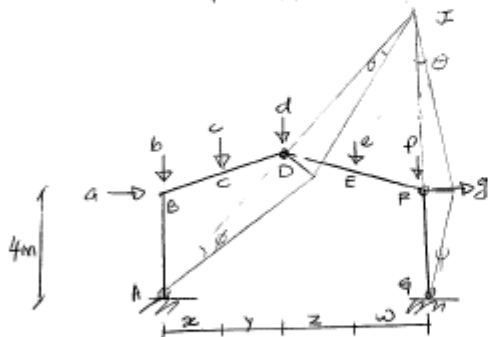
- This approach is best and systematic
- have to use the instantaneous centre of rotation when considering the panel mechanism (elementary mechanism) in pinned portal frames.

(b) Straight to geometrical method

- use when we do not know (or rather have not bothered to) all the independent elementary mechanisms.
- may have to use the instantaneous centre of rotation quite often.
- not systematic, but useful when we want to check & for a particular mechanism with a particular set of plastic hinges.
- use when plastic hinge positions given

⑥ Protonic Rule At Its Best.

The vertical deflection under a load on a member is equal to  $H\theta$  where  $H$  is the horizontal projection of the member from the point under concern to the point of rotation of the member whereas  $\theta$  is the rotation of the member. The point of rotation of a member could also be the instantaneous centre of rotation.



$\delta_{H_B} = 4\phi$  ;  $\delta_{V_B} = 0\phi = 0$   
 $\delta_{V_C} = x\phi$   
 $\delta_{V_D} = (x+y)\phi$  or  $(z+w)\theta$   
 $\delta_{V_E} = w\theta$   
 $\delta_{V_F} = 0(\phi)$  or  $0(\theta)$  ;  $\delta_{H_F} = 4\psi$

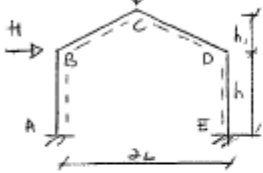
- o ABD rotates  $\phi$  about A
- o DF rotates  $\theta$  about I
- o FG rotates  $\psi$  about G

Also, to find angle relationship of inclined members :-  
 $(x+y)\phi = (z+w)\theta$  for relationship between  $\phi$  &  $\theta$ .

Just be wary that when computing external work, the load and displacement must be in the same direction, otherwise a negative external work term!

PITCHED-ROOF FRAMES

Because of the fact that the distance between eaves can change, this type of frame has certain collapse mechanisms which are not present in the rectangular portal frame.



Plastic hinges at B, C and D do not constitute a beam collapse mechanism as with portal frames as the vertical load can be transferred to the columns by simple truss action.

$$N = n - \alpha s$$

$$= 5 - 3$$

$$= 2$$

Here two independent elementary mechanisms, namely the sway and panel mechanism.

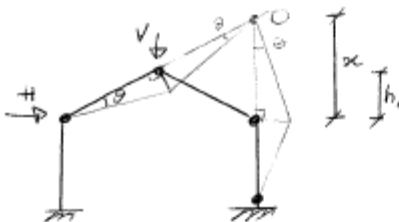
(1) Sway:



$$+H\delta h = -\delta M_B + \delta M_C - \delta M_D + \delta M_E \quad \text{--- (1)}$$

$$+H\delta h = +\delta M_P$$

(2) Panel mechanism: This mechanism is peculiar to pitched roof frames



- (i) Join extends of BC and ED to meet at the instantaneous centre of rotation O.
- (ii) Point C moves perpendicular to BC whilst point D moves perpendicular to ED.
- (iii) Let the lamina COD rotate by  $\psi$  at O.
- (iv) As with any instantaneous centre of rotation problem: -

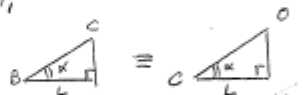
- (i) Distances
- (ii) Rotations (relative)
- (iii) Internal Work.
- (iv) External Work.

(i) Distances:

Similar triangles to find height to O:

$$\text{hence } \frac{h_1}{L} = \frac{x}{2L} \Rightarrow x = 2h_1$$

also  $BC = CO$  because



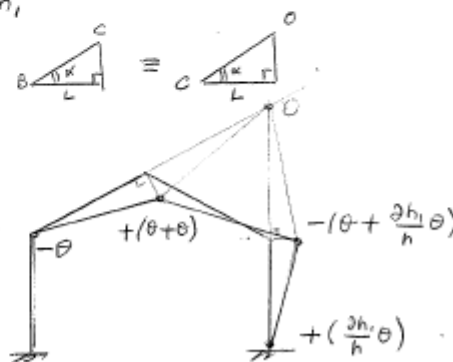
(ii) Relative rotations:

$$BC\theta = CO\psi$$

$$\text{and } DO\theta = ED\psi$$

$$2h_1\theta = h\psi$$

$$\psi = \frac{2h_1}{h}\theta$$



Signs of mid-hinges become obvious after drawing deformed shape.

(iii) Internal work:

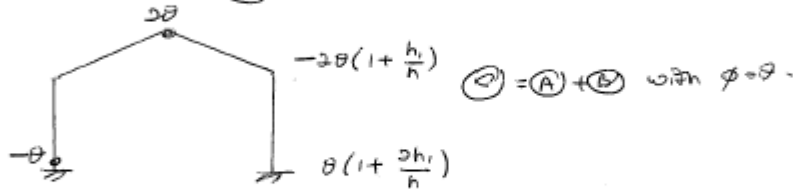
$$= \theta M_p + 2\theta M_p + (1 + \frac{2h_1}{h})\theta M_p + \frac{2h_1}{h}\theta M_p = (4 + \frac{4h_1}{h})\theta M_p$$

(iv) External work

$$= VL\theta \text{ (pneumatic rule).}$$

ⓐ Combined mechanism (not elementary mechanism).

In order to rid hinge at B, choose  $\phi = \theta$

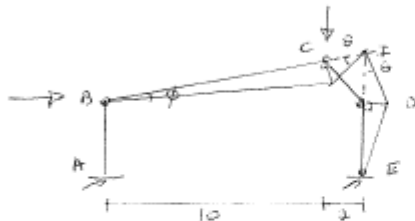


$$+Hh\theta + VL\theta = \theta M_p + 2\theta M_p + 2\theta(1 + \frac{h_1}{h})M_p + \theta(1 + \frac{2h_1}{h})M_p$$

$$\left( \begin{array}{l} +Hh + VL \\ \end{array} \right) = M_p (6 + \frac{4h_1}{h})$$

To obtain the external work terms of any combined mechanism, simply add all the external work terms unaltered from the independent elementary mechanisms used to form the combined mechanism. In the case of the pitched frame, there lies the possibility that the same load would appear twice in the external work terms. This occurs if there was a horizontal load at D causing work (external) to be done when either elementary mechanism is formed.

In the case of a panel mechanism as follows:



Let rotation about C as  $\theta$ .

To find rotation at B, use horizontal distances instead of inclined distances.

$$10\phi = 2\theta$$

$$\phi = \frac{2\theta}{10}$$

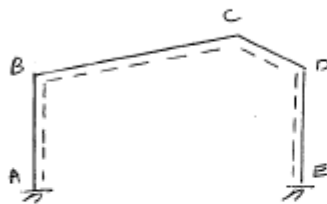
And this just as if BC were a beam



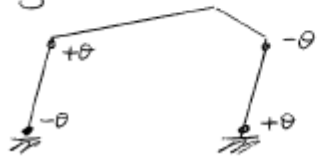
$$\begin{aligned} \text{rotation at C} &= \theta + \frac{\theta}{5} \\ &= \frac{6\theta}{5} \end{aligned}$$

7. (a)  $k_6 = 3$

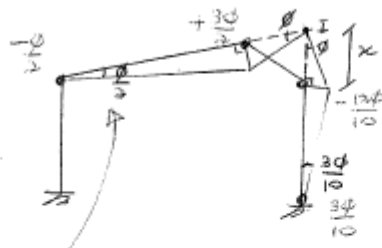
$$N = n - k_s = 5 - 3 = 2 \text{ i.e. sway and panel mechanisms.}$$



Sway:

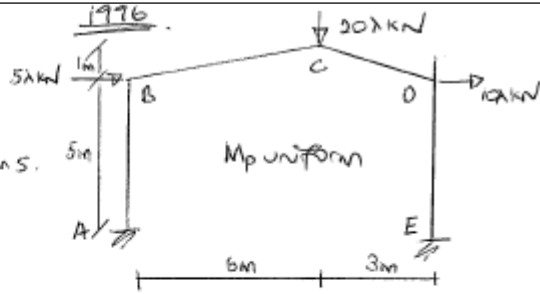


Panel:



CECL!  
Call this  $\alpha$  say.  
 $k_\alpha = 3 \neq$   
 $\lambda = \frac{\phi}{\alpha}$

i.e. Use horizontal distances instead of inclined distances.



- (a) Determine  $\lambda$  due to 3 possible collapse mechanisms.
- (b) For  $\lambda$  lowest draw corresponding beam.
- (c) If required collapse load-factor  $\lambda_c = 1.5$ , what is the corresponding

$$5\lambda(5\theta) + 10\lambda(5\theta) = -\theta M_A + \theta M_B - \theta M_C + \theta M_E \quad (1)$$

$$75\lambda\theta = 4M_p\theta$$

$$\lambda = \frac{4}{75} M_p$$

By similar triangles,

$$\frac{1}{6} = \frac{x}{9}$$

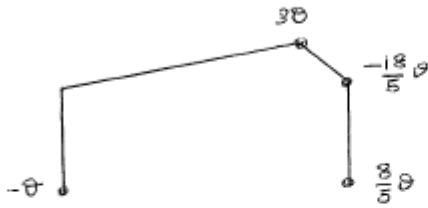
$$x = \frac{3}{2}$$

$$20\lambda \left(6 \frac{\phi}{2}\right) + 10\lambda \left(\frac{3\phi}{10} \times 5\right) = -\frac{\phi}{2} M_B + \frac{3\phi}{2} M_C - \frac{3\phi}{10} M_D + \frac{3\phi}{10} M_E \quad (2)$$

$$\lambda = \frac{6}{125} M_p$$

Combined mechanism:

Choose  $\theta = \frac{\Phi}{5}$  for no hinge at B.



$$75\lambda\theta + 20\lambda(6 \times \theta) + 10\lambda\left(\frac{3}{10}(2\theta) \times 5\right) = \frac{46}{5}\theta M_p$$

External work  
terms directly  
from the elementary  
mechanisms.

$$225\lambda = \frac{46}{5} M_p$$

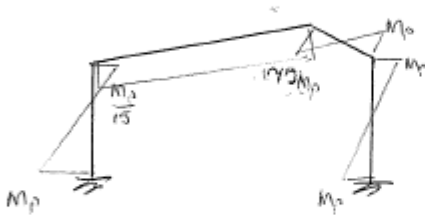
$$\lambda = \frac{46}{1125} M_p$$

(b) Static check for combined mechanism:

$$(1): 75\lambda\theta = -\theta(-M_p) + \theta M_B - \theta(-M_p) + \theta(M_p)$$

$$\text{with } \lambda = \frac{46}{1125} M_p$$

$$\therefore M_B = \frac{M_p}{15}$$

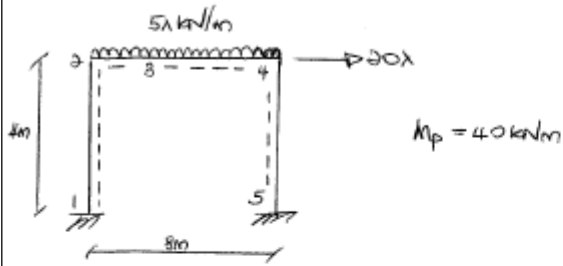


(c)

$$M_p = \frac{1125}{46} \times 1.5$$

$$= 36.68 \text{ kNm}$$

DISTRIBUTED LOAD (EXACT METHOD)



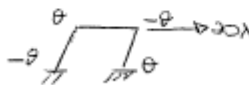
Note that point 3 is somewhere where the local  $m$  is max.

$$N = n - ds$$

$$= 5 - 3$$

$$= 2$$

(A) Sway Mechanism

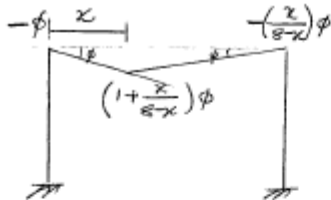


$$20\lambda(4\theta) = -\theta M_2 + \theta M_3 - \theta M_4 + M_5\theta \quad (1)$$

$$80\lambda\theta = 4M_p\theta \text{ with } M_p = 40 \text{ kNm}$$

$$\lambda = 2$$

(B) Beam Mechanism



The only difference is in the definition of  $x$ .

$$x\psi = (8-x)\psi$$

$$\psi = \frac{x}{(8-x)}\phi$$

$$5\lambda \left( \frac{1}{2} \times 8 \times x\psi \right) = -\phi M_2 + \left(1 + \frac{x}{8-x}\right)\phi M_3 - \left(\frac{x}{8-x}\right)\phi M_4 \quad (2)$$

5λ \* area displaced

For the purpose of performing the collapse analysis for the beam, it is evident that the hinge occurs in the midspan.

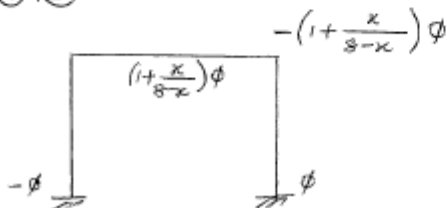
$$5\lambda \left( \frac{1}{2} \times 8 \times 4\phi \right) = \phi M_p + 2\phi M_p + \phi M_p$$

$$\lambda = 2$$

(C) Combined Mechanism

Choose  $\phi = \theta$  for no hinge at 2.

$$(C) = (A) + (B)$$



External work terms directly from elementary mechanisms; but keep  $x \Rightarrow$  yes

$$80\lambda\phi + 5\lambda\left(\frac{1}{3} \times 8x \times \phi\right) = 2M_p\phi + 2M_p\left(1 + \frac{x}{8-x}\right)\phi$$

$$\text{Now } M_p = 40 \text{ kNm}$$

$$80\lambda + 20\lambda x = 160 + \frac{80x}{8-x}$$

$$20\lambda(4+x) = 160 + \frac{80x}{8-x}$$

$$20\lambda = \frac{160}{4+x} + \frac{80x}{(4+x)(8-x)}$$

$$\lambda = \frac{8}{4+x} + \frac{4x}{(4+x)(8-x)}$$

$$= \frac{8}{(4+x)} + \frac{-\frac{4}{3}}{4+x} + \frac{\frac{8}{3}}{8-x} \quad (\text{partial fractions})$$

$$\text{For } \frac{d\lambda}{dx} = \frac{-8}{(4+x)^2} + \frac{\frac{4}{3}}{(4+x)^2} - \frac{\frac{8}{3}}{(8-x)^2} (-1) = 0$$

$$\frac{-\frac{20}{3}}{(4+x)^2} + \frac{\frac{8}{3}}{(8-x)^2} = 0$$

$$\frac{20}{3} \frac{1}{(4+x)^2} = \frac{8}{3} \frac{1}{(8-x)^2}$$

$$20(8-x)^2 = 8(4+x)^2$$

$$5(64 + x^2 - 16x) = 2(16 + x^2 + 8x)$$

$$320 + 5x^2 - 80x = 32 + 2x^2 + 16x$$

$$3x^2 - 96x + 288 = 0$$

$$x = 28.6 \text{ m}, \quad x = 3.35 \text{ m} \\ (\text{invalid})$$

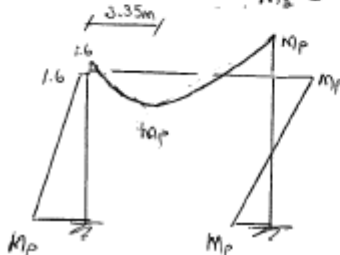
$$\therefore \lambda_{\text{opt}} = 1.48$$

Static Check:

$$(1): 80\lambda\theta = -\theta(-M_p) + \theta M_p - \theta(-M_p) + \theta M_p$$

$$\text{With } \lambda = 1.48, \quad M_p = 40$$

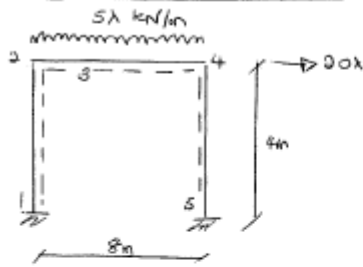
$$\therefore M_s = -1.6 \text{ kNm}$$



where  $M_p = 40$ .

Yield condition satisfied.

DISTRIBUTED LOAD (APPROXIMATE METHOD)



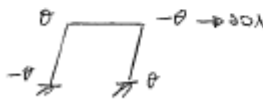
Note that point 3 is somewhere where the local bn is max.

$$N = n - \alpha_s$$

$$= 5 - 3$$

$$= 2$$

(A) Sway mechanism



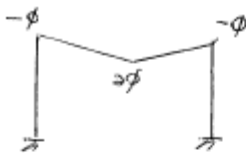
$$20\lambda(4\theta) = -\theta M_1 + \theta M_2 - \theta M_4 + \theta M_5 \quad \text{--- (1)}$$

$$80\lambda\theta = 4M_p\theta$$

$$\lambda = 2$$

(B) Beam mechanism

Assume hinge forms at mid-span.



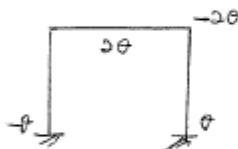
$$\underbrace{5\lambda \times \text{area displaced}}_{5\lambda \left(\frac{1}{2} \times 8 \times 4\phi\right)} = -\phi M_2 + 2\phi M_3 - \phi M_4 \quad \text{--- (2)}$$

$$80\lambda\phi = 4M_p\phi$$

$$\lambda = 2$$

(C) Combination of elementary mechanisms

Choose  $\phi = \theta$



$$80\lambda\theta + 80\lambda\theta = 6M_p\theta$$

$$\lambda = 1.5$$

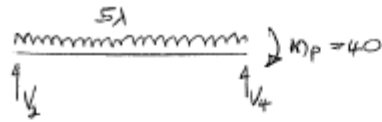
Static check:

Check for satisfaction of yield condition all along beam not merely  $M_2$ .

$$(1): 80\lambda\theta = -\theta(-M_p) + \theta M_2 - \theta(-M_p) + \theta(M_p)$$

with  $\lambda = 1.5$  and  $M_p = 40 \text{ kNm}$

$$\therefore M_2 = 0 \text{ kNm}$$



$$EI(\frac{8}{2}) + 40 = 8V_4 \Rightarrow V_4 = 25 \Rightarrow V_2 = 25 \text{ kNm}$$

General beam expression with  $x$  rightward from  $\partial_1$

$$-M + V_2x - \frac{5\lambda x^2}{2} = 0$$

$$M = -3.75x^2 + 25x$$

For  $\frac{dM}{dx} = -7.5x + 25 = 0$

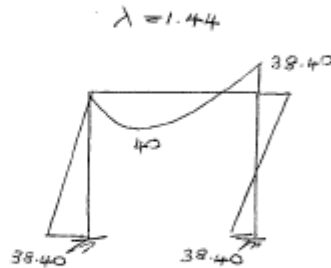
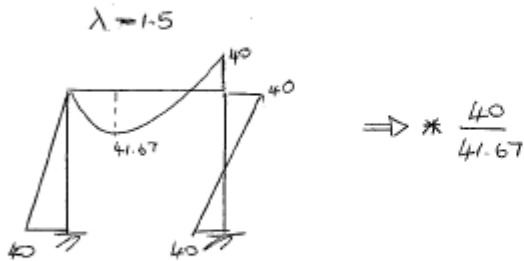
$$x = 3\frac{1}{3} \text{ m}$$

$$M_{\text{max}} = -3.75 \left(3\frac{1}{3}\right)^2 + 25 \left(3\frac{1}{3}\right) = 41.67 \text{ kNm}$$

Choose  $M_{\text{general}}$  as  $\curvearrowright$  to be the same convention as the plastic collapse analysis to ease matters.

If difficult to differentiate, use knowledge the  $M=0$  at shear force = 0. Draw  $\curvearrowright$  SFD and find zero SF by similar triangles. Replace this  $x$  position into expression for  $M$ .

Yield condition not satisfied.



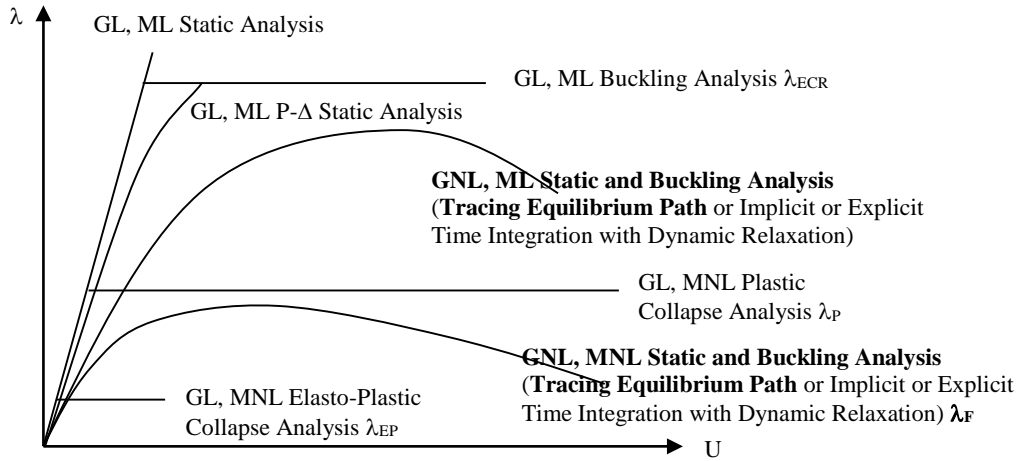
$$\Rightarrow * \frac{40}{41.67}$$

hence,

$$1.44 \leq \lambda_c \leq 1.5$$

### 3.4 GNL, MNL, Contact Nonlinear Static and Buckling Analysis by The Implicit Tracing The Equilibrium Path Method

#### 3.4.1 Mathematical Formulation of Tracing the Equilibrium Path



It is instructive to define a few important terms.

Definition of Equilibrium States and Paths	
Equilibrium state	A pair of $(\lambda, \{U\})$ satisfying the geometrically nonlinear equilibrium conditions between the external nodal $\{P\}$ loads and the component forces $\{f\}$ , given the compatibility relationship between $\{d\}$ and $\{U\}$ as well as the constitutive law relating $\{f\}$ to $\{d\}$
Equilibrium path	A continuous line of equilibrium states
Fundamental equilibrium path	An equilibrium path that includes the initial unloaded state $(\lambda=0, \{U\}=\{0\})$
Secondary equilibrium path	An equilibrium path that does not include the initial unloaded state $(\lambda=0, \{U\}=\{0\})$
Trivial fundamental path	An equilibrium path for which the displacements are zero for all levels of loading i.e. $(\lambda \neq 0, \{U\}=\{0\})$

The static equilibrium equation has been established, and is restated in all its simplicity.

$$[K_T] \delta\{U\} = \delta\{P\}$$

where  $[K_T] = [K_E] + [K_G]$

where  $[K_E] = [T]^T [[k_E]] [T]$

for which  $[k_E] = \int_{\Omega} [B]^T [D] [B] d\Omega$

and  $[K_G] = [T]^T [[k_G]] [T] + \left[ \frac{\partial^2 \langle d \rangle}{\partial \{U\} \partial \langle U \rangle} \{f\} \right]$

for which  $[k_G] = \int_{\Omega} \left[ \frac{\partial^2 \langle \varepsilon \rangle}{\partial \{d\} \partial \langle d \rangle} \{ \{ \sigma \}_n + \{ \sigma \}_i - [D] \{ \varepsilon \}_i \} \right] d\Omega - \left[ \frac{\partial^2 W_i}{\partial \{d\} \partial \langle d \rangle} \right] - \lambda \left[ \frac{\partial^2 W_n}{\partial \{d\} \partial \langle d \rangle} \right]$

and  $\{ \sigma \}_n = [D] [B] \{d\}$

and  $\{f\} = \left[ \int_{\Omega} [B]^T [D] [B] d\Omega \right] \{d\} + \left\{ \int_{\Omega} [B]^T \{ \sigma \}_i d\Omega \right\} - \left\{ \int_{\Omega} [B]^T [D] \{ \varepsilon \}_i d\Omega \right\} - \left\{ \int_{\Omega} [N]^T \{b\} d\Omega \right\}$

$[K_T]$  = tangent stiffness matrix

$[K_E]$  = instantaneous stiffness of the system with modified geometry as  $[T]$  dependent upon  $\{U\}$

$[K_G]$  = geometric stiffness matrix

$[K_T]$ ,  $[K_E]$  and  $[K_G]$  are all symmetric.

As stated, we have omitted the second order variation of work due to the external nodal loadings  $\{P\}$  from the above tangent stiffness matrix expression, i.e.

$$- \left[ \frac{\partial^2 W}{\partial \{U\} \partial \langle U \rangle} \right] = - \left[ \frac{\partial \{P\}}{\partial \langle U \rangle} \right] \quad \text{as} \quad \{P\} = \left\{ \frac{\partial W}{\partial \{U\}} \right\}$$

This is because, as mentioned, the externally applied loads at the nodes are in commercial codes always work-conjugate with the nodal DOFs  $\{U\}$ , failing which the above term must be incorporated. The second order variation of work due to loads applied on the finite elements is obviously still taken into account.

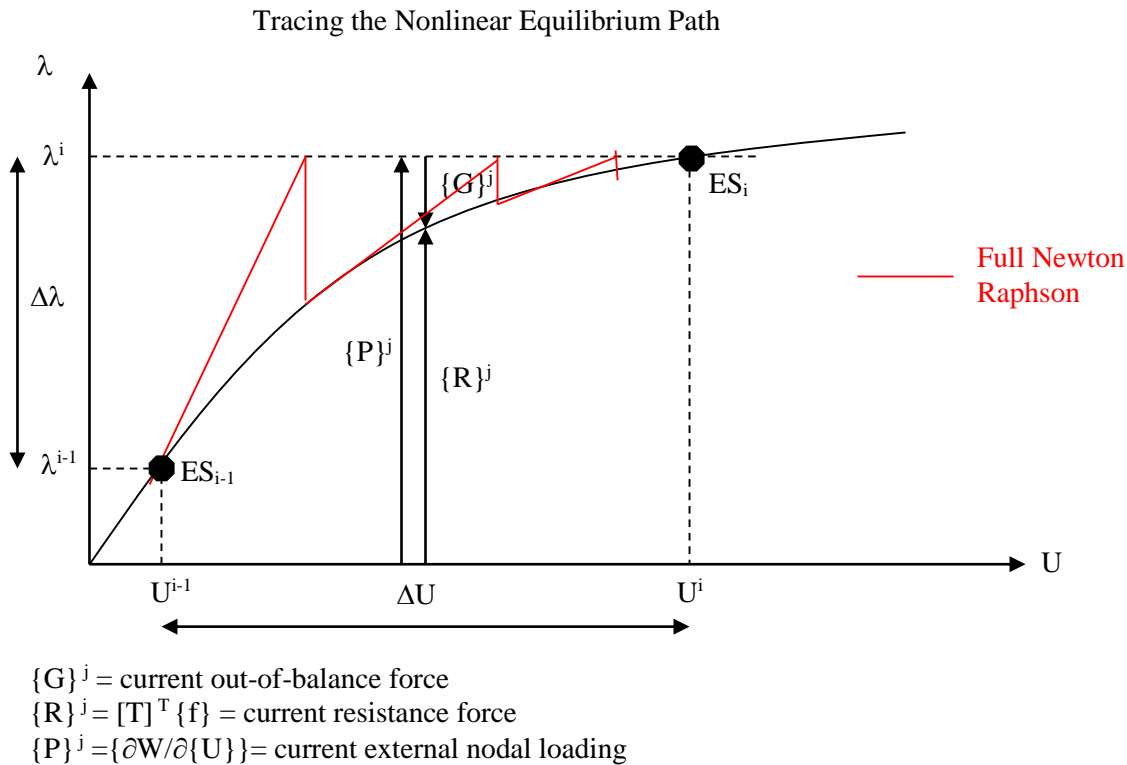
In order to find the buckling load, we could in theory perform a nonlinear eigenvalue solution. The nonlinear eigenvalue problem is expressed as

$$[K_T] \{ \phi \} = \{ 0 \}$$

The nontrivial solution is obtained by solving for the eigenvalue  $\lambda$  from

$$\det | [K_T] | = 0$$

This is quite a complex solution scheme is thus is not usually attempted. As closed-form mathematical solutions of realistic multi-degree of freedom nonlinear eigenvalue problems are highly complex, incremental methods to establish the equilibrium path is used. The incremental procedures can correspond to an increment of displacement or an increment of loading, i.e. displacement control or load control. The incremental approach is normally started from the initial unloaded equilibrium state, in which case the fundamental path is traced. In the vicinity of bifurcation states, it is essential that small incremental steps be used so as to avoid a jump from the fundamental path to a different path.



The vector  $\{f\}$  includes the fixed end forces which are negative terms here. It is equivalent then to add those terms to the  $\{P\}$  vector and call it the equivalent nodal loading vector if we desire; however the mathematics will work out nevertheless as the fixed end forces are included within  $\{f\}$  as negative terms. Now, in order to trace the nonlinear load path, we formulate a set of linear equations valid over a small load or displacement step.

$$[K_T] \delta\{U\} = \delta\{P\}$$

This is the linearized equilibrium equation valid as long as  $[K_T]$  is approximately constant over the displacement or load step. We can also rewrite the above equation as

$$[K_T] \delta\{U\} = -\{G\}$$

where  $\{G\}$  is the out-of-balance force between the equivalent loads and the resistance forces. In this way, there will be no accumulation of error as the load steps are traced.

To trace the nonlinear equilibrium path, we ascertain  $i$  successive equilibrium states

Between two successive equilibrium states  $j$  iterations are performed,

$$\Delta\{U\}^j \text{ is solved from } [K_T] \Delta\{U\}^j = -\{G\}^j \text{ where } \{G\}^j = \{R\}^j - \{P\}^j$$

$$\Delta\{U\} = \Delta\{U\} + \Delta\{U\}^j$$

The Full Newton-Raphson recalculates  $[K_T]$  at every  $j$  whilst the Modified Newton Raphson uses initial  $[K_T]$  at beginning of iteration  $i$

Next  $j$  until out-of-balance force  $\{G\} \approx 0$ , hence equilibrium state

Next  $i$  noting that change in out-of-balance force  $\delta\{G\} \approx 0$  signifies a limit point.

Iterative Method	Description	Advantages	Disadvantages
Newton-Raphson	$[K_T]$ calculated at every iteration in inner loop	Less iterations	Many $[K_T]^{-1}$ required for inner loop
Modified Newton-Raphson	$[K_T]$ calculated once before an iteration in inner loop	More iterations	Only one $[K_T]^{-1}$ required for inner loop

The modified Newton-Raphson is efficient when there is no strain hardening or an unloading path is not required, otherwise the Newton-Raphson is required for convergence.

We start with load control. Load control used for ascending portions of the equilibrium path. When close to a bifurcation point, load control is used with small steps. Then when close to a limit point, displacement control is used. Displacement control is also used for descending parts of the equilibrium path. Then, if we come to a limit point in the displacement sense, we revert to load control or use another displacement parameter.

### 3.4.2 Newton-Raphson Load Control, Displacement Control or Arc-Length Control Algorithm

#### *Advancing Phase*

1. Determine an increment (**of load, displacement or arc length**) to trace on the equilibrium path from  $ES_{i-1}$  to  $ES_i$
2. Determine an estimate of the tangent stiffness at  $ES_{i-1}$ ,  $K_{Ti-1}$
3. Determine the predicted displacement increment to move forward by solving the equilibrium equations
 
$$[K_{Ti-1}]\Delta\{U\}_{i-1}^P = -\{G\}_{i-1}$$
4. Calculate the element resisting force  $\{R\}_{i-1}$
5. Calculate the unbalanced force  $\{G\}_{i-1}$  and check for convergence. If converged, i.e.  $\{G\} \approx 0$ , then go to 1 with  $i = i + 1$ . If not converged go to 6.

#### *Iteration (or Correcting) Phase*

6. Determine an estimate of the tangent stiffness at  $ES_j$   
 $ES_j = ES_{i-1}$  then Modified Newton Raphson  
 $ES_j = ES_j$  then Full Newton Raphson
7. Determine displacement increment due to the unbalanced force
 
$$[K_{Ti-1}]\Delta\{U\}_j^C = -\{G\}_{j-1} \text{ for Modified Newton Raphson where } j - 1 = i - 1$$

$$[K_{Tj}]\Delta\{U\}_j^C = -\{G\}_{j-1} \text{ for Full Newton Raphson where } j - 1 = i - 1$$
8. Calculate the element resisting force  $\{R\}_j$
9. Calculate the unbalanced force  $\{G\}_j$  and check for convergence. If converged, i.e.  $\{G\} \approx 0$ , then go to 1 with  $i = i + 1$ . If not converged go to 6 with  $j = j + 1$ . If divergence occurs, then go to 1 with trying a smaller load step.

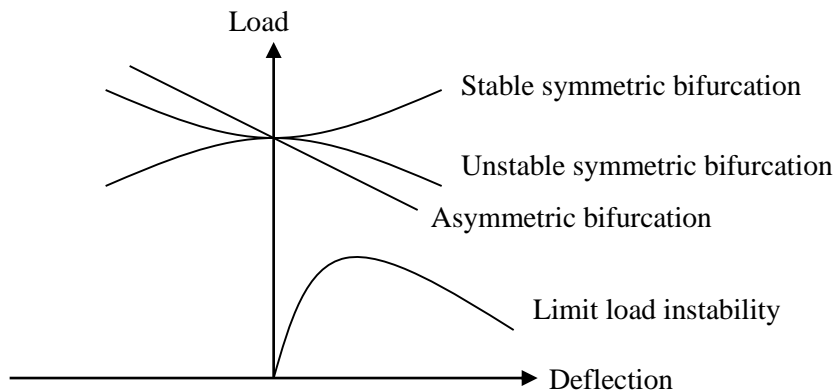
Note that no convergence can be achieved if the total applied load is greater than the buckling load. The Full Newton-Raphson procedure can be expensive and unnecessary when the solution is close to convergence.

### 3.4.3 Equilibrium Paths, Stability of Equilibrium Paths, Critical Points, Stability of Critical Points

Apart from the linear eigenvalue method (linear elastic buckling) and nonlinear tracing the equilibrium path, stability of an elastic system can be interpreted by means of the concept of minimum potential energy. An elastic system always tends to go to a state in which the total potential energy is at a minimum. The types of instability include: -

- (I) Bifurcation instability (For perfect systems – SOL 105)
  - (i) Stable symmetric bifurcation
  - (ii) Unstable symmetric bifurcation
  - (iii) Asymmetric bifurcation
- (II) Limit load instability (For imperfect systems – SOL 106)

Bifurcation instability can be analyzed using **linear buckling analysis** whilst limit load instability is analyzed by **tracing the equilibrium path**.



The **energy method** of stability analysis involves the following: -

- (i) Obtain the total potential energy function  $V = U - P\Delta$
- (ii) Obtain the equilibrium paths by solving for

$$\frac{\partial V}{\partial \theta} = 0$$

where for a SDOF system, a perfect system yields 2 solutions, one  $\theta = 0$  and the other  $P$  in terms of  $\theta$  whilst an imperfect system gives one solution for  $P$  in terms of  $\theta$ .

- (iii) Investigate the stability of the equilibrium paths

$$\frac{\partial^2 V}{\partial \theta^2} > 0 \quad \text{for regions of stability}$$

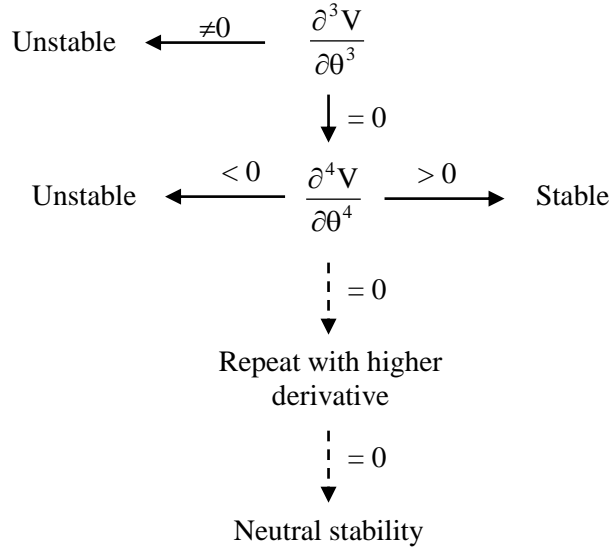
$$\frac{\partial^2 V}{\partial \theta^2} < 0 \quad \text{for regions of instability}$$

- (iv) Identify the critical points (i.e. the boundaries between stability and instability – bifurcation or limit points). For the perfect system, the critical point is the bifurcation point. This is obtained by inspection  $\theta = 0, P = P_{cr}$ . Alternatively, the two solutions of (ii) is put into

$$\frac{\partial^2 V}{\partial \theta^2} = 0$$

separately to yield two values defining the bifurcation point. We can also identify the limits points for imperfect systems by differentiating the equilibrium path equation, i.e.  $dP/d\theta = 0$ . Hence we shall obtain value for  $\theta$  at the limit point,  $\theta_{lp}$  which subsequently is replaced into  $P$  for the value of the critical point,  $P_{lp}$ .

- (v) Investigate the stability of the critical point. The bifurcation point ( $\theta = 0, P = P_{cr}$ ) or the limit point ( $\theta = \theta_{lp}, P = P_{lp}$ ) is replaced into the third derivative of  $V$ .



Increment of total potential energy,  $\Delta V = \delta V + \delta^2 V + \dots$

For equilibrium  $\delta V = 0$  (principle of minimum potential energy),

Increment of total potential energy around equilibrium state,  $\Delta V = \delta^2 V + \dots$

$$\begin{aligned}
 &= \frac{1}{2} \delta\{U\}^T \left[ \frac{\partial^2 V}{\partial \{U\} \partial \{U\}} \right] \delta\{U\} + \dots \\
 &= \frac{1}{2} \delta\{U\}^T [K_T] \delta\{U\} + \dots
 \end{aligned}$$

An equilibrium state is stable if  $\Delta V$  is positive for all possible infinitesimal disturbances  $\delta\{U\}$ . This implies that an agent external to the system will have to perform positive work in order to cause  $\delta\{U\}$ .

Stability of Equilibrium State ES		
$\delta^2 V$ positive definite	Thoroughly stable ES	Gaussian elimination on $[K_T]$ leads to all positive diagonals, i.e. $\delta^2 V = 0.5 \delta\{U\}^T [K_T] \delta\{U\} > 0$ for all $\delta\{U\}$ or $\det([K_T]) > 0$
$\delta^2 V$ admits negative values	Thoroughly unstable ES	Gaussian elimination leads to at least one negative diagonal term, i.e. $\delta^2 V = 0.5 \delta\{U\}^T [K_T] \delta\{U\} < 0$ for some $\delta\{U\} = \delta\{U_0\}$ or $\det([K_T]) < 0$

$\delta^2V$ positive semi-definite	Critically stable or unstable ES i.e. a critical point	Gaussian elimination leads to at least one zero diagonal term, i.e. $\delta^2V = 0.5 \delta\{U\}^T [K_T] \delta\{U\} = 0$ for some $\delta\{U\} = \delta\{U_0\}$ or $\det ([K_T]) = 0$
------------------------------------	---	--

A critical point (buckling point) can be a bifurcation or a limit point. At a critical point  $\det ([K_T]) = 0$ , i.e.  $K_T$  is singular indicating the presence of an infinitesimally adjacent equilibrium state at the same level of loading. A critical point is normally associated with one buckling mode  $\delta\{U_0\}$ . Bifurcation points are very rare in real structures due to the presence of imperfections in the geometry and due to pre-buckling displacements.

Nature of Critical Point		
Bifurcation point	A critical point is a bifurcation point if and only if the first order work done by $\{P_n\}$ over the buckling mode(s) $\delta\{U_0\}$ is zero. Loading can be increased further along at least one of the bifurcation paths.	$\{P_n\}^T \delta\{U_0\} = 0$
Limit point	A critical point is a limit point if and only if the first order work done by $\{P_n\}$ over the buckling mode(s) $\delta\{U_0\}$ is non-zero. Loading cannot be increased further.	$\{P_n\}^T \delta\{U_0\} \neq 0$

### 3.4.4 MSC.NASTRAN Decks

#### 3.4.4.1 GNL, MNL Load Control, Displacement Control or Arc-Length Control Static Analysis

All cards applicable to SOL 101 are also applicable to SOL 106.

<b>§ EXECUTIVE CONTROL SECTION</b>									
SOL 106									
<b>§ CASE CONTROL SECTION</b>									
DISPLACEMENT(<PRINT,PUNCH,PLOT>) = ALL/<Grid Set ID> SPCFORCES(<PRINT,PUNCH,PLOT>) = ALL/<Grid Set ID> OLOAD(<PRINT,PUNCH,PLOT>) = ALL/<Grid Set ID> NLSTRESS = (<PRINT,PUNCH,PLOT>) = ALL/<Element Set ID> ELSTRESS(<PRINT,PUNCH,PLOT>) = ALL/<Element Set ID> ELFORCE(<PRINT,PUNCH,PLOT>) = ALL/<Element Set ID> STRAIN(<PRINT,PUNCH,PLOT>) = ALL/<Element Set ID> ESE(<PRINT,PUNCH,PLOT>) = ALL/<Element Set ID> BOUTPUT = ALL \$ Slideline Contact Output Request \$									
<b>SUBCASE 1</b>									
LOAD = < ID of FORCEi, MOMENTi, PLOADi, GRAV, LOAD, SPCD Cards in Bulk Data > TEMP(LOAD) = < ID of TEMP, TEMPRB, TEMPP1 Cards in Bulk Data > SPC = < ID of SPC Cards in Bulk Data > NLPARM = < ID in Bulk Data NLPARM > \$									
<b>SUBCASE 2</b>									
LOAD = < ID of FORCEi, MOMENTi, PLOADi, GRAV, LOAD, SPCD Cards in Bulk Data > TEMP(LOAD) = < ID of TEMP, TEMPRB, TEMPP1 Cards in Bulk Data > SPC = < ID of SPC Cards in Bulk Data > NLPARM = < ID in Bulk Data NLPARM >									
<b>§ BULK DATA</b>									
PARAM, AUTOSPC, NO           \$ AUTOSPC NO By Default PARAM, FOLLOWK, YES       \$ Includes Follower Force Stiffness PARAM, LGDISP, 1           \$ Includes Large Displacement Effects i.e. [T] not constant PARAM, LANGLE, 2           \$ Rotation Vector Approach for Large Rotations PARAM, K6ROT, 100         \$ Shell normal rotation restrained in nonlinear analysis									
NLPARM	ID	NINC (<1000)	Incremental Time For Creep, DT	KMETHOD	KSTEP	MAXITER	CONV	INTOUT	
	EPSU	EPSP	EPSW	MAXDIV	MAXQN	MAXLS	FSTRESS	LSTOL	
	MAXBIS				MAXR		RTOLB		

Unlike linear analyses schemes, nonlinear analysis schemes (SOL 106 and SOL 129) employ subcases on an incremental basis, instead of separate load cases and boundary conditions. In linear analysis, subcases represent an independent loading condition. Each subcase is distinct from each other. Nonlinear static analysis permits only one independent loading condition per run. For SOL 106, the bulk data loads and prescribed displacements are measured from the initial configuration. Hence latter subcases should refer to different load cards that have magnitudes that include the magnitude of load cards from previous subcases. Hence, if the same point is being loaded or displaced in a subsequent subcase, the load or displacement value referred by the subsequent subcase should be relative to the initial undeflected value of zero and not that of the previous subcase. Subcases are hence

cumulative. Loads and boundary conditions at the end of a subcase are the initial conditions for the next subcase. Hence if the load description is inadvertently omitted in subsequent subcases, the load will automatically be removed in an incremental fashion. Only one independent loading history can be applied during an analysis. In general, a different loading sequence requires a complete new analysis. The load to be applied during a particular stage (i.e. subcase) is referred to by the LOAD Case Control Command. **NINC** in the NLPARM bulk data entry is an integer that specifies the number of increments in the particular subcase, by default 10. The more linear the problem is, the smaller the value of NINC that can be acceptable. But when nonlinearity is significant such as at the onset of plasticity, at regions of stress concentration where each load step causes high stress changes, at contact regions with high forces and at the onset of buckling, the incremental load should be small (i.e. NINC must be large). Hence different subcases should be used to model different regions along the load path. Where nonlinearity of stiffness is small, NINC can be small, and when nonlinearity is large, NINC must be large. The load specified in a particular subcase minus the load specified in the preceding subcase is equally divided by NINC to obtain the incremental load for the particular subcase. Clearly, if convergence is a problem, this incremental load should be made smaller (by increasing NINC and/or decreasing the magnitude of load specified in the particular subcase relative to the previous subcase) until convergence. Self-weight and/or prestressed elements must be simulated by incorporating an initial load case followed by whatever static loading load case. Each subcase should not have NINC exceeding 1000 to control the database size, output size and restarts.

The following can be performed with multiple subcases:

- (i) Loads can be changed, naturally
- (ii) Boundary conditions, i.e. SPC can be changed
- (iii) Solution strategy in NLPARM

The follower force is calculated and incorporated by the use of PARAM, FOLLOWK, YES. We know how the prestress affects the differential stiffness, namely a tensile prestress causing an increase in stiffness. The effect of the follower force on the stiffness is different. For example, for a cylinder under external pressure critical buckling load may be over-estimated (even though the mode shapes are similar) in a SOL 105 and the natural frequencies in vibration may be under-estimated (even though the mode shapes are similar) in a SOL 103 in the absence of follower stiffness. To the contrary, these observations are reversed in case of centrifugal loads. Centrifugal forces as a constant (static) load are applied by a Bulk Data RFORCE to any elements that have masses. The follower stiffness due to centrifugal load has the effect of lowering stiffness (although the centrifugal load tensioning effect increases stiffness), consequently lowering natural frequencies (even though the mode shapes are similar) in a SOL 103 and lowering the buckling loads (even though the mode shapes are similar) in a SOL 105. This effect increases as the RPM increases, and it becomes significant when the RPM is over 1000. For moderately geometric nonlinear analysis, exclusion of follower stiffness affects the rate of convergence, but the converged solution is correct. For severely geometric nonlinear analysis, it may not be possible to obtain a converged solution without including follower stiffness. As the geometric nonlinearity intensifies, so is the effect of follower stiffness. Therefore, inclusion of follower stiffness greatly enhances the convergence if the deformation involves severe geometric nonlinearity.

Output requests for each subcase are processed independently, but are appended after computation for output purposes. The **INTOUT** field is specified with YES, NO or ALL and determines whether the output is requested for each load increment within a subcase or just the last load step of the subcases.

- YES Output requested for every computed converged load increment within the subcases
- NO Output requested for only the last converged load increment of the subcases
- ALL Output requested for every computed and user specified load increment within the subcase

INTOUT is especially important for restarts. For Newton's iteration methods (i.e. without NLPCI) the option ALL is equivalent to YES but not when arc length methods (with NLPCI) are used.

#### 3.4.4.1.1 Increment Methods (Load Control, Displacement Control or Arc-Length Method)

**Load control** is specified by having load card definitions. Naturally, the LOAD case control command is required. Load cards relevant to SOL 101 is also relevant to SOL 106 except for DEFORM cards. The applicable load cards are FORCEi, MOMENTi, PLOADi. GRAV, TEMP, SPC, SPCD etc. Loads which are stationary in direction throughout the analysis include: -

- (i) FORCE, MOMENT, SLOAD
- (ii) PLOAD1
- (iii) GRAV

Loads which follow the motion of the grid or the element (i.e. follower forces that produce stiffness terms) include

- (i) FORCE1, FORCE2, MOMENT1, MOMENT2
- (ii) PLOAD, PLOAD2, PLOAD4, PLOADX1
- (iii) RFORCE
- (iv) TEMP, TEMPD, TEMPP1, TEMPP3, TEMPRB

**Displacement control** is specified by having SPCD card definitions, noting that grid points with displacements enforced by SPCD must also have an SPC entry. Note that enforced displacement can also be specified directly on the SPC bulk data entry, although this method is not recommended. Naturally, the LOAD case control command is required.

**Arc-length control** is specified by having load card definitions and also a NLPCI card with the same ID as the NLPARM card. Arc-length control cannot be used in conjunction with displacement control SPCD cards. The arc-length method is useful to trace unstable or post-buckling equilibrium paths defined by negative load control steps. The critical buckling load can be estimated by Newton’s load control method by performing the nonlinear static analysis until the solution cannot be obtained due to divergence, in which case the adaptive bisection method is activated in the vicinity of the critical buckling load and stops at the limit load close to the critical buckling load. But beyond that, the load control method does not work, and hence the arc-length method is required.

NLPCI	ID	TYPE	MINALR	MAXALR	SCALE		DESITER	MXINC	
-------	----	------	--------	--------	-------	--	---------	-------	--

**MAXR** on the NLPARM card is the maximum ratio for the adjusted arc-length increment relative to the initial value, by default 20.0. The TYPE field on the NLPCI card could be CRIS (default), RIKS or MRIKS.

#### 3.4.4.1.2 Stiffness Update Strategy (AUTO, SEMI or ITER using KSTEP)

The load is divided up into load steps. Each load step is then divided into iteration steps. **KMETHOD** specifies the method for controlling stiffness updates, whether **AUTO (default)**, **SEMI** or **ITER**.

With **AUTO**, NASTRAN automatically selects the most efficient strategy of when to update the tangent stiffness matrix based on convergence rates. The matrix could be updated in the middle of an iteration and will not be necessarily be updated at the beginning of the load step. AUTO is a good starting method. It essentially examines the solution convergence rate and uses the quasi-Newton, line search and/or bisection convergence acceleration methods to perform the solution as efficiently as possible without a stiffness matrix update. Highly nonlinear behaviour in some cases may not be handled effectively using AUTO. For AUTO (like SEMI), the stiffness matrix is updated on convergence if KSTEP is less than the number of iterations that was required for convergence with the current stiffness.

**SEMI** is similar to AUTO (it also uses the quasi-Newton, line search and/or bisection convergence acceleration methods) except that the tangent stiffness matrix will also be updated at the beginning of each load step, irrespective of the convergence status. Hence SEMI provides better convergence at the expense of higher cost. The SEMI method is an efficient method for nonlinear static iteration. For SEMI (like AUTO), the stiffness matrix is updated on convergence if KSTEP is less than the number of iterations that was required for convergence with the current stiffness.

With **ITER**, the stiffness matrix is updated at every **KSTEP** iteration. KSTEP specifies the number of iterations before the stiffness update, 5 by default. It is a ‘brute force’ method. It can be most suited for highly nonlinear problems. Full Newton-Raphson is obtained by selecting **KMETHOD = ITER** and **KSTEP = 1**. Modified Newton-Raphson is obtained by selecting **KMETHOD = ITER** and **KSTEP = MAXITER**.

### 3.4.4.1.3 Convergence Acceleration Techniques (Quasi-Newton MAXQN, Line Search using MAXLS and LSTOL, Bisection using MAXITER, RTOLB, MAXBIS and MAXDIV)

The convergence acceleration techniques include **quasi-Newton, line search and bisection**.

The stiffness updating schemes can be supplemented with **quasi-Newton** (QN) updates. **MAXQN** is the maximum number of quasi-Newton correction vectors to be saved on the database, equal to **MAXITER** by default. The BFGS update is performed if  $MAXQN > 0$ .

The **line search** is controlled by **MAXLS** and **LSTOL**. **MAXLS** is the maximum number of linear searches allowed for each iteration, default 4. **LSTOL** requires a real number between 0.01 and 0.9 to specify the tolerance for the line search operation, default 0.5. The line search operation will be conducted if the error defining the divergence rate is greater than **LSTOL**. Computing cost for each line search is comparable to that of an iteration.

**MAXITER** specifies the limit on number of iterations for each load increment, 25 by default. If the solution does not converge at **MAXITER** iterations, the load increment is **bisected** and the analysis is repeated. Bisection is also activated if **RTOLB**, by default 20.0 is exceeded. **RTOLB** is the maximum value of incremental rotation (in degrees) allowed per iteration before bisection is activated. **MAXBIS** specifies the maximum number of bisections for each load increment, 5 by default. If **MAXBIS** is positive, the stiffness matrix is updated on the first divergence and the load increment is bisected on the second divergence. If **MAXBIS** is negative, the load increment is bisected every time the solution diverges until the limit on bisection is reached. If  $|MAXBIS|$  has been attained and the solution still has not converged then the value on **MAXDIV**, which specifies the divergence criteria for an iteration, 3 by default, is considered. If **MAXDIV** is positive, the best attainable solution is computed and the analysis is continued to next load increment. If **MAXDIV** is negative, the analysis is terminated. Hence, if we want the analysis to terminate if convergence has not been achieved, **MAXDIV** must be negative, not the default value. The **recommended value** for **MAXDIV** is thus **-3**.

### 3.4.4.1.4 Convergence Criteria (CONV, EPSU, EPSP, EPSW)

The convergence test is performed at every iteration. **CONV** specifies the flags to select convergence criteria, **UPW** or any combination, note default **PW**. **EPSU** is the error tolerance for displacement error (U) convergence criteria. **EPSP** is the error tolerance for load equilibrium error (P) convergence criteria. **EPSW** is the error tolerance for work error (W) convergence criteria. If displacement control is used, then there is a need for tighter tolerances for convergence. There is a facility to provide a default value depending on the type of analysis, type of elements and desired accuracy by specifying the **NLTOL** parameter and leaving the **CONV**, **EPSU**, **EPSP** and **EPSW** fields in the **NLPARM** blank. Models with gap, contact or heat transfer elements will have tighter default convergences.

<b>\$ BULK DATA</b>
PARAM, NLTOL, ITOL

ITOL is an integer designating the level of tolerance as

- 0 (very high)
- 1 (high)
- 2 (engineering design)
- 3 (preliminary design)

Default convergence tolerances are as follows.

NLTOL	Designation	No Gaps, Contact or Heat Transfer Elements	With Gaps or Contact Elements	With Heat Transfer
0	Very High	EPSP=1.0E-3 EPSW=1.0E-7	EPSP=1.0E-3 EPSW=1.0E-7	EPSP=1.0E-3 EPSW=1.0E-7

				(Default)
1	High	EPSP=1.0E-2 EPSW=1.0E-3		
2	Engineering	EPSP=1.0E-2 EPSW=1.0E-2 (Default)	EPSP=1.0E-3 EPSW=1.0E-5 (Default)	
3	Preliminary	EPSP=1.0E-1 EPSW=1.0E-1		

The quality of the mesh is essential in nonlinear analysis. Artificial stress concentrations due to poor modelling such as when beams interface with a shell mesh without special handling techniques will cause convergence difficulty. The mesh should also be adequately fine for good stress recovery, hence a h-element convergence exercise must be undertaken. This could probably be performed by repetitive linear analysis, the resulting converged mesh can be used with confidence in a nonlinear analysis. Other steps that can be taken to improve convergence are increase the number of load increments, break applied load into multiple subcases, use a more general material stress-strain definition instead of a bilinear model, avoid poorly shaped elements in regions of high stresses and introduce initial load steps in the solution to establish equilibrium in the model prior to increasing the nonlinearity. Contact regions should have a fine mesh in order to capture the contact stresses. If large deformations are expected to distort elements such that their accuracy may be called into question, it may be worthwhile to manually distort the elements in the opposite direction somewhat before starting the solution so that the final shape will be closer to the ideal shape.

**3.4.4.1.5 Nonlinear Finite Elements in MSC.NASTRAN**

Element				Nature of Nonlinearity of Stiffness			
	Mass	Damping	Stiffness	Geometric Nonlinearity i.e. [T] Not Constant With {U}	Differential Stiffness i.e. From Element Force and Work Done	Large Strain Effect Hyperelastic i.e. [B] Not Constant With {d}	Material Nonlinearity i.e. [D] Not Constant With {ε}
CBAR PBAR MAT1 (MATT1)	Yes	No	Yes	No	Yes	No	No
CBUSH PBUSH and PBUSHT	No	Yes	Yes	No	No	No	Yes
CBUSH1D PBUSH1D	Yes	Yes	Yes	Yes	Yes	No	Yes
CROD PROD MAT1 (MATT1), MATS1	Yes	No	Yes	Yes	Yes	No	Yes
CONROD MAT1 (MATT1)	Yes	No	Yes	Yes	Yes	No	Yes
CTUBE PTUBE MAT1 (MATT1)	Yes	No	Yes	Yes	Yes	No	Yes
CBEAM PBEAM MAT1 (MATT1), MATS1	Yes	No	Yes	Yes	Yes	No	Yes
CQUAD4, CTRIA3	Yes	No	Yes	Yes	Yes	No	Yes

PSHELL MAT1 (MATT1), MAT2 (MATT2), MAT8, MATS1, CREEP							
CQUAD8, CTRIA6 PSHELL MAT1 (MATT1), MAT2	Yes	No	Yes	No	Yes	No	No
CQUAD4, CTRIA3 PLPLANE MATHP	Yes	No	Yes	Yes	Yes	Yes	Yes
CQUAD8, CTRIA6 PLPLANE MATHP	Yes	No	Yes	No	Yes	Yes	No
CHEXA, CPENTA, CTETRA PSOLID MAT1 (MATT1), MAT9 (MATT9), MATS1, CREEP	Yes	No	Yes	Yes	Yes	No	Yes
CHEXA, CPENTA, CTETRA PLSOLID MATHP	Yes	No	Yes	Yes	Yes	Yes	Yes

Note that the **CBAR** element is **not a nonlinear element** i.e. its coordinates are not updated as the element deforms.

The **CBUSH** is a **generalized nonlinear spring - linear damper** element. The **CBUSH1D** is a rod-type **nonlinear spring - nonlinear damper** element; it is a 1D version of the **CBUSH** element with added features. The **CBUSH** is **NOT geometrically nonlinear**, only materially. The **CBUSH1D** element can have geometric and material nonlinearity. The **CBUSH1D** element is the only element which can model **rotation damping** such as for modelling tuned pendulums mass dampers.

The **CROD**, **CONROD**, **CTUBE** elements can be used to model **cables** as these elements are geometrically nonlinear, incorporates the differential stiffness and can refer to different stress-strain curves for tension and compression.

**CGAP** element can also be used to work in the opposite sense to a contact element in order to function as a **cable** element. That is to say, the element can be made to work only in tension by specifying a separation distance corresponding to the taut condition, above which the element is to be turned on and resist tension.

The **CBEAM** element can model **plastic hinges** at its ends for **plastic collapse analysis** of frameworks. For this, the material type specified in the **MATS1** card must be **elastic-plastic (and perfectly plastic too) i.e. TYPE PLASTIC**, and strictly **not nonlinear elastic**. The **CBEAM** is assumed to have its nonlinearity concentrated at its ends. Obviously if material nonlinearity is enabled, there can be no pin flags. The user need not specify the cross-section axis about which the yielding occurs, since the implementation allows for combinations of bending moments in two directions plus an axial load. The flexibility of the plastic hinge is based upon eight idealized rods at each end, chosen to match the total area, center of gravity and moments of inertia of the cross section.

Note that rigid body elements **RBEi**, **RBAR** and **RROD** do not rotate in geometric nonlinear analysis i.e. their coordinates are not updated as the element deforms and hence are **not nonlinear elements**. Geometric stiffness is also not computed for rigid elements. **Offsets are not recommended** in nonlinear analysis, or even linearized buckling analysis. Overly stiff elements, as replacements are also not recommended as they may cause problems with convergence (**MAXRATIO** exceeded). Too stiff will give you mathematical problems and too flexible will create too soft a connection. Thankfully what you might consider "very stiff" is numerically still likely to be OK. In number terms you want something that is maybe 1000X stiffer than the local structure. If you are still unsure try 2

runs, with one having a bar 10 times stiffer than the other. If the answers are similar then you know it is stiff enough. To estimate the stiffness of the structure at that point connecting the gap, use simple beam formulae such as  $12EI/L^3$  or  $3EI/L^3$  or alternatively, apply an arbitrary load and ascertain the displacement from a SOL 101 static analysis.

Midside grids on solid elements are not allowed for nonlinear analysis.

### 3.4.4.1.6 Contact Nonlinearity

There are three primary types of contact elements, namely **point-to-point contact gap elements (CGAP)**, **line-to-line or surface-to-surface slide line contact elements (BLSEG)** and **general arbitrary line-to-line or surface-to-surface contact elements**.

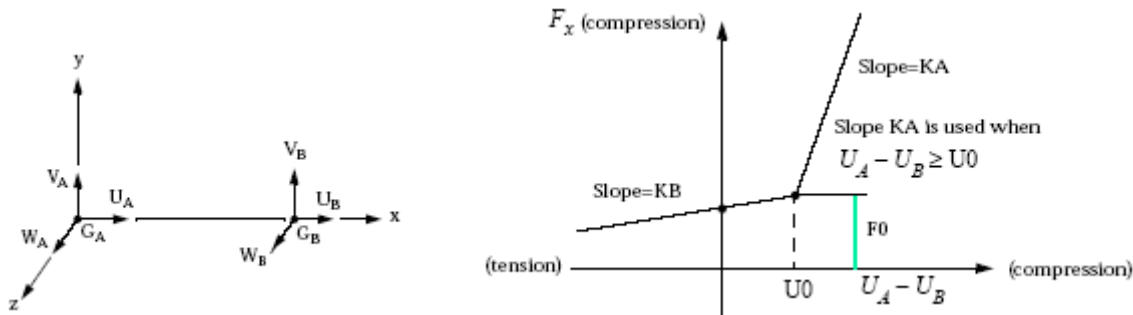
The **CGAP** element is a point-to-point contact element. Its element coordinate system is defined depending on whether the end grids points are coincident or not. If coincident, the orientation is defined by using the coordinate system CID, which if unspecified would default to the basic system. If the grid points are not coincident, the orientation is defined using the element x-axis using defined by the GA to GB grid orientation and the v vector is defined using X1, X2, X3 or G0 entries. Note also that no stress singularity will be introduced here by connecting many 1D gap elements to the shell or solid mesh. This is because of the multiple 1D element. Had there been just one 1D element connected to a shell or solid mesh, then certainly there will be stress singularity.

CGAP	EID	PID	GA	GB	X1	X2	X3	CID	
------	-----	-----	----	----	----	----	----	-----	--

The two basic properties of the CGAP element are its **initial gap** and its **compressive stiffness**. If the initial node-to-node separation becomes more positive, the gap has no stiffness and is for all intents and purposes dormant. As the separation becomes less positive and approaches zero or some predefined initial gap, the element wakes up and becomes a stiff spring, which resists further closure. The point at which the gap begins to resist this displacement is defined by the initial gap. This initial gap may be zero but the length of the element may not. The length of the gaps may be zero for solid elements by may not for shell elements, whereby the user may decide that due to mid-plane modelling, these two plates that might rest on each other, would by definition, be separated by half the sum of their thicknesses. By bridging this separation with gap elements assigned with initial gap of zero, the code will know that this initial position represents the two parts already in contact.

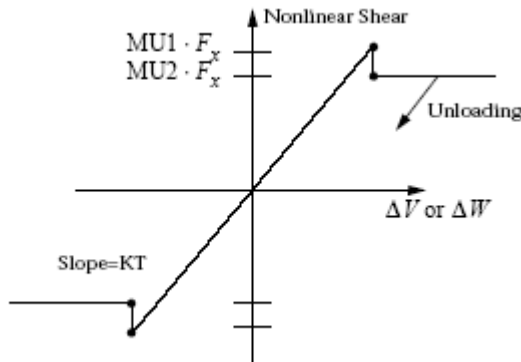
PGAP	PID	U0	F0	KA	KB	KT	MU1	MU2	
	TMAX	MAR	TRMIN						

The orientation is of the CGAP (whether coincident or not) is important to define the direction of opening and closing as depicted in the figures below. Hence GA and GB must be attached to the correct portions of the model in order to simulate the correct opening and closing behaviour.



The preload F0 is useful to model friction because the frictional force is a function of the total compressive force which in turn is a function of the preload. Hence in a SOL 129 analysis, if the only contribution of gravity is to add

a normal force which would result in frictional forces, the normal forces induced in the contact elements can be specified as preloads instead of modelling the gravity load case explicitly.



**Gap element stiffness** controls the numerical stability. The compressive stiffness must simulate the local stiffness of the elements in the contact pair. If the stiffness is too high, the element may bounce as the load is incremented near zero separation. The closed gap stiffness should not exceed the adjacent DOF stiffness **by 1000 times**. If the stiffness is too low, external forces may actually drive one node through the other. The CGAP element should be used when there is very little relative displacement or sliding normal to direction of closure is expected. The process of choosing a gap stiffness may be an iterative one as an initially soft gap if stiffened to the point where penetration is minimal but the nonlinear solution still converges. Alternatively, the adaptive gap stiffness technology adjusts the gap stiffness internally to achieve convergence without penetration within some predefined tolerance. In the adaptive solution, the method of specifying the initial gap stiffness is the opposite of the manual iterative process. Choose a stiffer gap and let the code soften it as is required numerically. The adaptive method is clearly more efficient. Note that the mesh on either contacting surfaces should correspond exactly so that the gap elements are well aligned. Relative slide should be insignificant as this can cause the gap element to go into tension when in reality it is still in contact. This problem arises if the force in the gap element acts in the direction of the element. A better method would then certainly be to define the stiffness of the gap element in a particular DOF only i.e. normal to the contact interface.

The gap element provides point-to-point contact. When the gap element is open, there is no contact and no friction. When the gap element is closed, there are three different conditions. The first case is when the gap is sliding (no friction). The second case occurs when the gap element is sticking (static friction). The third case occurs when the gap element is slipping (kinetic friction). Sometimes, it may be difficult to converge because of the switching among these conditions. Typical coefficients of friction are presented.

Material Contact	Coefficient of Friction
Steel on steel (dry)	0.3
Steel on steel (greasy)	0.05 to 0.1
Brake lining on cast iron	0.3 to 0.4
Rubber on steel	1.0
Tire on pavement (dry)	0.8 to 0.9
Wood on wood	0.2

On the PGAP Bulk Data entry, U0 and F0 are the initial gap opening and the preload, respectively. U0 is the separation of the gap element. If you are unsure about what preload to use, use the default value of zero. KA, KB, and KT are called the penalty values. KA is the axial stiffness when the gap is closed, KB is the axial stiffness when the gap is open, and the KT is the transverse gap stiffness. All you need to input is the KA value. KB is defaulted to be zero, and KT is defaulted as a function of KA. The selection of KA or a penalty value is critical to the convergence of the problem. The non-adaptive gap does not update this KA value. The new adaptive gap updates this KA value if you specify a positive value for TMAX. The default option for the new adaptive gap is NO adaptive stiffness update. This is when the TMAX value is equal to 0.0. If TMAX is a negative number, then MSC.Nastran uses the non-adaptive gap formulation. A good initial KA selection is roughly 1000 times the Young's modulus of the material that is in the neighborhood of the gap element. Fields 8 and 9 also require some

explanation. For the new adaptive value this is MU1, which is the static coefficient of friction, and MU2, which is the dynamic coefficient of friction. The non-adaptive gap elements use MUY and MUZ in the same fields instead of MU1 and MU2 values. Therefore, to compare the results using adaptive and non-adaptive gap elements, set both of these entries to the same values. On most problems, you will not know how to estimate the penetration depth or field 2 on the continuation entry. Therefore, if you skip the continuation entry, the default new adaptive gap is obtained, which is everything adaptive except the KA update. The recommended allowable penetration of TMAX is 10 percent of the thickness for the shell element, and for the solid element it is roughly 1/10,000 of the characteristic length for the problem. A small positive value will turn on the adaptive stiffness update, which will then converge at a faster rate. The maximum adjustment ratio or MAR in field 3 of the continuation entry is used only for the penalty value adjustment of the adaptive gap element. The default value of 100 is sufficient for most problems.

Further discussion of CGAP parameters is warranted. U0 is self explanatory - the initial open value of the gap. F0 - any preload you want to apply - be careful if KB is the only thing preventing rigid body motion. KA - this is the source of most convergence problems due to gap elements. It can be calculated from the local stiffness of the structure at the GRIDs to which the gap are applied. If you can't do this by hand (usually the case), then run a linear static (SOL 101) analysis with U0 temporarily set greater than 0.0 (or remove the gap element from the model for this run, if possible); this is so the gap stiffness you have already defined at KA does not influence the local stiffness. Then apply a unit load to both GRIDs of the gap in the direction of the gap X axis. Run the analysis and recover the displacement of both GRIDs in the gap X direction. Now take 1000 times the inverse of the displacement at the gap GRIDs and use the smallest value of the two for the value of KA. Now 2 questions arise. First, if the value of displacement in the gap X direction recovered from this run is, say, 3.4211378E-02 then I calculate KA so  $KA = 1000 * 1/3.4211378E-02 = 2.923E+04$ . Do I have to use this EXACT value ? No. The analysis is only sensitive to orders of magnitude of the value of KA. In the above case, therefore, I would use  $KA=3E+4$  as the initial KA value. Second, do I have to apply unit loads to EVERY gap GRID in the model (I may have many, many gaps) ? In general, no. Because I am looking for the order of magnitude of the stiffness for KA, it is only necessary to select one gap for each region where I judge the stiffness will be significantly different from other regions. That is to say, if the structure to which the gaps is attached is roughly the same stiffness no matter which gap GRIDs I select, then one gap will be enough to get a good KA value. Using engineering judgement, I can see if the structure will have significantly different stiffness in different areas of the model where gaps are connected. A value of  $3E+04$  will work just as well as  $2E+04$  or  $4E+04$  in the above example. KB - generally I leave this as default unless I have unusual situations such as a very large value of U0. To illustrate this, take the example of a gap that has an open value  $U0=1$ . I calculate the value of KA to be  $2E+16$ . I leave KB blank, so the default value becomes  $KA*1E-14 = 200$ . Now I apply my loads and eventually during the analysis, the gap closes. The gap will have moved 1.; gap force =  $KB*1. = 200$ . This may be a significant load compared with the applied load. In this case, I would force KB to 0.1 or smaller to avoid large gap forces due to large axial displacements in the gap. KT - generally I leave this at default as it is tied to KA via MU1. MU1 and MU2 are self explanatory. Friction will generally have a significant effect on the cost of the analysis. TMAX, MAR and TRMIN are useful if the local stiffness of the structure changes significantly as a result of the nonlinear deformations. They allow the gap stiffness to be adjusted during solution, but only approximate values can be calculated for these. For most cases, if the structure's stiffness at the gap GRIDs will not change significantly, I would not use adaptive gaps. The extra iteration of two that maybe needed to get convergence will in general be quicker than reforming the stiffness to get a not much better value for KA. Only if I expect local stiffness to change significantly would I use  $TMAX > 0.0$ . If TMAX is set to 0.0 (the default), the gap-induced stiffness update, gap-induced bisection, and sub-incremental process are enabled, but the penalty values (KA, KB, KT) remain unchanged. If TMAX is set to a small positive value, this has all the features of the gap when  $TMAX=0.0$ , and also enables the adaptive penalty capability where the penalty values are adjusted according to changes in the stiffness of the surrounding structure. A value for TMAX is calculated by examining the structure to which the gaps are attached. If these are shell elements, then a value of 10% of the thickness of the elements should be used. For other elements, such as beam elements, then an equivalent thickness is used, such as the depth of the beam in the axial direction of the gap. If the structure is a massive solid, then the ideal value of TMAX is two or three orders of magnitude less than the elastic deformation of the solid. This is not always easy to estimate, so a value of  $1 * 10E-4$  of the characteristic length of the model can be used. That is, determine the largest dimension of the model and use  $10E-4$  of that value. If TMAX

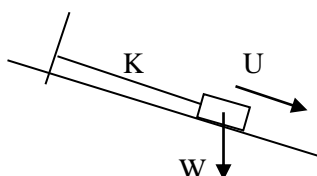
is too small, the solution will frantically try to adjust the penalty values to update the stiffnesses. If TMAX is too large; no update will occur and convergence may be elusive. MAR sets the maximum allowable adjustment ratio for the penalty values and must be in the range 1.0 to 10E6. The upper and lower bounds of the adjusted penalty values are K/MAR and K\*MAR, where K is KA or KT. TRMIN sets the lower bound for the allowable penetration and is a fraction of TMAX. It must be in the range 0.0 to 1.0. Penalty values are decreased if the penetration is less than the minimum allowable penetration which is calculated from TRMIN \* TMAX. What is allowable ? Back to good 'ol engineering judgement.

**Convergence** is often a problem in highly nonlinear problems such as in GAP-like problems. This following approach is normally a lot faster and more reliable than accepting the default NLPARM entries. The problem with gap analysis is that the non-linearity is a very severe On/Off situation. This can cause problems where you get numerical "chatter" when a gap is not open or tightly closed. This chatter makes Nastran think it is not converging and causes the loads to be bisected. Bisection can be the worst thing to happen, as it reduces the load and can mean the chatter gets worse. This causes another bisection and before you know it you are applying tiny load increments. Also, to help whenever a gap opens or closes, we must update the stiffness matrix every iteration. Hence use the full Newton Raphson. Finally to make the gap closure definite, apply all the load in 1 or 2 steps rather than the default 10. So in summary use the following settings on NLPARM for a pure gap problem. 1) NINC=1 or 2; 2) Use Newton Raphson. KMETHOD=ITER, KSTEP=1; 3) Switch off Bisection MAXBIS=0. If convergence is a problem such as in highly nonlinear problems, then the TSTEP method can always be used with KSTEP=1 such that stiffness is updated at every time step, hence there is no issue of convergence, just like in explicit nonlinear transient analysis. However, the time step size must still be small for accuracy.

The CGAP element is **not a geometrically nonlinear element**, it is a small displacement element, i.e. its coordinates are not updated as the element deforms. The orientation of the contact plane does not change during deflection.

Name	Characteristics	Friction Law	Geometric Nonlinearity
CGAP	Contact between two points. Extension has different springs for compression and tension. Shear force is less than the friction coefficient times the compression. Transverse finite compression stiffness is required.	Coulomb's Law with: kinetic friction ≠ static friction	No
Slideline	Contact between a point and a line.	Coulomb's Law with: kinetic friction = static friction	Yes

The **slide line contact elements BLSEG (with BCONP, BFRIC and BWIDTH)** are essentially contact curves that allow significant relative sliding between the contacting parts. Slide lines can also be used to model contact between surfaces by proper definition of the slide lines. This is done when two or more corresponding slide lines are positioned on the contacting parts such that they remain relatively coplanar throughout model deformations. The same stiffness considerations as those for gap elements apply the estimation of the stiffness may be more complicated than for gap elements. Friction between the sliding interfaces may be incorporated. The friction coefficient for FEA contact element should not be assumed to have a direct correlation to the friction coefficients pulled from data sheets. A handy test setup involves a mass on an inclined board supported by a spring.



$$\mu = \frac{W \sin \theta - KU}{W \cos \theta}$$

**General contact elements** are conceptually the simplest but the most computationally intensive. Sets of elements define the contacting parts. The contact stiffness is usually derived from the material properties of the elements in the contact pair – typically the Young’s Modulus and in some codes the material damping. The contact and separation directions are determined from the normals or boundaries of the contacting elements. These contact entities provide the smoothest and most realistic pressure distribution but the computational price is heavy.

#### 3.4.4.1.7 Material Nonlinearity

Material models can be

- elastic or inelastic** (the latter exhibiting different unloading path to loading path and hence plastic strain)
- linear or nonlinear** (the latter exhibiting a variable Young’s Modulus with respect to strain)
- strain-rate dependent or independent**
- temperature dependent or independent**
- isotropic, orthotropic or anisotropic** (defining properties in the three orthogonal directions)

**Inelastic, Nonlinear (Limited), Isotropic Material for Beams, Shells and Solids MATS1 (TYPE PLASTIC).** This material model can be used with CBEAM elements (with dedicated plastic hinges at their ends) to perform plastic collapse analysis of beam frameworks. The elastic-plastic material model requires the definition of the **yield stress**. The elastic-plastic material model also requires definition of the **yield criteria**, i.e. the criteria checked to initiate yield, namely Tresca, Von Mises, Mohr-Coulomb or Drucker-Prager. The **hardening rule** must also be specified, either no hardening (i.e. perfectly plastic), isotropic hardening or kinematic hardening. The isotropic hardening model does not take the Bauschinger effect into account and hence the compressive yield always equals the tensile yield. The kinematic hardening model will take into account the Bauschinger effect i.e. the reduction in the compressive yield once tensile yield has occurred and a stress reversal happens.

**Elastic, Nonlinear (General), Isotropic Material for Beams, Shells and Solids MATS1 (TYPE NLELAST).** The nonlinear material model requires the general definition of the **stress-strain curve** with a TABLES1 entry, i.e. the multi-linear stress-strain curve. To model a nonlinear elastic **cable**, a CROD element with the appropriate area (on a PROD card) can be defined together with a MAT1 and MATS1 card, both sharing the same ID. The MATS1 card references a TABLES1 card which defines the nonlinear stress-strain characteristics of the cable with three points, for instance (-1.0,0.0), (0.0,0.0) and (1.0,2.05E11) to define a steel tension only cable element.

**Hyperelastic Material MATHP.** Hyperelastic materials such as rubber, silicone and other elastomer behave differently than standard engineering materials. Their strain displacement relationship is nonlinear even at small strains and they are nearly incompressible. The Poisson’s ratio of hyperelastic materials may exceed 0.50, whereas specifying a Poisson’s ratio of 0.50 or greater will result in failure using any other solution method. If the elements undergo large net displacements, it is prudent to define **hyperelastic** elements, otherwise non-equilibrium loading effects may occur with small strain elements. Because of the corotational formulation where a large deformation is split into element rigid body deformation and element net deformation, small strain elements can be used to model large total deformation, but not large net element deformations. A fine mesh will usually ensure that element net deformations are small. If element net rotations exceed 20 degrees or if the element stretches by more than 10-20%, then large strain (hyperelastic) elements should be used. Material properties are usually entered as Mooney-Rivlin constants (consisting of distortional deformation constants and volumetric deformation constants) or as a set of stress-strain curves (of force versus stretch for simple tension, compression, shear and volumetric compression).

**Temperature Dependent Linear Elastic Material MATT1**

**Temperature Dependent Anisotropic Elastic Material for Shell MATT2 and Solid Elements MATT9**

**Creep Material CREEP**

### 3.4.4.2 Nonlinear Static and Linearized Eigenvalue Buckling Analysis

Buckling (i.e. instability) occurs when the tangent stiffness matrix becomes non-positive definite. To estimate the buckling load, the following methods can be used.

- I. A SOL 106 can be performed until a non-positive definite stiffness matrix is detected. The load steps can be reduced (by the adaptive bisection method) so the stage at which the tangent stiffness matrix becomes non-positive definite can be ascertained with greater precision, hence approximating the buckling load.
- II. Another method is to use the arc-length method to trace the limit state and the post-buckling path.
- III. Another option is to perform linearized buckling analysis at various stages of the equilibrium path based on the tangent stiffness and differential stiffness at that stage, so-called the linearized buckling analysis based on a deflected configuration. Note that this is not the true theoretical nonlinear eigenvalue extraction analysis. However, since the tangent stiffness and the differential stiffness are based on the deflected configuration from a nonlinear static analysis, we shall refer to this buckling analysis as the nonlinear buckling analysis.

The nonlinear buckling analysis computes a load factor based on the tangent stiffness matrix at not the initial undeflected configuration, but at a certain deflected position. The eigenvalue extraction method is the usual linear eigenvalue solution scheme. The nonlinear buckling solution is based on the extrapolation of two consecutive incremental solutions. The tangent stiffness matrix is proportional to the external loads, which implies that the critical load may be linearly extrapolated, i.e.

$$P_{cr} = P_n + \alpha \Delta P$$

The tangent stiffness matrix is proportional to the displacement increments, hence the critical displacements may be obtained by extrapolating from the current state, i.e.

$$U_{cr} = U_n + \lambda \Delta U$$

Since the tangent stiffness matrix is proportional to the displacement increments i.e. it changes linearly with displacements, the internal loads are a quadratic function of the displacements.

NASTRAN uses two converged solution points to form the differential stiffness matrix. Hence the buckling solution tends to be more accurate when these consecutive incremental steps are closer to the buckling point. Since we do not know where the buckling point is until the analysis is performed, the nonlinear buckling analysis is performed by dividing the load into a number of subcases and performing the buckling analysis in multiple subcases based on the tangent stiffness matrix at the current point. Hence, the deck would look exactly the same as a nonlinear static analysis with

- (i) the additional METHOD command in certain subcases referring to the EIGB (with SINV being the recommended extraction method)
- (ii) PARAM, BUCKLE, 2
- (iii) KSTEP = 1 in the NLPARM card to force the stiffness matrix to be updated at every solution step

<p><b>\$ CASE CONTROL SECTION</b></p> <p><b>Subcase 1</b>  LOAD = &lt; ... &gt;  NLPARM = &lt; ... &gt;  METHOD = &lt; ID of EIGB Card in Bulk Data &gt;</p> <p><b>Subcase 2</b>  LOAD = &lt; ... &gt;  NLPARM = &lt; ... &gt;  METHOD = &lt; ID of EIGB Card in Bulk Data &gt;</p> <p><b>Subcase 3</b>  LOAD = &lt; ... &gt;  NLPARM = &lt; ... &gt;  METHOD = &lt; ID of EIGB Card in Bulk Data &gt;</p>
--

<b>\$ BULK DATA</b>									
PARAM, BUCKLE, 2 \$ Buckling Parameter to Activate Nonlinear Buckling Analysis									
EIGB	ID								

To illustrate the nonlinear buckling analysis, if the first subcase has a load totaling 1000 and the second subcase 3000, i.e. an additional 2000. Say, the first subcase refers to a NLPARM entry with 5 increments (i.e. NINC = 5), hence the incremental load is 200. And say the second subcase refers to a NLPARM entry with 20 increments (i.e. NINC = 20), hence the incremental load is 2000/20 = 100. Performing a buckling analysis at the end of the first subcase (by having a METHOD command and PARAM, BUCKLE, 2) solves for  $\alpha$  from which the critical buckling load can be calculated as

$$P_{cr} = P_n + \alpha \Delta P = 1000 + 200\alpha$$

Likewise performing a buckling analysis at the end of the second subcase (by having a METHOD command and PARAM, BUCKLE, 2) solves for another  $\alpha$  from which the critical buckling load can be calculated as

$$P_{cr} = P_n + \alpha \Delta P = 3000 + 100\alpha$$

Evidently, a better estimate of the buckling load is attained when the equilibrium point from which buckling analysis is undertaken is close to the buckling point.

**3.4.4.3 Nonlinear Static and Linear Eigenvalue Modal Dynamic Analysis**

Linear modal analysis is performed on the nonlinear static solutions to include effects of prestress and other nonlinearities. The linear eigenvalue solution analysis is performed based on the tangent stiffness matrix at the end of the particular subcase or subcases where the METHOD statement appears. The deck would look exactly the same as a nonlinear static analysis with

- (i) the additional METHOD command in certain subcases referring to the bulk data EIGRL or EIGR entries to select the linear eigenvalue extraction method
- (ii) PARAM, NMLOOP, L with the loopid L of any positive value as this is not a restart

<b>\$ BULK DATA</b>									
PARAM, NMLOOP, L \$ Loopid L can be any positive integer as this is not a restart									

### 3.4.4.4 Restart From Nonlinear Static Analysis SOL 106 Into Nonlinear Static Analysis SOL 106

Restarts are allowed from converged solutions. A LOOPID is created after each converged load increment in static analysis. The restart .dat file should contain all the information from the previous analysis with the addition of the following cards.

<b>\$ FMS</b>	
RESTART	
<b>\$ BULK DATA</b>	
PARAM, LOOPID, L	\$ Specifies Converged Solution L to Start From
PARAM, SUBID, M	\$ Specifies the Subcase Sequence Number M to Start Into

SUBID is not the subcase ID but the subcase sequence number, which will be the subcase ID if the subcases have been incremented by 1 from 1. The SUBID value should be incremented by one from the last value printed in .f06. The LOOPID should be the last value stored for restart as printed in the .f06. On top of the above additional cards, additional cards which define the restart should be included. The Case Control Section should have the additional subcases starting with a subcase with the SUBID. The following changes are allowed in the model: -

- (i) Additional applied loads, naturally
- (ii) Changes to the boundary conditions i.e. SPC may be removed
- (iii) Addition of direct input matrices
- (iv) Changes to the grid points
- (v) Changes to the element, i.e. linear elements may be added or deleted, but should be drastic as to cause large initial imbalance of loads; also elastic material properties MAT1 may be changed.

### 3.4.4.5 Restart From Nonlinear Static SOL 106 Into Linear Solution Schemes SOL 107 to SOL 112

It is imperative to realize that linear restarts are incremental values with respect to the preload, not total values. Hence, the total values are obtained simply by adding the linear restart values to that obtained from the converged nonlinear static solution. It is advised to have KSTEP = 1 so that the tangent stiffness matrix is computed at every solution step and to ensure that the linear restarts are based on the very latest tangent stiffness matrix. The deck should obviously refer to the linear analysis being performed and not SOL 106.

<b>\$ FMS</b>	
RESTART	
<b>\$ BULK DATA</b>	
PARAM, NMLOOP, L	\$ Load step id at the end of the subcase from the SOL 106 run

### 3.4.4.6 Implicit Nonlinear Static (and Dynamic Analysis) SOL 400

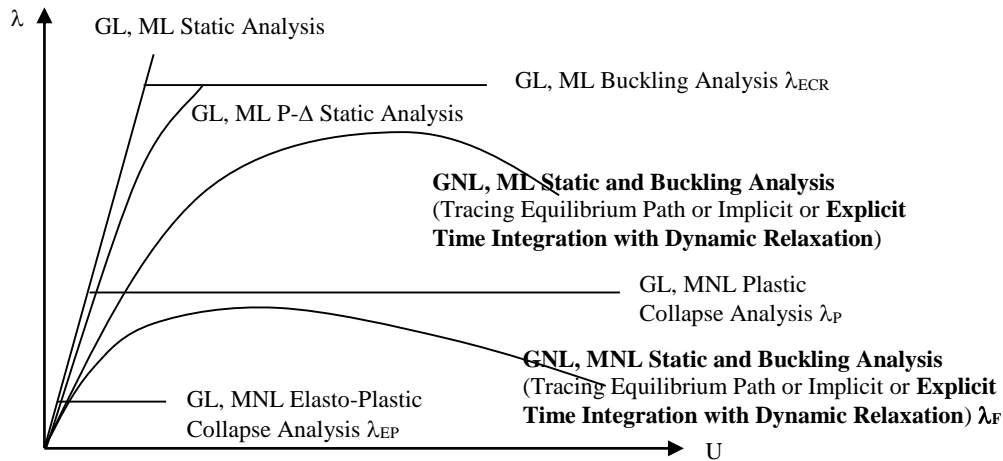
As described in Section 4.9.8.5.

### 3.4.4.7 Implicit Nonlinear Static (and Dynamic Analysis) SOL 600

As described in Section 4.9.8.6.

### 3.5 GNL, MNL Static and Buckling Analysis by Dynamic Relaxation

#### 3.5.1 Dynamic Relaxation of the Explicit Finite Difference Scheme Solving Newton's Dynamic Equilibrium ODE (LS-DYNA)



In dynamic relaxation analysis it is assumed that the loads are acting on the structure suddenly, so the structure is excited to vibrate around the equilibrium position and eventually come to rest on the equilibrium position. Within the solution scheme, it is similar to transient analysis except that

- (i) artificial viscous damping is applied at each time step
- (ii) mass scaling (artificial addition of mass) is employed

Termination occurs when the static solution is reached. If there is no damping applied to the structure, the oscillation of the structure will go on forever. Therefore, artificial damping is required in the form of reducing the calculated velocities of all the nodes by a factor at each timestep to allow the vibration to come to rest, and converge to the static solution.

Convergence is checked by a convergence parameter,

$$C = \text{current distortional kinetic energy} / \text{maximum distortional kinetic energy.}$$

$$\text{Distortional kinetic energy} = \text{total kinetic energy} - \text{total mass} * (\text{mass averaged velocity})^2 / 2.$$

The distortional kinetic energy is the component of kinetic energy that is deforming or distorting the model. In theory, the distortional KE should be zero when a static solution is reached.  $C$  typically vary between  $1E-3$  (loose) and  $1E-6$  (tight).

Loads and prescribed motions (such as displacements, velocities and accelerations) applied during the dynamic relaxation should always be ramped up from zero in order to reduce the oscillations. Instantaneously applied loads will induce over-excitation of higher modes, thus lengthening the time taken to converge and possibly introducing errors. In reality, the static loads are applied in an infinite time interval so as to not induce any dynamic effects. Hence, the load should be ramped up slowly (in a duration greater than the fundamental period) so as not to induce considerable dynamic effects.

If there are non-linear materials in the model, load curves which ramp up suddenly could induce large dynamic amplifications that could cause the non-linear materials to yield, when in reality they should remain elastic in the application of static loads. If any part of the model is required to yield (i.e. become non-elastic) as part of the equilibrium position then great care needs to be taken. This is a path-sensitive solution and the deformation should progress in a monotonic fashion, otherwise the degree of yielding will be incorrect. If all the material models within the finite element model are linear elastic, then the static solution (by dynamic relaxation) is path independent. As with all nonlinear static solutions that are based on solving the dynamic equilibrium equations, the solution is only valid if it is path independent, which in theory is only applicable to models limited to linear material properties. In a

true pseudo-static solution, the loading, deflections and the plastic behaviour increase monotonically. But the dynamic relaxation solution scheme will probably yield a sufficiently accurate solution so long as the dynamic oscillations are small at every stage of the analysis such that the variations of displacement (and hence elemental strain) are small so that excess plasticity is not generated. Dynamic relaxation can thus be used in models with nonlinear materials, but the time of application of the forcing function should be gradual so that the inertial part of the dynamic equilibrium equation does not incorrectly cause large displacements to occur and incorrectly cause the nonlinear materials to yield. If this happens, the material yields due to the dynamic effects of the solution scheme and not due to the underlying static loading, the latter of which is perfectly acceptable. The matter is further complicated if the material model have unloading curves as well as the plastic regions. To avoid the undesirable dynamic effects, there should thus be many time steps between each load increment so that there is plenty of opportunity for the velocities and hence accelerations to be damped down. Recall that artificial damping is applied at each time step. The time over which the loads are ramped up should aim to gently accelerate the model deformation and is dependent on the model. The time should not be so short that the model does not have time to react, effectively making the loading instantaneous. However, the time should not be too long, which would increase the time taken to converge. This is because the convergence parameter is based on the initial to the current kinetic energies. If even the initial kinetic energy in the model is too small (as a result of too gently accelerating the model) then for a certain convergence ratio, the current kinetic energy will have to be much smaller. A duration slightly greater than the fundamental period is appropriate.

As we are not interested in the dynamic response (since this is a static solution), the mass matrix can be artificially formed so as to maximize the time step which is limited by the lowest natural period in the model divided by  $\pi$ . Hence, mass scaling can be employed if damping is not sufficient to produce a converged static solution quickly. Mass scaling will also reduce the dynamic effects as the acceleration become smaller.

To perform dynamic relaxation, two steps are undertaken

- (i) first, run the dynamic relaxation analysis with as little damping as possible. If  $c$  is the damping constant corresponding to the fundamental frequency, defining
 
$$k = 1 - 2\zeta\omega_n dt$$
 let  $k = 0.9999999$ ; this allows the model to oscillate, enabling its natural frequency to be determined.
- (ii) then, calculate the constant  $k$  corresponding an under-damped system
 
$$k = 1 - 2\zeta\omega_n dt$$

$$\zeta = \text{desired fraction of critical damping}$$

$$\omega_n = \text{lowest natural frequency of oscillation (rad/s)}$$

$$dt = \text{timestep}$$
 effectively choosing a constant  $k$  that will result in the model being under-damped.

Another method of applying the artificial viscous damping is using DAMPING\_GLOBAL which applies global viscous damping proportional to the mass, i.e. damping force =  $c.v = 2\zeta m\omega.v = 2\zeta m 2\pi/T.v = 4\zeta\pi/T.m.v$ . The user specifies  $4\zeta\pi/T$  where  $T$  corresponds to the natural frequency of the most prominent mode excited by the excitation.

Ideally, critical damping will provide the most efficient dynamic relaxation. However, experience has shown that it is usually better to under-damp the model. An under-damped model will move just past the equilibrium position and then rebound to converge on the correct solution. This process is relatively easy to monitor and the equilibrium position becomes obvious. However, a critically damped model will not rebound, since it moves directly to the equilibrium position, and thus can often look similar to an over-damped model. Experience shows that damping in the order of about 5% of critical is about optimum and not much higher.

If the equilibrium position is path-sensitive (i.e. certain materials are required to yield), then ideally a critically damped model should be used. Alternatively, use plenty of time steps within each load increment so that the dynamic effects are very much reduced.

Ensure that all parts of the model have a velocity less than the terminal velocity. If parts of the model need to displace a relatively large distance before reaching equilibrium, then the model may reach terminal velocity. This is when the reduction in velocity due to relaxation damping just cancels out the increase in velocity due to loading (i.e. no resultant acceleration). This causes dynamic relaxation to take a long time because  $V_{\text{terminal}}$  limits the speed of deformation. To overcome this, ramp up the loading to greater than the real loading (2-3 times gravity) to deform faster, thus increasing  $V_{\text{terminal}}$ , then as equilibrium position reached, ramp load back down, ensuring no additional modes of deformation occurs that would not have occurred under normal magnitude loading.

$$V_{\text{terminal}} = F * dt * k / (m*(1-k))$$

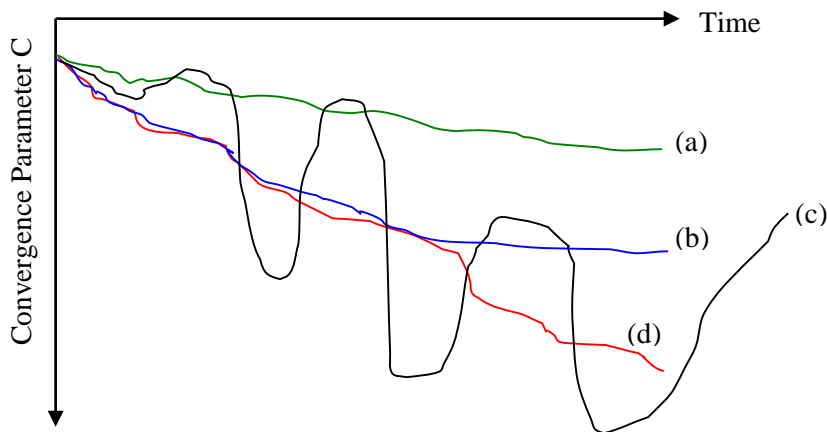
F = desired fraction of critical (normally 1.0)

dt = timestep

m = mass of body

k = damping constant

The effectiveness of the dynamic relaxation solution scheme is investigated by plotting the variation of the convergence parameter as shown below.



The most common problem with dynamic relaxations is that the solution fails to converge or appears to take too long to converge. Referring to the plot above, we can identify 4 cases

- (a) Solutions that never start to converge or take too long to converge. This can be caused by severe over-damping or by an insufficiently resisted (but loaded) mode of deformation. Apply a lower damping constant during the dynamic relaxation phase
- (b) Solutions that partly converge but never reach the convergence tolerance. This can be caused by hourglassing or high modes of oscillation such as single element modes. To solve these problems, try using a different hourglass control or significantly reduce the timestep by say a factor of 5 for the dynamic relaxation phase
- (c) Severe under-damping
- (d) The correct solution

### 3.5.2 LS-DYNA (GNL, MNL Explicit Transient) Dynamic Relaxation Cards

To specify termination time of zero for the explicit dynamic analysis to have no limit

\*CONTROL\_TERMINATION

<b>Termination Time Limit</b>	Termination Cycle Limit	Termination Min Time Step Size Limit	Termination Energy Ratio Limit	Termination Change in Total Mass From Mass Scaling			
-------------------------------	-------------------------	--------------------------------------	--------------------------------	--	--	--	--

To set structural timestep size control and invoke mass scaling if necessary

\*CONTROL\_TIMESTEP

Initial Time Step	<b>Factor For Time Step</b>	Basis	Shell Min Time Step	Min Time Step For Mass Scaling	Maximum Time Step Curve	Erosion Flag	Limit Mass Scaling
-------------------	-----------------------------	-------	---------------------	--------------------------------	-------------------------	--------------	--------------------

To define controls for dynamic relaxation

\*CONTROL\_DYNAMIC\_RELAXATION

To specify user-defined boundary conditions for the dynamic relaxation (stress initialization) phase,

\*LOAD\_NODE\_<POINT, SET> (HM: forces, moments)

\*SET\_NODE

\*DEFINE\_CURVE with SIDR = 1 for stress initialization phase

\*LOAD\_BEAM\_<ELEMENT, SET>

\*SET\_BEAM

\*DEFINE\_CURVE with SIDR = 1 for stress initialization phase

\*LOAD\_SHELL\_<ELEMENT, SET> (HM: pressure → ShellPres)

\*SET\_SHELL

\*DEFINE\_CURVE with SIDR = 1 for stress initialization phase

\*LOAD\_RIGID\_BODY

\*DEFINE\_CURVE with SIDR = 1 for stress initialization phase

\*LOAD\_SEGMENT\_<SET> (HM: pressure → SegmentPre)

\*SET\_SEGMENT

\*DEFINE\_CURVE with SIDR = 1 for stress initialization phase

To apply automatically computed gravitational loads, noting that by d-Alembert's principle, applying accelerations in a certain direction results in inertial loads acting in the opposite direction,

\*LOAD\_BODY\_Z with sf = 9.81 ms<sup>-2</sup>

\*DEFINE\_CURVE with SIDR = 1 for stress initialization phase

To prescribe displacements boundary conditions on a node, on a set of nodes, on a rigid body in the global axes system or on a rigid body in the rigid body local axes system,

\*BOUNDARY\_PRESCRIBED\_MOTION\_<NODE, SET, RIGID, RIGID\_LOCAL>

<b>NID, NSID, or PART ID</b>	<b>DOF</b>	<b>Displacement VAD</b>	<b>LCID</b>	<b>Load Curve Scale Factor SF</b>	<b>VID</b>	<b>DEATH</b>	<b>BIRTH</b>
----------------------------------	------------	-----------------------------	-------------	---	------------	--------------	--------------

The vector ID, VID is used to specify a direction vector if imposed motion not in global axes system.

\*SET\_NODE\_LIST

<b>NSID</b>	<b>DA1</b>	<b>DA2</b>	<b>DA3</b>	<b>DA4</b>			
<b>NID</b>	<b>NID</b>	<b>NID</b>	<b>NID</b>	<b>NID</b>	<b>NID</b>	<b>NID</b>	<b>NID</b>
<b>NID</b>	<b>NID</b>	<b>NID</b>	<b>NID</b>	...	...	...	...

\*DEFINE\_CURVE

<b>LCID</b>	<b>SIDR</b>	<b>SFA</b>	<b>SFO</b>	<b>OFFA</b>	<b>OFFO</b>	<b>DATTYP</b>	
<b>Abscissa Values</b>		<b>Ordinate Values</b>					
<b>Abscissa Values</b>		<b>Ordinate Values</b>					
...		...					

SIDR defines whether the curve is valid for the transient phase, stress initialization phase or both. Here obviously, SIDR = 1. The curve should define a constant value of displacement valid throughout the analysis. If the dynamic relaxation phase is to be followed by a transient seismic analysis, it is necessary to define zero velocity prescribed boundary conditions for the dynamic relaxation phase on the nodes at which the transient accelerations are applied so that the structure is supported during dynamic relaxation.

\*DEFINE\_VECTOR if DOF not global

<b>VID</b>	<b>XTail</b>	<b>YTail</b>	<b>ZTail</b>	<b>Xhead</b>	<b>Yhead</b>	<b>ZHead</b>	
------------	--------------	--------------	--------------	--------------	--------------	--------------	--

## 4 METHODS OF DYNAMIC ANALYSES

### 4.1 GL, ML Implicit Real Modal (Eigenvalue) Analysis

#### 4.1.1 Mathematical Formulation of Analysis

The natural frequencies of a structure are the frequencies at which the structure naturally tends to vibrate if subjected to a disturbance. Hence modal analysis warns if the dominant forcing frequencies are close to the lowest natural frequencies of the structure, indicating resonance behavior of the lowest modes of the structure.

The equation of motion for a free, undamped system is

$$[M]\{\ddot{u}(t)\} + [K]\{u(t)\} = \{0\}$$

We seek solutions of the form

$$\{u(t)\}_i = \text{Re al} \left[ \{\phi\}_i \xi_i e^{\lambda_i t} \right] \text{ for the } i^{\text{th}} \text{ mode of vibration}$$

where  $\xi_i = \xi_{Ri} + i\xi_{Ii}$  and  $\lambda_i = \alpha_i + i\omega_{di}$ .

Note that  $\alpha$  represents the decaying part and  $\omega_d$  the damped natural frequency.

Hence, substituting into the equation of motion

$$\begin{aligned} [M]\xi_i \lambda_i^2 \{\phi\}_i e^{\lambda_i t} + [C]\xi_i \lambda_i \{\phi\}_i e^{\lambda_i t} + [K]\xi_i \{\phi\}_i e^{\lambda_i t} &= \{0\} \\ \left[ \lambda_i^2 [M] + \lambda_i [C] + [K] \right] \{\phi\}_i &= \{0\} \end{aligned}$$

Since there is no damping

$$\alpha_i = 0 \quad \text{and} \quad \omega_{di} = \omega_{ni} \quad \text{and so} \quad \lambda_i = i\omega_{ni}$$

Thus

$$\left[ -\omega_{ni}^2 [M] + [K] \right] \{\phi\}_i = \{0\}$$

This is a real eigenvalue problem to be solved for  $\omega_{ni}$  and  $\{\phi\}_i$ .

For each mode  $i$ , NASTRAN outputs the modal frequency  $\omega_{ni}$  and the mode shape  $\{\phi\}_i$ .

For completion, the response due to mode  $i$ ,  $\{u(t)\}_i$  of a free undamped linear elastic structure subjected to an initial impact (defining an initial displacement and velocity) is

$$\begin{aligned} \{u(t)\}_i &= \{\phi\}_i \text{ Re al} \left[ \xi_{1i} e^{\lambda_{1i} t} + \xi_{2i} e^{\lambda_{2i} t} \right] \\ \{u(t)\}_i &= \{\phi\}_i \text{ Re al} \left[ (\xi_{1Ri} + i\xi_{1Ii}) (\cos \omega_{ni} t + i \sin \omega_{ni} t) + (\xi_{2Ri} + i\xi_{2Ii}) (\cos \omega_{ni} t - i \sin \omega_{ni} t) \right] \\ \{u(t)\}_i &= \{\phi\}_i \text{ Re al} \left[ ((\xi_{1Ri} + \xi_{2Ri}) \cos \omega_{ni} t - (\xi_{1Ii} - \xi_{2Ii}) \sin \omega_{ni} t) + i((\xi_{1Ii} + \xi_{2Ii}) \cos \omega_{ni} t + (\xi_{1Ri} - \xi_{2Ri}) \sin \omega_{ni} t) \right] \end{aligned}$$

For the free vibration response to be real for all  $t$ ,

$$\xi_{1Ii} = -\xi_{2Ii} \quad \text{and} \quad \xi_{1Ri} = \xi_{2Ri}$$

Since there are two less independent constants, let

$$\xi_{1Ii} = -\xi_{2Ii} = \xi_{Ii} \quad \text{and} \quad \xi_{1Ri} = \xi_{2Ri} = \xi_{Ri}$$

We notice that  $\xi_{1i}$  and  $\xi_{2i}$  are a complex conjugate pair

$$\xi_{1i} = \xi_{Ri} + i\xi_{Ii} \quad \text{and} \quad \xi_{2i} = \xi_{Ri} - i\xi_{Ii}$$

Hence

$$\{u(t)\}_i = \{\phi\}_i (2\xi_{Ri} \cos \omega_{ni} t - 2\xi_{Ii} \sin \omega_{ni} t)$$

Thus the total response due to the superposition of all modes

$$\{u(t)\} = [\Phi] \{ (2\xi_{Ri} \cos \omega_{ni} t - 2\xi_{Ii} \sin \omega_{ni} t) \}$$

Re writing the eigenvalue problem  $[[\mathbf{K}] - \omega_{ni}^2 [\mathbf{M}]]\{\phi\}_i = \{0\}$  as

$$[\mathbf{K}]\{\phi\}_i = \omega_{ni}^2 [\mathbf{M}]\{\phi\}_i$$

and premultiplying by  $\{\phi_i\}^T$

$$\{\phi_i\}^T [\mathbf{K}]\{\phi\}_i = \omega_{ni}^2 \{\phi_i\}^T [\mathbf{M}]\{\phi\}_i$$

$$K_i = \omega_{ni}^2 M_i$$

hence, the  $i^{\text{th}}$  generalized mass

$$M_i = \{\phi_i\}^T [\mathbf{M}]\{\phi_i\}$$

and the  $i^{\text{th}}$  generalized stiffness

$$K_i = \{\phi_i\}^T [\mathbf{K}]\{\phi_i\}$$

Note that the value of the generalized (or modal) mass and generalized (or modal) stiffness is arbitrary since it is dependent upon how the corresponding eigenvector has been normalized. However, for a particular mode,

$$K_i = \omega_{ni}^2 M_i$$

Also, the Rayleigh's quotient is obtained as

$$\omega_{ni}^2 = \frac{K_i}{M_i} = \frac{\{\phi_i\}^T [\mathbf{K}]\{\phi_i\}}{\{\phi_i\}^T [\mathbf{M}]\{\phi_i\}}$$

Because the normal modes are independent of each other, the orthogonality condition holds.

$$\{\phi_i\}^T [\mathbf{M}]\{\phi_j\} = 0$$

$$\& \quad \{\phi_i\}^T [\mathbf{K}]\{\phi_j\} = 0 \text{ if } i \neq j$$

Hence, we can obtain the diagonal modal mass and the diagonal modal stiffness matrices.

$$\text{modal mass matrix, } [\mathbf{M}] = [\Phi]^T [\mathbf{M}][\Phi]$$

$$\text{modal stiffness matrix, } [\mathbf{K}] = [\Phi]^T [\mathbf{K}][\Phi] = [\omega^2] [\mathbf{M}]$$

Again, the following relationship holds,

$$[\mathbf{K}] = [\omega^2] [\mathbf{M}]$$

A normal modal analysis indicates the best location for the accelerometers in dynamic testing. Design changes can be evaluated with a normal modal analysis, in that if a particular modification were to cause a change in the frequencies and mode shapes, then the response is also likely to change. This is done with the knowledge that the natural frequencies are a function of the structural properties and boundary conditions but the mode shapes are a function of only the boundary conditions. Modal strain energy is a useful quantity in identifying candidate elements for design changes to eliminate problematic low frequencies. Elements with large values of strain energy in a mode indicate the location of large elastic deformation (energy). Stiffening these elements will increase the natural frequency more than stiffening other elements.

It must be understood that the scaling (or normalization) of the normal modes are arbitrary, hence they do not indicate the response. This means that a different scaling method will yield a different modal (or generalized) mass, modal stiffness (but same modal frequency) and different modal response. However the response due to the particular mode in the physical coordinates will be unique irrespective of the method of scaling.

Even the comparison of magnitude of response between the different mode shapes or different modal masses **in itself** to determine relative importance of each mode is incomplete (as the amplitude and location of the excitation i.e. the modal mass is also important), although the response on different parts of the structure due to a particular

mode can be indicative of the more stressed parts due to that particular mode. But it remains that the mode shapes only represent the shapes of vibration that the structure vibrates in, and not the magnitude, which is dependent upon the amplitude and location of loading and the relation between the forcing frequencies and the natural frequencies.

Three methods of eigenvector scaling exists, namely

(i) MASS normalization

Ensures  $\{\phi_i\}^T[M]\{\phi_i\} = 1.0$ . Saves computational effort and storage. However, for very heavy structures,  $[M]$  becomes large, and so  $\{\phi_i\}$  can be very small. The magnitudes of the mode shapes of different modes cannot be compared to determine relative importance. The modal stiffness will be the square of the natural modal frequency because  $K_i = \omega_{ni}^2 M_i = \omega_{ni}^2(1) = \omega_{ni}^2$ .

(ii) MAX normalization

Scales the eigenvectors such that the maximum component is unity for each and every mode. Modal masses of the same order in themselves cannot be used to determine relative participation of individual modes (as the amplitude of the modal force is also of significance), however a small modal mass obtained from this normalization clearly indicates a local mode or an isolated mechanism.

(iii) POINT normalization

This allows the user to choose a specific displacement component at which the modal displacements are set to 1 or  $-1$ . Useful if user knows the maximum displacement location and component. However, this normalization is not always recommended because for complex structures, the chosen component may have very small values of displacement for higher modes causing larger numbers to be normalized by a small number, resulting in possible numerical roundoff errors and ridiculously higher modal masses. For instance, if the POINT normalization points to a DOF component which does not really exist in a particular mode, than all the other eigenvector terms will be normalized by a very small number, which will certainly result in numerical errors. In this method, the modal masses can be compared between modes if the DOF chosen for POINT normalization corresponds to the solitary point of load excitation, i.e. ensuring that the (amplitude of the) modal force is the same between different modes. In this case, the higher the modal mass, the lower will be the response.

The orthogonality of normal modes signifies that no mode can be obtained from a linear combination of other modes. The representation of a normal mode by using a modal mass and modal stiffness is useful for formulating equivalent dynamic models and in component mode synthesis.

Rayleigh's quotient as presented above is analogous to the equation of natural circular frequency  $\omega_n^2 = K/M$  for a SDOF system, here instead the natural circular frequency of the mode is the division of the modal stiffness to the modal mass, square rooted.

Identical eigenvalues (repeated roots) occur in structures that have a plane of symmetry or that have multiple identical pieces (such as appendages). The eigenvectors (mode shapes) for these repeated roots are not unique because many sets of eigenvectors can be found that are normal to each other. Consequently, small changes in model or different computers can make large changes in the eigenvectors for the repeated roots. Rigid body modes are a special case of repeated roots.

The modal dynamic analysis is based on only the instantaneous stiffness matrix at the initial undeflected stage. The modal dynamic P- $\Delta$  ( $K_G^A$  From  $K_T^A$ ) analysis is based on the instantaneous and geometric (or differential) stiffness matrices at the initial undeflected stage i.e. taking in to account the effect of the initial prestress and initial non-work conjugate external load on the stiffness of the structure in the computation of the structural frequencies and mode shapes.

$$\text{Modal Dynamic } [[K_E^A] - \omega_{ni}^2[M]]\{\phi\}_i = \{0\}$$

$$\text{Modal Dynamic P - Delta } [[K_T^A] - \omega_{ni}^2[M]]\{\phi\}_i = \{0\}$$

It is worth noting that only the stiffness and the mass distribution of the structure determine its modes. The static equilibrium displacement does not come into the equations. However, if geometrical non-linearity is taken into

account, the tangent stiffness of the structure will change from the initial undeflected configuration to its static equilibrium configuration, in which case the real modal analysis will be affected.

It is important to check for rigid body motion. The rigid body modes involve translation or rotation of the model, without any deformation i.e. stress free conditions indicating modelling errors is an inadequate constraint set or the analysis of unconstrained structures such as airplanes. Rigid body modes have a zero frequency. In practice, due to roundoff errors the frequency of these modes is a small number. The modes do not occur in such a pure form and are often coupled together in some way but there should always be 6 rigid-body modes and their natural frequencies should be close to 0.0 Hz ( $\sim 1.0E-4$ ) as their modal mass is greater than zero whilst their generalized stiffness is zero. The user should check that this number is several orders of magnitude lower than the lowest natural frequency. A zero frequency mode which does not also have zero strain energies is not a rigid body mode, instead could be a mechanism and as such should be investigated. The number of rigid body modes depends on the way the structure is supported. For example, an unsupported vehicle model would produce 6 rigid body modes (3 translations, 3 rotations), a model of half the vehicle with symmetry boundary conditions should produce 3 rigid body modes. A cantilever beam should have no rigid body modes. A common modelling error resulting in a mechanism is when a bar is cantilevered from a solid element; the bar has rotational stiffness and the solid has no rotational stiffness, resulting in a pinned connection when the two are joined. The user should check the natural frequency is of the right order of magnitude. For example, the lowest bending and torsion modes in a standard saloon vehicle are 20-30 Hz, while the lowest modes in multi-story buildings are 2-5 Hz. The natural modes should be animated, and the overall behavior should be assessed. It is important to distinguish between fundamental modes involving the whole structure, and local modes involving limited zones. The local modes can often be due to modelling problems (for example flapping panels in vehicle structures), and a judgment should be made whether they are unrealistic.

Modal analysis is extremely useful to check for unrestrained degrees-of-freedom. Note that in this case the analysis will often run but spurious mode shapes will often result involving a component that has not been properly attached to the main structure. It is often true that merely by post-processing the results from a modal analysis and studying the mode shapes most of the problems concerning the connectivity of the FE model become apparent. Alternatively, the edges of the finite element mesh can also be highlighted with a preprocessor and this could provide useful insight.

A matrix whose eigenvalues are all greater than zero is said to be positive definite. If the eigenvalues are zero and positive, the matrix is positive semi-definite. An unconstrained structure would have a positive semi-definite matrix. If all the rigid-body modes are constrained, the stiffness matrix will then be positive definite.

An extremely reliable mathematical tool that determines the number of eigenvalues that exists within a certain frequency range is the **Sturm Sequence Check**. This is printed under UIM 5010 and should be inspected always.

Modal testing and analysis correlation is done using orthogonality checking and Modal Assurance Criteria (MAC) using the postmaca.v2001 DMAP alter. It allows for the quick assessment of modal vectors obtained from test data. The orthogonality check indicates if a set of vectors is orthogonal to the mass matrix, and hence shows if the large mass terms have reasonable agreement between test and analysis. The MAC indicates a set of vectors is linearly independent, and hence indicates how well the modal vectors from the test and analysis agree with each other. As a general rule for the two checks, the diagonal terms should be greater than 0.9 (with lower order modes very close to unity) and off-diagonal terms should be less than 0.1. Note that both the analysis DOFs and test accelerometers should be in the same location and orientation.

Orthogonality Check

$$[\Phi]_t^T [M] [\Phi]_a = [I]$$

Modal Assurance Criteria,  $MAC_{ij}$

$$\frac{\left( (\phi_t^T)_i (\phi_a)_j \right)^2}{(\phi_t^T \phi_t)_i (\phi_a^T \phi_a)_j}$$

### 4.1.2 MSC.NASTRAN Decks

#### 4.1.2.1 GL, ML Real Modal Analysis

<b>\$ EXECUTIVE CONTROL SECTION</b>
SOL 103
<b>\$ CASE CONTROL SECTION</b>
<b>\$ Sets defining grid ids or element ids</b> SET < Number > = 1 THRU 100, 211, 343, < etc > <b>\$ Grid output of displacement for each mode i.e. eigenvector</b> <b>\$ SORT1 lists the results by eigenvalue whilst SORT2 lists the results by grid id</b> DISPLACEMENT(<SORT1/SORT2>,<PRINT,PUNCH,PLOT>) = ALL/<Grid Set ID> <b>\$ Grid output of real eigenvector for the a-set</b> SVECTOR(<PRINT,PUNCH>) = ALL/<Grid Set ID> <b>\$ Grid output of SPC forces</b> SPCFORCES(<SORT1/SORT2>,<PRINT,PUNCH,PLOT>) = ALL/<Grid Set ID> <b>\$ Element output of force, stress and strain</b> ELFORCE(<SORT1/SORT2>,<PRINT,PUNCH,PLOT>) = ALL/<Element Set ID> ELSTRESS(<SORT1/SORT2>,<PRINT,PUNCH,PLOT>) = ALL/<Element Set ID> STRAIN(<SORT1/SORT2>,<PRINT,PUNCH,PLOT>) = ALL/<Element Set ID> <b>\$ Analysis Cards</b> SPC = < ID of SPC Cards Defined in Bulk Data > METHOD = < ID IN EIGRL or EIGR > <b>\$ XY plot output</b> OUTPUT(XYPLOT) XYPUNCH <DISP/VELO/ACCE> RESPONSE <subcase>/<Grid ID>(<T1/T2/T3>) XYPUNCH <ELFORCE/ELSTRESS/STRAIN> RESPONSE <subcase>/<Element ID>(<Code Number>)

The recommended method of eigenvalue extraction is the **Lanczos method**, which combines the best characteristics of both the transformation (Givens, Householder, Modified Givens, Modified Householder) methods and iterative tracking (Inverse Power, Strum Modified Inverse Power) methods. The Lanczos method requires that the mass matrix be positive semi-definite and the stiffness be symmetric but does not miss modes. The Lanczos method is defined with an EIGRL entry which allows either **MASS (default)** or **MAX** eigenvector normalization.

<b>\$ BULK DATA</b>									
EIGRL	ID	Lower Frequency (Hz)	Upper Frequency (Hz)	Number of Eigenvalues	MSGLVL	MAXSET	SHFSCCL	Eigenvector Normalization Method	

A backup method that does not miss roots and is useful for finding out the first few modes for very large models that do not fit in memory is the Sturm Modified Inverse Power Method (SINV), which allows either **MASS (default)**, **MAX** or **POINT** eigenvector normalization.

<b>\$ BULK DATA</b>									
EIGR	ID	SINV	Lower Frequency (Hz)	Upper Frequency (Hz)		Number of Eigenvalues			
	Eigenvector Normalization Method	Grid ID for POINT	DOF for POINT						

#### 4.1.2.2 GL, ML P- $\Delta$ ( $K_G^A$ From $K_E^A$ ) Real Modal Analysis

It is often necessary to incorporate the reduction in bending stiffness of gravity load resisting columns for the analysis of lateral loads. The following procedure is undertaken.

##### Phase 1

Perform static analysis (with loads that cause the greatest negative or positive geometric stiffness) based on  $[K_E^A]$  but include the segyroa.v2001 alter prior to the Case Control Section in order to compute the geometric stiffness matrix  $[K_G^A]_1$  (and output into a .pch file) based on the generated element loads from the  $[K_E^A]$  static analysis.

##### Phase 2

A SOL 103 is undertaken based on  $[K_E^A] + [K_G^A]_1$  with the k2gg=ktjj statement in the Case Control Section and the outputted .pch file which contains the ktjj matrix in the Bulk Data. The responses at this stage represent the P- $\Delta$  ( $K_G^A$  From  $K_E^A$ ) real modal response.

The following equivalent alternative procedure can also be employed.

<pre> \$ CASE CONTROL SECTION  SUBCASE 1 LABEL = Static Preload Load Case LOAD = &lt; ID of FORCEi, MOMENTi, PLOADi, GRAV, LOAD, SPCD Cards in Bulk Data &gt; TEMP(Load) = &lt; ID of TEMP, TEMPRB, TEMPP1 Cards in Bulk Data &gt; DEFORM = &lt; ID of DEFORM Cards in Bulk Data &gt; SUBCASE 2 LABEL = P-<math>\Delta</math> Modal Analysis STATSUB(PRELOAD) = 1 METHOD = &lt; ID in EIGRL &gt;                 </pre>
---

The method is valid when **only the prestress is judged to affect the geometric stiffness** such as in the compressive preload of building columns due to gravitational loads and the prestressing of extremely taut cables that sag very little under gravity but not in systems such as suspension bridges. Where lateral loads are large enough to affect the geometry of the system with prestress, then a repetitive P- $\Delta$ , SOL 106, implicit dynamic relaxation SOL 129 or explicit dynamic relaxation must be employed. But in single P- $\Delta$  analysis, because cables do not have much elastic bending stiffness, the initial static preload subcase should only include the prestress and not gravity as including gravity is the same as solving two linear static problems of stiffness  $K_E^A$  with preload and gravity as the applied loads respectively. Clearly, in the gravity case, it is nonsensical as the cables do in reality have differential stiffness (from the prestress) to resist the gravitational force. Prestress in one direction (i.e. along the axis of cable) will cause a differential stiffness in the orthogonal direction. Gravity acts in the orthogonal direction and hence cannot be accounted for in the calculation of the prestress in this single P- $\Delta$  analysis. To quantitatively decide if gravity need not be considered in contributing to the differential stiffness of the cables, a static P- $\Delta$  analysis should be carried out, the first subcase being a SOL 101 with only the prestress as applied loads and the second subcase a P- $\Delta$  SOL 101 (i.e. utilizing the induced prestress from the first subcase to form a geometric stiffness matrix) with both the gravity and prestress included as applied loads. If the difference in the cable element forces between subcases 1 and 2 is negligible, then gravity has little influence in affecting the geometric stiffness. If there is a major difference in the cable element force, then clearly, gravity will affect the geometric stiffness and as such, a repetitive P- $\Delta$ , SOL 106, implicit dynamic relaxation or explicit dynamic relaxation must be used to converge to the true  $K_T$ . Likewise, in the single P- $\Delta$  analysis of multi-storey buildings, gravity (and only gravity) acts in axis of columns to generate prestress, and the differential stiffness is computed for the orthogonal direction reducing resistance to lateral wind forces, applied in the second subcase with gravity too.

The STATSUB(PRELOAD) computes the differential stiffness due to the prestress and also the follower force. The follower force is calculated and incorporated by the use of PARAM, FOLLOWK, YES. We know how the prestress affects the differential stiffness, namely a tensile prestress causing an increase in stiffness. The effect of the follower force on the stiffness is different. For example, for a cylinder under external pressure critical buckling load may be over-estimated (even though the mode shapes are similar) in a SOL 105 and the natural frequencies in vibration may be under-estimated (even though the mode shapes are similar) in a SOL 103 in the absence of follower stiffness. To the contrary, this observations are reversed in case of centrifugal loads. Centrifugal forces as a constant (static) load are applied by a Bulk Data RFORCE to any elements that have masses. The follower stiffness due to centrifugal load has the effect of lowering stiffness (although the centrifugal load tensioning effect increases stiffness), consequently lowering natural frequencies (even though the mode shapes are similar) in a SOL 103 and lowering the buckling loads (even though the mode shapes are similar) in a SOL 105. This effect increases as the RPM increases, and it becomes significant when the RPM is over 1000. For moderately geometric nonlinear analysis, exclusion of follower stiffness affects the rate of convergence, but the converged solution is correct. For severely geometric nonlinear analysis, it may not be possible to obtain a converged solution without including follower stiffness. As the geometric nonlinearity intensifies, so is the effect of follower stiffness. Therefore, inclusion of follower stiffness greatly enhances the convergence if the deformation involves severe geometric nonlinearity.

### 4.1.2.3 GL, ML P-Δ (K<sub>G</sub><sup>A</sup> From Exact or Approximate K<sub>T</sub><sup>A</sup>) Real Modal Analysis

It is often necessary to include the differential stiffness, especially if there are prestressed cables in the model and the mode shapes are sought.

$$\text{Modal Dynamic P - } \Delta [[K_T^A] - \omega_{ni}^2 [M]] \{\phi\}_i = \{0\}$$

To obtain K<sub>T</sub><sup>A</sup>, to be theoretically exact, a GNL SOL 106 (or implicit dynamic relaxation SOL 129 or explicit dynamic relaxation LS-DYNA) with prestress (as temperature loads say) and gravity must be undertaken. Alternatively, an approximation to K<sub>T</sub><sup>A</sup> can be obtained by repetitive P-Δ static analyses with the prestress (as temperature loads say) and gravity applied. The procedure to obtain this approximate K<sub>T</sub><sup>A</sup> will be presented. Note that the approximate K<sub>T</sub><sup>A</sup> will be the summation of the elastic stiffness K<sub>E</sub> at the undeflected (by the prestress and gravity) state but K<sub>G</sub> at the deflected (by the prestress and gravity) state. Hence if K<sub>E</sub> changes considerably during the application of the prestress, a full SOL 106 (or implicit dynamic relaxation SOL 129 or explicit dynamic relaxation LS-DYNA), which converges to the K<sub>E</sub> and K<sub>G</sub> at the deflected (by the prestress and gravity) state should be employed. Hence for the modelling of a suspension bridge where there is a great change in geometry (known in the bridge industry as **form-finding**, so-called because it is necessary to find the form or shape of the catenary suspension cables), it may be prudent to employ SOL 106 (or implicit dynamic relaxation SOL 129 or explicit dynamic relaxation LS-DYNA), but for a high tension low sag cable on say a tower with prestressed cables, the repetitive P-Δ static analysis may be adequate. The repetitive P-Δ analysis basically involves a number of iterations of linear static analyses to obtain an approximate K<sub>T</sub><sup>A</sup>. Note again that A refers to the initial undeflected (by the collapsing load) state, but deflected by the prestress and gravity. To perform the repetitive P-Δ analysis, a static analysis is performed based on K<sub>E</sub><sup>A</sup> with temperature loads and gravity to generate forces in the structural elements, which in turn provides input for the computation of K<sub>Gi</sub><sup>AKT</sup><sub>m</sub> where m is the iterations. Repetitive static analysis is performed with the prestress and gravity updating the stiffness matrix K<sub>E</sub><sup>A</sup> + K<sub>Gi</sub><sup>AKT</sup><sub>m-1</sub> + K<sub>Gi</sub><sup>AKT</sup><sub>m</sub> until convergence of displacements is obtained. The tangent stiffness at this stage is the approximate converged tangent stiffness matrix K<sub>T</sub><sup>A</sup> = K<sub>E</sub><sup>A</sup> + K<sub>Gi</sub><sup>AKT</sup>. The converged displacements represent the approximate P-Δ (K<sub>G</sub><sup>A</sup> From Approximate K<sub>T</sub><sup>A</sup>) static response to the initial prestress loads. The converged geometric stiffness at this stage would be that based upon the approximate tangent stiffness matrix K<sub>T</sub><sup>A</sup>, i.e. K<sub>Gi</sub><sup>AKT</sup>.

#### Phase 1

Perform static analysis (with prestress and gravity) based on [K<sub>E</sub><sup>A</sup>] but include the segyroa.v2001 alter prior to the Case Control Section in order to compute the geometric stiffness matrix [K<sub>G</sub><sup>A</sup>]<sub>1</sub> (and output into a .pch file) based on the generated element loads from the [K<sub>E</sub><sup>A</sup>] static analysis.

#### Phase 2

Perform static analysis (with prestress and gravity) based on [K<sub>E</sub><sup>A</sup>] + [K<sub>G</sub><sup>A</sup>]<sub>1</sub> by including the k2gg = ktjj statement in the Case Control Section, the outputted .pch file which contains the ktjj matrix in the Bulk Data and the segyroa.v2001 alter prior to the Case Control Section to compute the [K<sub>G</sub><sup>A</sup>]<sub>2</sub> (and output into the .pch file overwriting previous data) based on the generated element loads from the [K<sub>E</sub><sup>A</sup>] + [K<sub>G</sub><sup>A</sup>]<sub>1</sub> static analysis.

#### Phase 3

Repeatedly perform the Phase 2 static analysis (with prestress and gravity) based on [K<sub>E</sub><sup>A</sup>] + [K<sub>G</sub><sup>A</sup>]<sub>i</sub> for i = 2 to n where n represents the number of iterations required for the change in deflections between analyses to become negligible. This would signify that the change in the [K<sub>G</sub><sup>A</sup>] matrix become negligible and the correct [K<sub>G</sub><sup>A</sup>] is attained. The deflections and the other responses at this stage represent the P-Δ (K<sub>G</sub><sup>A</sup> From Approximate K<sub>T</sub><sup>A</sup>) static response to the prestress and gravity. The stiffness of the structure is K<sub>T</sub><sup>A</sup>.

#### Phase 4

A SOL 103 is undertaken with the k2gg=ktjj statement in the Case Control Section and the outputted .pch file which contains the latest ktjj matrix in the Bulk Data. The responses at this stage represent the P-Δ (K<sub>G</sub><sup>A</sup> From Approximate K<sub>T</sub><sup>A</sup>) real modal response.

### 4.1.3 Hand Methods Verification

#### 4.1.3.1 Natural Frequency and Free Vibration Response of SDOF Systems

Equation of motion

$$m\ddot{u}(t) + ku(t) = 0$$

Assume general solution

$$u(t) = Ge^{\lambda t} \text{ where } G = G_R + iG_I \text{ and } \lambda = \alpha + i\omega_d$$

Hence

$$mG\lambda^2 e^{\lambda t} + kGe^{\lambda t} = 0$$

$$(m\lambda^2 + k)Ge^{\lambda t} = 0$$

for LHS to be zero for all t

$$(m\lambda^2 + k) = 0 \quad \text{as} \quad Ge^{\lambda t} > 0$$

the roots of this quadratic characteristic equation are

$$\lambda_1 = +i\sqrt{\frac{k}{m}} \quad \lambda_2 = -i\sqrt{\frac{k}{m}}$$

$$\therefore \alpha = 0 \quad \text{and} \quad \omega_d = \omega_n = \sqrt{\frac{k}{m}} \text{ rad/s}$$

note that the relationships,

$$\text{natural frequency, } f_n = \frac{\omega_n}{2\pi} \text{ Hertz and the period, } T_n = \frac{2\pi}{\omega_n} \text{ s}$$

hence, the complementary function,

$$u(t) = G_1 e^{\lambda_1 t} + G_2 e^{\lambda_2 t}$$

$$u(t) = (G_{1R} + iG_{1I})(\cos \omega_n t + i \sin \omega_n t) + (G_{2R} + iG_{2I})(\cos \omega_n t - i \sin \omega_n t)$$

$$u(t) = [(G_{1R} + G_{2R})\cos \omega_n t - (G_{1I} - G_{2I})\sin \omega_n t] + i[(G_{1I} + G_{2I})\cos \omega_n t + (G_{1R} - G_{2R})\sin \omega_n t]$$

the free vibration response must be real for all t, hence

$$G_{1I} = -G_{2I} \quad \text{and} \quad G_{1R} = G_{2R}$$

since there are two less independent constants, let

$$G_{1I} = -G_{2I} = G_I \quad \text{and} \quad G_{1R} = G_{2R} = G_R$$

we notice that  $G_1$  and  $G_2$  are a complex conjugate pair

$$G_1 = G_R + iG_I \quad \text{and} \quad G_2 = G_R - iG_I$$

hence the general solution

$$u(t) = 2G_R \cos \omega_n t - 2G_I \sin \omega_n t$$

Substituting the integration constants with the initial conditions,

$$u(t) = u(0) \cos \omega_n t + \frac{\dot{u}(0)}{\omega_n} \sin \omega_n t$$

Hence the maximum dynamic displacement

$$u_{\max} = \sqrt{\left(\frac{\dot{u}(0)}{\omega_n}\right)^2 + u(0)^2}$$

A free vibrational dynamic response analysis involves initial displacement and velocity conditions but no forcing vector. It is important to realize that the vibration occurs about the static equilibrium position. Hence we always define  $u(t)$  to begin from the static equilibrium position. However, the dynamic analysis need not begin at this point. For example, in the instance of a mass  $m$  on a string of tensile stiffness  $k$  dropped from a level where the string is not taut, the dynamic analysis begins ( $t = 0.0$ ) when the string just becomes taut and hence  $u(t = 0.0) = -mg/k$  and  $du/dt (t = 0.0)$  will be the velocity of the mass when it reaches that particular taut string elevation. Likewise, when a mass  $m$  is dropped  $h$  meters onto the tip of a cantilever,  $u(t = 0.0) = -mgL^3/(3EI)$  and  $du/dt (t = 0.0) = (2gh)^{1/2}$ . The static displacement was found simply from the force  $mg$  divided by the stiffness  $3EI/L^3$ .

From the knowledge of the initial conditions, we can determine the maximum dynamic displacement by solving the free vibrational dynamic equation of motion. In summary, to determine the maximum dynamic displacement,

- (i) first identify the  $u(t) = 0$  reference as the position of static equilibrium;
- (ii) second, identify the  $t = 0$  level as when dynamic analysis begins, i.e. when a dynamic equation of motion can be written down
- (iii) evaluate the initial conditions  $u(t = 0.0)$  and  $du/dt (t = 0.0)$
- (iv) evaluate the natural circular frequency of the system
- (iv) the maximum dynamic displacement can be ascertained from the formula

To estimate the undamped natural circular frequency, we employ  $\omega_n=(k/m)^{0.5}$ . The single mass  $m$  is readily obtainable for SDOF systems. The elastic stiffness in the direction of the dynamic freedom  $k$  is obtained from either of the following methods.

#### 4.1.3.1.1 Natural Frequency Using the Unit Load Method (Virtual Work)

$P \Delta = f \delta$  expresses virtual work i.e. external work = internal work

$P' \Delta = f' \delta$  expresses the load method where

$P'$  = virtual external action, specified usually as unity for the unit load method

$\Delta$  = real external kinematic, the item to be found

$f'$  = virtual internal action, due to the virtual external actions  $P'$

$\delta$  = real internal kinematic, due to the real external actions on the structure

$1' \Delta = f_1' \delta$  expresses the unit load method

$1' \Delta_1 = f_1' \delta_1$  represents the unit load method with the real external actions also unity i.e. both the virtual external actions and real external actions are unity

$\Delta_1$  = external real kinematic due to unit external real action

$$= f_1' \delta_1$$

$$= \int (M_1)_v \left( \frac{M_1}{EI} ds \right)_R + \int (P_1)_v \left( \frac{P_1}{EA} ds \right)_R \text{ or } (P_1)_v \left( \frac{P_1 L}{EA} \right)_R + \int (T_1)_v \left( \frac{T_1}{GK_t} ds \right)_R + \int (V_1)_v \left( \frac{V_1 Q}{Glb} ds \right)_R$$

$$+ (P_{1spring})_v \left( \frac{P_{1spring}}{k_{spring}} \right)_R + (M_{1spring})_v \left( \frac{M_{1spring}}{k_{rotational\ spring}} \right)_R + (T_{1spring})_v \left( \frac{T_{1spring}}{k_{torsional\ spring}} \right)_R$$

$$= \int M_1 \frac{M_1}{EI} ds + \int P_1 \frac{P_1}{EA} ds \text{ or } P_1 \frac{P_1 L}{EA} + \int T_1 \frac{T_1}{GK_t} ds + \int V_1 \frac{V_1 Q}{Glb} ds + P_{1sp} \frac{P_{1sp}}{k_{sp}} + M_{1sp} \frac{M_{1sp}}{k_{rot\ sp}} + T_{1sp} \frac{T_{1sp}}{k_{tor\ sp}}$$

$$k = \frac{1}{\Delta_1}$$

To estimate the undamped natural circular frequency, we employ  $\omega_n=(k/m)^{0.5}$ .

If  $\alpha_s > 0$  and given BMD for non-unity external action, say for a load of 700.  $1' \Delta = f_1' \delta$  expresses the unit load method.  $\delta_{700}$  is given, and to find  $f_1$ , simply randomly release any indeterminacy to draw the virtual internal action

diagram  $f_1$  removing the real external load 700 and applying the virtual external unit load. Then,  $\Delta_{700} = f_1' \delta_{700}$  and finally,  $k = 700 / \Delta_{700}$ . To estimate the undamped natural circular frequency, we employ  $\omega_n = (k/m)^{0.5}$ .

#### 4.1.3.1.2 Natural Frequency Using Stiffness Formulae

It is worth noting that the equivalent stiffness of springs in parallel is the addition of the individual stiffnesses and the equivalent stiffness of springs in series is the inverse of the addition of the inverse of the individual stiffnesses. Stiffness in series occurs when the load path has to travel both stiffnesses sequentially. Stiffness in parallel occurs when the load path is given the option to be more attracted to the stiffer element. In series, there is no question of whether the load will travel the path or not, for it must, all loads must travel some path, and in series, there is no other option. A mass on the bottom of a vertically hanging spring at the free end of a bending beam cantilever can be idealized as a SDOF system with equivalent springs in series.

$$\frac{1}{k_e} = \frac{1}{k_{\text{spring}}} + \frac{L^3}{3EI}$$

Single story shear frames can be idealized as SDOF systems with the stiffness from the bending beam columns equivalent to a system of springs in parallel because of the axial rigidity of the horizontal member of the shear frame. By definition, there is full moment rigidity between the top of the columns and the rigid horizontal member. Standard fixed ended bending beam lateral stiffness used for shear frames with fixed bases is  $k = \text{number of columns} \times 12EI/L^3$ . Standard cantilever bending beam lateral stiffness used for shear frames with pinned bases,  $k = \text{number of columns} \times 3EI/L^3$ . An example of a shear frame includes water tank towers.

To estimate the undamped natural circular frequency, we employ  $\omega_n = (k/m)^{0.5}$ .

#### 4.1.3.1.3 Natural Frequency Using the Static Deflection (used when EI not readily available)

The natural frequency can be estimated from

$$f_n = \frac{1}{2\pi} \sqrt{\frac{k}{m}}$$

Replacing the mass term with weight,  $W$ , we have

$$f_n = \frac{\sqrt{g}}{2\pi} \sqrt{\frac{k}{mg}} = \frac{\sqrt{g}}{2\pi} \sqrt{\frac{k}{W}} = \frac{\sqrt{g}}{2\pi \sqrt{u_{\text{st}}}} = 15.76 \frac{1}{\sqrt{u_{\text{st}}}} \quad u_{\text{st}} \text{ in mm}$$

Which now relates the natural frequency to the static deflection  $u_{\text{st}}$  of a single lumped mass dynamic DOF. This formula is **exact for single lumped mass** systems.

### 4.1.3.2 Natural Frequencies of MDOF Systems

Either the **stiffness** or **flexibility formulation** to the equation of motion can be employed. The solution can be performed by either the exact classical determinant method, the approximate Stodola iterative method, the approximate Rayleigh Quotient method or the approximate Rayleigh-Ritz method.

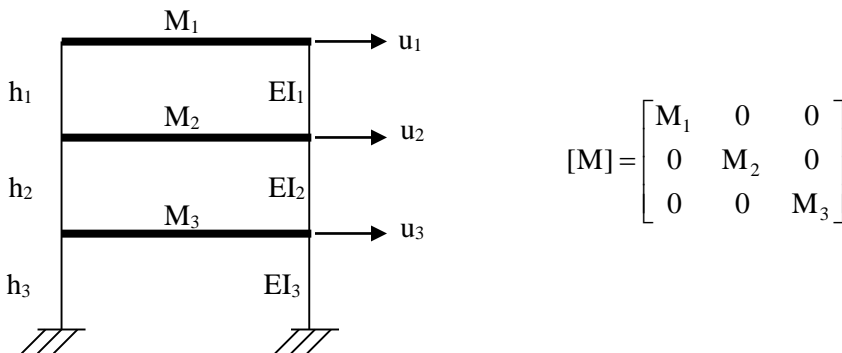
#### 4.1.3.2.1 Stiffness Formulation

Shear frames analysis assumes that the mass of the structure is concentrated at the floors, that the axial force in the columns are too small to consider axial deformation, and that the floor girders are infinitely stiff compared to the columns such that there is no rotation at the connection between the floor and the columns. The third assumption means that the stiffness (or flexibility) of the structure is only provided by the columns.

The free, undamped vibration of the shear frame is described by the equation of motion

$$[M] \{\ddot{u}(t)\} + [K] \{u(t)\} = \{0\}$$

The  $[K]$  matrix can be the instantaneous stiffness matrix  $[K_E^A]$  or the tangent stiffness matrix  $[K_T^A]$ , the A denoting at its initial undeflected configuration. In the instantaneous stiffness matrix, the stiffness coefficient  $k_{ij}$  is the force required at the  $i^{\text{th}}$  coordinate to maintain a unit displacement at the  $j^{\text{th}}$  coordinate while all other coordinates remain stationary. Formulate  $[K_E^A]$  column-by-column (each column corresponding to a unit displacement at the  $j^{\text{th}}$  coordinate) noting the forces required in all the  $i$  coordinates. Ensure  $[K_E^A]$  is symmetric.



A unit displacement of  $u_1$  would induce a force of  $2 \times 12EI_1/h_1^3$  at DOF 1 and a force of  $-2 \times 12EI_1/h_1^3$  at DOF 2 for all other DOFs to remain stationary. A unit displacement of  $u_2$  would induce a force of  $2 \times 12EI_1/h_1^3 + 2 \times 12EI_2/h_2^3$  at DOF 2, a force of  $-2 \times 12EI_1/h_1^3$  at DOF 1 and a force of  $-2 \times 12EI_2/h_2^3$  at DOF 3 for all other DOFs to remain stationary. A unit displacement of  $u_3$  would induce a force of  $2 \times 12EI_3/h_3^3$  at DOF 3 and a force of  $-2 \times 12EI_2/h_2^3$  at DOF 2 for all other DOFs to remain stationary. Hence, the instantaneous stiffness matrix,

$$[K_E^A] = \begin{bmatrix} \frac{24EI_1}{h_1^3} & -\frac{24EI_1}{h_1^3} & 0 \\ -\frac{24EI_1}{h_1^3} & \frac{24EI_1}{h_1^3} + \frac{24EI_2}{h_2^3} & -\frac{24EI_2}{h_2^3} \\ 0 & -\frac{24EI_2}{h_2^3} & \frac{24EI_2}{h_2^3} + \frac{24EI_3}{h_3^3} \end{bmatrix}$$

Note that the stiffness contributions from the columns at the same level are added because the stiffnesses are in parallel to each other. Also, had a base been pinned, then the lateral stiffness contribution would just be  $3EI/h^3$  instead of  $12EI/h^3$ .

It may also be prudent to include the reduction in stiffness from the P- $\Delta$  effect, i.e. a linearized geometric stiffness matrix. A unit displacement of  $u_1$  would induce a secondary moment of  $M_1g$  in the topmost columns (note all the topmost columns and not just one of them) for all other DOFs to remain stationary. This can be represented by a force  $M_1g/h_1$  at DOF 1 and a force  $-M_1g/h_1$  at DOF 2. Likewise, a unit displacement of  $u_2$  would induce a secondary moment of  $M_1g$  in the topmost columns and a secondary moment of  $(M_1+M_2)g$  in the intermediate columns. This can be represented by a force  $-M_1g/h_1$  at DOF 1, a force  $M_1g/h_1+(M_1+M_2)g/h_2$  at DOF 2 and a force  $-(M_1+M_2)g/h_2$  at DOF 3. Finally, a unit displacement of  $u_3$  would induce a secondary moment of  $(M_1+M_2)g$  in the intermediate columns and a secondary moment of  $(M_1+M_2+M_3)g$  in the lowermost columns. This can be represented by a force  $-(M_1+M_2)g/h_2$  at DOF 2 and a force  $(M_1+M_2)g/h_2+(M_1+M_2+M_3)g/h_3$  at DOF 3. Hence, the geometric stiffness matrix,

$$[K_{Gn}^A] = \begin{bmatrix} \frac{M_1g}{h_1} & -\frac{M_1g}{h_1} & 0 \\ -\frac{M_1g}{h_1} & \frac{M_1g}{h_1} + \frac{(M_1+M_2)g}{h_2} & -\frac{(M_1+M_2)g}{h_2} \\ 0 & -\frac{(M_1+M_2)g}{h_2} & \frac{(M_1+M_2)g}{h_2} + \frac{(M_1+M_2+M_3)g}{h_3} \end{bmatrix}$$

It is important to point out that the instantaneous stiffness matrix represents the forces required to produce and maintain the unit displacements in the pertinent DOFs. The geometric stiffness matrix on the other hand represents the forces which are generated due to the unit displacements in the pertinent DOFs. Hence the equation of motion is

$$\begin{aligned} [M] \{\ddot{u}(t)\} + [K_E^A] \{u(t)\} &= [K_{Gn}^A] \{u\} \\ [M] \{\ddot{u}(t)\} + [[K_E^A]-[K_{Gn}^A]] \{u(t)\} &= \{0\} \\ [M] \{\ddot{u}(t)\} + [K_T] \{u(t)\} &= \{0\} \end{aligned}$$

Letting  $\{u\}_i = \{\phi\}_i G_i e^{\lambda_i t}$  leads to the real eigenvalue problem

$$[[K] - \omega_{ni}^2 [M]] \{\phi\}_i = 0$$

The total solution of the free vibrational problem is given by the linear superposition of the individual modes of vibration.

$$\{u\} = \left[ \begin{array}{c} \{ \phi \}_1 \dots \{ \phi \}_i \dots \{ \phi \}_n \end{array} \right] \left\{ \begin{array}{c} A_1 \sin(\omega_1 t - \alpha_1) \\ \vdots \\ A_i \sin(\omega_i t - \alpha_i) \\ \vdots \\ A_n \sin(\omega_n t - \alpha_n) \end{array} \right\}$$

The constants  $A_i$  and  $\alpha_i$  are the constants of integration to be determined from the initial displacement and velocity conditions.

Note that the flexibility matrix  $[F]$  of the frame can be obtained from a **linear static analysis program** by successively applying unit loads at each storey and on each occasion measuring the total displacement at all the storey levels. The matrix  $[F]$  is then inverted to obtain the stiffness matrix  $[K]$ .

#### 4.1.3.2.2 Flexibility Formulation

Stiffness formulation,

$$[[\mathbf{K}] - \omega_{ni}^2 [\mathbf{M}]] \{\phi\}_i = \{0\}$$

Multiply by  $[\mathbf{F}]$  or by  $-\frac{1}{\omega_{ni}^2} [\mathbf{F}]$ ,

$$[[\mathbf{F}][\mathbf{K}] - \omega_{ni}^2 [\mathbf{F}][\mathbf{M}]] \{\phi\}_i = \{0\} \quad \text{or} \quad [[\mathbf{F}][\mathbf{M}] - \frac{1}{\omega_{ni}^2} [\mathbf{F}][\mathbf{K}]] \{\phi\}_i = \{0\}$$

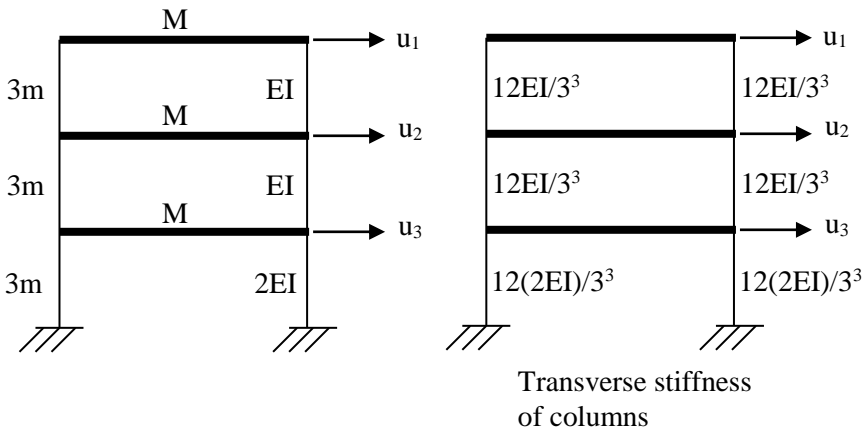
$$[[\mathbf{I}] - \omega_{ni}^2 [\mathbf{F}][\mathbf{M}]] \{\phi\}_i = \{0\} \quad \text{or} \quad [[\mathbf{F}][\mathbf{M}] - \frac{1}{\omega_{ni}^2} [\mathbf{I}]] \{\phi\}_i = \{0\} \quad (\text{Flexibility formulations})$$

These are eigenvalue problems.

Flexibility coefficient  $f_{ij}$  is the displacement produced at the  $i^{\text{th}}$  coordinate due to a unit force applied at the  $j^{\text{th}}$  coordinate only. Formulate  $[\mathbf{F}]$  column-by-column (each column corresponding to a unit force at the  $j^{\text{th}}$  coordinate) noting the displacements induced in all the  $i$  coordinates. In formulating these columns in  $[\mathbf{F}]$ , 3 cases are identified: -

- Unit force above the displacement of the DOF sought  $\rightarrow$  Displacement of the DOF is the flexibility of all that including and below the displacement DOF
- Unit force inline with the displacement of the DOF sought  $\rightarrow$  Displacement of the DOF is the flexibility of all that including and below the displacement DOF
- Unit force below the displacement of the DOF sought  $\rightarrow$  Displacement of the DOF is the flexibility of all that including and below the unit force

In short, the displacement at the particular DOF sought after is the cumulative flexibility (inverse of stiffness) of all the shear frame levels including and below the displacement DOF or the unit force, whichever is lower. Ensure  $\underline{\mathbf{F}}$  is symmetric.



$$\frac{1}{12EI/3^3 + 12EI/3^3} = \frac{9}{8EI}$$

$$\frac{1}{12EI/3^3 + 12EI/3^3} = \frac{9}{8EI}$$

$$\frac{1}{12(2EI)/3^3 + 12(2EI)/3^3} = \frac{9}{16EI}$$

Displacement contribution of floor level due to unit load at the particular level

$$[\mathbf{F}] = \begin{bmatrix} \frac{9}{8EI} + \frac{9}{8EI} + \frac{9}{16EI} & \frac{9}{8EI} + \frac{9}{16EI} & \frac{9}{16EI} \\ \frac{9}{8EI} + \frac{9}{16EI} & \frac{9}{8EI} + \frac{9}{16EI} & \frac{9}{16EI} \\ \frac{9}{16EI} & \frac{9}{16EI} & \frac{9}{16EI} \end{bmatrix} = \frac{9}{16EI} \begin{bmatrix} 5 & 3 & 1 \\ 3 & 3 & 1 \\ 1 & 1 & 1 \end{bmatrix}$$

$$[\mathbf{M}] = \begin{bmatrix} \mathbf{M} & 0 & 0 \\ 0 & \mathbf{M} & 0 \\ 0 & 0 & \mathbf{M} \end{bmatrix}$$

#### 4.1.3.2.3 Natural Frequencies Using the Exact Classical Determinant Method

The **stiffness formulated** real eigenvalue problem is expressed

$$[[\mathbf{K}] - \omega_{ni}^2 [\mathbf{M}]]\{\phi\}_i = \{0\}$$

This equation has one additional unknown and hence does not have a unique solution. For a 3 DOF dynamic system, there will be 3  $\phi$  terms and the  $\omega_{ni}^2$  term, i.e. one additional unknown. For there to be a solution that is nontrivial (i.e. that not all  $\phi$  terms zero), the determinant must be zero. The eigenvalue problem is solved for  $\omega_{ni}^2$  by employing the classical determinant computation for a nontrivial solution,

$$\text{Det} [[\mathbf{K}] - \omega_{ni}^2 [\mathbf{M}]] = 0$$

This leads to a polynomial in  $\omega_{ni}^2$  the order of which corresponds to the number of dynamic degrees of freedom. For instance, for a 3 DOF dynamic system, the order of polynomial in  $\omega_{ni}^2$  will be cubic, i.e. up to the  $\omega_{ni}^6$  term. They can be solved for the 3 natural circular frequencies  $\omega_1$ ,  $\omega_2$  and  $\omega_3$ . Then, in order to obtain the an eigenvector corresponding to each eigenvalue, we replace each eigenvalue in turn into

$$[[\mathbf{K}] - \omega_{ni}^2 [\mathbf{M}]]\{\phi\}_i = \{0\}$$

Now that we have found  $\omega_{ni}^2$  based on a zero determinant, the number of independent equations becomes one less, i.e. for the 3 DOF dynamic system, 2 independent equations. Hence for each  $\omega_{ni}^2$  we can solve for the relative values of  $\phi$ . This is where we have to decide on how to normalize the eigenvectors, i.e. whether MAX, MASS or POINT normalization.

Note that the first mode or fundamental mode refers to the mode corresponding to the lowest frequency. The other modes are referred to as higher harmonics.

The **flexibility formulated** real eigenvalue problem is expressed

$$[[\mathbf{I}] - \omega_{ni}^2 [\mathbf{F}][\mathbf{M}]]\{\phi\}_i = \{0\} \quad \text{or} \quad [[\mathbf{F}][\mathbf{M}] - \frac{1}{\omega_{ni}^2} [\mathbf{I}]]\{\phi\}_i = \{0\}$$

These are eigenvalue problems. For a nontrivial solution,

$$\text{DET}[[\mathbf{I}] - \omega_{ni}^2 [\mathbf{F}][\mathbf{M}]] = 0 \quad \text{or} \quad \text{DET}[[\mathbf{F}][\mathbf{M}] - \frac{1}{\omega_{ni}^2} [\mathbf{I}]] = 0$$

#### 4.1.3.2.4 Natural Frequencies Using the Approximate Stodola Iterative Method

With this method, only the fundamental natural circular frequency and the fundamental mode can be obtained fairly accurately. Higher natural circular frequencies and modes can also be obtained inefficiently with the use of the sweeping matrix to purify the eigenvalue problem off the earlier modes of vibration. However, this method is subjected to cumulative errors and so the errors increase in estimating the frequencies and mode shapes of higher modes of vibration.

Stiffness formulation,

$$[\underline{\mathbf{K}} - \omega^2 \underline{\mathbf{M}}] \underline{\phi} = \underline{\mathbf{0}}$$

Multiply by  $\underline{\mathbf{F}}$  or by  $-\frac{1}{\omega^2} \underline{\mathbf{F}}$ ,

$$[\underline{\mathbf{FK}} - \omega^2 \underline{\mathbf{FM}}] \underline{\phi} = \underline{\mathbf{0}} \quad \text{or} \quad [\underline{\mathbf{FM}} - \frac{1}{\omega^2} \underline{\mathbf{FK}}] \underline{\phi} = \underline{\mathbf{0}}$$

$$[\underline{\mathbf{I}} - \omega^2 \underline{\mathbf{FM}}] \underline{\phi} = \underline{\mathbf{0}} \quad \text{or} \quad [\underline{\mathbf{FM}} - \frac{1}{\omega^2} \underline{\mathbf{I}}] \underline{\phi} = \underline{\mathbf{0}} \quad (\text{Flexibility formulations})$$

Employ the latter flexibility formulation,

$$[\underline{\mathbf{FM}} - \frac{1}{\omega^2} \underline{\mathbf{I}}] \underline{\phi} = \underline{\mathbf{0}}$$

$$\underline{\mathbf{FM}} \underline{\phi} = \frac{1}{\omega^2} \underline{\phi}$$

Stodola's method,

$$\underline{\mathbf{FM}} \underline{\phi} = \frac{1}{\omega^2} \underline{\phi} \text{ is akin to } \underline{\mathbf{A}} \underline{\mathbf{x}} = \lambda \underline{\mathbf{x}}$$

Guess  $\underline{\mathbf{x}}^{(0)}$

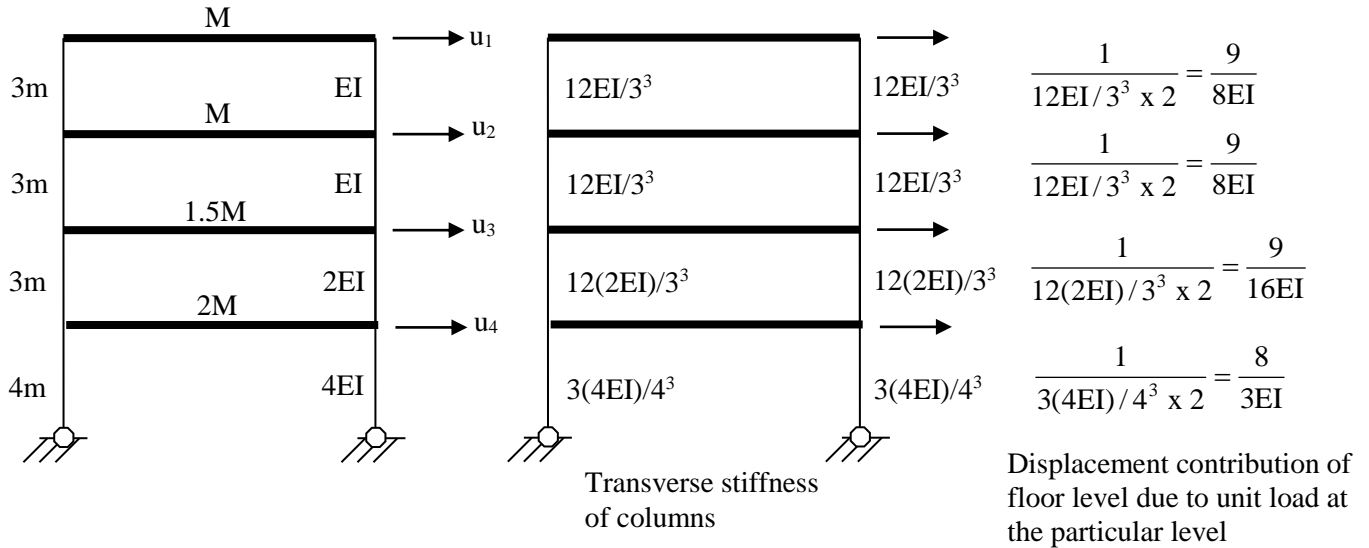
For  $i = 0$  to  $n$

Compute  $\underline{\mathbf{A}} \underline{\mathbf{x}}^{(i)}$

Normalise first coordinate of  $\underline{\mathbf{A}} \underline{\mathbf{x}}^{(i)}$  to obtain  $\lambda^{(i+1)}$  and  $\underline{\mathbf{x}}^{(i+1)}$

Next  $i$

The final  $\lambda^{(n+1)}$  is the  $\frac{1}{\omega_1^2}$  and  $\underline{\mathbf{x}}^{(n+1)}$  the fundamental mode  $\underline{\phi}_1$ .



The figure above shows a 4-degree of freedom shear frame. The flexibility formulation is described by

$$[\underline{FM} - \frac{1}{\omega^2} \underline{I}] \underline{\phi} = \underline{0}$$

$$\underline{FM} \underline{\phi} = \frac{1}{\omega^2} \underline{\phi}$$

Stodola's method,

$$\underline{FM} \underline{\phi} = \frac{1}{\omega^2} \underline{\phi} \text{ is akin to } \underline{Ax} = \lambda \underline{x}$$

Guess  $\underline{x}^{(0)}$

For  $i = 0$  to  $n$

    Compute  $\underline{Ax}^{(i)}$

    Normalise first coordinate of  $\underline{Ax}^{(i)}$  to obtain  $\lambda^{(i+1)}$  and  $\underline{x}^{(i+1)}$

Next  $i$

The final  $\lambda^{(n+1)}$  is the  $\frac{1}{\omega_1^2}$  and  $\underline{x}^{(n+1)}$  the fundamental mode  $\underline{\phi}_1$ .

For the shear frame above,

$$\underline{F} = \begin{bmatrix} \frac{9}{8EI} + \frac{9}{8EI} + \frac{9}{16EI} + \frac{8}{3EI} & \frac{9}{8EI} + \frac{9}{16EI} + \frac{8}{3EI} & \frac{9}{16EI} + \frac{8}{3EI} & \frac{8}{3EI} \\ \frac{9}{8EI} + \frac{9}{16EI} + \frac{8}{3EI} & \frac{9}{8EI} + \frac{9}{16EI} + \frac{8}{3EI} & \frac{9}{16EI} + \frac{8}{3EI} & \frac{8}{3EI} \\ \frac{9}{16EI} + \frac{8}{3EI} & \frac{9}{16EI} + \frac{8}{3EI} & \frac{9}{16EI} + \frac{8}{3EI} & \frac{8}{3EI} \\ \frac{8}{3EI} & \frac{8}{3EI} & \frac{8}{3EI} & \frac{8}{3EI} \end{bmatrix} = \frac{1}{48EI} \begin{bmatrix} 263 & 209 & 155 & 128 \\ 209 & 209 & 155 & 128 \\ 155 & 155 & 155 & 128 \\ 128 & 128 & 128 & 128 \end{bmatrix}$$

$$\underline{M} = \begin{bmatrix} M & 0 & 0 & 0 \\ 0 & M & 0 & 0 \\ 0 & 0 & \frac{3}{2}M & 0 \\ 0 & 0 & 0 & 2M \end{bmatrix}$$

Hence,

$$\underline{A} = \underline{FM} = \frac{1}{48EI} \begin{bmatrix} 263 & 209 & 155 & 128 \\ 209 & 209 & 155 & 128 \\ 155 & 155 & 155 & 128 \\ 128 & 128 & 128 & 128 \end{bmatrix} \begin{bmatrix} M & 0 & 0 & 0 \\ 0 & M & 0 & 0 \\ 0 & 0 & \frac{3}{2}M & 0 \\ 0 & 0 & 0 & 2M \end{bmatrix}$$

$$= \frac{M}{48EI} \begin{bmatrix} 263 & 209 & 232.5 & 256 \\ 209 & 209 & 232.5 & 256 \\ 155 & 155 & 232.5 & 256 \\ 128 & 128 & 192 & 256 \end{bmatrix}$$

$$\text{Guess } \underline{x}^{(0)} = \begin{bmatrix} 1 \\ 0.8000 \\ 0.7000 \\ 0.6000 \end{bmatrix}, \quad \underline{Ax}^{(0)} = \frac{M}{48EI} \begin{bmatrix} 263 & 209 & 232.5 & 256 \\ 209 & 209 & 232.5 & 256 \\ 155 & 155 & 232.5 & 256 \\ 128 & 128 & 192 & 256 \end{bmatrix} \begin{bmatrix} 1 \\ 0.8000 \\ 0.7000 \\ 0.6000 \end{bmatrix} = \frac{M}{EI} \begin{bmatrix} 15.5531 \\ 14.4281 \\ 12.4031 \\ 10.8000 \end{bmatrix} = \frac{15.5531M}{EI} \begin{bmatrix} 1 \\ 0.9277 \\ 0.7975 \\ 0.6944 \end{bmatrix}$$

$$\underline{x}^{(1)} = \begin{bmatrix} 1 \\ 0.9277 \\ 0.7975 \\ 0.6944 \end{bmatrix}, \quad \underline{Ax}^{(1)} = \frac{M}{48EI} \begin{bmatrix} 263 & 209 & 232.5 & 256 \\ 209 & 209 & 232.5 & 256 \\ 155 & 155 & 232.5 & 256 \\ 128 & 128 & 192 & 256 \end{bmatrix} \begin{bmatrix} 1 \\ 0.9277 \\ 0.7975 \\ 0.6944 \end{bmatrix} = \frac{M}{EI} \begin{bmatrix} 17.0846 \\ 15.9596 \\ 13.7909 \\ 12.0338 \end{bmatrix} = \frac{17.0846M}{EI} \begin{bmatrix} 1 \\ 0.9342 \\ 0.8072 \\ 0.7044 \end{bmatrix}$$

$$\underline{x}^{(2)} = \begin{bmatrix} 1 \\ 0.9342 \\ 0.8072 \\ 0.7044 \end{bmatrix}, \quad \underline{Ax}^{(2)} = \frac{M}{48EI} \begin{bmatrix} 263 & 209 & 232.5 & 256 \\ 209 & 209 & 232.5 & 256 \\ 155 & 155 & 232.5 & 256 \\ 128 & 128 & 192 & 256 \end{bmatrix} \begin{bmatrix} 1 \\ 0.9342 \\ 0.8072 \\ 0.7044 \end{bmatrix} = \frac{M}{EI} \begin{bmatrix} 17.2132 \\ 16.0882 \\ 13.9123 \\ 12.1432 \end{bmatrix} = \frac{17.2132M}{EI} \begin{bmatrix} 1 \\ 0.9346 \\ 0.8082 \\ 0.7055 \end{bmatrix}$$

$$\underline{x}^{(3)} = \begin{bmatrix} 1 \\ 0.9346 \\ 0.8082 \\ 0.7055 \end{bmatrix}, \quad \underline{Ax}^{(3)} = \frac{M}{48EI} \begin{bmatrix} 263 & 209 & 232.5 & 256 \\ 209 & 209 & 232.5 & 256 \\ 155 & 155 & 232.5 & 256 \\ 128 & 128 & 192 & 256 \end{bmatrix} \begin{bmatrix} 1 \\ 0.9346 \\ 0.8082 \\ 0.7055 \end{bmatrix} = \frac{M}{EI} \begin{bmatrix} 17.2261 \\ 16.1011 \\ 13.9246 \\ 12.1544 \end{bmatrix} = \frac{17.2261M}{EI} \begin{bmatrix} 1 \\ 0.9347 \\ 0.8083 \\ 0.7056 \end{bmatrix}$$

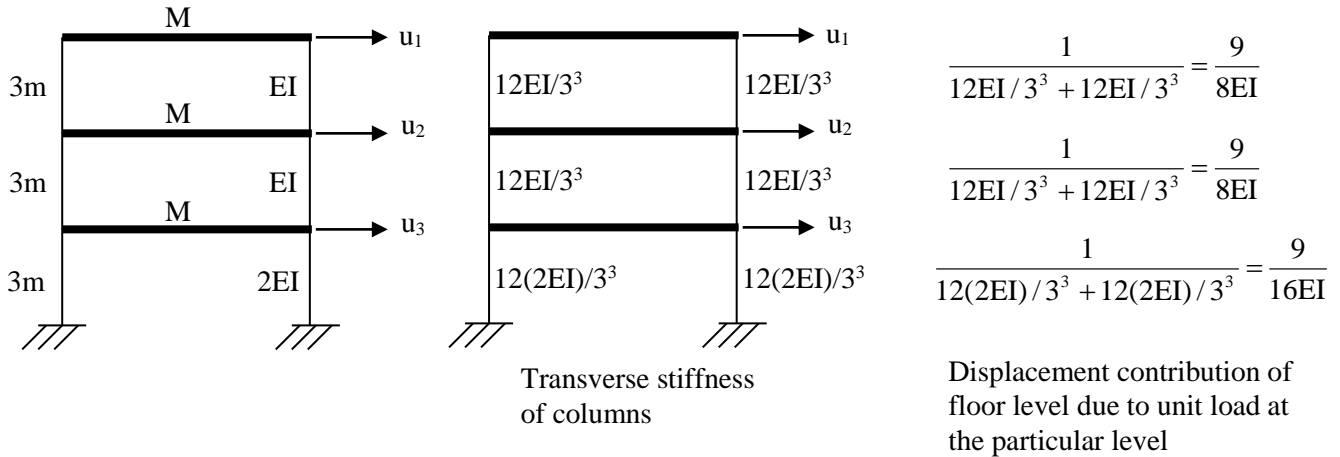
Convergence is achieved to two decimal places. Thus,

$$\frac{1}{\omega_1^2} = \frac{17.2261M}{EI},$$

$$\text{fundamental frequency } \omega_1 = \sqrt{\frac{EI}{17.2261M}} = 0.2409 \sqrt{\frac{EI}{M}}$$

$$\text{and the fundamental mode } \underline{\phi}_1 = \begin{bmatrix} 1 \\ 0.93 \\ 0.81 \\ 0.71 \end{bmatrix}.$$

For higher modes the sweeping matrix can be employed. This method is computationally intensive and the rate of convergence depends very much on whether the initial guessed mode shape approximates the actual mode shape sought after. Also the errors are cumulative as the sweeping matrix is a function of the previous mode shape. Hence, higher modes are less accurate. As will be demonstrated hereafter, the first and second modes converge to the exact solution to 3 decimal places, whilst the third mode shape is only accurate to 2 decimal places.



The figure above shows a 3-degree of freedom shear frame. The flexibility formulation is described by

$$\underline{\underline{FM}}\underline{\underline{\phi}} = \frac{1}{\omega^2}\underline{\underline{\phi}}$$

$$\underline{\underline{Ax}} = \lambda\underline{\underline{x}}$$

$$\underline{\underline{A}} = \underline{\underline{FM}} = \frac{9}{16EI} \begin{bmatrix} 5 & 3 & 1 \\ 3 & 3 & 1 \\ 1 & 1 & 1 \end{bmatrix} \begin{bmatrix} M & 0 & 0 \\ 0 & M & 0 \\ 0 & 0 & M \end{bmatrix}$$

Fundamental mode : Operate on  $\underline{\underline{A}} = \underline{\underline{FM}}$

$$\text{Guess } \underline{\underline{x}}^{(0)} = \begin{bmatrix} 1 \\ 0.7 \\ 0.3 \end{bmatrix}, \quad \underline{\underline{Ax}}^{(3)} = \frac{4.1984M}{EI} \begin{bmatrix} 1.0000 \\ 0.7320 \\ 0.2680 \end{bmatrix}$$

Convergence is achieved to 4 decimal places after 3 iterations. Thus,  $1/\omega_1^2 = 4.1984M/EI$ ,

fundamental frequency  $\omega_1 = \sqrt{\frac{EI}{4.1984M}} = 0.4880\sqrt{\frac{EI}{M}}$  and the fundamental mode  $\underline{\underline{\phi}}_1^T = [1 \quad 0.7320 \quad 0.2680]$

Sweeping matrix,  $\underline{\underline{S}}_1 = \underline{\underline{I}} - \frac{1}{M_1}\underline{\underline{\phi}}_1\underline{\underline{\phi}}_1^T\underline{\underline{M}}$  where  $M_1 = \underline{\underline{\phi}}_1^T\underline{\underline{M}}\underline{\underline{\phi}}_1$

Second mode : Operate on  $\underline{\underline{A}} = \underline{\underline{FMS}}_1$

$$\text{Guess } \underline{\underline{x}}^{(0)} = \begin{bmatrix} 1 \\ -0.8 \\ -0.8 \end{bmatrix}, \quad \underline{\underline{Ax}}^{(12)} = \frac{0.5625M}{EI} \begin{bmatrix} 1.0000 \\ -0.9994 \\ -0.9995 \end{bmatrix}$$

Convergence is achieved to 4 decimal places after 12 iterations. Thus,  $1/\omega_2^2 = 0.5625M/EI$ ,

$\omega_2 = \sqrt{\frac{EI}{0.5625M}} = 1.3333\sqrt{\frac{EI}{M}}$  and the second mode  $\underline{\underline{\phi}}_2^T = [1 \quad -0.9994 \quad -0.9995]$

Sweeping matrix,  $\underline{\underline{S}}_2 = \underline{\underline{S}}_1 - \frac{1}{M_2}\underline{\underline{\phi}}_2\underline{\underline{\phi}}_2^T\underline{\underline{M}}$  where  $M_2 = \underline{\underline{\phi}}_2^T\underline{\underline{M}}\underline{\underline{\phi}}_2$

Third mode : Operate on  $\underline{\underline{A}} = \underline{\underline{FMS}}_2$

$$\text{Guess } \underline{\underline{x}}^{(0)} = \begin{bmatrix} 1 \\ -2 \\ 3 \end{bmatrix}, \quad \underline{\underline{Ax}}^{(3)} = \frac{0.3014M}{EI} \begin{bmatrix} 0.9999 \\ -2.7358 \\ 3.7360 \end{bmatrix}$$

Convergence is achieved to 4 decimal places after 3 iterations. Thus,  $1/\omega_3^2 = 0.3014M/EI$ ,

$\omega_3 = \sqrt{\frac{EI}{0.3014M}} = 1.8215\sqrt{\frac{EI}{M}}$  and the third mode  $\underline{\underline{\phi}}_3^T = [0.9999 \quad -2.7358 \quad 3.7360]$

### 4.1.3.2.5 Natural (Fundamental) Frequency Using the Approximate Rayleigh Quotient Method

The **stiffness formulated** eigenvalue problem can be solved by employing the Rayleigh Quotient method. The basis of the method is to equate the maximum kinetic energy during motion to the maximum potential energy to obtain an estimate of the natural circular frequency with an assumed mode shape or displacement function. With this method, **only the fundamental natural circular frequency can be obtained fairly accurately**. Vibration analysis by Rayleigh's Quotient method will yield a fundamental natural circular frequency  $\omega_1$  which is higher than the actual because of the approximation made by the mode shape  $\phi(x)$ . Higher natural circular frequencies can be obtained only if the exact higher mode shapes are known.

#### Improved Rayleigh Quotient Method

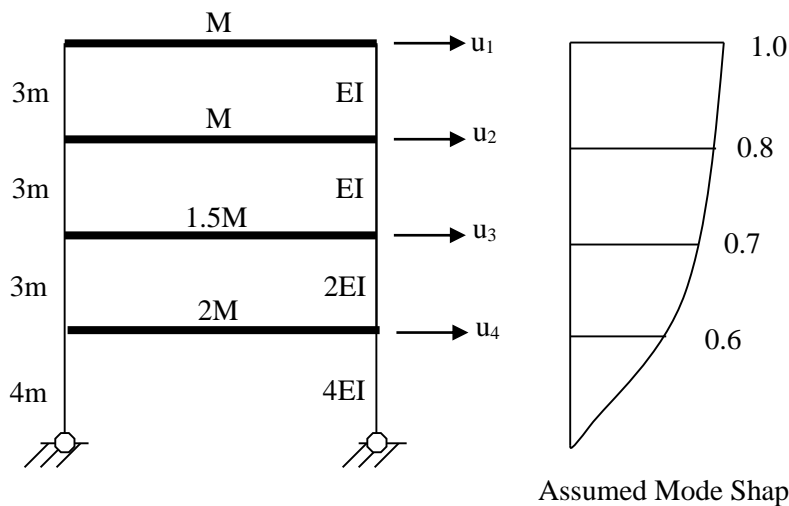
- (a) Guess mode shape based on the displacements produced by applying inertial forces as static loads. That is to say, load the structure with the inertial loads associated with an assumed displacement. This load then results in a new improved displacement configuration. Loop for even better estimate or simply goto (b).
- (b) Apply Rayleigh's formula to obtain an estimate of  $\omega_i$

$$\omega_i^2 = \frac{\text{Generalised Stiffness of Mode } i, K_i}{\text{Generalised Mass of Mode } i, M_i} = \frac{\{\phi_i\}^T [K] \{\phi_i\}}{\{\phi_i\}^T [M] \{\phi_i\}} = \frac{\sum k_i \Delta \phi_i^2}{\sum m_i \phi_i^2}$$

- (c) From the obtained estimate of the eigenvalue, obtain a better estimate of the eigenvector from

$$[[K] - \omega_i^2 [M]] \{\phi\}_i = 0$$

with the eigenvector normalized in the same method as before. Loop to (b) for a new estimate of the eigenvalue based on the new eigenvector. This is repeated until convergence. The stiffness of the calculated system is always greater than the stiffness of the exact system as we are modelling a system of infinite DOFs with a finite number of DOFs. The value of  $\omega_1$  decreases as the mode shape becomes closer to the actual fundamental mode shape. Hence, the calculated natural circular frequency will always be greater than the exact value. Seek to obtain the lowest possible estimate of  $\omega$  for convergence.



Freedom	Assumed Mode Shape	Force on the Freedoms $M_i \phi_i \omega^2$	Force on Shear Frame (Cumulative)	Displacement Contribution of Floor Level	Displacement of Shear Frame (Cumulative)	Improved Mode Shape
1	1.0	$M\omega^2$	$M\omega^2$	$M\omega^2/(24EI/27)$	$15.55M\omega^2/EI$	1
2	0.8	$0.8M\omega^2$	$1.8M\omega^2$	$1.8M\omega^2/(24EI/27)$	$14.43M\omega^2/EI$	0.93
3	0.7	$1.5M(0.7\omega^2)$	$2.85M\omega^2$	$2.85M\omega^2/(48EI/27)$	$12.40M\omega^2/EI$	0.80
4	0.6	$2M(0.6\omega^2)$	$4.05M\omega^2$	$4.05M\omega^2/(24EI/64)$	$10.80M\omega^2/EI$	0.69

$$\mathbf{K} = \begin{bmatrix} 2 \times \frac{12EI}{3^3} & -2 \times \frac{12EI}{3^3} & 0 & 0 \\ -2 \times \frac{12EI}{3^3} & 4 \times \frac{12EI}{3^3} & -2 \times \frac{12EI}{3^3} & 0 \\ 0 & -2 \times \frac{12EI}{3^3} & 2 \times \frac{12EI}{3^3} + 2 \times \frac{12(2EI)}{3^3} & -2 \times \frac{12(2EI)}{3^3} \\ 0 & 0 & -2 \times \frac{12(2EI)}{3^3} & 2 \times \frac{12(2EI)}{3^3} + 2 \times \frac{3(4EI)}{4^3} \end{bmatrix} = EI \begin{bmatrix} \frac{24}{27} & -\frac{24}{27} & 0 & 0 \\ -\frac{24}{27} & \frac{48}{27} & -\frac{24}{27} & 0 \\ 0 & -\frac{24}{27} & \frac{8}{3} & -\frac{48}{27} \\ 0 & 0 & -\frac{48}{27} & \frac{155}{72} \end{bmatrix}$$

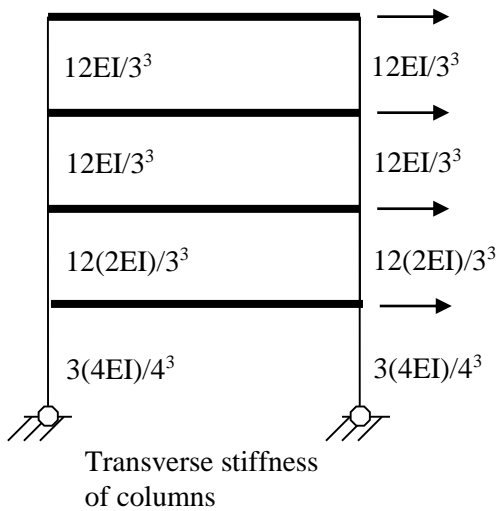
$$\mathbf{M} = \begin{bmatrix} M & 0 & 0 & 0 \\ 0 & M & 0 & 0 \\ 0 & 0 & 1.5M & 0 \\ 0 & 0 & 0 & 2M \end{bmatrix} \quad \phi_1 = \begin{bmatrix} 1 \\ 0.93 \\ 0.80 \\ 0.69 \end{bmatrix}$$

Hence, the fundamental natural circular frequency  $\omega_1$  is given by

$$\omega_1^2 = \frac{K_1}{M_1} = \frac{\{\phi_1\}^T [\mathbf{K}] \{\phi_1\}}{\{\phi_1\}^T [\mathbf{M}] \{\phi_1\}} = \frac{0.2194EI}{3.7771M} = 0.0581 \frac{EI}{M} \quad \therefore \omega_1 = 0.2410 \sqrt{\frac{EI}{M}}$$

The alternative approach to the calculation is to use the following formula. However, the former approach above is more recommended as defining the storey stiffnesses below can be tricky.

$$\omega_1^2 = \frac{\sum k_i \Delta \phi_i^2}{\sum m_i \phi_i^2}$$



$$\omega_1^2 = \frac{\sum k_i \Delta \phi_i^2}{\sum m_i \phi_i^2} = \frac{\left(2 \times \frac{12EI}{3^3}\right)(1.0 - 0.93)^2 + \left(2 \times \frac{12EI}{3^3}\right)(0.93 - 0.80)^2 + \left(2 \times \frac{12(2EI)}{3^3}\right)(0.80 - 0.69)^2 + \left(2 \times \frac{3(4EI)}{4^3}\right)(0.69)^2}{M \times 1.0^2 + M \times 0.93^2 + 1.5M \times 0.80^2 + 2M \times 0.69^2}$$

$$= \frac{0.2194EI}{3.7771M} = 0.05809 \frac{EI}{M}$$

$$\omega_1 = \sqrt{0.05809 \frac{EI}{M}} = 0.2410 \sqrt{\frac{EI}{M}}$$

### Rayleigh Quotient Method – No Improvement To Guessed Mode Shape

The Rayleigh Quotient expression can also be rewritten in terms of the static displacements as follows. This is employed in Earthquake Engineering codes of practice for the fundamental period of structures.

$$T_1 = 2\pi \sqrt{\frac{\sum W_i \delta_i^2}{g \sum W_i \delta_i}}$$

The static deflections due to the horizontal application of the weight of the structure are obtained from a static analysis program. It need not be the gravity forces that are applied, but any inertial force that produces a deflected shape corresponding to the mode shape of interest. The static horizontal deflected shape of the structure resembles the fundamental mode shape of the vibrational analysis because the  $\rho_0/K_i$  term is largest for the fundamental mode since higher modes are less significant in contributing to the static response. **This method however does not employ the repetitive improved estimates of the Improved Rayleigh Quotient method until convergence of the mode shape. Hence if the mode shape estimate is incorrect, so will be the natural frequency.** Of course, the static displacement should be calculated assuming a weight corresponding to the loading for which the frequency is required, i.e. usually a dead load with an allowance for the expected live load. Vertical bending modes of single span beams and plates can be found knowing the static deflections at various points (hence assuming lumped mass DOFs at those points). For the horizontal mode of vibration of an entire structure, the gravity force must be applied laterally. For multi-span beams, say a two span continuous beam, the fundamental mode is an antisymmetric mode. Hence, if the static loads were applied all in the same direction, we would be predicting the frequency of the symmetric mode, which is higher. This is an example where the assumed mode shape was totally incorrect. The repetitive improved estimates of the Improved Rayleigh Quotient method above would have detected this. The static load should have been applied downwards in one span and upwards in the other to produce a deflected shape that somewhat resembles the fundamental asymmetric mode.

### Lumped Mass Rayleigh Quotient Method – Lumped Mass & No Improvement To Guessed Mode Shape

The above Rayleigh Quotient expression can also be rewritten in terms of the static displacement and **lumping the mass to a single mass DOF**. For SDOF systems, we have said that the natural frequency can be estimated from

$$f_n = \frac{1}{2\pi} \sqrt{\frac{k}{m}}$$

This is the Rayleigh Quotient expression for SDOF systems if you like. Replacing the mass term with weight,  $W$ , we have

$$f_n = \frac{\sqrt{g}}{2\pi} \sqrt{\frac{k}{mg}} = \frac{\sqrt{g}}{2\pi} \sqrt{\frac{k}{W}} = \frac{\sqrt{g}}{2\pi \sqrt{u_{st}}} = 15.76 \frac{1}{\sqrt{u_{st}}} \quad u_{st} \text{ in mm}$$

Which now relates the natural frequency to the static deflection  $u_{st}$  of a single lumped mass dynamic DOF. This formula is **exact ONLY for single lumped mass** systems. We can approximately extend this to MDOF systems but the numerical factor 15.76 will be different generally between 16 and 20; 18 is quite practical. **But of course, this is a fudge to account for the fact that we are not taking static deflections at various mass DOFs, but simply at one solitary mass DOF.** The advantage of this method is that it is simple. If the static deflection is known from various standard static deflection equations, the natural frequency can be determined, albeit very approximately. Vertical bending modes of single span beams and plates can easily be found knowing the midpoint static deflection (hence assuming a lumped mass DOF in the middle). For the horizontal mode of vibration of an entire structure, the gravity force must be applied laterally and the lateral deflection at the top of the equivalent vertical cantilever is employed (hence assuming that the lumped mass DOF is at the top of the building).

#### 4.1.3.2.6 Natural Frequencies Using the Rayleigh-Ritz Method

The Rayleigh Quotient method gives the first mode of vibration only. Ritz extended this method to give a few more modes.

The full eigenvalue problem is expressed as

$$([K] - \omega_i^2[M]) \{\phi_i\} = \{0\} \quad i = 1 \text{ to the number of DOF in original system, } n$$

But with the approximation of  $\{\phi\} = [\Psi]\{z\}$ , the reduced eigenvalue problem can be expressed as

$$([K^*] - \omega_i^2[M^*]) \{z_i\} = \{0\} \quad i = 1 \text{ to the number of Ritz vectors in reduced system, } s < n$$

Hence, the following procedure is undertaken

- (a)  $[K]$  and  $[M]$  are established
- (b) The Ritz vectors  $[\Psi] = [\{\Psi_1\}, \{\Psi_2\}, \dots, \{\Psi_s\}]$  are assembled, where  $s < n$
- (c) Compute  $[K^*] = [\Psi]^T[K][\Psi]$  and  $[M^*] = [\Psi]^T[M][\Psi]$
- (d) Solve the reduced eigenvalue problem

$$\begin{aligned} &([K^*] - \omega_i^2[M^*]) \{z_i\} = \{0\} \\ &\text{Det} ([K^*] - \omega_i^2[M^*]) = 0 \\ &\text{Hence, } \omega_i \text{ and } \{z_i\} \text{ obtained, } i = 1 \text{ to } s \end{aligned}$$

- (e) The  $s$  (not  $n$ ) approximate mode shapes in the original system is obtained

$$\{\phi_i\} = [\Psi]\{z_i\} \text{ obtained, } i = 1 \text{ to } s$$

- (f) The number of good approximation of modes =  $s / 2$ ; Hence, Ritz extended Rayleigh's method to give  $s / 2$  modes with good accuracy

### 4.1.3.3 Natural Frequencies of Distributed Systems

#### 4.1.3.3.1 Natural (Fundamental) Frequency Using the Approximate Rayleigh Quotient Method

The Rayleigh Quotient Method is approximate because of the approximation of the mode shape. The closer the mode shape resembles the true mode shape, the more accurate the natural frequency estimation.

For the flexural Bernoulli-Euler beam of length  $L$  with additional lumped masses and stiffnesses the natural circular frequency  $\omega_i$  is given by

$$\omega_i^2 = \frac{\text{Generalised Stiffness } K_i}{\text{Generalised Mass } M_i} = \frac{\int_0^L EI(x) \{\phi''(x)\}^2 dx + \sum_{j=1}^{n_2} k_j \phi_j^2}{\int_0^L m(x) \{\phi(x)\}^2 dx + \sum_{i=1}^{n_1} m_i \phi_i^2}$$

The number of coefficients in the polynomial approximation of the mode shape  $\phi(x)$  = the number of geometric and static boundary conditions + 1  
 One is added because one coefficient will cancel out in Rayleigh's formula.

Geometric boundary conditions:

Fixed end	→	$\phi(x) = 0$ and $\phi'(x) = 0$
Pinned end	→	$\phi(x) = 0$
Free end in rotation and translation	→	None
Free end with spring $k_s$	→	None
Free end in translation only	→	$\phi'(x) = 0$

Static boundary conditions:

Note that $M(x) = EI(x)\phi''(x)$ and $V(x) = M'(x) = EI(x)\phi'''(x)$		
Fixed end	→	None
Pinned end	→	$\phi''(x) = 0$
Free end in rotation and translation	→	$\phi''(x) = 0$ and $\phi'''(x) = 0$
Free end with spring $k_s$	→	$\phi''(x) = 0$
Free end in translation only	→	None

#### 4.1.3.4 Natural Frequencies By Exactly Solving the Partial Differential Equilibrium Equation

In reality, all systems have distributed mass, damping and stiffness properties. The finite element method discretizes the continuous system with a finite number of degrees of freedom resulting in a set of second order ordinary differential equations (ODEs). Continuous systems on the other hand result in one partial differential equation of at least second order. The reason for this is that on top of having the time variable, continuous systems also include the spatial variable as there are not discrete DOFs. Because of the mathematical complexity of generating and solving (integrating) these partial differential equations, this method is limited to simple structures.

##### 4.1.3.4.1 The Bernoulli-Euler Beam

The **Bernoulli-Euler beam** equation of motion, which is based on simple bending theory **assuming that plane sections remain plane, no shear deformation and no axial force effects** results in the equation of motion

$$EI \frac{\partial^4 u}{\partial x^4} + \bar{m} \frac{\partial^2 u}{\partial t^2} = P(x, t) \quad \bar{m} = \text{mass per unit length}$$

where  $u$  is the transverse displacement. Note that the Timoshenko beam equation extends the Bernoulli-Euler beam theory to include shear deformations and rotary inertia and should be used if such effects matter. Solving the corresponding free vibration PDE analytically by the method of separation of variables leads to two ODEs, which yield the following natural circular frequencies and mode shapes

$$\omega_n = (a_n L)^2 \sqrt{\frac{EI}{\bar{m} L^4}}$$

$$\phi(x) = A \sin ax + B \cos ax + C \sinh ax + D \cosh ax$$

By applying various boundary conditions to these equations, various solutions may be found. The modal mass is

$$M_i = \bar{m} \int_0^L \phi(x)^2 dx$$

Note that  $i$  refers to the natural modes,  $i = 1, 2, 3 \dots$  etc.

Boundary Conditions	$(a_i L)^2$ Term	Natural Frequencies	Mode Shapes	Modal Mass
Fixed-Free (Cantilever)	$\cos(aL)\cosh(aL) - 1 = 0$ thus $(a_i L)^2 = 3.5160,$ 22.0345, 61.6972 ...	$\omega_{ni} = (a_i L)^2 \sqrt{\frac{EI}{\bar{m} L^4}}$	$\phi_i(x) = \cosh a_i x - \cos a_i x - \sigma_i (\sinh a_i x - \sin a_i x)$ $\sigma_i = \frac{\cosh a_i L + \cos a_i L}{\sinh a_i L + \sin a_i L}$	$0.25\bar{m}L$
Simply Supported	$\sin(aL) = 0$ thus, $(a_i L)^2 = (i\pi)^2, i = 1,$ 2, 3 ...	$\omega_{ni} = (a_i L)^2 \sqrt{\frac{EI}{\bar{m} L^4}}$	$\phi_i(x) = \sin \frac{a_i x}{L} = \sin \frac{i\pi x}{L}$	$0.50\bar{m}L$
Fixed-Simply Support (Propped Cantilever)	$\tan(aL) - \tanh(aL) = 0$ thus $(a_i L)^2 = 15.4118,$ 49.9648, 104.2477 ...	$\omega_{ni} = (a_i L)^2 \sqrt{\frac{EI}{\bar{m} L^4}}$	$\phi_i(x) = -\cosh a_i x + \cos a_i x + \sigma_i (\sinh a_i x - \sin a_i x)$ $\sigma_i = \frac{-\cosh a_i L + \cos a_i L}{-\sinh a_i L + \sin a_i L}$	$M_1 = 0.439\bar{m}L$ $M_2 = 0.437\bar{m}L$ $M_3 = 0.437\bar{m}L$
Free-Free	$\cos(aL)\cosh(aL) - 1 = 0$ thus $(a_i L)^2 = 22.3733,$ 61.6728, 120.9034 ...	$\omega_{ni} = (a_i L)^2 \sqrt{\frac{EI}{\bar{m} L^4}}$	$\phi_i(x) = \cosh a_i x + \cos a_i x - \sigma_i (\sinh a_i x + \sin a_i x)$ $\sigma_i = \frac{\cosh a_i L - \cos a_i L}{\sinh a_i L - \sin a_i L}$	
Fixed-Fixed (Encastre)	$\cos(aL)\cosh(aL) - 1 = 0$ thus $(a_i L)^2 = 22.3733,$ 61.6728, 120.9034 ...	$\omega_{ni} = (a_i L)^2 \sqrt{\frac{EI}{\bar{m} L^4}}$	$\phi_i(x) = \cosh a_i x - \cos a_i x - \sigma_i (\sinh a_i x - \sin a_i x)$ $\sigma_i = \frac{-\cosh a_i L + \cos a_i L}{-\sinh a_i L + \sin a_i L}$	$M_1 = 0.394\bar{m}L$ $M_2 = 0.439\bar{m}L$ $M_3 = 0.437\bar{m}L$

The modal mass for the simply supported beam is **half** the total mass for all the modes and that for the cantilever is **quarter** the total mass for all modes.

Length =  $L$  (m) (typical units)  
 Flexural rigidity =  $EI$  (N m<sup>2</sup>)  
 Mass/unit length =  $m$  (kg/m)  
 $f_n = \frac{k_n}{2\pi} \sqrt{\left(\frac{EI}{mL^4}\right)}$  Hz: values of  $k_n$  given below

	Mode	Shape	$k_n$	Nodal points at $x/L =$
Simply-supported	1		9.87	0 1
	2		39.5	0 0.5 1
	3		88.8	0 0.333 0.667 1
	$n$	$x = \sin\left(n\pi \frac{x}{L}\right)$	$n^2\pi^2$	$0 \frac{1}{n} \dots \frac{n-1}{n} 1$
Encastré	1		22.4	0 1
	2		61.7	0 0.5 1
	3		121	0 0.359 0.641 1
Cantilever	1		3.52	0
	2		22.0	0 0.774
	3		61.7	0 0.5 0.868

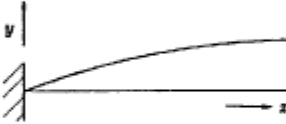
The natural frequencies of a simply-supported Bernoulli-Euler beam **with axial force** (positive P being tension) are

$$f_{ni} = \frac{(i\pi)^2}{2\pi} \sqrt{\frac{EI}{mL^4}} \sqrt{\left(1 + \frac{PL^2}{EIi^2\pi^2}\right)}$$

### 4.1.3.4.2 The Shear Beam

In reality, both shear and bending deformations must be accounted for when computing the frequencies of the beam. Shear deformation become prominent in deep (with respect to the span) beams. Hence the equivalent building cantilever beam model tends to be more of a shear mode. We are talking about the global behaviour of the building and not the shear deformation of individual column members, which are generally flexural. Note that shear frequencies are proportional to  $1/L$  whilst bending frequencies are proportional to  $1/L^2$ .

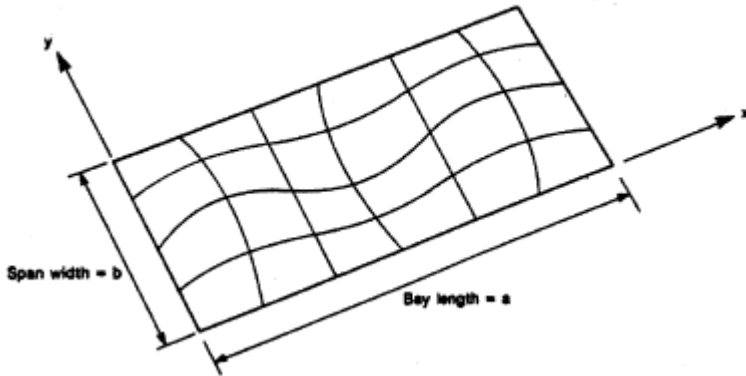
$$\begin{aligned} \text{Length} &= L && \text{(m) (typical units)} \\ \text{Shear rigidity} &= GA_s && \text{(N)} \\ \text{Mass/unit length} &= m && \text{(kg/m)} \\ f_n &= \frac{k_n}{2\pi} \sqrt{\left(\frac{GA_s}{mL^2}\right)} \text{ Hz: values of } k_n \text{ given below} \end{aligned}$$

Mode	Shape	$k_n$	Nodal points at $x/L =$
1		1.57	0
2		4.71	0 0.667
3		7.85	0 0.4 0.8
$n$	$y = \sin\left((2n-1)\frac{\pi x}{2L}\right)$	$(2n-1)\frac{\pi}{2}$	0 $\frac{2}{(2n-1)}$ $\frac{4}{(2n-1)}$ $\frac{6}{(2n-1)}$ etc.

The **Southwell-Dunkerly** formula can then be used to combine the effects of both bending and shear deformations (of course both deformations have to occur in the same mode to be compatible) to obtain a frequency estimate as follows.

$$\frac{1}{f_n^2} = \frac{1}{f_{n \text{ bending}}^2} + \frac{1}{f_{n \text{ shear}}^2}$$

### 4.1.3.4.3 Anisotropic Plate Simply-Supported



The mode shapes are described by

$$\mu = \sin\left(2\pi m_a \frac{x}{a}\right) \sin\left(2\pi m_b \frac{y}{b}\right)$$

For  $m_b = 1$  (higher modes in this direction of much higher frequencies), the natural frequencies are

$$f_n = \frac{\pi}{2a^2} \sqrt{\frac{m_a^4 D_x + 2Hm_a^2 \left(\frac{a}{b}\right)^2 + D_y \left(\frac{a}{b}\right)^4}{m}}$$

Note only bending deformation accounted for; no shear deformation.

$f_n$  = natural frequency (Hz)

$a$  = length of bay in x transverse direction

$b$  = length of bay in y primary span direction

$m_a$  = number of half sinewaves of the mode in x direction

$D_x$  = flexural rigidity for bending in the x direction (transverse direction)

$D_y$  = flexural rigidity for bending in the y direction (primary span direction)

$H$  = torsional stiffness parameter

$m$  = mass per unit area

The modal mass is then

$$M = \int_0^a \int_0^b m \mu_i^2 dy dx$$

For MAX normalized mode shapes, the **modal masses for ALL modes** of the **simply supported anisotropic plate** are **quarter** of the total mass.

#### Flat Slab

$$D_x = D_y = H = \frac{Eh^3}{12(1-\nu^2)}$$

$D_x$  and  $D_y$  are flexural rigidity per unit width

For unit width beam, the flexural rigidity,  $D = EI = Eh^3/12$  per unit width whilst for unit width plate, the flexural rigidity,  $D = EI = Eh^3/[12(1-\nu^2)]$  per unit width. The torsional rigidity  $H$  should be such that it is equal to the bending rigidity  $D$  so that there is equal bending stiffness of the plate about any horizontal axis. **The natural**

**frequency of a square flat slab plate simply supported all round is**  $f = \frac{\pi}{a^2} \sqrt{\frac{Eh^3}{12m(1-\nu^2)}}$ .

### One-way Composite Spanning

$$D_x = H = \frac{Eh^3}{12(1-\nu^2)}$$

where  $h$  is the effective thickness of the concrete slab, and

$$D_y = \frac{EI_y}{a_y}$$

where  $EI_y$  is the composite stiffness of one beam and  $a_y$  the beam spacing.

### Two-way Composite Spanning

$$D_x = \frac{EI_x}{a_x}$$

$$D_y = \frac{EI_y}{a_y}$$

$$H = \frac{Eh^3}{12(1-\nu^2)}$$

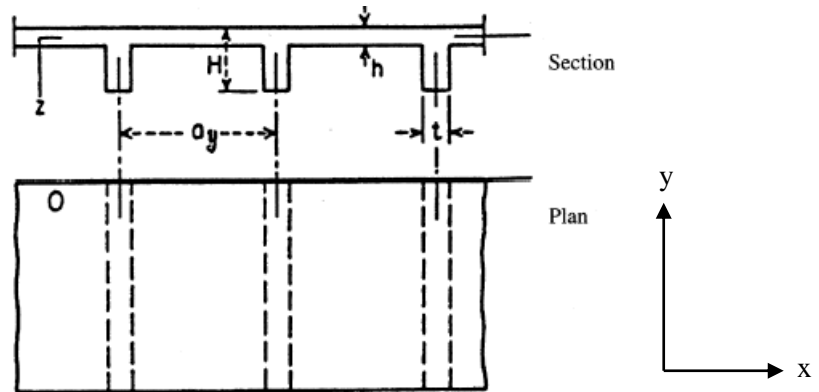
where  $EI_x$  is the composite stiffness of one beam in the transverse direction and  $a_x$  the beam spacing in this direction.

### Ribbed Section in One Direction

$$D_x = \frac{Ea_y h^3}{12(a_y - t + \alpha^2 t)}$$

$$D_y = \frac{EI_y}{a_y}$$

$$H = \frac{Eh^3}{12(1-\nu^2)} + \frac{C_y}{a_y}$$



where  $C_y$  is the torsional rigidity of each rib. For a rectangular rib of longer dimension  $a$  and shorter dimension  $b$ , (ref. Roark and Young):

$$C_y = Gab^3 \left[ \frac{1}{3} - 0.21 \frac{b}{a} \left( 1 - \frac{b^4}{12a^4} \right) \right]$$

### Ribbed Section in Two Directions

$$D_x = \frac{EI_x}{a_x}$$

$D_x$  is the flexural rigidity per unit width for bending about y-axis (or bending in x-z plane).

$$D_y = \frac{EI_y}{a_y}$$

$D_y$  is the flexural rigidity per unit width for bending about x-axis (or bending in y-z plane);  $I_y = t(H-h)^3/12 + A_{web}(\text{lever arm})^2 + (a_y \cdot h^3/12)[a_x/(a_x - t_{ortho} + t_{ortho} \cdot \alpha_{ortho}^3)] + A_{slab}(\text{lever arm})^2$ ; Note the factor  $[a_x/(a_x - t_{ortho} + t_{ortho} \cdot \alpha_{ortho}^3)]$  to account for the effect of the orthogonal ribs on the bending stiffness. Thus here  $\alpha_{ortho} = h/H_{ortho}$  where ( $H_{ortho} - h$ ) is the depth of the orthogonal ribs and  $t_{ortho}$  is the thickness of the orthogonal ribs.

$$H = \frac{Eh^3}{12(1-\nu^2)} + \frac{C_x}{a_x} + \frac{C_y}{a_y}$$

### 4.1.3.5 Approximate Formulae

#### 4.1.3.5.1 Multi-Storey Buildings

A good approximate fundamental frequency formula for single-storey buildings, multi-storey buildings and towers is (Bachmann and EC1-2.4:1995)

$$f = 46 / h \text{ (Hz)}$$

where h is the height (m).

Alternatively, EC8 recommends for buildings up to 80m,

$$T_1 = C_t \cdot H^{3/4}$$

where

$$T_1 \quad \text{fundamental period of building, in s,}$$

$$C_t = \begin{cases} 0,085 & \text{for moment resistant space steel frames,} \\ 0,075 & \text{for moment resistant space concrete frames} \\ & \text{and for eccentric braced steel frames,} \\ 0,050 & \text{for all other structures,} \end{cases}$$

$$H \quad \text{height of the building, in m.}$$

and  $C_t$  for structures with concrete or masonry shear walls is given by

$$C_t = 0,075 / \sqrt{A_c}$$

with

$$A_c = \Sigma [A_i \cdot (0,2 + (l_{wi}/H))^2]$$

where

$$A_c \quad \text{combined effective area of the shear walls in the first storey of the building, in m}^2,$$

$$A_i \quad \text{effective cross-sectional area of the shear wall i in the first storey of the building, in m}^2,$$

$$l_{wi} \quad \text{length of the shear wall i in the first storey in the direction parallel to the applied forces, in m,}$$

with the restriction that  $l_{wi}/H$  shall not exceed 0,9.

Another approximations is

$$T_1 = 2 \cdot \sqrt{d}$$

where

$$T_1 \quad \text{fundamental period of building, in s,}$$

$$d \quad \text{lateral displacement of the top of the building, in m, due to the gravity loads applied horizontally.}$$

#### 4.1.3.5.2 Cable Stayed Bridges

A good approximate fundamental frequency formula for cable stayed bridges is (Bachmann)

$$f = 110 / L$$

where L is the length of the main span (m).

#### **4.1.3.5.3 Highway Bridges**

A good approximate fundamental frequency formula for highway bridges is (Bachmann)

$$f = 100 / L$$

where L is the length of the main span (m).

## 4.2 GL, ML Implicit Direct Complex Modal (Eigenvalue) Analysis

### 4.2.1 Mathematical Formulation of Analysis

The equation of motion for a free, damped system is

$$[M]\{\ddot{u}(t)\} + [C]\{\dot{u}(t)\} + [K]\{u(t)\} = \{0\}$$

We seek solutions of the form

$$\{u(t)\}_i = \text{Re al}[\{\phi\}_i \xi_i e^{\lambda_i t}] \text{ for the } i^{\text{th}} \text{ mode of vibration}$$

where  $\xi_i = \xi_{Ri} + i\xi_{Ii}$  and  $\lambda_i = \alpha_i + i\omega_{di}$

Note that  $\alpha$  represents the decaying part and  $\omega_d$  the damped natural frequency.

Hence, substituting into the equation of motion

$$\begin{aligned} [M]\xi_i \lambda_i^2 \{\phi\}_i e^{\lambda_i t} + [C]\xi_i \lambda_i \{\phi\}_i e^{\lambda_i t} + [K]\xi_i \{\phi\}_i e^{\lambda_i t} &= \{0\} \\ [\lambda_i^2 [M] + \lambda_i [C] + [K]]\{\phi\}_i &= \{0\} \end{aligned}$$

This is a complex eigenvalue problem to be solved for  $\lambda_i$  and  $\{\phi\}_i$ .

For completion, the response due to mode  $i$ ,  $\{u(t)\}_i$  of a free damped linear elastic structure subjected to an initial impact (defining an initial displacement and velocity) is

$$\begin{aligned} \{u(t)\}_i &= \{\phi\}_i \text{Re al} \left[ \xi_{1i} e^{\lambda_{1i} t} + \xi_{2i} e^{\lambda_{2i} t} \right] \\ \{u(t)\}_i &= \{\phi\}_i \text{Re al} \left[ (\xi_{1Ri} + i\xi_{1Ii}) e^{\alpha_i t} (\cos \omega_{di} t + i \sin \omega_{di} t) + (\xi_{2Ri} + i\xi_{2Ii}) e^{\alpha_i t} (\cos \omega_{di} t - i \sin \omega_{di} t) \right] \\ \{u(t)\}_i &= \{\phi\}_i \text{Re al} \left[ e^{\alpha_i t} \left[ (\xi_{1Ri} + \xi_{2Ri}) \cos \omega_{di} t - (\xi_{1Ii} - \xi_{2Ii}) \sin \omega_{di} t + i((\xi_{1Ii} + \xi_{2Ii}) \cos \omega_{di} t + (\xi_{1Ri} - \xi_{2Ri}) \sin \omega_{di} t) \right] \right] \end{aligned}$$

For the free vibration response to be real for all  $t$ ,

$$\xi_{1Ii} = -\xi_{2Ii} \quad \text{and} \quad \xi_{1Ri} = \xi_{2Ri}$$

Since there are two less independent constants, let

$$\xi_{1Ii} = -\xi_{2Ii} = \xi_{Ii} \quad \text{and} \quad \xi_{1Ri} = \xi_{2Ri} = \xi_{Ri}$$

We notice that  $\xi_{1i}$  and  $\xi_{2i}$  are a complex conjugate pair

$$\xi_{1i} = \xi_{Ri} + i\xi_{Ii} \quad \text{and} \quad \xi_{2i} = \xi_{Ri} - i\xi_{Ii}$$

Hence

$$\{u(t)\}_i = \{\phi\}_i e^{\alpha_i t} (2\xi_{Ri} \cos \omega_{di} t - 2\xi_{Ii} \sin \omega_{di} t)$$

Thus the total response due to the superposition of all modes

$$\{u(t)\} = [\Phi] \left\{ e^{\alpha_i t} (2\xi_{Ri} \cos \omega_{di} t - 2\xi_{Ii} \sin \omega_{di} t) \right\}$$

In the real eigenvalue analysis, for each mode  $i$ , NASTRAN outputs,

one real root  $\omega_{ni}$  representing the undamped natural circular frequency

one real eigenvector  $\{\phi\}_i$  representing the real mode shape

Complex eigenvalue analysis with viscous (and structural optional) damping, for each mode  $i$ , NASTRAN outputs,

two complex roots which are a complex conjugate pair,  $\alpha_i + i\omega_{di}$  and  $\alpha_i - i\omega_{di}$ , where

$\alpha_i$  is negative and represents the decaying constant

$\omega_{di}$  is positive and represents the damped natural circular frequency

two complex eigenvectors which are a complex conjugate pair,  $\{\phi_R + i\phi_I\}_i$  and  $\{\phi_R - i\phi_I\}_i$

Complex eigenvalue analysis with only structural (and no viscous) damping, for each mode  $i$ , NASTRAN outputs,

one complex root,  $\alpha_i + i\omega_{di}$ , where

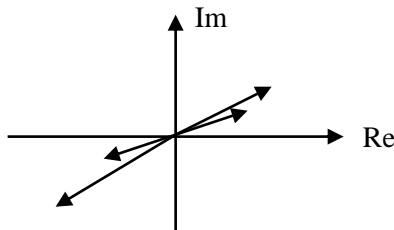
$\alpha_i$  is negative and represents the decaying constant

$\omega_{di}$  is positive and represents the damped natural circular frequency

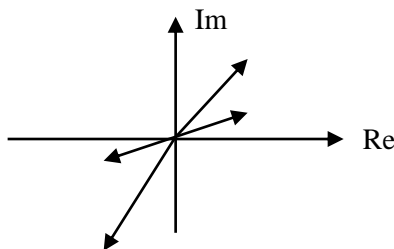
one complex eigenvector,  $\{\phi_R + i\phi_I\}_i$

### 4.2.2 Complexity of Modes of Vibration

A pure real mode has all its terms in phase with each other. Different modes will of course be out of phase with each other, but every point in a particular mode will vibrate in phase. And so, for a mode, all points in the structure reach its maximum and minimum at the same phase instant. A complex mode on the other hand will have different points of the structure reaching its maximum at different phase instants, i.e. different points of the structure are out of phase with each other for a particular mode. Of course, different modes are still out of phase with each other. The degree to which these points are out of phase with each other is a measure of the complexity of the mode. An Argand diagram with all the terms of the complex eigenvector plotted will exhibit a narrowband if the mode is only slightly complex. The diagram below shows plots for 4 eigenvector terms. Since there is only a slight phase difference between the terms (angle between the arrows), the 4 terms define an almost real complex eigenvector.



The following eigenvector plot on the other hand is highly complex because of the large phase angle difference between the terms of the eigenvector.



The animation of the complex modes is quite indicative of the complexity of the mode. In complex modal analysis, each mode has two complex conjugate eigenvectors. Each eigenvector has a real and imaginary part. The animation of such a complex mode is only of value when we plot the magnitude of either (of the two complex conjugate) eigenvectors. The phase information (which is obtained when the magnitude and argument of the real and imaginary components are obtained) is essential in order to determine the relative phase of the motion of different parts of the structure. In a real mode, there is no phase information, and hence the animation of a real mode will show all parts of the structure vibrating in-phase with each other. Explicit viscous dampers will cause parts of the structure to vibrate clearly out-of-phase. This clearly occurs when explicit viscous dampers are used to damp prestressed cable vibrations. A cable with a damper element of a very high damping coefficient attached to its center will behave as two separate cables, the damper element effectively producing a fixity at the center of the cable. This changes the fundamental mode shape of the cable from one of a low frequency to two cable mode shapes of higher fundamental frequency.

### 4.2.3 Complex Modal Analysis To Determine Modal Damping Values

Because the solution by complex modal analysis yields a decaying constant  $\alpha_i$  for each and every mode, the modal damping can be obtained as modal structural damping,  $G_i = 2\alpha_i/\omega_{di}$ .

### 4.2.4 MSC.NASTRAN Decks

#### 4.2.4.1 GL, ML Complex Modal Analysis

```

$ EXECUTIVE CONTROL SECTION
SOL 107
$ CASE CONTROL SECTION
$ Sets defining grid ids or element ids
SET < Number > = 1 THRU 100, 211, 343, < etc >
$ Grid output of displacement for each mode i.e. eigenvector
$ SORT1 lists the results by eigenvalue whilst SORT2 lists the results by grid id
DISPLACEMENT(<SORT1/SORT2>,<PRINT,PUNCH,PLOT>,<REAL/PHASE>) = ALL/<Grid Set ID>
$ Grid output of displacement for each normalized mode i.e. normalized eigenvector
SDISPLACEMENT(<SORT1/SORT2>,<PRINT,PUNCH>,<REAL/PHASE>) = ALL/<Grid Set ID>
$ Grid output of real eigenvector for the a-set
SVECTOR(<PRINT,PUNCH>) = ALL/<Grid Set ID>
$ Grid output of SPC forces
SPCFORCES(<SORT1/SORT2>,<PRINT,PUNCH,PLOT>,<REAL/PHASE>) = ALL/<Grid Set ID>
$ Element output of force, stress and strain
ELFORCE(<SORT1/SORT2>,<PRINT,PUNCH,PLOT>,<REAL/PHASE>) = ALL/<Element Set ID>
ELSTRESS(<SORT1/SORT2>,<PRINT,PUNCH,PLOT>,<REAL/PHASE>) = ALL/<Element Set ID>
STRAIN(<SORT1/SORT2>,<PRINT,PUNCH,PLOT>,<REAL/PHASE>) = ALL/<Element Set ID>
$ Analysis Requests
SPC = < ID of SPC Cards Defined in Bulk Data >
CMETHOD = < ID IN EIGC >
$ XY plot output
OUTPUT(XY PLOT)
XYPUNCH <DISP/VELO/ACCE> RESPONSE <subcase>/<Grid ID>(<T1/T2/T3><RM/IP>)
XYPUNCH <ELFORCE/ELSTRESS/STRAIN> RESPONSE <subcase>/<Element ID>(<Code Number>)
    
```

The EIGC bulk data card is required.

EIGC	SID	METHOD	NORM	G	C	E	ND0		
------	-----	--------	------	---	---	---	-----	--	--

The METHOD commonly used is CLAN. NORM, G, and C have to do with the specification of the method of normalization. The eigenvectors may be normalized either to a unit value at grid point G for coordinate C, or for the largest term to be of unit magnitude. E is used to specify the convergence criterion of the solution. Each method has a different default value for this criterion, and each is adequate for most problems. The following continuation is repeated for each desired search region. (J = 1 to n, where n is the number of search regions).

	ALPHAAJ	OMEGAAJ	ALPHABJ	OMEGABJ	LJ	NEJ	NDJ		
--	---------	---------	---------	---------	----	-----	-----	--	--

As mentioned, replacing the following into the free damped equation of motion

$$u(t) = Real\left(\sum\{\phi_i\}e^{(\alpha_i + i\omega_i)t}\right)$$

results in the following complex eigenvalue problem

$$[K + pB + p^2M]\{\phi\} = 0$$

where

$$p = \alpha + i\omega$$

If  $\alpha=0$ , the radian frequency,  $\omega$  of complex eigenvalue analysis is the same as that of real eigensolutions. The real part,  $\alpha$ , is a measure of the decay rate of a damped structure, or if negative, the rate of divergence of an unstable system. The imaginary part,  $\omega$ , is the modified frequency in radians/unit time. However, roots with negative values of  $\omega$  should be treated as special terms. The recommended practice is to specify one point  $\alpha_1=0.0$  and  $\omega_1$  at the lower bound of the expected range of eigenvalues, but not at 0.0. A second shift may be input at  $\alpha_2=0.0$  and  $\omega_2$  at the upper bound of the expected range. All ALPHABj and OMEGABj must be blank.

The eigenvalue output for a sample problem is shown below.

COMPLEX EIGENVALUE SUMMARY					
ROOT NO.	EXTRACTION ORDER	EIGENVALUE		FREQUENCY (CYCLES)	DAMPING COEFFICIENT
		(REAL)	(IMAG)		
1	9	-5.806441E+01	5.750383E+03	9.152019E+02	2.019497E-02
2	8	-6.294888E+01	6.293917E+03	1.001708E+03	2.000309E-02
3	7	-6.910709E+01	6.844852E+03	1.089392E+03	2.019243E-02
4	1	-3.300980E+02	1.667092E+04	2.653260E+03	3.960164E-02
5	5	-3.565692E+02	1.823559E+04	2.902285E+03	3.910694E-02
. . .					

The column labeled (REAL) contains  $\alpha_1$ , and the column labeled (IMAG) contains  $\omega_1$ . The column labeled (FREQUENCY) contains the circular frequency. The last column is the damping coefficient computed from the equation

$$(g) = -2\alpha / |\omega|$$

which is approximately twice the value of the conventional modal damping ratio. Note that if the magnitude of this term is computed to be less than  $5.0 \times 10^{-4}$ , it is reset to zero. For small values, the damping coefficient is twice the fraction of critical damping for the mode. The eigenvalues are sorted on  $\omega$ , with the negative values sorted first (there are none in this example), sorted on increasing magnitude, followed by the eigenvalues with positive  $\omega$ , again sorted on magnitude. Roots with equal  $\omega$  values are sorted next on  $\alpha$ .

#### 4.2.4.2 GL, ML P- $\Delta$ ( $K_G^A$ From $K_E^A$ ) Complex Modal Analysis

It is often necessary to incorporate the reduction in bending stiffness of gravity load resisting columns for the analysis of lateral loads. The following procedure is undertaken.

##### Phase 1

Perform static analysis (with loads that cause the greatest negative or positive geometric stiffness) based on  $[K_E^A]$  but include the segyroa.v2001 alter prior to the Case Control Section in order to compute the geometric stiffness matrix  $[K_G^A]_1$  (and output into a .pch file) based on the generated element loads from the  $[K_E^A]$  static analysis.

##### Phase 2

A SOL 107 is undertaken based on  $[K_E^A] + [K_G^A]_1$  with the k2gg=ktjj statement in the Case Control Section and the outputted .pch file which contains the ktjj matrix in the Bulk Data. The responses at this stage represent the P- $\Delta$  ( $K_G^A$  From  $K_E^A$ ) complex modal response.

The following equivalent alternative procedure can also be employed.

<pre> \$ CASE CONTROL SECTION  SUBCASE 1 LABEL = Static Preload Load Case LOAD = &lt; ID of FORCEi, MOMENTi, PLOADi, GRAV, LOAD, SPCD Cards in Bulk Data &gt; TEMP(LOAD) = &lt; ID of TEMP, TEMPRB, TEMPP1 Cards in Bulk Data &gt; DEFORM = &lt; ID of DEFORM Cards in Bulk Data &gt; SUBCASE 2 LABEL = P-<math>\Delta</math> Complex Modal Analysis STATSUB(PRELOAD) = 1 CMETHOD = &lt; ID in EIGC &gt;                 </pre>
---

The method is valid when **only the prestress is judged to affect the geometric stiffness** such as in the compressive preload of building columns due to gravitational loads and the prestressing of extremely taut cables that sag very little under gravity but not in systems such as suspension bridges. Where lateral loads are large enough to affect the geometry of the system with prestress, then a repetitive P- $\Delta$ , SOL 106, implicit dynamic relaxation SOL 129 or explicit dynamic relaxation must be employed. But in single P- $\Delta$  analysis, because cables do not have much elastic bending stiffness, the initial static preload subcase should only include the prestress and not gravity as including gravity is the same as solving two linear static problems of stiffness  $K_E^A$  with preload and gravity as the applied loads respectively. Clearly, in the gravity case, it is nonsensical as the cables do in reality have differential stiffness (from the prestress) to resist the gravitational force. Prestress in one direction (i.e. along the axis of cable) will cause a differential stiffness in the orthogonal direction. Gravity acts in the orthogonal direction and hence cannot be accounted for in the calculation of the prestress in this single P- $\Delta$  analysis. To quantitatively decide if gravity need not be considered in contributing to the differential stiffness of the cables, a static P- $\Delta$  analysis should be carried out, the first subcase being a SOL 101 with only the prestress as applied loads and the second subcase a P- $\Delta$  SOL 101 (i.e. utilizing the induced prestress from the first subcase to form a geometric stiffness matrix) with both the gravity and prestress included as applied loads. If the difference in the cable element forces between subcases 1 and 2 is negligible, then gravity has little influence in affecting the geometric stiffness. If there is a major difference in the cable element force, then clearly, gravity will affect the geometric stiffness and as such, a repetitive P- $\Delta$ , SOL 106, implicit dynamic relaxation or explicit dynamic relaxation must be used to converge to the true  $K_T$ . Likewise, in the single P- $\Delta$  analysis of multi-storey buildings, gravity (and only gravity) acts in axis of columns to generate prestress, and the differential stiffness is computed for the orthogonal direction reducing resistance to lateral wind forces, applied in the second subcase with gravity too.

The STATSUB(PRELOAD) computes the differential stiffness due to the prestress and also the follower force. The follower force is calculated and incorporated by the use of PARAM, FOLLOWK, YES. We know how the prestress affects the differential stiffness, namely a tensile prestress causing an increase in stiffness. The effect of the follower force on the stiffness is different. For example, for a cylinder under external pressure critical buckling load may be over-estimated (even though the mode shapes are similar) in a SOL 105 and the natural frequencies in vibration may be under-estimated (even though the mode shapes are similar) in a SOL 103 in the absence of follower stiffness. To the contrary, these observations are reversed in case of centrifugal loads. Centrifugal forces as a constant (static) load are applied by a Bulk Data RFORCE to any elements that have masses. The follower stiffness due to centrifugal load has the effect of lowering stiffness (although the centrifugal load tensioning effect increases stiffness), consequently lowering natural frequencies (even though the mode shapes are similar) in a SOL 103 and lowering the buckling loads (even though the mode shapes are similar) in a SOL 105. This effect increases as the RPM increases, and it becomes significant when the RPM is over 1000. For moderately geometric nonlinear analysis, exclusion of follower stiffness affects the rate of convergence, but the converged solution is correct. For severely geometric nonlinear analysis, it may not be possible to obtain a converged solution without including follower stiffness. As the geometric nonlinearity intensifies, so is the effect of follower stiffness. Therefore, inclusion of follower stiffness greatly enhances the convergence if the deformation involves severe geometric nonlinearity.

#### 4.2.4.3 GL, ML P- $\Delta$ ( $K_G^A$ From Exact or Approximate $K_T^A$ ) Complex Modal Analysis

The above top deck solves the linear modal complex eigenvalue problem. It is often necessary to include the differential stiffness, especially if there are prestressed cables in the model and the mode shapes are sought. To obtain  $K_T^A$ , to be theoretically exact, a GNL SOL 106 (or implicit dynamic relaxation SOL 129 or explicit dynamic relaxation LS-DYNA) with prestress (as temperature loads say) and gravity must be undertaken. Alternatively, an approximation to  $K_T^A$  can be obtained by repetitive P- $\Delta$  static analyses with the prestress (as temperature loads say) and gravity applied. The procedure to obtain this approximate  $K_T^A$  will be presented. Note that the approximate  $K_T^A$  will be the summation of the elastic stiffness  $K_E$  at the undeflected (by the prestress and gravity) state but  $K_G$  at the deflected (by the prestress and gravity) state. Hence if  $K_E$  changes considerably during the application of the prestress, a full SOL 106 (or implicit dynamic relaxation SOL 129 or explicit dynamic relaxation LS-DYNA), which converges to the  $K_E$  and  $K_G$  at the deflected (by the prestress and gravity) state should be employed. Hence for the modelling of a suspension bridge where there is a great change in geometry (known in the bridge industry as **form-finding**, so-called because it is necessary to find the form or shape of the catenary suspension cables), it may be prudent to employ SOL 106 (or implicit dynamic relaxation SOL 129 or explicit dynamic relaxation LS-DYNA), but for a high tension low sag cable on say a tower with prestressed cables, the repetitive P- $\Delta$  static analysis may be adequate. The repetitive P- $\Delta$  analysis basically involves a number of iterations of linear static analyses to obtain an approximate  $K_T^A$ . Note again that A refers to the initial undeflected (by the collapsing load) state, but deflected by the prestress and gravity. To perform the repetitive P- $\Delta$  analysis, a static analysis is performed based on  $K_E^A$  with temperature loads and gravity to generate forces in the structural elements, which in turn provides input for the computation of  $K_{Gi}^{AKT_m}$  where m is the iterations. Repetitive static analysis is performed with the prestress and gravity updating the stiffness matrix  $K_E^A + K_{Gi}^{AKT_{m-1}} + K_{Gi}^{AKT_m}$  until convergence of displacements is obtained. The tangent stiffness at this stage is the approximate converged tangent stiffness matrix  $K_T^A = K_E^A + K_{Gi}^{AKT}$ . The converged displacements represent the approximate P- $\Delta$  ( $K_G^A$  From Approximate  $K_T^A$ ) static response to the initial prestress loads. The converged geometric stiffness at this stage would be that based upon the approximate tangent stiffness matrix  $K_T^A$ , i.e.  $K_{Gi}^{AKT}$ .

##### Phase 1

Perform static analysis (with prestress and gravity) based on  $[K_E^A]$  but include the segyroa.v2001 alter prior to the Case Control Section in order to compute the geometric stiffness matrix  $[K_G^A]_1$  (and output into a .pch file) based on the generated element loads from the  $[K_E^A]$  static analysis.

##### Phase 2

Perform static analysis (with prestress and gravity) based on  $[K_E^A] + [K_G^A]_1$  by including the k2gg = ktjj statement in the Case Control Section, the outputted .pch file which contains the ktjj matrix in the Bulk Data and the segyroa.v2001 alter prior to the Case Control Section to compute the  $[K_G^A]_2$  (and output into the .pch file overwriting previous data) based on the generated element loads from the  $[K_E^A] + [K_G^A]_1$  static analysis.

##### Phase 3

Repeatedly perform the Phase 2 static analysis (with prestress and gravity) based on  $[K_E^A] + [K_G^A]_i$  for  $i = 2$  to  $n$  where  $n$  represents the number of iterations required for the change in deflections between analyses to become negligible. This would signify that the change in the  $[K_G^A]$  matrix become negligible and the correct  $[K_G^A]$  is attained. The deflections and the other responses at this stage represent the P- $\Delta$  ( $K_G^A$  From Approximate  $K_T^A$ ) static response to the prestress and gravity. The stiffness of the structure is  $K_T^A$ .

##### Phase 4

A SOL 107 is undertaken with the k2gg=ktjj statement in the Case Control Section and the outputted .pch file which contains the latest ktjj matrix in the Bulk Data. The responses at this stage represent the P- $\Delta$  ( $K_G^A$  From Approximate  $K_T^A$ ) complex modal response.

## 4.2.5 Hand Methods Verification

### 4.2.5.1 Determination of Damped Natural Frequency and the Maximum Dynamic Displacement, $u_{\max}$ for Free Damped Vibration Due to Initial Displacement and/or Initial Velocity by Classically Solving the SDOF Linear ODE and Maximizing the Solution

Equation of motion (linear second order ODE)

$$m\ddot{u}(t) + c\dot{u}(t) + ku(t) = 0$$

Assume  $u(t) = \text{Re al} [Ge^{\lambda t}]$  where  $G = G_R + iG_I$  and  $\lambda = \alpha + i\omega_d$

$$mG\lambda^2 e^{\lambda t} + cG\lambda e^{\lambda t} + kGe^{\lambda t} = 0$$

$$(m\lambda^2 + c\lambda + k)Ge^{\lambda t} = 0$$

for LHS to be zero for all t

$$(m\lambda^2 + c\lambda + k) = 0 \quad \text{as} \quad Ge^{\lambda t} > 0$$

the roots of this quadratic characteristic equation are

$$\lambda_1 = -\frac{c}{2m} + \sqrt{\left(\frac{c}{2m}\right)^2 - \frac{k}{m}} \quad \lambda_2 = -\frac{c}{2m} - \sqrt{\left(\frac{c}{2m}\right)^2 - \frac{k}{m}}$$

Hence the general solution is the superposition of the two possible solutions,

$$u(t) = \text{Re al} [G_1 e^{\lambda_1 t} + G_2 e^{\lambda_2 t}]$$

The exact form depends on the value of the viscous damping coefficient t, c.

Case : critically damped  $c = c_{cr} = 2\sqrt{km} = 2m\omega_n$ , the two roots are real and repeated,

$$\lambda_1 = \lambda_2 = -\frac{c_{cr}}{2m} = -\frac{2\sqrt{km}}{2m}$$

Hence,

$$u(t) = (G_1 + G_2 t) e^{-\frac{c_{cr}}{2m} t}$$

There will be no oscillatory motion, instead simply an exponential decay.

Case : overdamped  $c > c_{cr}$ , the two roots will be real and distinct,

$$u(t) = G_1 e^{\lambda_1 t} + G_2 e^{\lambda_2 t}$$

Again, there will be no oscillatory motion, instead exponential decay in a longer time.

Case : under - damped,  $c < c_{cr}$ , the roots are complex conjugates,

$$\lambda_1 = -\frac{c}{2m} + i\sqrt{\frac{k}{m} - \left(\frac{c}{2m}\right)^2} \quad \lambda_2 = -\frac{c}{2m} - i\sqrt{\frac{k}{m} - \left(\frac{c}{2m}\right)^2}$$

employing Euler's equations,

$$e^{i\theta} = \cos \theta + i \sin \theta$$

$$e^{-i\theta} = \cos \theta - i \sin \theta$$

hence, writing  $\omega_d = \sqrt{\frac{k}{m} - \left(\frac{c}{2m}\right)^2}$

$$u(t) = \text{Re al} \left[ (G_{1R} + iG_{1I})e^{-\frac{c}{2m}t} (\cos \omega_d t + i \sin \omega_d t) + (G_{2R} + iG_{2I})e^{-\frac{c}{2m}t} (\cos \omega_d t - i \sin \omega_d t) \right]$$

$$u(t) = \text{Re al} \left[ e^{-\frac{c}{2m}t} \left[ (G_{1R} + G_{2R}) \cos \omega_d t - (G_{1I} - G_{2I}) \sin \omega_d t + i((G_{1I} + G_{2I}) \cos \omega_d t + (G_{1R} - G_{2R}) \sin \omega_d t) \right] \right]$$

for the free vibration response to be real for all t,

$$G_{1I} = -G_{2I} \quad \text{and} \quad G_{1R} = G_{2R}$$

since there are two less independent constants, let

$$G_{1I} = -G_{2I} = G_I \quad \text{and} \quad G_{1R} = G_{2R} = G_R$$

we notice that  $G_1$  and  $G_2$  are a complex conjugate pair

$$G_1 = G_R + iG_I \quad \text{and} \quad G_2 = G_R - iG_I$$

hence

$$u(t) = e^{-\frac{c}{2m}t} \left[ (2G_R \cos \omega_d t - 2G_I \sin \omega_d t) \right]$$

defining the damping ratio  $\zeta$  such that

$$c = \zeta c_{cr} = \zeta 2\sqrt{km} = \zeta 2m\omega_n$$

the damped natural circular frequency,

$$\omega_d = \sqrt{\frac{k}{m} - \left(\frac{\zeta 2\sqrt{km}}{2m}\right)^2} = \sqrt{\frac{k}{m} - \frac{\zeta^2 k}{m}} = \sqrt{\frac{k}{m}(1 - \zeta^2)} = \omega_n \sqrt{1 - \zeta^2}$$

hence,

$$u(t) = e^{-\zeta\omega_n t} \left[ (2G_R \cos \omega_d t - 2G_I \sin \omega_d t) \right]$$

where  $\omega_d = \omega_n \sqrt{1 - \zeta^2}$  and  $2G_R, -2G_I$  being the constants of integration from the initial conditions.

Note also that we often define the decaying constant

$$\alpha = -\frac{c}{2m}$$

hence since  $c = \zeta 2m\omega_n$

$$\alpha = -\frac{\zeta 2m\omega_n}{2m}$$

$$\alpha = -\zeta\omega_n$$

Damping causes the damped natural frequencies to be a little less than the undamped natural frequencies, but the difference is negligible in real structures, which are under-damped. Hence, the old classroom example of measuring the natural frequency of a pendulum in air and in water gives a lower frequency in water simply because of the added water mass in the dynamic model.

We have established that for under - damped free vibrations

$$u(t) = e^{-\zeta\omega_n t} \left[ (2G_R \cos \omega_d t - 2G_I \sin \omega_d t) \right]$$

With initial displacement and velocity conditions,

$$u(t) = e^{-\zeta\omega_n t} \left( u(0) \cos \omega_d t + \frac{\dot{u}(0) + u(0)\zeta\omega_n}{\omega_d} \sin \omega_d t \right) \text{ where } \omega_d = \omega_n \sqrt{1 - \zeta^2}$$

Hence, the maximum dynamic displacement

$$u_{\max} = \sqrt{u(0)^2 + \left( \frac{\dot{u}(0) + u(0)\zeta\omega_n}{\omega_d} \right)^2}$$

The motion is oscillatory with a period of  $T_d = \frac{2\pi}{\omega_d}$ , the amplitude decreasing exponentially.

The damping ratio  $\zeta$  can be estimated experimentally from two displacement peaks separated by  $mT_d$ ,

$$\frac{u_n}{u_{n+m}} = \frac{e^{-\zeta\omega_n t_1}}{e^{-\zeta\omega_n (t_1 + mT_d)}} = e^{\zeta\omega_n mT_d} = e^{\zeta\omega_n m \frac{2\pi}{\omega_d}} = e^{\zeta\omega_n m \frac{2\pi}{\omega_n \sqrt{1-\zeta^2}}} = e^{\zeta m \frac{2\pi}{\sqrt{1-\zeta^2}}} = e^{\frac{2\pi\zeta m}{\sqrt{1-\zeta^2}}}$$

The logarithmic decrement is defined as the natural log of the ratio between successive peaks ( $m = 1$ ),

$$\delta = \ln \frac{u_n}{u_{n+1}} = \frac{2\pi\zeta}{\sqrt{1-\zeta^2}} \approx 2\pi\zeta$$

### 4.3 GL, ML Implicit (Real) Modal Frequency Response Analysis

#### 4.3.1 Nature of the Dynamic Loading Function

The solution method can be used to solve dynamic systems subjected to: -

- (a) **Deterministic periodic harmonic long duration** loading functions

A deterministic periodic forcing function has regularly repeating amplitude. The sine or cosine function is said to be harmonic. Because the periodic function repeats itself, any initial starting transient response is insignificant and the steady state response is of interest, hence the solution is performed in the frequency domain. The starting transient normally decays away after 50-100 cycles of oscillation for light damping. The steady-state oscillatory response occurs at the same frequency as the loading phase shifted due to damping.

**In this LINEAR FREQUENCY DOMAIN solution**, not only that the static response has to be added separately, but also the mean of the dynamic excitation has also got to be added separately as a static response. This is because the mean of the dynamically applied force is not included in the dynamic excitations. **Hence the total response in this frequency domain dynamic analysis = static response to mean of dynamic excitation + dynamic response + static response to static loads.**

#### 4.3.2 Mathematical Formulation of Analysis

In the modal frequency analysis, the solution of a particular forcing frequency is obtained through the summation of the individual modal responses. With the knowledge of the modal frequencies and corresponding mode shapes, the coupled system of simultaneous dynamic equilibrium equations can be uncoupled by premultiplying the dynamic equation of motion by  $[\Phi]^T$  as shown below. This means that the simultaneous ODEs no longer need to be solved simultaneously and so the MDOF system of equations is reduced to a SDOF system of equations, which can be solved independently of each other. The computational benefit comes from not having to run a rigorous simultaneous equation solver. The knowledge of the modal frequencies and the corresponding mode shapes are a prerequisite to this implicit modal frequency response analysis, hence the implicit real (note not complex) eigenvalue analysis must be performed first. Because of the fact that the modes are real and do not take into account the explicit elemental (structural and viscous) damping within the structure, the coupled ODEs cannot be uncoupled by  $[\Phi]^T$ . The system of coupled ODEs remains in the existence of structural and/or viscous damping and the simultaneous equation solver must be invoked. The only difference then between SOL 111 and SOL 108 is the fact that the former solves the equations in the modal coordinates instead of the physical coordinates. Hence, as long as sufficient modes are included (to represent both the static and dynamic response of the system), SOL 111 will give the same solution as SOL 108 even with large values of structural and/or viscous damping. We know that large values of elemental damping will modify the mode shape and frequencies. However, a SOL 111 can still be performed because a true (real) modal approach is not undertaken, instead the coupled ODEs are solved using a direct approach, but in the modal coordinates. However, the use of the **FREQ4** card, which bases the excitation frequencies to be solved for on the real natural frequencies may prove to be insufficient. This is because with high values of elemental viscous damping, certain local modes can be totally eliminated. For instance, viscous dampers with high coefficients of damping on cables can considerably alter the natural frequency of the local mode and even eliminate a local mode altogether. In this case, the **FREQ4** card will not capture the response at the damped natural frequency. Hence, these damped natural frequencies need to be known (by performing a SOL 107) before choosing the excitation frequencies to be solved for using **FREQ2** cards. To reiterate, SOL 111 reverts to a direct solution technique (akin to SOL 108) when there is either viscous or structural element damping as the equations of motion cannot be orthogonalized. But the unknowns are still the modal responses and not the physical responses. And because with damping the modes are really complex modes, there is greater difficulty in capturing all the response using the real modes. Hence, even more modes are thus required to capture the response accurately in SOL 111 with element damping especially if the elemental damping is high enough to cause significant complex modes. Thus if elemental damping is high and the modes are complex, the direct method SOL 108 may be more appropriate. If a true modal approach is intended for the solution of coupled ODEs with structural and/or viscous damping, then a complex modal forced frequency response analysis is necessary, although this is quite impractical.

The modal matrix from the free, undamped modal analysis is

$$[\Phi] = [\{\phi\}_1 \quad \dots \quad \{\phi\}_i \quad \dots \quad \{\phi\}_n]$$

The coupled system of ODEs of the undamped forced vibration equation of motion is

$$[M]\{\ddot{u}(t)\} + [K]\{u(t)\} = \{P(t)\}$$

In the frequency domain, let

$$\begin{aligned} \{u(t)\} &= \text{Re al} \left[ [\Phi] \{\xi(\omega)\} e^{i\omega t} \right] \text{ where } \{\xi(\omega)\} \text{ is a complex modal displacement response function vector} \\ \{P(t)\} &= \text{Re al} \left[ \{P(\omega)\} e^{i\omega t} \right] \text{ where } \{P(\omega)\} \text{ is a harmonic loading function vector} \end{aligned}$$

This transformation is worth a little explanation. The harmonic forcing function in the time domain  $P(t)$  is transformed into the frequency domain simply by multiplying

$$\{P(t)\} = \text{Re al} \left[ \{P(\omega)\} e^{i\omega t} \right]$$

$\{P(\omega)\}$  is the complex harmonic forcing function. The harmonic term is  $e^{i\omega t}$ .  $\{P(\omega)\}$  can be frequency dependent and/or can even be complex in general. If  $\{P(\omega)\}$  is complex, this refers to harmonic loading functions which are out of phase with respect to each other. We usually assume that  $\{P(\omega)\}$  is frequency independent and also just real, such that  $\{P(\omega)\} = \{p_0\}$ . The frequency domain complex forcing function  $\{P(\omega)\}$  is specified in NASTRAN with the RLOAD1 and RLOAD2 cards. The harmonic term is inferred naturally. Note that in the modal approach of the response analysis, the complex modal response is  $\xi_i(\omega)$  and that the total complex response function is  $F(\omega)$ .

$$\{F(\omega)\} = [\Phi] \{\xi(\omega)\}$$

It must be stressed that the specified frequency domain excitation is the complex harmonic forcing function  $\{P(\omega)\}$  and that the corresponding complex total response vector is  $\{F(\omega)\}$ . If  $\{P(\omega)\}$  is complex, then  $\{F(\omega)\}$  will be complex. If  $\{P(\omega)\}$  is only real, then  $\{F(\omega)\}$  will be real if there is no damping in the system but will be complex if there is damping in the system. The curves for  $\{F(\omega)\}$  versus  $\omega$  is what is produced by the NASTRAN output in a frequency domain analysis. It can be viewed in its real and imaginary components versus  $\omega$ , or in its magnitude and phase versus  $\omega$ , the latter of which is what should be observed to ascertain the response. To summarize

Frequency domain loading function from the time domain loading function

$$\{P(t)\} = \text{Re al} \left[ \{P(\omega)\} e^{i\omega t} \right]$$

where  $\{P(\omega)\}$  is the complex loading function vector

Frequency domain complex modal response to  $\{P(\omega)\}$  is

$$\{\xi(\omega)\} \text{ which is complex in general}$$

Frequency domain complex total response function vector

$$\{F(\omega)\} = [\Phi] \{\xi(\omega)\}$$

where  $\{F(\omega)\}$  is complex in general

Time domain total response from the frequency domain complex total response

$$\{u(t)\} = \text{Re al} \left[ \{F(\omega)\} e^{i\omega t} \right]$$

We have specified that

$$\{u(t)\} = \text{Re al} \left[ [\Phi] \{\xi(\omega)\} e^{i\omega t} \right]$$

This transforms the physical coordinates  $\{u(\omega)\}$  to modal coordinates  $\{\xi(\omega)\}$ . The mode shapes  $[\Phi]$  are used to transform the problem in terms of the behavior of the modes as opposed to the behavior of the grid points. This equation represents an equality if all the modes are used, but since all the modes are rarely used, the equation usually represents an approximation.

Hence, the equation for harmonic motion in terms of the modal coordinates is

$$\begin{aligned} -[M][\Phi] \{\xi(\omega)\} \omega^2 e^{i\omega t} + [K][\Phi] \{\xi(\omega)\} e^{i\omega t} &= \{P(\omega)\} e^{i\omega t} \\ -\omega^2 [M][\Phi] \{\xi(\omega)\} + [K][\Phi] \{\xi(\omega)\} &= \{P(\omega)\} \end{aligned}$$

Premultiplying by  $[\Phi]^T$  reduces the coupled system of ODEs to a system of uncoupled ODEs

$$\begin{aligned} -\omega^2 [\Phi]^T [M][\Phi] \{\xi(\omega)\} + [\Phi]^T [K][\Phi] \{\xi(\omega)\} &= [\Phi]^T \{P(\omega)\} \\ -\omega^2 [M] \{\xi(\omega)\} + [K] \{\xi(\omega)\} &= \{P(\omega)\} \end{aligned}$$

where

$$\text{the diagonal generalised (modal) mass matrix, } [M] = [\Phi]^T [M][\Phi]$$

$$\text{the diagonal generalised (modal) stiffness matrix, } [K] = [\Phi]^T [K][\Phi] = [\omega_n^2] [M]$$

$$\text{the generalised (modal) force vector, } \{P(\omega)\} = [\Phi]^T \{P(\omega)\}$$

The matrices  $[M]$  and  $[K]$  are diagonal because of the orthogonality condition of the normal modes

$$\{\phi_i\}^T [M] \{\phi_j\} = 0 \quad \text{and} \quad \{\phi_i\}^T [K] \{\phi_j\} = 0 \quad \text{if} \quad i \neq j$$

Accordingly, the generalised mass solitary term and the generalised stiffness solitary term associated with a particular mode 'i' are

$$M_i = \{\phi_i\}^T [M] \{\phi_i\} \quad \text{and} \quad K_i = \{\phi_i\}^T [K] \{\phi_i\} = \omega_{ni}^2 M_i$$

And because these matrices are diagonal, the equations become uncoupled and is easy to solve for  $\{\xi(\omega)\}$ .

Hence, the set of uncoupled SDOF systems is

$$\begin{aligned} -\omega^2 M_i \xi_i(\omega) + K_i \xi_i(\omega) &= P_i(\omega) \\ \xi_i(\omega) &= \frac{P_i(\omega)}{-\omega^2 M_i + K_i} \quad \text{for } i = 1 \text{ to } n \text{ modes} \end{aligned}$$

which is solved for the individual modal responses  $\xi_i(\omega)$ .

Finally, the total physical response is the superposition of the individual modal responses

$$\begin{aligned} \{u(t)\} &= \text{Re al} \left[ [\Phi] \{\xi(\omega)\} e^{i\omega t} \right] \\ \{u(t)\} &= \text{Re al} \left[ \{F(\omega)\} e^{i\omega t} \right] \end{aligned}$$

In modal frequency response analysis, mode truncation refers to not utilizing all the natural modes in computing the response of the structure. At a minimum all the modes that have resonant frequencies that lie within the range of the forcing frequencies have to be retained. For better accuracy, all the modes up to at least 2 to 3 times the highest forcing frequency should be retained. For example, if a structure is excited between 200 and 2000 Hz, all modes from 0 to at least 4000 Hz should be retained as the forcing frequencies still excite the higher modes although not resonating with them, i.e. off-resonant excitation. The recommendation of using modes up to 2 or 3 times the highest excitation frequency assumes that the static response can be captured adequately using this finite number of modes. Clearly, if the distribution of applied loads is multiple concentrated forces, then the finite number of modes may still not be sufficient to capture the difficult static shape. In this case, it may be prudent to use static residual vectors instead of increasing the number of vibration modes solely to capture the static response.

The following damping models are supported by the solution scheme

I.	elemental damping	
	i. viscous damping	Yes
	ii. structural damping	Yes
II.	modal damping	
	i. viscous damping	Yes
	ii. structural damping	Yes
III.	global proportional viscous damping	
	i. mass proportional damping	No
	ii. stiffness proportional damping	Yes
	iii. Rayleigh damping	No

If explicit viscous damping element contributions are made to the damping matrix  $[C]$  or if elemental structural damping is specified such that a complex stiffness matrix exists, then neither the damping nor the stiffness matrices can be diagonalized by the modal matrix. In this case the modal frequency response analysis solves the still coupled problem using a direct frequency approach but in terms of the modal coordinates  $\{\xi(\omega)\}$  instead of the physical coordinates  $\{u(t)\}$ . Since the number of modes used in a solution is typically much less than the number of physical variables, using the coupled solution of the modal equations is less costly than using physical variables. Hence, with elemental viscous and/or elemental structural damping, the coupled system of ODEs of the damped harmonically forced vibration equation of motion is given by

$$[M]\{\ddot{u}(t)\} + [C]\{\dot{u}(t)\} + [K]\{u(t)\} = \{P(t)\}$$

where

$$[K] = (1 + iG)[K] + i \sum G_E [K_E]$$

$$[C] = \sum [C_E]$$

Hence,

$$[-\omega^2 [\Phi]^T [M] [\Phi] + i\omega [\Phi]^T [C] [\Phi] + [\Phi]^T [K] [\Phi]] \{\xi(\omega)\} = [\Phi]^T \{P(\omega)\}$$

The modal frequency response analysis solves the still coupled problem using a direct frequency approach but in terms of the modal coordinates  $\{\xi(\omega)\}$  instead of the physical coordinates  $\{u(t)\}$ .

If however only viscous modal damping  $\zeta_i$  is specified, the generalized damping matrix  $[\Phi]^T [C] [\Phi]$  remains diagonal and so the uncoupled equations of motion can be maintained. The uncoupled equations of motion become

$$-\omega^2 M_i \xi_i(\omega) + i(\zeta_i 2M_i \omega_{n_i}) \omega \xi_i(\omega) + K_i \xi_i(\omega) = P_i(\omega) \quad \text{for } i = 1 \text{ to } n \text{ modes}$$

$$\xi_i(\omega) = \frac{P_i(\omega)}{-\omega^2 M_i + i(\zeta_i 2M_i \omega_{n_i}) \omega + K_i}$$

which is solved for the individual modal responses  $\xi_i(\omega)$ .

The animation of the forced frequency response is quite indicative of the nature of the response of the structure to harmonic excitations. The forced frequency response analysis will yield for each node, both real and imaginary responses. The animation of the forced response of the structure as a whole (at any particular frequency of excitation) is only of value when we plot the magnitude of the response, and not the individual real or imaginary components. The phase information (which is obtained when the magnitude and argument of the real and imaginary components are obtained) is essential in order to determine the relative phase of the motion of different parts of the structure. Explicit viscous dampers will cause parts of the structure to vibrate clearly out-of-phase.

If only structural modal damping  $G_i$  is specified, modal damping is processed as a complex stiffness of each individual mode and so the uncoupled equations of motion can still be maintained. The uncoupled equations of motion become

$$-\omega^2 M_i \xi_i(\omega) + (1 + iG_i(\omega)) K_i \xi_i(\omega) = P_i(\omega) \quad \text{for } i = 1 \text{ to } n \text{ modes}$$

$$\xi_i(\omega) = \frac{P_i(\omega)}{-\omega^2 M_i + (1 + iG_i(\omega)) K_i}$$

which is solved for the individual modal responses  $\xi_i(\omega)$ .

It is important to know how to convert between structural damping and equivalent viscous damping for a particular mode. For a particular mode,

$$\begin{aligned} \text{Viscous damping, } F_{\text{viscous}} &= \zeta_i (\text{critical damping}) (\text{modal velocity}) \\ &= \zeta_i (2M_i \omega_{ni}) (i\omega \xi_i \{\phi_i\}) \end{aligned}$$

$$\text{Structural damping, } F_{\text{structural}} = iG_i K_i \xi_i \{\phi_i\}$$

For the two forms to be equal,  $F_{\text{viscous}} = F_{\text{structural}}$

$$\zeta_i (2M_i \omega_{ni}) (i\omega \xi_i \{\phi_i\}) = iG_i K_i \xi_i \{\phi_i\}$$

In the special case that  $\omega = \omega_{ni}$

$$\begin{aligned} \zeta_i (2M_i \omega_{ni}^2) &= G_i K_i \\ \zeta_i (2M_i K_i / M_i) &= G_i K_i \\ 2\zeta_i &= G_i \end{aligned}$$

Hence, the relationship  $G_i = 2\zeta_i$  can be used to specify an equivalent viscous damping for structural damping, but is only exact when the forcing frequency  $\omega =$  the natural modal frequency  $\omega_{ni}$  which occurs at resonance, i.e. when damping is of primary importance.

The complex response function due to a loading  $\{P(\omega)\}$  is defined as

$$\{F(\omega)\} = \frac{\{P(\omega)\}}{-\omega^2 [M] + i\omega [C] + [K]}$$

The complex transfer function is defined as the complex frequency response function due to unit harmonic excitations

$$[H(\omega)] = \frac{1}{-\omega^2 [M] + i\omega [C] + [K]}$$

This is the so-called *transfer function* that transfers the excitation to the response as follows

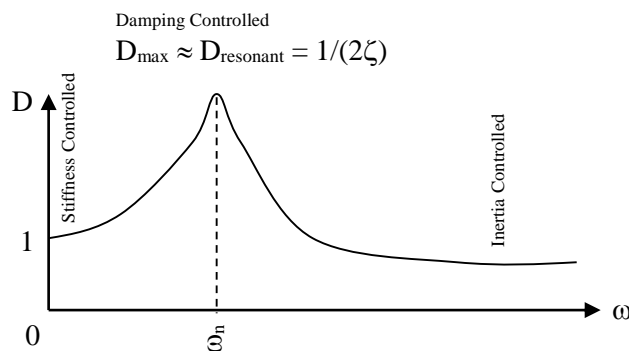
$$\{u(t)\} = \text{Re al} \left[ [H(\omega)] \{P(\omega)\} e^{i\omega t} \right]$$

The (magnitude of the) dynamic amplification function  $D(\omega)$  is defined as the magnitude of the complex response function  $\{F(\omega)\}$  divided by the static displacement.

### 4.3.3 Capability of A Finite Number of Modes To Model The Static and Dynamic Response of Structure

When running a modal based dynamic response analysis, it is imperative to know if the chosen number of modes within the modal dynamic analysis is capable of representing both the static and dynamic response of the structure. **First and foremost, the chosen modes must cover and extend beyond the excitation frequency range such that both the resonant response of the modes within the range and the off-resonant response of the modes beyond (from say a 1/3<sup>rd</sup> of lowest excitation frequency to 3x the highest excitation frequency) the range are captured. This will sufficiently model the dynamic response. Considerations then must be made for the finite number of modes to capture the static response.**

It is often said in dynamic analyses that if the chosen finite number of modes are capable of representing the static response, then they will usually also be able to represent the dynamic response of the structure. We shall consider the frequency domain as this enables us to plot the FRF (and hence of course also the transfer function and the dynamic amplification function). Let us picture the (magnitude of the) dynamic magnification function, here shown below for a single mode, i.e. a SDOF system.



The finite number of modes should be able to represent the true static displacement at zero excitation frequency and the maximum (magnitude of the) dynamic amplification. Obtaining just the correct maximum (magnitude of the) dynamic amplification is not proof that the chosen finite number of modes is sufficient. This is because the response  $D(\omega)$  at the frequency corresponding to the maximum dynamic response is controlled only by the damping within the structure. Note that the corresponding value  $F(\omega)$  is also a function of the modal stiffness (or modal mass), the natural frequency and the (amplitude of the) modal force. Hence if the static response is inaccurate, so will be the dynamic response. Thus it is best to compare the response function  $F(\omega)$  between the modal model and the full MDOF model.

To compare individual components of the modal model, the following approach is undertaken. First, the accuracy of the stiffness representation is investigated. This corresponds to the static displacement. When the excitation frequency is zero, if the modal approach with SOL 111 achieves the same  $F(\omega)$  response as that from a static analysis SOL 101, then the chosen finite modes are capable of representing the stiffness within the system and hence are capable of modelling the static response for the system. The mathematics of converting the static equilibrium equations in physical coordinates to equations in modal coordinates (and hence with a certain degree of modal truncation unless the number of modal coordinates equals the number of physical coordinates) is presented in **Section 3.1.4**.

Thereafter, the damping representation is evaluated by comparing the response  $F(\omega)$  at the frequency of maximum amplification. Finally, the inertial representation is evaluated by comparing the response  $F(\omega)$  at high excitation frequencies. If the responses obtained from the modal approach when the excitation frequency is off-resonant is similar to that obtained from the multi degree of freedom model, then the chosen finite number of modes are capable also of modelling the mass and stiffness distribution within the system.

Hence, in order to quantitatively decide whether the chosen number of finite modes is capable of representing a multi degree of freedom system the response between a direct solution SOL 108 and the modal solution SOL 111 is compared. The complex frequency response function  $F(\omega)$  can be plotted for the response at the DOF of interest from both a SOL 108 and a SOL 111. A XYPLOT showing the contribution of individual modal responses  $F(\omega)$  superposed on a plot containing the total physical response is most useful in visually determining the contribution of each and every mode to the static and dynamic response at particular frequencies of excitation. In MSC.NASTRAN, it is possible to plot the response function  $F(\omega)$  for individual natural modes using SOL 111 (even if there is structural and/or viscous damping as SOL 111 then performs a coupled ODE solution process, but with the unknowns as the modal responses instead of the physical responses) by delimiting the mode calculated using EIGRL or using LFREQ (lower limit of the frequency range), HFREQ (upper limit of the frequency range) or LMODES (number of lowest modes retained). Alternatively, selective modes which are not sequential can be deleted by the user by using the alter delmodea.v2001 and the associated bulk data entry DMI. The degree of similarity between the two traces is an indication of the ability of the finite number of modes to represent the response of the system. The number of modes should be increased or decreased accordingly. Note that the static response at zero excitation frequency obtained from both SOL 111 and SOL 108 can be compared with the true static solution from a SOL 101. It will be found that SOL 108 will yield the same static response as SOL 101 (when there is no structural damping within the finite element model) whilst SOL 111 will yield a result that is lower due to the nature of the finite number of modes presenting a stiffer response. Incidentally, since SOL 108 does not allow the automatic specification of the frequency points to correspond to the natural frequencies of the structure, the user would have to perform a SOL 103 and manually specify to increase the resolution near the vicinity of the natural frequencies.

It is essential that the sufficient modes be incorporated when derived quantities are intended. For instance, to evaluate the modal damping of a particular mode, both the static response and the dynamic response must be accurately represented. If the static response is not sufficiently captured, then the dynamic response will not be accurate either as the response of the  $FRF = P/K$  times  $D(\omega)$ . If the distribution of the excitation force is concentrated at multiple points, then it is likely that the difficult static shape requires many modes of vibration. In this case, it may be better to utilize static residual vectors to capture the response more directly. Alternatively of course, the direct frequency approach SOL 108 may be used, in which case the static response and the dynamic response of all modes are automatically captured, but it requires effort in capturing the peak response (by requesting fine frequency intervals near the peaks). But when using the modal method, damping estimates using the half power bandwidth on the FRF of the  $D(\omega)$  or using  $1/(2\zeta)$  on the  $D(\omega)$  depend on the capability of the modes to accurately represent the static and dynamic response. Where in doubt, use a SOL 101 solution to check the static response. And a SOL 107 solution should be used to check the modal damping estimates.

The relative contribution of each mode to the total static and dynamic response can also be determined. This is known as the modal responses, i.e. the value of the modal variables in the modal solution scheme. The Case Control Cards SDISP, SVELO and SACCE will produce the modal solution set output,  $\{\xi_i(\omega)\}$ . These are plots of the modal response (for each mode) in terms of frequency of excitation, i.e. the frequency domain modal response. That is to say, SDISP(PUNCH) (or SVELO or SACCE) will output one value for each mode at each excitation frequency. These are the modal responses in **modal space**. They must be multiplied by the corresponding mode shapes in order to obtain the modal responses in **physical space** i.e.

$$\{F_i(\omega)\} = \{\phi_i\}\xi_i(\omega)$$

Another method of determining the modal contribution of individual modes to a particular excitation is by using the modal strain energy. Firstly, to evaluate the ability of the natural modes to represent the static response, a SOL 101 is run with the amplitude of the dynamic loads applied as a static load and the results are written to a DMIG file using the alter pchdispa.v2001. Then a SOL 103 is run with the DMIG included and also the alter modevala.v2001 to ascertain how well each and every mode can represent the static solution. The strain energy for each mode can be compared to the strain energy in all the modes calculated and also the input vector. Note that the eigenvector scaling must be set to the default MASS (not MAX) for this alter to be valid. Secondly, to evaluate the ability of the natural modes to represent the dynamic response, the alter mfreqa.v2001 is utilized for SOL 111. The results are presented in a matrix of strain energies with the rows representing the excitation frequencies and the columns

representing the natural modes. The frequency interval between the rows and between the columns corresponds to the excitation frequency interval and the natural mode frequency interval. Of course, the dominant modes that represent the static response is not necessarily the same as the dominant modes that represent the dynamic response at different excitation frequencies. This is simply because the dynamic response is also a function of the loading frequency and resonance frequency, on top of the static response. Including the dominant modes that represent the static response will however improve the accuracy of representing the dynamic response  $F(\omega)$  as it is the function of the amplification  $D(\omega)$  and the static response  $P/K$ .

Note that the capability of a finite number of modes to represent the static and dynamic response of the structure is **limited to a particular force excitation direction and distribution**. If the force changes its location or direction, then the prominence of the different modes which will be different. This is simply because changing the location or direction of the force will cause a different set of modal forces and hence a different level of excitation of the different modes. The capability of a finite number of modes to represent the static and dynamic response of the structure depends also on the level of elemental structural and elemental viscous damping present within the system. This is because, the level of elemental damping affects the complexity of the modes, hence possibly requiring more real modes if the modal complexity is high. Thus damping should be included when performing the study to determine the required number of modes.

For accurate results of modal methods, **static residual vectors (PARAM, RESVEC, YES)** can be calculated except when using the seismic large mass method for enforced motion. The residual vector method is more efficient than the mode acceleration method and can be applied to both superelements and the residual structure when substructuring is employed. Clearly though, there should be sufficient modes comfortably beyond within the excitation frequency bandwidth to capture the dynamic response, and the static residual vectors should only be used as a final step to append the quasi-static responses of high frequency (relative to the excitation frequencies) modes.

Note that SOL 111 reverts to a direct solution technique (akin to SOL 108) when there is either viscous or structural element damping as the equations of motion cannot be orthogonalized. But the unknowns are still the modal responses and not the physical responses. And because with damping the modes are really complex modes, there is greater difficulty in capturing all the response using the real modes. Hence, even more modes are thus required to capture the response accurately in SOL 111 with element damping especially if the elemental damping is high enough to cause significant complex modes. Thus if elemental damping is high and the modes are complex, the direct method SOL 108 may be more appropriate.

Another method of determining the adequacy of the finite number of modes is to evaluate the **cumulative effective mass** of the chosen number of modes. The effective mass has got a specific meaning in seismic analysis, but can be used for other dynamic analyses as well as a measure of determining the adequacies of the finite number of modes. A cumulative effective mass that approaches unity suggests adequacy of the chosen modes to model the **spatial distribution** of the loading. This parameter of course does not say much about the adequacy of the chosen modes to model the **frequency content of the loading**. Essentially, and to reiterate, the chosen number of modes must be sufficient to model both the **frequency content** and also the **spatial distribution** of the loading. It is found that for a high cumulative effective mass, uniformly distributed loads such as in seismic analyses require only a few modes whereas a concentrated patch requires more modes and finally a highly concentrated load requires a much greater number of modes to capture the effect of the spatial distribution of the loading.

#### 4.3.4 Complex Response $F(\omega)$ and Amplification $D(\omega)$ With Elemental and/or Modal Structural Damping

The response at zero excitation frequency from a forced frequency response analysis (SOL 111 or SOL 108) will not be equal to the true static response (from a SOL 101 solution) if there is elemental or modal structural damping within the model. Intuitively, we know this to be true simply due to the fact that structural damping is independent of forcing frequency. Hence, there is no reason for it to be zero at an excitation frequency of zero. We shall illustrate this mathematically for modal structural damping although the same concept applies when there exist elemental structural damping. We know that the (magnitude of the) dynamic amplification factor for a mode when there is modal viscous damping is

$$D_i(\omega) = \frac{1}{\sqrt{\left(1 - \omega^2 / \omega_{ni}^2\right)^2 + \left(2\zeta_i \omega / \omega_{ni}\right)^2}}$$

If however we have modal structural damping, the modal equation of motion will be

$$-\omega^2 M_i \xi_i(\omega) + i(\zeta_i 2M_i \omega_{ni}) \omega \xi_i(\omega) + (1 + iG_i) K_i \xi_i(\omega) = P_i(\omega)$$

$$\xi_i(\omega) = \frac{P_i(\omega)}{-\omega^2 M_i + i(\zeta_i 2M_i \omega_{ni}) \omega + (1 + iG_i) K_i}$$

$$\xi_i(\omega) = \frac{P_i(\omega)}{-\omega^2 M_i + i(C_i \omega + G_i K_i) + K_i}$$

By complex arithmetic, we arrive to

$$\xi_i(\omega) = \frac{P_i(\omega) / K_i}{\sqrt{\left(1 - \omega^2 / \omega_{ni}^2\right)^2 + \left(G_i K_i + 2\zeta_i \omega / \omega_{ni}\right)^2}} e^{-i\theta_i}$$

And hence the (magnitude of the) modal dynamic amplification factor will be

$$D_i(\omega) = \frac{1}{\sqrt{\left(1 - \omega^2 / \omega_{ni}^2\right)^2 + \left(G_i K_i + 2\zeta_i \omega / \omega_{ni}\right)^2}}$$

At zero excitation frequency, the (magnitude of the) dynamic amplification is thus not unity, but instead

$$D_i(\omega) = \frac{1}{\sqrt{1 + \left(G_i K_i\right)^2}}$$

As an aside, the (magnitude of the) dynamic amplification at resonance is

$$D_i(\omega) = \frac{1}{G_i K_i + 2\zeta_i}$$

Thus, in general, with structural damping, the amplification at zero frequency is less than one simply due to the nature of structural damping being independent of excitation frequency. This should obviously not be the case for a true static solution since the static response is independent of damping. Hence, the response obtained at zero frequency from a forced response analysis of a system with structural damping is not the true static solution. This means that in order to derive the (magnitude of the) dynamic amplification function in a model with structural damping, it is necessary to perform a static solution SOL 101 to ascertain the actual static displacement and then divide the magnitude of the complex response function  $F(\omega)$  from a SOL 108 solution by this value.

#### 4.3.5 Representation of A MDOF System As A SDOF system

A SDOF dynamic model is represented by a modal mass  $M$ , modal stiffness and modal damping. This SDOF model can even be modeled as a mass attached to a parallel spring and damper although hand calculations are sufficient to predict the response of a SDOF system exactly. The natural frequency is a function of the modal mass and modal stiffness. The modal masses, modal stiffnesses (or natural frequencies) of a MDOF system can be obtained from a real eigenvalue analysis SOL 103 or a back calculation from a SOL 111 analysis. The modal damping can be obtained from a complex modal analysis SOL 107.

It will be shown that modes with small values of modal damping can be approximated simply as real modes (without its imaginary component). Hence, a real modal mass can be used. If however, the mode includes large values of modal damping, its complex modal mass must be evaluated and subsequently a complex modal forced response analysis must ensue.

#### Estimation of Real Modal Mass From A Forced Frequency Response Analysis Back-Calculation On A System Without Any Form of Damping

This procedure is shown just to illustrate the dynamic response function. It is certainly as easy to obtain the modal mass from a real eigenvalue analysis. To determine the modal mass from a forced response back-calculation, the following procedure is undertaken. We know that

$$F(\omega) = \frac{P}{K} D(\omega)$$

$$\text{Hence, the static displacement} = \frac{P}{K} = \frac{P}{\omega^2 M}$$

In order to compute the modal mass from a back-calculation of the forced response analysis, a SOL 111 should be performed with EIGRL limiting the calculated modes to only that being considered. Then the relationship above can be used to estimate the modal mass. Note that the static displacement obtained will be due only to the eigenvector being considered. The modal mass obtained using this method will correspond exactly to that calculated from

$$\text{Modal Mass, } M_i = \{\phi_i\}^T [M] \{\phi_i\}$$

#### Modal Mass of Modes With Small Values of Damping

We know that

$$F(\omega) = \frac{P}{K} D(\omega)$$

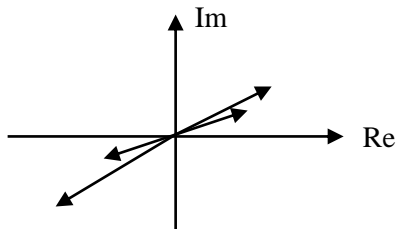
$$\text{Hence, the static displacement} = \frac{P}{K} = \frac{P}{\omega^2 M}$$

This shows that the modal mass is a function of the static displacement and not the (magnitude of the) dynamic amplification at resonance. At resonance, only damping controls the (magnitude of the) dynamic amplification response  $D(\omega)$  of the structure. It is however, not true to say that the dynamic response  $F(\omega)$  is controlled just by damping as it is also a function of the modal stiffness (or modal mass). At off-resonant frequencies stiffness, damping and inertia effects become prominent. The static displacement of the structure with or without damping in reality will be the same as long as elemental damping does not significantly alter the mode shape. At zero frequency of excitation, damping in reality does not affect the response because there are no dynamic effects. Hence, from the equation above, it becomes apparent that the modal mass  $M$  does not change as long as the natural frequency of the mode does not change significantly. As a rule, as long as the mode shapes and the natural

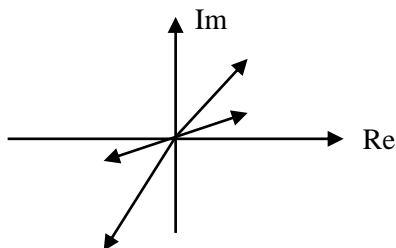
frequency does not change too much with explicit damping elements (the mode shapes will not change with other forms of damping, such as modal damping; note that the frequency does not change much unless the modal damping values are very high), then the modal mass will stay unchanged. This could be an argument to prove that the modal mass for a mode of a system with low values of damping stays unchanged from the same mode without damping, which is readily obtainable from a SOL 103 solution.

### Modal Mass of Modes With Large Values of Damping

However, how do we obtain the modal mass from a complex mode if the eigenvector changes considerably from that without explicit element dampers? A pure real mode has all its terms in phase with each other. Different modes will of course be out of phase with each other, but every point in a particular mode will vibrate in phase. And so, for a mode, all points in the structure reach its maximum and minimum at the same phase instant. A complex mode on the other hand will have different points of the structure reaching its maximum at different phase instants, i.e. different points of the structure are out of phase with each other for a particular mode. Of course, different modes are still out of phase with each other. The degree to which these points are out of phase with each other is a measure of the complexity of the mode. An Argand diagram with all the terms of the complex eigenvector plotted will exhibit a narrowband if the mode is only slightly complex. The diagram below shows plots for 4 eigenvector terms. Since there is only a slight phase difference between the terms (angle between the arrows), the 4 terms define an almost real complex eigenvector.



The following eigenvector plot on the other hand is highly complex because of the large phase angle difference between the terms of the eigenvector.



The eigenvectors of cable elements for instance can change considerably when explicit dampers with high coefficients are placed onto them. Then the modal damping values can become very high (such as even 15 to 20% of critical). If this occurs, the real modal mass is a poor representation of the mode. Instead, a complex modal mass must be evaluated. Hence, a real modal approach should thus not be used in this case. Instead a (rather mathematically involved) complex modal forced response analysis is required. Alternatively, a full MDOF analyses should be undertaken to investigate the response.

SOL 111 reverts to a direct solution technique (akin to SOL 108) when there is either viscous or structural element damping as the equations of motion cannot be orthogonalized. But the unknowns are still the modal responses and not the physical responses. And because with damping the modes are really complex modes, there is greater difficulty in capturing all the response using the real modes. Hence, even more modes are thus required to capture the response accurately in SOL 111 with element damping. Thus if elemental damping is high, the direct method SOL 108 may be more appropriate.

### 4.3.6 MSC.NASTRAN Decks

#### 4.3.6.1 GL, ML Modal Forced Frequency Response Analysis

<b>\$ EXECUTIVE CONTROL SECTION</b>									
SOL 111									
<b>\$ CASE CONTROL SECTION</b>									
<b>\$ Sets defining grid ids or element ids</b>									
SET < Number > = 1 THRU 100, 211, 343, < etc >									
<b>\$ Grid output of displacement, velocity and acceleration for excitation frequencies</b>									
<b>\$ SORT1 lists the results by frequency whilst SORT2 lists the results by grid id</b>									
DISPLACEMENT (<SORT1/SORT2>,<PRINT,PUNCH,PLOT>,<REAL/PHASE>) = ALL/<Grid Set ID>									
VELOCITY (<SORT1/SORT2>,<PRINT,PUNCH,PLOT>,<REAL/PHASE>) = ALL/<Grid Set ID>									
ACCELERATION (<SORT1/SORT2>,<PRINT,PUNCH,PLOT>,<REAL/PHASE>) = ALL/<Grid Set ID>									
<b>\$ Grid output of applied load vector</b>									
OLOAD (<SORT1/SORT2>,<PRINT,PUNCH,PLOT>,<REAL/PHASE>) = ALL/<Grid Set ID>									
<b>\$ Grid output of modal responses (in modal space)</b>									
SDISPLACEMENT (<SORT1/SORT2>,<PRINT,PUNCH>,<REAL/PHASE>) = ALL/< Mode Number >									
SVELOCITY (<SORT1/SORT2>,<PRINT,PUNCH>,<REAL/PHASE>) = ALL/< Mode Number >									
SACCELERATION (<SORT1/SORT2>,<PRINT,PUNCH>,<REAL/PHASE>) = ALL/< Mode Number >									
<b>\$ Grid output of real eigenvector for the a-set</b>									
SVECTOR (<PRINT,PUNCH>) = ALL/<Grid Set ID>									
<b>\$ Grid output of SPC forces</b>									
SPCFORCES (<SORT1/SORT2>,<PRINT,PUNCH,PLOT>,<REAL/PHASE>) = ALL/<Grid Set ID>									
<b>\$ Element output of force, stress and strain</b>									
ELFORCE (<SORT1/SORT2>,<PRINT,PUNCH,PLOT>,<REAL/PHASE>) = ALL/<Element Set ID>									
ELSTRESS (<SORT1/SORT2>,<PRINT,PUNCH,PLOT>,<REAL/PHASE>) = ALL/<Element Set ID>									
STRAIN (<SORT1/SORT2>,<PRINT,PUNCH,PLOT>,<REAL/PHASE>) = ALL/<Element Set ID>									
<b>\$ Analysis Cards</b>									
SPC = < ID of SPC Cards Defined in Bulk Data >									
METHOD = < ID IN EIGRL >									
FREQUENCY = < ID OF FREQ <sub>i</sub> >									
<b>\$ XY plot output</b>									
OUTPUT (XYPLOT)									
XYPUNCH < DISP/VELO/ACCE > RESPONSE < subcase > / < Grid ID > (< T1/T2/T3 > < RM/IP >)									
XYPUNCH < SDISP/SVELO/SACCE > RESPONSE < subcase > / < Grid ID > (< T1/T2/T3 > < RM/IP >)									
XYPUNCH < ELFORCE/ELSTRESS/STRAIN > RESPONSE < subcase > / < Element ID > (< Code Number >)									
<b>\$ BULK DATA</b>									
EIGRL	ID	Lower Frequency (Hz)	Upper Frequency (Hz)	Number of Eigenvalues				Eigenvalue Normalization Method	
FREQ1	ID	f <sub>start</sub>	Δf	Number of Δf					
FREQ4	ID	f <sub>lower bound</sub>	f <sub>upper bound</sub>	FSPD	NFM				

All FREQ<sub>i</sub> entries with the same selected ID, selected by the FREQUENCY entry in the Case Control Section, will be combined. The **FREQ1** bulk data entry selects the frequencies at which the frequency response analysis is performed. It is important to specify a fine enough frequency step size Δf to adequately predict peak response. Use at least five to ten points across the half-power bandwidth. For maximum efficiency, an uneven frequency step size should be used. Smaller frequency spacing should be used in regions near resonant frequencies, and larger frequency step sizes should be used in regions away from resonant frequencies. **FREQ4** defines a frequency spread FSPD for each and every normal mode that occurs within the bounds of the frequency range with NFM evenly

spaced frequencies per spread. Hence, to choose 11 equally spaced frequencies across a frequency band of  $0.7f_n$  to  $1.3f_n$  for each natural frequency within  $f_{\text{lower bound}}$  and  $f_{\text{upper bound}}$ ,  $FSPD = 0.30$  and  $NFM = 11$ . The spread should definitely be greater than the half-power bandwidth, which for a SDOF system is approximately  $2\zeta f_n$  because  $\zeta \approx (f_2 - f_1)/2f_n$  hence the spread  $f_2 - f_1 \approx 2\zeta f_n$ .

**FREQ3** specifies excitation frequencies in the range between two modal frequencies. The increments between excitation frequencies are calculated linearly or logarithmically. These frequencies may be clustered towards the end points of the range or towards the center by specifying a cluster parameter.

Printed .f06 frequency response output can be in SORT1 or SORT2 format. In the SORT1 format, the results are listed by frequency i.e. for each frequency the results of all grid points are given, whilst in the SORT2 format, the results are listed by grid point i.e. for each grid point the results of all frequencies are given. In the modal frequency response analysis, PARAM, CURVPLOT, 1 and PARAM, DDRMM, -1 are required to obtain SORT1 output. To define frequency frozen structural plots,

<b>\$ CASE CONTROL SECTION</b>
DISPLACEMENT (PLOT, PHASE) =ALL
<b>\$ BULK DATA</b>
PARAM, DDRMM, -1 PARAM, CURVPLOT, 1

For each frequency of excitation, the magnitude of the response at each and every point in the structure is animated with the phase information. It is meaningless and impossible to plot the real and imaginary components, as the animation requires the phase difference between different points in the structure. It is prudent to limit the frequencies of excitation so as to limit the amount of output.

#### 4.3.6.1.1 Applied Load Excitations

Applied load excitations are as described in direct forced frequency response analysis.

#### 4.3.6.1.2 Enforced Motion

Enforced motion is as described in direct forced frequency response analysis.

#### 4.3.6.1.3 Damping

Viscous and structural modal damping is defined as follows. TYPE refers to the type of damping units, i.e. whether structural damping G (default), critical damping CRIT or quality factor Q. The values of  $f_i$  and  $g_i$  define pairs of frequencies and damping. Straight-line interpolation is used for modal frequencies between consecutive  $f_i$  values. Linear extrapolation is used for modal frequencies outside the entered range. ENDT ends the table input. If PARAM, KDAMP, 1 then the modal damping is processed as critical damping and if PARAM, KDAMP, -1 then the modal damping is processed as structural damping, NASTRAN internally making use of  $\zeta_i = G_i/2$  and  $Q_i = 1/G_i$  to convert to the required coefficient from that specified by TYPE.

<b>\$ CASE CONTROL SECTION</b>									
SDAMPING = < ID IN TABDMP1 >									
<b>\$ BULK DATA</b>									
PARAM, KDAMP, 1 \$ modal damping processed as critical damping									
PARAM, KDAMP, -1 \$ modal damping processed as structural damping, complex stiffness									
TABDMP1	ID	TYPE							
	f1	g1	f2	g2	F3	g3	f4	g4	
	f5	g5	f6	g6	...	...	ENDT		

### 4.3.6.2 GL, ML P- $\Delta$ ( $K_G^A$ From $K_E^A$ ) Modal Forced Frequency Response Analysis

It is often necessary to incorporate the reduction in bending stiffness of gravity load resisting columns for the analysis of lateral loads. The following procedure is undertaken.

#### Phase 1

Perform static analysis (with loads that cause the greatest negative or positive geometric stiffness) based on  $[K_E^A]$  but include the segyroa.v2001 alter prior to the Case Control Section in order to compute the geometric stiffness matrix  $[K_G^A]_1$  (and output into a .pch file) based on the generated element loads from the  $[K_E^A]$  static analysis.

#### Phase 2

A SOL 111 is undertaken based on  $[K_E^A] + [K_G^A]_1$  with the k2gg=ktjj statement in the Case Control Section and the outputted .pch file which contains the ktjj matrix in the Bulk Data. The responses at this stage represent the P- $\Delta$  ( $K_G^A$  From  $K_E^A$ ) response to the dynamic excitation.

The following equivalent alternative procedure can also be employed.

<pre> \$ CASE CONTROL SECTION  SUBCASE 1 LABEL = Static Preload Load Case LOAD = &lt; ID of FORCEi, MOMENTi, PLOADi, GRAV, LOAD, SPCD Cards in Bulk Data &gt; TEMP(Load) = &lt; ID of TEMP, TEMPRB, TEMPP1 Cards in Bulk Data &gt; DEFORM = &lt; ID of DEFORM Cards in Bulk Data &gt; SUBCASE 2 LABEL = P-<math>\Delta</math> Modal Frequency Response Analysis STATSUB(PRELOAD) = 1 DLOAD = &lt; ID OF RLOAD1 or RLOAD2 &gt;                 </pre>
--

The method is valid when **only the prestress is judged to affect the geometric stiffness** such as in the compressive preload of building columns due to gravitational loads and the prestressing of extremely taut cables that sag very little under gravity but not in systems such as suspension bridges. Where lateral loads are large enough to affect the geometry of the system with prestress, then a repetitive P- $\Delta$ , SOL 106, implicit dynamic relaxation SOL 129 or explicit dynamic relaxation must be employed. But in single P- $\Delta$  analysis, because cables do not have much elastic bending stiffness, the initial static preload subcase should only include the prestress and not gravity as including gravity is the same as solving two linear static problems of stiffness  $K_E^A$  with preload and gravity as the applied loads respectively. Clearly, in the gravity case, it is nonsensical as the cables do in reality have differential stiffness (from the prestress) to resist the gravitational force. Prestress in one direction (i.e. along the axis of cable) will cause a differential stiffness in the orthogonal direction. Gravity acts in the orthogonal direction and hence cannot be accounted for in the calculation of the prestress in this single P- $\Delta$  analysis. To quantitatively decide if gravity need not be considered in contributing to the differential stiffness of the cables, a static P- $\Delta$  analysis should be carried out, the first subcase being a SOL 101 with only the prestress as applied loads and the second subcase a P- $\Delta$  SOL 101 (i.e. utilizing the induced prestress from the first subcase to form a geometric stiffness matrix) with both the gravity and prestress included as applied loads. If the difference in the cable element forces between subcases 1 and 2 is negligible, then gravity has little influence in affecting the geometric stiffness. If there is a major difference in the cable element force, then clearly, gravity will affect the geometric stiffness and as such, a repetitive P- $\Delta$ , SOL 106, implicit dynamic relaxation or explicit dynamic relaxation must be used to converge to the true  $K_T$ . Likewise, in the single P- $\Delta$  analysis of multi-storey buildings, gravity (and only gravity) acts in axis of columns to generate prestress, and the differential stiffness is computed for the orthogonal direction reducing resistance to lateral wind forces, applied in the second subcase with gravity too.

When a static subcase is specified for linear transient response analysis (SOLs 109 and 112) with STATSUB(PRELOAD), the data recovery is controlled by PARAM, ADSTAT. By default (YES) the static solution will be superimposed on the dynamic response solution (displacement, stress and SPCForce). The relative solution can be obtained in reference to the static solution point by PARAM, ADSTAT, NO. No provision is made for frequency response analysis, because the static responses contribute only to the zero frequency response.

The STATSUB(PRELOAD) computes the differential stiffness due to the prestress and also the follower force. The follower force is calculated and incorporated by the use of PARAM, FOLLOWK, YES. We know how the prestress affects the differential stiffness, namely a tensile prestress causing an increase in stiffness. The effect of the follower force on the stiffness is different. For example, for a cylinder under external pressure critical buckling load may be over-estimated (even though the mode shapes are similar) in a SOL 105 and the natural frequencies in vibration may be under-estimated (even though the mode shapes are similar) in a SOL 103 in the absence of follower stiffness. To the contrary, these observations are reversed in case of centrifugal loads. Centrifugal forces as a constant (static) load are applied by a Bulk Data RFORCE to any elements that have masses. The follower stiffness due to centrifugal load has the effect of lowering stiffness (although the centrifugal load tensioning effect increases stiffness), consequently lowering natural frequencies (even though the mode shapes are similar) in a SOL 103 and lowering the buckling loads (even though the mode shapes are similar) in a SOL 105. This effect increases as the RPM increases, and it becomes significant when the RPM is over 1000. For moderately geometric nonlinear analysis, exclusion of follower stiffness affects the rate of convergence, but the converged solution is correct. For severely geometric nonlinear analysis, it may not be possible to obtain a converged solution without including follower stiffness. As the geometric nonlinearity intensifies, so is the effect of follower stiffness. Therefore, inclusion of follower stiffness greatly enhances the convergence if the deformation involves severe geometric nonlinearity.

### 4.3.6.3 GL, ML P- $\Delta$ ( $K_G^A$ From Exact or Approximate $K_T^A$ ) Modal Forced Frequency Response Analysis

It is often necessary to include the differential stiffness, especially if there are prestressed cables in the model. To obtain  $K_T^A$ , to be theoretically exact, a GNL SOL 106 (or implicit dynamic relaxation SOL 129 or explicit dynamic relaxation LS-DYNA) with prestress (as temperature loads say) and gravity must be undertaken. Alternatively, an approximation to  $K_T^A$  can be obtained by repetitive P- $\Delta$  static analyses with the prestress (as temperature loads say) and gravity applied. The procedure to obtain this approximate  $K_T^A$  will be presented. Note that the approximate  $K_T^A$  will be the summation of the elastic stiffness  $K_E$  at the undeflected (by the prestress and gravity) state but  $K_G$  at the deflected (by the prestress and gravity) state. Hence if  $K_E$  changes considerably during the application of the prestress, a full SOL 106 (or implicit dynamic relaxation SOL 129 or explicit dynamic relaxation LS-DYNA), which converges to the  $K_E$  and  $K_G$  at the deflected (by the prestress and gravity) state should be employed. Hence for the modelling of a suspension bridge where there is a great change in geometry (known in the bridge industry as **form-finding**, so-called because it is necessary to find the form or shape of the catenary suspension cables), it may be prudent to employ SOL 106 (or implicit dynamic relaxation SOL 129 or explicit dynamic relaxation LS-DYNA), but for a high tension low sag cable on say a tower with prestressed cables, the repetitive P- $\Delta$  static analysis may be adequate. The repetitive P- $\Delta$  analysis basically involves a number of iterations of linear static analyses to obtain an approximate  $K_T^A$ . Note again that A refers to the initial undeflected (by the collapsing load) state, but deflected by the prestress and gravity. To perform the repetitive P- $\Delta$  analysis, a static analysis is performed based on  $K_E^A$  with temperature loads and gravity to generate forces in the structural elements, which in turn provides input for the computation of  $K_{Gi}^{AKT_m}$  where m is the iterations. Repetitive static analysis is performed with the prestress and gravity updating the stiffness matrix  $K_E^A + K_{Gi}^{AKT_{m-1}} + K_{Gi}^{AKT_m}$  until convergence of displacements is obtained. The tangent stiffness at this stage is the approximate converged tangent stiffness matrix  $K_T^A = K_E^A + K_{Gi}^{AKT}$ . The converged displacements represent the approximate P- $\Delta$  ( $K_G^A$  From Approximate  $K_T^A$ ) static response to the initial prestress loads. The converged geometric stiffness at this stage would be that based upon the approximate tangent stiffness matrix  $K_T^A$ , i.e.  $K_{Gi}^{AKT}$ .

#### Phase 1

Perform static analysis (with prestress and gravity) based on  $[K_E^A]$  but include the segyroa.v2001 alter prior to the Case Control Section in order to compute the geometric stiffness matrix  $[K_G^A]_1$  (and output into a .pch file) based on the generated element loads from the  $[K_E^A]$  static analysis.

#### Phase 2

Perform static analysis (with prestress and gravity) based on  $[K_E^A] + [K_G^A]_1$  by including the k2gg = ktjj statement in the Case Control Section, the outputted .pch file which contains the ktjj matrix in the Bulk Data and the segyroa.v2001 alter prior to the Case Control Section to compute the  $[K_G^A]_2$  (and output into the .pch file overwriting previous data) based on the generated element loads from the  $[K_E^A] + [K_G^A]_1$  static analysis.

#### Phase 3

Repeatedly perform the Phase 2 static analysis (with prestress and gravity) based on  $[K_E^A] + [K_G^A]_i$  for  $i = 2$  to  $n$  where  $n$  represents the number of iterations required for the change in deflections between analyses to become negligible. This would signify that the change in the  $[K_G^A]$  matrix become negligible and the correct  $[K_G^A]$  is attained. The deflections and the other responses at this stage represent the P- $\Delta$  ( $K_G^A$  From Approximate  $K_T^A$ ) static response to the prestress and gravity. The stiffness of the structure is  $K_T^A$ .

#### Phase 4

A SOL 111 is undertaken with the k2gg=ktjj statement in the Case Control Section and the outputted .pch file which contains the latest ktjj matrix in the Bulk Data. The responses at this stage represent the P- $\Delta$  ( $K_G^A$  From Approximate  $K_T^A$ ) response to the dynamic excitation.

### 4.3.7 Hand Methods Verification

#### 4.3.7.1 Determination of Maximum Dynamic Displacement for Deterministic Frequency Domain Loading by Transforming the Coupled MDOF Linear Damped ODEs To a Set of Independent (Uncoupled) SDOF ODEs and Solving the Independent Equations in a Manner Similar to Solving a SDOF ODE

Linear frequency domain hand methods are capable of analyzing: -

#### Multi-Modal Response To Deterministic Periodic Harmonic Long Duration Loading Functions

A coupled MDOF system of linear ODEs must be uncoupled to a set of independent SDOF system of linear ODEs if any feasible hand method computation is to be employed. These independent SDOF ODEs can be solved using standard techniques of solving SDOF linear dynamic ODEs. The final stage to the analysis is to employ a modal superposition method to express the total response as a summation of the results from the solution of the individual modal equations. Note that since the modal frequencies and the corresponding mode shapes are required to uncouple the coupled MDOF ODEs, the real eigenvalue analysis must be performed first. It was shown that a system of coupled MDOF ODEs could be reduced to a system of independent SDOF ODEs by employing the orthogonality properties of real modes

$$-\omega^2 M_i \xi_i(\omega) + i C_i \omega \xi_i(\omega) + K_i \xi_i(\omega) = P_i(\omega)$$

where the generalized (or modal) terms are obtained from solving the real eigenvalue problem

$$\begin{aligned} M_i &= \{\phi_i\}^T [M] \{\phi_i\} \\ C_i &= \{\phi_i\}^T [C] \{\phi_i\} = \zeta_i 2M_i \omega_{ni} \\ K_i &= \{\phi_i\}^T [K] \{\phi_i\} = \omega_{ni}^2 M_i \\ P_i(\omega) &= \{\phi_i\}^T \{P(\omega)\} \end{aligned}$$

The modal properties (i.e. modal masses, modal frequencies and hence modal stiffness) can be obtained by performing a real modal analysis SOL 103 and if required the modal damping can also be incorporated from a complex modal analysis SOL 107. The normalization of the mode shapes can be arbitrary. The normalization technique employed will not affect the value of the modal frequencies but of course will determine the values of the modal masses (and hence modal damping and stiffnesses) and the (amplitude of the) modal force. Although the normalization technique is arbitrary, it is recommended that the normalization employed would facilitate the calculation of the (amplitude of the) modal force since this is a hand calculation. To facilitate the computation, it is wise to choose the normalization to be unity at the DOF of application of the external excitation. Either way, the modal force (for a particular mode) for discrete loading points is calculated as follows

$$P_i(\omega) = \{\phi_i\}^T \{P(\omega)\}$$

Had the loading been continuous, a continuous modal force can also be calculated by hand (or a spreadsheet) as follows

$$P_i(\omega) = \int_0^L \phi_i(x) \{P(x, \omega)\} dx$$

For the special case, which is most common in reality, when the complex harmonic force vector is independent of the frequency of excitation and simply real, we have  $\{P(\omega)\} = \{p_0\}$  and hence,

$$\begin{aligned} \{P(t)\} &= \text{Re al} \left[ \{P(\omega)\} e^{i\omega t} \right] \\ &= \text{Re al} \left[ \{p_0\} e^{i\omega t} \right] \end{aligned}$$

$$\begin{aligned} \text{hence } P_i(\omega) &= \{\phi_i\}^T \{p_0\} \\ &= P_{0i} \end{aligned}$$

There will be  $n$  uncoupled ODEs for  $n$  natural modes. These are now simply SDOF ODEs, which can be solved using complex arithmetic. Hence, the complex modal response (in modal space)

$$\xi_i(\omega) = \frac{P_i(\omega)}{-\omega^2 M_i + iC_i \omega + K_i} = \frac{P_{0i}}{-\omega^2 M_i + iC_i \omega + K_i}$$

From complex number theory

$$x + iy = \left( \sqrt{x^2 + y^2} \right) e^{i\theta}, \theta = \tan^{-1}(y/x)$$

Changing the denominator to a polar complex form

$$\xi_i(\omega) = \frac{P_{0i}}{\sqrt{(K_i - M_i \omega^2)^2 + (C_i \omega)^2}} e^{i\theta_i}, \theta_i = \tan^{-1} \frac{C_i \omega}{K_i - M_i \omega^2} = \tan^{-1} \left( \frac{2\zeta_i \omega / \omega_{ni}}{1 - \omega^2 / \omega_{ni}^2} \right)$$

$$\xi_i(\omega) = \frac{P_{0i} / K_i}{\sqrt{(1 - \omega^2 / \omega_{ni}^2)^2 + (2\zeta_i \omega / \omega_{ni})^2}} e^{-i\theta_i}, \theta_i = \tan^{-1} \left( \frac{2\zeta_i \omega / \omega_{ni}}{1 - \omega^2 / \omega_{ni}^2} \right)$$

This can be written very illustratively as

$$\xi_i(\omega) = D_i(\omega) \frac{P_{0i}}{K_i} e^{-i\theta_i}, \theta_i = \tan^{-1} \left( \frac{2\zeta_i \omega / \omega_{ni}}{1 - \omega^2 / \omega_{ni}^2} \right)$$

where the real modal amplification factor and its maximum are

$$D_i(\omega) = \frac{1}{\sqrt{(1 - \omega^2 / \omega_{ni}^2)^2 + (2\zeta_i \omega / \omega_{ni})^2}}; \quad D_{i \max} = \frac{1}{2\zeta_i \sqrt{1 - \zeta_i^2}}$$

Thus, the steady-state solution in the time domain

$$\begin{aligned} \{u(t)\} &= \text{Re al} \left[ [\Phi] \{ \xi(\omega) \} e^{i\omega t} \right] \\ \{u(t)\} &= \text{Re al} \left[ [\Phi] \left\{ D(\omega) \frac{P_0}{K} e^{-i\theta} \right\} e^{i\omega t} \right] \\ \{u(t)\} &= \text{Re al} \left[ [\Phi] \left\{ D(\omega) \frac{P_0}{K} e^{i(\omega t - \theta)} \right\} \right] \\ \{u(t)\} &= [\Phi] \left\{ D(\omega) \frac{P_0}{K} \cos(\omega t - \theta) \right\} \end{aligned}$$

Note that this expression is to be interpreted as

$$\{u(t)\} = \left[ \begin{array}{cccc} \{\phi\}_1 & \dots & \{\phi\}_i & \dots & \{\phi\}_n \end{array} \right] \left\{ \begin{array}{c} D_1(\omega) \frac{P_{01}}{K_1} \cos(\omega t - \theta_1) \\ \dots \\ D_i(\omega) \frac{P_{0i}}{K_i} \cos(\omega t - \theta_i) \\ \dots \\ D_n(\omega) \frac{P_{0n}}{K_n} \cos(\omega t - \theta_n) \end{array} \right\}$$

Note that  $\rho_{0i}$  corresponds to the amplitude of the modal loading function  $P_i(\omega)$  and not simply the amplitude of the loading function  $\{P(\omega)\}$ , i.e.  $p_0$  at any particular node. Of course, if the normalization of the mode was such that it was unity at the DOF of application of the external force with amplitude  $p_0$  then,  $\rho_{0i}$  will be equal to  $p_0$ .

For a 2 DOF system, this expression would be

$$\begin{Bmatrix} u_1(t) \\ u_2(t) \end{Bmatrix} = \begin{bmatrix} \phi_{11} & \phi_{12} \\ \phi_{21} & \phi_{22} \end{bmatrix} \begin{Bmatrix} D_1(\omega) \frac{\rho_{01}}{K_1} \cos(\omega t - \theta_1) \\ D_2(\omega) \frac{\rho_{02}}{K_2} \cos(\omega t - \theta_2) \end{Bmatrix}$$

The above computation takes into account the phase difference between the responses of different modes. It is important to point out that the maximum of the modal responses  $\xi_i(\omega)$  do not occur at the same time. The frequency domain response ODE can only be solved for a particular excitation frequency  $\omega$  at a time. For a particular  $\omega$  there will be different responses  $\xi_i(\omega)$  from different modes, differing in amplitude of response  $D_i(\omega)$ , static displacement and in phase  $\theta_i$ . Because there is a difference in phase angle between the responses of each and every mode from

$$\theta_i = \tan^{-1} \frac{2\zeta_i \omega / \omega_{ni}}{(1 - \omega^2 / \omega_{ni}^2)}$$

the exact solution involves maximizing a complicated trigonometric expression with many phase angles. The exact solution can be obtained by expanding the general  $u(t)$  expression to include all the modes considered, and only then maximised.

However, this may prove to be mathematically involved if differentiation is to be performed analytically by hand (the computerized method of course performs the response calculation at discrete frequency points as it is not just the maximum that is of interest). An alternative would be to instead of maximising the physical response, maximise the modal responses and then only superpose the modal responses for the physical response.

$$D_{i\max} = \frac{1}{2\zeta\sqrt{(1-\zeta^2)}}$$

$$\xi_{i\max} = D_{i\max}(\omega) \frac{\rho_{0i}}{K_i}$$

This is equivalent to the response spectrum method (only that the procedure is employed on a deterministic loading function instead of a random function). The square root of sum of squares (SRSS) of the maximum modal contributions as follows, depicted for a 2 DOF dynamic system.

$$\begin{Bmatrix} u_{1\max} \\ u_{2\max} \end{Bmatrix} = \begin{Bmatrix} \sqrt{(\phi_{11}\xi_{1\max})^2 + (\phi_{12}\xi_{2\max})^2} \\ \sqrt{(\phi_{21}\xi_{1\max})^2 + (\phi_{22}\xi_{2\max})^2} \end{Bmatrix}$$

Alternatively, the Complete Quadratic Combination (CQC) method is used if the modal natural frequencies are too close to each other (within about 10 %). This is based on random vibration theory. Of course, the upper limit combination would be to choose all the eigenvectors to have the maximum modal response at the same time.

Often, we need to ascertain other types of response such as velocity and acceleration.

We know that,

$$\{u(t)\} = \text{Re al} \left[ [\Phi] \left\{ D(\omega) \frac{\rho_0}{K} e^{i(\omega t - \theta)} \right\} \right]$$

Hence the velocity,

$$\{\dot{u}(t)\} = \text{Re al} \left[ [\Phi] \left\{ i\omega D(\omega) \frac{P_0}{K} e^{i(\omega t - \theta)} \right\} \right]$$

$$\{\dot{u}(t)\} = -\omega [\Phi] \left\{ D(\omega) \frac{P_0}{K} \sin(\omega t - \theta) \right\}$$

And the acceleration,

$$\{\ddot{u}(t)\} = \text{Re al} \left[ [\Phi] \left\{ -\omega^2 D(\omega) \frac{P_0}{K} e^{i(\omega t - \theta)} \right\} \right]$$

$$\{\ddot{u}(t)\} = -\omega^2 [\Phi] \left\{ D(\omega) \frac{P_0}{K} \cos(\omega t - \theta) \right\}$$

The differentiation of the complex vector representing the displacement is equivalent to multiplying the length of the vector by  $\omega$  and turning it ahead by 90 degrees. Multiplying any complex number by imaginary  $i$  is equivalent to a rotation of 90 degrees. Hence the velocity leads the displacement by 90 degrees and the acceleration leads the velocity by 90 degrees. The magnitude of the velocity is  $\omega$  times that of the displacement and the magnitude of the acceleration is  $\omega$  times that of the velocity. In all cases, it is implicitly understood that it is the real part of the complex number that represents the physical harmonic motion.

Note that the total response is obtained by multiplying the eigenvectors by their corresponding modal amplitude factor, which is an indication of the prominence of the mode in the response. It is often the case that lower modes of vibration will have greater prominence. Hence, only a few of the initial prominent modes need to be evaluated in the expression. However, an important point to observe is that since the velocity and acceleration total responses in the time domain are a function of the frequencies and the square of the frequencies respectively on top of the usual modal amplitude factors, this would mean that the prominence of higher modes become more significant when velocities and accelerations are computed.

Ideally, the responses in the time domain should be maximised to obtain the maximum response. But if this proves to be difficult, the modal responses can be maximised and combined using some superposition method such as SRSS or CQC (effectively a response spectrum analysis on a deterministic loading function). For whatever response be it the displacement, velocity acceleration or force, the individual modal responses should first be calculated in terms of time  $t$ , then maximised, then only combined for the physical response with some method of superposition. Do not maximise the modal displacement response and base the other velocity and acceleration responses on that.



$$\omega_n := \begin{bmatrix} 5.728219619 & 0. \\ 0. & 11.45643924 \end{bmatrix}$$

$$\Phi := \begin{bmatrix} 2 & -1 \\ 1 & 1 \end{bmatrix}$$

$$\Phi := \begin{bmatrix} 1 & -1 \\ \frac{1}{2} & 1 \end{bmatrix}$$

**Uncoupling The Equations of Motion**

```

> MODALMASS:=evalf(Transpose(Phi).MASS.Phi);
MODALSTIFFNESS:=evalf(Transpose(Phi).KE.Phi);
MODALFORCE:=evalf(Transpose(Phi).P(w));
    
```

$$MODALMASS := \begin{bmatrix} 600000. & 0. \\ 0. & .120000010^7 \end{bmatrix}$$

$$MODALSTIFFNESS := \begin{bmatrix} .1968750010^8 & 0. \\ 0. & .15750000010^9 \end{bmatrix}$$

$$MODALFORCE := \begin{bmatrix} 10000. \\ -10000. \end{bmatrix}$$

**Modal Responses  $Re[\xi_i] = D_i(\omega) P_{oi}/K_i \cos(\omega t - \theta_i)$**

```

> D(w):=Vector(DOF):
for i from 1 to DOF do
  D(w)[i]:=1/((1-w^2/lambda[i,i])^2+(2*MODALDAMPING[i,i]*w/lambda[i,i]^(1/2))^2)^(1/2);
end do;
xi:=Vector(DOF):
for i from 1 to DOF do
  xi[i]:=D(w)[i]*MODALFORCE[i,1]/MODALSTIFFNESS[i,i]*cos(w*t-
arctan(2*MODALDAMPING[i,i]*w/lambda[i,i]^(1/2)/(1-w^2/lambda[i,i])));
end do;
xi:=evalf(xi);
    
```

$$D(4.5826)_1 := 2.775090553$$

$$D(4.5826)_2 := 1.190424609$$

$$\xi := \begin{bmatrix} .001409569805\cos(4.5826t - .04441628701) \\ -.00007558251486\cos(4.5826t - .009523591344) \end{bmatrix}$$

**Physical Response in Time Domain**

```

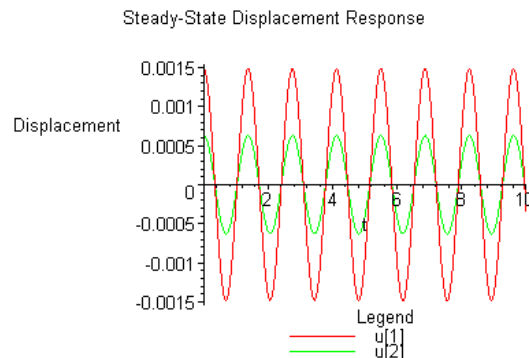
> u(t):=Vector(DOF):
u(t):=Phi.xi;
    
```

$$u(t) := \begin{bmatrix} .001409569805\cos(4.5826t - .04441628701) + .00007558251486\cos(4.5826t - .009523591344) \\ .0007047849025\cos(4.5826t - .04441628701) - .00007558251486\cos(4.5826t - .009523591344) \end{bmatrix}$$

**Plot of Response in Time Domain**

```

> variablelegend:=seq(convert(u[i],string),i=1..DOF):
plot([seq(u(t)[i],i=1..DOF)], t=0..10, Displacement,title="Steady-State Displacement
Response", legend=[variablelegend]);
    
```



An absolutely equivalent method of solving the equations in the frequency domain is to work in real and imaginary terms instead of in terms of magnitude and phase.

As before, the complex modal response (in modal space) is

$$\begin{aligned}\xi_i(\omega) &= \frac{p_{0i}}{-\omega^2 M_i + iC_i \omega + K_i} \\ &= \frac{p_{0i}}{-\omega^2 M_i + K_i + iC_i \omega} \\ &= \frac{p_{0i}/K_i}{\left(1 - \omega^2 / \omega_{ni}^2\right) + i(2\zeta_i \omega / \omega_{ni})}\end{aligned}$$

Instead of the polar form, this can be written in terms of the real and imaginary parts

$$\begin{aligned}\xi_i(\omega) &= \frac{p_{0i}}{K_i} \left[ \frac{\left(1 - \omega^2 / \omega_{ni}^2\right)}{\left(1 - \omega^2 / \omega_{ni}^2\right)^2 + (2\zeta_i \omega / \omega_{ni})^2} - i \frac{(2\zeta_i \omega / \omega_{ni})}{\left(1 - \omega^2 / \omega_{ni}^2\right)^2 + (2\zeta_i \omega / \omega_{ni})^2} \right] \\ \xi_i(\omega) &= \xi_{i\text{REAL}}(\omega) - i\xi_{i\text{IMAG}}(\omega)\end{aligned}$$

Thus, the steady-state solution in the time domain

$$\begin{aligned}\{u(t)\} &= \text{Re al} \left[ [\Phi] \{ \xi_{i\text{REAL}}(\omega) - i\xi_{i\text{IMAG}}(\omega) \} e^{i\omega t} \right] \\ \{u(t)\} &= \text{Re al} \left[ [\Phi] \{ \xi_{i\text{REAL}}(\omega) - i\xi_{i\text{IMAG}}(\omega) \} (\cos \omega t + i \sin \omega t) \right] \\ \{u(t)\} &= [\Phi] \{ \xi_{i\text{REAL}}(\omega) \} \cos \omega t + \{ \xi_{i\text{IMAG}}(\omega) \} \sin \omega t\end{aligned}$$

Note that this expression is to be interpreted as

$$\{u(t)\} = \left[ \begin{array}{cccc} \{ \phi \}_1 & \dots & \{ \phi \}_i & \dots & \{ \phi \}_n \end{array} \right] \left\{ \begin{array}{l} \frac{p_{01}}{K_1} (D_{1\text{REAL}}(\omega) \cos \omega t + D_{1\text{IMAG}}(\omega) \sin \omega t) \\ \dots \\ \frac{p_{0i}}{K_i} (D_{i\text{REAL}}(\omega) \cos \omega t + D_{i\text{IMAG}}(\omega) \sin \omega t) \\ \dots \\ \frac{p_{0n}}{K_n} (D_{n\text{REAL}}(\omega) \cos \omega t + D_{n\text{IMAG}}(\omega) \sin \omega t) \end{array} \right\}$$

where

$$\begin{aligned}D_{i\text{REAL}}(\omega) &= \frac{\left(1 - \omega^2 / \omega_{ni}^2\right)}{\left(1 - \omega^2 / \omega_{ni}^2\right)^2 + (2\zeta_i \omega / \omega_{ni})^2} \\ D_{i\text{IMAG}}(\omega) &= \frac{(2\zeta_i \omega / \omega_{ni})}{\left(1 - \omega^2 / \omega_{ni}^2\right)^2 + (2\zeta_i \omega / \omega_{ni})^2}\end{aligned}$$

**This method is very useful because the final expression being in cos and sin means that we can very quickly find the maximum response (i.e. the steady-state response) as  $\text{MAX}(A \cos \omega t + B \sin \omega t) = (A^2 + B^2)^{1/2}$ . At a particular DOF  $j$ , the steady state response will then be**

$$\text{Steady - State Response, } u_{j\text{MAX}} = \sqrt{\left( \sum_i^n \frac{p_{0i}}{K_i} \phi_{ij} D_{i\text{REAL}}(\omega) \right)^2 + \left( \sum_i^n \frac{p_{0i}}{K_i} \phi_{ij} D_{i\text{IMAG}}(\omega) \right)^2}$$

This procedure is now implemented in the above MAPLE example, showing identical results in the end.

**System and Frequency Domain Excitation Description - User Input**

```
> restart;
with(LinearAlgebra):
DOF:=2:
EI:=560000000:
M:=400000:
L:=4:
MASS:=Matrix([[M,0],[0,2*M]]);
KE:=Matrix([[3*EI/L^3,-3*EI/L^3],[-3*EI/L^3,9*EI/L^3]]);
MODALDAMPING:=Matrix([[0.01,0],[0,0.01]]);
# Excitation - P(w) is the magnitude of the excitation, i.e. P(t)=Re[P(w)EXP(iwt)]
w:=4.5826:
P(w):=Matrix([[10000],[0]]);
```

$$MASS := \begin{bmatrix} 400000 & 0 \\ 0 & 800000 \end{bmatrix}$$

$$KE := \begin{bmatrix} 26250000 & -26250000 \\ -26250000 & 78750000 \end{bmatrix}$$

$$MODALDAMPING := \begin{bmatrix} .01 & 0 \\ 0 & .01 \end{bmatrix}$$

$$P(4.5826) := \begin{bmatrix} 10000 \\ 0 \end{bmatrix}$$

**Modal Properties of System - Solution of Real Eigenvalue Problem  $[K-\lambda M]\{\phi\}=\{0\}$**

- Note that Eigensolution may not arrange the roots sequentially
- MAX normalization of the Eigenvectors

```
> Eigensolution:=Eigenvectors(MatrixInverse(MASS).KE):
lambda:=Matrix(Eigensolution[1],shape=diagonal):
wn:=map(sqrt,evalf(lambda));
Phi:=Eigensolution[2];
for j from 1 to DOF do
  eig:=0:
  for i from 1 to DOF do
    eig:=eig,Phi[i,j];
  end do;
  for i from 1 to DOF do
    Phi[i,j]:=Phi[i,j]/max(eig);
  end do;
end do;
Phi:=Phi;
```

$$wn := \begin{bmatrix} 5.728219619 & 0. \\ 0. & 11.45643924 \end{bmatrix}$$

$$\Phi := \begin{bmatrix} 2 & -1 \\ 1 & 1 \end{bmatrix}$$

$$\Phi := \begin{bmatrix} 1 & -1 \\ \frac{1}{2} & 1 \end{bmatrix}$$

**Uncoupling The Equations of Motion**

```
> MODALMASS:=evalf(Transpose(Phi).MASS.Phi);
MODALSTIFFNESS:=evalf(Transpose(Phi).KE.Phi);
MODALFORCE:=evalf(Transpose(Phi).P(w));
```

$$MODALMASS := \begin{bmatrix} 600000. & 0. \\ 0. & .120000010^7 \end{bmatrix}$$

$$MODALSTIFFNESS := \begin{bmatrix} .1968750010^8 & 0. \\ 0. & .15750000010^9 \end{bmatrix}$$

$$MODALFORCE := \begin{bmatrix} 10000. \\ -10000. \end{bmatrix}$$

**Modal Responses**  $Re[\xi_i] = Poi/Ki \{ DiREAL(w) \cos(wt) - DiIMAG(w) \sin(wt) \}$

```
> DREAL(w) := Vector(DOF) :
DIMAG(w) := Vector(DOF) :
for i from 1 to DOF do
  DREAL(w) [i] := (1-w^2/lambda[i,i]) / ((1-
w^2/lambda[i,i])^2 + (2*MODALDAMPING[i,i]*w/lambda[i,i]^(1/2))^2);
  DIMAG(w) [i] := (2*MODALDAMPING[i,i]*w/lambda[i,i]^(1/2)) / ((1-
w^2/lambda[i,i])^2 + (2*MODALDAMPING[i,i]*w/lambda[i,i]^(1/2))^2);
end do;
xi := Vector(DOF) :
for i from 1 to DOF do
xi[i] := MODALFORCE[i,1] / MODALSTIFFNESS[i,i] * (DREAL(w) [i] * cos(w*t) + DIMAG(w) [i] * sin(w*t));
end do;
xi := evalf(xi);
```

$$DREAL(4.5826)_1 := 2.772353645$$

$$DIMAG(4.5826)_1 := .001344426180\sqrt{525}\sqrt{16}$$

$$DREAL(4.5826)_2 := 1.190370624$$

$$DIMAG(4.5826)_2 := .0002473924464\sqrt{525}\sqrt{4}$$

$$\xi := \begin{bmatrix} .001408179629\cos(4.5826t) + .00006258727349\sin(4.5826t) \\ -.00007557908724\cos(4.5826t) - .719806102510^{-6}\sin(4.5826t) \end{bmatrix}$$

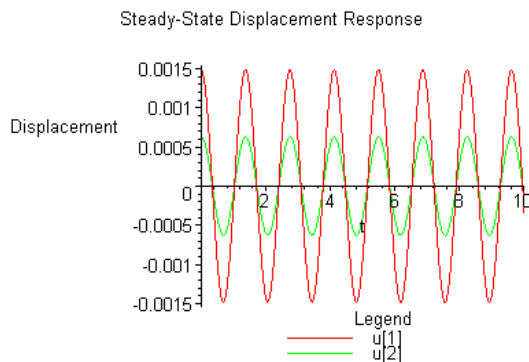
**Physical Response in Time Domain**

```
> u(t) := Vector(DOF) :
u(t) := Phi.xi;
```

$$u(t) := \begin{bmatrix} .001483758716\cos(4.5826t) + .00006330707959\sin(4.5826t) \\ .0006285107273\cos(4.5826t) + .00003057383064\sin(4.5826t) \end{bmatrix}$$

**Plot of Response in Time Domain**

```
> variablelegend := seq(convert(u[i], string), i=1..DOF) :
plot([seq(u(t) [i], i=1..DOF)], t=0..10, Displacement, title="Steady-State Displacement
Response", legend=[variablelegend]);
```



## 4.4 GL, ML Implicit (Complex) Modal Frequency Response Analysis

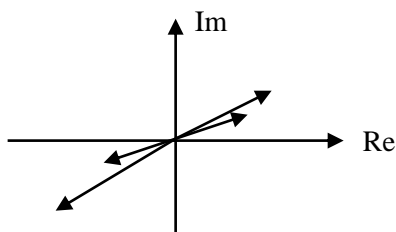
### 4.4.1 Mathematical Formulation of Analysis

SOL 111 performs a modal forced frequency response analysis. It utilizes the real modal properties to decouple the equations of motion when there is no elemental structural and/or viscous damping within the system. With the existence of elemental structural and/or viscous, the real modal properties cannot decouple the couple ODEs. In this case, SOL 111 then performs the forced frequency response analysis using a direct approach on the coupled ODEs, but in the modal coordinates instead of the physical coordinates. With sufficient modes (sufficient modal variables), a SOL 111 solution will yield the same answer as a SOL 108 solution. However, the use of the `FREQ4` card, which bases the excitation frequencies to be solved for on the real natural frequencies may prove to be insufficient. This is because with high values of elemental viscous damping, certain local modes can be totally eliminated. For instance, viscous dampers with high coefficients of damping on cables can considerably alter the natural frequency of the local mode and even eliminate a local mode altogether. In this case, the `FREQ4` card will not capture the response at the damped natural frequency. Hence, these damped natural frequencies need to be known (by performing a SOL 107) before choosing the excitation frequencies to be solved for using `FREQ2` cards.

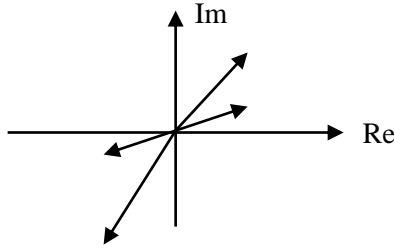
If however, a modal approach is still intended with the existence of structural and/or viscous damping, the complex modal properties must be employed. It is thus necessary to find new orthogonality properties of modes (complex modes now) in order to be able to diagonalize the matrices. The response analysis is called the complex modal forced response analysis.

The mathematical formulation of the solution scheme is quite involved. In principle, in order to employ a modal approach, we need to reduce a set of coupled ODEs to a set of uncoupled ODEs that can be solved independently of each other. In order to do that, we need to establish orthogonality conditions. A similar procedure employed for establishing real modal orthogonality conditions can again be utilized to determine the complex modal orthogonality conditions.

The decision of whether such an involved process is required lies with the degree of complexity of the modes. If the modes are only slightly complex, then a real modal approach might well be justified. In order to ascertain the level of complexity of a particular mode, each term within the complex eigenvector is plotted on an Argand diagram i.e. the imaginary component versus the real component. An almost real mode shape does not necessarily have vector terms near 0 or 180 degrees. What matters is the relative phase between different terms. A pure real mode has all its terms in phase which each other. Different modes will of course be out of phase with each other, but every point in a particular mode will vibrate in phase. And so, for a mode, all points in the structure reach its maximum and minimum at the same phase instant. A complex mode on the other hand will have different points of the structure reaching its maximum at different phase instants, i.e. different points of the structure are out of phase with each other for a particular mode. Of course, different modes are still out of phase with each other. The degree to which these points are out of phase with each other is a measure of the complexity of the mode. An Argand diagram with all the terms of the complex eigenvector plotted will exhibit a narrowband if the mode is only slightly complex. The diagram below shows plots for 4 eigenvector terms. Since there is only a slight phase difference between the terms (angle between the arrows), the 4 terms define an almost real complex eigenvector.



The following eigenvector plot on the other hand is highly complex because of the large phase angle difference between the terms of the eigenvector and as such a complex modal approach needs to be undertaken if a modal approach is intended at all. A direct approach is most recommended to avoid the mathematical complexities.



The modal approach in the frequency domain based on real modal properties is first described. This is the approach used by SOL 111 only when there is no elemental structural or elemental viscous damping.

The coupled system of ODEs of the undamped forced vibration equation of motion is

$$[M]\{\ddot{u}(t)\} + [K]\{u(t)\} = \{P(t)\}$$

To solve the equation in the frequency domain, we let

$$\{u(t)\} = \text{Re al} \left[ [\Phi]\{\xi(\omega)\}e^{i\omega t} \right]$$

Hence

$$\begin{aligned} -[M][\Phi]\{\xi(\omega)\}\omega^2 e^{i\omega t} + [K][\Phi]\{\xi(\omega)\}e^{i\omega t} &= \{P(\omega)\}e^{i\omega t} \\ -\omega^2 [M][\Phi]\{\xi(\omega)\} + [K][\Phi]\{\xi(\omega)\} &= \{P(\omega)\} \end{aligned}$$

It can be shown that the orthogonality condition of the normal modes is

$$\{\phi_i\}^T [[M] + [K]]\{\phi_j\} = 0 \quad \text{if} \quad i \neq j$$

Hence, premultiplying by  $[\Phi]^T$  reduces the coupled system of ODEs to a system of uncoupled ODEs

$$\begin{aligned} -\omega^2 [\Phi]^T [M][\Phi]\{\xi(\omega)\} + [\Phi]^T [K][\Phi]\{\xi(\omega)\} &= [\Phi]^T \{P(\omega)\} \\ -\omega^2 [M]\{\xi(\omega)\} + [K]\{\xi(\omega)\} &= \{P(\omega)\} \end{aligned}$$

The matrices  $[M]$  and  $[K]$  are thus diagonal.

The modal approach in the frequency domain based on complex modal properties is now described.

Complex eigenvalue analysis with viscous (and structural optional) damping, for each mode  $i$ , NASTRAN outputs,

two complex roots which are a complex conjugate pair,  $\alpha_i + i\omega_{di}$  and  $\alpha_i - i\omega_{di}$ , where

$\alpha_i$  is negative and represents the decaying constant

$\omega_{di}$  is positive and represents the damped natural circular frequency

two complex eigenvectors which are a complex conjugate pair,  $\{\phi_R + i\phi_I\}_i$  and  $\{\phi_R - i\phi_I\}_i$

Complex eigenvalue analysis with only structural (and no viscous) damping, for each mode  $i$ , NASTRAN outputs,

one complex root,  $\alpha_i + i\omega_{di}$ , where

$\alpha_i$  is negative and represents the decaying constant

$\omega_{di}$  is positive and represents the damped natural circular frequency

one complex eigenvector,  $\{\phi_R + i\phi_I\}_i$

The coupled system of ODEs of the damped forced vibration equation of motion is

$$[M]\{\ddot{u}(t)\} + [C]\{\dot{u}(t)\} + [K]\{u(t)\} = \{P(t)\}$$

where  $[K] = (1 + iG)[K] + i \sum G_E [K_E]$

It can be shown that the orthogonality conditions with viscous (and structural optional) damping are

$$\begin{aligned} \{\phi_R + i\phi_I\}_i^T [((\alpha_i + i\omega_{di}) + (\alpha_j + i\omega_{dj}))][M] + [C]\{\phi_R + i\phi_I\}_j &= 0, \quad \text{and} \\ \{\phi_R + i\phi_I\}_i^T [((\alpha_i + i\omega_{di})^* (\alpha_j + i\omega_{dj}))][M] - [K]\{\phi_R + i\phi_I\}_j &= 0, \quad \text{if } i \neq j \end{aligned}$$

Note that the orthogonality condition with only structural (and no viscous) damping is

$$\{\phi_R + i\phi_I\}_i^T [[M] + [K]]\{\phi_R + i\phi_I\}_j = 0, \quad \text{if } i \neq j$$

Clearly, the orthogonality conditions are far more complicated, making the mathematics defining the complex modal forced frequency response analysis very difficult. It will not be attempted here.

## 4.5 GL, ML Implicit Direct Frequency Response Analysis

### 4.5.1 Nature of the Dynamic Loading Function

The solution method can be used to solve dynamic systems subjected to: -

- (a) **Deterministic periodic harmonic long duration** loading functions

A deterministic periodic forcing function has regularly repeating amplitude. The sine or cosine function is said to be harmonic. Because the periodic function repeats itself, any initial starting transient response is insignificant and the steady state response is of interest, hence the solution is performed in the frequency domain. The starting transient normally decays away after 50-100 cycles of oscillation for light damping. The steady-state oscillatory response occurs at the same frequency as the loading phase shifted due to damping.

**In this LINEAR FREQUENCY DOMAIN solution**, not only that the static response has to be added separately, but also the mean of the dynamic excitation has also got to be added separately as a static response. This is because the mean of the dynamically applied force is not included in the dynamic excitations. **Hence the total response in this frequency domain dynamic analysis = static response to mean of dynamic excitation + dynamic response + static response to static loads.**

### 4.5.2 Mathematical Formulation of Analysis

This method is not a modal method and so the solution is not a reduced solution and is therefore computationally very expensive as it involves the full mass, stiffness and damping matrices. For small models this type of solution is probably better than a modal frequency response analysis and certainly more accurate. However, for large models it is too inefficient and can only be used to compute response at a handful of frequency locations, where there is doubt in the modal frequency response results. In general, modal frequency response analysis is used when

- (i) the model is large
- (ii) many excitation frequencies need to be solved for

On the other hand, direct frequency response analysis is employed when

- (i) the model is small
- (ii) only a few excitation frequencies need to be solved for
- (iii) the response due to high frequency excitation is required, as this requires many modes to be computed in the modal frequency response analysis, the computation of the modes being the costly operation in the modal approach
- (iv) high accuracy is required as the direct approach does not involve mode truncation.

The coupled system of ODEs of the undamped harmonically forced vibration equation of motion are given by

$$[M]\{\ddot{u}(t)\} + [K]\{u(t)\} = \{P(t)\}$$

In the frequency domain, let

$$\{u(t)\} = \text{Re al} \left[ \{F(\omega)\} e^{i\omega t} \right] \text{ where } \{F(\omega)\} \text{ is a complex displacement response function vector}$$

$$\{P(t)\} = \text{Re al} \left[ \{P(\omega)\} e^{i\omega t} \right] \text{ where } \{P(\omega)\} \text{ is a complex forcing function vector}$$

This transformation is worth a little explanation. The harmonic forcing function in the time domain  $P(t)$  is transformed into the frequency domain simply by multiplying

$$\{P(t)\} = \text{Re al} \left[ \{P(\omega)\} e^{i\omega t} \right]$$

$\{P(\omega)\}$  is the complex harmonic forcing function. The harmonic term is  $e^{i\omega t}$ .  $\{P(\omega)\}$  can be frequency dependent and/or can even be complex in general. If  $\{P(\omega)\}$  is complex, this refers to harmonic loading functions which are out of phase with respect to each other. We usually assume that  $\{P(\omega)\}$  is frequency independent and also just real, such that  $\{P(\omega)\} = \{p_0\}$ . The frequency domain complex forcing function  $\{P(\omega)\}$  is specified in NASTRAN with

the RLOAD1 and RLOAD2 cards. The harmonic term is inferred naturally. It must be stressed that the specified frequency domain excitation is the complex harmonic forcing function  $\{P(\omega)\}$  and that the corresponding complex total response vector is  $\{F(\omega)\}$ . If  $\{P(\omega)\}$  is complex, then  $\{F(\omega)\}$  will be complex. If  $\{P(\omega)\}$  is only real, then  $\{F(\omega)\}$  will be real if there is no damping in the system but will be complex if there is damping in the system. The curves for  $\{F(\omega)\}$  versus  $\omega$  is what is produced by the NASTRAN output in a frequency domain analysis. It can be viewed in its real and imaginary components versus  $\omega$ , or in its magnitude and phase versus  $\omega$ , the latter of which is what should be observed to ascertain the response. To summarize

Frequency domain loading function from the time domain loading function

$$\{P(t)\} = \text{Re al} \left[ \{P(\omega)\} e^{i\omega t} \right]$$

where  $\{P(\omega)\}$  is the complex loading function vector

Frequency domain complex total response function vector is

$$\{F(\omega)\} \text{ which is complex in general}$$

Time domain total response from the frequency domain complex total response

$$\{u(t)\} = \text{Re al} \left[ \{F(\omega)\} e^{i\omega t} \right]$$

Hence on substitution,

$$\begin{aligned} -[M]\{F(\omega)\}\omega^2 e^{i\omega t} + [K]\{F(\omega)\}e^{i\omega t} &= \{P(\omega)\}e^{i\omega t} \\ [-\omega^2[M] + [K]]\{F(\omega)\} &= \{P(\omega)\} \\ \{F(\omega)\} &= \frac{\{P(\omega)\}}{-\omega^2[M] + [K]} \end{aligned}$$

This equation is solved at each and every specified discrete forcing frequency  $\omega$  using complex arithmetic.

Because the terms are vectors and matrices, there is the requirement for simultaneous equation solvers to ascertain  $\{F(\omega)\}$ , this being the reason that the direct approach is far more expensive computationally compared to the modal approach.

Finally the total response is

$$\{u(t)\} = \text{Re al} \left[ \{F(\omega)\} e^{i\omega t} \right]$$

The following damping models are supported by the solution scheme

- |      |                                     |     |
|------|-------------------------------------|-----|
| I.   | elemental damping                   |     |
|      | i. viscous damping                  | Yes |
|      | ii. structural damping              | Yes |
| II.  | modal damping                       |     |
|      | i. viscous damping                  | No  |
|      | ii. structural damping              | No  |
| III. | global proportional viscous damping |     |
|      | i. mass proportional damping        | No  |
|      | ii. stiffness proportional damping  | Yes |
|      | iii. Rayleigh damping               | No  |

With damping, the coupled system of ODEs of the damped harmonically forced vibration equation of motion are given by

$$[M]\{\ddot{u}(t)\} + [C]\{\dot{u}(t)\} + [K]\{u(t)\} = \{P(t)\}$$

where

$$[K] = (1 + iG)[K] + i \sum G_E [K_E]$$

$$[C] = \sum [C_E]$$

Hence,

$$-[M]\{F(\omega)\}\omega^2 e^{i\omega t} + i\omega[C]\{F(\omega)\}e^{i\omega t} + [K]\{F(\omega)\}e^{i\omega t} = \{P(\omega)\}e^{i\omega t}$$

$$[-\omega^2[M] + i\omega[C] + [K]]\{F(\omega)\} = \{P(\omega)\}$$

$$\{F(\omega)\} = \frac{\{P(\omega)\}}{-\omega^2[M] + i\omega[C] + [K]}$$

This equation is solved at each and every specified discrete forcing frequency  $\omega$  using complex arithmetic. Unlike the modal frequency response analysis, the direct frequency response analysis requires the solution of simultaneous equations at each forcing frequency, hence explaining its additional cost.

Finally the total response is

$$\{u(t)\} = \text{Re al} \left[ \{F(\omega)\}e^{i\omega t} \right]$$

In direct frequency response analysis, it is not necessary to assume an equivalent viscous form for structural damping as the solution is complex. Hence the element structural damping coefficient  $G_{\text{element}}$  or  $G$  parameters do not form a damping matrix  $[C]$ , instead they form a complex stiffness matrix.

The complex response function due to a loading  $\{P(\omega)\}$  is defined as

$$\{F(\omega)\} = \frac{\{P(\omega)\}}{-\omega^2[M] + i\omega[C] + [K]}$$

The complex transfer function is defined as the complex frequency response function due to unit harmonic excitations

$$[H(\omega)] = \frac{1}{-\omega^2[M] + i\omega[C] + [K]}$$

This is the so-called *transfer function* that transfers the excitation to the response as follows

$$\{u(t)\} = \text{Re al} \left[ [H(\omega)]\{P(\omega)\}e^{i\omega t} \right]$$

The (magnitude of the) dynamic amplification function  $D(\omega)$  is defined as the magnitude of the complex response function  $\{F(\omega)\}$  divided by the static displacement.

The animation of the forced frequency response is quite indicative of the nature of the response of the structure to harmonic excitations. The forced frequency response analysis will yield for each node, both real and imaginary responses. The animation of the forced response of the structure as a whole (at any particular frequency of excitation) is only of value when we plot the magnitude of the response, and not the individual real or imaginary components. The phase information (which is obtained when the magnitude and argument of the real and imaginary components are obtained) is essential in order to determine the relative phase of the motion of different parts of the structure. Explicit viscous dampers will cause parts of the structure to vibrate clearly out-of-phase.

### 4.5.3 MSC.NASTRAN Decks

#### 4.5.3.1 GL, ML Direct Forced Frequency Response Analysis

<b>\$ EXECUTIVE CONTROL SECTION</b>									
SOL 108									
<b>\$ CASE CONTROL SECTION</b>									
<b>\$ Sets defining grid ids or element ids</b>									
SET < Number > = 1 THRU 100, 211, 343, < etc >									
<b>\$ Grid output of displacement, velocity and acceleration for excitation frequencies</b>									
<b>\$ SORT1 lists the results by frequency whilst SORT2 lists the results by grid id</b>									
DISPLACEMENT (<SORT1/SORT2>,<PRINT,PUNCH,PLOT>,<REAL/PHASE>) = ALL/<Grid Set ID>									
VELOCITY (<SORT1/SORT2>,<PRINT,PUNCH,PLOT>,<REAL/PHASE>) = ALL/<Grid Set ID>									
ACCELERATION (<SORT1/SORT2>,<PRINT,PUNCH,PLOT>,<REAL/PHASE>) = ALL/<Grid Set ID>									
<b>\$ Grid output of applied load vector</b>									
OLOAD (<SORT1/SORT2>,<PRINT,PUNCH,PLOT>,<REAL/PHASE>) = ALL/<Grid Set ID>									
<b>\$ Grid output of d-set displacement, velocity and acceleration</b>									
SDISPLACEMENT (<SORT1/SORT2>,<PRINT,PUNCH>,<REAL/PHASE>) = ALL/<Grid Set ID>									
SVELOCITY (<SORT1/SORT2>,<PRINT,PUNCH>,<REAL/PHASE>) = ALL/<Grid Set ID>									
SACCELERATION (<SORT1/SORT2>,<PRINT,PUNCH>,<REAL/PHASE>) = ALL/<Grid Set ID>									
<b>\$ Grid output of SPC forces</b>									
SPCFORCES (<SORT1/SORT2>,<PRINT,PUNCH,PLOT>,<REAL/PHASE>) = ALL/<Grid Set ID>									
<b>\$ Element output of force, stress and strain</b>									
ELFORCE (<SORT1/SORT2>,<PRINT,PUNCH,PLOT>,<REAL/PHASE>) = ALL/<Element Set ID>									
ELSTRESS (<SORT1/SORT2>,<PRINT,PUNCH,PLOT>,<REAL/PHASE>) = ALL/<Element Set ID>									
STRAIN (<SORT1/SORT2>,<PRINT,PUNCH,PLOT>,<REAL/PHASE>) = ALL/<Element Set ID>									
<b>\$ Analysis Cards</b>									
SPC = < ID of SPC Cards Defined in Bulk Data >									
FREQ = < ID OF FREQi >									
<b>\$ XY plot output</b>									
OUTPUT (XYPLOT)									
XYPUNCH <DISP/VELO/ACCE> RESPONSE <subcase>/<Grid ID>(<T1/T2/T3><RM/IP>)									
XYPUNCH <ELFORCE/ELSTRESS/STRAIN> RESPONSE <subcase>/<Element ID>(<Code Number>)									
<b>\$ BULK DATA</b>									
FREQ1	ID	$f_{start}$	$\Delta f$	Number of $\Delta f$					

All FREQi entries with the same selected ID, selected by the FREQUENCY entry in the Case Control Section, will be combined. The **FREQ1** bulk data entry selects the frequencies at which the frequency response analysis is performed. The **FREQ** and **FREQ2** cards can also be used to define points within the regions of resonance (evaluated by a separate modal analysis prior to the forced response analysis). It is important to specify a fine enough frequency step size  $\Delta f$  to adequately predict peak response. Use at least five to ten points across the half-power bandwidth. For maximum efficiency, an uneven frequency step size should be used. Smaller frequency spacing should be used in regions near resonant frequencies, and larger frequency step sizes should be used in regions away from resonant frequencies. Adaptive excitation frequency Bulk Data entries, which depend on the modal frequencies FREQ3, FREQ4 and FREQ5 cannot be used as the modal frequencies are not calculated in the direct response analysis. This is one of the drawbacks of the direct method SOL 108 as opposed to the modal method SOL 112, i.e. it is necessary to spend effort in capturing the peak. SOL 112 does not suffer from this drawback because the solution set is the modal responses and hence the peak is naturally captured. But in SOL 108, it is especially difficult to capture peak when the modal damping is low since the peak is very spiky. Again five to ten points across the half-power bandwidth must be ensured. To check if the peak has been truly captured, a SOL 107 can be used to estimate the modal damping. Then assuming small modal damping the maximum dynamic

amplification would be  $1/2\zeta$ . Note that the dynamic amplification curve is obtained from the plotted FRF from NASTRAN by dividing by the static response P/K. It should be okay to use the zero frequency SOL 108 response to estimate the static response P/K, although this assumes that the frequency is close enough to zero and that there is little structural damping in the system. There are of course no modal truncation concerns in this direct approach. The exact estimate of the static response P/K would clearly be to perform a static analysis SOL 101 with a magnitude equal to the amplitude of the frequency domain (sinusoidal) forcing function.

Printed .f06 frequency response output can be in SORT1 or SORT2 format. In the SORT1 format, the results are listed by frequency i.e. for each frequency the results of all grid points are given, whilst in the SORT2 format, the results are listed by grid point i.e. for each grid point the results of all frequencies are given.

To define frequency frozen structural plots,

<b>\$ CASE CONTROL SECTION</b>
DISPLACEMENT (PLOT, PHASE) =ALL
<b>\$ BULK DATA</b>
PARAM, DDRMM, -1 PARAM, CURVPLOT, 1

For each frequency of excitation, the magnitude of the response at each and every point in the structure is animated with the phase information. It is meaningless and impossible to plot the real and imaginary components, as the animation requires the phase difference between different points in the structure. It is prudent to limit the frequencies of excitation so as to limit the amount of output.

### 4.5.3.1.1 Applied Load Excitations

To define a frequency dependent dynamic excitation, both spatial distribution and the frequency variation (i.e. the temporal distribution) must be defined. The RLOAD1 entry defines dynamic excitation in real and imaginary format whilst the RLOAD2 entry defines dynamic excitation in magnitudes and phases. It is important to realize that  $P(f)$  is defined with the right-hand-side of the equation of motion in the frequency domain being Real  $[P(f)e^{i2\pi ft}]$ . Hence  $P(f)$  is the complex loading function in the frequency domain.

$$\text{RLOAD1: } \{P(f)\} = \{A[C(f)+iD(f)e^{i(\theta - 2\pi f\tau)}]\}$$

$$\text{RLOAD2: } \{P(f)\} = \{AB(f)e^{i(\phi(f) + \theta - 2\pi f\tau)}\}$$

Note that  $C(f) + iD(f) = B(f)e^{i\phi(f)}$

$f$  = frequency in cycles per unit time

$A$  = amplitude scalar multiplier defined by DAREA for a DOF

$\tau$  = time delay in an applied load defined by DELAY for a DOF

$\theta$  = phase lead angle in degrees defined by DPHASE for a DOF

$C(f)$  = frequency dependent real coefficient defined by Real TABLED1

$D(f)$  = frequency dependent imaginary coefficient defined by Imaginary TABLED1

$B(f)$  = frequency dependent amplitude curve defined by Amplitude TABLED1

$\phi(f)$  = frequency dependent phase angles curve in degrees defined by Phase TABLED1

<b>\$ CASE CONTROL SECTION</b>									
DLOAD = < ID OF RLOAD1 or RLOAD2 >									
<b>\$ BULK DATA</b>									
RLOAD1	ID	DAREA ID	DELAY ID	DPHASE ID	Real TABLED1 ID	Imaginary TABLED1 ID			
RLOAD2	ID	DAREA ID	DELAY ID	DPHASE ID	Amplitude TABLED1 ID	Phase TABLED1 ID			
DAREA	ID	GRID ID	Component Number	Scale Factor	GRID ID	Component Number	Scale Factor		
DELAY	ID	GRID ID	Component Number	Time Delay $\tau$	GRID ID	Component Number	Time Delay $\tau$		
DPHASE	ID	GRID ID	Component Number	Phase Lead $\theta$ (degrees)	GRID ID	Component Number	Phase Lead $\theta$ (degrees)		
TABLED1	ID	XAXIS	YAXIS						
	x1	y1	x2	y2	x3	y3	x4	Y4	
	x5	y5	x6	y6	...	...	ENDT		

Any number of DAREA, DELAY and DPHASE entries may be defined. All those with the same ID will be subjected to the dynamic excitation definition of Real/Amplitude TABLED1 and Imaginary/Phase TABLED1 as defined within the same RLOAD1/RLOAD2 entry. The XAXIS and YAXIS in the TABLED1 entry refers to either LINEAR or LOG interpolation between and beyond the extremities of the specified  $\{x_i, y_i\}$  pairs of {frequency, amplitude} or {frequency, phase angles}. Note that the frequencies are specified in cycles per unit time and the phase angles are specified in degrees.

In order to verify the applied loading, the response at 0.0 Hz without structural damping should be checked to match the results from a static analysis, the discrepancy arising from mode truncation.

It must be understood that use of complex numbers is only to ease mathematical manipulation. The harmonic excitation is understood to consist only of the real component of the complex number and likewise with the response. At a component of a DOF,

$$\begin{aligned} P(t) &= \text{Re al} \left[ P(\omega) e^{i\omega t} \right] \quad \text{where } P(\omega) \text{ is complex} \\ &= \text{Re al} \left[ A(C + iDe^{i(0-\omega\tau)}) e^{i\omega t} \right] \end{aligned}$$

If we required a simple  $P(t) = 1.0\sin\omega t$  loading function,

Let  $A = 1.0$ ,  $D = -1.0$  and all else zero, so that

$$\begin{aligned} P(t) &= \text{Re al} \left[ 1(0 - i1e^{i(0-\omega 0)}) e^{i\omega t} \right] \\ &= \text{Re al} \left[ -ie^{i\omega t} \right] \\ &= \text{Re al} \left[ -i(\cos \omega t + i \sin \omega t) \right] \\ &= \text{Re al} \left[ -i \cos \omega t + \sin \omega t \right] \\ &= \sin \omega t \end{aligned}$$

If we required a simple  $P(t) = 1.0\cos\omega t$  loading function,

Let  $A = 1.0$ ,  $C = 1.0$  and all else zero, so that

$$\begin{aligned} P(t) &= \text{Re al} \left[ 1(1 - i0e^{i(0-\omega 0)}) e^{i\omega t} \right] \\ &= \text{Re al} \left[ 1e^{i\omega t} \right] \\ &= \text{Re al} \left[ 1(\cos \omega t + i \sin \omega t) \right] \\ &= \text{Re al} \left[ \cos \omega t + i \sin \omega t \right] \\ &= \cos \omega t \end{aligned}$$

If we require  $P(t) = 1.0\sin\omega t + 1.0\cos\omega t$ ,

Let  $A = 1.0$ ,  $C = 1.0$ ,  $D = -1.0$  and all else zero, so that

$$\begin{aligned} P(t) &= \text{Re al} \left[ 1(1 - i1e^{i(0-\omega 0)}) e^{i\omega t} \right] \\ &= \text{Re al} \left[ 1(1 - i) e^{i\omega t} \right] \\ &= \text{Re al} \left[ (1 - i)(\cos \omega t + i \sin \omega t) \right] \\ &= \text{Re al} \left[ \cos \omega t + i \sin \omega t - i \cos \omega t + \sin \omega t \right] \\ &= \sin \omega t + \cos \omega t \end{aligned}$$

Notice that  $\cos\omega t$  is basically 90 degrees out of phase with  $\sin\omega t$ . If we require a function which is out of phase by  $\alpha$ , for instance  $P(t) = 1.0\sin(\omega t + \alpha)$ ,

Let  $A = 1.0$ ,  $D = -1.0$ ,  $\theta = \alpha$  and all else zero, so that

$$\begin{aligned} P(t) &= \text{Re al} \left[ (0 - i) e^{i(\alpha - \omega t)} e^{i\omega t} \right] \\ &= \text{Re al} \left[ -i e^{i(\omega t + \alpha)} \right] \\ &= \text{Re al} \left[ -i (\cos(\omega t + \alpha) + i \sin(\omega t + \alpha)) \right] \\ &= \text{Re al} \left[ -i \cos(\omega t + \alpha) + \sin(\omega t + \alpha) \right] \\ &= \sin(\omega t + \alpha) \end{aligned}$$

Likewise, the steady-state response should be interpreted.

$$\begin{aligned} u(t) &= \text{Re al} \left[ F(\omega) e^{i\omega t} \right] \quad \text{where } F(\omega) \text{ is complex} \\ &= \text{Re al} \left[ \left( D(\omega) \frac{P_0}{k} e^{-i\theta} \right) e^{i\omega t} \right] \\ &= \text{Re al} \left[ D(\omega) \frac{P_0}{k} e^{i(\omega t - \theta)} \right] \\ &= \text{Re al} \left[ D(\omega) \frac{P_0}{k} (\cos(\omega t - \theta) + i \sin(\omega t - \theta)) \right] \\ &= D(\omega) \frac{P_0}{k} \cos(\omega t - \theta) \end{aligned}$$

It is suggested that the  $P(\omega)$  be inputted in Complex Cartesian format (i.e. RLOAD1) and that the response  $u(t)$  be interpreted in Complex Polar format. Remember that it is  $P(\omega)$  that is inputted in RLOAD1 (and not  $P(t)$ ) and that it is  $F(\omega)$  which is outputted by NASTRAN in terms of preferably magnitude and phase. The NASTRAN output is

$$\text{Magnitude} = D(\omega) \frac{P_0}{k} \quad \text{and} \quad \text{Phase} = \theta$$

Note that  $D(\omega)$  is the (magnitude of the) dynamic amplification factor.  $F(\omega)$  can of course still be outputted in real and imaginary components if desired, but it is far more indicative if it is outputted in terms of magnitude and phase. All instances of phase refer to the clockwise angle from the real axis in the complex plane. Hence, we can make the following conclusions from the steady-state harmonic analysis,

- (i) if  $P(\omega)$  is only positive real such that  $P(t) = 1.0\cos\omega t$ , then the response will be

$$u(t) = D(\omega) \frac{P_0}{k} \cos(\omega t - \theta)$$

which means that the response lags the loading by  $\theta$ . There will be a phase lag if and only if there is damping within the system.

- (ii) if  $P(\omega)$  is only negative imaginary such that  $P(t) = 1.0\sin\omega t$ , then the response will be

$$u(t) = D(\omega) \frac{P_0}{k} \sin(\omega t - \theta)$$

which means that the response again lags the loading by  $\theta$ . There will be a phase lag if and only if there is damping within the system.

- (iii) if  $P(\omega)$  is both real and imaginary, such that  $P(t) = 1.0\sin\omega t + 1.0\cos\omega t$ , then the response will be

$$u(t) = D(\omega) \frac{P_0}{k} [\sin(\omega t - \theta) + \cos(\omega t - \theta)]$$

which means that the response again lags the loading by  $\theta$ . There will be a phase lag if and only if there is damping within the system.

Thus, it can be concluded that there will only be a phase lag in the response if there is damping within the system.

Defining the spatial distribution using DAREA only enables the specification of dynamic concentrated forces and moments. To accommodate more complicated loadings, the LSEQ entry is used to refer to static load entries that define the spatial distribution of the dynamic loads.

<b>\$ CASE CONTROL SECTION</b>									
LOADSET = < ID OF LSEQ > DLOAD = < ID OF RLOAD1/RLOAD2 >									
<b>\$ BULK DATA</b>									
LSEQ	ID	DAREA Reference Link	Static Load ID	Temp Load ID					
RLOAD1	ID	DAREA Reference Link	DELAY ID	DPHASE ID	Real TABLED1 ID	Imaginary TABLED1 ID			
RLOAD2	ID	DAREA Reference Link	DELAY ID	DPHASE ID	Amplitude TABLED1 ID	Phase TABLED1 ID			

The DAREA Reference Link links the RLOAD1/RLOAD2 entry to the LSEQ which can now be used to refer to static load set ids which define the spatial distribution of the dynamic loads. The static load set id can refer to one or more static load entry types. Obviously, there is not a DAREA entry anymore. It is replaced by an LSEQ bulk data entry, a LOADSET case control entry and the pertinent bulk data static load entries such as FORCE, PLOADi or GRAV.

A new automatic feature will be activated *if and only if* the user does *not* have a LOADSET/LSEQ selection. With the new enhancement, it is no longer necessary for the user to explicitly specify LOADSET/LSEQ combination in order to employ static loading data in dynamic analysis. Instead, when the user selects a dynamic load, all static loads and thermal loads that have the same ID as the DAREA ID on the dynamic load entry are automatically selected.

The frequency dependent load card RLOAD1/RLOAD2 is selected using the DLOAD case control command. If more than one RLOAD1/RLOAD2 entry is required, then a dynamic load set combination is required. This is done using a DLOAD bulk data entry that linearly combines multiple RLOAD1/RLOAD2 entries.

<b>\$ CASE CONTROL SECTION</b>									
DLOAD = < ID OF DLOAD >									
<b>\$ BULK DATA</b>									
DLOAD	ID	Overall Scale Factor	Scale Factor	RLOAD1 / RLOAD2 ID	Scale Factor	RLOAD1 / RLOAD2 ID	..etc..		

#### 4.5.3.1.2 Enforced Motion

Four methods can be used for enforced motion, namely: -

- (i) The direct absolute response approach
- (ii) The direct relative response approach
- (iii) The indirect large mass method (absolute response approach)
- (iv) The indirect large spring method (absolute response approach)

The direct absolute response approach makes no assumptions. The direct relative response approach makes the following assumptions<sup>3</sup>: -

- (i) base movements in any given direction are identical i.e. that the base supports cannot move independently
- (ii) no mass or damping coupling between the structure and the ground (the off diagonal terms in the unsupported mass matrix that couple the structure and the ground movements are zero or are insignificant)
- (ii) no damping into the ground

In both the direct absolute and direct relative approaches, the equation of motion is the same on the LHS, hence the same resonant frequencies and mode shapes are obtained, only the applied loading vector on the RHS differ. The two approaches will also give the same stresses within the elements. With the assumption of no coupling of mass and damping, the absolute response is found by applying a base displacement and the relative response by applying a base displacement. The absolute displacement response and relative displacement response only differ by a rigid body movement.

##### 4.5.3.1.2.1 Direct Enforced Motion (Absolute Response Approach)

The direct approach of applying enforced motion is the most accurate method. Denoting the free DOFs as f and the constrained DOFs (whether with enforced motion or zero constraints) as s, P the force and q the reaction, the dynamic equilibrium equation can be partitioned as

$$\left( -\omega^2 \begin{bmatrix} M_{ff} & M_{fs} \\ M_{sf} & M_{ss} \end{bmatrix} + i\omega \begin{bmatrix} B_{ff} & B_{fs} \\ B_{sf} & B_{ss} \end{bmatrix} + \begin{bmatrix} K_{ff} & K_{fs} \\ K_{sf} & K_{ss} \end{bmatrix} \right) \begin{Bmatrix} U_f \\ U_s \end{Bmatrix} = \begin{Bmatrix} P_f \\ P_s + q_s \end{Bmatrix}$$

With zero constraints, i.e.

$$(U_s = \{0\})$$

the dynamic equation of motion reduces to the usual

$$(-\omega^2 M_{ff} + i\omega B_{ff} + K_{ff})U_f = P_f$$

with the corresponding reactions

$$q_s = -P_s + (-\omega^2 M_{sf} + i\omega B_{sf} + K_{sf})U_f$$

But, with enforced motion, the dynamic equation of motion is

$$(-\omega^2 M_{ff} + i\omega B_{ff} + K_{ff})U_f = P_f - (-\omega^2 M_{fs} + i\omega B_{fs} + K_{fs})U_s$$

with the corresponding reactions

<sup>3</sup> NAFEMS. *A Finite Element Primer*. NAFEMS Ltd., Great Britain, 1992.

$$q_s = -P_s + (-\omega^2 M_{sf} + i\omega B_{sf} + K_{sf})U_f + (-\omega^2 M_{ss} + i\omega B_{ss} + K_{ss})U_s$$

Hence, in general the user specifies the either the support displacement, velocity or acceleration, as all three motions are related to each other in the sense that the velocity is the first derivative and the acceleration is the second derivative of the displacement.

$$u(t) = U(\omega) \cdot e^{i\omega t} \quad \dot{u}(t) = i\omega U(\omega) \cdot e^{i\omega t} \quad \ddot{u}(t) = -\omega^2 U(\omega) \cdot e^{i\omega t}$$

But for most structural problems, the damping component  $B_{sf}$  (not  $B_{ss}$  in the reaction expression) can be ignored and for lumped mass formulations (or at least no coupling to the support freedoms),  $M_{sf}$  is zero, hence reducing the equivalent forcing function to

$$P_f(t) - K_{fs} u_s(t)$$

and hence, only the base displacement excitation needs to be incorporated. However, these approximations need not necessarily be employed in which case the absolute approach has **no inherent assumptions**. Note that the response will be obtained in absolute terms. This solution method is general and is valid even if different supports are moving with different independent excitations.

#### 4.5.3.1.2.2 Direct Enforced Motion (Relative Response Approach)

Described for the time domain in the direct transient response section.

The DLOAD Case Control Command, optionally the DLOAD bulk data entry, RLOAD1/RLOAD2, DELAY, DPHASE and TABLED1 is used in the same way as they were when load excitations were applied. One difference is the TYPE Field 8 of RLOAD1/RLOAD2 where enforced motion in terms of DISP, VELO or ACCE is specified. Another difference for the direct enforced motion lies in the EXCITEID Field 3 of RLOAD1/RLOAD2, where instead of referencing a DAREA card (hence not requiring a DAREA card at all for enforced motion), the EXCITEID Field references an SPCD entry, which in turn will reference a GRID ID and an associated DOF component in which the enforced motion is to be applied. Now at the same time, in line with methods of applying enforced motion in static analysis, the DOF component of the GRID ID with enforced motion must be constrained with an SPC bulk data entry which of course must be referenced by an SPC Case Control Command. Modal augmentation vectors by PARAM, RESVEC, YES must be used for modal methods. This is because since there no rigid body modes (as they are constrained by the enforced motion), there can be no motion of the enforced points unless RESVEC is used.

**4.5.3.1.2.3 Indirect Large Mass Method (Absolute Response Approach) – Base Acceleration Specified**

If a very large mass  $m_0$ , which is several orders of magnitude larger than the mass of the entire structure, is connected to a DOF where a dynamic load is applied, then the acceleration of the DOF is approximately

$$\ddot{u}(t) = \frac{P(t)}{m_0}$$

Hence, the (large) force required to produce the desired acceleration at the DOF is

$$P(t) = m_0 \ddot{u}(t)$$

The stiffness, damping and the inertial force of the mass of the structure at the DOF contributes little in comparison to the force provided by the large mass, hence the acceleration response is due primarily to the inertial force of the large mass. The larger the mass in comparison, the more accurate the acceleration excitation. However the magnitude is limited by numeric overflow in the computer. MSC recommends that the value of  $m_0$  be approximately  $10^6$  times the mass of the entire structure for an enforced translational DOF and  $10^6$  times the mass moment of inertia of the entire structure for a rotational DOF (for 6 digits of numerical accuracy). The disadvantage of the large mass method is that it involves a loss of numerical conditioning and hence a loss of accuracy of the response. If the large mass is  $10^6$  times the mass of the structure, this is equivalent to losing 6 significant figures in the definition of the mass and stiffness matrices.

The following procedure is employed to specify prescribed motion in forced frequency response analysis: -

- (i) remove constraints from the enforced DOFs
- (ii) place large masses or inertia scalar elements CMASSi or CONMi with values approximately  $10^6$  times the mass or mass moment of inertia of the entire structure
- (iii) if a sinusoidal displacement motion is to be prescribed

$$\text{Prescribed displacement } u(t) = B \sin(2\pi ft)$$

$$\text{Hence, prescribed acceleration } \ddot{u}(t) = -B4\pi^2 f^2 \sin(2\pi ft)$$

$$\begin{aligned} \text{Hence, load with large mass method } P(t) &= P(f) \sin(2\pi ft) \\ &= -m_0 B 4\pi^2 f^2 \sin(2\pi ft) \end{aligned}$$

$$\text{Hence, } P(f) = -m_0 B 4\pi^2 f^2$$

Clearly, if a sinusoidal (of amplitude B) velocity or acceleration was to be prescribed the amplitude of the force  $P(f)$  would simply be  $m_0 B 2\pi f$  or  $m_0 B$  respectively.

The scale factor  $A=Bm_0$  can be entered in the DAREA entry. The factors  $-4\pi^2 f^2$  and  $2\pi f$  are frequency-dependent factors which has to be entered using the TABLED4 entry, illustrated for the former as follows,

TABLED4	ID	X1=0.0	X2=1.0	X3=0.0	X4=10000.0				
	A0=0.0	A1=0.0	A2=-4π <sup>2</sup>	A3	A4	A5	... etc ...	ENDT	

The TABLED4 entry has the following algorithm,

$$y = \sum_{i=0}^N A_i \left( \frac{x - X1}{X2} \right)^i$$

In this case,

$$y = -4\pi^2 \left( \frac{x - 0.0}{1.0} \right)^2$$

Only the coefficient A2 is of a non-zero value to generate a frequency dependent coefficient to the second degree. Likewise a prescribed sinusoidal velocity will have a frequency dependency to the first degree and a prescribed sinusoidal acceleration will not have a frequency dependency. Note that when  $x < X3$ ,  $x = X3$  and when  $x > X4$ ,  $x = X4$ . This has the effect of placing bounds on the table, there is no extrapolation outside the table boundaries. ENDT ends the table input.

The DLOAD Case Control Command, optionally the DLOAD bulk data entry, RLOAD1/RLOAD2, DAREA, DELAY, DPHASE and TABLED1 is used in the same way as they were when load excitations were applied.

To ensure that the chosen mass values are high enough two modal analyses (SOL 103) should be run, one with the enforced DOFs constrained and the other with the large masses attached and the DOFs left unconstrained. The flexible frequencies (not the rigid mode frequencies) between the two analyses should be well comparable (to within 4 or 5 significant figures), otherwise the mass values should be increased.

In modal methods, further considerations must be made to the rigid body modes. Globally unconstrained structures will have rigid body modes. Releasing a global DOF and placing a large mass there to enforce an applied motion will result in that DOF being unconstrained and hence will result in a rigid body mode (stress free mode). This mode can safely be discarded in the solution by using LFREQ or simply not calculating it in EIGRL. If however two large masses are placed at two different locations to simulate enforced motion in the same direction, there will be a further low-frequency mode that represents the motion of one large mass relative to the other. This mode does contribute to the stresses and cannot be ignored. It must be captured within EIGRL and LFREQ. To avoid this problem, a solution will be to place only one large mass at an arbitrary location and connect with RBE2 elements all DOFs that are to be subjected to that enforced motion.

#### **4.5.3.1.2.4 Indirect Large Spring Method (Absolute Response Approach) – Base Displacement Specified**

Described for the time domain in the direct transient response section.

### 4.5.3.2 GL, ML P- $\Delta$ ( $K_G^A$ From $K_E^A$ ) Direct Forced Frequency Response Analysis

It is often necessary to incorporate the reduction in bending stiffness of gravity load resisting columns for the analysis of lateral loads. The following procedure is undertaken.

#### Phase 1

Perform static analysis (with loads that cause the greatest negative or positive geometric stiffness) based on  $[K_E^A]$  but include the segyroa.v2001 alter prior to the Case Control Section in order to compute the geometric stiffness matrix  $[K_G^A]_1$  (and output into a .pch file) based on the generated element loads from the  $[K_E^A]$  static analysis.

#### Phase 2

A SOL 108 is undertaken based on  $[K_E^A] + [K_G^A]_1$  with the k2gg=ktjj statement in the Case Control Section and the outputted .pch file which contains the ktjj matrix in the Bulk Data. The responses at this stage represent the P- $\Delta$  ( $K_G^A$  From  $K_E^A$ ) response to the dynamic excitation.

The following equivalent alternative procedure can also be employed.

<pre> \$ CASE CONTROL SECTION  SUBCASE 1 LABEL = Static Preload Load Case LOAD = &lt; ID of FORCEi, MOMENTi, PLOADi, GRAV, LOAD, SPCD Cards in Bulk Data &gt; TEMP(Load) = &lt; ID of TEMP, TEMPRB, TEMPP1 Cards in Bulk Data &gt; DEFORM = &lt; ID of DEFORM Cards in Bulk Data &gt; SUBCASE 2 LABEL = P-<math>\Delta</math> Direct Frequency Response Analysis STATSUB(PRELOAD) = 1 DLOAD = &lt; ID OF RLOAD1 or RLOAD2 &gt; </pre>
---

The method is valid when **only the prestress is judged to affect the geometric stiffness** such as in the compressive preload of building columns due to gravitational loads and the prestressing of extremely taut cables that sag very little under gravity but not in systems such as suspension bridges. Where lateral loads are large enough to affect the geometry of the system with prestress, then a repetitive P- $\Delta$ , SOL 106, implicit dynamic relaxation SOL 129 or explicit dynamic relaxation must be employed. But in single P- $\Delta$  analysis, because cables do not have much elastic bending stiffness, the initial static preload subcase should only include the prestress and not gravity as including gravity is the same as solving two linear static problems of stiffness  $K_E^A$  with preload and gravity as the applied loads respectively. Clearly, in the gravity case, it is nonsensical as the cables do in reality have differential stiffness (from the prestress) to resist the gravitational force. Prestress in one direction (i.e. along the axis of cable) will cause a differential stiffness in the orthogonal direction. Gravity acts in the orthogonal direction and hence cannot be accounted for in the calculation of the prestress in this single P- $\Delta$  analysis. To quantitatively decide if gravity need not be considered in contributing to the differential stiffness of the cables, a static P- $\Delta$  analysis should be carried out, the first subcase being a SOL 101 with only the prestress as applied loads and the second subcase a P- $\Delta$  SOL 101 (i.e. utilizing the induced prestress from the first subcase to form a geometric stiffness matrix) with both the gravity and prestress included as applied loads. If the difference in the cable element forces between subcases 1 and 2 is negligible, then gravity has little influence in affecting the geometric stiffness. If there is a major difference in the cable element force, then clearly, gravity will affect the geometric stiffness and as such, a repetitive P- $\Delta$ , SOL 106, implicit dynamic relaxation or explicit dynamic relaxation must be used to converge to the true  $K_T$ . Likewise, in the single P- $\Delta$  analysis of multi-storey buildings, gravity (and only gravity) acts in axis of columns to generate prestress, and the differential stiffness is computed for the orthogonal direction reducing resistance to lateral wind forces, applied in the second subcase with gravity too.

When a static subcase is specified for linear transient response analysis (SOLs 109 and 112) with STATSUB(PRELOAD), the data recovery is controlled by PARAM, ADSTAT. By default (YES) the static solution will be superimposed on the dynamic response solution (displacement, stress and SPCForce). The relative solution can be obtained in reference to the static solution point by PARAM, ADSTAT, NO. No provision is made for frequency response analysis, because the static responses contribute only to the zero frequency response.

The STATSUB(PRELOAD) computes the differential stiffness due to the prestress and also the follower force. The follower force is calculated and incorporated by the use of PARAM, FOLLOWK, YES. We know how the prestress affects the differential stiffness, namely a tensile prestress causing an increase in stiffness. The effect of the follower force on the stiffness is different. For example, for a cylinder under external pressure critical buckling load may be over-estimated (even though the mode shapes are similar) in a SOL 105 and the natural frequencies in vibration may be underestimated (even though the mode shapes are similar) in a SOL 103 in the absence of follower stiffness. To the contrary, these observations are reversed in case of centrifugal loads. Centrifugal forces as a constant (static) load are applied by a Bulk Data RFORCE to any elements that have masses. The follower stiffness due to centrifugal load has the effect of lowering stiffness (although the centrifugal load tensioning effect increases stiffness), consequently lowering natural frequencies (even though the mode shapes are similar) in a SOL 103 and lowering the buckling loads (even though the mode shapes are similar) in a SOL 105. This effect increases as the RPM increases, and it becomes significant when the RPM is over 1000. For moderately geometric nonlinear analysis, exclusion of follower stiffness affects the rate of convergence, but the converged solution is correct. For severely geometric nonlinear analysis, it may not be possible to obtain a converged solution without including follower stiffness. As the geometric nonlinearity intensifies, so is the effect of follower stiffness. Therefore, inclusion of follower stiffness greatly enhances the convergence if the deformation involves severe geometric nonlinearity.

### 4.5.3.3 GL, ML P- $\Delta$ ( $K_G^A$ From Exact or Approximate $K_T^A$ ) Direct Forced Frequency Response Analysis

It is often necessary to include the differential stiffness, especially if there are prestressed cables in the model. To obtain  $K_T^A$ , to be theoretically exact, a GNL SOL 106 (or implicit dynamic relaxation SOL 129 or explicit dynamic relaxation LS-DYNA) with prestress (as temperature loads say) and gravity must be undertaken. Alternatively, an approximation to  $K_T^A$  can be obtained by repetitive P- $\Delta$  static analyses with the prestress (as temperature loads say) and gravity applied. The procedure to obtain this approximate  $K_T^A$  will be presented. Note that the approximate  $K_T^A$  will be the summation of the elastic stiffness  $K_E$  at the undeflected (by the prestress and gravity) state but  $K_G$  at the deflected (by the prestress and gravity) state. Hence if  $K_E$  changes considerably during the application of the prestress, a full SOL 106 (or implicit dynamic relaxation SOL 129 or explicit dynamic relaxation LS-DYNA), which converges to the  $K_E$  and  $K_G$  at the deflected (by the prestress and gravity) state should be employed. Hence for the modelling of a suspension bridge where there is a great change in geometry (known in the bridge industry as **form-finding**, so-called because it is necessary to find the form or shape of the catenary suspension cables), it may be prudent to employ SOL 106 (or implicit dynamic relaxation SOL 129 or explicit dynamic relaxation LS-DYNA), but for a high tension low sag cable on say a tower with prestressed cables, the repetitive P- $\Delta$  static analysis may be adequate. The repetitive P- $\Delta$  analysis basically involves a number of iterations of linear static analyses to obtain an approximate  $K_T^A$ . Note again that A refers to the initial undeflected (by the collapsing load) state, but deflected by the prestress and gravity. To perform the repetitive P- $\Delta$  analysis, a static analysis is performed based on  $K_E^A$  with temperature loads and gravity to generate forces in the structural elements, which in turn provides input for the computation of  $K_{Gi}^{AKT_m}$  where m is the iterations. Repetitive static analysis is performed with the prestress and gravity updating the stiffness matrix  $K_E^A + K_{Gi}^{AKT_{m-1}} + K_{Gi}^{AKT_m}$  until convergence of displacements is obtained. The tangent stiffness at this stage is the approximate converged tangent stiffness matrix  $K_T^A = K_E^A + K_{Gi}^{AKT}$ . The converged displacements represent the approximate P- $\Delta$  ( $K_G^A$  From Approximate  $K_T^A$ ) static response to the initial prestress loads. The converged geometric stiffness at this stage would be that based upon the approximate tangent stiffness matrix  $K_T^A$ , i.e.  $K_{Gi}^{AKT}$ .

#### Phase 1

Perform static analysis (with prestress and gravity) based on  $[K_E^A]$  but include the segyroa.v2001 alter prior to the Case Control Section in order to compute the geometric stiffness matrix  $[K_G^A]_1$  (and output into a .pch file) based on the generated element loads from the  $[K_E^A]$  static analysis.

#### Phase 2

Perform static analysis (with prestress and gravity) based on  $[K_E^A] + [K_G^A]_1$  by including the k2gg = ktjj statement in the Case Control Section, the outputted .pch file which contains the ktjj matrix in the Bulk Data and the segyroa.v2001 alter prior to the Case Control Section to compute the  $[K_G^A]_2$  (and output into the .pch file overwriting previous data) based on the generated element loads from the  $[K_E^A] + [K_G^A]_1$  static analysis.

#### Phase 3

Repeatedly perform the Phase 2 static analysis (with prestress and gravity) based on  $[K_E^A] + [K_G^A]_i$  for  $i = 2$  to  $n$  where  $n$  represents the number of iterations required for the change in deflections between analyses to become negligible. This would signify that the change in the  $[K_G^A]$  matrix become negligible and the correct  $[K_G^A]$  is attained. The deflections and the other responses at this stage represent the P- $\Delta$  ( $K_G^A$  From Approximate  $K_T^A$ ) static response to the prestress and gravity. The stiffness of the structure is  $K_T^A$ .

#### Phase 4

A SOL 108 is undertaken with the k2gg=ktjj statement in the Case Control Section and the outputted .pch file which contains the latest ktjj matrix in the Bulk Data. The responses at this stage represent the P- $\Delta$  ( $K_G^A$  From Approximate  $K_T^A$ ) response to the dynamic excitation.

#### 4.5.4 Hand Methods Verification

##### 4.5.4.1 The Theory of the Dynamic Magnification Factor for Undamped Motion and Hence the Determination of Maximum Dynamic Displacement, $u_{\max}$ for Deterministic Harmonic Loading by Classically Solving the SDOF Linear Undamped ODE and Maximizing the Solution

Equation of motion

$$m\ddot{u}(t) + ku(t) = \text{Re al} \left[ p_0 e^{i\omega t} \right]$$

Assume solution

$$u(t) = u_c(t) + u_p(t)$$

For homogenous part,

$$m\ddot{u}_c(t) + ku_c(t) = 0$$

assume  $u_c(t) = \text{Re al} \left[ G e^{\lambda t} \right]$  where  $G = G_R + iG_I$  and  $\lambda = \alpha + i\omega_d$

$$mG\lambda^2 e^{\lambda t} + kGe^{\lambda t} = 0$$

$$(m\lambda^2 + k)Ge^{\lambda t} = 0$$

for LHS to be zero for all t

$$(m\lambda^2 + k) = 0 \quad \text{as} \quad Ge^{\lambda t} > 0$$

the roots of this quadratic characteristic equation are

$$\lambda_1 = +i\sqrt{\frac{k}{m}} \quad \lambda_2 = -i\sqrt{\frac{k}{m}}$$

$$\therefore \alpha = 0 \quad \text{and} \quad \omega_d = \omega_n = \sqrt{\frac{k}{m}} \text{ rad/s}$$

hence, the complementary function,

$$u_c(t) = \text{Re al} \left[ G_1 e^{\lambda_1 t} + G_2 e^{\lambda_2 t} \right]$$

$$u_c(t) = \text{Re al} \left[ (G_{1R} + iG_{1I})(\cos \omega_n t + i \sin \omega_n t) + (G_{2R} + iG_{2I})(\cos \omega_n t - i \sin \omega_n t) \right]$$

$$u_c(t) = \text{Re al} \left[ ((G_{1R} + G_{2R}) \cos \omega_n t - (G_{1I} - G_{2I}) \sin \omega_n t) + i((G_{1I} + G_{2I}) \cos \omega_n t + (G_{1R} - G_{2R}) \sin \omega_n t) \right]$$

for the free vibration response to be real for all t,

$$G_{1I} = -G_{2I} \quad \text{and} \quad G_{1R} = G_{2R}$$

since there are two less independent constants, let

$$G_{1I} = -G_{2I} = G_I \quad \text{and} \quad G_{1R} = G_{2R} = G_R$$

we notice that  $G_1$  and  $G_2$  are a complex conjugate pair

$$G_1 = G_R + iG_I \quad \text{and} \quad G_2 = G_R - iG_I$$

hence

$$u_c(t) = 2G_R \cos \omega_n t - 2G_I \sin \omega_n t$$

For the inhomogenous part,

assume  $u_p(t) = \text{Re al} \left[ F(\omega) e^{i\omega t} \right]$  hence on substitution,

$$-m\omega^2 F(\omega) + kF(\omega) = p_0$$

$$F(\omega) = \frac{p_0}{k - m\omega^2} = \frac{p_0/k}{1 - (\omega/\omega_n)^2}$$

thus

$$u_p(t) = \text{Re al} \left[ F(\omega) e^{i\omega t} \right] = \frac{p_0/k}{1 - (\omega/\omega_n)^2} \cos \omega t$$

Hence, the general solution is

$$u(t) = 2G_R \cos \omega_n t - 2G_I \sin \omega_n t + \frac{p_0/k}{1 - (\omega/\omega_n)^2} \cos \omega t$$

$$\text{where } 2G_R = \frac{\dot{u}(0)}{\omega_n} - \frac{\omega p_0/k}{(1 - \omega^2/\omega_n^2)\omega_n} \quad \text{and} \quad -2G_I = u(0)$$

Notice that the initial conditions were obtained from the general solution, and not from considering the complementary function alone.

Investigating the frequency of the response, the starting transient solution  $u_c(t)$  is at the frequency and is in phase with the structure's  $\omega_n$ , whilst the steady-state solution  $u_p(t)$  is at the frequency and is in phase with the loading's  $\omega$ . Since there is no damping, there is no imaginary component in the complex response function  $F(\omega)$ .

Investigating the amplitude of the response, the steady-state solution has a static displacement amplitude  $p_0/k$  scaled by the (magnitude of the) dynamic amplification factor  $1/(1 - \omega^2/\omega_n^2)$ . Hence, the (magnitude of the) dynamic amplification factor  $D(\omega)$  increases as  $\omega/\omega_n$  approaches unity, and resonance occurs. With no damping, the maximum (magnitude of the) dynamic amplification occurs exactly when  $\omega = \omega_n$ .

#### 4.5.4.2 The Theory of the Dynamic Magnification Factor for Damped Motion and Hence Determination of Maximum Dynamic Displacement, $u_{\max}$ for Deterministic Harmonic Loading by Classically Solving the SDOF Linear Damped ODE and Maximizing the Solution

Equation of motion

$$m\ddot{u}(t) + c\dot{u}(t) + ku(t) = \text{Re al} [p_0 e^{i\omega t}]$$

Assume solution

$$u(t) = u_c(t) + u_p(t)$$

For homogenous part,

$$m\ddot{u}_c(t) + c\dot{u}_c(t) + ku_c(t) = 0$$

assume  $u_c(t) = \text{Re al} [Ge^{\lambda t}]$  where  $G = G_R + iG_I$  and  $\lambda = \alpha + i\omega_d$

$$mG\lambda^2 e^{\lambda t} + cG\lambda e^{\lambda t} + kGe^{\lambda t} = 0$$

$$(m\lambda^2 + c\lambda + k)Ge^{\lambda t} = 0$$

for LHS to be zero for all t

$$(m\lambda^2 + c\lambda + k) = 0 \quad \text{as} \quad Ge^{\lambda t} > 0$$

the roots of this quadratic characteristic equation are

$$\lambda_1 = -\frac{c}{2m} + \sqrt{\left(\frac{c}{2m}\right)^2 - \frac{k}{m}} \quad \lambda_2 = -\frac{c}{2m} - \sqrt{\left(\frac{c}{2m}\right)^2 - \frac{k}{m}}$$

hence, the complementary function,

$$u_c(t) = \text{Re al} [G_1 e^{\lambda_1 t} + G_2 e^{\lambda_2 t}]$$

in the under-damped case,  $c < c_{cr}$ , the roots are complex conjugates,

$$\lambda_1 = -\frac{c}{2m} + i\sqrt{\frac{k}{m} - \left(\frac{c}{2m}\right)^2} \quad \lambda_2 = -\frac{c}{2m} - i\sqrt{\frac{k}{m} - \left(\frac{c}{2m}\right)^2}$$

employing Euler's equations,

$$e^{i\theta} = \cos \theta + i \sin \theta$$

$$e^{-i\theta} = \cos \theta - i \sin \theta$$

hence, writing  $\omega_d = \sqrt{\frac{k}{m} - \left(\frac{c}{2m}\right)^2}$

$$u_c(t) = \text{Re al} \left[ (G_{1R} + iG_{1I}) e^{-\frac{c}{2m}t} (\cos \omega_d t + i \sin \omega_d t) + (G_{2R} + iG_{2I}) e^{-\frac{c}{2m}t} (\cos \omega_d t - i \sin \omega_d t) \right]$$

$$u_c(t) = \text{Re al} \left[ e^{-\frac{c}{2m}t} \left[ (G_{1R} + G_{2R}) \cos \omega_d t - (G_{1I} - G_{2I}) \sin \omega_d t + i((G_{1I} + G_{2I}) \cos \omega_d t + (G_{1R} - G_{2R}) \sin \omega_d t) \right] \right]$$

for the free vibration response to be real for all t,

$$G_{1I} = -G_{2I} \quad \text{and} \quad G_{1R} = G_{2R}$$

since there are two less independent constants, let

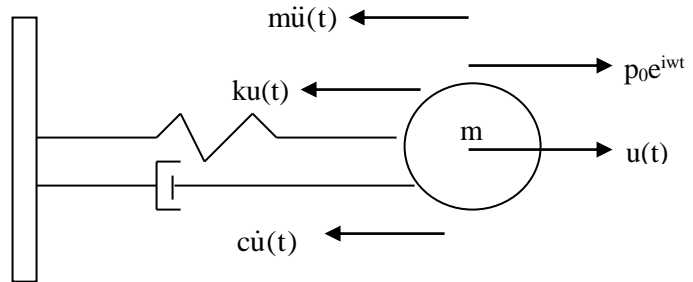
$$G_{1I} = -G_{2I} = G_I \quad \text{and} \quad G_{1R} = G_{2R} = G_R$$

we notice that  $G_1$  and  $G_2$  are a complex conjugate pair

$$G_1 = G_R + iG_I \quad \text{and} \quad G_2 = G_R - iG_I$$

hence

$$u_c(t) = e^{-\frac{c}{2m}t} \left[ (2G_R \cos \omega_d t - 2G_I \sin \omega_d t) \right]$$



defining the damping ratio  $\zeta$  such that

$$c = \zeta c_{cr} = \zeta 2\sqrt{km} = \zeta 2m\omega_n$$

the damped natural circular frequency,

$$\omega_d = \sqrt{\frac{k}{m} - \left(\frac{\zeta 2\sqrt{km}}{2m}\right)^2} = \sqrt{\frac{k}{m} - \frac{\zeta^2 k}{m}} = \sqrt{\frac{k}{m}(1 - \zeta^2)} = \omega_n \sqrt{1 - \zeta^2}$$

hence, the complementary function

$$u_c(t) = e^{-\zeta\omega_n t} [(2G_R \cos \omega_d t - 2G_I \sin \omega_d t)]$$

where  $\omega_d = \omega_n \sqrt{1 - \zeta^2}$  and  $2G_R, -2G_I$  being the constants of integration from the initial conditions.

For the inhomogeneous part,

assume  $u_p(t) = \text{Re al} [F(\omega)e^{i\omega t}]$  hence on substitution,

$$-m\omega^2 F(\omega) + ic\omega F(\omega) + kF(\omega) = p_0$$

$$F(\omega) = \frac{P_0}{k - m\omega^2 + ic\omega}$$

from complex number theory

$$x + iy = \left(\sqrt{x^2 + y^2}\right) e^{i\theta}, \theta = \tan^{-1}(y/x)$$

changing the denominator to a polar complex form

$$F(\omega) = \frac{P_0}{\sqrt{(k - m\omega^2)^2 + (c\omega)^2}} e^{i\theta}, \theta = \tan^{-1} \frac{c\omega}{k - m\omega^2} = \tan^{-1} \left( \frac{2\zeta\omega/\omega_n}{1 - \omega^2/\omega_n^2} \right)$$

$$F(\omega) = \frac{P_0/k}{\sqrt{(1 - \omega^2/\omega_n^2)^2 + (2\zeta\omega/\omega_n)^2}} e^{-i\theta}, \theta = \tan^{-1} \left( \frac{2\zeta\omega/\omega_n}{1 - \omega^2/\omega_n^2} \right)$$

thus,

$$u_p(t) = \text{Re al} [F(\omega)e^{i\omega t}]$$

$$u_p(t) = \frac{P_0/k}{\sqrt{(1 - \omega^2/\omega_n^2)^2 + (2\zeta\omega/\omega_n)^2}} \cos(\omega t - \theta)$$

Hence the general solution,

$$u(t) = e^{-\zeta\omega_n t} [(2G_R \cos \omega_d t - 2G_I \sin \omega_d t)] + \frac{P_0/k}{\sqrt{(1 - \omega^2/\omega_n^2)^2 + (2\zeta\omega/\omega_n)^2}} \cos(\omega t - \theta)$$

$$\text{where } \omega_d = \omega_n \sqrt{1 - \zeta^2}, \theta = \tan^{-1} \frac{2\zeta\omega/\omega_n}{(1 - \omega^2/\omega_n^2)}$$

The starting transient is insignificant because the term  $e^{-\zeta\omega_n t}$  will cause it to vanish. Investigating the frequency of the response, the insignificant starting transient is at the damped natural frequency of the structure,  $\omega_d = \omega_n(1 - \zeta^2)^{1/2}$  and the steady-state solution is at the frequency of but out of phase with the loading's  $\omega$  by  $\theta$ . The complex response function  $F(\omega)$  may contain both real and imaginary components depending on the complex loading function  $P(\omega)$  and the existence of damping within the system, i.e.

- (i) If  $P(\omega)$  is real and there is no damping within the system,  $F(\omega)$  is real
- (ii) If  $P(\omega)$  is complex and there is no damping within the system,  $F(\omega)$  is complex
- (iii) If  $P(\omega)$  is real and there is damping within the system,  $F(\omega)$  is complex
- (iv) If  $P(\omega)$  is complex and there is damping within the system,  $F(\omega)$  is complex

The complex expression for  $F(\omega)$  is often expressed in magnitude and phase  $\theta$ . If  $P(\omega)$  is only real, the value of the phase angle  $\theta$  gives an indication of the damping inherent within the system.

Recapping basic complex number theory,

a complex number contains real and imaginary components

$$z = x + iy$$

it can be written in a polar form by computing the magnitude and the phase

$$z = \left( \sqrt{x^2 + y^2} \right) e^{i\theta}, \quad \theta = \tan^{-1}(y/x)$$

$$z = \left( \sqrt{x^2 + y^2} \right) (\cos \theta + i \sin \theta), \quad \theta = \tan^{-1}(y/x)$$

The Cartesian form is visualized on a Cartesian diagram of real x- and imaginary y-axes. The polar form is visualized on the same Cartesian diagram with the magnitude being the radius from the origin and the phase being the angle of the radius from the real x-axis. It is implicitly understood that when a complex vector is used to represent a harmonic motion, it is the horizontal projection of the complex vector (i.e. the real component) that represents the motion.

Investigating the amplitude of the response, the steady-state solution has a static displacement amplitude  $p_0/k$  scaled by the (magnitude of the) dynamic amplification factor,  $D(\omega)$ .

$$D(\omega) = \frac{1}{\sqrt{\left(1 - \omega^2 / \omega_n^2\right)^2 + \left(2\zeta\omega / \omega_n\right)^2}}$$

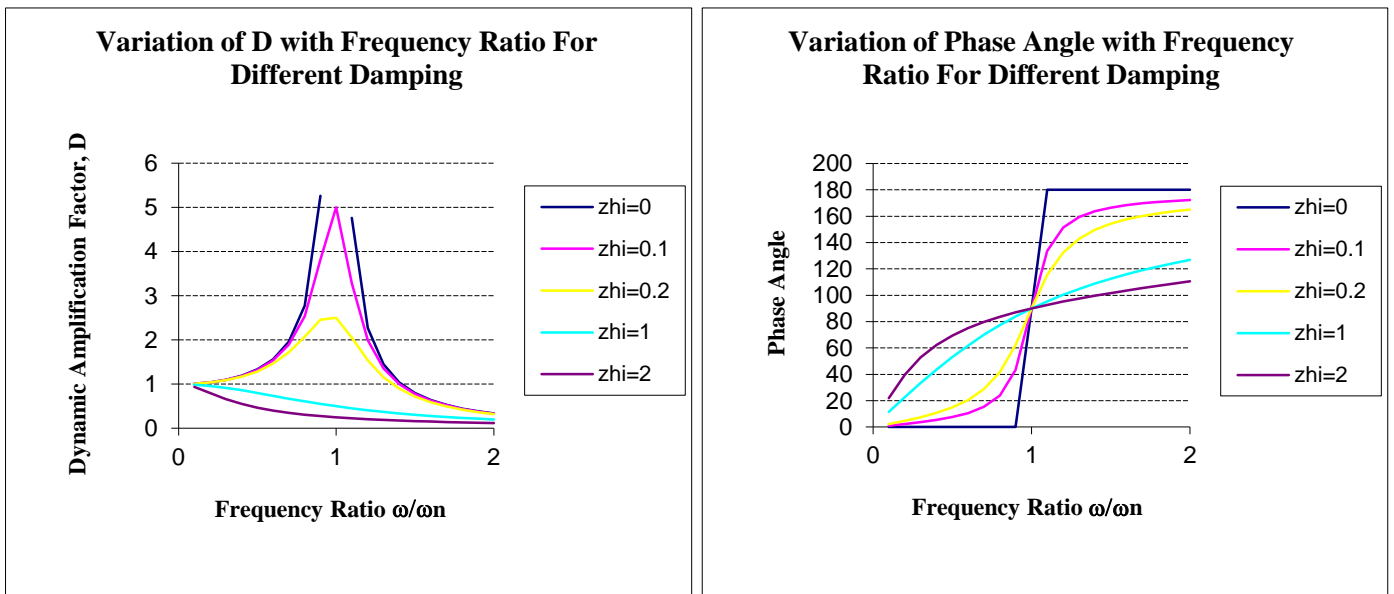
The following cases are identified: -

- (i) If  $\omega/\omega_n \ll 1$  (very low frequency loading), the (magnitude of the) dynamic amplification  $D(\omega)$  approaches 1, stiffness forces dominate and static solution obtained with the displacement response in phase with loading. Performing a frequency response analysis at a frequency of 0.0 Hertz gives the same results as a static analysis. The phase angle  $\theta$  approaches  $0^\circ$ .
- (ii) When  $\omega = \omega_n$ , the (magnitude of the) dynamic amplification factor  $D = 1/(2\zeta)$ . Resonance by definition occurs. Stiffness and inertial forces cancel each other and applied force is balanced by damping (hence the greater the damping, the smaller the response). Although the maximum amplification is not at its greatest, it is close enough to the maximum for even moderate amounts of damping. The phase angle  $\theta$  is  $90^\circ$ .
- (iii) If  $\omega/\omega_n = (1-2\zeta^2)^{1/2}$  (note how this is slightly different from  $\omega_d = \omega_n(1-\zeta^2)^{1/2}$  meaning which the maximum amplification does not actually occur exactly when the forcing frequency equals the damped natural frequency, never mind the undamped natural frequency,  $\omega_n$ ), the maximum (magnitude of the) dynamic amplification occurs.  $D = 1/(2\zeta(1-\zeta^2)^{0.5})$ .
- (iv) If  $\omega/\omega_n \gg 1$  (very high frequency loading), the (magnitude of the) dynamic amplification  $D(\omega)$  approaches 0, inertial forces dominate and no displacement obtained, i.e. loading is changing too fast for the structure to respond. The displacement response will be  $180^\circ$  out of phase with loading (i.e. displacement response will have opposite sign to loading force).

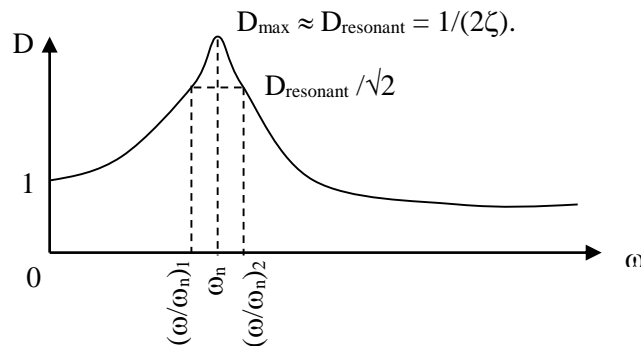
Hence, the increase in maximum response for a dynamic analysis compared to a static analysis comes from the (magnitude of the) dynamic amplification factor, which is a function of the forcing amplitude and the ratio between the forcing frequencies and the natural frequencies. If the structure is excited close to a resonance, then the stiffness force (potential or strain energy) and the inertia forces (kinetic energy) cancel out and the response amplitude is greater in order to maintain equilibrium. The amplitude of vibration is then controlled by the level of damping. The external forces are balanced by the damping forces. The frequencies at which resonance occurs, that is when the stiffness and the inertia forces cancel are called the natural frequencies of the system. This is evident from the eigenvalue problem  $[K]\{\phi\} = \omega^2[M]\{\phi\}$  where frequencies are found such that the inertia and stiffness forces cancel. It is the frequencies at which a free undamped system will vibrate if disturbed from equilibrium. Damping

causes the peak amplitude to occur at a slightly lower frequency so that the damped resonant frequency is slightly lower than the undamped natural frequency, but since typical structures are under-damped this change is so small it can be neglected. If the system is excited at some frequency other than resonance, then the amplitude of the response is largely controlled by the stiffness and inertia forces. In this case, they do not cancel each other and so the damping force is generally not as significant.

When damping is not considered, the maximum (magnitude of the) dynamic amplification occurs at resonance when the forcing frequency,  $\omega$  exactly matches the natural circular frequency,  $\omega_n$ . In that case, the amplification is infinite. This is not the case when damping is considered, i.e. maximum (magnitude of the) dynamic amplification does not occur exactly at resonance when the forcing frequency,  $\omega$  matches the natural circular frequency,  $\omega_n$  or when  $\omega$  matches the damped natural circular frequency,  $\omega_d = \omega_n(1-\zeta^2)^{1/2}$  for that matter, instead the maximum (magnitude of the) dynamic amplification occurs when  $\omega = \omega_n(1-2\zeta^2)^{1/2}$ .



The shape of the (magnitude of the) dynamic amplification factor  $D(\omega)$  versus frequency ratio  $\omega/\omega_n$  depends on the level of damping, as of course does the maximum (magnitude of the) dynamic amplification.



Measuring the bandwidth at  $1/\sqrt{2}$  of peak resonant amplitude for convenience, we can write for when

$$D_{resonant} = \frac{1}{\sqrt{2}} \frac{1}{2\zeta}$$

$$\frac{1}{\sqrt{(1 - \omega^2/\omega_n^2)^2 + (2\zeta\omega/\omega_n)^2}} = \frac{1}{\sqrt{2}} \frac{1}{2\zeta}$$

Squaring both sides and solving for the frequency ratio,

$$(\omega/\omega_n)^2 = 1 - 2\zeta^2 \pm 2\zeta\sqrt{1 + \zeta^2}$$

Ignoring higher order terms of  $\zeta^2$ , hence the assumption that this final equation is valid for only small damping  $\zeta$ ,

$$\begin{aligned} (\omega/\omega_n)^2 &= 1 - 2\zeta^2 \pm 2\zeta \\ \therefore (\omega/\omega_n)_1^2 &= 1 - 2\zeta^2 + 2\zeta & (\omega/\omega_n)_2^2 &= 1 - 2\zeta^2 - 2\zeta \\ \therefore (\omega/\omega_n)_1 &= 1 + \zeta - \zeta^2 & (\omega/\omega_n)_2 &= 1 - \zeta - \zeta^2 \end{aligned}$$

Finally, subtracting one root from each other

$$\zeta = \frac{(\omega/\omega_n)_2 - (\omega/\omega_n)_1}{2} = \frac{\omega_2 - \omega_1}{2\omega_n} = \frac{f_2 - f_1}{2f_n}$$

Remember that only when damping is small that the maximum (magnitude of the) dynamic amplification can be approximated to occur at resonance, by definition when the forcing frequency equals the undamped natural frequency. When damping is high, it is imperative that the (magnitude of the) dynamic amplification expression be differentiated or use is made of  $\omega_d = \omega_n(1-2\zeta^2)^{1/2}$  as the point at which the maximum (magnitude of the) dynamic amplification occurs.

#### 4.5.4.3 The Theory of Vibration (Base) Isolation and the Force Transmitted Into Rigid Foundation by the Damped Structure Subjected to Deterministic Harmonic Loading

Knowing the displacement response of a linear damped SDOF system subjected to deterministic harmonic loading also means that we can derive the velocity response. This means that we can evaluate the force transmitted through the spring-damper system. Considering the steady-state response due to a harmonic excitation of  $p_0 \sin \omega t$ ,

$$u(t) = D(\omega) p_0 / k \sin(\omega t - \theta)$$

where

$$D(\omega) = \frac{1}{\sqrt{(1 - \omega^2/\omega_n^2)^2 + (2\zeta\omega/\omega_n)^2}} \text{ and } \theta = \tan^{-1} \frac{2\zeta\omega/\omega_n}{(1 - \omega^2/\omega_n^2)}$$

Hence the force in the spring - damper system

$$\begin{aligned} \text{Force}(t) &= ku(t) + c\dot{u}(t) \\ &= D(\omega) p_0 / k (k \sin(\omega t - \theta) + c\omega \cos(\omega t - \theta)) \\ &= D(\omega) p_0 / k \sqrt{k^2 + c^2\omega^2} \sin(\omega t - \theta + \beta) \quad \text{where } \tan\beta = c\omega/k = 2\zeta\omega/\omega_n \\ &= D(\omega) p_0 \sqrt{1 + (2\zeta\omega/\omega_n)^2} \sin(\omega t - \theta + \beta) \quad \text{where } \tan\beta = c\omega/k = 2\zeta\omega/\omega_n \end{aligned}$$

Now, we define an expression for the relative transmissibility as the force response amplitude divided by the amplitude of the enforcing harmonic force,

$$\begin{aligned} T_r &= \frac{\text{Force Response Amplitude}}{P_0} \\ &= \frac{D p_0 \sqrt{1 + (2\zeta\omega/\omega_n)^2}}{P_0} \\ &= \frac{\sqrt{1 + (2\zeta\omega/\omega_n)^2}}{\sqrt{(1 - \omega^2/\omega_n^2)^2 + (2\zeta\omega/\omega_n)^2}} \end{aligned}$$

This is the force transmissibility expression. It will be shown that this expression can also represent the displacement and acceleration transmissibility's. This expression of force transmissibility is useful to calculate the force in the spring-damper system due to both stiffness and viscous damping. This can be used to calculate the force induced into a foundation by a vibrating structure. For instance, we can evaluate the force induced by a rotating machine into the supporting structure. And hence, we can design the supporting system of the rotation machine such that it induces the least amount of vibrations into the supporting structure (and hence the rigid foundation). The concepts behind vibration isolation (i.e. by investigating the transmissibility expression) is the same whether we are investigating

- (i) the force transmitted into the supporting structure (and hence the rigid foundation) due to a component subjected to harmonic force, or
- (ii) the displacement and acceleration response of a component subjected to harmonic displacement or acceleration at the rigid foundation

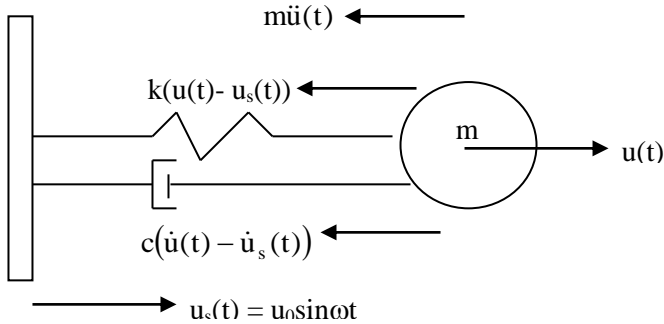
On investigating the transmissibility expression, we can design the supporting system for vibration isolation. The transmissibility is unity when the supporting system is infinitely stiff with respect to the loading frequency. The transmissibility is also unity when the frequency ratio is  $\sqrt{2}$ . If the supporting system is designed such that the frequency ratio is less than  $\sqrt{2}$  but greater than 0, the transmissibility is greater than one, which means that the supporting system actually makes matters worse as far as vibration isolation is concerned. When the frequency ratio is greater than  $\sqrt{2}$ , it is seen that the transmissibility is smaller than unity and hence, the supporting system functions as a vibration isolator. Damping is seen to be advantages only in the region when the frequency ratio is

less than  $\sqrt{2}$  (where a spring mounting supporting system makes matters worse) and not when the frequency ratio is greater than  $\sqrt{2}$  (where a spring mounting supporting system acts as an effective vibration isolator). This is not so important actually as the undesirable effects of high values of damping at frequency ratios greater than  $\sqrt{2}$  is not so great especially at even higher frequency ratios, i.e. achieved by making the supporting system even more flexible. Also, in the unfortunate circumstance that the resonance region of frequency ratio less than  $\sqrt{2}$  is somehow attained; high levels of damping are extremely effective. For good isolation, it is often recommended to design the supporting system for a frequency ratio of at least 3.

Note that the above force transmissibility expression is only valid if the foundation is rigid. If the foundation is not rigid, then the supporting system must be even more flexible in order to provide the same level of protection as when the foundation is rigid.

#### 4.5.4.4 The Theory of Vibration (Base) Isolation and the Determination of Maximum Dynamic Displacement, $u_{\max}$ for Deterministic Harmonic Support Motion (Displacement, Velocity or Acceleration) by Classically Solving the SDOF Linear Damped ODE (in Absolute and Relative Terms) and Maximizing the Solution

If instead of a harmonic force, the SDOF dynamic system can be subjected to a harmonic displacement such as a support motion. Let us consider the equation of motion in absolute terms at first.



Equation of motion

$$m\ddot{u}(t) + c(\dot{u}(t) - \dot{u}_s(t)) + k(u(t) - u_s(t)) = 0$$

Re placing  $u_s(t) = u_0 \sin \omega t$

$$m\ddot{u}(t) + c\dot{u}(t) + ku(t) = ku_0 \sin \omega t + c\omega u_0 \cos \omega t$$

$$m\ddot{u}(t) + c\dot{u}(t) + ku(t) = p_0 \sin(\omega t + \beta)$$

$$\text{where } p_0 = u_0 \sqrt{k^2 + (c\omega)^2} = u_0 k \sqrt{1 + (2\zeta\omega / \omega_n)^2}$$

$$\tan \beta = c\omega / k = 2\zeta\omega / \omega_n$$

This equation is similar to that of the harmonic loading except that there is a phase angle  $\beta$  in the loading. Hence the steady state solution is also similar except for the addition of the  $\beta$  phase angle.

$$u(t) = \frac{p_0 / k}{\sqrt{(1 - \omega^2 / \omega_n^2)^2 + (2\zeta\omega / \omega_n)^2}} \sin(\omega t + \beta - \theta) \quad \theta = \tan^{-1} \frac{2\zeta\omega / \omega_n}{(1 - \omega^2 / \omega_n^2)}$$

But now,  $p_0/k$  is not the static displacement any longer. Replacing the expression for  $p_0$

$$u(t) = \frac{u_0 \sqrt{1 + (2\zeta\omega / \omega_n)^2}}{\sqrt{(1 - \omega^2 / \omega_n^2)^2 + (2\zeta\omega / \omega_n)^2}} \sin(\omega t + \beta - \theta) \quad \theta = \tan^{-1} \frac{2\zeta\omega / \omega_n}{(1 - \omega^2 / \omega_n^2)}$$

The amplitude of the response is thus

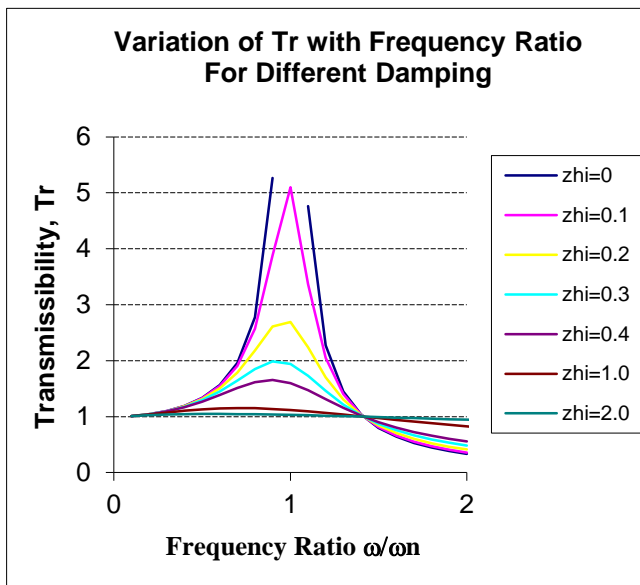
$$F = \frac{u_0 \sqrt{1 + (2\zeta\omega / \omega_n)^2}}{\sqrt{(1 - \omega^2 / \omega_n^2)^2 + (2\zeta\omega / \omega_n)^2}}$$

Now, we define an expression for the relative transmissibility as the displacement response amplitude  $F$  divided by the amplitude of the enforcing harmonic displacement,

$$T_r = \frac{F}{u_0} = \frac{\sqrt{1 + (2\zeta\omega / \omega_n)^2}}{\sqrt{(1 - \omega^2 / \omega_n^2)^2 + (2\zeta\omega / \omega_n)^2}}$$

This is the displacement transmissibility expression. The acceleration transmissibility is exactly similar. A plot of  $T_r$  versus  $\omega / \omega_n$  is somewhat similar to that of (the magnitude of the) dynamic amplification  $D$  versus  $\omega / \omega_n$ , except that all the curves of different  $\zeta$  pass through the same point of  $T_r = 1.0$  when  $\omega / \omega_n = \sqrt{2}$ . Noting the curves after

this point it is observed that damping tends to reduce the effectiveness of vibration isolation for frequency ratios greater than  $\sqrt{2}$ .



This formula is effective to determine the stiffness and damping (hence natural frequency) of an isolation system knowing the input displacement or acceleration and the maximum acceptable dynamic displacement or acceleration that the structural component can be subjected to.

Remember that only when damping is small that the maximum transmissibility can be approximated to occur at resonance. When damping is high, it is imperative that the transmissibility expression be differentiated (also use cannot be made of  $\omega = \omega_n(1-2\zeta^2)^{1/2}$  as this is based on differentiating and maximizing the (magnitude of the) dynamic amplification factor, D).

On investigating the transmissibility expression, we can design the supporting system for vibration isolation. The transmissibility is unity when the supporting system is infinitely stiff with respect to the loading frequency. The transmissibility is also unity when the frequency ratio is  $\sqrt{2}$ . If the supporting system is designed such that the frequency ratio is less than  $\sqrt{2}$  but greater than 0, the transmissibility is greater than one, which means that the supporting system actually makes matters worse as far as vibration isolation is concerned. When the frequency ratio is greater than  $\sqrt{2}$ , it is seen that the transmissibility is smaller than unity and hence, the supporting system functions as a vibration isolator. Damping is seen to be advantages only in the region when the frequency ratio is less than  $\sqrt{2}$  (where a spring mounting supporting system makes matters worse) and not when the frequency ratio is greater than  $\sqrt{2}$  (where a spring mounting supporting system acts as an effective vibration isolator). This is not so important actually as the undesirable effects of high values of damping at frequency ratios greater than  $\sqrt{2}$  is not so great especially at even higher frequency ratios, i.e. achieved by making the supporting system even more flexible. Also, in the unfortunate circumstance that the resonance region of frequency ratio less than  $\sqrt{2}$  is somehow attained; high levels of damping are extremely effective. For good isolation, it is often recommended to design the supporting system for a frequency ratio of at least 3.

Note that the above relationships were based on the absolute terms of acceleration, velocity and displacement, not the relative. The expression for  $u$  as depicted in the diagrams is always the absolute displacement. The notion of relative terms only arises when we have support motion. Note that in absolute terms, we need the support displacement and velocity in the equation of motion whilst in relative terms we need only the support acceleration in the equation of motion. Finding an expression for the relative displacement can be useful especially if we want to calculate the shear and bending forces induced in the isolating system. Of course we could subtract the absolute quantities, but this may prove difficult, as there is a phase difference between the input and response quantities.

In absolute terms, the equation of motion

$$m\ddot{u}(t) + c(\dot{u}(t) - \dot{u}_s(t)) + k(u(t) - u_s(t)) = 0$$

In relative terms

$$u_r(t) = u(t) - u_s(t)$$

Hence,

$$m(\ddot{u}_r(t) + \ddot{u}_s(t)) + c\dot{u}_r(t) + ku_r(t) = 0$$

$$m\ddot{u}_r(t) + c\dot{u}_r(t) + ku_r(t) = -m\ddot{u}_s(t)$$

Replacing  $u_s(t) = u_0 \sin \omega t$

$$m\ddot{u}_r(t) + c\dot{u}_r(t) + ku_r(t) = m\omega^2 u_0 \sin \omega t$$

This equation is similar to that of the harmonic loading except that the harmonic force excitation amplitude is now  $m\omega^2 u_0$ . Hence the steady state solution for the relative displacement is

$$\begin{aligned} u_r(t) &= \frac{mu_0\omega^2/k}{\sqrt{(1-\omega^2/\omega_n^2)^2 + (2\zeta\omega/\omega_n)^2}} \sin(\omega t - \theta) \quad \theta = \tan^{-1} \frac{2\zeta\omega/\omega_n}{(1-\omega^2/\omega_n^2)} \\ &= \frac{u_0\omega^2/\omega_n^2}{\sqrt{(1-\omega^2/\omega_n^2)^2 + (2\zeta\omega/\omega_n)^2}} \sin(\omega t - \theta) \quad \theta = \tan^{-1} \frac{2\zeta\omega/\omega_n}{(1-\omega^2/\omega_n^2)} \end{aligned}$$

## 4.6 GL, ML Frequency Domain Analysis – Deterministic and Random Dynamic Response Analysis

### 4.6.1 Mathematical Preliminaries of Representing Dynamic Characteristics in the Frequency Domain

The **complex frequency response function (FRF)** due to a loading  $\{P(\omega)\}$  is defined as

$$\{F(\omega)\} = \frac{\{P(\omega)\}}{-\omega^2 [M] + i\omega[C] + [K]}$$

The **complex transfer function (a.k.a. the dynamic flexibility matrix)** is defined as the complex frequency response function due to unit harmonic excitations

$$[H(\omega)] = \frac{1}{-\omega^2 [M] + i\omega[C] + [K]}$$

This is the so-called **transfer function** that transfers the excitation to the response as follows

$$\{u(t)\} = \text{Re al} \left[ [H(\omega)] \{P(\omega)\} e^{i\omega t} \right]$$

The displacement transfer function  $H(\omega)$  (steady state displacement response per unit harmonic force) is known as the **receptance**. The velocity transfer function  $\omega H(\omega)$  (steady state velocity response per unit harmonic force) is known as the **mobility**. The acceleration transfer function  $\omega^2 H(\omega)$  (steady state acceleration response per unit harmonic force) is known as the **inertance**.

The transfer function or the dynamic flexibility matrix  $[H(\omega)]$  is actually the Fourier Transform of the **unit impulse response matrix  $[h(t-\tau)]$  (a.k.a. dynamic stiffness matrix)** defined for the (implicit) time domain (for modal solutions; not direct solutions).

The **(magnitude of the) dynamic amplification factor  $D(\omega)$**  is defined as the magnitude of the complex response function  $\{F(\omega)\}$  divided by the static displacement.

In (implicit) time domain solutions based on modal methods, the **unit impulse response matrix (a.k.a. dynamic stiffness matrix)** is the crucial matrix that transforms the excitation to the response as described by the Duhamel's or convolution integral expression as follows

$$\{u(t)\} = \int_0^t [h(t-\tau)] \{P(\tau)\} d\tau$$

This impulse response matrix  $[h(t-\tau)]$  (a.k.a. dynamic stiffness matrix) is actually the Inverse Fourier Transform of the dynamic flexibility matrix or the transfer function  $[H(\omega)]$  defined for the frequency domain. A unit impulse is theoretically a force time history that occurs over zero time, but has a unit value of the integral of force/time curve. That obviously implies infinite force, which can't exist in reality, but is a very useful approximation when the time of the impulse is short compared to the periods of interest in the response. The response in the time domain to an impulse excitation can be calculated using the Duhamel's Integral (Convolution Integral). A unit impulse excitation will produce what is known as the unit impulse response matrix function (a.k.a. dynamic stiffness) in the time domain. Now, the unit impulse response matrix function (a.k.a. dynamic stiffness) is the Inverse Fourier Transform of the dynamic flexibility matrix (i.e. the transfer function). Conversely, the dynamic flexibility matrix (i.e. the transfer function) is the Fourier Transform of the unit impulse response matrix function (a.k.a. dynamic stiffness).

### 4.6.2 GL, ML Vibration Testing

The purpose of the vibration testing is to **establish the modal properties** (modal frequencies, modal mass and modal damping) of the system for correlation with the finite element model. Vibration testing is also used to **establish the response** to certain excitations to be compared to that of the finite element model to verify the analysis procedure.

The vibration test could either be

- (i) Impact (Hammer or Heel-Drop) Test (Artificial Excitation) – For Model Correlation
- (ii) Shaker Table Test (Artificial Excitation) – For Model Correlation
- (iii) Response Measurements (Actual Excitation) – For Analysis Procedure Verification

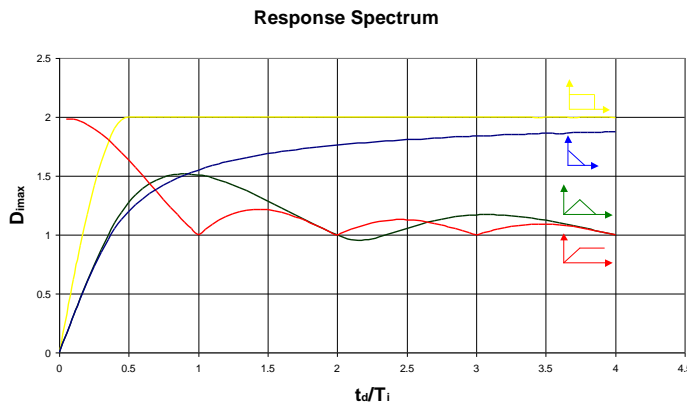
**For model correlation**, the vibration tests can be used to measure the applied excitation and the structural response. **For analysis procedure verification**, the vibration test measures the RESPONSE of the structure to the induced excitations, not the actual excitations themselves.

#### 4.6.2.1 Vibration Testing for Model Correlation

Vibration Test	FE Equivalent	Response	Derived information
Impact Test and Logarithmic Decrement	SOL 109 with impact force excitation	Time history signal of ensuing free vibration, the frequency content of which can be obtained by FFT. Note that this is NOT the frequency response function FRF, $F(\omega)$ . The phase information is random.	With knowledge of frequency content, time history signal can be signal processed (i.e. filtered) to yield single mode time history, which by logarithmic decrement provides modal damping
Impact Test and Transfer Function	SOL 109 with impact force excitation	Time history signal of ensuing free vibration and the knowledge of the excitation function can be used to derive unit impulse response matrix (a.k.a. dynamic stiffness matrix), $h(t-\tau)$ from $\{u(t)\} = \int_0^t [h(t-\tau)]\{P(\tau)\}d\tau$ which can transformed by Forward FFT to obtain the complex transfer function $H(\omega)$ (a.k.a. the dynamic flexibility matrix)	$H(\omega)$ (with real and imaginary or magnitude and phase info) provides frequency content, modal damping and modal mass. $H(\omega)$ (with only magnitude info) provides frequency content and approximate modal damping by half-power bandwidth.
Shaker Table Test and Frequency Response Function	SOL 108 with wide-band harmonic excitation	Frequency response function FRF, $F(\omega)$	$F(\omega)$ (with real and imaginary or magnitude and phase info) provides frequency content, modal damping and modal mass. $F(\omega)$ (with only magnitude info) provides frequency content and approximate modal damping by half-power bandwidth.
Shaker Table Test and Transfer Function	SOL 108 with wide-band harmonic excitation	Frequency response function FRF, $F(\omega)$ which divided by the excitation static force provides the transfer function $H(\omega)$	$H(\omega)$ (with real and imaginary or magnitude and phase info) provides frequency content, modal damping and modal mass. $H(\omega)$ (with only magnitude info) provides frequency content and approximate modal damping by half-power bandwidth.

### 4.6.2.1.1 Impact Test and Logarithmic Decrement

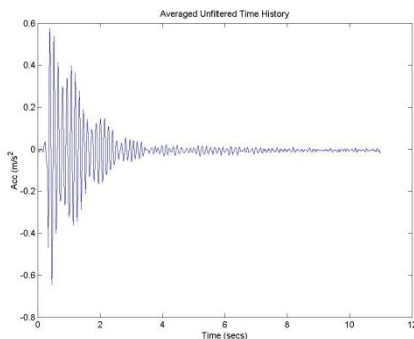
The impact excites the natural modes of vibration. An impact test produces an impulse, which excites the modes, of course some more than others.



It is really not necessary to know which modes are excited more as we are really only interested in finding out the natural frequencies of the structure, not the response.

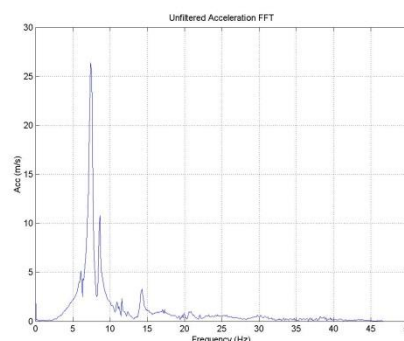
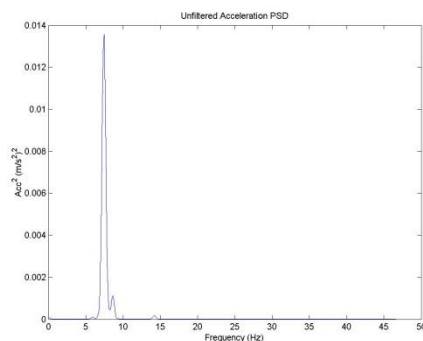
To perform signal processing of the impact test

- (I) First, read in all the acceleration time history signals



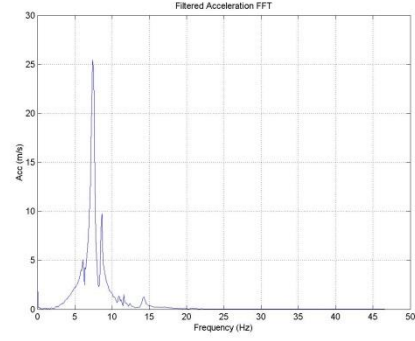
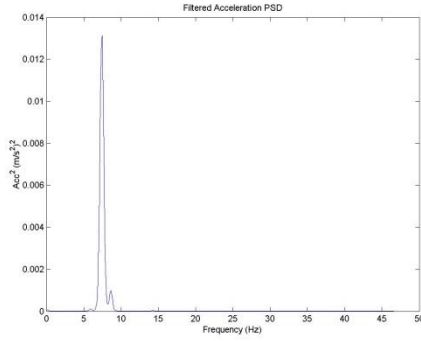
- (II) For each acceleration time history signal

- (i) Plot the signal;  $\Delta t = t_2 - t_1$ ; sampling frequency =  $1/\Delta t$
- (ii) FFT/PSD (use linear scale instead of logarithmic) the signal to establish its **frequency content**

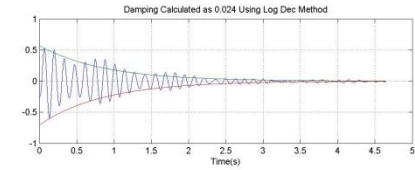
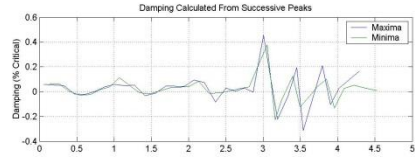
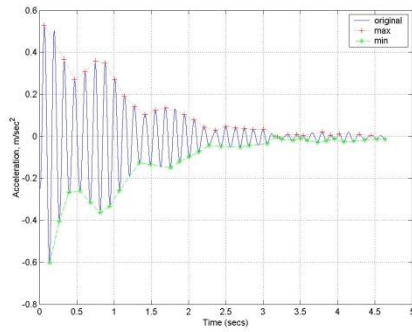


For each mode of interest

- (iii) Design a filter to filter the mode of interest for damping estimation. Employ the Butterworth IIR Algorithm, specify the sampling frequency, specify the order and whether it is a low-pass, high-pass or band-pass filter
- (iv) Filter the signal and plot the (single frequency) filtered signal
- (v) FFT/PSD the (single frequency) filtered signal to ascertain the effectiveness and accuracy of the filter



- (vi) Perform a logarithmic decrement on the (single frequency) filtered signal to determine **the modal damping** of the mode of interest



Next mode of interest  
Next acceleration time history signal

The impact test establishes the natural frequencies and the damping of the structure and is useful for model correlation. Clearly, this method is reliable only if the modes are well spaced out.

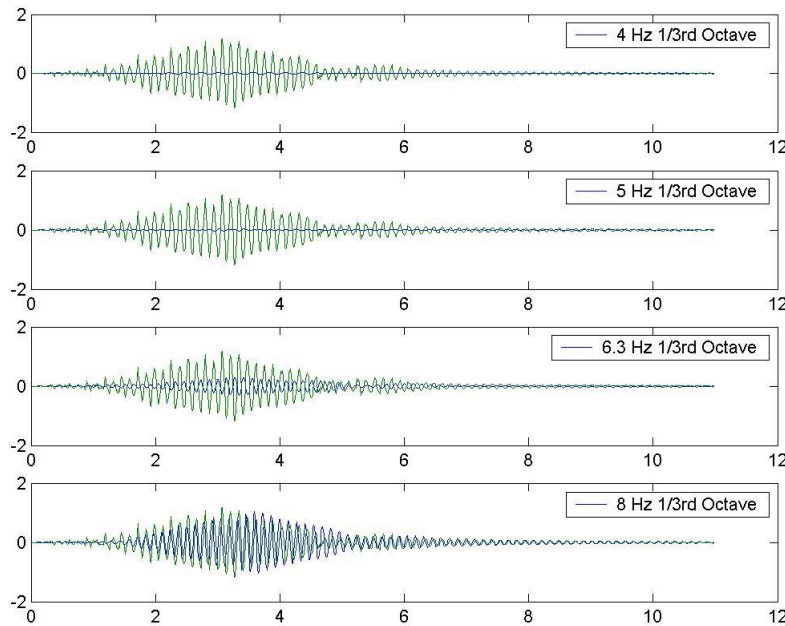
### 4.6.2.2 Vibrating Testing For Analysis Procedure Verification

Response measurements are made to verify the FE analysis procedure. Note that the starting transient occurs at the natural frequencies of the structure whilst the **steady-state response is at the frequencies of excitation**.

To perform signal processing of the response measurements, first read in all the acceleration or velocity time history signals.

For **each** time history

- (I) Compare the **peak** of the **UNFILTERED** time history with established criteria.
- (II) Compute the **(1.0s say) RMS** of the **ULFILTERED** time history. Compare the maximum RMS (of the RMS values from each 1.0s window) with established criteria. Note that the RMS over the entire duration will be lower than over short intervals such as 1.0s.
- (III) To compare the **peak** and the **(1.0s say) RMS** of the **FILTERED** time history with established criteria,
  - (i) Plot the signal;  $\Delta t = t_2 - t_1$ ; sampling frequency =  $1/\Delta t$ .
  - (ii) Design a filter to filter the signal into its  $1/3^{\text{rd}}$  octave bands. Employ the Butterworth IRR Algorithm, specify the sampling frequency, specify the order and band-pass filter.
  - (iii) Filter the signal and plot the filtered signals.



- (iv) Compute the peaks of each  $1/3^{\text{rd}}$  octave band filtered signal. Compare the peak values from each  $1/3^{\text{rd}}$  octave band filtered signal with established (frequency dependent) criteria.
- (v) Compute the RMS of each filtered signal in time intervals of 1.0s say. Compute the maximum RMS (of the RMS values from each 1.0s time interval) for one RMS value for each  $1/3^{\text{rd}}$  octave band. Note that the RMS over the entire duration will be lower than over short intervals such as 1.0s. Compute the maximum RMS (of the RMS values for each  $1/3^{\text{rd}}$  octave band) and compare with established (frequency dependent) criteria. Note also that the unfiltered RMS will be larger than the filtered RMS.

Next time history signal

### 4.6.3 GL, ML Steady-State Response of Deterministic Periodic (Not Necessarily Harmonic) Long Duration Excitation Utilizing Fourier Series (or Generally Utilizing Fast Fourier Transforms FFT)

The solution method can be used to solve dynamic systems subjected to: -

- (a) **Deterministic periodic non-harmonic long duration** loading functions

**In this LINEAR FREQUENCY DOMAIN solution**, not only that the static response has to be added separately, but also the mean of the dynamic excitation has also got to be added separately as a static response. This is because the mean of the dynamically applied force is not included in the dynamic excitations. **Hence the total response in this frequency domain dynamic analysis = static response to mean of dynamic excitation + dynamic response + static response to static loads.**

#### 4.6.3.1 Fourier Series

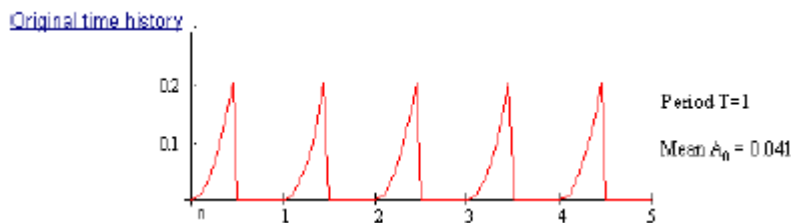
The French Mathematician J. Fourier (1768-1830) postulated that any deterministic periodic function can be expressed as the summation of a number of sinusoidal waves of varying frequency, amplitude and phase. A **deterministic periodic** (of period T) function that is not necessarily harmonic can thus be expressed as a summation of an infinite number of sine and cosine terms, i.e. a **Fourier Series**. Forced responses (steady-state) are performed in the frequency domain with these individual harmonics (with the correct amplitudes and phase differences) as the excitations. Note that since this method is performed in the frequency domain, the response calculated is the steady-state response. Hence, it is assumed that the excitation is **periodic and long enough** for **steady-state conditions** to be achieved. The total steady-state response is thus the summation of the responses of the individual harmonics.

A **general deterministic periodic (of period T) function that is not necessarily harmonic** can be expressed as a summation of an infinite number of sine and cosine terms, i.e. a **Continuous Fourier Series**.

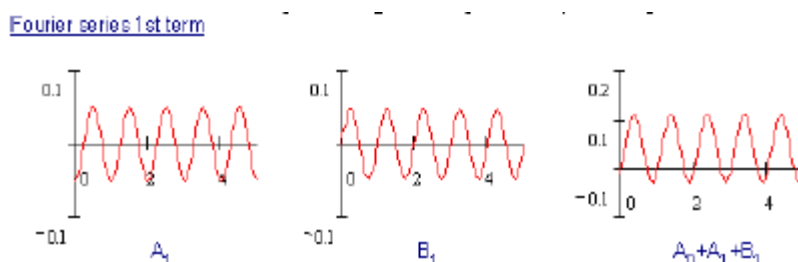
$$P(t) = a_0 + \sum_{n=1}^{\infty} [a_n \cos n\omega t + b_n \sin n\omega t]$$

$$a_0 = \frac{1}{T} \int_0^T P(t) dt \quad a_n = \frac{2}{T} \int_0^T P(t) \cos n\omega t dt \quad b_n = \frac{2}{T} \int_0^T P(t) \sin n\omega t dt$$

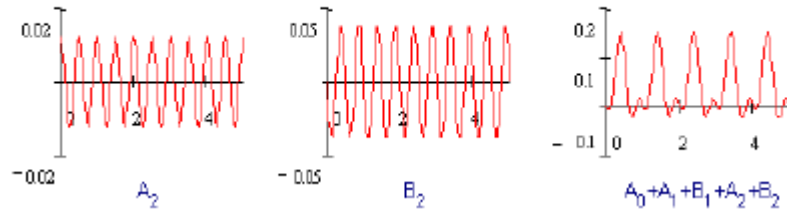
The constant  $a_0$  is the mean component of the force. The coefficients  $a_n$  and  $b_n$  which is constant for each harmonic  $n$ , is the amplitudes of the harmonics. Usually only the first few harmonics need to be included as the response to higher harmonics may be negligible. An illustration is presented for a saw tooth function.



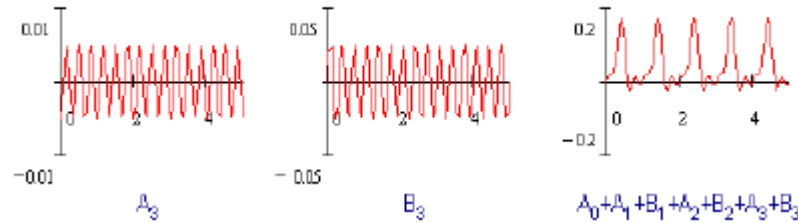
The Fourier Series representation is as follows. Even with only 3 Fourier terms, the representation is pretty good.



#### Fourier series 2nd term



#### Fourier series 3rd term



The total response will then be the summation of all the responses due to the individual harmonics. For a SDOF system, the steady-state response due to the constant  $a_0$  force is

$$u_{\text{mean}}(t) = \frac{a_0}{k}$$

The steady-state response due to a  $a_n \cos n\omega t$  force

$$u_{\cos}(t) = \frac{a_n / k}{\sqrt{(1 - (n\omega^2)/\omega_n^2)^2 + (2\zeta n\omega/\omega_n)^2}} \cos(n\omega t - \theta) \quad \theta = \tan^{-1} \frac{2\zeta n\omega/\omega_n}{(1 - (n\omega^2)/\omega_n^2)}$$

The steady-state response due to a  $b_n \sin n\omega t$  force

$$u_{\sin}(t) = \frac{b_n / k}{\sqrt{(1 - (n\omega^2)/\omega_n^2)^2 + (2\zeta n\omega/\omega_n)^2}} \sin(n\omega t - \theta) \quad \theta = \tan^{-1} \frac{2\zeta n\omega/\omega_n}{(1 - (n\omega^2)/\omega_n^2)}$$

The total SDOF steady-state response is thus the summation of the above three components for all harmonics  $m$ .

$$u(t) = u_{\text{mean}}(t) + \sum_{n=1}^{\infty} [u_{\cos}(t) + u_{\sin}(t)]$$

#### 4.6.3.2 Discrete Fourier Series

In the Fourier Series Analysis, the original continuous loading function  $P(t)$  can be represented exactly by a continuous function if an infinite (Fourier) series is adopted. Now, if the function  $P(t)$  is supplied only at  $N$  equally spaced time intervals ( $\Delta t = T/N$ )  $t_0, t_1, t_2, \dots, t_{N-1}$ , where  $t_j = j\Delta t$ , the Discrete Fourier Series results

$$P(t_j) = a_0 + \sum_{n=1}^{\infty} [a_n \cos n\omega t_j + b_n \sin n\omega t_j]$$

$$a_0 = \frac{1}{T} \sum_{j=0}^{N-1} P(t_j)$$

$$a_n = \frac{2}{T} \sum_{j=0}^{N-1} P(t_j) \cos n\omega t_j \Delta t$$

$$b_n = \frac{2}{T} \sum_{j=0}^{N-1} P(t_j) \sin n\omega t_j \Delta t$$

Whereas the **Fourier Series** could represent a deterministic **continuous and periodic** function exactly if an **infinite number of harmonics** were utilized, the **Discrete Fourier Series** can represent a deterministic **discrete and non-periodic** function exactly **only at the discrete points** if an **infinite number of harmonics** are adopted.

#### 4.6.3.3 Discrete Fourier Series in Complex Notation

In practice the Fourier coefficients  $a_0$ ,  $a_n$  and  $b_n$  prove very cumbersome to manipulate algebraically. Complex number theory helps with this aspect as all three coefficients may be replaced by one complex coefficient  $C_n$ . Recapping basic complex number theory,

a complex number contains real and imaginary components

$$z = x + iy$$

it can be written in a polar form by computing the magnitude and the phase

$$z = \left( \sqrt{x^2 + y^2} \right) e^{i\theta}, \quad \theta = \tan^{-1}(y/x)$$

$$z = \left( \sqrt{x^2 + y^2} \right) (\cos \theta + i \sin \theta), \quad \theta = \tan^{-1}(y/x)$$

Writing

$$\begin{aligned} [a_n \cos n\omega t + b_n \sin n\omega t] &= \text{Re al} [a_n \cos n\omega t + ia_n \sin n\omega t - ib_n \cos n\omega t - i^2 b_n \sin n\omega t] \\ &= \text{Re al} [(a_n - ib_n)(\cos n\omega t + i \sin n\omega t)] \\ &= \text{Re al} [\Lambda_n e^{in\omega t}] \end{aligned}$$

the Discrete Fourier Series can be rewritten in complex notation as follows

$$P(t_j) = a_0 + \text{Re al} \left[ \sum_{n=1}^{\infty} \Lambda_n e^{in\omega t_j} \right]$$

$$\Lambda_n = a_n - ib_n$$

but since

$$a_n = \frac{2}{T} \sum_{j=0}^{N-1} P(t_j) \cos n\omega t_j \Delta t \quad \text{and} \quad b_n = \frac{2}{T} \sum_{j=0}^{N-1} P(t_j) \sin n\omega t_j \Delta t$$

we have

$$\begin{aligned} \Lambda_n &= a_n - ib_n \\ &= \frac{2}{T} \sum_{j=0}^{N-1} P(t_j) e^{-in\omega t_j} \Delta t \end{aligned}$$

and thus the Discrete Fourier Series can be rewritten in complex notation as follows

$$P(t_j) = a_0 + \text{Re al} \left[ \sum_{n=1}^{\infty} \Lambda_n e^{in\omega t_j} \right]$$

$$\Lambda_n = \frac{2}{T} \sum_{j=0}^{N-1} P(t_j) e^{-in\omega t_j} \Delta t$$

#### 4.6.3.4 Double Sided Discrete Fourier Series in Complex Notation

The Discrete Fourier Series in Complex Notation expression may be simplified even further by the introduction of negative frequencies. These have the effect of **cancelling the imaginary components and hence allowing the Real[...]function to be dropped** as presented below.

$$P(t_j) = a_0 + \frac{1}{2} \sum_{n=1}^{\infty} \Lambda_n e^{in\omega t_j} + \frac{1}{2} \sum_{n=-1}^{-\infty} \Lambda_n e^{in\omega t_j}$$

$$\Lambda_n = \frac{2}{T} \sum_{j=0}^{N-1} P(t_j) e^{-in\omega t_j} \Delta t$$

To prove that the Double Sided expression is the same as the single sided with Re [...] expression, the following back analysis is performed.

$$\begin{aligned} P(t_j) &= a_0 + \frac{1}{2} \sum_{n=1}^{\infty} \Lambda_n e^{in\omega t_j} + \frac{1}{2} \sum_{n=-1}^{-\infty} \Lambda_n e^{in\omega t_j} \\ &= a_0 + \frac{1}{2} \sum_{n=1}^{\infty} (a_n - ib_n) (\cos n\omega t_j + i \sin n\omega t_j) + \frac{1}{2} \sum_{n=-1}^{-\infty} (a_n - ib_n) (\cos n\omega t_j + i \sin n\omega t_j) \\ &= a_0 + \frac{1}{2} \sum_{n=1}^{\infty} (a_n - ib_n) (\cos n\omega t_j + i \sin n\omega t_j) + \frac{1}{2} \sum_{n=1}^{\infty} (a_n + ib_n) (\cos n\omega t_j - i \sin n\omega t_j); \text{ Note } \Lambda_{-n} = a_n + ib_n \\ &= a_0 + \frac{1}{2} \sum_{n=1}^{\infty} (2a_n \cos n\omega t_j + 2b_n \sin n\omega t_j) \\ &= a_0 + \sum_{n=1}^{\infty} (a_n \cos n\omega t_j + b_n \sin n\omega t_j) \\ &= a_0 + \text{Re al} \left[ \sum_{n=1}^{\infty} \Lambda_n e^{in\omega t_j} \right] \end{aligned}$$

Hence, proven. We then change the limits of the summation the Fourier coefficients so that  $a_0$  and  $\Lambda_n$  can be replaced with the single complex Fourier coefficient  $C_n$ . Hence from

$$P(t_j) = a_0 + \frac{1}{2} \sum_{n=1}^{\infty} \Lambda_n e^{in\omega t_j} + \frac{1}{2} \sum_{n=-1}^{-\infty} \Lambda_n e^{in\omega t_j}$$

$$\Lambda_n = \frac{2}{T} \sum_{j=0}^{N-1} P(t_j) e^{-in\omega t_j} \Delta t$$

we thus have

$$P(t_j) = \sum_{n=-\infty}^{\infty} C_n e^{in\omega t_j}$$

$$C_n = \frac{1}{2} \Lambda_n = \frac{1}{T} \sum_{j=0}^{N-1} P(t_j) e^{-in\omega t_j} \Delta t$$

where **even the  $a_0$  term is accounted for** by  $C_n$ . Knowing that  $t_j = j\Delta t$ ,  $T = N\Delta t$  and  $\omega = 2\pi/T$

$$P(t_j) = \sum_{n=-\infty}^{\infty} C_n e^{2\pi i(nj/N)}$$

$$C_n = \frac{1}{N} \sum_{j=0}^{N-1} P(t_j) e^{-2\pi i(nj/N)}$$

Hence we have derived the Double Sided Discrete Fourier Series in Complex Notation. This expression is said to be double sided because it uses both positive and negative frequencies to represent the Fourier coefficients. From the Double Sided Discrete Fourier Series in Complex Notation, we now define the Discrete Fourier Transform of the series  $P(t_j)$  as  $C_n$ .

$$C_n = \frac{1}{N} \sum_{j=0}^{N-1} P(t_j) e^{-2\pi i(nj/N)}$$

Because the **phase information is also stored**, the time signal can be regenerated from the Discrete Fourier Transform using the Discrete Inverse Fourier Transform

$$P(t_j) = \sum_{n=-\infty}^{\infty} C_n e^{2\pi i(nj/N)}$$

Whereas the **Fourier Series** could represent a deterministic **continuous and periodic** function exactly if **an infinite number of harmonics** were utilized, the **Double Sided Discrete Fourier Series in Complex Notations** can represent a deterministic **discrete and non-periodic** function exactly **only at the discrete points** if **an infinite number of harmonics** are adopted.

#### 4.6.3.5 Normalized Double Sided Discrete Fourier Series in Complex Notation

Each Fourier coefficient  $C_n$  is obtained for a frequency of  $n/T$  Hz, the frequency interval between each coefficient  $\Delta f$  is therefore  $1/T$  Hz. This causes problems as the frequency at which the coefficients are calculated is dependent on the period  $T$  chosen. It is common practice to **normalize** the Fourier Transform coefficients  $C_n$  to eliminate the dependence on  $T$ . The normalized coefficients take the form of a **density function** and the Fourier coefficient is obtained from the area under the density curve for the range  $\Delta f = 1/T$  in question. The Inverse Fourier Transform is thus

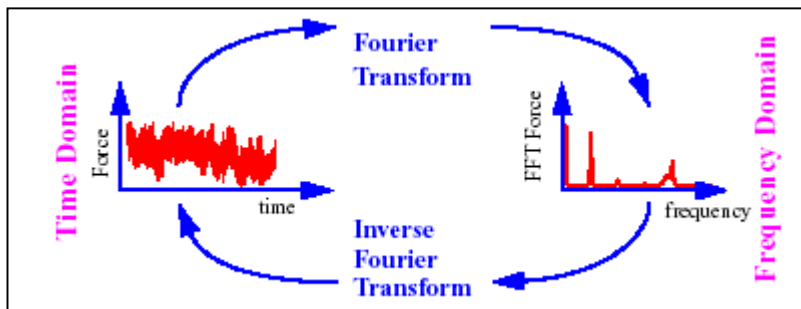
$$P(t_j) = \frac{1}{T} \sum_{n=-\infty}^{\infty} c_n e^{2\pi i(nj/N)} \quad \text{instead of} \quad P(t_j) = \sum_{n=-\infty}^{\infty} C_n e^{2\pi i(nj/N)}$$

Note that here  $T$  is period, not duration!

and the Fourier Transform Density Function is

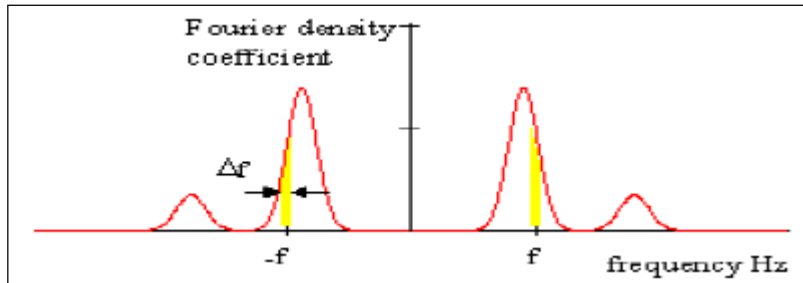
$$c_n = \frac{T}{N} \sum_{j=0}^{N-1} P(t_j) e^{-2\pi i(nj/N)} \quad \text{instead of} \quad C_n = \frac{1}{N} \sum_{j=0}^{N-1} P(t_j) e^{-2\pi i(nj/N)}$$

The Fourier Transform Density Function and Inverse Fourier Transform transformations are illustrated.

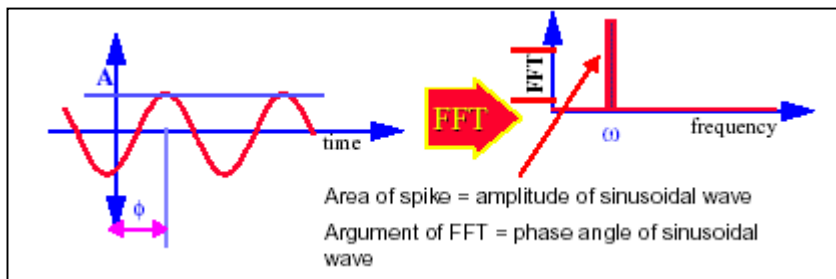


Whereas the **Fourier Series** could represent a deterministic **continuous and periodic** function exactly if **an infinite number of harmonics** were utilized, the **Normalized Double Sided Discrete Fourier Series in Complex Notations** can represent a deterministic **discrete and non-periodic** function exactly **only at the discrete points** if **an infinite number of harmonics** are adopted.

With the definition of the Fourier Density Function, the amplitude and phase of a frequency component with frequency  $f$  is now obtained by taking the magnitude and argument of the sum of area under the density curve within  $\Delta f$  at  $f$  and  $-f$ .



The area under the Fourier Density Function is given as a complex number; the amplitude content can be obtained by taking the modulus of this complex area and the phase content from the argument or this complex area. The Fourier Density Function of a stationary random signal is a plot of amplitude (and phase) against frequency. A sine wave of frequency  $\omega$ , amplitude  $A$  and initial phase angle  $\phi$  is represented in the frequency domain by a spike occurring at  $\omega$  along the frequency axis. If the magnitude of the complex Fourier Density Function is plotted, then the **area** under the spike is found to be the **amplitude**  $A$  of the sine wave. When the argument of the complex Fourier Density Function is plotted then the **area** is found to be **initial phase angle**  $\phi$  of the sine wave. Therefore, if we want to find the amplitude and phase of the sinusoidal waves in a particular frequency range, say between 2 and 2.5 Hz, we can measure the area under the curve in that frequency range.



#### 4.6.3.6 Symmetrical Normalized Double Sided Discrete Fourier Series in Complex Notation

In order to **maintain the symmetry with its transform pair**, i.e. the Discrete Fourier Transform Density Function

$$c_n = \frac{T}{N} \sum_{j=0}^{N-1} P(t_j) e^{-2\pi i(nj/N)}$$

the Discrete Inverse Fourier Transform is **limited to only N terms (i.e. from 0 to N-1)** as follows

$$P(t_j) = \frac{1}{T} \sum_{n=0}^{N-1} c_n e^{2\pi i(nj/N)}$$

It is paramount to realize that in the Discrete Inverse Fourier Transform summation indicated above, the frequencies increase up to only  $N/2$  and not  $N-1$ . This is because it can be shown that for  $n > N/2$ , the

corresponding frequencies are equal to the negative frequencies of order  $N-n$ . This fact restricts the harmonic frequency components that may be represented in the series to a maximum of  $N/2$ . The frequency corresponding to this maximum order  $\omega_{N/2} = (N/2)\omega$  is known as the Nyquist frequency (a.k.a. folding frequency). Moreover, if there are harmonic components above  $\omega_{N/2}$  in the original function, these higher components will introduce distortions in the lower harmonic components of the series, a phenomenon known as aliasing. Hence, it is recommended that the number of sampled points,  $N$  should be at least twice the highest harmonic component present in the function.

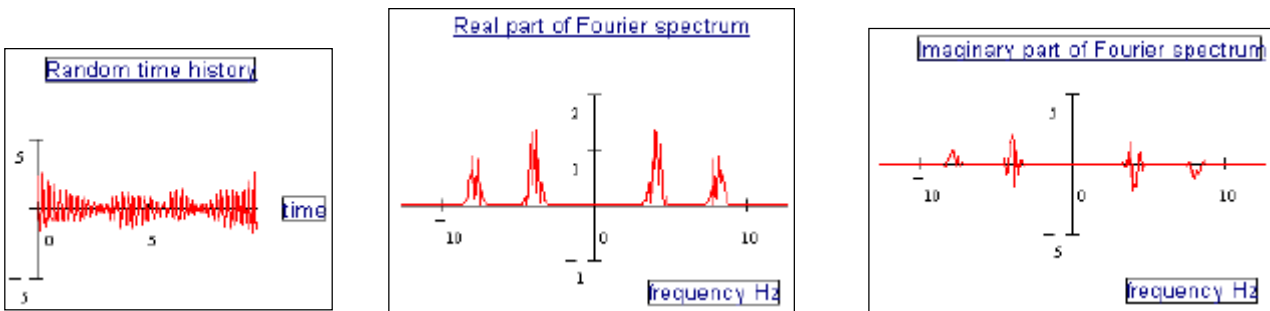
Whereas the **Fourier Series** could represent a deterministic **continuous and periodic** function exactly if an **infinite number of harmonics** were utilized, the **Symmetrical Normalized Double Sided Discrete Fourier Series in Complex Notations** can represent a deterministic **discrete and non-periodic** function *approximately only at the discrete points* since **the number of harmonics is limited to  $N/2$  i.e. from  $-N/2$  to  $N/2$  instead of  $\infty$  i.e. from  $-\infty$  to  $\infty$  and if components of frequency higher than the Nyquist,  $\omega_{N/2} = (N/2)\omega = (N/2)(2\pi/T) = \pi N/T = \pi/\Delta t$  exist in the time signal, aliasing (distortions in the lower harmonic components) occurs, noting however that the latter reason is user avoidable.**

#### 4.6.3.7 Symmetrical Normalized Single Sided Discrete Fourier Series in Complex Notation

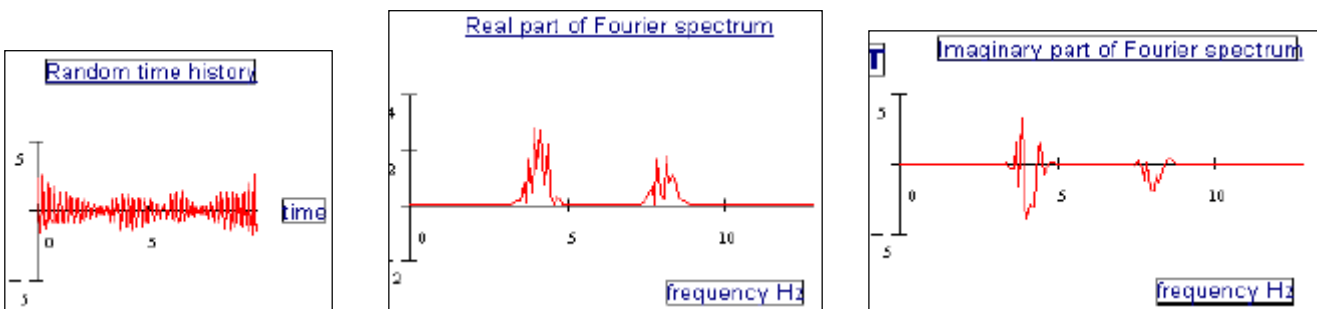
The Single Sided Fourier Transform Density Function contains the same information as the Double Sided Fourier Transform Density Function but is often more convenient to use as negative frequencies are not considered. In order to maintain the same intensity of the original time signal, the Single Sided Fourier Transform Density Function is doubled. The Single Sided Discrete Fourier Transform Density Function of the series  $P(t_j)$  and the corresponding Single Sided Discrete Inverse Fourier Transform are respectively

$$c_n = \frac{2T}{N} \sum_{j=0}^{N/2} P(t_j) e^{-2\pi i(nj/N)} \quad \text{and} \quad P(t_j) = \frac{1}{T} \sum_{n=0}^{N-1} c_n e^{2\pi i(nj/N)}$$

The following time history will produce the following Double Sided Fourier Transform Density Functions.



And the time history will instead produce the following Single Sided Fourier Transform Density Functions.



#### 4.6.3.8 Practicalities of the Specification of the Fast Fourier Transform (FFT) Representation

An extremely efficient computational algorithm, which employs the Discrete Fourier Transform concept is the Fast Fourier Transform (FFT). Note that whereas the Fourier Series can represent **deterministic periodic** functions, the **Fast Fourier Transform FFT** can represent **deterministic non-periodic** functions. Again, since the FFT method is performed in the frequency domain, the response calculated is the steady-state response. Hence, it is assumed that the excitation is **periodic and long enough** for **steady-state conditions** to be achieved. The concept of Fourier Series and the Fast Fourier Transform representations is presented.

Fourier Series Method → Represents **Deterministic, Periodic** Functions

Fast Fourier Transform Method → Represents **Deterministic, Non-periodic** Functions

However, since the analysis is performed in the frequency domain, the response is steady-state and hence we shall use the Fast Fourier Transform FFT method to solve excitations which are **deterministic, periodic and long duration** for steady-state conditions to be achieved. Hence, forced response due to an **impulse** must be performed in the time domain and cannot be performed in the frequency domain although  $h(t-\tau)$  and  $H(\omega)$  are a Fourier Transform pair. This means that although the excitation in the time and frequency domains and the structural characteristics ( $h(t-\tau)$  and  $H(\omega)$ ) are interchangeable with the Fourier Transforms, the response in the time and frequency domain are only comparable if the excitation is **deterministic, periodic and long duration** for steady state conditions to be achieved, a condition which is not achieved for an impulsive excitation.

**The FFT must follow certain rules. The time signal should follow the  $2^N$  rule, N an integer. This means that the number of data points within the time signal should be 32, 64, 128, 256, 512, 1024, 2048 ... 131072 for the FFT to be computed. Three considerations should be made in choosing the parameters digitizing a time history signal. Firstly, if N is the number of sample intervals, it can be shown mathematically that the Discrete Inverse Fourier Transform representation is restricted to a maximum of N/2 harmonic components in the series, i.e. N/2 spectral lines.**

$$\text{Number of points in positive FFT} = \frac{1}{2} \times \text{number of points in time signal, N}$$

**This occurs because for  $n > N/2$ , the corresponding frequencies are equal to the negative of frequencies order N-n. Secondly, the maximum harmonic component that can be represented is  $(N/2)\omega$ , where  $\omega$  here is  $2\pi/T$ , T being the entire duration of loading.**

$$\omega_y = \frac{N}{2} \omega = \frac{N}{2} \frac{2\pi}{T} = \frac{N}{2} \frac{2\pi}{N\Delta t} = \frac{\pi}{\Delta t}$$

$$f_y = \frac{\omega_y}{2\pi} = \frac{1}{2\Delta t}$$

In other words,

$$\text{Nyquist Frequency, } f_y = \frac{1}{2} \times \text{sampling frequency}$$

$$= \frac{1}{2} \times \frac{1}{\text{time step, } \Delta t}$$

**The frequency of this maximum harmonic component is called the Nyquist frequency or the folding frequency. Thirdly, if harmonic components above the Nyquist frequency were present in the original function, it would introduce distortions in the lower harmonic components of the series, a phenomenon called aliasing. The sampling frequency must then be two times the highest frequency component so that the Nyquist frequency (which is half the sampling frequency) becomes equal to the highest frequency component of interest. This is also obvious from observation of the function. A triangular pulse of a frequency of 100Hz**

(period 0.01s) requires at least 3 sampling points to define the triangular shape. Three sampling points here means that the sampling frequency will be 200Hz (0.005s). The Nyquist frequency will then be 200Hz/2 = 100Hz, which again is the frequency of that of the triangular pulse. Hence the FFT should represent all the frequency components of the original time signal to avoid aliasing.

USER CHOICE (CHOOSE 2 OF 4)				CONSEQUENCE			Remark
Time Step, $\Delta t$ (s)	Sampling Frequency = $1/\Delta t$ (Hz)	Number of Time Steps, N	Duration = $N\Delta t$ (s)	Nyquist Frequency = Sampling Frequency / 2 (Hz)	Number of Spectral Lines = $N / 2$	$\Delta f = \text{Nyquist Frequency} / \text{Number of Spectral Lines}$ (Hz)	
0.02	50	1024	20.48	25	512	0.049	Original
0.02	50	2048	40.96	25	1024	0.024	More resolution
0.04	25	1024	40.96	12.5	512	0.024	More resolution, lower Nyquist
0.01	100	1024	10.24	50	512	0.098	Less resolution, higher Nyquist

We can make a couple of conclusions. First, the time step should be chosen to capture all frequency components of the time signal so that the Nyquist frequency (which is half the sampling frequency) is at least equal to the highest frequency component to avoid aliasing. To be sure of this, one may filter the signal electronically to remove all frequencies above the Nyquist frequency. Second, the more the number of time steps, N and/or the larger the time step  $\Delta t$  (so long as the sampling frequency  $1/\Delta t$  is still at least twice the highest frequency component in the time signal to avoid aliasing) the better the resolution as  $\Delta f = 1/T$ .

Hence, for example, if say we are interested in capturing a time signal with frequency components up to say 25Hz, we thus specify a digitizing sampling frequency of 50Hz (so that the Nyquist frequency which is half the sampling frequency equals the highest frequency of interest) i.e. a time step of 0.02s whilst filtering all frequencies above 25Hz to avoid aliasing. Then, we choose the number of time steps, N of 1024, 2048, 4096 etc ... and hence the duration  $N\Delta t$  so that an acceptable resolution is obtained on the Fourier Transform Density Function knowing that the number of spectral lines is  $N/2$ .

#### 4.6.3.9 MSC.NASTRAN Fast Fourier Transform Analysis Methodology

The Fourier Transform method provides an efficient alternative method of determining the **steady-state** transient response of the equations of motion. It avoids the lengthy time integration of the transient equations of motion with the repetitive periodic input of the loading function. Time-dependent applied loads are transformed to the frequency domain using the Double Sided Fourier Transform Density Function

$$c_n = \frac{T}{N} \sum_{j=0}^{N-1} P(t_j) e^{-2\pi i(nj/N)}$$

before all frequency dependent matrix calculations are completed in the frequency domain.

$$\{u(\omega_n)\} = [H(\omega)]\{c_n\}$$

Then using the Inverse Fourier Transform

$$P(t_j) = \frac{1}{T} \sum_{n=0}^{N-1} u(\omega_n) e^{2\pi i(nj/N)}$$

the frequency response solution variables are then transformed back into the time domain. The steady-state response to the forcing function  $P(t_j)$  is thus

$$\begin{aligned} \{u(t_j)\} &= \text{Re al} \left[ [H(\omega)] P(t_j) \right] \\ &= \text{Re al} \left[ \frac{1}{T} \sum_{n=0}^{N-1} \frac{c_n e^{2\pi i(nj/N)}}{-\omega^2 [M] + i\omega [C] + [K]} \right] \end{aligned}$$

Fourier transform methods have been implemented in MSC.NASTRAN to integrate the equations of motion in order to obtain the aeroelastic response of fixed wing aircraft. This capability is especially important for this type of analysis since the unsteady aerodynamic matrices are known only in the frequency domain. The Fourier transform method may also be used to solve for the transient response of conventional structural models (no aerodynamic effects) subjected to periodic loads. This capability is available in **SOL 108** and **SOL 111** for frequency response output data. For transient type output, **SOL 146** must be used. The transformation is performed quite simply when the requested load is the time dependent TLOADi form instead of a frequency dependent RLOADi entry.

In MSC.NASTRAN, two forms of the Fourier transform are available, namely the **Fourier series** and the **Fourier integral**. Both methods require necessary numerical compromises and hence produce numerical approximations.

In the **Fourier series**, the basic time interval is  $0 < t < T$ , with the function periodic. The circular frequencies are given by

$$\begin{cases} \omega_n = 2\pi n \Delta f \\ \Delta f = \frac{1}{T} \end{cases}$$

where  $T$  is a large time equal to the period of the lowest forcing frequency. The load transformation for a load at point  $a$  is given for each requested frequency by

$$\bar{P}_a(\omega_n) = \int_0^T P_a(t) e^{-i\omega_n t} dt$$

The response at point  $j$  is given by

$$\tilde{u}_j(\omega_n) = H_{ja}(\omega_n)\tilde{P}_a(\omega_n)$$

where  $H_{ja}(\omega_n)$  is the frequency response of any physical variable due to unit load. The response in the time domain is given by

$$u_j(t) = \frac{\Delta\omega}{\pi} \left[ \left(\frac{1}{2}\right)\tilde{u}_j(0) + \sum_{n=1}^{\infty} Re(\tilde{u}_j(\omega_n)e^{i\omega_n t}) \right]$$

In the **Fourier Integral**, the time interval is the limit as  $T \rightarrow \infty$ ,  $\Delta f \rightarrow 0$ , and  $2\pi n\Delta f \rightarrow \omega$  of the Fourier series. Here,  $\omega$  is a continuous variable. The corresponding load transformation, frequency response and time domain response relationships are presented.

$$\tilde{P}_a(\omega) = \int_0^{\infty} P_a(t)e^{-i\omega t} dt$$

$$\tilde{u}_j(\omega) = H_{ja}(\omega)\tilde{P}_a(\omega)$$

$$u_j(t) = \left(\frac{1}{\pi}\right) \int_0^{\infty} Re(\tilde{u}_j(\omega)e^{i\omega t}) d\omega$$

The approach that must be undertaken by the user in MSC.NASTRAN is described.

(a) The **solution scheme** must be SOL 108, SOL 111 or SOL 145. The SOL 145 requires the cards of SOL 111 with the addition of TSTEP Case Control and Bulk Data cards.

(b) **The user must define a time domain function that vanishes for  $t > T$ .** Note that  $T$  is the interval of the periodic function. For piecewise linear tabular functions (TLOAD1), a table of pairs  $(x_i, Y_i)$  ( $i = 1, N$ ) prescribes  $N-1$  time intervals. If an X1 shift and an X2 scale factor are included, the time-dependent load at point  $a$  is given by

$$P_a(t) = A_a Y_T \left( \frac{t - \tau_a - X1}{X2} \right)$$

where  $A_a$  is an amplitude factor and  $\tau_a$  is a delay factor that may depend upon the loading point. Likewise, the general function (TLOAD2) is defined by

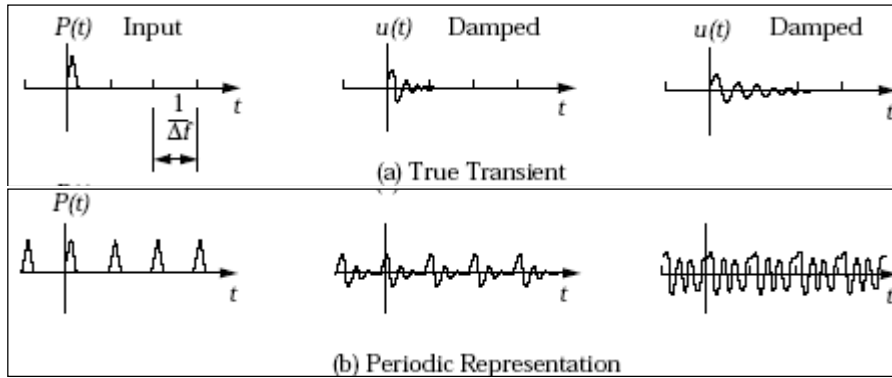
$$P_a(t) = \begin{matrix} A_a \bar{t}^n e^{\alpha \bar{t}} \cos(2\pi f \bar{t} + \phi) & 0 < t < T_2 - T_1 \\ 0 & \text{Otherwise} \end{matrix} \quad \text{where } \bar{t} = t - T_1 - \tau_a$$

The value of  $n$  must be an integer for transient analysis by the Fourier method. **Do not mix loading functions of RLOADi with TLOADi.**

(c) Use constant frequency spacing,  $\Delta f = 1/T$

(d) Three approximation methods are available to evaluate the **inverse Fourier transform** which may be selected by the user via the parameter IFTM, namely Method 0, Method 1 and Method 2.

Consider the response of a simple damped oscillator to a pulse. The upper three curves show the pulse and the response of the system if it is very stable and slightly stable. Using the Fourier method, the pulse is replaced by a series of pulses, with period .



As can be seen, this method gives good results if the system is damped, but an incorrect impression if the system is lightly damped. Thus, in order for the results of the Fourier method to be valid:

1. The system should be reasonably well damped.
2. The forcing function should be zero for some time interval to allow decay.
3. The frequency interval

$$\Delta f \leq 1 / (T_{pulse} + T_{decay})$$

In general, Methods 1 and 2 are more accurate than Method 0. However, these methods introduce positive artificial damping into the result that may lead to erroneous conclusions in stability studies.

**Note that an alternative to the Fourier Method is to perform a SOL 108 or SOL 111 with multiple RLOADi entries to define the different harmonics of the signal, with the correct phase difference. This of course depends on knowing the harmonics which could be derived by manually performing an FFT on the periodic signal.**

#### 4.6.4 GL, ML Steady-State Response of Random, Gaussian, and Stationary (and Ergodic) Excitations Utilizing Power Spectral Density (PSD) Functions

The solution method can be used to solve dynamic systems subjected to: -

- (a) **Random stationary (and ergodic) long duration** loading functions

**In this LINEAR FREQUENCY DOMAIN solution**, not only that the static response has to be added separately, but also the mean of the dynamic excitation has also got to be added separately as a static response. This is because the mean of the dynamically applied force is not included in the dynamic excitations. **Hence the total response in this frequency domain dynamic analysis = static response to mean of dynamic excitation + dynamic response + static response to static loads.**

##### 4.6.4.1 Statistic of Time Domain Function

The **statistics of a random function P(t)** of duration T can be characterized by

- (a) The **mean**, which is usually zero

$$\bar{P} = \frac{1}{T} \int_0^T P(t) dt$$

- (b) The **root mean square (RMS)** and root mean quad (RMQ), the latter gives greater weight to higher values

$$RMS = \sqrt{\frac{1}{T} \int_0^T P^2(t) dt} \quad RMQ = \left( \frac{1}{T} \int_0^T P^4(t) dt \right)^{1/4}$$

Note that the RMS of a continuous simple harmonic motion is amplitude/ $\sqrt{2}$ .

- (c) The **standard deviation**, which is equal to the RMS when the mean is zero

$$\sigma = \sqrt{\frac{1}{T} \int_0^T [P(t) - \bar{P}]^2 dt} = \sqrt{(RMS)^2 - (\bar{P})^2}$$

- (d) The **Gaussian (a.k.a. normal) probability density function PDF to define the amplitude of the (narrowband and broadband) random function P(t)**. The area under the PDF defines the probability of occurrence. Random loading functions P(t) usually follow the Gaussian (or normal) PDF distribution which is a function of the mean and the standard deviation. The Gaussian is bell-shaped and is symmetrical about the mean.

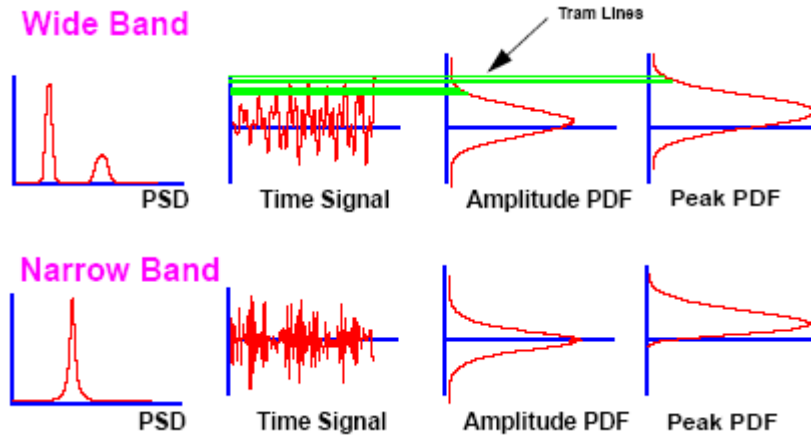
$$\begin{aligned} \text{Gaussian} \quad \text{Pr obability}(P_1 \leq P \leq P_2) &= \int_{P_1}^{P_2} \text{PDF}(P) dP \\ &= \frac{1}{\sqrt{2\pi}\sigma} \int_{P_1}^{P_2} e^{-\frac{1}{2}(P-\bar{P})^2/\sigma^2} dP \end{aligned}$$

On integration of the Gaussian, it is shown that, the probability of P lying within 1 standard deviation from the mean is 68.3%, within 2 standard deviations is 95.4% and within 3 standard deviations is 99.7%.

- (e) The **Rayleigh distribution to define the peaks A of the (narrowband) random vibration functions P(t)**. The Rayleigh distribution is a function of the standard deviation.

$$\begin{aligned} \text{Rayleigh} \quad \text{Pr obability}(A_1 \leq A \leq A_2) &= \int_{A_1}^{A_2} \text{PDF}(A) dA \\ &= \int_{A_1}^{A_2} \frac{A}{\sigma^2} e^{-A^2/2\sigma^2} dA, \quad A > 0 \end{aligned}$$

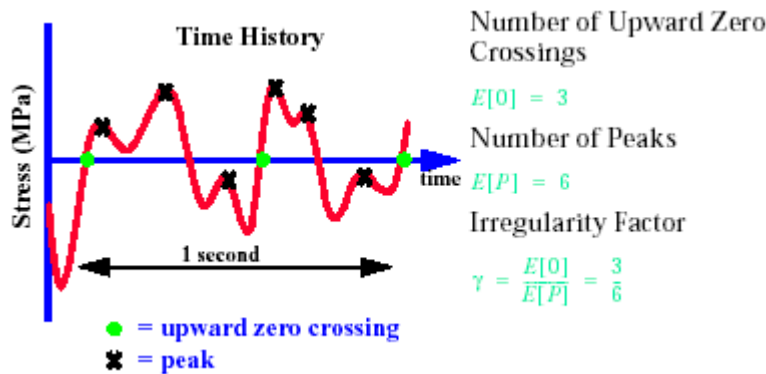
The best way to visualize the amplitude and peak PDFs is to draw tram lines horizontally through the time history and then count either the number of times the signal crosses the tram lines or the number of times a peak occurs in-between the tram lines. The complete PDFs are obtained by repeating this process for all horizontal levels in the signal.



- (f) The **irregularity factor characterizing the frequency content and bandedness** of the time signal  $P(t)$  in the time domain. The irregularity factor is defined as

$$\text{Irregularity factor, } \gamma = \frac{E[0]}{E[P]}; 0 < \gamma < 1$$

where  $E(0)$  is the expected number of upward mean crossings and  $E(P)$  is the expected number of peaks.



Note that  $\gamma = 0.0$  indicates white noise and  $\gamma = 1.0$  indicates a pure sine wave. Practical values are presented.

$\gamma = 1.0$	Sine wave
$\gamma \approx 1.0$	Narrowband process
$\gamma \approx 0.7$ to $0.95$	Broadband process
$\gamma < 0.7$	White noise process

A **narrowband process** is typically recognized in the time history by the amplitude modulation, often referred to as a beat envelope. An important observation made of narrowband processes is that the peak and trough of the time signal amplitude envelope is **symmetrical** about the time axis. This occurs because the frequency content is in a narrowband and is thus almost similar to each other, and so the time signal always passes through the mean (zero amplitude usually) in every cycle. It is interesting to note that the amplitude probability density function (PDF) of a narrowband signal is Gaussian whilst the peak PDF is Rayleigh in distribution. The time signal of a **broadband process** is **not symmetrical** about the time axis. This occurs

because the frequency content is in a broadband and is thus dissimilar to each other, and so the time signal will not pass through the mean (zero amplitude usually) in every cycle. Hence, a broadband process is typically characterized in the time domain by its positive valleys and negative peaks. It is interesting to note that the **amplitude PDF** of a wide band signal is **Gaussian**.

- (g) The **auto-covariance (a.k.a. auto-correlation) characterizing the bandedness** of the time signal P(t) in the time domain. The auto-covariance function is defined

$$C_{yy}(\tau) = E\{y(t) \cdot y(t + \tau)\} - E\{y(t)\}^2$$

$$E\{y(t)\} = \frac{1}{T} \cdot \int_{-T/2}^{T/2} y(t) dt$$

The notation  $C_{yy}$  indicates the auto-covariance function for a single process  $y$ . The notation is introduced to distinguish between the **cross-covariance** function ( $C_{xy}$ ) for two random processes  $x$  and  $y$  defined as follows.

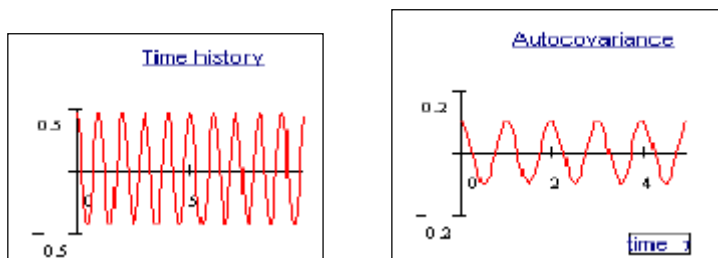
$$C_{yx}(\tau) = E\{y(t) \cdot x(t + \tau)\} - E\{y(t) \cdot x(t)\}$$

For a zero mean time history, the auto-covariance can be rewritten as the infinite time average as follows.

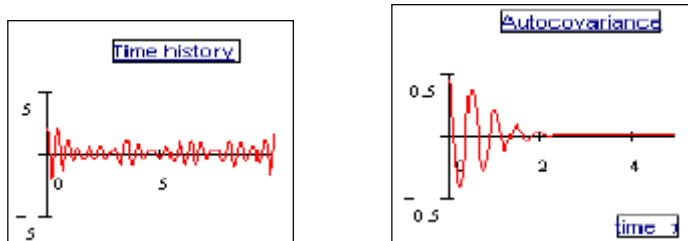
$$C_{yy}(\tau) = \lim_{T \rightarrow \infty} \left[ \frac{1}{T} \cdot \int_{-T/2}^{T/2} y(t) \cdot y(t + \tau) dt \right]$$

A wide-banded process loses similarity within a short time shift and hence the auto-correlation function becomes zero quickly. A narrowbanded process does not lose similarity and hence it takes a long time for the auto-correlation function to become zero. For periodic processes with period  $T$ , the auto-covariance function is also periodic with the same period. For stationary processes the auto-covariance function is even, i.e.  $C_{yy}(\tau) = C_{yy}(-\tau)$ , and may be expressed as a single sided function.

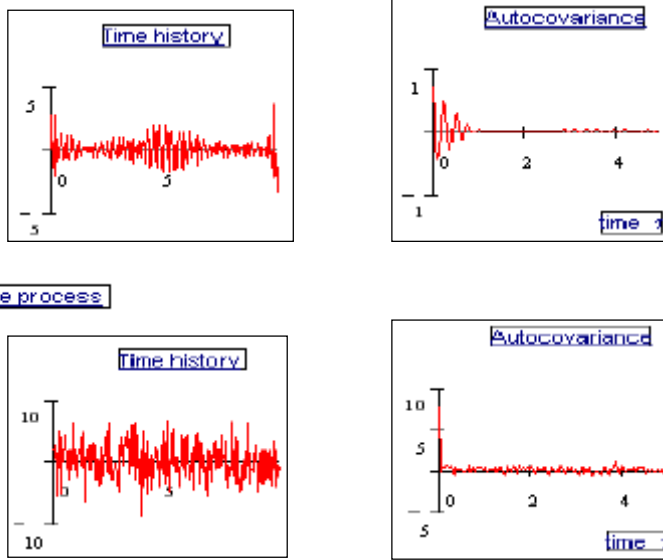
Sine wave



Narrow band process



Broad band process



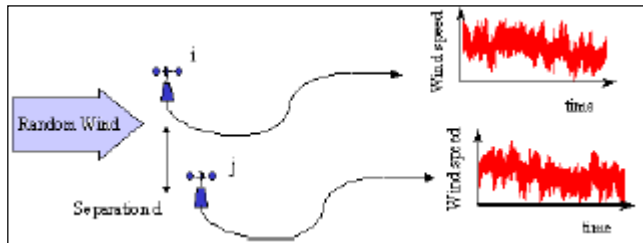
It is often convenient to normalize the covariance function in order to compare different time histories with different scales of measurement. This is achieved by dividing the covariance by the variance. The normalized covariance function is defined below, it has the same shape as the covariance function except that the ordinate is scaled to have a value of 1 for  $\tau=0$ .

$$\rho_{yy}(\tau) = \frac{C_{yy}(\tau)}{C_{yy}(0)} = \frac{C_{yy}(\tau)}{\sigma_y^2}$$

The time scale is defined as the area under the normalized covariance function as below. For a random time history this roughly equates to the mean zero crossing period of the time history. For a periodic time history this is not the case however as  $T_y \rightarrow 0$ .

$$T_y = \int_0^{\infty} \rho_{xy}(\tau) \cdot d\tau$$

- (h) The **cross-covariance function characterizing the correlation between two time signals**. We are interested in the sequential relationship between the two time histories. The figure shows two anemometers measuring wind speed placed side by side with separation  $d$ . From each anemometer a time history of the wind speed is produced. If the two anemometers are far enough apart then the wind speed witnessed by one will be completely independent of the other, they are said to be uncorrelated. As they are moved closer together then a correlation between the two time histories will be noted. Correlation occurs because the random turbulent wind incident on anemometer  $x$  is sufficiently large to also be influencing anemometer  $y$ .



The covariance function may be used to find the sequential relationships between the two time histories.

$$C_{yx}(\tau) = E\{y(t) \cdot x(t + \tau)\} - E\{y(t)\} \cdot E\{x(t)\}$$

The notation  $C_{yx}$  is used to describe the cross-covariance function between the two random processes  $x$  and  $y$ . It effectively tells us what the effect on  $y$  would be should a random process hit  $x$ .

#### 4.6.4.2 Definition of the Power Spectral Density (PSD)

A random stationary forcing function has an imprecisely known magnitude, however all samples of the forcing function have the same statistical characteristics. The statistics of stationary and ergodic processes can be described by one sample that is sufficiently long in duration. The PSD represents the random function.

Consider the transformation from a **single sided Fourier Density Spectra** (as described in **Section 4.6.3.7**) to a **single sided PSD**. The mean amplitude of the component sinusoidal waves over a frequency range  $\Delta f$  is obtained from the Fourier spectra by taking the modulus of the area under the curve expressed as follows.

$$\text{Amplitude}(f_n) = \Delta f \cdot c_n(f_n)$$

The area under a PSD represents the mean squared amplitude of the component sinusoidal waves where  $\text{MeanSquare}(f_n) = \frac{1}{2}[\text{Amplitude}(f_n)]^2$ . We can equate the mean square amplitudes calculated from the PSD and the Fourier spectra and hence determine the transformation between the two, as follows.

$$\Delta f \cdot G(f_n) = \frac{1}{2} \cdot \Delta f^2 \cdot |c_n(f_n)|^2$$

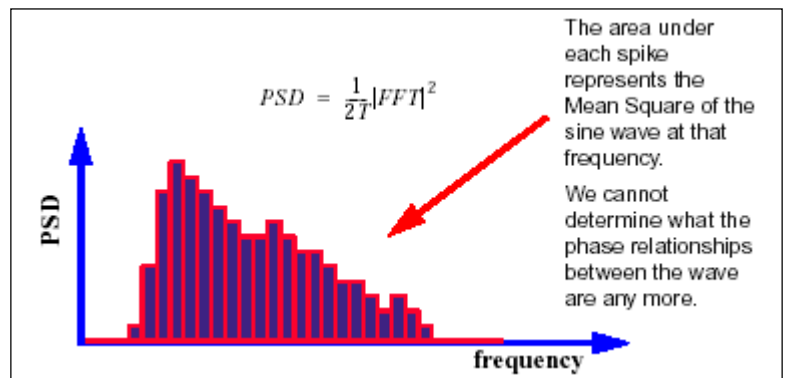
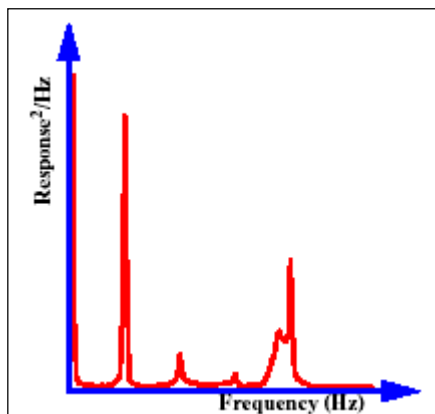
$$\therefore G(f_n) = \frac{1}{2 \cdot T} \cdot |c_n(f_n)|^2$$

Note that here T is period, not duration!

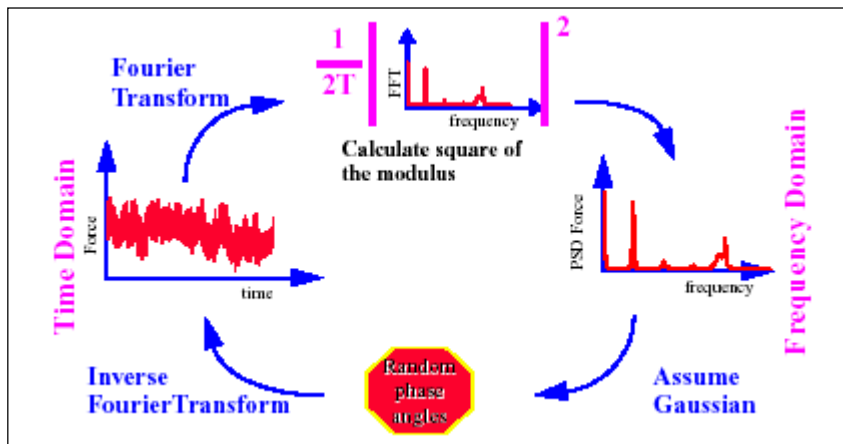
The transformation from a **double sided Fourier Density Spectra** (as described in **Section 4.6.3.6**) to a **double sided PSD** is expressed as follows.

$$S(f_n) = \frac{1}{T} \cdot |c_n(f_n)|^2$$

The PSD discards the initial phase information (of the individual harmonic components) of the FFT storing only the **amplitude squared** and corresponding frequency information. The PSD is hence the **modulus squared of the FFT**. Because there is no phase information, the PSD is no longer complex unlike the FFT.



PSDs are given in many of the design standards where random loading is involved. If the designer wishes to determine how a non-linear structure will react to a typical random load history it is necessary to **regenerate a characteristic time history from the design PSD**, this can then be analyzed using a dynamic analysis program in the time domain. The PSD contains information on the amplitude and frequency content of the sinusoidal waves but does not show the phase relationships. The discarding of the phase information means that the original signal cannot be reproduced exactly deterministically. However, a random phase description can be applied (using the Inverse Fourier Transform) in order to recreate a signal that is statistically similar. Hence, this means that the creation of a PSD from a time signal should assume that the original signal is random in the first place.



In the past, the time signal used to be transformed to the auto-covariance function, then subsequently into the PSD. Now, with the arrival of the Fast Fourier Transform FFT, the PSD is generated directly from the time signal.

The **auto- and cross-spectral density functions** are defined from the **auto- and cross-covariance functions using the Fourier Transform** are follows.

$$S_{yy}(f) = \int_{-\infty}^{\infty} C_{yy}(\tau) \cdot e^{-i2\pi f\tau} d\tau$$

$$S_{yx}(f) = \int_{-\infty}^{\infty} C_{yx}(\tau) \cdot e^{-i2\pi f\tau} d\tau$$

In fact, the **Fourier transform pair** can be used to transform between the **covariance functions** and the **PSDs**.

$$S_{yy}(f) = \int_{-\infty}^{\infty} C_{yy}(\tau) \cdot e^{-i2\pi f\tau} d\tau \quad C_{yy}(\tau) = \int_{-\infty}^{\infty} S_{yy}(f) \cdot e^{i2\pi f\tau} df$$

$$S_{yx}(f) = \int_{-\infty}^{\infty} C_{yx}(\tau) \cdot e^{-i2\pi f\tau} d\tau \quad C_{yx}(\tau) = \int_{-\infty}^{\infty} S_{yx}(f) \cdot e^{i2\pi f\tau} df$$

The **auto-covariance** function is similar to a time history representation of the PSD. In effect it is the time history of the mean square amplitude of the sinusoidal waves with a zero phase angle.

The **correlation between two random processes** can be described using the **coherence** function. The coherence represents the degree of correlation between two random processes. Two uncorrelated events show zero coherence where as two fully correlated events show unit coherence. The coherence function is defined below as a ratio of the cross-power spectral density function to the geometric mean of the two auto-power spectral density functions.

$$\gamma_{xy}(f) = \frac{|S_{xy}(f)|}{\sqrt{S_{xx}(f) \cdot S_{yy}(f)}}$$

Many design standards quote the auto-power spectral density function which the designer should use to verify the design. Where there are correlated multiple events it is often easier to express the correlation in terms of the coherence function than to specify many cross-power spectral density functions separately. The designer may then derive his own cross-spectral density functions by rearranging the above equation. For certain analyses, such as wind turbulence, the coherence function is expressed as a function of frequency and separation distance.

The **regeneration of a time history** from the double sided PSD is as follows (noting that  $y(f_n)$  is another notation for  $c(f_n)$ ).

$$\begin{aligned}
 y(t)_n &= \text{Inverse Fourier Transform of } y(f_n) \\
 y(f)_n &= T \cdot (A_n - i \cdot B_n) \\
 A_n &= \sqrt{\frac{S(f_n)}{T \cdot (1 + \varphi_n^2)}} \quad B_n = A_n \varphi_n^2 \quad \varphi_n = \tan(\phi_{rnd}_n)
 \end{aligned}$$

The **regeneration of a time history** from the single sided PSD is as follows (noting that  $y(f_n)$  is another notation for  $c(f_n)$ ).

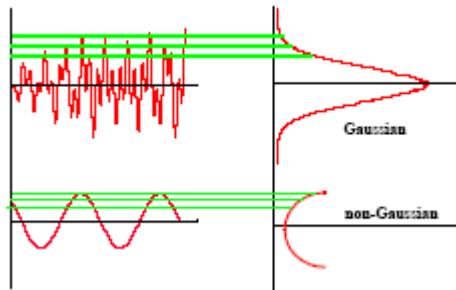
$$\begin{aligned}
 y(t)_n &= \text{Inverse Fourier Transform of } y(f_n) \\
 y(f)_n &= 2 \cdot T \cdot (A_n - i \cdot B_n) \\
 A_n &= \sqrt{\frac{G(f_n)}{2 \cdot T \cdot (1 + \varphi_n^2)}} \quad B_n = A_n \varphi_n^2 \quad \varphi_n = \tan(\phi_{rnd}_n)
 \end{aligned}$$

**Practical ball park PSD vibration levels** are presented. A PSD of  $0.001 \text{ g}^2/\text{Hz}$  over 25 to 250 Hz would be experienced inside a civil airliner. A PSD of  $0.01 \text{ g}^2/\text{Hz}$  would be the level most electronic equipment is tested. A PSD of  $0.1 \text{ g}^2/\text{Hz}$  would make one feel quite uncomfortable and is typical in military vehicles. A PSD of  $1.0 \text{ g}^2/\text{Hz}$  would certainly make one extremely uncomfortable.

#### 4.6.4.3 Validity of the PSD Representation

The specification of a PSD in place of a time signal (for a frequency domain analysis) is valid only when: -

- (i) The signal is **random (narrowband or broadband)** in phase, i.e. the initial phase between the different harmonic components is random. This may not be always true, in which case the signal is deterministic, and the analysis should thus be performed using deterministic methods in the time or frequency domain. If the time signal has a discernible spike or a superimposed dominating sine wave, then it is unlikely that that will be random. Performing a frequency domain random analysis on a deterministic signal is conservative. For instance, the PSD of a sine wave with an amplitude of say 140MPa is simply a spike. We know that the RMS of the sinusoidal time signal is 0.7071 times the amplitude, hence 100MPa. This RMS will be represented by the square root of the area under the PSD. We also know that generating a random time signal from a PSD will predict a peak amplitude of 3 (to 4.5) times the RMS, hence 300MPa here. This is because the amplitude distribution of a narrow or broadband signal is Gaussian. This is much higher than the 140MPa value of the original signal. Thus the frequency domain approach will be conservative.
- (ii) The signal is **Gaussian** in its amplitude probability distribution. This is usually the case. Gaussian means that the peak and amplitude probability density function are gaussian in nature or follow a bell shaped curve as shown here. If you draw tram lines through a signal and count the number of times the signal passes through it and plot that as a density function it is gaussian if it follows a bell shape. An example of a non- gaussian signal is a pure sine wave. However adding multiple sine wave together quickly becomes gaussian.



- (iii) The signal is statistically **stationary (and ergodic)**. This means that the statistics of the signal does not change with time. This is usually the case. This ensures that the time signal is long enough to be represented by the PSD. Stationarity refers to the fact that the average of the instantaneous displacements of an ensemble of time history samples at a particular arbitrary time  $t_i$  is the same as the average at any other time  $t_i$ . In addition, if the average obtained with respect to time for any time history sample within the ensemble of time histories is equal to the average across the ensemble at an arbitrary time  $t_i$ , the random process is called ergodic. Thus in a stationary, ergodic process, a single record may be used to obtain the statistical description of the random function.

#### 4.6.4.4 Generation and Specification of the PSD

The following aspects are considered in the generation of a PSD from a time signal: -

- (i) The number of points in the PSD,  $NFFT = \text{number of data points} / 2$
- (ii) Employ the Welch Method
- (iii) Employ the Hanning Window. The Hanning window shape accounts for the fact that the signals within the buffers are not periodic, i.e. that they do not start and end at the zero. Incomplete cycles cause spectral leakage, which gives errors in the PSD frequencies and amplitudes. This arises because of Fourier's assumption that the time history is periodic. Spectral leakage tends to occur with rectangular window functions.
- (iv) The size of the buffer or window,  $NWIND (<NFFT)$  is optimized to balance the statistical accuracy and the statistical resolution. A PSD is obtained for each buffer sample of the time signal and is averaged to obtain the averaged PSD. The method of averaging the PSDs should simply be a linear. Other existing methods such as the peak-hold method are theoretically incorrect and should not be used. If the buffer size is too big, then there will not be enough buffer samples to average over and obtain a smooth PSD curve. If the PSD curve is found to be not so smooth, then it can be concluded that there is too much scatter and the buffer size should be reduced. If the buffer size is too small, then there will not be enough point within the buffer to compute a PSD with sufficient resolution. Note that the number of points on the PSD is half the number of points in the time signal. Clearly a balance is sought between statistical accuracy and statistical resolution. The method would be to start with a small buffer size, gradually increasing the buffer size noting the increase in resolution, until too much scatter is observed, suggesting the lack of buffer samples to average over.
- (v) Let there be no overlap between the buffers. Let there be light!
- (vi) There should not be buffer data normalization. A buffer data normalization will allow for the correction of the mean offset of the time signal within each buffer. This mean offset however causes a large peak at the zero Hz frequency. This is even theoretically incorrect, and hence buffer data normalization should never be used. As for the global mean of the time signal, that should be removed before computing the PSD anyway.
- (vii) Do not employ zero-padded buffers as this artificially adds zero value points to the time signal when the number of data points within the signal does not follow the rule  $2^n$ ; this has the effect of changing the statistics of the original signal.

The specification of a PSD should be supplemented with: -

- (i) The mean of the time signal as a PSD does not contain information about the mean

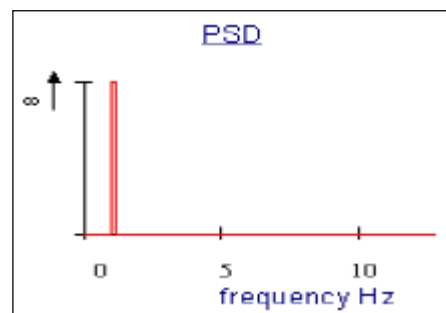
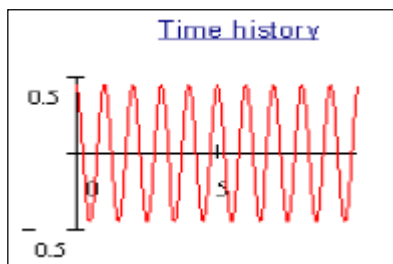
A good method to check whether a PSD has been specified correctly from a time signal is to convert the PSD back into a time signal and comparing the statistics of the new signal to that of the original signal.

#### 4.6.4.5 Statistical Information Provided by the PSD

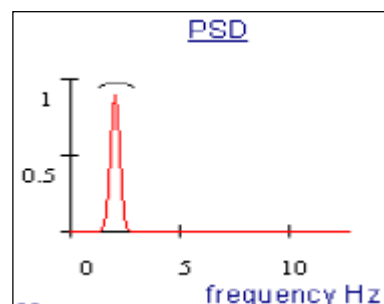
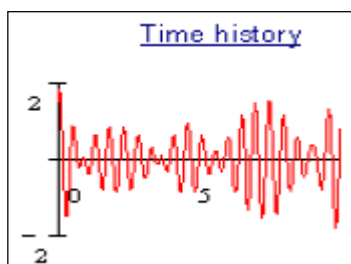
The PSD provides the following information: -

- (i) A description of the **frequency content** within the signal. The PSD of a **constant amplitude sine wave** is an infinite amplitude spike. The sine wave cannot be reproduced, as it is not random. A sinusoidal time history appears as a single spike on the PSD plot. The spike is centered at the frequency of the sine wave and the area of the spike represents the mean square amplitude of the wave. In theory this spike should be infinitely tall and infinity narrow for a pure sine wave, however because of the numerical analysis the spike will have a finite width and will therefore have a finite height. Remember, with PSD plots we are interested in the area under the graph and not the height of the graph. The PSD of a **narrowband** process is a finite amplitude spike within a narrow frequency band. The regenerated amplitude envelope of the time signal will be irregular, but the signal will consist of only a few dominant frequencies. The PSD of a **broadband** process is a multitude of finite amplitude spikes within a broad frequency band. The PSD of a **white noise** is flat, i.e. the frequency content of the signal shows a similar weighting to all frequencies.

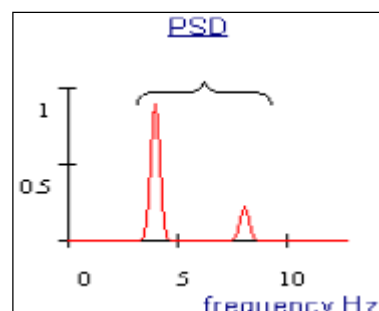
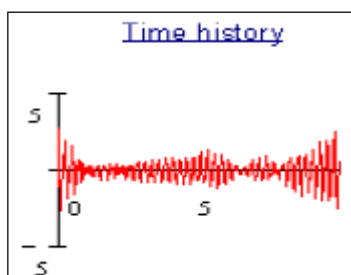
##### Sine wave



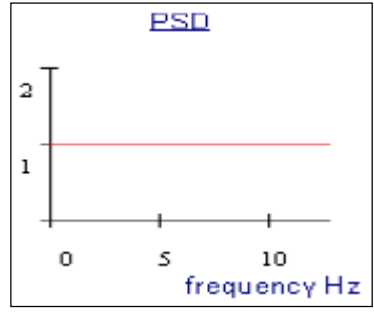
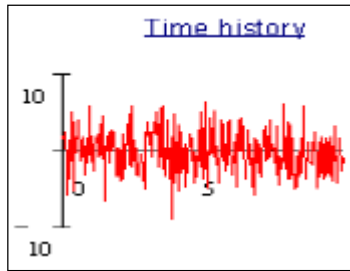
##### Narrow band process



##### Broad band process

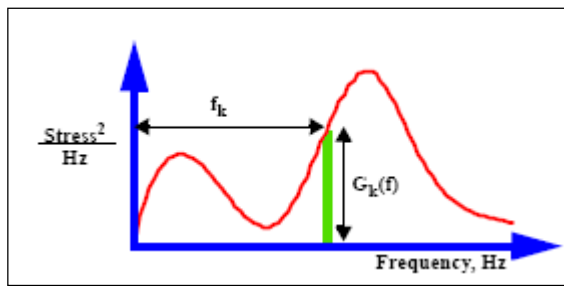


##### White noise process



To quantitatively describe the frequency content or bandedness of the PSD, the **irregularity factor**,  $\gamma$  can be calculated based on the moments of the PSD. The  $n^{\text{th}}$  moment of the PSD is

$$m_n = \int_0^{\infty} f^n \cdot G(f) df = \sum f^n \cdot G(f) \cdot \delta f$$



Hence, the irregularity factor is defined as follows

$$\text{Irregularity factor, } \gamma = \frac{E[0]}{E[P]}; 0 < \gamma < 1$$

$$\text{Expected number of zero crossings, } E[0] = \sqrt{\frac{m_2}{m_0}}$$

$$\text{Expected number of peaks, } E[P] = \sqrt{\frac{m_4}{m_2}}$$

In theory all possible moments are required to fully characterize the original process. However, in practice we find that  $m_0$ ,  $m_1$ ,  $m_2$ , and  $m_4$  are sufficient. With higher moments of a PSD, greater weighting is given to higher frequencies. The number of zero crossings  $E[0]$  is usually the number of mean crossings as the mean is non-existent in the PSD.

- (ii) The **bandedness** can be described using the **auto-covariance** functions which is defined using the Inverse Fourier Transform of the **auto-spectral density (PSD)**.

$$C_{yy}(\tau) = \int_{-\infty}^{\infty} S_{yy}(f) \cdot e^{i2\pi f\tau} df$$

- (iii) The **correlation between two random processes** can be described using the **cross-covariance** functions which is defined using the Inverse Fourier Transform of the **cross-spectral densities (CPSD)**.

$$C_{yx}(\tau) = \int_{-\infty}^{\infty} S_{yx}(f) \cdot e^{i2\pi f\tau} df$$

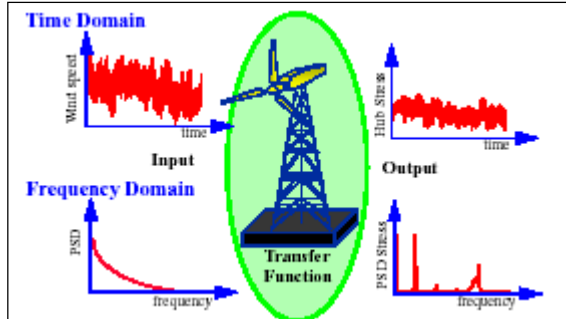
- (iv) The **correlation between two random processes** can be described using the **coherence** function. The coherence represents the degree of correlation between two random processes. Two uncorrelated events show zero coherence where as two fully correlated events show unit coherence. The coherence function is defined below as a ratio of the cross-power spectral density function to the geometric mean of the two auto-power spectral density functions.

$$\gamma_{xy}(f) = \frac{|S_{xy}(f)|}{\sqrt{S_{xx}(f) \cdot S_{yy}(f)}}$$

- (v) The **RMS** of the time signal is the square root of the area under the PSD, defining the intensity of the signal. If the mean of the PSD has been removed, the RMS ( $\sqrt{m_0}$ ) is equal to the standard deviation. The mean is almost always removed in dynamic analysis and is dealt with statically.
- (vi) The **peak amplitude** of the random signal used to generate the PSD is approximately 3 to 4.5 times the RMS. This is because the amplitude distribution of a narrow or broadband signal is Gaussian. Hence, the peak range is approximately 6 to 9 times the RMS.

#### 4.6.4.6 MSC.NASTRAN Random Analysis Methodology

In random forcing functions, the instantaneous magnitude is not known at any given time. Random vibration excitations include that from earthquake ground motions, wind, ocean waves, acoustic excitations and jet engine noises. A power spectral density (PSD) function defines these random excitations. Frequency response analysis is used to generate transfer functions  $[H(\omega)]$ , which are the ratio of the output to the unit inputs. The **input PSDs** are then multiplied to the square of these transfer functions  $[H(\omega)]$  to form response PSDs.



The double sided PSD response to a double sided PSD excitation is

$$S^F(f) = g \cdot g^* \cdot S^y(f) \text{ or } S^F(f) = |g|^2 \cdot S^y(f)$$

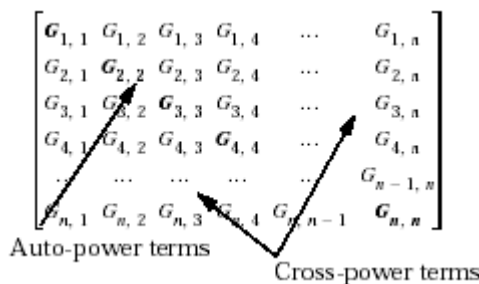
whilst a single sided PSD response to a single sided PSD excitation is

$$G^F(f) = g \cdot g^* \cdot G^y(f) \text{ or } G^F(f) = |g|^2 \cdot G^y(f)$$

If two processes are correlated then the sequencing effect of the two processes may act to either increase or decrease the overall effects. Thus, the input PSDs must be in the form of **auto-** and **cross-spectral** density functions. The double sided and single sided PSD computations are as follows, respectively.

$$S^F(f) = \sum_i \sum_j g_i \cdot \bar{g}_j \cdot S_{ij}^y(f) \qquad G^F(f) = \sum_i \sum_j g_i \cdot g_j^* \cdot G_{ij}^y(f)$$

The auto- and cross-power spectral density functions may be expressed in matrix form, this permits the rapid calculation of responses using matrix algebra. The auto-power spectral values are located along the leading diagonal while the cross-power terms are located in the remaining cells.



Hence the single sided PSD computation is as follows.

$$G^F(f) = [\underline{g}]^T \cdot [G(f)] \cdot [\underline{\bar{g}}]$$

To get the transfer function into the correct units for a PSD analysis the response parameter (per unit input loading) has to be squared. This is because the units of PSDs are units of interest squared, per hertz. If one takes the example of an offshore platform the input loading is typically expressed as a sea state spectrum. The process which this PSD defines is the sea surface elevation profile. In the time domain this is the sea surface elevation variation with time. The units of the input PSD are therefore given as  $\text{m}^2/\text{Hz}$  (in SI units). Since the response parameter of interest is stress (or strain) the output PSD is usually expressed as  $\text{MPa}^2/\text{Hz}$ . The units of the transfer function are therefore given as  $(\text{MPa}/\text{Hz})^2$ .

Most of the computational time is spent in solving the structural model. In the time domain, the structural model is solved for each time history of input; hence two load cases would take twice as long to calculate as one. In the frequency domain the linear transfer function is only calculated once, hence two load cases take little more time to analyze than one, and each additional load case can be done virtually instantaneously. The structural calculation is effectively separated from the response analysis when working in the frequency domain.

The output from a random response analysis consists of the **response PSD, auto-covariance functions, number of zero crossings** with positive slope per unit time and **RMS** values of the response.

In MSC.Nastran, random response analysis is treated as a data reduction procedure that is applied to the results of a frequency response analysis. First, the frequency response analysis is performed for sinusoidal loading conditions,  $\{P_a\}$ , each a separate subcase, at a sequence of frequencies  $\omega_j$ . Normal data reduction procedures are then applied to the output of the frequency response analysis module, resulting in a set of output quantities  $u_{j,a}(\omega_j)$ , corresponding to an output  $j$  and subcase  $a$ . The calculations of power spectral densities and autocorrelation functions for the output quantities are performed in the random analysis module.

Each loading condition subcase represents a unique random load source, which may be applied to many grid points. Typically, these loads are chosen to be unit loads such as unit "g" loads or unit pressures. The probabilistic magnitude of each load source is defined by spectral density functions on RANDPS input data. If the load subcases are correlated, the coupling spectral density is also defined on one or more RANDPS functions. An example of coupled spectral density would be the forces on four wheels of a vehicle traveling over a rough road.

**Figure 6-8** is a simplified flow diagram for the random analysis module. The inputs to the module are the frequency responses,  $H_{j,a}(\omega_j)$ , of quantities  $u_j$  to loading conditions  $\{P_a\}$  at frequencies  $\omega_j$ , and the auto- and cross-spectral densities of the loading conditions  $S_a$  and  $S_{ab}$ . The response quantities,  $s_j$ , may be displacements, velocities, accelerations, internal forces, or stresses. The power spectral densities of the response quantities are calculated by different procedures depending on whether the loading conditions are correlated or uncorrelated. The spectral densities due to all sources, considered independent, will be combined into one set of outputs.

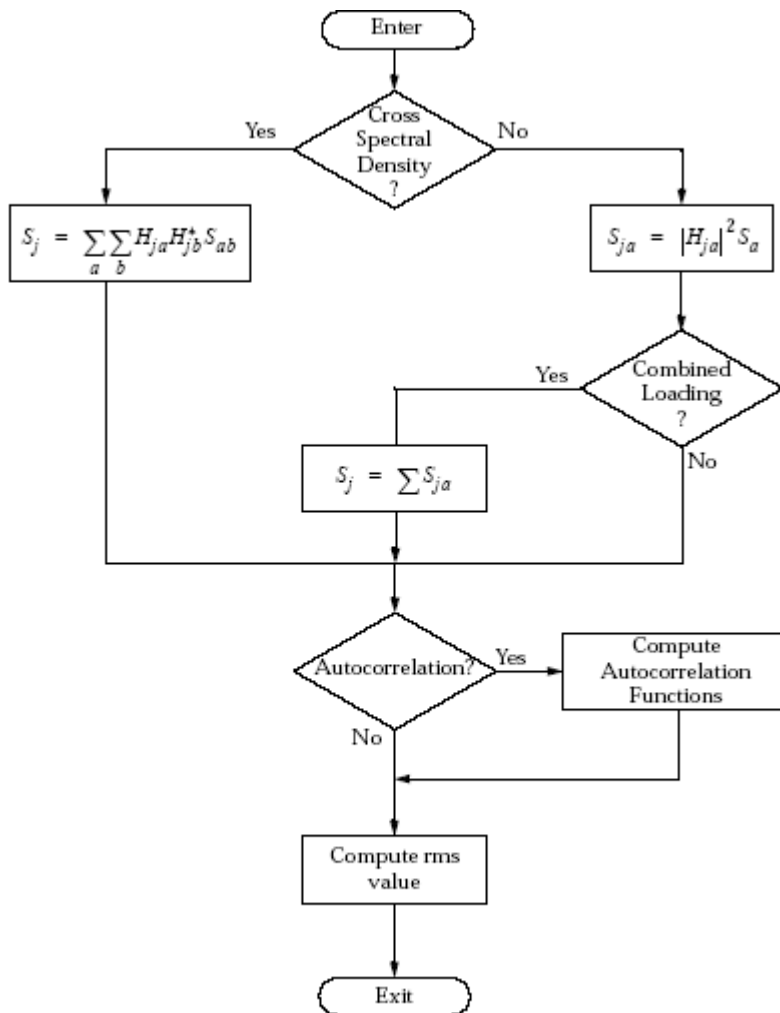


Figure 6-8 Flow Diagram for Random Analysis Module

### Theory

The application of these frequency response techniques to the analysis of random processes requires that the system be linear and that the excitation be stationary with respect to time. The theory includes a few important theorems that will be reviewed.

An important quantity in random analysis theory is the autocorrelation function  $R_j(\tau)$ , of a physical variable,  $u_j$ , which is defined by

$$R_j(\tau) = \lim_{T \rightarrow \infty} \frac{1}{T} \int_0^T u_j(t) u_j(t - \tau) dt \quad \text{Eq. 6-41}$$

Note that  $R_j(0)$  is the time average value of  $u_j^2$ , which is an important quantity in the analysis of structural failure. The one-sided power spectral density  $S_j(\omega)$  of  $u_j$  is defined by

$$S_j(\omega) = \lim_{T \rightarrow \infty} \frac{2}{T} \left| \int_0^T e^{-i\omega t} u_j(t) dt \right|^2 \quad \text{Eq. 6-42}$$

It may be shown (using the theory of Fourier integrals) that the autocorrelation function and the power spectral density are Fourier transforms of each other. Thus, we define the autocorrelation function in terms of frequency response functions

$$R_j(\tau) = \frac{1}{2\pi} \int_0^{\infty} S_j(\omega) \cos(\omega\tau) d\omega \quad \text{Eq. 6-43}$$

from the mean-square theorem, the rms (root mean squared) magnitude,  $u_j$ , is

$$\bar{u}_j^2 = R_j(0) = \frac{1}{2\pi} \int_0^{\infty} S_j(\omega) d\omega \quad \text{Eq. 6-44}$$

The transfer function theorem states that, if  $H_{ja}(\omega)$  is the frequency response of any physical variable,  $u_j$ , due to an excitation source,  $Q_a$ , which may be a point force, a loading condition or some other form of excitation, i.e., if

$$u_j(\omega) = H_{ja}(\omega) \cdot Q_a(\omega) \quad \text{Eq. 6-45}$$

where  $u_j(\omega)$  and  $Q_a(\omega)$  are the Fourier transforms of  $u_j$  and  $Q_a$ , then the power spectral density of the response  $S_j(\omega)$ , is related to the power spectral density of the source,  $S_a(\omega)$ , by

$$S_j(\omega) = |H_{ja}(\omega)|^2 \cdot S_a(\omega) \quad \text{Eq. 6-46}$$

**Eq. 6-46** is an important result because it allows the statistical properties (e.g., the autocorrelation function) of the response of a system to random excitation to be evaluated via the techniques of frequency response. Another useful result is that, if sources  $Q_1$ ,  $Q_2$ ,  $Q_3$ , etc., are statistically independent, i.e., if the cross-correlation function between any pair of sources

$$R_{ab}(\tau) = T \lim_{T \rightarrow \infty} \frac{1}{T} \int_0^T q_a(t) q_b(t - \tau) d\tau \quad \text{Eq. 6-47}$$

is null, then the power spectral density of the total response is equal to the sum of the power spectral densities of the responses due to individual sources. Thus

$$S_j(\omega) = \sum_a S_{ja}(\omega) = \sum_a |H_{ja}(\omega)|^2 S_a(\omega) \quad \text{Eq. 6-48}$$

If the sources are statistically correlated, the degree of correlation can be expressed by a cross-spectral density,  $S_{ab}$ , and the spectral density of the response may be evaluated from

$$S_j = \sum_a \sum_b H_{ja} H_{jb}^* S_{ab} \quad \text{Eq. 6-49}$$

where  $H_{jb}^*$  is the complex conjugate of  $H_{jb}$ .

In applying the theory, it is not necessary to consider the sources to be forces at individual points. Rather, an ensemble of applied forces that are completely correlated (i.e., a loading condition) should be treated as a single source. For example, a plane pressure wave from a specified direction may be treated as a source. Furthermore, the response may be any physical variable including internal forces and stresses as well as displacements, velocities, and accelerations.

The power spectral densities,  $S_j$ , are plotted versus frequency using the XYOUT commands (XYPLOT, XYPRINT, XYPEAK, AND XYPUNCH). The autocorrelation functions,  $R_j(\tau)$ , are plotted versus selected time delays,  $\tau$ , using XYOUT requests.

Because of the potential computational costs, cross-correlations and cross-spectral densities.

## 4.7 GL, ML Implicit (Real) Modal Transient Response Analysis

### 4.7.1 Nature of the Dynamic Loading Function

The solution can be used to ascertain the modal properties of the system by performing a time domain impulse analysis to excite the modes of interest. The duration of the impulse must be sufficiently long to excite the first fundamental mode, which is usually of concern. This would result in a response that includes the first fundamental mode and most likely higher modes as well. The first fundamental mode is readily ascertained from inspection of the response time history curve at any node. Higher natural frequencies can also be ascertained by performing an FFT on the response curve.

The solution method can be used to solve dynamic systems subjected to: -

- (a) **Deterministic non-periodic short duration impulse (a.k.a. blast) loading functions with subsequent wave propagation**
- (b) **Random non-stationary short duration impulse loading functions**

The force amplitude does not repeat itself regularly but rises from zero to a series of maxima and minima until settling down to a constant value. The starting transient is significant and so the solution is carried out in the time domain. Estimates of the induced stress in a **linear elastic** body due to an **impulsive blast** may be made easily in some cases with a simpler static method of analysis. **Section 4.7.4** describes this concept further.

If the forcing function is a random non-stationary forcing function such that the random forces start from a low-level building up to a maximum then dying away, such as in a seismic event, then exact solution methods are not established. Instead, we could either analyze a set of such events using deterministic transient solution methods and then average or envelope the results or alternatively use the crude response spectrum method which envelopes the response spectra of a series of time histories.

**In this LINEAR TIME DOMAIN solution**, the static response must be added to the dynamic response if the dynamic analysis is performed about the initial undeflected (by the static loads) state with only the dynamic loads applied, hence causing the dynamic response to be measured relative to the static equilibrium position. **Hence, the total response = the dynamic response + the static response to static loads.**

**Alternatively, in this LINEAR TIME DOMAIN solution**, if the dynamic analysis is performed with the deflected static shape as initial input and the static loads maintained throughout the dynamic excitations, the total or absolute response (static and dynamic) is obtained straight away from the dynamic analysis. **Hence total response = dynamic response (which already includes the static response to static loads).**

### 4.7.2 Mathematical Formulation of Analysis

With the knowledge of the modal frequencies and corresponding mode shapes, the coupled system of simultaneous dynamic equilibrium equations can be uncoupled by premultiplying the dynamic equation of motion by  $[\Phi]^T$  as shown below. This means that the simultaneous ODEs no longer need to be solved simultaneously and so the MDOF system of equations is reduced to a SDOF system of equations, which can be solved independently of each other. The computational benefit comes from not having to run a rigorous simultaneous equation solver. The knowledge of the modal frequencies and the corresponding mode shapes are a prerequisite to this implicit modal transient response analysis, hence the implicit real (note not complex) eigenvalue analysis must be performed first. Because of the fact that the modes are real and do not take into account the explicit elemental (viscous) damping within the structure, the coupled ODEs cannot be uncoupled by  $[\Phi]^T$ . The system of coupled ODEs remains in the existence of viscous damping and the simultaneous equation solver must be invoked. The only difference then between SOL 112 and SOL 109 is the fact that the former solves the equations in the modal coordinates instead of the physical coordinates. Hence, as long as sufficient modes are included (to represent both the static and dynamic response of the system), SOL 112 will give the same solution as SOL 109 even with large values of viscous damping. We know that large values of elemental damping will modify the mode shape and frequencies. However,

a SOL 112 can still be performed because a true (real) modal approach is not undertaken, instead the coupled ODEs are solved using a direct approach, but in the modal coordinates. However, the use of the **FREQ4** card, which bases the excitation frequencies to be solved for on the real natural frequencies may prove to be insufficient. This is because with high values of elemental viscous damping, certain local modes can be totally eliminated. For instance, viscous dampers with high coefficients of damping on cables can considerably alter the natural frequency of the local mode and even eliminate a local mode altogether. In this case, the **FREQ4** card will not capture the response at the damped natural frequency. Hence, these damped natural frequencies need to be known (by performing a SOL 107) before choosing the excitation frequencies to be solved for using **FREQ2** cards. To reiterate, SOL 112 reverts to a direct solution technique (akin to SOL 109) when there is either viscous or structural element damping as the equations of motion cannot be orthogonalized. But the unknowns are still the modal responses and not the physical responses. And because with damping the modes are really complex modes, there is greater difficulty in capturing all the response using the real modes. Hence, even more modes are thus required to capture the response accurately in SOL 112 with element damping especially if the elemental damping is high enough to cause significant complex modes. Thus if elemental damping is high and the modes are complex, the direct method SOL 109 may be more appropriate. If a true modal approach is intended for the solution of coupled ODEs with elemental viscous damping, then a complex modal forced transient response analysis is necessary, although this is quite impractical.

The modal matrix from the free, undamped vibration analysis

$$[\Phi] = [\{\phi\}_1 \dots \{\phi\}_i \dots \{\phi\}_n] \text{ for the } n \text{ modes}$$

The coupled system of ODEs are given by

$$[M]\{\ddot{u}(t)\} + [K]\{u(t)\} = \{P(t)\}$$

Let  $\{u(t)\} = [\Phi]\{\xi(t)\}$

$$[M][\Phi]\{\ddot{\xi}(t)\} + [K][\Phi]\{\xi(t)\} = \{P(t)\}$$

Premultiplying by  $[\Phi]^T$  reduces the coupled system of ODEs to a system of uncoupled ODEs

$$[\Phi]^T [M][\Phi]\{\ddot{\xi}(t)\} + [\Phi]^T [K][\Phi]\{\xi(t)\} = [\Phi]^T \{P(t)\}$$

Hence the generalised mass matrix and the generalised stiffness matrix for the entire system is

$$\text{the diagonal modal (generalized) mass matrix, } [M] = [\Phi]^T [M][\Phi]$$

$$\text{the diagonal modal (generalized) stiffness matrix, } [K] = [\Phi]^T [K][\Phi] = [\omega_n^2] [M]$$

$$\text{the modal (generalized) force vector, } \{P(t)\} = [\Phi]^T \{P(t)\}$$

The generalized mass matrix and the generalized stiffness matrix are diagonal because of the orthogonality condition of the normal modes

$$\{\phi_i\}^T [M] \{\phi_j\} = 0 \quad \text{if } i \neq j$$

$$\{\phi_i\}^T [K] \{\phi_j\} = 0 \quad \text{if } i \neq j$$

And because these matrices are diagonal, the equations become uncoupled.

Accordingly, the generalized mass solitary term and the generalized stiffness solitary term associated with a particular mode 'i' are

$$M_i = \{\phi_i\}^T [M] \{\phi_i\}$$

$$K_i = \{\phi_i\}^T [K] \{\phi_i\} = \omega_{ni}^2 M_i$$

The uncoupled system of equations are thus

$$[M]\{\ddot{\xi}(t)\} + [K]\{\xi(t)\} = \{P(t)\}$$

These are a set of SDOF ordinary differential equations

$$M_i \ddot{\xi}_i(t) + K_i \xi_i(t) = P_i(t) \text{ for the } i^{\text{th}} \text{ mode}$$

The central difference numerical integration of the uncoupled equations are then trivial

$$\dot{\xi}_n = \frac{1}{2\Delta t} (\xi_{n+1} - \xi_{n-1})$$

$$\ddot{\xi}_n = \frac{1}{\Delta t^2} (\xi_{n+1} - 2\xi_n + \xi_{n-1})$$

and replacing into the dynamic equation of motion averaging the applied force over 3 adjacent time steps

$$M_i \frac{1}{\Delta t^2} (\xi_{n+1} - 2\xi_n + \xi_{n-1}) + \frac{1}{3} K_i (\xi_{n+1} + \xi_n + \xi_{n-1}) = \frac{1}{3} (P_{n+1} + P_n + P_{n-1})$$

Collecting terms and making  $\xi_{n+1}$  the subject

$$A_1 \xi_{n+1} = A_2 + A_3 \xi_n + A_4 \xi_{n-1}$$

$$A_1 = \frac{1}{\Delta t^2} M_i + \frac{1}{3} K_i$$

$$A_2 = \frac{1}{3} (P_{n+1} + P_n + P_{n-1})$$

$$A_3 = \frac{2}{\Delta t^2} M_i - \frac{1}{3} K_i$$

$$A_4 = -\frac{1}{\Delta t^2} M_i - \frac{1}{3} K_i$$

Once individual modal responses are computed  $\{\xi(t)\}$ , the physical response is thus

$$\{u(t)\} = [\Phi] \{\xi(t)\}$$

Since the numerical integration is performed on a *small* number (as not all the modes are usually included) of *uncoupled* equations, there is not a large computational penalty for changing  $\Delta t$  as there is in direct transient response analysis. A constant  $\Delta t$  is still recommended.

In modal transient response analysis, mode truncation refers to not utilizing all the natural modes in computing the response of the structure. At a minimum all the modes that have resonant frequencies that lie within the range of the forcing frequencies have to be retained. For better accuracy, all the modes up to at least 2 to 3 times the highest forcing frequency should be retained. For example, if a structure is excited between 200 and 2000 Hz, all modes from 0 to at least 4000 Hz should be retained as the forcing frequencies still excite the higher modes although not resonating with them i.e. off-resonant excitation. It is thus necessary to evaluate the frequency content of the transient loads and determine the frequency above which no modes are noticeably excited. Truncating high-frequency modes truncates high frequency response. The recommendation of using modes up to 2 or 3 times the highest excitation frequency assumes that the static response can be captured adequately using this finite number of modes. Clearly, if the distribution of applied loads is multiple concentrated forces, then the finite number of modes may still not be sufficient to capture the difficult static shape. In this case, it may be prudent to use static residual vectors instead of increasing the number of vibration modes solely to capture the static response.

The following damping models are supported by the solution scheme

I.	elemental damping	
	i. viscous damping	Yes
	ii. structural damping	Specified but converted to viscous
II.	modal damping	
	i. viscous damping	Yes
	ii. structural damping	Specified but converted to viscous
III.	global proportional viscous damping	
	i. mass proportional damping	No
	ii. stiffness proportional damping	Specified but converted to viscous
	iii. Rayleigh damping	No

If explicit viscous damping element contributions are made to the damping matrix [C] or if elemental structural damping is specified, then the damping stiffness matrix cannot be diagonalized by the modal matrix. In this case the modal transient response analysis solves the still coupled problem using a direct transient approach but in terms

of the modal coordinates  $\{\xi(t)\}$  instead of the physical coordinates  $\{u(t)\}$ . Since the number of modes used in a solution is typically much less than the number of physical variables, using the coupled solution of the modal equations is less costly than using physical variables.

Elemental viscous damping makes contributions to the  $[C]$  matrix.

$$[\Phi]^T [M][\Phi]\{\ddot{\xi}(t)\} + [\Phi]^T [C][\Phi]\{\dot{\xi}(t)\} + [\Phi]^T [K][\Phi]\{\xi(t)\} = [\Phi]^T \{P(t)\}$$

Elemental structural damping will modify the damping matrix as follows

$$[\Phi]^T [M][\Phi]\{\ddot{\xi}(t)\} + [\Phi]^T \left[ C + \frac{1}{\omega_4} \sum G_E [K_E] \right] [\Phi]\{\dot{\xi}(t)\} + [\Phi]^T [K][\Phi]\{\xi(t)\} = [\Phi]^T \{P(t)\}$$

where the parameter  $\omega_4$  converts the structural damping into equivalent viscous damping as the transient response analysis does not permit the use of complex coefficients.

Stiffness proportional global viscous damping modifies the dynamic equilibrium equations as follows

$$[\Phi]^T [M][\Phi]\{\ddot{\xi}(t)\} + [\Phi]^T \left[ C + \frac{G}{\omega_3} [K] \right] [\Phi]\{\dot{\xi}(t)\} + [\Phi]^T [K][\Phi]\{\xi(t)\} = [\Phi]^T \{P(t)\}$$

where the parameter  $\omega_3$  converts the structural damping into equivalent viscous damping as the transient response analysis does not permit the use of complex coefficients.

Hence, with elemental viscous, elemental structural and global structural damping, the uncoupled system of ODEs are given by

$$[\Phi]^T [M][\Phi]\{\ddot{\xi}(t)\} + [\Phi]^T \left[ C + \frac{1}{\omega_4} \sum G_E [K_E] + \frac{G}{\omega_3} [K] \right] [\Phi]\{\dot{\xi}(t)\} + [\Phi]^T [K][\Phi]\{\xi(t)\} = [\Phi]^T \{P(t)\}$$

The fundamental structural response is solved at discrete times, typically at fixed integration time steps  $\Delta t$ .

Using a central finite difference representation for the velocity and acceleration,

$$\begin{aligned} \{\dot{\xi}_n\} &= \frac{1}{2\Delta t} \{\xi_{n+1} - \xi_{n-1}\} \\ \{\ddot{\xi}_n\} &= \frac{1}{\Delta t^2} \{\xi_{n+1} - 2\xi_n + \xi_{n-1}\} \end{aligned}$$

and replacing into the dynamic equation of motion averaging the applied force over 3 adjacent time steps

$$\begin{aligned} \frac{1}{\Delta t^2} [\Phi]^T [M][\Phi]\{\xi_{n+1} - 2\xi_n + \xi_{n-1}\} + \frac{1}{2\Delta t} [\Phi]^T \left[ C + \frac{1}{\omega_4} \sum G_E [K_E] + \frac{G}{\omega_3} [K] \right] [\Phi]\{\xi_{n+1} - \xi_{n-1}\} \\ + \frac{1}{3} [\Phi]^T [K][\Phi]\{\xi_{n+1} + \xi_n + \xi_{n-1}\} = \frac{1}{3} [\Phi]^T \{P_{n+1} + P_n + P_{n-1}\} \end{aligned}$$

Collecting terms and making  $\{\xi_{n+1}\}$  the subject

$$\begin{aligned} [A_1]\{\xi_{n+1}\} &= [A_2] + [A_3]\{\xi_n\} + [A_4]\{\xi_{n-1}\} \\ [A_1] &= [\Phi]^T \left[ \frac{1}{\Delta t^2} [M] + \frac{1}{2\Delta t} \left[ C + \frac{1}{\omega_4} \sum G_E [K_E] + \frac{G}{\omega_3} [K] \right] + \frac{1}{3} [K] \right] [\Phi] \\ [A_2] &= \frac{1}{3} [\Phi]^T \{P_{n+1} + P_n + P_{n-1}\} \\ [A_3] &= [\Phi]^T \left[ \frac{2}{\Delta t^2} [M] - \frac{1}{3} [K] \right] [\Phi] \\ [A_4] &= [\Phi]^T \left[ -\frac{1}{\Delta t^2} [M] + \frac{1}{2\Delta t} \left[ C + \frac{1}{\omega_4} \sum G_E [K_E] + \frac{G}{\omega_3} [K] \right] - \frac{1}{3} [K] \right] [\Phi] \end{aligned}$$

The modal transient response analysis solves the still coupled problem using a direct transient approach but in terms of the modal coordinates  $\{\xi(t)\}$  (modal responses in modal space) instead of the physical coordinates  $\{u(t)\}$ . A constant  $\Delta t$  is obviously computationally beneficial. Hence, if discrete damping is desired, direct transient response analysis is recommended.

If however only viscous modal damping  $\zeta_i$  is specified, the generalized damping matrix  $[\Phi]^T[C][\Phi]$  remains diagonal and so the uncoupled equations of motion can be maintained. The uncoupled equations of motion become

$$M_i \ddot{\xi}_i(t) + (\zeta_i 2M_i \omega_{ni}) \dot{\xi}_i(t) + K_i \xi_i(t) = P_i(t) \quad \text{for the } i^{\text{th}} \text{ mode}$$

which is solved for the individual modal responses  $\xi_i(t)$  using the Duhamel's Integral

$$\begin{aligned} \xi_i(\tau = t) = e^{-\zeta_i \omega_{ni} t} & \left( \xi_i(\tau = 0) \cos \omega_{di} t + \frac{\dot{\xi}_i(\tau = 0) + \xi_i(\tau = 0) \zeta_i \omega_{ni}}{\omega_{di}} \sin \omega_{di} t \right) \\ & + \frac{1}{M_i \omega_{di}} \int_{\tau=0}^{\tau=t} P_i(\tau) e^{-\zeta_i \omega_{ni} (t-\tau)} \sin \omega_{di} (t-\tau) d\tau \end{aligned}$$

$$\text{where } \omega_{di} = \omega_{ni} \sqrt{1 - \zeta_i^2}$$

If structural modal damping  $G_i$  is specified, it is converted to an equivalent viscous modal damping

$$\zeta_i = G_i / 2$$

### 4.7.3 Capability of A Finite Number of Modes To Model The Static and Dynamic Response of Structure

**First and foremost, the chosen modes must cover and extend beyond the excitation frequency range such that both the resonant response of the modes within the range and the off-resonant response of the modes beyond (from say a 1/3<sup>rd</sup> of lowest excitation frequency to 3x the highest excitation frequency determined by FFT as frequency content not obvious) the range are captured. This will sufficiently model the dynamic response. Considerations then must be made for the finite number of modes to capture the static response.**

Modal truncation can be specified by delimiting the number of modes used in the response calculations from that calculated by EIGRL. To delimit the natural modes employed, LFREQ (lower limit of the frequency range), HFREQ (upper limit of the frequency range) or LMODES (number of lowest modes retained) can be used.

To determine if enough modes have been selected **to represent the static response** of the structure, a dynamic load curve ramped up gradually from zero to a constant value can be applied to a SOL 112 and the final static equilibrium response after all the dynamic amplification effects have subsided can be compared to the static response from a SOL 101 solution. Often, if the finite number of modes is found to be capable of representing the static response, then they will usually be found to be sufficient to represent the dynamic response as well.

To determine if enough modes have been chosen **to represent the static and dynamic response** of the structure, a SOL 112 solution can be compared to that of a SOL 109 and the response time history traces compared.

The relative contribution of each mode to the total static and dynamic response can also be determined. This is known as the modal responses, i.e. the value of the modal variables in the modal solution scheme. The Case Control Cards SDISP, SVELO and SACCE will produce the modal solution set output,  $\{\xi_i(t)\}$ . These are plots of the modal response (for each mode) in terms of time, i.e. the time domain modal response. That is to say, SDISP(PUNCH) (or SVELO or SACCE) will output one value for each mode at each time step. These are the modal responses in **modal space**. They must be multiplied by the corresponding mode shapes in order to obtain the modal responses in **physical space** i.e.

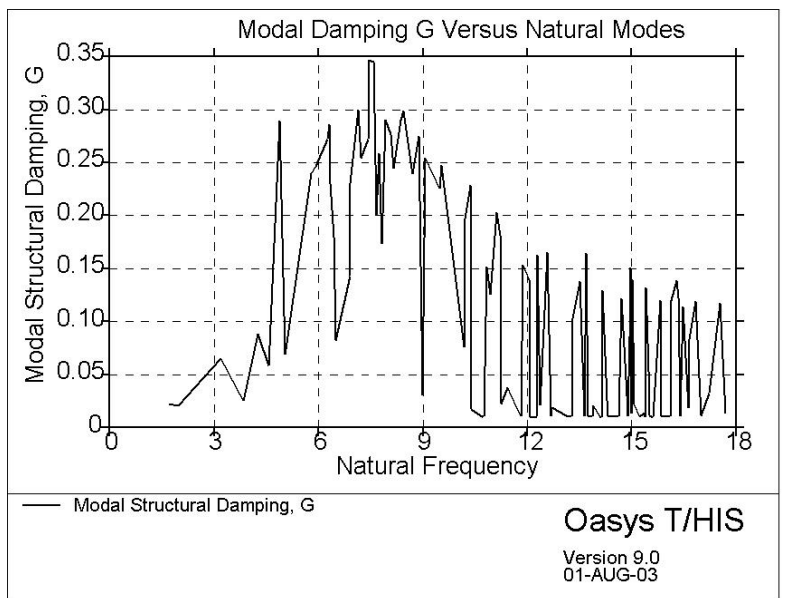
$$\{u_i(t)\} = \{\phi_i\} \xi_i(t)$$

Another method of determining the modal contribution of individual modes to a particular excitation is by using the modal strain energy. Firstly, to evaluate the ability of the natural modes to represent the static response, a SOL 101 is run with the amplitude of the dynamic loads applied as a static load and the results are written to a DMIG file using the alter pchdispa.v2001. Then a SOL 103 is run with the DMIG included and also the alter modevala.v2001 to ascertain how well each and every mode can represent the static solution. The strain energy for each mode can be compared to the strain energy in all the modes calculated and also the input vector. Note that the eigenvector scaling must be set to the default MASS (not MAX) for this alter to be valid. Secondly, to evaluate the ability of the natural modes to represent the dynamic response, the alter mtranea.v2001 is utilized for SOL 112.

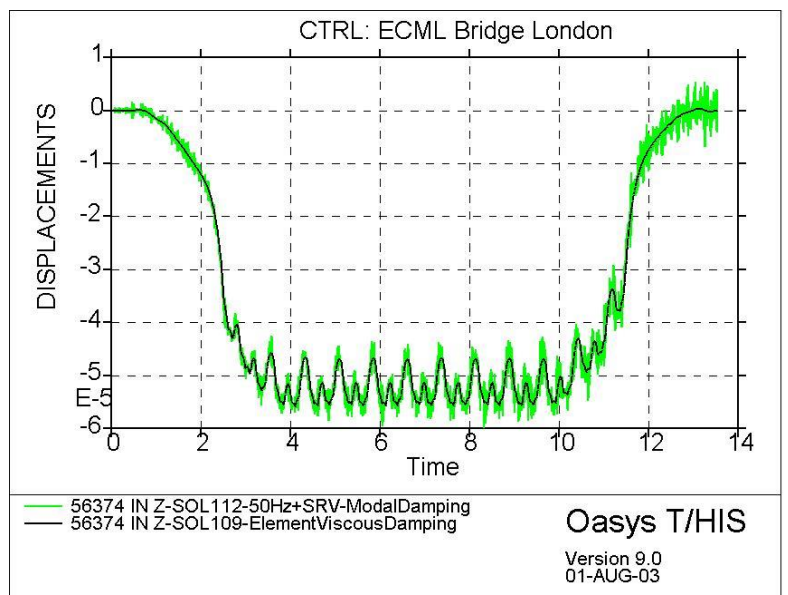
Note that the capability of a finite number of modes to represent the static and dynamic response of the structure is **limited to a particular force excitation direction and distribution**. If the force changes its location or direction, then the prominence of the different modes which will be different. This is simply because changing the location or direction of the force will cause a different set of modal forces and hence a different level of excitation of the different modes. The capability of a finite number of modes to represent the static and dynamic response of the structure depends also on the level of elemental structural (although cannot be accounted for exactly in the time domain) and elemental viscous damping present within the system. This is because, the level of elemental damping affects the complexity of the modes, hence possibly requiring more real modes if the modal complexity is high. Thus damping should be included when performing the study to determine the required number of modes.

The above method assumes that the direct solution SOL 109 is exact and hence we only have to match that using a certain number of modes. **However, there is an instance when the solution from the direct approach SOL 109 is inaccurate. This occurs when there is elemental structural damping.** This problem does not occur in the

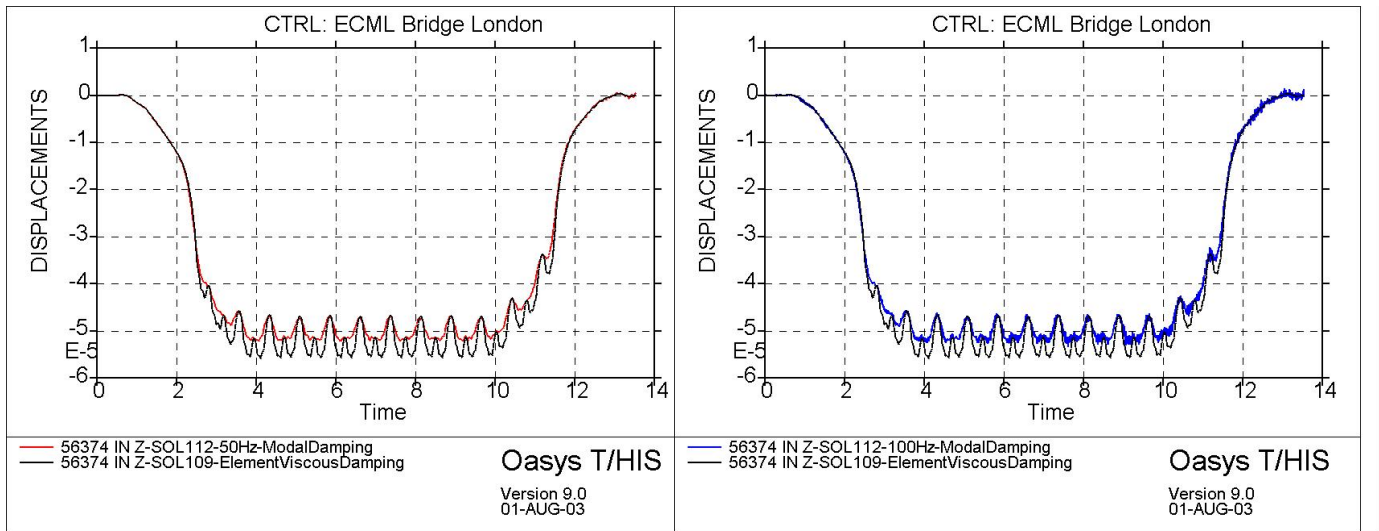
frequency domain and the approach of comparing the modal estimate to the correct direct solution can be always made. It can also always be made in the time domain if the only form of damping is viscous. However, time domain solutions cannot model structural damping exactly, hence having to convert the structural damping into equivalent viscous damping. But this conversion ties the equivalence to **one** natural frequency (PARAM, W3 or PARAM, W4). Hence the damping will only be accurate for the mode with the natural frequency corresponding to (PARAM, W3 or PARAM, W4), that to only at that excitation frequency, but then again damping is most critical at resonance. But the fact of the matter is that the direct solution will not be accurate when there is structural damping. Hence, noting that the direct solution is not a good benchmark to measure against, a modal approach must be used. Employing SOL 112, a solution would be to insert modal damping estimates based on a SOL 107 calculation. Hence different modes will be damped accurately (but again not at all excitation frequencies, this usually being an acceptable inaccuracy). The following graph shows the modal structural damping for a bridge with a floating track slab resting on isolation pads.



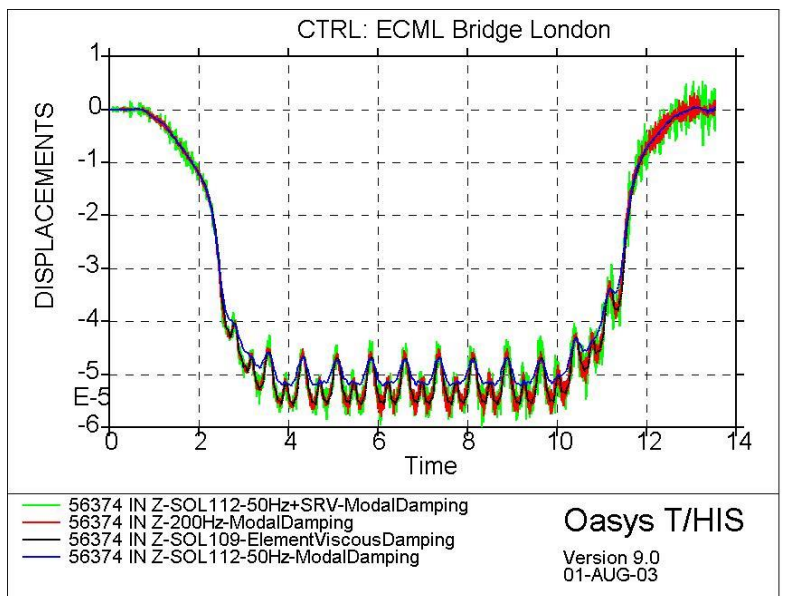
The graph below shows significant high frequency response when modal damping (with no elemental structural damping) is applied in a SOL 112 solution compared to a highly attenuated high frequency response in a SOL 109 direct solution which incorporates equivalent viscous damping for elemental structural damping tied in at the frequency of the first mode. Thus clearly, a modal approach must be used when structural damping is present. Alternatively of course, a direct time domain analysis can be performed if Rayleigh damping (which damps two modes accurately and interpolates for the modal damping within the range) is incorporated.



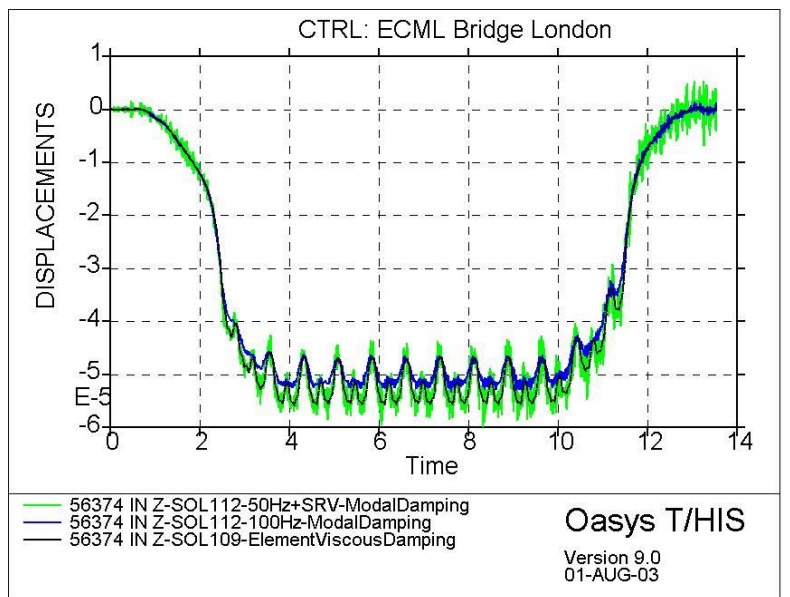
But let us go with the modal solution. Now since no comparison to a direct approach can be made, the verification the sufficiency of the chosen number of modes becomes difficult. A solution may be to run repetitive modal SOL 112 analysis (of course with the modal damping from SOL 107 incorporated, but no elemental structural damping achieved by simply excluding PARAM, W3 and/or PARAM, W4) with increasing number of modes until convergence of the results occurs. But the question then becomes, does the results converge to the true solution? It would then be prudent to compare the modal results with gradually increasing number of modes with the SOL 109 solution with 'tied in' equivalent viscous damping, bearing in mind that we would expect to see high frequency response in the modal solution. The following graphs show such a comparison.



A significant observation can be made by looking at these graphs. Although the chosen modes cover and extend beyond the excitation frequency range such that both the resonant response of the modes within the range and the off-resonant response of the modes beyond the range are captured, clearly something is amiss for there to be such a difference in the response. Now if the chosen modes cover the excitation frequency range adequately, the only reason for there to be any inaccuracy in the modal solution is if the modes still (for whatever reason) are not sufficient to capture the static response. This can occur if the distribution of the force is such that the static response (i.e. the static deflected shape of the structure to the applied loads) is too complicated for it to be represented by the dynamic eigenvectors. In the above example, the dynamic eigenvectors were not sufficiently enough to capture the static response of a passing train on a bridge. Because of the nature of the load distribution being concentrated loads applied at certain closely spaced intervals, the static response is clearly a wave-like shape of a low wavelength. Imagine the static response of the bridge to the train passing to be the train stationary at intervals along the bridge. The graph above did not have sufficient modes to capture this somewhat difficult shape that can possibly be captured by higher frequency modes. This proves to be correct and the comparison is shown below where the SOL 112 solution with modes up to 200Hz seem to converge to the correct solution.



Clearly then, instead of laboriously calculating modes of such high frequency to capture the static response, surely it is better to use static residual vectors instead that capture the static response straight away. Indeed! So long as the dynamic modes are chosen to cover and extend beyond the excitation frequency range (say 2x or 3x the highest excitation frequency determined by FFT for time domain loading functions as frequency content not always obvious) such that both the resonant response of the modes within the range and the off-resonant response of the modes beyond the range are captured, it is highly recommended to append the static residual vectors to the total response. **Static residual vectors (PARAM, RESVEC, YES)** can be calculated except when using the seismic large mass method for enforced motion. The residual vector method is more efficient than the mode acceleration method and can be applied to both superelements and the residual structure when substructuring is employed. Clearly though, there should be sufficient modes comfortably beyond within the excitation frequency bandwidth to capture the dynamic response, and the static residual vectors should only be used as a final step to append the quasi-static responses of high frequency (relative to the excitation frequencies) modes. There is no question of damping associated with these static vectors, as by definition they are the static response of high frequency modes i.e. the response of high frequency modes to low (relatively that is) frequency excitation. The response then is quasi-static and by definition independent of the damping of the mode. The effect (i.e. the no amplification response or rather the quasi-static response) of these truncated high frequency modes can thus be approximated by residual vectors. These vectors are by default created using the applied loads and solving for the static response in a static solution. The following graph shows the effect of using these static residual vectors in the above train passing problem.



Clearly, the true solution was obtained using modes up to just 50Hz with PARAM, RESVEC, YES included. Even the SOL 112 solution with 100Hz (without RESVEC) was still not able to capture the true response, but is moving in the right direction since as shown modes up to 200Hz may just be sufficient to capture the static response. Hence RESVEC is highly recommended. Only when the static response is adequately captured will derived quantities from the response be accurate. For instance, modal damping estimates from signal filtering the response (to only include the mode of interest and doing a logarithmic decrement calculation) will only be accurate when the static response is adequately captured. There are of course much better methods of computing the modal damping.

Note that SOL 112 reverts to a direct solution technique (akin to SOL 109) when there is either viscous or structural element damping as the equations of motion cannot be orthogonalized. But the unknowns are still the modal responses and not the physical responses. And because with damping the modes are really complex modes, there is greater difficulty in capturing all the response using the real modes. Hence, even more modes are thus required to capture the response accurately in SOL 112 with element damping especially if the elemental damping is high enough to cause significant complex modes. Thus if elemental damping is high and the modes are complex,

the direct method SOL 109 may be more appropriate although of course modal damping cannot be utilized and hence there is a genuine difficulty in modelling structural damping accurately.

The convergence of *average* stress values is quite similar to the convergence of velocities<sup>4</sup>. However, for structures with any form of stress concentrations, it is not the *average* stress that is of concern, but the *peak* stresses. These involve small local regions of high strain energy with low relative velocities around the stress concentration. It follows from the consideration of the Rayleigh quotient that such behavior will be associated with high frequency modes and the low frequency ones will not excite the stress concentrations very strongly. Hence, if any form of **condensation** (reduced number of modes, Guyan reduction, dynamic substructuring or large time steps that filter high frequency modes in implicit time integration schemes) is used to calculate the dynamic response, then this will filter out the *peak* stresses. This condition arises when the stresses are determined directly from the displacement response. The peak stresses will be under-estimated even if mesh refinement was undertaken, since the error is directly related to the degree of condensation of the high frequency modes and not upon the mesh density. The user can test the accuracy of the dynamic stress recovery process by simulating the static response in the dynamic solution (zero frequency excitation for the frequency domain or dynamic relaxation for time domain). This can then be compared to the stress distribution produced directly from a true static analysis. If the comparison is good, then the dynamic stress recovery procedure is verified.

We shall discuss the **methods of improving the modal solution** accuracy. We shall discuss the

**I. matrix method or the mode displacement method**

**II. mode acceleration method**

**III. mode truncation augmentation method i.e. the static residual RESVEC method (MT)**

The dynamic equilibrium equation is presented.

$$[M]\{\ddot{u}(t)\} + [C]\{\dot{u}(t)\} + [K]\{u(t)\} = \{P(t)\} = \{P_0\}P(t)$$

The applied loading is composed of two parts,  $\{P_0\}$  is the invariant spatial portion and  $P(t)$  is the time varying portion.

The **matrix method (default) (PARAM, DDRMM, 1)** computes displacements and stresses per mode and then computes physical displacements and stresses as the summation. Cost is proportional to number of modes. Since the number of modes is usually much less than the number of excitation frequencies (or time steps in the time domain), the matrix method is usually more efficient. The **mode displacement method (PARAM, DDRMM, -1)** computes the total physical displacements for each excitation frequency (or time step in time domain) from the modal displacements, and then computes the element stresses from the total physical displacements. Cost is proportional to the number of excitation frequencies (or time steps in time domain).

The coupled system of ODEs are given by

$$[M]\{\ddot{u}(t)\} + [C]\{\dot{u}(t)\} + [K]\{u(t)\} = \{P(t)\}$$

Let  $\{u(t)\} = [\Phi]\{\xi(t)\}$

$$[M][\Phi]\{\ddot{\xi}(t)\} + [C][\Phi]\{\dot{\xi}(t)\} + [K][\Phi]\{\xi(t)\} = \{P(t)\}$$

Premultiplying by  $[\Phi]^T$

$$[\Phi]^T [M][\Phi]\{\ddot{\xi}(t)\} + [\Phi]^T [C][\Phi]\{\dot{\xi}(t)\} + [\Phi]^T [K][\Phi]\{\xi(t)\} = [\Phi]^T \{P(t)\}$$

These equations are solved for  $\{\xi(t)\}$  as a set of SDOF systems if the damping matrix can be orthogonalized, otherwise directly using a simultaneous equation solver. Finally the physical response is recovered as follows.

$$\{u(t)\} = [\Phi]\{\xi(t)\}$$

$$\{\dot{u}(t)\} = [\Phi]\{\dot{\xi}(t)\}$$

$$\{\ddot{u}(t)\} = [\Phi]\{\ddot{\xi}(t)\}$$

<sup>4</sup> NAFEMS. *A Finite Element Primer*. NAFEMS Ltd., Great Britain, 1992.

A key concept of the matrix method or the mode displacement method is that the displacement, velocity and acceleration modal responses were obtained from equations which were decoupled (or attempted to be decoupled) by pre-multiplication by  $\{\Phi\}^T$ . The load vector was also pre-multiplied by  $\{\Phi\}^T$ . This clearly thus limits the representation of the applied loading to be dependent on the chosen number of dynamic modes. The choice of the number of modes retained is typically driven by the need to span the frequency content of interest. That is, the frequency of the highest mode retained should sufficiently exceed the frequency content of the applied time history by a predetermined margin (say 2x or 3x highest excitation frequency). However, this criterion only addresses the time dependent portion of the applied loading,  $P(t)$  and ignores the spatial portion  $\{P_0\}$ . These result in accuracies especially if the spatial distribution of the loading is concentrated and repetitive such that the lower dynamic modes have difficulty in capturing the response. The truncated spatial portion of the applied loading due to the finite number of dynamic modes can be quantified as follows. The exact spatial loading is  $\{P_0\}$ . To obtain the modal representation of the spatial loading, the static equation must be considered.

The static equation

$$[K]\{u\} = \{P_0\}$$

Let  $\{u\} = [\Phi]\{\xi\}$

$$[K][\Phi]\{\xi\} = \{P_0\}$$

To obtain  $\{\xi\}$ , premultiplying by  $[\Phi]^T$

$$[\Phi]^T [K][\Phi]\{\xi\} = [\Phi]^T \{P_0\}$$

$$\{\xi\} = \frac{[\Phi]^T \{P_0\}}{[\Phi]^T [K][\Phi]} = \frac{[\Phi]^T \{P_0\}}{\{\omega^2\}}$$

Hence, on substitution

$$[K][\Phi] \frac{[\Phi]^T \{P_0\}}{\{\omega^2\}} = \{P_0\}$$

But from eigenvalue problem  $[K][\Phi] = [M][\Phi]\{\omega^2\}$ , hence the modal representation of spatial load

$$[M][\Phi]\{\omega^2\} \frac{[\Phi]^T \{P_0\}}{\{\omega^2\}} = \{P_0\}$$

$$[M][\Phi][\Phi]^T \{P_0\} = \{P_0\}$$

We conclude that the truncated part of the spatial portion of the applied load is

$$\{P_T\} = \{P_0\} - [M][\Phi][\Phi]^T \{P_0\}$$

Clearly, as the number of modes is increased, the truncated part  $\{P_T\}$  becomes smaller. However, the number of modes required for an accurate solution can become significant, possibly negating the computational advantages gained by the modal truncation method.

**Mode acceleration method (PARAM, DDRMM, -1 and PARAM, MODACC, 0)** is a method of improving the modal solution in the time or frequency domain. A much better estimate of the peak stress can be obtained using the mode acceleration method. Here the acceleration and velocity response is first obtained. The modal solutions are expanded to analysis set vectors and multiplied by the mass, damping and direct input matrices to generate equivalent loading vectors. These vectors are added to the applied load function to generate a pseudo load matrix for all selected frequencies (or time steps in the time domain). The static problem is then solved using a static analysis procedure. The stresses are found from solving this static problem. The mode acceleration method considers higher modes and hence gives more accurate answers than the matrix method or the mode displacement method especially if the number of retained modes is small in comparison to the number of DOFs. The accuracy of the dynamic stress distribution will then be comparable to that of a static analysis. The method works because the high frequency modes that define the stress concentration have a constant response over the low frequency excitation range that has been considered for the dynamic calculation, and since the stresses are found from an

instantaneous static sum, the constant component of the high frequency response have been included. In other words, the higher modes respond in a quasi-static manner to lower frequency excitations. Hence, at lower frequency excitations, the inertia and damping forces contain little contribution from higher modes. Also, the relative accelerations around the stress concentration are low and all that is required is a reasonably accurate estimate of the overall structural accelerations. This will be given by the lower modes<sup>5</sup>. The overall performance and accuracy of the mode acceleration method falls somewhere between the standard modal output and the expensive direct solution method. It is then of course not cost-effective when only the peak displacements are important.

The logic of the mode acceleration method is clear, if the number of modes retained accurately spans the frequency range of interest, any loading represented by the non-retained modes will produce a quasi-static response. Consequently, the response due to the non-retained modes will have no dynamic amplification. That is to say, the modes not retained will cause no appreciable velocity or acceleration response and hence the velocity and acceleration response can be obtained using the matrix or mode displacement method whilst the displacement response is obtained using a more direct approach.

From

$$[\Phi]^T [M][\Phi]\{\ddot{\xi}(t)\} + [\Phi]^T [C][\Phi]\{\dot{\xi}(t)\} + [\Phi]^T [K][\Phi]\{\xi(t)\} = [\Phi]^T \{P(t)\}$$

The modal velocity and acceleration response is determined as before

$$\{\dot{u}(t)\} = [\Phi]\{\dot{\xi}(t)\}$$

$$\{\ddot{u}(t)\} = [\Phi]\{\ddot{\xi}(t)\}$$

However, the displacement response is obtained directly from

$$\{u(t)\} = [K]^{-1} \{P(t)\} - [K]^{-1} [M][\Phi]\{\ddot{\xi}(t)\} - [K]^{-1} [C][\Phi]\{\dot{\xi}(t)\}$$

In modal acceleration method, damping need not be specified for the higher unretained modes as the displacement response is independent of damping of the higher unretained modes, but of course dependent on damping of retained modes.

**A key concept of the mode acceleration method is that although the velocity and acceleration modal responses were obtained from equations which were decoupled (or attempted to be decoupled) by pre-multiplication by  $\{\Phi\}^T$  with the load vector also pre-multiplied by  $\{\Phi\}^T$ , the displacement response was obtained directly from the equilibrium equation without pre-multiplication by  $\{\Phi\}^T$ . This is done because it is assumed that there is no appreciable velocity or acceleration response due to the applied loading from the unretained modes, but there will be an appreciable quasi-static displacement response due to the applied loading from the unretained modes. Hence not only are modal coordinates used to determine the modal velocity and acceleration responses, but the contribution of velocity and acceleration in the direct displacement response expression is also in modal terms as shown above.**

**Mode truncation augmentation method i.e. the static residual RESVEC method (PARAM, RESVEC, YES or PARAM, RESVNER, YES)** is an excellent method of improving the modal solution in the time or frequency domain. It attempts to correct for the inadequate representation of the spatial loads in the modal domain by creating additional “pseudo eigen” or static residual vectors to include in the modal set for the response analysis. The terminology of “pseudo eigen” is used because the static residual vectors are orthogonal to on the mass and stiffness matrices but do not satisfy the eigenvalue problem. The mode truncation vectors are created using a mathematically consistent Rayleigh-Ritz approximation where the assumed Ritz basis vectors are derived using the spatial force truncation vector  $\{P_T\}$  presented above. The mode truncation vectors are orthogonal to the retained eigenvectors since the force truncation vector does not contain any components of the retained eigenvectors. For the response solution the mode truncation vectors and associated Rayleigh-Ritz frequencies are appended to the retained eigenvectors and the modal response analysis proceeds as if the augmented vector set were all eigenvectors. A mode truncation vector is first determined by solving for the displacement vector  $\{X\}$

$$[K]\{X\} = \{P_T\}$$

<sup>5</sup> NAFEMS. *A Finite Element Primer*. NAFEMS Ltd., Great Britain, 1992.

Form,

$$[\bar{K}] = [X]^T [K] [X]$$

$$[\bar{M}] = [X]^T [M] [X]$$

and solve the reduced eigenvalue problem

$$[\bar{K}]\{\Phi_R\} = [\bar{M}]\{\Phi_R\}\omega_S^2$$

Finally, the static residual vectors can be determined from

$$\{\Phi_S\} = \{X\}\{\Phi_R\}^T$$

These static residual vectors are simply appended to the retained modal set for the response calculations. There will be one static residual vector for each spatial load vector, i.e. one for each time step.

Finally, the static residual vectors can be determined from

$$\{\Phi_{\text{AUGMENTED}}\} = \{\Phi_{\text{RETAINED DYNAMIC MODES}}\} + \{\Phi_S\}$$

The coupled system of ODEs are given by

$$[M]\{\ddot{u}(t)\} + [C]\{\dot{u}(t)\} + [K]\{u(t)\} = \{P(t)\}$$

Let  $\{u(t)\} = [\Phi]\{\xi(t)\}$

$$[M][\Phi]\{\ddot{\xi}(t)\} + [C][\Phi]\{\dot{\xi}(t)\} + [K][\Phi]\{\xi(t)\} = \{P(t)\}$$

Premultiplying by  $[\Phi]^T$

$$[\Phi]^T [M][\Phi]\{\ddot{\xi}(t)\} + [\Phi]^T [C][\Phi]\{\dot{\xi}(t)\} + [\Phi]^T [K][\Phi]\{\xi(t)\} = [\Phi]^T \{P(t)\}$$

These equations are solved for  $\{\xi(t)\}$  as a set of SDOF systems if the damping matrix can be orthogonalized, otherwise directly using a simultaneous equation solver. Finally the physical response is recovered as follows.

$$\{u(t)\} = [\Phi]\{\xi(t)\}$$

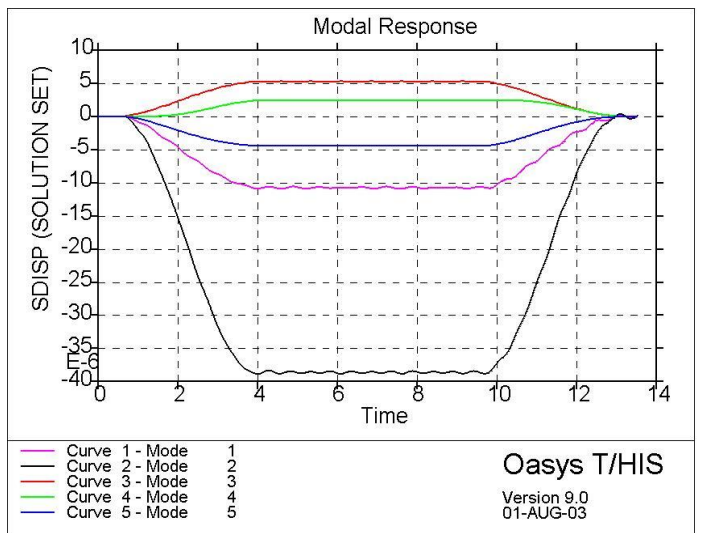
$$\{\dot{u}(t)\} = [\Phi]\{\dot{\xi}(t)\}$$

$$\{\ddot{u}(t)\} = [\Phi]\{\ddot{\xi}(t)\}$$

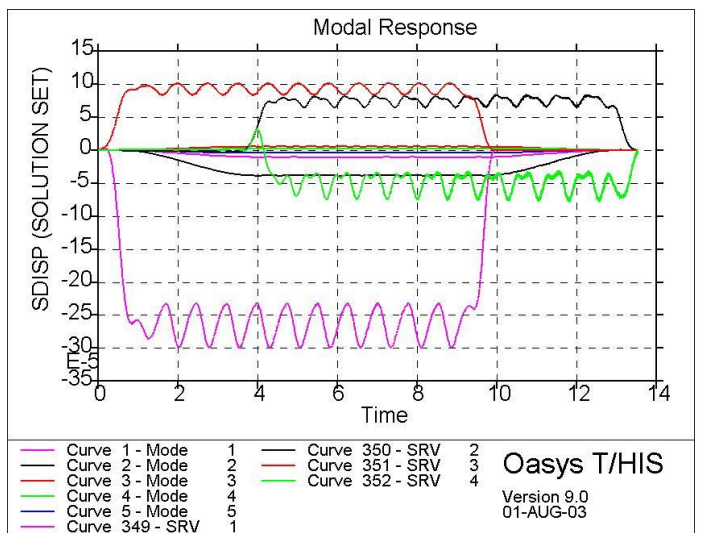
PARAM, RESVEC, YES augments static residual vectors due to the applied loads (one residual vector for each time step). PARAM, RESVINER, YES augments static residual vectors due to inertial loads i.e. unit accelerations of mass (6 residual vectors created for inertial loads in the 6 DOFs). RESVINER is not as good as RESVEC unless the loading is gravitational loads. The Rayleigh-Ritz frequencies are printed in the .f06 file. These frequencies will be higher than those of the real dynamic modes. Modal augmentation vectors by PARAM, RESVEC, YES are must be used for modal methods (in the time or frequency domain) with enforced motion. This is because since there no rigid body modes (as they are constrained by the enforced motion), there can be no motion of the enforced points unless RESVEC is used.

**A key concept of the mode truncation method is that the truncated force captured by the static residual vectors include dynamic effects from the non-retained modes, including velocity and acceleration effects. This is unlike the mode acceleration method which does not consider the velocity and acceleration response of the unretained modes, only the displacement response. The mode truncation method attempts to average in a consistent mathematical sense the response of all the modes not retained into a single static residual vector (for each load case or time step) which contributes to the static displacement and the dynamic velocity and acceleration response. The mode acceleration method forces the higher unretained modes to respond only statically. Hence the mode acceleration method is a subset of the mode truncation method. Also, since dynamic response is accounted for, unlike the mode acceleration method, damping must be specified for the higher unretained modes in the mode truncation method. This effect should however be small as sufficient dynamic modes (say 2x or 3x highest excitation frequency) should be requested to capture the amplified response where damping really matters.**

A highly illustrative concept is **the modal response concept**. This can be punched using SDISP, SVELO or SACCE. These are really the plots of the solution set. Below is a plot of the dynamic modal responses without the static residual vectors multipliers. Note that the eigenvectors were normalized using MAX, thus the plot shows the significant modes. These plots will be meaningless if MASS normalization was used.



The following graph then shows the solution set responses including both the dynamic modal responses and the static residual vectors multipliers (although the comparison should only be made if the method of eigenvector normalization is consistent). Clearly the static residual vectors are quite significant in this particular case.



Another method of determining the adequacy of the finite number of modes is to evaluate the **cumulative effective mass (NASTRAN Case Control Command MEFFMASS)** of the chosen number of modes. The effective mass has got a specific meaning in seismic analysis, but can be used for other dynamic analyses as well as a measure of determining the adequacies of the finite number of modes. A cumulative effective mass that approaches unity suggests adequacy of the chosen modes to model the **spatial distribution** of the loading. This parameter of course does not say much about the adequacy of the chosen modes to model the **frequency content of the loading**. Essentially, and to reiterate, the chosen number of modes must be sufficient to model both the **frequency content** and also the **spatial distribution** of the loading. It is found that for a high cumulative effective mass, uniformly distributed loads such as in seismic analyses require only a few modes whereas a concentrated patch requires more modes and finally a highly concentrated load requires a much greater number of modes to capture the effect of the spatial distribution of the loading.

### 4.7.4 Concepts of Equivalent Static Force

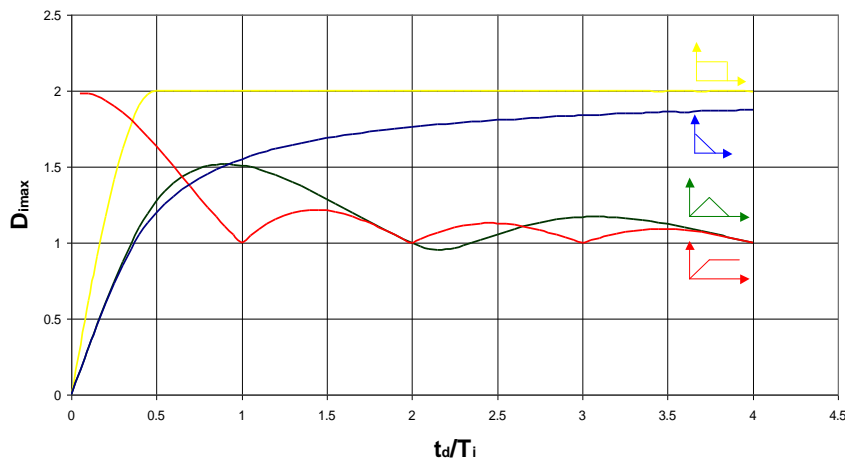
In large structural engineering projects, it may be more convenient to derive appropriate equivalent static forces for the dynamic effects of certain types of excitations. Codes of practice usually derive equivalent static loads from dynamic considerations for application in linear static analyses of large structural engineering finite element models. This may be used for instance in the impact analysis of a train in the design of an underground station. The impacting train imposes an impulse  $I = F\Delta t = m\Delta v$  onto the structure, where  $m$  and  $\Delta v$  are known. Knowing that  $F\Delta t$  is the area under the impulse curve, making an estimate of the shape of the impulse curve and the duration  $\Delta t$ , we can thus estimate the peak amplitude,  $p_0$ . Hence, the impulse curve is defined. Now, we know that the true dynamic response is given for mode  $i$  as

$$\xi_i(t) = D_i(t) \frac{\rho_{0i}}{K_i} = D_i(t) \frac{\rho_{0i}}{\omega_{ni}^2 M_i}$$

$$\{u_i(t)\} = \{\phi_i\} \xi_i(t)$$

To derive an equivalent static response to a dynamic excitation we need to make the **assumption** that the **DYNAMIC AMPLIFICATION** and the **SHAPE** of the response are governed primarily by the **FUNDAMENTAL MODE**. Let us illustrate this concept. A set of static equilibrium equations can be transformed from physical coordinates into modal coordinates by the same methods transforming dynamic equilibrium equations into modal coordinates. This is described in **Section 3.1.4**. If ALL the modes are included, then there will be the same number of modal DOFs to the physical DOFs and the computational problem size is exactly the same. The response will also be exactly the same between the physical model and the modal model. This concept is also demonstrated when we observe the 0.0 Hz (or close to) point on the frequency response function (FRF) of a SOL 108 and SOL 111 analyses. The SOL 108 uses all the modes (because it solves the frequency domain dynamic equilibrium equations in the physical coordinates) whilst SOL 111 employs only the user-selected modes. Hence, a SOL 108 FRF a 0.0 Hz (assuming no structural damping) would give the same response as a static analysis SOL 101, whilst a SOL 111 would not. As more modes are employed the SOL 111 result will approach that of the true static response. These concepts are presented in **Section 4.3.3**. Now we know that the static response will include all the modes. So, what about the dynamic amplification? Because the method of solution of a set of static equilibrium equations is direct (and not modal), different modes cannot be amplified uniquely. We are thus resolved to amplifying all the modes by the same dynamic amplification factor,  $D_i(t)$ . We choose the **FUNDAMENTAL MODE** because it features most prominently in the static response by virtue of having the largest  $\rho_{0i}/K_i$  term as higher modes will have larger modal stiffness  $K_i$  terms. This is another way of simply saying that is because the static deformed shape usually somewhat resembles that of the fundamental mode because the static response of higher modes are much smaller. Hence the dynamic amplification  $D_1(t)$  is based upon the ratio of the duration of the impulse,  $\Delta t$  with respect to the period of the fundamental period,  $T_1$ . And thus we can estimate the **maximum** dynamic amplification  $D_{1max}$ . The equivalent modal static force will thus be  $D_{1max}\rho_{0i}$  and a linear static analysis is subsequently carried out with loading of  $D_{1max}p_0$  (where  $p_0$  is the amplitude of the applied dynamic force) to approximate the dynamic response.

Response Spectrum



Reiterating, performing an equivalent static analysis to approximate the dynamic response makes the assumption that the **DYNAMIC AMPLIFICATION** of ALL the modes is based upon that of **ONLY** the **FUNDAMENTAL MODE** and hence ignoring the **POTENTIALLY LARGE AMPLIFICATIONS OF HIGHER MODES**.

Even if the highest amplification factor  $\text{MAX}[D_{i\text{max}}]$  considering all modes  $i$  (note that the amplification factor is theoretically limited to 2.0) were to be employed, it is not necessary that the static solution will always be safe. This is because, due to the fact that all the modes have to be amplified by the same amplification, the **SHAPE** of the response will be governed by the fundamental mode (due to its lowest  $K_i$  term). The familiar higher mode rippled shape (which may certainly cause greater stressing in some elements) will not be observed as that would require a greater amplification of a particular higher mode and not (the fundamental mode and) all higher modes, the consequence of which is a canceling of response that cause the ripple effect. Take for instance the green triangular impulse loading function of duration  $t_d$ . If  $t_d/T_1 \approx 1.0$ , then the greatest dynamic amplification  $D_i$  is observed on the fundamental mode and higher modes observe lower amplifications. The **AMPLITUDE** and **SHAPE** of the response will be governed by the fundamental mode and hence the equivalent static procedure **may be justified**. However, if  $t_d/T_1$  is  $\ll 1.0$ , then the greatest amplification  $D_i$  is observed by some higher mode  $i$  which has  $t_d/T_i \approx 1.0$  and not by the fundamental mode. Note that if  $t_d/T_1$  is  $< 0.2$ , then the **maximum** modal response due to the first mode can be approximated as follows.

$$\xi_1(\tau = t) = h(t - \tau) \int_{\tau=0}^{\tau=t} p(\tau) d\tau$$

$$\xi_{1\text{max}} = \frac{1}{M_1 \omega_{n1}} \int_{\tau=0}^{\tau=t} \phi_i p(\tau) d\tau \quad \text{undamped}$$

$$\xi_{1\text{max}} = \frac{1}{M_1 \omega_{d1}} \int_{\tau=0}^{\tau=t} \phi_i p(\tau) d\tau \quad \text{damped}$$

where  $\phi_i$  = modal component at excitation point

The maximum modal displacement response is  $I/(\omega_{d1} M_1)$ . The magnitude of the impulse  $I$  can be calculated as  $m\Delta v$  where  $m$  is the small mass and  $\Delta v$  the change of velocity at impact. If there is no rebound  $\Delta v$  is the approach velocity. The maximum modal velocity response is approximately  $I/M_1$  and acceleration is approximately  $I\omega_{d1}/M_1$ . Anyway, using the amplification of the fundamental mode to represent the amplification of all modes (in the equivalent static procedure) will not be conservative. Even if the amplification for this particular higher mode was used to represent the amplification for all the modes (including the fundamental mode), there is no guarantee that the stressing of all the elements within the system will be on the conservative side. This is because, as mentioned, the **exclusive** amplification of that particular (rippling) mode shape (or eigenvector) which observed the greatest amplification cannot be made in an equivalent static procedure. Instead the amplification of all the modes with this single amplification factor causes the ripple effect (which may have caused certain elements to witness greater stresses) to be ineffectual as a canceling of response occurs. Hence, if  $t_d/T_1$  is  $\ll 1.0$ , the equivalent static procedure may **NOT** be safe.

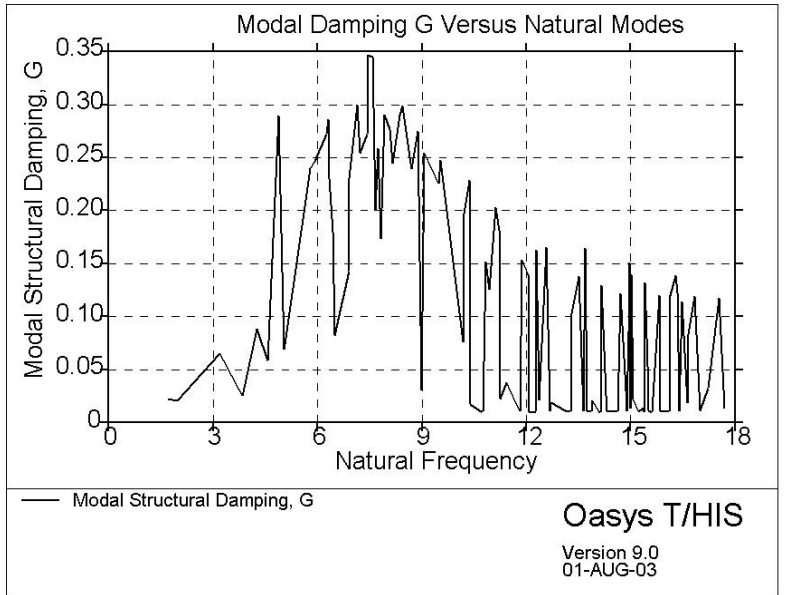
#### 4.7.5 Structural Damping in Time Domain Analyses

Direct **frequency domain** solution SOL 108 can handle both elemental structural and elemental viscous damping exactly. All modes are correctly damped at all excitation frequencies. Modal frequency domain solution SOL 111 reverts to a direct approach (but in the modal coordinates) when there is either elemental structural or elemental viscous damping. Clearly, the solution is not exact because of modal truncation. If the number of modes were increased to equal the number of DOFs, then the solution will be exact as obtained by SOL 108. But if a finite number of modes less than the number of DOFs are used, then the solution will be approximate. If the modes are only slightly complex, then the real modes (which are used in SOL 111) can easily capture the true complex modes. But if the modes are very complex (quantified on the complexity plot), then even more (real) modes are necessary to capture the true complex modes. In either case, SOL 111 can be used (as it reverts to a direct approach) so long as the number of modes is sufficient to capture the static and dynamic response accurately.

A further method can be employed if the modes are only mildly complex, i.e. the response calculations can be performed using SOL 111 with modal damping estimates obtained from SOL 107. SOL 107 can be used to calculate the modal damping from a model with elemental structural and/or viscous damping. These modal damping (in structural or viscous form) estimates can be employed within a SOL 111 analysis, but of course removing the elemental structural and/or viscous damping so not as to double count. SOL 111 in this case will not revert to SOL 108 as there is only modal damping. Note that the modal damping can be processed as either structural or viscous damping (according to PARAM, KDAMP). This conversion of modal damping from structural to viscous and vice versa is actually only perfectly accurate when the frequency of excitation matches the natural frequency of the mode (at resonance), but of course this is acceptable as only that is the instance when the damping estimate is most critical. Hence this method will damp the different modes accurately, but not at all excitation frequencies. The benefit of this approach is only computation speed as the solution can be performed in modal space using a modal approach. If the modes are found to be complex, then the user can always revert to the direct SOL 108 which can handle both structural and viscous damper elements accurately anyway.

**Time domain** solution cannot handle structural damping exactly, only viscous damping. A direct transient analysis SOL 109 or a modal transient analysis SOL 112 correctly models elemental viscous damping at all modes and at all excitation frequencies. SOL 109 and SOL 112 however do not model elemental structural damping (specified on the GE field of the MAT1 card or can be specified also using CELAS or CBUSH) exactly. If structural damping is specified at the element levels, then the incorrect modal damping will result because the conversion from structural to viscous damping will only be valid for one modal natural frequency,  $w_4$  as specified by PARAM, W4. A solution may be to use a modal approach. Now, the modal transient response analysis SOL 112 reverts to a direct approach (but in the modal coordinates) when there is either elemental structural or elemental viscous damping. Clearly, the solution is not exact because of modal truncation added to the fact that elemental structural damping cannot be incorporated exactly in a time domain solution. If the number of modes were increased to equal the number of DOFs, then the solution will be exactly as obtained by SOL 108, but still not exact theoretically due to the incorrect modelling of elemental structural damping. Certainly, if a finite number of modes less than the number of DOFs are used, then the solution will be even more approximate. If the modes are only slightly complex, then the real modes (which are used in SOL 112) can easily capture the true complex modes. But if the modes are very complex (quantified on the complexity plot), then even more (real) modes are necessary to capture the true complex modes. In either case, SOL 112 can be used (as it reverts to a direct approach) so long as the number of modes is sufficient to capture the static and dynamic response accurately, but this still does not correctly model structural damping in the time domain solution. **Modelling elemental structural damping mechanism in the time domain using an equivalent viscous damping will certainly over-damp higher modes of vibration.** A method can be employed if the modes are only slightly complex i.e. the response calculations can be performed using SOL 112 with modal damping estimates obtained from SOL 107. SOL 107 can be used to calculate the modal damping from a model with elemental structural and/or viscous damping. These modal damping (of course internally converted to the mathematical viscous form irrespective of whether specified as modal viscous damping or modal structural damping) estimates can be employed within a SOL 112 analysis, but of course removing the elemental structural and/or viscous damping so not as to double count. SOL 112 in this case will not revert to SOL 109 as there is only

modal damping. Note that the modal damping must be processed as viscous damping in this time domain solution. This conversion of modal damping from structural to viscous and vice versa is actually only perfectly accurate when the frequency of excitation matches the natural frequency of the mode (at resonance), but of course this is acceptable as only that is the instance when the damping estimate is most critical. Hence, this modal method SOL 112 **offers the advantage of more correctly modelling the elemental structural damping** on the different modes, although the modes are not damped accurately at all excitation frequencies. Since modal damping is explicitly calculated and applied, all the modes are correctly damped by the elemental structural damping here in the time domain. Note that this method of employing modal damping is valid only if the modes are **only slightly complex as the modal damping values are applied onto the real modes**. If the modes are highly complex, then elemental structural damping cannot be incorporated exactly in the time domain.



The graph shows two traces, the first obtained from a SOL 109 solution with equivalent elemental viscous damping for elemental structural damping tied in at the first mode, and the second showing the solution obtained using a SOL 112 with no elemental damping (hence equations can be orthogonalized) but with modal damping. Clearly, there is significant response from the higher frequency modes, a feature that will be masked if equivalent viscous damping and the direct solution were used.

### 4.7.6 MSC.NASTRAN Decks

#### 4.7.6.1 GL, ML Modal Forced Transient Response Analysis

<b>\$ EXECUTIVE CONTROL SECTION</b>									
SOL 112									
<b>\$ CASE CONTROL SECTION</b>									
<b>\$ Sets defining grid ids or element ids</b> SET < Number > = 1 THRU 100, 211, 343, < etc >									
<b>\$ Grid output of displacement, velocity and acceleration with time</b>									
<b>\$ SORT1 lists the results by time whilst SORT2 lists the results by grid id</b>									
DISPLACEMENT(<SORT1/SORT2>,<PRINT,PUNCH,PLOT>) = ALL/<Grid Set ID>									
VELOCITY(<SORT1/SORT2>,<PRINT,PUNCH,PLOT>) = ALL/<Grid Set ID>									
ACCELERATION(<SORT1/SORT2>,<PRINT,PUNCH,PLOT>) = ALL/<Grid Set ID>									
<b>\$ Grid output of applied load vector</b>									
OLOAD(<SORT1/SORT2>,<PRINT,PUNCH,PLOT>) = ALL/<Grid Set ID>									
<b>\$ Grid output of modal responses (in modal space)</b>									
SDISPLACEMENT(<SORT1/SORT2>,<PRINT,PUNCH>) = ALL/< Mode Number >									
SVELOCITY(<SORT1/SORT2>,<PRINT,PUNCH>) = ALL/< Mode Number >									
SACCELERATION(<SORT1/SORT2>,<PRINT,PUNCH>) = ALL/< Mode Number >									
<b>\$ Grid output of real eigenvector for the a-set</b>									
SVECTOR(<PRINT,PUNCH>) = ALL/<Grid Set ID>									
<b>\$ Grid output of SPC forces</b>									
SPCFORCES(<SORT1/SORT2>,<PRINT,PUNCH,PLOT>) = ALL/<Grid Set ID>									
<b>\$ Element output of force, stress and strain</b>									
ELFORCE(<SORT1/SORT2>,<PRINT,PUNCH,PLOT>) = ALL/<Element Set ID>									
ELSTRESS(<SORT1/SORT2>,<PRINT,PUNCH,PLOT>) = ALL/<Element Set ID>									
STRAIN(<SORT1/SORT2>,<PRINT,PUNCH,PLOT>) = ALL/<Element Set ID>									
<b>\$ Analysis Cards</b>									
SPC = < ID of SPC Cards Defined in Bulk Data >									
METHOD = < ID IN EIGRL >									
TSTEP = < ID IN TSTEP >									
<b>\$ XY plot output</b>									
OUTPUT(XYPLOT)									
XYPUNCH <DISP/VELO/ACCE> RESPONSE <subcase>/<Grid ID>(<T1/T2/T3>)									
XYPUNCH <SDISP/SVELO/SACCE> RESPONSE <subcase>/<Grid ID>(<T1/T2/T3>)									
XYPUNCH <ELFORCE/ELSTRESS/STRAIN> RESPONSE <subcase>/<Element ID>(<Code Number>)									
<b>\$ BULK DATA</b>									
TSTEP	ID	Number of Steps, N1	Time Step, Δt1	Output Every N01 Steps					
		Number of Steps, N2	Time Step, Δt2	Output Every N02 Steps					
		... etc ...							

The integration time step must be small enough to represent accurately both the variation in the loading and also to represent the maximum frequency of interest. If a loading has a frequency content of 500 Hz then the time step should be less than 1/500 s. A very high frequency transient excitation will have very sharp spikes (i.e. very low period). It is necessary for the integration time step to subdivide this. Another reason is the fact that the solution algorithm smoothes the force by taking the average of 3 times steps. Hence, it is important to avoid defining

discontinuous forcing functions. If the analysis calls for sharp impulses, it is best to smooth the impulse over at least one integration time step. It is also recommended to use at least 10 solution time steps per period of response for the cut-off maximum frequency of interest. Hence if the highest frequency of interest is 500 Hz, then the time step should be  $1/(500 \times 10)$  or smaller. Since the solution algorithm is an implicit time integration scheme, the size of the time step is limited for accuracy purposes and not for the stability of the scheme, which becomes the governing criteria in explicit time integration schemes.

Since the numerical integration is performed on a *small* number (as not all the modes are usually included) of *uncoupled* equations, there is not a large computational penalty for changing  $\Delta t$  as there is in direct transient response analysis. A constant  $\Delta t$  is still recommended because an artificial spike occurs each time  $\Delta T$  is changed, especially if NOLINI is present.

As for the duration of analysis, it is important that it be long enough such that the lowest flexible mode oscillates at least through one cycle. So if the first fundamental natural frequency is 0.5 Hz, the duration of analysis should be at the least 2.0 s.

In both direct and modal transient response analysis, the cost of integration is directly proportional to the number of time steps. If on one hand, a small time step is required to subdivide the smallest period, a long enough duration of analysis is required to properly capture long period response. This is so because in many cases, the peak dynamic response does not occur at the peak value of load nor necessarily during the duration of the loading. A good rule is to always solve for at least one cycle of response for the longest period mode after peak excitation.

To specify the optional initial displacement and velocity conditions (note that initial accelerations is assumed to be zero),

\$ CASE CONTROL SECTION									
IC = < ID OF TIC >									
\$ BULK DATA									
TIC	SID	Grid ID	Component Number	Initial Displacement	Initial Velocity				

**In this LINEAR TIME DOMAIN solution**, the static response must be added to the dynamic response if the dynamic analysis is performed about the initial undeflected (by the static loads) state with only the dynamic loads applied, hence causing the dynamic response to be measured relative to the static equilibrium position. **Hence, the total response = the dynamic response + the static response to static loads.** Time domain dynamic excitation functions should always be applied from the amplitude of 0.0 (and realistically de-ramped to 0.0 as well). This is because inherently, the dynamic excitation function has to be extrapolated within the analysis code to be from 0.0. Hence, that initial jolt should better be representative of reality irrespective of whether load excitations or enforced motion is being applied.

**Alternatively, in this LINEAR TIME DOMAIN solution**, if the dynamic analysis is performed with the deflected static shape as initial input and the static loads maintained throughout the dynamic excitations, the total or absolute response (static and dynamic) is obtained straight away from the dynamic analysis. **Hence total response = dynamic response (which already includes the static response to static loads).** Of course, if the transient dynamic analysis follows a static analysis (by say SOL 101, SOL 106, implicit dynamic relaxation by SOL 129 or explicit dynamic relaxation), then the dynamic excitation function should be ramped up from the static amplitude and not from 0.0 (and realistically de-ramped to the static load as well), so that again there would be no jolt unrepresentative of reality.

#### 4.7.6.1.1 Applied Load Excitations

Applied load excitations are as described in direct forced transient response analysis.

#### 4.7.6.1.2 Nonlinear Transient Load

Nonlinear transient loads are as described in nonlinear forced transient response analysis.

#### 4.7.6.1.3 Enforced Motion

Enforced motion is as described in direct forced transient response analysis.

#### 4.7.6.1.4 Damping

Viscous and structural modal damping is defined as follows. TYPE refers to the type of damping units, i.e. whether structural damping G (default), critical damping CRIT or quality factor Q. The values of  $f_i$  and  $g_i$  define pairs of frequencies and damping. Straight-line interpolation is used for modal frequencies between consecutive  $f_i$  values. Linear extrapolation is used for modal frequencies outside the entered range. ENDT ends the table input.

<b>\$ CASE CONTROL SECTION</b>									
SDAMPING = < ID IN TABDMP1 >									
<b>\$ BULK DATA</b>									
TABDMP1	ID	TYPE							
	f1	g1	f2	g2	f3	g3	f4	g4	
	f5	g5	f6	g6	...	...	ENDT		

Because time domain solutions (be it a modal method or a direct method) cannot handle structural damping, an equivalent viscous damping is required. Hence, if structural damping is specified at the element levels, then the incorrect modal damping will result because the conversion from structural to viscous damping will only be valid for one modal natural frequency,  $w_4$  as specified by PARAM, W4 (Note that element viscous damping damps different modes accurately). Hence, if the model has any structural damping, then it should be specified as modal damping. Modal damping can be calculated using SOL 107 and specified as either modal structural or modal viscous damping (hence a modal method of analysis i.e. SOL 112 must be used). Of course, the modal damping will be converted to modal viscous damping for solution in the time domain. This conversion is only perfectly accurate when the frequency of excitation matches the natural frequency of the mode (at resonance), but of course this is acceptable as only that is the instance when the damping estimate is most critical. Note that in the frequency domain, for the modal solution (SOL 111), the modal damping specified will be converted to either modal viscous or modal structural damping depending on PARAM, KDAMP.

#### 4.7.6.2 GL, ML P- $\Delta$ ( $K_G^A$ From $K_E^A$ ) Modal Forced Transient Response Analysis

It is often necessary to incorporate the reduction in bending stiffness of gravity load resisting columns for the analysis of lateral loads. The following procedure is undertaken.

##### Phase 1

Perform static analysis (with loads that cause the greatest negative or positive geometric stiffness) based on  $[K_E^A]$  but include the segyroa.v2001 alter prior to the Case Control Section in order to compute the geometric stiffness matrix  $[K_G^A]_1$  (and output into a .pch file) based on the generated element loads from the  $[K_E^A]$  static analysis.

##### Phase 2

A SOL 112 with a general loading function is undertaken based on  $[K_E^A] + [K_G^A]_1$  with the k2gg=ktjj statement in the Case Control Section and the outputted .pch file which contains the ktjj matrix in the Bulk Data. The responses at this stage represent the P- $\Delta$  ( $K_G^A$  From  $K_E^A$ ) response to the dynamic excitation.

The following equivalent alternative procedure can also be employed.

<pre> \$ CASE CONTROL SECTION  SUBCASE 1 LABEL = Static Preload Load Case LOAD = &lt; ID of FORCEi, MOMENTi, PLOADi, GRAV, LOAD, SPCD Cards in Bulk Data &gt; TEMP(Load) = &lt; ID of TEMP, TEMPRB, TEMPP1 Cards in Bulk Data &gt; DEFORM = &lt; ID of DEFORM Cards in Bulk Data &gt; SUBCASE 2 LABEL = P-<math>\Delta</math> Modal Transient Response Analysis STATSUB(PRELOAD) = 1 DLOAD = &lt; ID OF TLOAD1 or TLOAD2 &gt;                 </pre>
--

The method is valid when **only the prestress is judged to affect the geometric stiffness** such as in the compressive preload of building columns due to gravitational loads and the prestressing of extremely taut cables that sag very little under gravity but not in systems such as suspension bridges. Where lateral loads are large enough to affect the geometry of the system with prestress, then a repetitive P- $\Delta$ , SOL 106, implicit dynamic relaxation SOL 129 or explicit dynamic relaxation must be employed. But in single P- $\Delta$  analysis, because cables do not have much elastic bending stiffness, the initial static preload subcase should only include the prestress and not gravity as including gravity is the same as solving two linear static problems of stiffness  $K_E^A$  with preload and gravity as the applied loads respectively. Clearly, in the gravity case, it is nonsensical as the cables do in reality have differential stiffness (from the prestress) to resist the gravitational force. Prestress in one direction (i.e. along the axis of cable) will cause a differential stiffness in the orthogonal direction. Gravity acts in the orthogonal direction and hence cannot be accounted for in the calculation of the prestress in this single P- $\Delta$  analysis. To quantitatively decide if gravity need not be considered in contributing to the differential stiffness of the cables, a static P- $\Delta$  analysis should be carried out, the first subcase being a SOL 101 with only the prestress as applied loads and the second subcase a P- $\Delta$  SOL 101 (i.e. utilizing the induced prestress from the first subcase to form a geometric stiffness matrix) with both the gravity and prestress included as applied loads. If the difference in the cable element forces between subcases 1 and 2 is negligible, then gravity has little influence in affecting the geometric stiffness. If there is a major difference in the cable element force, then clearly, gravity will affect the geometric stiffness and as such, a repetitive P- $\Delta$ , SOL 106, implicit dynamic relaxation or explicit dynamic relaxation must be used to converge to the true  $K_T$ . Likewise, in the single P- $\Delta$  analysis of multi-storey buildings, gravity (and only gravity) acts in axis of columns to generate prestress, and the differential stiffness is computed for the orthogonal direction reducing resistance to lateral wind forces, applied in the second subcase with gravity too.

When a static subcase is specified for linear transient response analysis (SOLs 109 and 112) with STATSUB(PRELOAD), the data recovery is controlled by PARAM, ADSTAT. By default (YES) the static solution will be superimposed on the dynamic response solution (displacement, stress and SPCForce). The relative solution can be obtained in reference to the static solution point by PARAM, ADSTAT, NO. No provision is made for frequency response analysis, because the static responses contribute only to the zero frequency response. For linear dynamic response, the static solution can be superimposed after the dynamic solution procedure. The preload effect is reflected only in the stiffness and the actual static load is omitted in the dynamic response analysis. The total displacement can be obtained by superposing the static solution to the transient response analysis.

$$\{u\}_{total} = [\Phi]\{q\} + \{u\}_{static}$$

And the stress output is obtained as

$$\sigma = [S]\{u_{static} + u_{dynamic}\}$$

The STATSUB(PRELOAD) computes the differential stiffness due to the prestress and also the follower force. The follower force is calculated and incorporated by the use of PARAM, FOLLOWK, YES. We know how the prestress affects the differential stiffness, namely a tensile prestress causing an increase in stiffness. The effect of the follower force on the stiffness is different. For example, for a cylinder under external pressure critical buckling load may be over-estimated (even though the mode shapes are similar) in a SOL 105 and the natural frequencies in vibration may be under-estimated (even though the mode shapes are similar) in a SOL 103 in the absence of follower stiffness. To the contrary, these observations are reversed in case of centrifugal loads. Centrifugal forces as a constant (static) load are applied by a Bulk Data RFORCE to any elements that have masses. The follower stiffness due to centrifugal load has the effect of lowering stiffness (although the centrifugal load tensioning effect increases stiffness), consequently lowering natural frequencies (even though the mode shapes are similar) in a SOL 103 and lowering the buckling loads (even though the mode shapes are similar) in a SOL 105. This effect increases as the RPM increases, and it becomes significant when the RPM is over 1000. For moderately geometric nonlinear analysis, exclusion of follower stiffness affects the rate of convergence, but the converged solution is correct. For severely geometric nonlinear analysis, it may not be possible to obtain a converged solution without including follower stiffness. As the geometric nonlinearity intensifies, so is the effect of follower stiffness. Therefore, inclusion of follower stiffness greatly enhances the convergence if the deformation involves severe geometric nonlinearity.

### 4.7.6.3 GL, ML P- $\Delta$ ( $K_G^A$ From Exact or Approximate $K_T^A$ ) Modal Forced Transient Response Analysis

It is often necessary to include the differential stiffness, especially if there are prestressed cables in the model. To obtain  $K_T^A$ , to be theoretically exact, a GNL SOL 106 (or implicit dynamic relaxation SOL 129 or explicit dynamic relaxation LS-DYNA) with prestress (as temperature loads say) and gravity must be undertaken. Alternatively, an approximation to  $K_T^A$  can be obtained by repetitive P- $\Delta$  static analyses with the prestress (as temperature loads say) and gravity applied. The procedure to obtain this approximate  $K_T^A$  will be presented. Note that the approximate  $K_T^A$  will be the summation of the elastic stiffness  $K_E$  at the undeflected (by the prestress and gravity) state but  $K_G$  at the deflected (by the prestress and gravity) state. Hence if  $K_E$  changes considerably during the application of the prestress, a full SOL 106 (or implicit dynamic relaxation SOL 129 or explicit dynamic relaxation LS-DYNA), which converges to the  $K_E$  and  $K_G$  at the deflected (by the prestress and gravity) state should be employed. Hence for the modelling of a suspension bridge where there is a great change in geometry (known in the bridge industry as **form-finding**, so-called because it is necessary to find the form or shape of the catenary suspension cables), it may be prudent to employ SOL 106 (or implicit dynamic relaxation SOL 129 or explicit dynamic relaxation LS-DYNA), but for a high tension low sag cable on say a tower with prestressed cables, the repetitive P- $\Delta$  static analysis may be adequate. The repetitive P- $\Delta$  analysis basically involves a number of iterations of linear static analyses to obtain an approximate  $K_T^A$ . Note again that A refers to the initial undeflected (by the collapsing load) state, but deflected by the prestress and gravity. To perform the repetitive P- $\Delta$  analysis, a static analysis is performed based on  $K_E^A$  with temperature loads and gravity to generate forces in the structural elements, which in turn provides input for the computation of  $K_{Gi}^{AKT_m}$  where m is the iterations. Repetitive static analysis is performed with the prestress and gravity updating the stiffness matrix  $K_E^A + K_{Gi}^{AKT_{m-1}} + K_{Gi}^{AKT_m}$  until convergence of displacements is obtained. The tangent stiffness at this stage is the approximate converged tangent stiffness matrix  $K_T^A = K_E^A + K_{Gi}^{AKT}$ . The converged displacements represent the approximate P- $\Delta$  ( $K_G^A$  From Approximate  $K_T^A$ ) static response to the initial prestress loads. The converged geometric stiffness at this stage would be that based upon the approximate tangent stiffness matrix  $K_T^A$ , i.e.  $K_{Gi}^{AKT}$ .

#### Phase 1

Perform static analysis (with prestress and gravity) based on  $[K_E^A]$  but include the segyroa.v2001 alter prior to the Case Control Section in order to compute the geometric stiffness matrix  $[K_G^A]_1$  (and output into a .pch file) based on the generated element loads from the  $[K_E^A]$  static analysis.

#### Phase 2

Perform static analysis (with prestress and gravity) based on  $[K_E^A] + [K_G^A]_1$  by including the k2gg = ktjj statement in the Case Control Section, the outputted .pch file which contains the ktjj matrix in the Bulk Data and the segyroa.v2001 alter prior to the Case Control Section to compute the  $[K_G^A]_2$  (and output into the .pch file overwriting previous data) based on the generated element loads from the  $[K_E^A] + [K_G^A]_1$  static analysis.

#### Phase 3

Repeatedly perform the Phase 2 static analysis (with prestress and gravity) based on  $[K_E^A] + [K_G^A]_i$  for  $i = 2$  to  $n$  where  $n$  represents the number of iterations required for the change in deflections between analyses to become negligible. This would signify that the change in the  $[K_G^A]$  matrix become negligible and the correct  $[K_G^A]$  is attained. The deflections and the other responses at this stage represent the P- $\Delta$  ( $K_G^A$  From Approximate  $K_T^A$ ) static response to the prestress and gravity. The stiffness of the structure is  $K_T^A$ .

#### Phase 4

A SOL 112 with a general loading function is undertaken with the k2gg=ktjj statement in the Case Control Section and the outputted .pch file which contains the latest ktjj matrix in the Bulk Data. The responses at this stage represent the P- $\Delta$  ( $K_G^A$  From Approximate  $K_T^A$ ) response to the dynamic excitation.

#### 4.7.7 Hand Methods Verification

##### 4.7.7.1 Determination of Maximum Dynamic Displacement for Deterministic Time Domain Loading by Transforming the Coupled MDOF Linear Undamped ODEs To a Set of Independent (Uncoupled) SDOF ODEs and Solving the Independent Equations in a Manner Similar to Solving a SDOF ODE

Linear time domain hand methods are capable of analyzing: -

##### **Multi-Modal Response to Deterministic Non-Periodic Short Duration Impulse and Hence Random Non-Stationary Short Duration Impulse by Enveloping Deterministic Responses**

A coupled MDOF system of linear ODEs must be uncoupled to a set of independent SDOF system of linear ODEs if any feasible hand method computation is to be employed. These independent SDOF ODEs can be solved using standard techniques of solving SDOF linear dynamic ODEs. The final stage to the analysis is to employ a modal superposition method to express the total response as a summation of the results from the solution of the individual modal equations. Note that since the modal frequencies and the corresponding mode shapes are required to uncouple the coupled MDOF ODEs, the real eigenvalue analysis must be performed first. It was shown that a system of coupled MDOF ODEs could be reduced to a system of independent SDOF ODEs by employing the orthogonality properties of real modes

$$M_i \ddot{\xi}_i(t) + C_i \dot{\xi}_i(t) + K_i \xi_i(t) = P_i(t) \quad \text{for the } i^{\text{th}} \text{ mode}$$

where the generalized (or modal) terms are obtained from solving the real eigenvalue problem

$$M_i = \{\phi_i\}^T [M] \{\phi_i\}$$

$$C_i = \zeta_i 2M_i \omega_{ni}$$

$$K_i = \{\phi_i\}^T [K] \{\phi_i\} = \omega_{ni}^2 M_i$$

$$P_i(t) = \{\phi_i\}^T \{P(t)\}$$

The modal properties (i.e. modal masses, modal frequencies and hence modal stiffness) can be obtained by performing a real modal analysis SOL 103 and if required the modal damping can also be incorporated from a complex modal analysis SOL 107. The normalization of the mode shapes can be arbitrary. The normalization technique employed will not affect the value of the modal frequencies but of course will determine the values of the modal masses (and hence modal damping and stiffnesses) and the (amplitude of the) modal force. Although the normalization technique is arbitrary, it is recommended that the normalization employed would facilitate the calculation of the (amplitude of the) modal force since this is a hand calculation. To facilitate the computation, it is wise to choose the normalization to be unity at the DOF of application of the external excitation. Either way, the modal force (for a particular mode) for discrete loading points is calculated as follows

$$P_i(t) = \{\phi_i\}^T \{P(t)\}$$

Had the loading been continuous, a continuous modal force can also be calculated by hand (or a spreadsheet) as follows

$$P_i(t) = \int_0^L \phi_i(x) \{P(x, t)\} dx$$

There will be n uncoupled ODEs for n natural modes. These are now simply SDOF ODEs, which can be solved using Duhamel's integral. For a particular mode i, for a general loading function  $P_i(t)$ , from SDOF response analysis, we can establish

$$\begin{aligned} D_i(t) &= \text{dynamic amplification factor in the time domain} \\ D_{i\max} &= \text{maximum dynamic amplification factor in the time domain} \end{aligned}$$

Note that in general,  $D_i(t)$  is a function of the natural circular frequency  $\omega_{ni}^2 = K_i/M_i$  or the damped natural circular frequency  $\omega_d$ , the time duration of loading  $t_d$  and the general time  $t$ .  $D_{imax}$  is a function of the natural circular frequency  $\omega_{ni}^2 = K_i/M_i$  or the damped natural circular frequency  $\omega_d$  and the time duration of loading  $t_d$ . From this, we can establish the modal responses

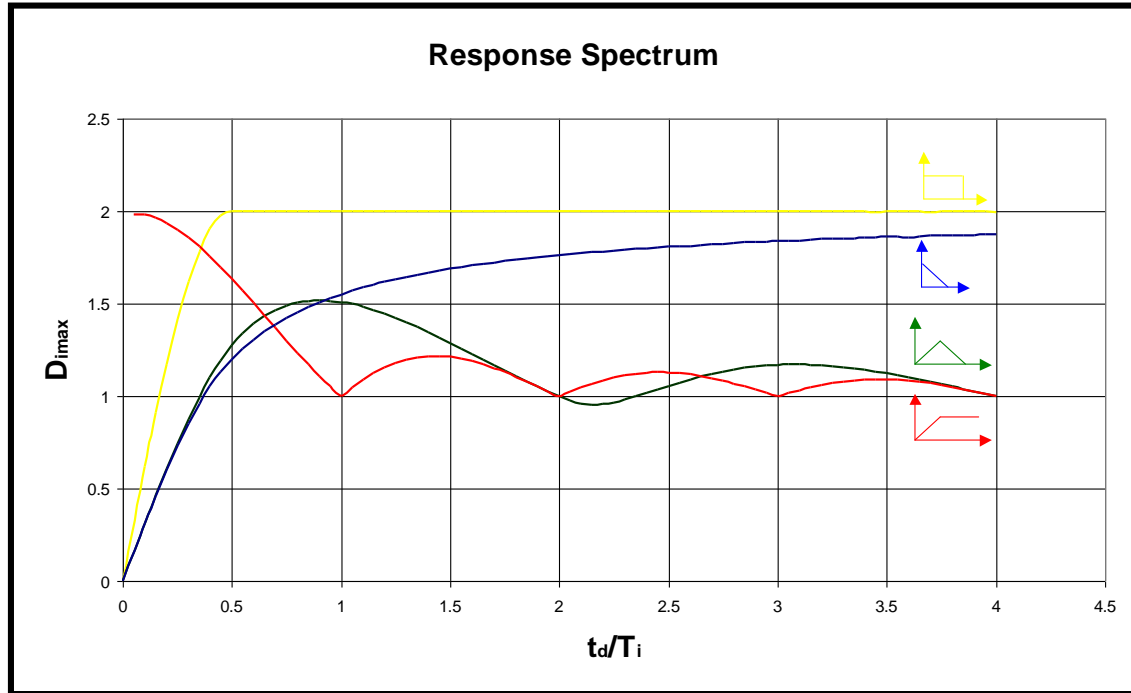
$$\begin{aligned} \xi_i(t) &= \text{modal displacement response (in modal space) in the time domain, } D_i(t)(\rho_{0i}/K_i) \\ \xi_{imax} &= \text{maximum modal displacement response in the time domain, } D_{imax}(\rho_{0i}/K_i) \end{aligned}$$

Note that  $\rho_{0i}$  corresponds to the amplitude of the modal loading function  $P_i(t)$  and not simply the amplitude of the loading function  $\{P(t)\}$ , i.e.  $p_0$  at any particular node. Of course, if the normalization of the mode was such that it was unity at the DOF of application of the external force with amplitude  $p_0$  then,  $\rho_{0i}$  will be equal to  $p_0$ .

The dynamic amplification factor can be derived for standard short duration loadings as follows.

Excitation	Undamped (Unless Specified Otherwise) Dynamic Amplification Factor of Mode i, $D_i(t)$	Undamped (Unless Specified Otherwise) Maximum Dynamic Amplification Factor of Mode i, $D_{imax}$
An Instantaneous Continuous Constant Force of Amplitude $p_0$	$D_i(t) = 1 - \cos \omega_n t$	$D_{imax} = 2$
An Instantaneous Rectangular Force of Duration $t_d$ and of Amplitude $p_0$	$\tau < t_d \quad D_i(t) = 1 - \cos \omega_n t$ $\tau > t_d \quad D_i(t) = \left( -2 \sin \omega_n \frac{2t - t_d}{2} \sin \omega_n \frac{-t_d}{2} \right)$	$\tau < t_d \quad D_{imax} = 2$ $\tau > t_d \quad D_{imax} = 2 \sin \omega_n \frac{t_d}{2}$
An Instantaneous Right Angled Triangular Force of Duration $t_d$ and of Amplitude $p_0$	$\tau < t_d \quad D_i(t) = (1 - \cos \omega_n t) + \frac{1}{t_d} \left( \frac{\sin \omega_n t}{\omega_n} - t \right)$ $\tau > t_d \quad D_i(t) = \frac{1}{\omega_n t} (\sin \omega_n t - \sin \omega_n (t - t_d)) - \cos \omega_n t$	Plot $D_i(t)$ versus $t_d/T$ to determine maximum response
An Instantaneous Isosceles Triangular Force of Duration $t_d$ and of Amplitude $p_0$	$\tau < t_d/2 \quad D_i(t) = \frac{2}{\omega_n t_d} (\omega_n t - \sin \omega_n t)$ $t_d/2 < \tau < t_d \quad D_i(t) = \frac{2}{\omega_n t_d} [\omega_n (t_d - t) + 2 \sin \omega_n (t - t_d/2) - \sin \omega_n t]$ $\tau > t_d \quad D_i(t) = \frac{2}{\omega_n t_d} [2 \sin \omega_n (t - t_d/2) - \sin \omega_n t - \sin \omega_n (t - t_d)]$	Plot $D_i(t)$ versus $t_d/T$ to determine maximum response
An Instantaneous Half Sine Force of Frequency $\omega$ and of Amplitude $p_0$	$\tau < t_d \quad D_i(t) = \left( \frac{1}{1 - \omega^2/\omega_n^2} \right) \left( \sin \omega t - \frac{\omega}{\omega_n} \sin \omega_n t \right)$ $\tau > t_d \quad D_i(t) = - \left( \frac{\omega/\omega_n}{1 - \omega^2/\omega_n^2} \right) (\sin \omega_n t + \sin \omega_n (t - t_d))$	Plot $D_i(t)$ versus $t_d/T$ to determine maximum response

The above table shows that the maximum dynamic amplification that can be produced is **two times the static displacement!** This occurs for the instantaneous applied continuous constant force. The response spectrum showing the maximum responses from plots of  $D_i(t)$  versus  $t_d/T_i$  for various  $t_d/T_i$  is presented.



The response from an impulse is even easier to obtain as the unit impulse function can be brought outside the integral (i.e. the Duhamel's or Convolution Integral). The maximum modal response (in modal space) from an impulse ( $t_i/T < 0.2$ ), can be obtained simply as follows.

$$\xi_i(\tau = t) = h(t - \tau) \int_{\tau=0}^{\tau=t} p(\tau) d\tau$$

$$\xi_{i_{max}} = \frac{1}{M_i \omega_{ni}} \int_{\tau=0}^{\tau=t} \phi_i p(\tau) d\tau \quad \text{undamped}$$

$$\xi_{i_{max}} = \frac{1}{M_i \omega_{di}} \int_{\tau=0}^{\tau=t} \phi_i p(\tau) d\tau \quad \text{damped}$$

where  $\phi_i$  = modal component at excitation point

The above expression may seem to differ from the dynamic amplification approach where the denominator contains the modal stiffness, i.e. modal mass times the square of the natural circular frequency. This is because the above expression requires the explicit integration of the forcing function. The dynamic amplification approach differs in the sense that the integral (i.e. Duhamel's Integral) is already classically integrated to obtain the expression  $D(t)$ . Another equivalent interpretation of the above relationship is from the basic consideration of the conservation of momentum. The impacting particle (of small relative mass compared to mass of structure) imposes an impulse  $I$  onto the structure. The magnitude of  $I$  can be calculated as  $m\Delta v$  where  $m$  is the small mass and  $\Delta v$  the change of velocity at impact. If there is no rebound  $\Delta v$  is the approach velocity. Conservation of momentum at impact requires the initial velocity of the structural mass to be  $I/M$ . A lightly damped system then displays damped free vibration with an initial displacement of approximately  $I/(\omega_d M)$ , or an initial velocity of approximately  $I/M$  or an initial acceleration of approximately  $I\omega_d/M$ .

And the modal response (in modal space) from a general loading function that cannot be classically integrated can be obtained by employing a numerical integration technique such as Simpson's Rule.

$$\xi_i(\tau = t) = \frac{1}{M_i \omega_{ni}} \int_{\tau=0}^{\tau=t} \phi_i p(\tau) \sin \omega_{ni} (t - \tau) d\tau$$

$$= \sin \omega_{ni} t \frac{1}{M_i \omega_{ni}} \int_{\tau=0}^{\tau=t} \phi_i p(\tau) \cos \omega_{ni} \tau d\tau - \cos \omega_{ni} t \frac{1}{M_i \omega_{ni}} \int_{\tau=0}^{\tau=t} \phi_i p(\tau) \sin \omega_{ni} \tau d\tau$$

Once the individual modal responses  $\{\xi(t)\}$  are computed, the physical response can be calculated from

$$\{u(t)\} = [\Phi]\{\xi(t)\}$$

For a 2 DOF system, this expression would be

$$\begin{Bmatrix} u_1(t) \\ u_2(t) \end{Bmatrix} = \begin{bmatrix} \phi_{11} & \phi_{12} \\ \phi_{21} & \phi_{22} \end{bmatrix} \begin{Bmatrix} \xi_1(t) \\ \xi_2(t) \end{Bmatrix}$$

The above computation takes into account the phase difference between the responses of different modes. It is important to point out that the maximum of the modal responses do not occur at the same time. As shown above, the exact solution can be obtained by expanding the general  $u(t)$  expression to include all the modes considered, and only then maximised.

However, this may prove to be mathematically involved if differentiation is to be performed analytically by hand (the computerized method of course performs the response calculation at discrete time points as it is not just the maximum that is of interest). An alternative would be to instead of maximising the physical response, maximise the modal responses and then only superpose the modal responses for the physical response. This is equivalent to the response spectrum method (only that the procedure is employed on a deterministic loading function instead of a random function). The square root of sum of squares (SRSS) of the maximum modal contributions as follows, depicted for a 2 DOF dynamic system.

$$\begin{Bmatrix} u_{1\max} \\ u_{2\max} \end{Bmatrix} = \begin{Bmatrix} \sqrt{(\phi_{11}\xi_{1\max})^2 + (\phi_{12}\xi_{2\max})^2} \\ \sqrt{(\phi_{21}\xi_{1\max})^2 + (\phi_{22}\xi_{2\max})^2} \end{Bmatrix}$$

If the modal natural frequencies are too close to each other (within about 10%), then the Complete Quadratic Combination (CQC), which is based on random vibration theory should be used. These methods of approximating the maximum multi-modal responses are effectively response spectrum analyses on a deterministic loading function (as opposed to a non-stationary random loading function which is normally associated with response spectrum analysis).

The upper limit would be to choose all the eigenvectors to have the maximum modal response at the same time. This is obtained by multiplying the moduli as follows.

$$\{u(t)\} = [\Phi]\{\xi_{i\max}\}$$

Often, we need to ascertain other types of response. The modal velocities and accelerations can easily be obtained by differentiating the  $\{\xi(t)\}$  vector with respect to time  $t$  and hence,

$$\begin{aligned} \{\dot{u}(t)\} &= [\Phi]\{\dot{\xi}(t)\} \\ \{\ddot{u}(t)\} &= [\Phi]\{\ddot{\xi}(t)\} \end{aligned}$$

Finally, the SRSS superposition, again depicted for the 2 DOF system,

$$\begin{aligned} \begin{Bmatrix} \dot{u}_1(t) \\ \dot{u}_2(t) \end{Bmatrix} &= \begin{bmatrix} \phi_{11} & \phi_{12} \\ \phi_{21} & \phi_{22} \end{bmatrix} \begin{Bmatrix} \dot{\xi}_1(t) \\ \dot{\xi}_2(t) \end{Bmatrix} \\ \therefore \begin{Bmatrix} \ddot{u}_{1\max} \\ \ddot{u}_{2\max} \end{Bmatrix} &= \begin{Bmatrix} \sqrt{(\phi_{11}\ddot{\xi}_{1\max})^2 + (\phi_{12}\ddot{\xi}_{2\max})^2} \\ \sqrt{(\phi_{21}\ddot{\xi}_{1\max})^2 + (\phi_{22}\ddot{\xi}_{2\max})^2} \end{Bmatrix} \end{aligned}$$

For whatever response be it the displacement, velocity acceleration or force, the individual modal responses should first be calculated in terms of time  $t$ , then maximised, then only combined for the physical response with some method of superposition. Do not maximise the modal displacement response and base the other responses on that.

It must be understood that the scaling (or normalization) of the normal modes are arbitrary, hence their do not indicate the response. This means that a different scaling method will yield a different modal (or generalized) mass, modal stiffness (but same modal frequency) and (amplitude of) modal force. It follows that the modal response  $\xi_i(t)$  from a particular mode will be not be unique and will be dependent upon how the eigenvectors are scaled. However, the response in the physical coordinates for each and every mode will be unique irrespective of how the eigenvectors are scaled. This can be proven just by studying the modal equations above. The equation of dynamic equilibrium for a mode is given by

$$M_i \ddot{\xi}_i(t) + K_i \xi_i(t) = P_i(t)$$

$$\{\phi_i\}^T [M] \{\phi_i\} \ddot{\xi}_i(t) + \{\phi_i\}^T [K] \{\phi_i\} \xi_i(t) = \{\phi_i\}^T \{P(t)\}$$

It is evident that for each mode  $i$ , the modal mass  $M_i$ , modal stiffness  $K_i$  and the amplitude of the modal force  $\rho_{0i}$  is all dependent upon an arbitrarily scaled eigenvector. The modal frequency  $\omega_{ni}^2 = K_i/M_i$  on the other hand is unique to the mode. It follows that the maximum dynamic amplification factor  $D_{imax}$  is also unique to the mode since it is a function of the natural circular frequency  $\omega_{ni}^2 = K_i/M_i$  and the time duration of loading  $t_d$ . However, the maximum modal displacement response,  $\xi_{imax} = D_{imax}(\rho_{0i}/K_i)$  is dependent upon the scaling of the eigenvector. The response in the physical coordinates  $\{u_{imax}\} = \{\phi_i\} \xi_{imax}$ . Say an eigenvector was to be arbitrarily scaled up by say 3. Hence,

$$\begin{aligned} \text{New } M_i &= 9M_i \\ \text{New } K_i &= 9K_i \\ \text{New } \omega_{ni}^2 &= \omega_{ni}^2 \\ \text{New } D_{imax} &= D_{imax} \\ \text{New } \xi_{imax} &= D_{imax} 3\rho_{0i} / (9K_i) \\ &= D_{imax} \rho_{0i} / (3K_i) \\ \text{New } \{u_{imax}\} &= 3\{\phi_i\} \xi_{imax} \\ &= 3\{\phi_i\} D_{imax} \rho_{0i} / (3K_i) \\ &= \{\phi_i\} D_{imax} \rho_{0i} / K_i \\ &= \{u_{imax}\} \text{ as before} \end{aligned}$$

As a final note, if the eigenvector  $i$  was scaled such that its component is unity at the DOF which corresponds to both the solitary point of application of load and the response, then

$$\{u_{imax}\}_{\text{response point of interest}} = \{\phi_i\}_{\text{response point of interest}} \xi_{imax}$$

$$\text{As eigenvector term unity at point of interest } \{\phi_i\}_{\text{response point of interest}} = 1.0$$

$$\begin{aligned} \{u_{imax}\}_{\text{response point of interest}} &= 1.0 \xi_{imax} \\ &= \frac{1.0 D_{imax} \rho_{0i}}{K_i} \end{aligned}$$

$$\text{As eigenvector term unity at solitary point of application of load } \rho_{0i} = 1.0 p_0$$

$$\begin{aligned} \{u_{imax}\}_{\text{response point of interest}} &= \frac{1.0 D_{imax} 1.0 p_0}{K_i} \\ &= \frac{D_{imax} p_0}{K_i} \end{aligned}$$

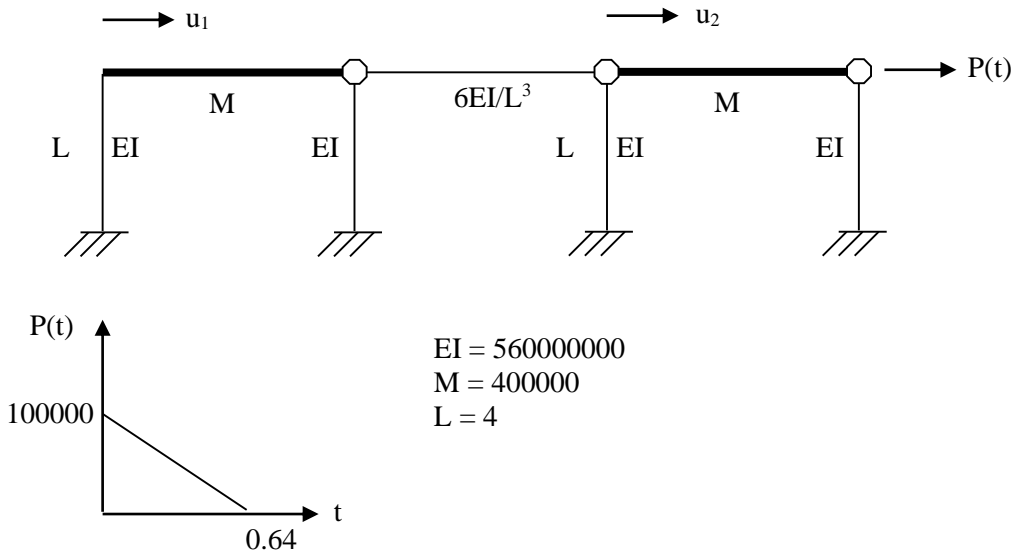
$$\text{Since } K_i = \omega_{ni}^2 M_i$$

$$\{u_{imax}\}_{\text{response point of interest}} = \frac{D_{imax} p_0}{\omega_{ni}^2 M_i}$$

The significance of this result is that if the eigenvector  $i$  was scaled such that its component is unity at the DOF which corresponds to both the solitary point of application of load and the response, the physical response due to the particular mode can be seen to be just proportional to the dynamic amplification  $D_{i\max}$  (which is a function of the excitation frequency and the natural frequency  $\omega_{ni}$ ) and the amplitude of the loading function  $p_0$ , and inversely proportional to square of the natural frequency  $\omega_{ni}$  and the modal mass  $M_i$ . The dynamic displacement response is then basically the static deflection scaled by the maximum dynamic amplification factor.

Another important significance is that with this normalization technique applied to all the modes, the relative importance of different modes to a certain force excitation at a certain location can be determined. That is to say, **if all the eigenvectors were scaled such that its component is unity at the DOF which corresponds to both the solitary point of application of load and the response (using POINT normalization), then the greater the modal mass, the less important is the mode as the response is inversely proportional to the modal mass.** Unlike natural frequencies, the relative importance of modes is not a structural property. It is dependent upon the location of the excitation force and the location of the response.

A forced response analysis of a shear frame (be it to model a building or water tank) connected by a mass-less flexible beam is illustrated in MAPLE 7. All units in SI.



**System and Frequency Domain Excitation Description - User Input**

```
> restart;
with(LinearAlgebra):
DOF:=2:
EI:=560000000:
M:=400000:
L:=4:
MASS:=Matrix([[M,0],[0,M]]);
KE:=Matrix([[30*EI/L^3,-6*EI/L^3],[-6*EI/L^3,30*EI/L^3]]);
# Excitation - Po is the amplitude of the excitation, i.e. P(t)=Po*function of t
P(t):=Matrix([[0],[100000]]);
td:=0.64;
```

$$MASS := \begin{bmatrix} 400000 & 0 \\ 0 & 400000 \end{bmatrix}$$

$$KE := \begin{bmatrix} 262500000 & -52500000 \\ -52500000 & 262500000 \end{bmatrix}$$

$$P(t) := \begin{bmatrix} 0 \\ 100000 \end{bmatrix}$$

$td := .64$

**Modal Properties of System - Solution of Real Eigenvalue Problem  $[K-\lambda M]\{\phi\}=\{0\}$**

- Note that Eigensolution may not arrange the roots sequentially
- MAX normalization of the Eigenvectors

```
> Eigensolution:=Eigenvectors(MatrixInverse(MASS).KE):
lambda:=Matrix(Eigensolution[1],shape=diagonal):
wn:=map(sqrt,evalf(lambda));
Phi:=Eigensolution[2];
for j from 1 to DOF do
  eig:=0:
  for i from 1 to DOF do
    eig:=eig,Phi[i,j];
  end do;
  for i from 1 to DOF do
    Phi[i,j]:=Phi[i,j]/max(eig);
  end do;
end do;
```

Phi:=Phi;

$$wn := \begin{bmatrix} 22.91287847 & 0. \\ 0. & 28.06243040 \end{bmatrix}$$

$$\Phi := \begin{bmatrix} 1 & -1 \\ 1 & 1 \end{bmatrix}$$

$$\Phi := \begin{bmatrix} 1 & -1 \\ 1 & 1 \end{bmatrix}$$

**Uncoupling The Equations of Motion**

> MODALMASS:=evalf(Transpose(Phi).MASS.Phi);  
 MODALSTIFFNESS:=evalf(Transpose(Phi).KE.Phi);  
 MODALFORCE:=evalf(Transpose(Phi).P(t));

$$MODALMASS := \begin{bmatrix} 800000. & 0. \\ 0. & 800000. \end{bmatrix}$$

$$MODALSTIFFNESS := \begin{bmatrix} .42000000010^9 & 0. \\ 0. & .63000000010^9 \end{bmatrix}$$

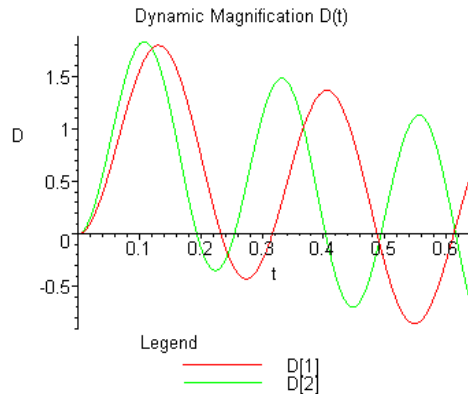
$$MODALFORCE := \begin{bmatrix} 100000. \\ 100000. \end{bmatrix}$$

**Modal Responses  $\xi_i = D_i(t)P_{oi}/K_i$**

> D(t):=Vector(DOF):  
 for i from 1 to DOF do  
   D(t)[i]:=1-cos(wn[i,i]\*t)+1/td\*(sin(wn[i,i]\*t)/wn[i,i]-t);  
 end do;  
 variablelegend:=seq(convert(D[i],string),i=1..DOF):  
 plot([seq(D(t)[i],i=1..DOF)], t=0..td, D,title="Dynamic Magnification D(t)",  
 legend=[variablelegend]);  
 xi:=Vector(DOF):  
 for i from 1 to DOF do  
   xi[i]:=D(t)[i]\*MODALFORCE[i,1]/MODALSTIFFNESS[i,i];  
 end do;  
 xi:=evalf(xi);

$$D(t)_1 := 1 - \cos(22.91287847t) + .06819309072\sin(22.91287847t) - 1.562500000t$$

$$D(t)_2 := 1 - \cos(28.06243040t) + .05567942541\sin(28.06243040t) - 1.562500000t$$



$\xi :=$

$$[.0002380952381 - .0002380952381\cos(22.91287847t) + .00001623645017\sin(22.91287847t) - .0003720238095t]$$

$$[.0001587301587 - .0001587301587\cos(28.06243040t) + .883800403210^{-5}\sin(28.06243040t) - .0002480158730t]$$

**Physical Response in Time Domain**

> u(t):=Vector(DOF):  
 u(t):=Phi.xi;

$u(t) :=$

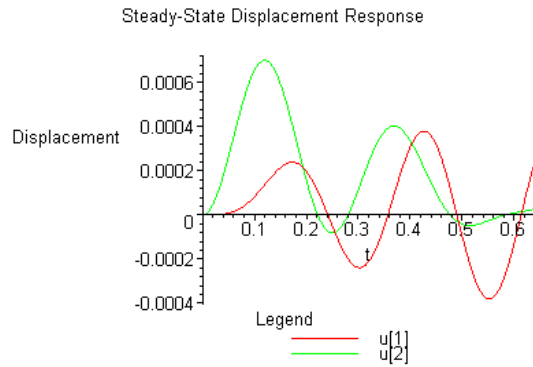
$$\begin{aligned}
 & [.0000793650794 - .0002380952381 \cos(22.91287847t) + .00001623645017 \sin(22.91287847t) \\
 & - .0001240079365t + .0001587301587 \cos(28.06243040t) - .883800403210^{-5} \sin(28.06243040t)] \\
 & [.0003968253968 - .0002380952381 \cos(22.91287847t) + .00001623645017 \sin(22.91287847t) \\
 & - .0006200396825t - .0001587301587 \cos(28.06243040t) + .883800403210^{-5} \sin(28.06243040t)]
 \end{aligned}$$

**Plot of Response in Time Domain**

```

> variablelegend:=seq(convert(u[i],string),i=1..DOF):
plot([seq(u(t)[i],i=1..DOF)], t=0..td, Displacement,title="Steady-State Displacement
Response", legend=[variablelegend]);

```



#### 4.7.7.2 Determination of Max Dynamic Displacement for Deterministic Time Domain Support Motion (Displacement, Velocity or Acceleration) by Transforming the Coupled MDOF Linear Undamped ODEs (In Relative Terms) To a Set of Independent (Uncoupled) SDOF ODEs (In Relative Terms) and Solving the Independent Equations in a Manner Similar to Solving a SDOF ODE

Linear time domain hand methods are capable of analyzing: -

##### **Multi-Modal Response to Deterministic Non-Periodic Short Duration Impulse Enforced Motion and Hence Random Non-Stationary Short Duration Impulse Enforced Motion by Enveloping Deterministic Responses**

For a MDOF system, the equation of motion for support excitation in relative terms is

$$[M]\{\ddot{u}(t)\} + [C]\{\dot{u}(t)\} + [K]\{u(t)\} = -[M]\{1\}\ddot{u}_s(t)$$

Note that  $\{D\} = \{1\}$  is a unity vector corresponding to the rigid body motion. The support excitation causes all the masses to produce an inertial force opposing its motion (D'Alembert's Principle).

This coupled MDOF system could be reduced to a system of independent SDOF ODEs by employing the orthogonality properties of real modes

$$M_i \ddot{\xi}_i(t) + C_i \dot{\xi}_i(t) + K_i \xi_i(t) = P_i(t) \quad \text{for the } i^{\text{th}} \text{ mode}$$

where the generalized (or modal) terms are obtained from solving the real eigenvalue problem

$$M_i = \{\phi_i\}^T [M] \{\phi_i\}$$

$$C_i = \zeta_i 2M_i \omega_{ni}$$

$$K_i = \{\phi_i\}^T [K] \{\phi_i\} = \omega_{ni}^2 M_i$$

$$P_i(t) = -\{\phi_i\}^T [M] \{1\} \ddot{u}_s(t)$$

The modal properties (i.e. modal masses, modal frequencies and hence modal stiffness) can be obtained by performing a real modal analysis SOL 103 and if required the modal damping can also be incorporated from a complex modal analysis SOL 107. The normalization of the mode shapes can be arbitrary. The normalization technique employed will not affect the value of the modal frequencies but of course will determine the values of the modal masses (and hence modal damping and stiffnesses) and the (amplitude of the) modal force. Note that the modal force (for a particular mode) for discrete loading points is calculated as follows

$$P_i(t) = -\{\phi_i\}^T [M] \{1\} \ddot{u}_s(t)$$

There will be n uncoupled ODEs for n natural modes. These are now simply SDOF ODEs, which can be solved using Duhamel's integral.

$$M_i \ddot{\xi}_i(t) + C_i \dot{\xi}_i(t) + K_i \xi_i(t) = -\{\phi_i\}^T [M] \{1\} \ddot{u}_s(t)$$

For a particular mode i, for a general loading function  $P_i(t)$ , from SDOF response analysis, we can establish

$$\begin{aligned} D_i(t) &= \text{dynamic amplification factor in the time domain} \\ D_{i\max} &= \text{maximum dynamic amplification factor in the time domain} \end{aligned}$$

Note that in general,  $D_i(t)$  is a function of the natural circular frequency  $\omega_{ni}^2 = K_i/M_i$  or the damped natural circular frequency  $\omega_d$ , the time duration of loading  $t_d$  and the general time t.  $D_{i\max}$  is a function of the natural circular frequency  $\omega_{ni}^2 = K_i/M_i$  or the damped natural circular frequency  $\omega_d$  and the time duration of loading  $t_d$ . From this, we can establish the modal responses

$$\xi_i(t) = D_i(t) \frac{p_{0i}}{K_i} = -D_i(t) \frac{\{\phi_i\}^T [M] \{1\} \ddot{u}_0}{\omega_{ni}^2 M_i} \quad \ddot{u}_0 = \text{amplitude}$$

Thus whereby we had the following for the modal response in load excitations

$$\xi_i(t) = D_i(t) \frac{p_{0i}}{K_i} = D_i(t) \frac{\{\phi_i\}^T \{p_0\}}{\omega_{ni}^2 M_i}$$

we now have the following for enforced base motion

$$\xi_i(t) = D_i(t) \frac{p_{0i}}{K_i} = -D_i(t) \frac{\{\phi_i\}^T [M] \{1\} \ddot{u}_0}{\omega_{ni}^2 M_i}$$

An interesting observation is that whereby for load excitations the amplitude of the forcing vector  $\{p_0\}$  may be sparse with only possibly one point with a value, that for enforced motion is quite different  $[M]\{1\} \ddot{u}_0$  with all components having a value.

Let us also define the modal participation factor for enforced motion as

$$\Gamma_i = -\frac{\{\phi_i\}^T [M] \{1\}}{M_i} = -\frac{\{\phi_i\}^T [M] \{1\}}{\{\phi_i\}^T [M] \{\phi_i\}}$$

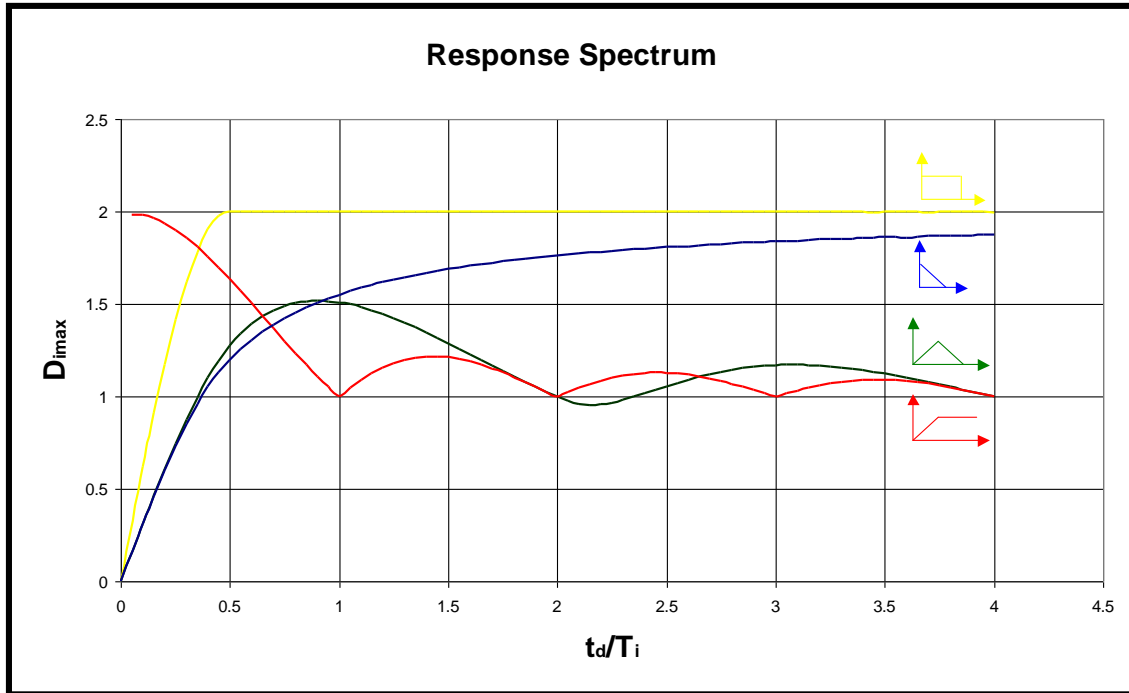
Hence, the modal response for enforced motion excitations

$$\xi_i(t) = D_i(t) \Gamma_i \frac{\ddot{u}_0}{\omega_{ni}^2}$$

The dynamic amplification factor can be derived for standard short duration loadings as follows.

Excitation	Undamped (Unless Specified Otherwise) Dynamic Amplification Factor of Mode i, $D_i(t)$	Undamped (Unless Specified Otherwise) Maximum Dynamic Amplification Factor of Mode i, $D_{i\max}$
An Instantaneous Continuous Constant Force of Amplitude $p_0$	$D_i(t) = 1 - \cos \omega_n t$	$D_{i\max} = 2$
An Instantaneous Rectangular Force of Duration $t_d$ and of Amplitude $p_0$	$\tau < t_d \quad D_i(t) = 1 - \cos \omega_n t$ $\tau > t_d \quad D_i(t) = \left( -2 \sin \omega_n \frac{2t - t_d}{2} \sin \omega_n \frac{-t_d}{2} \right)$	$\tau < t_d \quad D_{i\max} = 2$ $\tau > t_d \quad D_{i\max} = 2 \sin \omega_n \frac{t_d}{2}$
An Instantaneous Right Angled Triangular Force of Duration $t_d$ and of Amplitude $p_0$	$\tau < t_d \quad D_i(t) = (1 - \cos \omega_n t) + \frac{1}{t_d} \left( \frac{\sin \omega_n t}{\omega_n} - t \right)$ $\tau > t_d \quad D_i(t) = \frac{1}{\omega_n t} (\sin \omega_n t - \sin \omega_n (t - t_d)) - \cos \omega_n t$	Plot $D_i(t)$ versus $t_d/T$ to determine maximum response
An Instantaneous Isosceles Triangular Force of Duration $t_d$ and of Amplitude $p_0$	$\tau < t_d/2 \quad D_i(t) = \frac{2}{\omega_n t_d} (\omega_n t - \sin \omega_n t)$ $t_d/2 < \tau < t_d \quad D_i(t) = \frac{2}{\omega_n t_d} [\omega_n (t_d - t) + 2 \sin \omega_n (t - t_d/2) - \sin \omega_n t]$ $\tau > t_d \quad D_i(t) = \frac{2}{\omega_n t_d} [2 \sin \omega_n (t - t_d/2) - \sin \omega_n t - \sin \omega_n (t - t_d)]$	Plot $D_i(t)$ versus $t_d/T$ to determine maximum response
An Instantaneous Half Sine Force of Frequency $\omega$ and of Amplitude $p_0$	$\tau < t_d \quad D_i(t) = \frac{1}{(1 - \omega^2/\omega_n^2)} \left( \sin \omega t - \frac{\omega}{\omega_n} \sin \omega_n t \right)$ $\tau > t_d \quad D_i(t) = -\frac{\omega/\omega_n}{(1 - \omega^2/\omega_n^2)} (\sin \omega_n t + \sin \omega_n (t - t_d))$	Plot $D_i(t)$ versus $t_d/T$ to determine maximum response

The above table shows that the maximum dynamic amplification that can be produced is **two times the static displacement!** This occurs for the instantaneous applied continuous constant force. The response spectrum showing the maximum responses from plots of  $D_i(t)$  versus  $t_d/T_i$  for various  $t_d/T_i$  is presented.



Once the individual modal responses  $\{\xi(t)\}$  are computed, the physical response can be calculated from

$$\{u(t)\} = [\Phi]\{\xi(t)\}$$

For a 2 DOF system, this expression would be

$$\begin{Bmatrix} u_1(t) \\ u_2(t) \end{Bmatrix} = \begin{bmatrix} \phi_{11} & \phi_{12} \\ \phi_{21} & \phi_{22} \end{bmatrix} \begin{Bmatrix} \xi_1(t) \\ \xi_2(t) \end{Bmatrix}$$

The above computation takes into account the phase difference between the responses of different modes. It is important to point out that the maximum of the modal responses do not occur at the same time. As shown above, the exact solution can be obtained by expanding the general  $u(t)$  expression to include all the modes considered, and only then maximised.

However, this may prove to be mathematically involved if differentiation is to be performed analytically by hand (the computerized method of course performs the response calculation at discrete time points as it is not just the maximum that is of interest). An alternative would be to instead of maximising the physical response, maximise the modal responses and then only superpose the modal responses for the physical response. This is equivalent to the response spectrum method (only that the procedure is employed on a deterministic loading function instead of a random function). The square root of sum of squares (SRSS) of the maximum modal contributions as follows, depicted for a 2 DOF dynamic system.

$$\begin{Bmatrix} u_{1\max} \\ u_{2\max} \end{Bmatrix} = \begin{Bmatrix} \sqrt{(\phi_{11}\xi_{1\max})^2 + (\phi_{12}\xi_{2\max})^2} \\ \sqrt{(\phi_{21}\xi_{1\max})^2 + (\phi_{22}\xi_{2\max})^2} \end{Bmatrix}$$

If the modal natural frequencies are too close to each other (within about 10%), then the Complete Quadratic Combination (CQC), which is based on random vibration theory should be used. These methods of approximating the maximum multi-modal responses are effectively response spectrum analyses on a deterministic loading

function (as opposed to a non-stationary random loading function which is normally associated with response spectrum analysis).

The upper limit would be to choose all the eigenvectors to have the maximum modal response at the same time. This is obtained by multiplying the moduli as follows.

$$\{u(t)\} = [\Phi] \{\xi_{i \max}\}$$

Often, we need to ascertain other types of response. The modal velocities and accelerations can easily be obtained by differentiating the  $\{\xi(t)\}$  vector with respect to time  $t$  and hence,

$$\begin{aligned} \{\dot{u}(t)\} &= [\Phi] \{\dot{\xi}(t)\} \\ \{\ddot{u}(t)\} &= [\Phi] \{\ddot{\xi}(t)\} \end{aligned}$$

Finally, the SRSS superposition, again depicted for the 2 DOF system,

$$\begin{aligned} \begin{Bmatrix} \ddot{u}_1(t) \\ \ddot{u}_2(t) \end{Bmatrix} &= \begin{bmatrix} \phi_{11} & \phi_{12} \\ \phi_{21} & \phi_{22} \end{bmatrix} \begin{Bmatrix} \ddot{\xi}_1(t) \\ \ddot{\xi}_2(t) \end{Bmatrix} \\ \therefore \begin{Bmatrix} \ddot{u}_{1 \max} \\ \ddot{u}_{2 \max} \end{Bmatrix} &= \begin{Bmatrix} \sqrt{(\phi_{11} \ddot{\xi}_{1 \max})^2 + (\phi_{12} \ddot{\xi}_{2 \max})^2} \\ \sqrt{(\phi_{21} \ddot{\xi}_{1 \max})^2 + (\phi_{22} \ddot{\xi}_{2 \max})^2} \end{Bmatrix} \end{aligned}$$

For whatever response be it the displacement, velocity acceleration or force, the individual modal responses should first be calculated in terms of time  $t$ , then maximised, then only combined for the physical response with some method of superposition. Do not maximise the modal displacement response and base the other responses on that.

#### 4.7.7.3 Determination of Maximum Dynamic Displacement for Deterministic Time Domain Loading by Transforming the Coupled Distributed System Linear Damped ODEs (from the governing PDE) To A Set of Independent (Uncoupled) SDOF ODEs and Solving the Independent Equations in a Manner Similar to Solving a SDOF ODE

In reality, all systems have distributed mass, damping and stiffness properties. The finite element method discretizes the continuous system with a finite number of degrees of freedom resulting in a set of ordinary differential equations (ODEs) when Newton's equation of motion is applied. Continuous systems on the other hand result in one partial differential equation. Since the integration of the partial differential equation (PDE) is far more complicated, the modelling of a structure as a continuous system is limited to simple structures. The Bernoulli-Euler beam equation of motion, which is based on simple bending theory assuming that plane sections remain plane results in the equation of motion

$$EI \frac{\partial^4 u}{\partial x^4} + \bar{m} \frac{\partial^2 u}{\partial t^2} = P(x, t)$$

where  $u$  is the transverse displacement. Note that the Timoshenko beam equation extends the Bernoulli-Euler beam theory to include shear deformations and rotary inertia and should be used if such effects matter. Solving the corresponding free vibration PDE analytically by the method of separation of variables leads to two ODEs, which yield the following natural circular frequencies and mode shapes

$$\omega_n = a^2 L^2 \sqrt{\frac{EI}{\bar{m}L^4}} \quad \phi(x) = A \sin ax + B \cos ax + C \sinh ax + D \cosh ax$$

The values of  $a$  and the integration constants depend on the boundary conditions and is presented in **Section 4.1.3.4**. The orthogonality property for continuous systems can be shown to be essentially similar to that of the discrete systems. Hence, if for a discrete system the uncoupled equation of motion for the  $i^{\text{th}}$  mode is

$$M_i \ddot{\xi}_i(t) + (\zeta_i 2M_i \omega_{ni}) \dot{\xi}_i(t) + K_i \xi_i(t) = P_i(t)$$

$$\{\phi_i\}^T [M] \{\phi_i\} \ddot{\xi}_i(t) + (\zeta_i 2\{\phi_i\}^T [M] \{\phi_i\} \omega_{ni}) \dot{\xi}_i(t) + \{\phi_i\}^T [K] \{\phi_i\} \xi_i(t) = \{\phi_i\}^T \{P(t)\}$$

Likewise, the uncoupled equation of motion for the  $i^{\text{th}}$  mode of a continuous system (in particular that of a beam) is

$$M_i \ddot{\xi}_i(t) + (\zeta_i 2M_i \omega_{ni}) \dot{\xi}_i(t) + K_i \xi_i(t) = P_i(t)$$

$$M_i \ddot{\xi}_i(t) + (\zeta_i 2M_i \omega_{ni}) \dot{\xi}_i(t) + \omega_{ni}^2 M_i \xi_i(t) = P_i(t)$$

$$\left[ \int_0^L \bar{m} \phi_i^2(x) dx \right] \ddot{\xi}_i(t) + \left[ \zeta_i 2 \left( \int_0^L \bar{m} \phi_i^2(x) dx \right) \omega_{ni} \right] \dot{\xi}_i(t) + \omega_{ni}^2 \left[ \int_0^L \bar{m} \phi_i^2(x) dx \right] \xi_i(t) = \int_0^L \phi_i(x) \{P(x, t)\} dx$$

where the modal mass, modal damping, modal stiffness and modal force is clearly determined. There will be  $n$  uncoupled ODEs for  $n$  natural modes. These are now simply SDOF ODEs, which can be solved using Duhamel's integral. For a particular mode  $i$ , for a general loading function  $P_i(t)$ , from SDOF response analysis, we can establish

$$D_i(t) = \text{dynamic amplification factor in the time domain}$$

Note that in general,  $D_i(t)$  is a function of the natural circular frequency  $\omega_{ni}^2 = K_i/M_i$ , the time duration of loading  $t_d$  and the general time  $t$ . From this, we can establish the modal responses

$$\xi_i(t) = \text{modal displacement response in the time domain, } D_i(t)(\rho_{0i}/K_i)$$

Note that  $\rho_{0i}$  corresponds to the amplitude of the modal loading function  $P_i(t)$ .

The final step is to obtain the physical displacements  $u(x, t)$  from the summation of the  $n$  modal responses as follows.

$$u(x, t) = \sum_{i=1}^n \phi_i(x) \xi_i(t)$$

As a final note, the element stresses (here the bending moments and shear forces) can be obtained from the Bernoulli-Euler beam equations

$$M(x, t) = EI \frac{\partial^2 u}{\partial x^2} \quad V(x, t) = EI \frac{\partial^3 u}{\partial x^3}$$

## 4.8 GL, ML Implicit Direct Transient Response Analysis

### 4.8.1 Nature of the Dynamic Loading Function

The solution can be used to ascertain the modal properties of the system by performing a time domain impulse analysis to excite the modes of interest. The duration of the impulse must be sufficiently long to excite the first fundamental mode, which is usually of concern. This would result in a response that includes the first fundamental mode and most likely higher modes as well. The first fundamental mode is readily ascertained from inspection of the response time history curve at any node. Higher natural frequencies can also be ascertained by performing an FFT on the response curve.

The solution method can be used to solve dynamic systems subjected to: -

- (a) **Deterministic non-periodic short duration impulse (a.k.a. blast)** loading functions with subsequent **wave propagation**
- (b) **Random non-stationary short duration impulse** loading functions

The force amplitude does not repeat itself regularly but rises from zero to a series of maxima and minima until settling down to a constant value. The starting transient is significant and so the solution is carried out in the time domain. Estimates of the induced stress in a **linear elastic** body due to an **impulsive blast** may be made easily in some cases with a simpler static method of analysis. **Section 4.7.4** describes this concept further.

If the forcing function is a random non-stationary forcing function such that the random forces start from a low-level building up to a maximum then dying away, such as in a seismic event, then exact solution methods are not established. Instead, we could either analyze a set of such events using deterministic transient solution methods and then average or envelope the results or alternatively use the crude response spectrum method which envelopes the response spectra of a series of time histories.

**In this LINEAR TIME DOMAIN solution**, the static response must be added to the dynamic response if the dynamic analysis is performed about the initial undeflected (by the static loads) state with only the dynamic loads applied, hence causing the dynamic response to be measured relative to the static equilibrium position. **Hence, the total response = the dynamic response + the static response to static loads.**

**Alternatively, in this LINEAR TIME DOMAIN solution**, if the dynamic analysis is performed with the deflected static shape as initial input and the static loads maintained throughout the dynamic excitations, the total or absolute response (static and dynamic) is obtained straight away from the dynamic analysis. **Hence total response = dynamic response (which already includes the static response to static loads).**

### 4.8.2 Mathematical Formulation of Analysis

In general, modal transient response analysis is used when

- (i) the model is large
- (ii) many time steps need to be solved for

On the other hand, direct frequency response analysis is employed when

- (i) the model is small
- (ii) only a few time steps need to be solved for
- (iii) the response due to high frequency excitation is required, as this requires many modes to be computed in the modal transient response analysis, the computation of the modes being the costly operation in the modal approach
- (iv) high accuracy is required as the direct approach does not involve mode truncation

The coupled system of ODEs of the damped vibration equation of motion are given by

$$[M]\{\ddot{u}(t)\} + [C]\{\dot{u}(t)\} + [K]\{u(t)\} = \{P(t)\}$$

The fundamental structural response is solved at discrete times, typically at fixed integration time steps  $\Delta t$ .

Using a central finite difference representation for the velocity and acceleration,

$$\{\dot{u}_n\} = \frac{1}{2\Delta t} \{u_{n+1} - u_{n-1}\}$$

$$\{\ddot{u}_n\} = \frac{1}{\Delta t^2} \{u_{n+1} - 2u_n + u_{n-1}\}$$

and replacing into the dynamic equation of motion averaging the applied force over 3 adjacent time steps

$$\frac{1}{\Delta t^2} [M]\{u_{n+1} - 2u_n + u_{n-1}\} + \frac{1}{2\Delta t} [C]\{u_{n+1} - u_{n-1}\} + \frac{1}{3} [K]\{u_{n+1} + u_n + u_{n-1}\} = \frac{1}{3} \{P_{n+1} + P_n + P_{n-1}\}$$

Collecting terms and making  $\{u_{n+1}\}$  the subject

$$[A_1]\{u_{n+1}\} = [A_2] + [A_3]\{u_n\} + [A_4]\{u_{n-1}\}$$

$$[A_1] = \left[ \frac{1}{\Delta t^2} [M] + \frac{1}{2\Delta t} [C] + \frac{1}{3} [K] \right]$$

$$[A_2] = \frac{1}{3} \{P_{n+1} + P_n + P_{n-1}\}$$

$$[A_3] = \left[ \frac{2}{\Delta t^2} [M] - \frac{1}{3} [K] \right]$$

$$[A_4] = \left[ -\frac{1}{\Delta t^2} [M] + \frac{1}{2\Delta t} [C] - \frac{1}{3} [K] \right]$$

The initial conditions  $\{u_0\}$  and  $\{\dot{u}_0\}$  are used to determine the values of  $\{u_{-1}\}$ ,  $\{P_0\}$  and  $\{P_{-1}\}$ ,

$$\{u_{-1}\} = \{u_0\} - \{\dot{u}_0\}\Delta t$$

$$\{P_0\} = [K]\{u_0\} + [C]\{\dot{u}_0\}$$

$$\{P_{-1}\} = [K]\{u_{-1}\} + [C]\{\dot{u}_0\}$$

Direct response analysis involves the solution of coupled simultaneous geometrically linear dynamic equilibrium equations. The direct transient solution involves decomposing  $[A_1]$  and applying to the right-hand-side of the equation. The solution behaves like a succession of static solutions with each time step performing a forward-backward substitution (FBS) on a new load vector. If  $\Delta t$  is constant during the entire analysis, the  $[A_1]$  matrix needs to be decomposed only once. Each progressive step in the analysis is only an FBS of a new load vector. If  $\Delta t$  is changed,  $[A_1]$  needs to be decomposed again, which can be costly in large problems.

The following damping models are supported by the solution scheme

- |      |                                     |                                    |
|------|-------------------------------------|------------------------------------|
| I.   | elemental damping                   |                                    |
|      | i. viscous damping                  | Yes                                |
|      | ii. structural damping              | Specified but converted to viscous |
| II.  | modal damping                       |                                    |
|      | i. viscous damping                  | No                                 |
|      | ii. structural damping              | No                                 |
| III. | global proportional viscous damping |                                    |
|      | i. mass proportional damping        | No                                 |
|      | ii. stiffness proportional damping  | Specified but converted to viscous |
|      | iii. Rayleigh damping               | No                                 |

Elemental viscous damping makes contributions to the [C] matrix.

$$[M]\{\ddot{u}(t)\} + [C]\{\dot{u}(t)\} + [K]\{u(t)\} = \{P(t)\}$$

Elemental structural damping will modify the damping matrix as follows

$$[M]\{\ddot{u}(t)\} + \left[ [C] + \frac{1}{\omega_4} \sum G_E [K_E] \right] \{\dot{u}(t)\} + [K]\{u(t)\} = \{P(t)\}$$

where the parameter  $\omega_4$  converts the structural damping into equivalent viscous damping as the transient response analysis does not permit the use of complex coefficients.

Stiffness proportional global viscous damping modifies the dynamic equilibrium equations as follows

$$[M]\{\ddot{u}(t)\} + \left[ [C] + \frac{G}{\omega_3} [K] \right] \{\dot{u}(t)\} + [K]\{u(t)\} = \{P(t)\}$$

where the parameter  $\omega_3$  converts the structural damping into equivalent viscous damping as the transient response analysis does not permit the use of complex coefficients.

### 4.8.3 MSC.NASTRAN Decks

#### 4.8.3.1 GL, ML Direct Forced Transient Response Analysis

<b>\$ EXECUTIVE CONTROL SECTION</b>									
SOL 109									
<b>\$ CASE CONTROL SECTION</b>									
<b>\$ Sets defining grid ids or element ids</b> SET < Number > = 1 THRU 100, 211, 343, < etc > <b>\$ Grid output of displacement, velocity and acceleration with time</b> <b>\$ SORT1 lists the results by time whilst SORT2 lists the results by grid id</b> DISPLACEMENT(<SORT1/SORT2>,<PRINT,PUNCH,PLOT>) = ALL/<Grid Set ID> VELOCITY(<SORT1/SORT2>,<PRINT,PUNCH,PLOT>) = ALL/<Grid Set ID> ACCELERATION(<SORT1/SORT2>,<PRINT,PUNCH,PLOT>) = ALL/<Grid Set ID> <b>\$ Grid output of applied load vector</b> OLOAD(<SORT1/SORT2>,<PRINT,PUNCH,PLOT>) = ALL/<Grid Set ID> <b>\$ Grid output of d-set displacement, velocity and acceleration</b> SDISPLACEMENT(<SORT1/SORT2>,<PRINT,PUNCH>) = ALL/<Grid Set ID> SVELOCITY(<SORT1/SORT2>,<PRINT,PUNCH>) = ALL/<Grid Set ID> SACCELERATION(<SORT1/SORT2>,<PRINT,PUNCH>) = ALL/<Grid Set ID> <b>\$ Grid output of SPC forces</b> SPCFORCES(<SORT1/SORT2>,<PRINT,PUNCH,PLOT>) = ALL/<Grid Set ID> <b>\$ Element output of force, stress and strain</b> ELFORCE(<SORT1/SORT2>,<PRINT,PUNCH,PLOT>) = ALL/<Element Set ID> ELSTRESS(<SORT1/SORT2>,<PRINT,PUNCH,PLOT>) = ALL/<Element Set ID> STRAIN(<SORT1/SORT2>,<PRINT,PUNCH,PLOT>) = ALL/<Element Set ID> <b>\$ Analysis Cards</b> SPC = < ID of SPC Cards Defined in Bulk Data > TSTEP = < ID IN TSTEP > <b>\$ XY plot output</b> OUTPUT(XYPLOT) XYPUNCH <DISP/VELO/ACCE> RESPONSE <subcase>/<Grid ID>(<T1/T2/T3>) XYPUNCH <ELFORCE/ELSTRESS/STRAIN> RESPONSE <subcase>/<Element ID>(<Code Number>)									
<b>\$ BULK DATA</b>									
TSTEP	ID	Number of Steps, N1	Time Step, Δt1	Output Every N01 Steps					
		Number of Steps, N2	Time Step, Δt2	Output Every N02 Steps					
		... etc ...							

The integration time step must be small enough to represent accurately both the variation in the loading and also to represent the maximum frequency of interest. If a loading has a frequency content of 500 Hz then the time step should be less than 1/500 s. A very high frequency transient excitation will have very sharp spikes (i.e. very low period). It is necessary for the integration time step to subdivide this. Another reason is the fact that the solution algorithm smoothes the force by taking the average of 3 times steps. Hence, it is important to avoid defining discontinuous forcing functions. If the analysis calls for sharp impulses, it is best to smooth the impulse over at least one integration time step. It is also recommended to use at least 10 solution time steps per period of response for the cut-off maximum frequency of interest. Hence if the highest frequency of interest is 500 Hz, then the time step should be 1/(500x10) or smaller. Since the solution algorithm is an implicit time integration scheme, the size

of the time step is limited for accuracy purposes and not for the stability of the scheme, which becomes the governing criteria in explicit time integration schemes.

It is recommended that the time step not be changed in a linear direct transient analysis. This is because a decomposition of the dynamic matrix is required each time  $\Delta t$  is changed and this can be a costly operation. Also, a constant  $\Delta t$  is recommended because an artificial spike occurs each time  $\Delta T$  is changed, especially if NOLINI is present.

As for the duration of analysis, it is important that it be long enough such that the lowest flexible mode oscillates at least through one cycle. So if the first fundamental natural frequency is 0.5 Hz, the duration of analysis should be at the least 2.0 s.

In both direct and modal transient response analysis, the cost of integration is directly proportional to the number of time steps. If on one hand, a small time step is required to subdivide the smallest period, a long enough duration of analysis is required to properly capture long period response. This is so because in many cases, the peak dynamic response does not occur at the peak value of load nor necessarily during the duration of the loading. A good rule is to always solve for at least one cycle of response for the longest period mode after peak excitation.

To specify the optional initial displacement and velocity conditions (note that initial accelerations is assumed to be zero),

<b>\$ CASE CONTROL SECTION</b>									
IC = < ID OF TIC >									
<b>\$ BULK DATA</b>									
TIC	SID	Grid ID	Component Number	Initial Displacement	Initial Velocity				

**In this LINEAR TIME DOMAIN solution**, the static response must be added to the dynamic response if the dynamic analysis is performed about the initial undeflected (by the static loads) state with only the dynamic loads applied, hence causing the dynamic response to be measured relative to the static equilibrium position. **Hence, the total response = the dynamic response + the static response to static loads.** Time domain dynamic excitation functions should always be applied from the amplitude of 0.0 (and realistically de-ramped to 0.0 as well). This is because inherently, the dynamic excitation function has to be extrapolated within the analysis code to be from 0.0. Hence, that initial jolt should better be representative of reality irrespective of whether load excitations or enforced motion is being applied.

**Alternatively, in this LINEAR TIME DOMAIN solution**, if the dynamic analysis is performed with the deflected static shape as initial input and the static loads maintained throughout the dynamic excitations, the total or absolute response (static and dynamic) is obtained straight away from the dynamic analysis. **Hence total response = dynamic response (which already includes the static response to static loads).** Of course, if the transient dynamic analysis follows a static analysis (by say SOL 101, SOL 106, implicit dynamic relaxation by SOL 129 or explicit dynamic relaxation), then the dynamic excitation function should be ramped up from the static amplitude and not from 0.0 (and realistically de-ramped to the static load as well), so that again there would be no jolt unrepresentative of reality.

### 4.8.3.1.1 Applied Load Excitations

To define a time dependent dynamic excitation, both spatial distribution and the time variation (i.e. the temporal distribution) must be defined.

$$TLOAD1: \quad \{P(t)\} = \{AF(t - \tau)\}$$

$$TLOAD2: \quad \{P(t)\} = \begin{cases} 0 & , \quad t < (T1 + \tau) \text{ or } t > (T2 + \tau) \\ A\tilde{t}^B e^{C\tilde{t}} \cos(2\pi F\tilde{t} + P) & , \quad (T1 + \tau) \leq t \leq (T2 + \tau) \end{cases}$$

where  $\tilde{t} = t - T1 - \tau$

t = time

A = amplitude scalar multiplier defined by DAREA for a DOF

$\tau$  = time delay in an applied load defined by DELAY for a DOF

F(t) = time dependent force variation defined by TABLED1

T1 = time constant defined by T1 in TLOAD2

T2 = time constant defined by T2 in TLOAD2

F = frequency (cycles per unit time) defined by F in TLOAD2

P = phase angle (degrees) defined by P in TLOAD2

C = exponential coefficient defined by C in TLOAD2

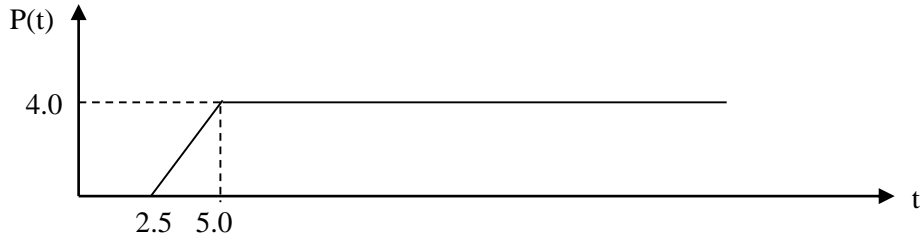
B = growth coefficient defined by B in TLOAD2

\$ CASE CONTROL SECTION									
DLOAD = < ID OF TLOAD1 or TLOAD2 >									
\$ BULK DATA									
TLOAD1	ID	DAREA ID	DELAY ID	TYPE	F(t) TABLED1 ID				
TLOAD2	ID	DAREA ID	DELAY ID	TYPE	T1	T2	F	P	
	C	B							
DAREA	ID	GRID ID	Component Number	Scale Factor	GRID ID	Component Number	Scale Factor		
DELAY	ID	GRID ID	Component Number	Time Delay $\tau$	GRID ID	Component Number	Time Delay $\tau$		
TABLED1	ID	XAXIS	YAXIS						
	x1	y1	x2	y2	x3	y3	x4	Y4	
	x5	y5	x6	y6	...	...	ENDT		

TYPE is the TLOAD1 and TLOAD2 entries defined the type of excitation, i.e. 0 for Force or Moment.

Any number of DAREA and DELAY entries may be defined. All those with the same ID will be subjected to the same dynamic excitation defined in the TLOAD1 and TLOAD2 entries. The XAXIS and YAXIS in the TABLED1 entry refers to either LINEAR or LOG interpolation between and beyond the extremities of the specified  $\{x_i, y_i\}$  pairs of  $\{\text{time, amplitude}\}$ .

Hence to define a force that ramps up and is constant thereafter as shown

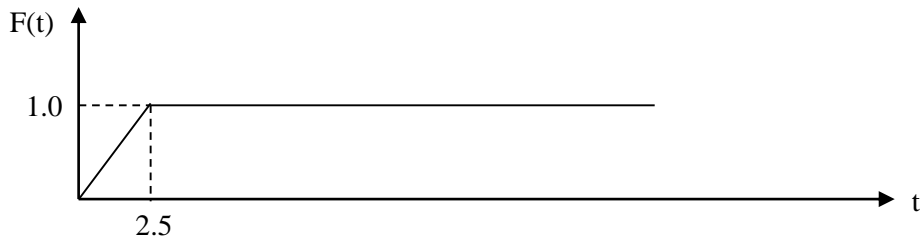


we define for TLOAD1

A = 4.0 in DAREA

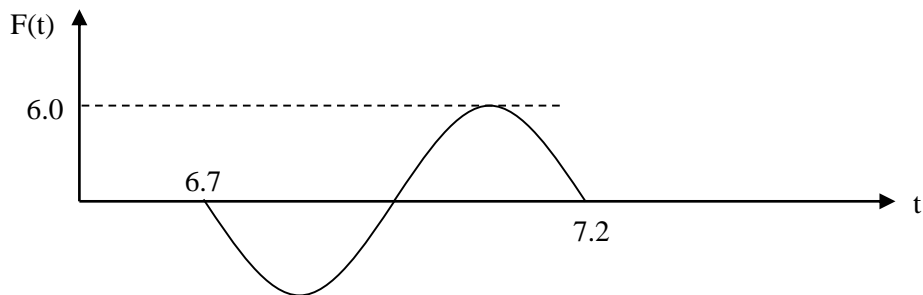
$\tau = 2.5$  in DELAY

F(t) in a TABLED1 entry



Hence, using a TABLED1 we can define very general transient force excitations.

To define a sinusoidal harmonic load  $P(t) = -6.0\sin(\omega(t-6.7))$  with a period  $T = 0.5\text{s}$  for one cycle (i.e. from  $t = 6.7\text{s}$  to  $t = 7.2\text{s}$ ),



$T = 0.5\text{s}$

hence,  $f = 2.0\text{ Hz}$

we define for TLOAD2,

A = 6.0 in DAREA

$\tau = 6.7$  in DELAY

T1 = 0.0

T2 = 0.5

F = 2.0

P = 90.0 degrees

C = 0.0 in TLOAD2

B = 0.0 in TLOAD2

Hence,

$$\{P(t)\} = \begin{cases} 0 & , \quad t < (T1 + \tau) \text{ or } t > (T2 + \tau) \\ A\tilde{t}^B e^{C\tilde{t}} \cos(2\pi F\tilde{t} + P) & , \quad (T1 + \tau) \leq t \leq (T2 + \tau) \end{cases}$$

where  $\tilde{t} = t - T1 - \tau$

$$\{P(t)\} = \begin{cases} 0 & , \quad t < 6.7 \text{ or } t > 7.2 \\ 6.0 \cos(2\pi 2(t - 6.7) + 90.0) & , \quad 6.7 \leq t \leq 7.2 \end{cases}$$

Since,  $\sin \theta = \cos (90.0 - \theta)$

$$\{P(t)\} = \begin{cases} 0 & , \quad t < 6.7 \text{ or } t > 7.2 \\ -6.0 \sin(2\pi 2(t - 6.7)) & , \quad 6.7 \leq t \leq 7.2 \end{cases}$$

In order to verify the applied loading, the response to the load applied suddenly (over one or two time steps) should be checked to double the results from a static analysis with the same loading.

Defining the spatial distribution using DAREA only enables the specification of dynamic concentrated forces and moments. To accommodate more complicated loadings, the LSEQ entry is used to refer to static load entries that define the spatial distribution of the dynamic loads.

§ CASE CONTROL SECTION									
LOADSET = < ID OF LSEQ >									
DLOAD = < ID OF TLOAD1/TLOAD2 >									
§ BULK DATA									
LSEQ	ID	DAREA Reference Link	Static Load ID	Temp Load ID					
TLOAD1	ID	DAREA Reference Link	DELAY ID	TYPE	F (t) TABLED1 ID				
TLOAD2	ID	DAREA Reference Link	DELAY ID	TYPE	T1	T2	F	P	
	C	B							

The DAREA Reference Link links the TLOAD1/TLOAD2 entry to the LSEQ which can now be used to refer to static load set ids which define the spatial distribution of the dynamic loads. The static load set id can refer to one or more static load entry types. Obviously, there is not a DAREA entry anymore. It is replaced by an LSEQ bulk data entry, a LOADSET case control entry and the pertinent bulk data static load entries such as FORCE, PLOADi or GRAV. The time dependent load card TLOAD1/TLOAD2 is selected using the DLOAD case control command.

A new automatic feature will be activated *if and only if* the user does *not* have a LOADSET/LSEQ selection. With the new enhancement, it is no longer necessary for the user to explicitly specify LOADSET/LSEQ combination in order to employ static loading data in dynamic analysis. Instead, when the user selects a dynamic load, all static loads and thermal loads that have the same ID as the DAREA ID on the dynamic load entry are automatically selected.

If more than one TLOAD1/TLOAD2 entry is required, then a dynamic load set combination is required. This is done using a DLOAD bulk data entry that linearly combines multiple TLOAD1/TLOAD2 entries.

<b>\$ CASE CONTROL SECTION</b>										
DLOAD = < ID OF DLOAD >										
<b>\$ BULK DATA</b>										
DLOAD	ID	Overall Scale Factor	Scale Factor	TLOAD1 / TLOAD2 ID	Scale Factor	TLOAD1 / TLOAD2 ID	..etc..			

#### 4.8.3.1.2 Nonlinear Transient Load

Nonlinear transient loads are as described in nonlinear forced transient response analysis.

### 4.8.3.1.3 Enforced Motion

Four methods can be used for enforced motion, namely: -

- (i) The direct absolute response approach
- (ii) The direct relative response approach
- (iii) The indirect large mass method (absolute response approach)
- (iv) The indirect large spring method (absolute response approach)

The direct absolute response approach makes no assumptions. The direct relative response approach makes the following assumptions <sup>6</sup>: -

- (i) base movements in any given direction are identical i.e. that the base supports cannot move independently
- (ii) no mass or damping coupling between the structure and the ground (the off diagonal terms in the unsupported mass matrix that couple the structure and the ground movements are zero or are insignificant)
- (ii) no damping into the ground

In both the direct absolute and direct relative approaches, the equation of motion is the same on the LHS, hence the same resonant frequencies and mode shapes are obtained, only the applied loading vector on the RHS differ. The two approaches will also give the same stresses within the elements. With the assumption of no coupling of mass and damping, the absolute response is found by applying a base displacement and the relative response by applying a base displacement. The absolute displacement response and relative displacement response only differ by a rigid body movement.

#### 4.8.3.1.3.1 Direct Enforced Motion (Absolute Response Approach)

The direct approach of applying enforced motion is the most accurate method. Denoting the free DOFs as f and the constrained DOFs (whether with enforced motion or zero constraints) as s, P the force and q the reaction, the dynamic equilibrium equation can be partitioned as

$$\begin{bmatrix} M_{ff} & M_{fs} \\ M_{sf} & M_{ss} \end{bmatrix} \begin{Bmatrix} \ddot{u}_f \\ \ddot{u}_s \end{Bmatrix} + \begin{bmatrix} B_{ff} & B_{fs} \\ B_{sf} & B_{ss} \end{bmatrix} \begin{Bmatrix} \dot{u}_f \\ \dot{u}_s \end{Bmatrix} + \begin{bmatrix} K_{ff} & K_{fs} \\ K_{sf} & K_{ss} \end{bmatrix} \begin{Bmatrix} u_f \\ u_s \end{Bmatrix} = \begin{Bmatrix} P_f(t) \\ P_s(t) + q_s(t) \end{Bmatrix}$$

With zero constraints, i.e.

$$u_s = \dot{u}_s = \ddot{u}_s = \{0\}$$

the dynamic equation of motion reduces to the usual

$$M_{ff} \ddot{u}_f + B_{ff} \dot{u}_f + K_{ff} u_f = P_f(t)$$

with the corresponding reactions

$$q_s(t) = -P_s(t) + (M_{sf} \ddot{u}_f + B_{sf} \dot{u}_f + K_{sf} u_f)$$

But, with enforced motion, the dynamic equation of motion is

$$M_{ff} \ddot{u}_f + B_{ff} \dot{u}_f + K_{ff} u_f = P_f(t) - (M_{sf} \ddot{u}_s + B_{sf} \dot{u}_s + K_{fs} u_s)$$

with the corresponding reactions

<sup>6</sup> NAFEMS. *A Finite Element Primer*. NAFEMS Ltd., Great Britain, 1992.

$$q_s(t) = -P_s(t) + [M_{sf} \ M_{ss}] \begin{Bmatrix} \ddot{u}_f \\ \ddot{u}_s \end{Bmatrix} + [B_{sf} \ B_{ss}] \begin{Bmatrix} \dot{u}_f \\ \dot{u}_s \end{Bmatrix} + [K_{sf} \ K_{ss}] \begin{Bmatrix} u_f \\ u_s \end{Bmatrix}$$

Hence, in general the user specifies the either the support displacement, velocity or acceleration (as all three motions are related to each other in the sense that the velocity is the first derivative and the acceleration is the second derivative of the displacement) and the equation of motion is solved as usual. But for most structural problems, the damping component  $B_{sf}$  (not  $B_{ss}$  in the reaction expression) can be ignored and for lumped mass formulations (or at least no coupling to the support freedoms),  $M_{sf}$  is zero, hence reducing the equivalent forcing function to

$$P_f(t) - K_{fs} u_s(t)$$

and hence, only the base displacement excitation need to be incorporated. However, these approximations need not necessarily be employed in which case the absolute approach has **no inherent assumptions**. Note that the response will be obtained in absolute terms. This solution method is general and is valid even if different supports are moving with different independent excitations.

#### 4.8.3.1.3.2 Direct Enforced Motion (Relative Response Approach)

The dynamic equation of motion in absolute terms with enforced motion has been shown to be

$$M_{ff} \ddot{u}_f + B_{ff} \dot{u}_f + K_{ff} u_f = P_f(t) - (M_{sf} \ddot{u}_s + B_{sf} \dot{u}_s + K_{fs} u_s)$$

Assuming that the **base movements in any given direction are identical i.e. that the base supports cannot move independently** (arising in only seismic problems, not any other), the structural movements can be expressed relative to the base as

$$u_{rel} = u_f - u_s$$

Thus

$$M_{ff} \ddot{u}_{rel} + B_{ff} \dot{u}_{rel} + K_{ff} u_{rel} = P_f(t) - (M_{sf} \ddot{u}_s + B_{sf} \dot{u}_s + K_{fs} u_s) - (M_{ff} \ddot{u}_s + B_{ff} \dot{u}_s + K_{ff} u_s)$$

Using the fact that  $Ku_s = 0$  and **assuming further that the mass and damping are diagonal (or at least no coupling to the support freedoms)**, the equation of motion becomes

$$M_{ff} \ddot{u}_{rel} + B_{ff} \dot{u}_{rel} + K_{ff} u_{rel} = P_f(t) - (M_{ff} \ddot{u}_s + B_{ff} \dot{u}_s)$$

**Assuming further that there is no damping into the ground**, we obtain the common form

$$M_{ff} \ddot{u}_{rel} + B_{ff} \dot{u}_{rel} + K_{ff} u_{rel} = P_f(t) - M_{ff} \ddot{u}_s$$

The DLOAD Case Control Command, optionally the DLOAD bulk data entry, TLOAD1/TLOAD2, DELAY and TABLED1 is used in the same way as they were when load excitations were applied. One difference is the TYPE field of TLOAD1/TLOAD2 where instead of load excitation LOAD, enforced motion in terms of DISP, VELO or ACCE is specified. Another difference for the direct enforced motion lies in the EXCITEID Field 3 of TLOAD1/TLOAD2, where instead of referencing a DAREA card (hence not requiring a DAREA card at all for enforced motion), the EXCITEID Field references an SPCD entry, which in turn will reference a GRID ID and an associated DOF component in which the enforced motion is to be applied. Now at the same time, in line with methods of applying enforced motion in static analysis, the DOF component of the GRID ID with enforced motion must be constrained with an SPC bulk data entry which of course must be referenced by an SPC Case Control Command. Modal augmentation vectors by PARAM, RESVEC, YES must be used for modal methods. This is because since there no rigid body modes (as they are constrained by the enforced motion), there can be no motion of the enforced points unless RESVEC is used.

#### 4.8.3.1.3.3 Indirect Large Mass Method (Absolute Response Approach) – Base Acceleration Specified

If a very large mass  $m_0$ , which is several orders of magnitude larger than the mass of the entire structure, is connected to a DOF where a dynamic load is applied, then the acceleration of the DOF is approximately

$$\ddot{u}(t) = \frac{P(t)}{m_0}$$

Hence, the (large) force required to produce the desired acceleration at the DOF is

$$P(t) = m_0 \ddot{u}(t)$$

The stiffness, damping and the inertial force of the mass of the structure at the DOF contributes little in comparison to the force provided by the large mass, hence the acceleration response is due primarily to the inertial force of the large mass. The larger the mass in comparison, the more accurate the acceleration excitation. However the magnitude is limited by numeric overflow in the computer. MSC recommends that the value of  $m_0$  be approximately  $10^6$  times the mass of the entire structure for an enforced translational DOF and  $10^6$  times the mass moment of inertia of the entire structure for a rotational DOF (for 6 digits of numerical accuracy). The disadvantage of the large mass method is that it involves a loss of numerical conditioning and hence a loss of accuracy of the response. If the large mass is  $10^6$  times the mass of the structure, this is equivalent to losing 6 significant figures in the definition of the mass and stiffness matrices.

The following procedure is employed to specify prescribed motion in forced transient response analysis: -

- (i) remove constraints from the enforced DOFs
- (ii) place large masses or inertia scalar elements CMASSi or CONMi with values approximately  $10^6$  times the mass or mass moment of inertia of the entire structure
- (iii) indicate in Field 5 of TLOAD1 or TLOAD2 whether the enforced motion is a displacement, velocity or acceleration; NASTRAN automatically differentiates a specified velocity once or a specified displacement twice to obtain an acceleration; Hence, to maintain accuracy, it is best to specify an acceleration in the first place
- (iv) apply a dynamic load to each enforced DOF equal to
  - $P(t) = m_0 \ddot{u}(t)$  if acceleration prescribed motion
  - $P(t) = m_0 \dot{u}(t)$  if velocity prescribed motion
  - $P(t) = m_0 u(t)$  if displacement prescribed motion

The DLOAD Case Control Command, optionally the DLOAD bulk data entry, TLOAD1/TLOAD2, DAREA, DELAY and TABLED1 is used in the same way as they were when load excitations were applied. The key difference is the TYPE field of TLOAD1/TLOAD2 where instead of load excitation LOAD, enforced motion in terms of DISP, VELO or ACCE is specified.

To ensure that the chosen mass values are high enough two modal analyses (SOL 103) should be run, one with the enforced DOFs constrained and the other with the large masses attached and the DOFs left unconstrained. The flexible frequencies (not the rigid mode frequencies) between the two analyses should be well comparable (to within 4 or 5 significant figures), otherwise the mass values should be increased.

In modal methods, further considerations must be made to the rigid body modes. Globally unconstrained structures will have rigid body modes. Releasing a global DOF and placing a large mass there to enforce an applied motion will result in that DOF being unconstrained and hence will result in a rigid body mode (stress free mode). This mode can safely be discarded in the solution by using LFREQ or simply not calculating it in EIGRL. If however two large masses are placed at two different locations to simulate enforced motion in the same direction, there will be a further low-frequency mode that represents the motion of one large mass relative to the other. This mode does contribute to the stresses and cannot be ignored. It must be captured within EIGRL and LFREQ. To avoid this problem, a solution will be to place only one large mass at an arbitrary location and connect with RBE2 elements all DOFs that are to be subjected to that enforced motion.

#### 4.8.3.1.3.4 Indirect Large Spring Method (Absolute Response Approach) – Base Displacement Specified

A stiff spring may be used to simulate an enforced displacement.

$$P(t) = k_0 u(t)$$

where  $k_0$  is the stiffness of the stiff spring and  $u(t)$  is the enforced displacement. The large stiffness method certainly works, but the large mass method is preferred because it is easier to estimate a good value for the large mass than to estimate a good value for the stiff spring. In addition and more importantly, the large mass method is far superior when modal methods are used. If very stiff springs are used for modal analysis rather than very large masses, the vibration modes corresponding to the very stiff springs have very high frequencies and in all likelihood, are not included among the modes used in the response analysis. This is the main reason that large masses should be used instead of stiff springs.

The stiff spring method is however advantageous in the case of (time domain) enforced displacement because it avoids the roundoff error that occurs while differentiating the displacement to obtain acceleration in the large mass method. The stiff spring method also avoids the problem of rigid-body drift when applying enforced motion on statically determinate support points (Rigid-body drift means that the displacement increases continuously with time, which is often caused by the accumulation of small numerical errors when integrating the equations of motion).

#### 4.8.3.1.4 Damping

To specify stiffness proportional global viscous damping on all the deformable elements, the following parameters are used.

<b>\$ BULK DATA</b>
PARAM,G,<Structural Damping Coefficient> PARAM,W3,<Circular Frequency at which Structural Damping Equals Viscous Damping>

To specify elemental structural damping on selected deformable elements, PARAM, W4 is used in conjunction with the GE field on the MATi or entries in the CBUSH or CELAS elements to convert the structural damping into equivalent viscous damping.

<b>\$ BULK DATA</b>
PARAM,W4,<Circular Frequency at which Structural Damping Equals Viscous Damping>

If PARAM, W3 and/or PARAM, W4 is not specified, it defaults to 0.0, hence ignoring all the elemental structural damping cards.

Because time domain solutions cannot handle structural damping, an equivalent viscous damping is required. Hence, if structural damping is specified at the element levels, then the incorrect modal damping will result because the conversion from structural to viscous damping will only be valid for one modal natural frequency,  $w_4$  as specified by PARAM, W4 (Note that element viscous damping damps different modes accurately). Hence, if the model has any structural damping, then it should be specified as modal damping. Modal damping can be calculated using SOL 107 and specified as either modal structural or modal viscous damping (hence a modal method of analysis i.e. SOL 112 must be used). Of course, the modal damping will be converted to modal viscous damping for solution in the time domain. This conversion is only perfectly accurate when the frequency of excitation matches the natural frequency of the mode (at resonance), but of course this is acceptable as only that is the instance when the damping estimate is most critical. Note that in the frequency domain, for the modal solution (SOL 111), the modal damping specified will be converted to either modal viscous or modal structural damping depending on PARAM, KDAMP.

### 4.8.3.2 GL, ML P- $\Delta$ ( $K_G^A$ From $K_E^A$ ) Direct Forced Transient Response Analysis

It is often necessary to incorporate the reduction in bending stiffness of gravity load resisting columns for the analysis of lateral loads. The following procedure is undertaken.

#### Phase 1

Perform static analysis (with loads that cause the greatest negative or positive geometric stiffness) based on  $[K_E^A]$  but include the segyroa.v2001 alter prior to the Case Control Section in order to compute the geometric stiffness matrix  $[K_G^A]_1$  (and output into a .pch file) based on the generated element loads from the  $[K_E^A]$  static analysis.

#### Phase 2

A SOL 109 with a general loading function is undertaken based on  $[K_E^A] + [K_G^A]_1$  with the k2gg=ktjj statement in the Case Control Section and the outputted .pch file which contains the ktjj matrix in the Bulk Data. The responses at this stage represent the P- $\Delta$  ( $K_G^A$  From  $K_E^A$ ) response to the dynamic excitation.

The following equivalent alternative procedure can also be employed.

<pre> \$ CASE CONTROL SECTION  SUBCASE 1 LABEL = Static Preload Load Case LOAD = &lt; ID of FORCEi, MOMENTi, PLOADi, GRAV, LOAD, SPCD Cards in Bulk Data &gt; TEMP(Load) = &lt; ID of TEMP, TEMPRB, TEMPP1 Cards in Bulk Data &gt; DEFORM = &lt; ID of DEFORM Cards in Bulk Data &gt; SUBCASE 2 LABEL = P-<math>\Delta</math> Direct Transient Response Analysis STATSUB(PRELOAD) = 1 DLOAD = &lt; ID OF TLOAD1 or TLOAD2 &gt;                 </pre>
---

The method is valid when **only the prestress is judged to affect the geometric stiffness** such as in the compressive preload of building columns due to gravitational loads and the prestressing of extremely taut cables that sag very little under gravity but not in systems such as suspension bridges. Where lateral loads are large enough to affect the geometry of the system with prestress, then a repetitive P- $\Delta$ , SOL 106, implicit dynamic relaxation SOL 129 or explicit dynamic relaxation must be employed. But in single P- $\Delta$  analysis, because cables do not have much elastic bending stiffness, the initial static preload subcase should only include the prestress and not gravity as including gravity is the same as solving two linear static problems of stiffness  $K_E^A$  with preload and gravity as the applied loads respectively. Clearly, in the gravity case, it is nonsensical as the cables do in reality have differential stiffness (from the prestress) to resist the gravitational force. Prestress in one direction (i.e. along the axis of cable) will cause a differential stiffness in the orthogonal direction. Gravity acts in the orthogonal direction and hence cannot be accounted for in the calculation of the prestress in this single P- $\Delta$  analysis. To quantitatively decide if gravity need not be considered in contributing to the differential stiffness of the cables, a static P- $\Delta$  analysis should be carried out, the first subcase being a SOL 101 with only the prestress as applied loads and the second subcase a P- $\Delta$  SOL 101 (i.e. utilizing the induced prestress from the first subcase to form a geometric stiffness matrix) with both the gravity and prestress included as applied loads. If the difference in the cable element forces between subcases 1 and 2 is negligible, then gravity has little influence in affecting the geometric stiffness. If there is a major difference in the cable element force, then clearly, gravity will affect the geometric stiffness and as such, a repetitive P- $\Delta$ , SOL 106, implicit dynamic relaxation or explicit dynamic relaxation must be used to converge to the true  $K_T$ . Likewise, in the single P- $\Delta$  analysis of multi-storey buildings, gravity (and only gravity) acts in axis of columns to generate prestress, and the differential stiffness is computed for the orthogonal direction reducing resistance to lateral wind forces, applied in the second subcase with gravity too.

When a static subcase is specified for linear transient response analysis (SOLs 109 and 112) with STATSUB(PRELOAD), the data recovery is controlled by PARAM, ADSTAT. By default (YES) the static solution will be superimposed on the dynamic response solution (displacement, stress and SPCForce). The relative solution can be obtained in reference to the static solution point by PARAM, ADSTAT, NO. No provision is made for frequency response analysis, because the static responses contribute only to the zero frequency response. For linear dynamic response, the static solution can be superimposed after the dynamic solution procedure. The preload effect is reflected only in the stiffness and the actual static load is omitted in the dynamic response analysis. The total displacement can be obtained by superposing the static solution to the transient response analysis.

$$\{u\}_{total} = \{u\}_{dynamic} + \{u\}_{static}$$

And the stress output is obtained as

$$\sigma = [S]\{u_{static} + u_{dynamic}\}$$

The STATSUB(PRELOAD) computes the differential stiffness due to the prestress and also the follower force. The follower force is calculated and incorporated by the use of PARAM, FOLLOWK, YES. We know how the prestress affects the differential stiffness, namely a tensile prestress causing an increase in stiffness. The effect of the follower force on the stiffness is different. For example, for a cylinder under external pressure critical buckling load may be over-estimated (even though the mode shapes are similar) in a SOL 105 and the natural frequencies in vibration may be under-estimated (even though the mode shapes are similar) in a SOL 103 in the absence of follower stiffness. To the contrary, this observations are reversed in case of centrifugal loads. Centrifugal forces as a constant (static) load are applied by a Bulk Data RFORCE to any elements that have masses. The follower stiffness due to centrifugal load has the effect of lowering stiffness (although the centrifugal load tensioning effect increases stiffness), consequently lowering natural frequencies (even though the mode shapes are similar) in a SOL 103 and lowering the buckling loads (even though the mode shapes are similar) in a SOL 105. This effect increases as the RPM increases, and it becomes significant when the RPM is over 1000. For moderately geometric nonlinear analysis, exclusion of follower stiffness affects the rate of convergence, but the converged solution is correct. For severely geometric nonlinear analysis, it may not be possible to obtain a converged solution without including follower stiffness. As the geometric nonlinearity intensifies, so is the effect of follower stiffness. Therefore, inclusion of follower stiffness greatly enhances the convergence if the deformation involves severe geometric nonlinearity.

### 4.8.3.3 GL, ML P- $\Delta$ ( $K_G^A$ From Exact or Approximate $K_T^A$ ) Direct Forced Transient Response Analysis

It is often necessary to include the differential stiffness, especially if there are prestressed cables in the model. To obtain  $K_T^A$ , to be theoretically exact, a GNL SOL 106 (or implicit dynamic relaxation SOL 129 or explicit dynamic relaxation LS-DYNA) with prestress (as temperature loads say) and gravity must be undertaken. Alternatively, an approximation to  $K_T^A$  can be obtained by repetitive P- $\Delta$  static analyses with the prestress (as temperature loads say) and gravity applied. The procedure to obtain this approximate  $K_T^A$  will be presented. Note that the approximate  $K_T^A$  will be the summation of the elastic stiffness  $K_E$  at the undeflected (by the prestress and gravity) state but  $K_G$  at the deflected (by the prestress and gravity) state. Hence if  $K_E$  changes considerably during the application of the prestress, a full SOL 106 (or implicit dynamic relaxation SOL 129 or explicit dynamic relaxation LS-DYNA), which converges to the  $K_E$  and  $K_G$  at the deflected (by the prestress and gravity) state should be employed. Hence for the modelling of a suspension bridge where there is a great change in geometry (known in the bridge industry as **form-finding**, so-called because it is necessary to find the form or shape of the catenary suspension cables), it may be prudent to employ SOL 106 (or implicit dynamic relaxation SOL 129 or explicit dynamic relaxation LS-DYNA), but for a high tension low sag cable on say a tower with prestressed cables, the repetitive P- $\Delta$  static analysis may be adequate. The repetitive P- $\Delta$  analysis basically involves a number of iterations of linear static analyses to obtain an approximate  $K_T^A$ . Note again that A refers to the initial undeflected (by the collapsing load) state, but deflected by the prestress and gravity. To perform the repetitive P- $\Delta$  analysis, a static analysis is performed based on  $K_E^A$  with temperature loads and gravity to generate forces in the structural elements, which in turn provides input for the computation of  $K_{Gi}^{AKT_m}$  where m is the iterations. Repetitive static analysis is performed with the prestress and gravity updating the stiffness matrix  $K_E^A + K_{Gi}^{AKT_{m-1}} + K_{Gi}^{AKT_m}$  until convergence of displacements is obtained. The tangent stiffness at this stage is the approximate converged tangent stiffness matrix  $K_T^A = K_E^A + K_{Gi}^{AKT}$ . The converged displacements represent the approximate P- $\Delta$  ( $K_G^A$  From Approximate  $K_T^A$ ) static response to the initial prestress loads. The converged geometric stiffness at this stage would be that based upon the approximate tangent stiffness matrix  $K_T^A$ , i.e.  $K_{Gi}^{AKT}$ .

#### Phase 1

Perform static analysis (with prestress and gravity) based on  $[K_E^A]$  but include the segyroa.v2001 alter prior to the Case Control Section in order to compute the geometric stiffness matrix  $[K_G^A]_1$  (and output into a .pch file) based on the generated element loads from the  $[K_E^A]$  static analysis.

#### Phase 2

Perform static analysis (with prestress and gravity) based on  $[K_E^A] + [K_G^A]_1$  by including the k2gg = ktjj statement in the Case Control Section, the outputted .pch file which contains the ktjj matrix in the Bulk Data and the segyroa.v2001 alter prior to the Case Control Section to compute the  $[K_G^A]_2$  (and output into the .pch file overwriting previous data) based on the generated element loads from the  $[K_E^A] + [K_G^A]_1$  static analysis.

#### Phase 3

Repeatedly perform the Phase 2 static analysis (with prestress and gravity) based on  $[K_E^A] + [K_G^A]_i$  for  $i = 2$  to  $n$  where  $n$  represents the number of iterations required for the change in deflections between analyses to become negligible. This would signify that the change in the  $[K_G^A]$  matrix become negligible and the correct  $[K_G^A]$  is attained. The deflections and the other responses at this stage represent the P- $\Delta$  ( $K_G^A$  From Approximate  $K_T^A$ ) static response to the prestress and gravity. The stiffness of the structure is  $K_T^A$ .

#### Phase 4

A SOL 109 with a general loading function is undertaken with the k2gg=ktjj statement in the Case Control Section and the outputted .pch file which contains the latest ktjj matrix in the Bulk Data. The responses at this stage represent the P- $\Delta$  ( $K_G^A$  From Approximate  $K_T^A$ ) response to the dynamic excitation.

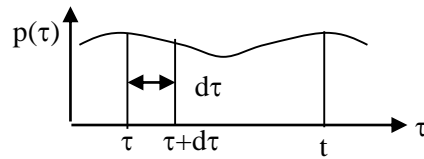
#### 4.8.4 Hand Methods Verification

##### 4.8.4.1 Determination of Maximum Dynamic Displacement, $u_{\max}$ by Solving the SDOF Undamped/Damped Linear Equation of Motion ODE for Deterministic Time Domain Loading With/Without Initial Conditions Using the Convolution Integral (Duhamel's integral)

The Duhamel's integral can be used to calculate the response of SDOF systems to general loading functions. It inherently includes both the steady state and the transient components of the motion in the response corresponding to no initial conditions. However, the method is only valid for linear elastic structures as superposition of response is utilized.

The impulse of a force is defined as the product of the force  $p(\tau)$  and its duration time  $d\tau$ . An impulsive force acts only for a short duration of time. We define time a general time variable  $\tau$  where

- $\tau = 0$  Initial displacement and velocity conditions
- $\tau = \tau$  Time of application of impulsive force for duration  $d\tau$
- $\tau = t$  Time dynamic response sought



From Newton's Laws of Motion, an impulse on a mass  $m$  will result in a change of momentum and hence change of velocity.

$$mdv = p(\tau)d\tau$$

$$dv = \frac{p(\tau)d\tau}{m}$$

This incremental velocity can be considered as the initial velocity of a free vibrational analysis. Recall the transient state solution for a free vibrational analysis with initial displacement and velocity conditions.

$$u(t) = \frac{\dot{u}(0)}{\omega_n} \sin \omega_n t + u(0) \cos \omega_n t$$

Hence the response due to the initial velocity  $dv$  (with no initial displacement) at time  $\tau$  at a later time  $t$ ,

$$du(\tau = t) = \frac{p(\tau)d\tau}{m\omega_n} \sin \omega_n (t - \tau)$$

We denote the start of the application of the impulsive forces at time  $\tau$  (for duration  $d\tau$ ) and the response to be evaluated at time  $t$ . A general loading function can be regarded as a series of short impulses at successive incremental times of  $d\tau$ , each impulse producing its own differential response at time  $t$ . Thus, the total response at  $t$  will be the superposition of all the impulses acting from time  $\tau = 0$  to  $\tau = t$ .

$$\int_{\tau=0}^{\tau=t} du(\tau = t)d\tau = \int_{\tau=0}^{\tau=t} \frac{p(\tau)d\tau}{m\omega_n} \sin \omega_n (t - \tau)$$

$$u(\tau = t) = \frac{1}{m\omega_n} \int_{\tau=0}^{\tau=t} p(\tau) \sin \omega_n (t - \tau) d\tau$$

This is known as the Duhamel's integral and it **inherently includes both the transient state and steady state components** of the response. Because it **utilizes superposition** of the responses, it is only valid for linear elastic structural behavior. To also incorporate initial conditions at time  $\tau = 0$ ,

$$u(\tau = t) = \frac{\dot{u}(\tau = 0)}{\omega_n} \sin \omega_n t + u(\tau = 0) \cos \omega_n t + \frac{1}{m\omega_n} \int_{\tau=0}^{\tau=t} p(\tau) \sin \omega_n (t - \tau) d\tau$$

Including viscous damping, the corresponding expression becomes

$$u(\tau = t) = e^{-\zeta\omega_n t} \left( u(\tau = 0) \cos \omega_d t + \frac{\dot{u}(\tau = 0) + u(\tau = 0)\zeta\omega_n}{\omega_d} \sin \omega_d t \right) + \frac{1}{m\omega_d} \int_{\tau=0}^{\tau=t} p(\tau) e^{-\zeta\omega_n(t-\tau)} \sin \omega_d(t-\tau) d\tau$$

$$\text{where } \omega_d = \omega_n \sqrt{1 - \zeta^2}$$

Hence, the general Duhamel's Integral expression excluding the initial conditions,

$$u(\tau = t) = \int_{\tau=0}^{\tau=t} p(\tau) h(t - \tau) d\tau$$

$$\text{where } h(t - \tau) = \frac{1}{m\omega_n} \sin \omega_n(t - \tau) \text{ without damping}$$

$$\text{and } h(t - \tau) = \frac{1}{m\omega_d} e^{-\zeta\omega_n(t-\tau)} \sin \omega_d(t - \tau) \text{ with damping}$$

Incidentally,  $h(t-\tau)$  is known as the unit impulse response function. Now it is just a matter of evaluating this integral and expression either classically or numerically for a variety of loading functions to determine the response.

Other quantities such as velocity and acceleration can be obtained simply by differentiating the displacement expression with respect to  $t$ . Sometimes this simply results in a multiplication by  $\omega_n$  (or  $\omega_d$ ) for velocity and  $\omega_n^2$  (or  $\omega_d^2$ ) for acceleration.

#### (i) An Instantaneous Impulsive Force of Duration $t_1 < T$

An impulse is a very large load acting for a very short time. So long as  $t_1/T < 0.2$ , we can approximate the force as an impulse. The lower the  $t_1/T$ , the more impulse-like the loading becomes. An impulse analysis is easier because  $h(t-\tau)$  can be approximated outside the integral whereas in the non-impulse loading  $h(t-\tau)$  must be evaluated inside the integral. The remainder within the integral reduces to simply the area (or impulse) under the loading force  $p(\tau)$ .

$$u(\tau = t) = h(t - \tau) \int_{\tau=0}^{\tau=t} p(\tau) d\tau$$

$$u(\tau = t) = \frac{1}{m\omega_n} \sin \omega_n(t - \tau) \int_{\tau=0}^{\tau=t} p(\tau) d\tau \quad \text{undamped}$$

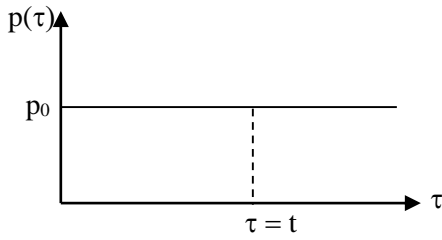
$$u(\tau = t) = \frac{1}{m\omega_d} e^{-\zeta\omega_n(t-\tau)} \sin \omega_d(t - \tau) \int_{\tau=0}^{\tau=t} p(\tau) d\tau \quad \text{damped}$$

$$u_{\max} = \frac{1}{m\omega_n} \int_{\tau=0}^{\tau=t} p(\tau) d\tau \quad \text{undamped}$$

$$u_{\max} = \frac{1}{m\omega_d} \int_{\tau=0}^{\tau=t} p(\tau) d\tau \quad \text{damped}$$

Another equivalent interpretation of the above relationship is from the basic consideration of the conservation of momentum. The impacting particle (of small relative mass compared to mass of structure) imposes an impulse  $I$  onto the structure. The magnitude of  $I$  can be calculated as  $m\Delta v$  where  $m$  is the small mass and  $\Delta v$  the change of velocity at impact. If there is no rebound  $\Delta v$  is the approach velocity. Conservation of momentum at impact requires the initial velocity of the structural mass to be  $I/M$ . A lightly damped system then displays damped free vibration with an initial displacement of approximately  $I/(\omega_d M)$ , or an initial velocity of approximately  $I/M$  or an initial acceleration of approximately  $I\omega_d/M$ .

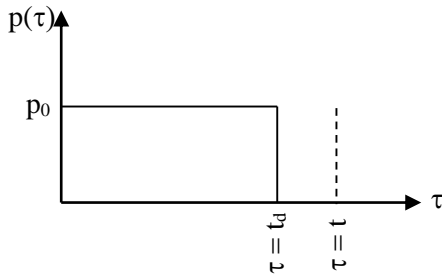
**(ii) An Instantaneous Continuous Constant Force of Amplitude  $p_0$**



With no damping,

$$\begin{aligned}
 u(\tau = t) &= \int_{\tau=0}^{\tau=t} p(\tau) \frac{1}{m\omega_n} \sin \omega_n (t - \tau) d\tau \\
 &= \int_{\tau=0}^{\tau=t} p_0 \frac{1}{m\omega_n} \sin \omega_n (t - \tau) d\tau \\
 &= \frac{p_0}{m\omega_n^2} \left[ \cos \omega_n (t - \tau) \right]_0^t \\
 &= \frac{p_0}{k} (1 - \cos \omega_n t) \\
 u_{\max} &= \frac{2p_0}{k} \quad \text{when} \quad \cos \omega_n t = -1
 \end{aligned}$$

The maximum dynamic displacement is twice the static displacement. This means that a constant force applied suddenly will produce a maximum displacement of twice that which will be produced if the force was applied statically (i.e. slowly such that there are no dynamic effects). This is also true for internal forces and stresses.

**(iii) An Instantaneous Rectangular Force of Duration  $t_d$  of Amplitude  $p_0$** 


With no damping,

For  $\tau < t_d$

$$u(\tau = t) = \frac{p_0}{k} (1 - \cos \omega_n t)$$

$$\dot{u}(\tau = t) = \frac{p_0}{k} \omega_n \sin \omega_n t$$

$$u_{\max} = \frac{2p_0}{k}$$

For  $\tau = t_d$

$$u(\tau = t_d) = \frac{p_0}{k} (1 - \cos \omega_n t_d)$$

$$\dot{u}(\tau = t_d) = \frac{p_0}{k} \omega_n \sin(\omega_n t_d)$$

For  $\tau > t_d$ , we utilize the initial conditions as at  $\tau = t_d$ , hence replacing  $t$  by  $t - t_d$

$$u(\tau = t) = \frac{\dot{u}(\tau = t_d)}{\omega_n} \sin \omega_n (t - t_d) + u(\tau = t_d) \cos \omega_n (t - t_d) + \frac{1}{m\omega_n} \int_{\tau=t_d}^{\tau=t} p(\tau) \sin \omega_n (t - \tau) d\tau$$

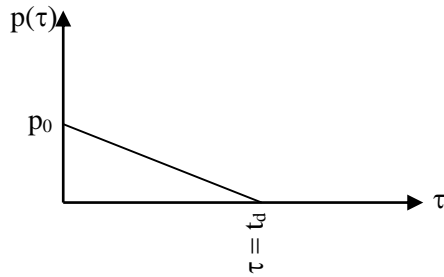
$$u(\tau = t) = \frac{p_0}{k} \sin(\omega_n t_d) \sin \omega_n (t - t_d) + \frac{p_0}{k} (1 - \cos \omega_n t_d) \cos \omega_n (t - t_d) + 0$$

$$u(\tau = t) = \frac{p_0}{k} (\cos \omega_n (t - t_d) - \cos \omega_n t)$$

$$u(\tau = t) = \frac{p_0}{k} \left( -2 \sin \omega_n \frac{2t - t_d}{2} \sin \omega_n \frac{-t_d}{2} \right)$$

$$u_{\max} = 2 \frac{p_0}{k} \sin \omega_n \frac{t_d}{2} \quad \text{when} \quad \sin \omega_n \frac{2t - t_d}{2} = 1$$

It is found that the maximum dynamic response is a function of  $\omega_n t_d$  or  $t_d/T$ . For  $t_d/T \geq 0.5$ , the maximum dynamic response is the same as it would have been had the force loading been infinite. This means that the maximum amplification occurs during the application of loading. However, if the loading is very short duration, such that  $t_d/T < 0.4$ , then the maximum response may occur after the loading, during the subsequent free vibration.

**(iv) An Instantaneous Right Angled Triangular Force of Amplitude  $p_0$** 


With no damping,

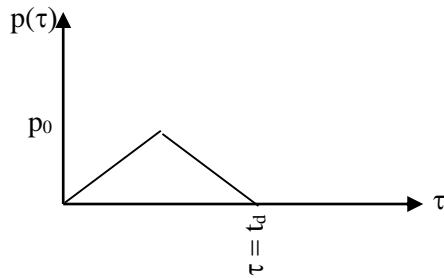
For  $\tau < t_d$

$$u(\tau = t) = \frac{p_0}{k} (1 - \cos \omega_n t) + \frac{p_0}{k t_d} \left( \frac{\sin \omega_n t}{\omega_n} - t \right)$$

For  $\tau > t_d$ ,

$$u(\tau = t) = \frac{p_0}{k \omega_n t} (\sin \omega_n t - \sin \omega_n (t - t_d)) - \frac{p_0}{k} \cos \omega_n t$$

As always, a plot of  $y(t)$  versus  $t_d/T$  would be very beneficial. For large values for instance in this case, the maximum dynamic displacement response approaches twice the static displacement value.

**(v) An Instantaneous Isosceles Triangular Force of Amplitude  $p_0$** 


With no damping,

For  $\tau < t_d / 2$

$$u(\tau = t) = \frac{2p_0}{k \omega_n t_d} (\omega_n t - \sin \omega_n t)$$

For  $t_d / 2 < \tau < t_d$

$$u(\tau = t) = \frac{2p_0}{k \omega_n t_d} [\omega_n (t_d - t) + 2 \sin \omega_n (t - t_d / 2) - \sin \omega_n t]$$

For  $\tau > t_d$ ,

$$u(\tau = t) = \frac{2p_0}{k \omega_n t_d} [2 \sin \omega_n (t - t_d / 2) - \sin \omega_n t - \sin \omega_n (t - t_d)]$$

An impacting particle (of small relative mass compared to mass of structure) imposes an impulse  $I = F\Delta t$  onto the structure. The magnitude of  $I = F\Delta t$  can be calculated as  $m\Delta v$  where  $m$  is the small mass and  $\Delta v$  the change of velocity at impact. If there is no rebound  $\Delta v$  is the approach velocity. Knowing that  $F\Delta t$  is the area under the impulse curve, making an estimate of the shape of the impulse curve and the duration  $\Delta t$ , we can thus estimate the peak amplitude. Hence, the impulse curve is defined.

**(vi) An Instantaneous Half Sine Force of Frequency  $\omega$  and Amplitude  $p_0$** 

With no damping,

For  $\tau < t_d$

$$u(\tau = t) = \frac{p_0}{k(1 - \omega^2 / \omega_n^2)} \left( \sin \omega t - \frac{\omega}{\omega_n} \sin \omega_n t \right)$$

For  $\tau > t_d$ ,

$$u(\tau = t) = -\frac{p_0 \omega / \omega_n}{k(1 - \omega^2 / \omega_n^2)} (\sin \omega_n t + \sin \omega_n (t - t_d))$$

An impacting particle (of small relative mass compared to mass of structure) imposes an impulse  $I = F\Delta t$  onto the structure. The magnitude of  $I = F\Delta t$  can be calculated as  $m\Delta v$  where  $m$  is the small mass and  $\Delta v$  the change of velocity at impact. If there is no rebound  $\Delta v$  is the approach velocity. Knowing that  $F\Delta t$  is the area under the impulse curve, making an estimate of the shape of the impulse curve and the duration  $\Delta t$ , we can thus estimate the peak amplitude. Hence, the impulse curve is defined.

**(vii) General Piecewise Linear Loading Functions**

General piecewise linear functions can be integrated and can be shown to produce response given by the following.

Without damping,

$$u(\tau = t) = \frac{1}{m\omega_n} (A(t) \sin \omega_n t - B(t) \cos \omega_n t)$$

$$\text{where } A(t) = \int_{\tau=0}^{\tau=t} p(\tau) \cos \omega_n \tau d\tau = \sum_{i=1}^{i=n} A(t_{i-1}) + \int_{t_{i-1}}^{t_i} p(\tau) \cos \omega_n \tau d\tau$$

$$\text{and } B(t) = \int_{\tau=0}^{\tau=t} p(\tau) \sin \omega_n \tau d\tau = \sum_{i=1}^{i=n} B(t_{i-1}) + \int_{t_{i-1}}^{t_i} p(\tau) \sin \omega_n \tau d\tau$$

where  $n$  is the number of linear segments.

If the loading is segmented piecewise linearly by  $\Delta t_i$ , the loading function within each segment is

$$p(\tau) = p(t_{i-1}) + \frac{\Delta p_i}{\Delta t_i} (\tau - t_{i-1}) \quad \text{for } t_{i-1} \leq \tau \leq t_i$$

where  $\Delta p_i = p(t_i) - p(t_{i-1})$  and  $\Delta t_i = t_i - t_{i-1}$

On substitution into the above integrals, and with integration,

$$\begin{aligned} A(t_i) &= A(t_{i-1}) + \frac{1}{\omega_n} \left( p(t_{i-1}) - t_{i-1} \frac{\Delta p_i}{\Delta t_i} \right) (\sin \omega_n t_i - \sin \omega_n t_{i-1}) \\ &\quad + \frac{\Delta p_i}{\omega_n^2 \Delta t_i} [\cos \omega_n t_i - \cos \omega_n t_{i-1} + \omega_n (t_i \sin \omega_n t_i - t_{i-1} \sin \omega_n t_{i-1})] \\ B(t_i) &= B(t_{i-1}) + \frac{1}{\omega_n} \left( p(t_{i-1}) - t_{i-1} \frac{\Delta p_i}{\Delta t_i} \right) (\cos \omega_n t_{i-1} - \cos \omega_n t_i) \\ &\quad + \frac{\Delta p_i}{\omega_n^2 \Delta t_i} [\sin \omega_n t_i - \sin \omega_n t_{i-1} - \omega_n (t_i \cos \omega_n t_i - t_{i-1} \cos \omega_n t_{i-1})] \end{aligned}$$

The above expressions represent the response at a time during the application of the loading. If the response during the ensuing free vibration is sought, then the expression must be evaluated at the end point of the loading and the initial conditions expression must be used.

**(viii) General Nonlinear Loading Functions**

General loading functions that cannot be classically integrated must be integrated numerically using integration techniques such as Simpson’s Rule.

Without damping,

$$\begin{aligned}
 u(\tau = t) &= \frac{1}{m\omega_n} \int_{\tau=0}^{\tau=t} p(\tau) \sin \omega_n (t - \tau) d\tau \\
 &= \sin \omega_n t \frac{1}{m\omega_n} \int_{\tau=0}^{\tau=t} p(\tau) \cos \omega_n \tau d\tau - \cos \omega_n t \frac{1}{m\omega_n} \int_{\tau=0}^{\tau=t} p(\tau) \sin \omega_n \tau d\tau
 \end{aligned}$$

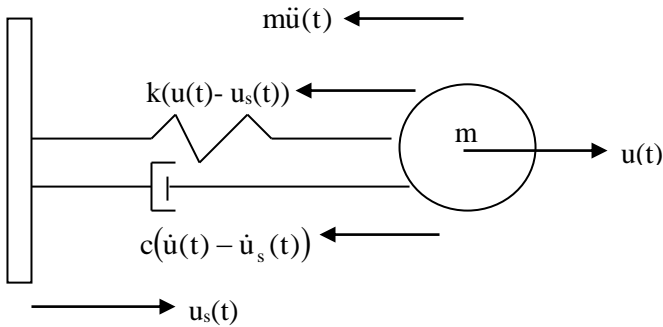
The integrals can be evaluated numerically with Simpson’s Rule which is piecewise parabolic.

$$\text{Integral} = \frac{h}{3} (I_1 + 4I_2 + 2I_3 + \dots + 2I_{n-2} + 4I_{n-1} + I_n)$$

In order to use Simpson’s Rule effectively, divide the integral functions into segments, within which the function can be well approximated by a cubic variation. Having three terms  $I_1$ ,  $4I_2$  and  $I_3$  is sufficient to model a cubic function exactly. Thus basically, we segment the integral function into piecewise cubic functions and apply Simpson’s Rule separately on each segment, summing the results in the end.

The above expressions represent the response at a time during the application of the loading. If the response during the ensuing free vibration is sought, then the expression must be evaluated at the end point of the loading and the initial conditions expression must be used.

#### 4.8.4.2 Determination of Maximum Dynamic Displacement, $u_{\max}$ by Solving the SDOF Undamped/Damped Linear Equation of Motion ODE (In Relative Terms) for Deterministic Time Domain Support Motion (Displacement, Velocity or Acceleration) With/Without Initial Conditions Using the Convolution Integral (Duhamel's integral)



In absolute terms, the equation of motion

$$m\ddot{u}(t) + c(\dot{u}(t) - \dot{u}_s(t)) + k(u(t) - u_s(t)) = 0$$

In relative terms

$$u_r(t) = u(t) - u_s(t)$$

Hence,

$$m(\ddot{u}_r(t) + \ddot{u}_s(t)) + c\dot{u}_r(t) + ku_r(t) = 0$$

$$m\ddot{u}_r(t) + c\dot{u}_r(t) + ku_r(t) = -m\ddot{u}_s(t)$$

Note that in absolute terms, we need the support displacement and velocity in the equation of motion whilst in relative terms we need only the support acceleration in the equation of motion. This resulting equation of motion above is similar to that which considers time domain force loading  $p(t)$ , and thus can be solved in exactly the same manner taking

$$p(t) = -m\ddot{u}_s(t)$$

The response will be obtained in relative terms as follows.

With damping,

$$\begin{aligned} u_r(\tau = t) &= \frac{1}{m\omega_d} \int_{\tau=0}^{\tau=t} p(\tau) e^{-\xi\omega_n(t-\tau)} \sin \omega_d(t-\tau) d\tau \\ &= \frac{1}{m\omega_d} \int_{\tau=0}^{\tau=t} -m\ddot{u}_s(\tau) e^{-\xi\omega_n(t-\tau)} \sin \omega_d(t-\tau) d\tau \\ &= \frac{1}{\omega_d} \int_{\tau=0}^{\tau=t} -\ddot{u}_s(\tau) e^{-\xi\omega_n(t-\tau)} \sin \omega_d(t-\tau) d\tau \\ u_{r\max}(\tau = t) &= \frac{1}{\omega_d} \text{MAX} \left[ \int_{\tau=0}^{\tau=t} \ddot{u}_s(\tau) e^{-\xi\omega_n(t-\tau)} \sin \omega_d(t-\tau) d\tau \right] \\ &= \frac{1}{\omega_d} S_v \end{aligned}$$

where  $S_v$  = pseudo spectral velocity

## 4.9 GNL, MNL Implicit and Explicit Direct Transient Response Analysis

### 4.9.1 Nature of the Dynamic Loading Function

The solution can be used to ascertain the modal properties of the system by performing a time domain impulse analysis to excite the modes of interest. The duration of the impulse must be sufficiently long to excite the first fundamental mode, which is usually of concern. This would result in a response that includes the first fundamental mode and most likely higher modes as well. The first fundamental mode is readily ascertained from inspection of the response time history curve at any node. Higher natural frequencies can also be ascertained by performing an FFT on the response curve.

The solution method can be used to solve dynamic systems subjected to: -

- (a) **Deterministic non-periodic short duration impulse (a.k.a. blast)** loading functions with subsequent **wave propagation**
- (b) **Random non-stationary short duration impulse** loading functions
- (c) **Projectile (a.k.a. impact)** excitations with subsequent **wave propagation** (Explicit Analysis Only)
- (d) **Brittle snap or redundancy check** excitations (Explicit Analysis Only)

In blast, impact and brittle snap problems, the force amplitude does not repeat itself regularly but rises from zero to a maximum or a series of maxima until settling down to a constant value. The starting transient is significant and so the solution is carried out in the time domain.

If the forcing function is a random non-stationary forcing function such that the random forces start from a low-level building up to a maximum then dying away, such as in a seismic event, then exact solution methods are not established. Instead, we could either analyze a set of such events using deterministic transient solution methods and then average or envelope the results or alternatively use the crude response spectrum method which envelopes the response spectra of a series of time histories.

**In this NONLINEAR TIME DOMAIN solution**, the static response must be added to the dynamic response if the dynamic analysis is performed about the initial undeflected (by the static loads) state with only the dynamic loads applied, hence causing the dynamic response to be measured relative to the static equilibrium position. **Hence, the total response = the dynamic response + the static response to static loads.**

**Alternatively, in this NONLINEAR TIME DOMAIN solution**, if the dynamic analysis is performed with the deflected static shape as initial input and the static loads maintained throughout the dynamic excitations, the total or absolute response (static and dynamic) is obtained straight away from the dynamic analysis. **Hence total response = dynamic response (which already includes the static response to static loads).**

### 4.9.2 Deterministic Non-Periodic Short Duration Impulse (a.k.a. Blast) Loading Functions With Subsequent Wave Propagation

Estimates of the induced stress in a **linear elastic** body due to an **impulsive blast** may be made easily in some cases with a simpler static method of analysis. **Section 4.7.4** describes this concept further.

Key wavefront parameters are

- $p_s$  peak overpressure
- $T_s$  positive phase duration
- $i_s$  specific impulse (area under pressure-time curve)
- $t_a$  arrival time of blast wave

These are well established

Rankine-Hugonot 1870

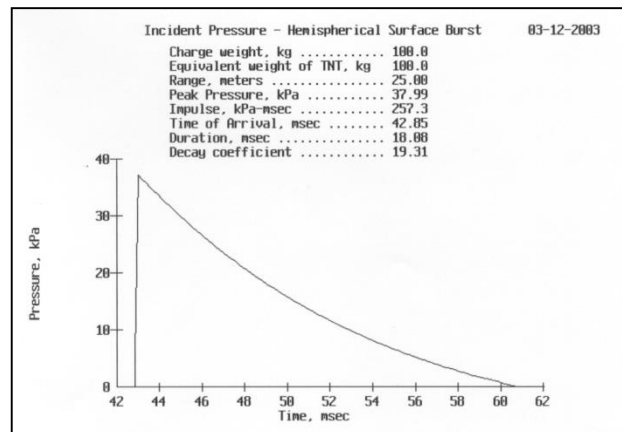
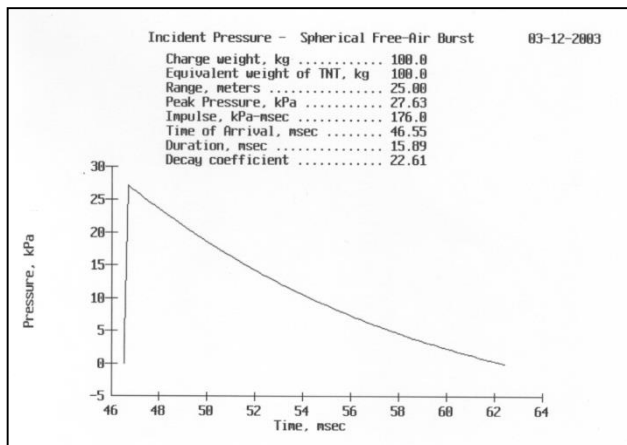
$$W = \text{charge weight} \quad R = \text{distance from charge}$$

Blast wave scaling laws

$$R_1/R_2 = (W_1/W_2)^{1/3}$$

$$\text{Scaled distance } Z = R/W^{1/3}$$

Spherical airburst – baseline condition and Hemispherical surface burst – typical condition for terrorist attack.



### 4.9.3 Projectile Crash (a.k.a. Impact) (and Impulsive Blast) Analysis With Subsequent Wave Propagation

A projectile crash analysis involves the specification of an initial velocity. Hence the a structure is given an initial momentum. The motion is then subsequently retarded when it impacts another elastic body. The impulse (i.e. force) generated depends on the duration taken to retard the momentum, i.e. the impulsive force is the change in momentum divided by the duration. This duration is a function of the stiffness of the elastic body. **This is essentially the difference between a projectile crash analysis and a blast analysis, the latter of which has a predefined impulsive force which is independent of the stiffness of the retarding elastic body.** Now a consequence of the fact that the force in a projectile analysis being dependent upon the stiffness of the elastic body is that the result of the analysis is very much dependent upon the assumptions made of these stiffnesses. A blast analysis presents a predefined impulsive force and the response of the different modes of the structure is simply dependent upon the predefined magnitude of the impulsive force and the dynamic amplification (which is dependent upon  $t_d/T_i$  where  $t_d$  is the duration of the impulse and  $T_i$  the period of the mode, noting that the theoretical maximum dynamic amplification is only 2.0). Now on the other hand, a projectile impact analysis does not predefine the magnitude of the impulsive force. It just defines the momentum. The impulsive force is the change of momentum divided by the duration of the impulse. A stiff retarding structure will offer a short retarding duration and hence resulting in large internal force magnitudes. The impulsive dynamic amplification will still be at most 2.0, but the magnitude of the force could be quite considerable. Hence the definition of the stiffness of the structure retarding the motion is of paramount importance in any projectile impact analysis.

Any **projectile crash** will set off a wave propagation. (Note that an **impulsive blast** will also set off a wave propagation). As the wave propagates through the structure, parts of the structure that are initially at rest are suddenly forced into motion as the wavefront passes. The highest frequency wave that can be propagated depends upon the distance between consecutive nodes. If the highest frequency to be propagated is  $f$  Hz and the wave velocity is  $v$  m/s, then the wavelength is  $\ell = v/f$ . There should be at least 4 nodes over this wavelength for the wave to propagate<sup>7</sup>. **(Another way of looking at this concept is when stresses resulting from an impulsive blast is to be obtained using modal methods, of course limited to linear analyses; in order for stresses originating from high excitation frequencies to be captured, the mesh has got to be sufficiently fine to represent the higher natural modes as they are the ones that will be amplified the most).** A uniform mesh of elements that have all sides of the same length will allow waves to propagate equally in any direction. If a change in mesh density is used within the model, then this gives rise to a change in the effective numerical impedance where the mesh density changes. A fine to coarse mesh transition acts as a filter for the high frequency waves that can be transmitted by the fine mesh but not by the coarse mesh. Hence, spurious high frequency internal wave reflections occur back into the fine mesh at these mesh density changes. Hence a **uniform mesh** is paramount to wave propagation problems. Wave propagation analysis is performed using an explicit time integration scheme with the time step slightly less than the time it takes the wavefront to travel between two adjacent nodes. If the time step is longer than that, there is an effective truncation of the highest frequency that can be propagated, and if shorter then an excessive amount of computation is carried out unnecessarily. Condensation techniques that truncate high frequency modes of the structure should NOT be used for wave propagations problems. Although high frequency modes of the equations of motion have no physical meaning that are important numerically for wave propagation problems, if they are not included then the wavefront gets dispersed and ceases to be as sharp as they should be. **Hence it can be concluded that unlike other dynamic analysis problems, higher modes of vibration is paramount in wave propagation problems (i.e. projectile impact and impulsive blast analysis).**

**Strain-rate** effects often are important for **projectile crash** (and **impulsive blast** for that matter as that is also a form of wave propagation problem) analysis. The **Cowper-Symonds** rules are a common simplified method of accounting for strain-rate effects in a MNL solution. Strain-rates will affect the stress-strain curve in a number of ways, namely

<sup>7</sup> NAFEMS. *A Finite Element Primer*. NAFEMS Ltd., Great Britain, 1992.

- I. The ‘static’ (i.e. low strain-rate, about 1E-6) stress-strain curve is modified by the Cowper-Symond factor (which is completely defined by the parameters C and P), i.e. a higher strain-rate yields higher stress values.

$$\frac{\sigma_d}{\sigma_s} = 1 + \left( \frac{\dot{\epsilon}}{C} \right)^{\frac{1}{P}}$$

- II. The ultimate failure strain is also dependent upon the strain-rate, i.e. a higher strain-rate causes a lower failure strain.  
 III. The Cowper-Symond values itself are strain dependent.

For S275 and S355 steel, typical Cowper-Symond C and P parameters are as follows.

	0-3%	5%	UTS (19.9%)
C (K)	40.4	300	6844
P (n)	5	2.5	3.91

These result in the following Cowper-Symond factors.

**Strain level:**

Rate [s <sup>-1</sup> ]:	0-3%	5%	UTS (19.9%)
1.00E-06	1.03011	1.00041	1.00305
1.00E-04	1.07564	1.00257	1.00991
1.00E-02	1.18999	1.01619	1.03218
1.00E+00	1.47723	1.10213	1.10450
1.00E+02	2.19874	1.64439	1.33932

However, the strain-rate of the material during testing must also be taken into account. This occurs because the strain-rate at the necking area is greater than elsewhere. (Note that we have already taken the fact that the necking area is smaller in the derivation of the ‘static’ stress-strain curve, this being the engineering stress-strain to the true stress-strain conversion). The following enhancement factors would be applicable for the standard test rates for “static tests”.

0-3%	5%	UTS (19.9%)
1.080	1.015	1.030

The absolute strain-rate enhancement, taking the test rate into account, is presented in the table below.

**Strain level:**

Rate [s <sup>-1</sup> ]:	0-3%	5%	UTS (19.9%)
1.00E-06	0.95381	0.98562	0.97384
1.00E-04	0.99596	0.98775	0.98050
1.00E-02	1.10184	1.00117	1.00212
1.00E+00	1.36780	1.08584	1.07233
1.00E+02	2.03587	1.62009	1.30031

For the S275 and S355 carbon steels the failure true strain of 19.9% is derived from the basic tensile test on a standard test coupon. This elongation is measured over the whole test specimen and is therefore not representative of the actual strain in the necked region of the test specimen. The strain in the necking region is based on the reduction in cross-sectional area of the specimen at the necking point. Unfortunately, this is not usually measured during the standard tensile test, but is typically about 50-60% for these carbon steels.

BS 6399-1 specifies accidental vehicle impact loads as follows.

$$F = \frac{0.5mv^2}{\delta_c + \delta_b}$$

$m$  is the gross mass of the vehicle (in kg);  
 $v$  is the velocity of the vehicle (in m/s) normal to the barrier;  
 $\delta_c$  is the deformation of the vehicle (in mm);  
 $\delta_b$  is the deflection of the barrier (in mm).

**11.2** Where the car park has been designed on the basis that the gross mass of the vehicles using it will not exceed 2500 kg the following values are used to determine the force  $F$ :

$m$  = 1 500 kg<sup>1)</sup>;  
 $v$  = 4.5 m/s;  
 $\delta_c$  = 100 mm unless better evidence is available.

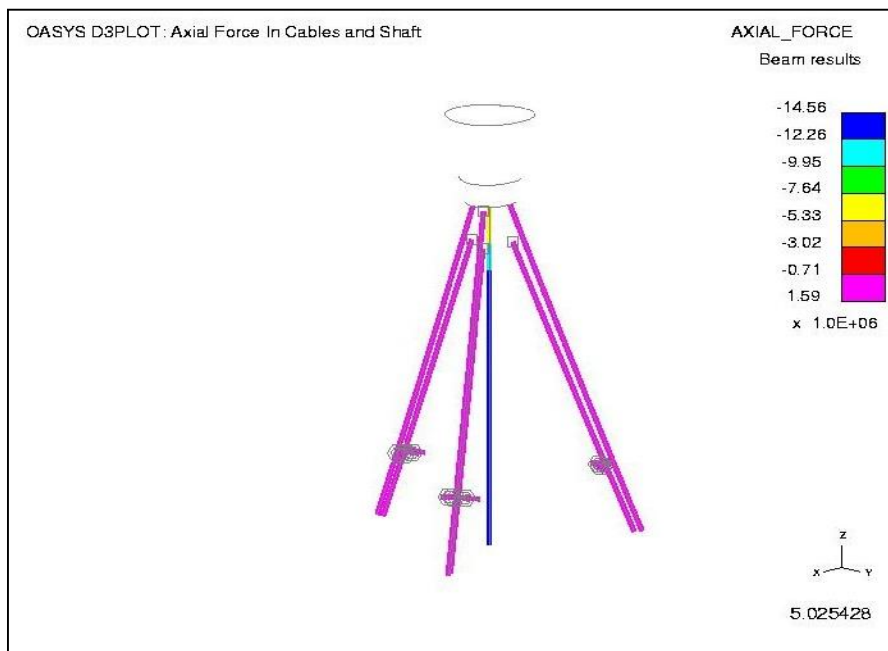
For a rigid barrier, for which  $\delta_b$  may be taken as zero, the force  $F$  appropriate to vehicles up to 2 500 kg gross mass is taken as 150 kN.

**11.3** Where the car park has been designed for vehicles whose gross mass exceeds 2500 kg the following values are used to determine the force  $F$ :

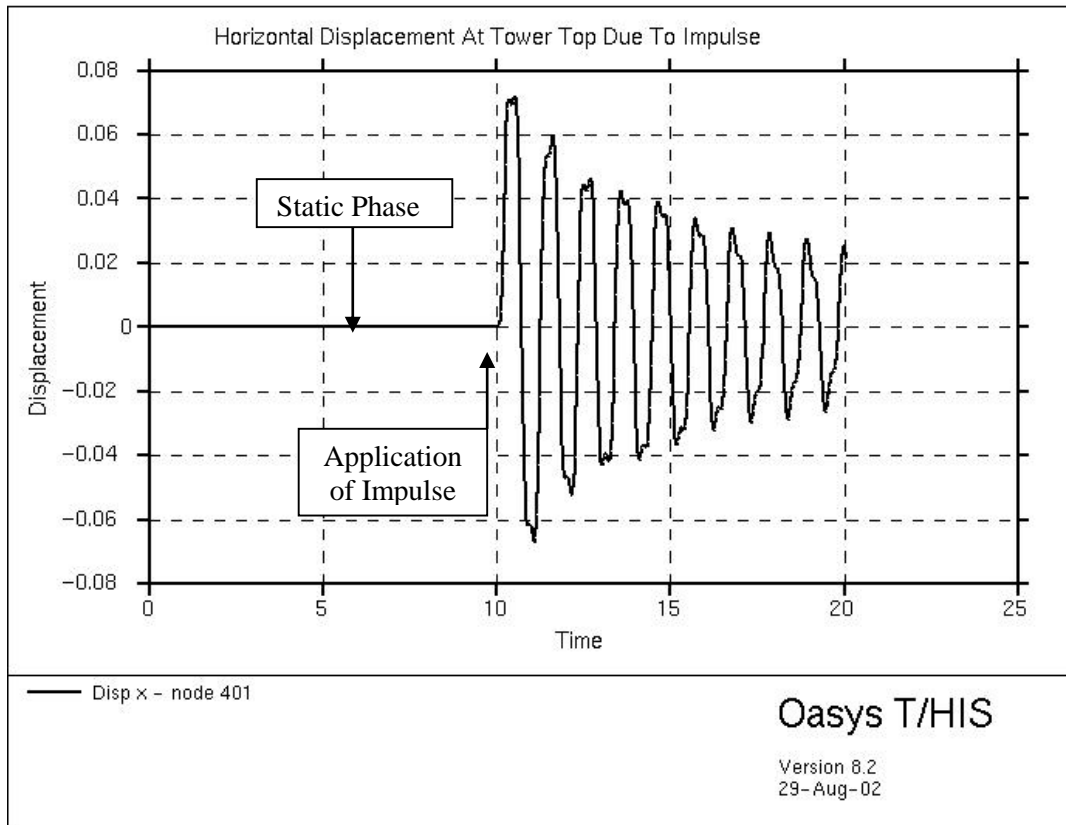
$m$  = the actual mass of the vehicle for which the car park is designed (in kg);  
 $v$  = 4.5 m/s;  
 $\delta_c$  = 100 mm unless better evidence is available.

#### 4.9.4 Brittle Snap or Redundancy Check Excitation

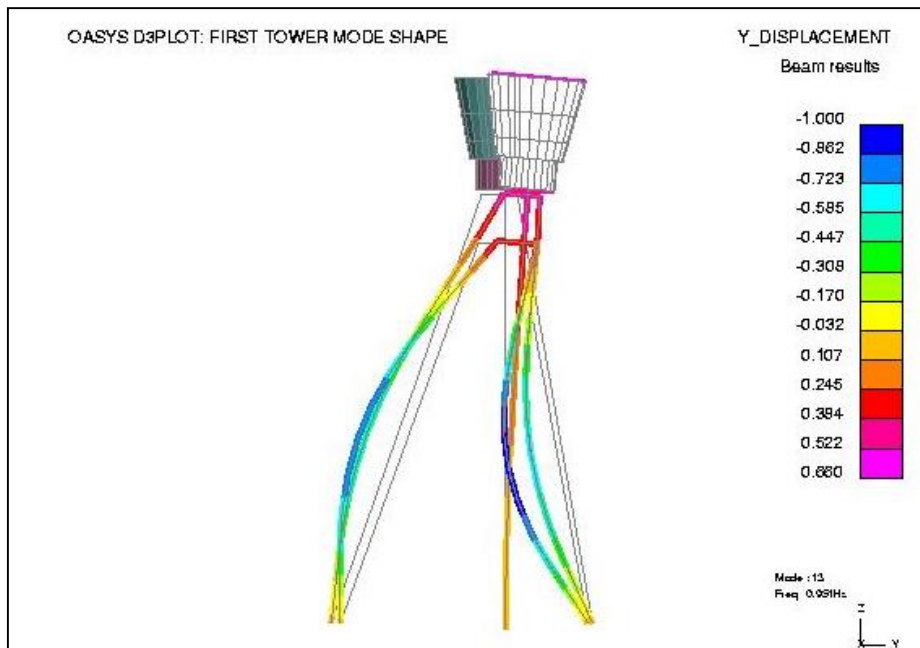
A brittle snap or redundancy check analysis include the analysis of sudden fracture of structural members from the static equilibrium configuration such as the sudden snapping of a prestressed structural cable, and evaluates the redundancy available within the structure. This analysis always involves a two-stage procedure. The first stage involves a static solution by a linear static method or a nonlinear static method (either Newton's tracing the equilibrium path SOL 106, an implicit dynamic relaxation by SOL 129 or an explicit dynamic relaxation method LS-DYNA) in order to obtain the deflected configuration and the stiffness of the structure in the deflected configuration  $K_T$  by the prestress (prestressing of structural members such as cables contribute greatly to a large change in stiffness within the static solution and hence will require a nonlinear static method) and gravity. The second stage involves a restart into a nonlinear transient dynamic solution scheme with no additional dynamic excitation but with a change in the structure (in the deletion of a member that fails in brittle fashion simulating a redundancy check) or a change in boundary condition (to simulate the effect of the loss of a support or anchor attached to a prestressed cable etc.). An example would be the gradual prestressing of structural cable elements within a suspension bridge or a cable prestressed tower until a static solution (by SOL 106, implicit SOL 129 or explicit LS-DYNA) is achieved. The cables can be prestressed using a gradual temperature load case (or a gradual enforced displacement on the cable anchorage points) plus gravitational loads until the correct level of prestress is achieved (by SOL 106, implicit SOL 129 or explicit LS-DYNA). Then with a restart into an explicit transient dynamic scheme of LS-DYNA, the boundary condition supporting the cable is released or a cable element is deleted, causing the structure to experience an out-of-balance of forces and hence vibrate to a new static equilibrium configuration.



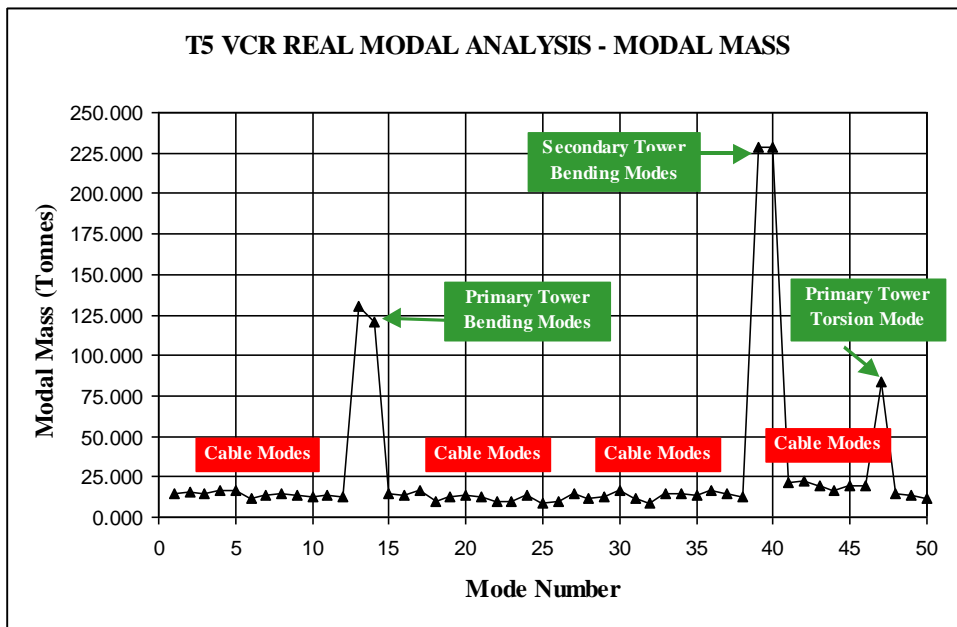
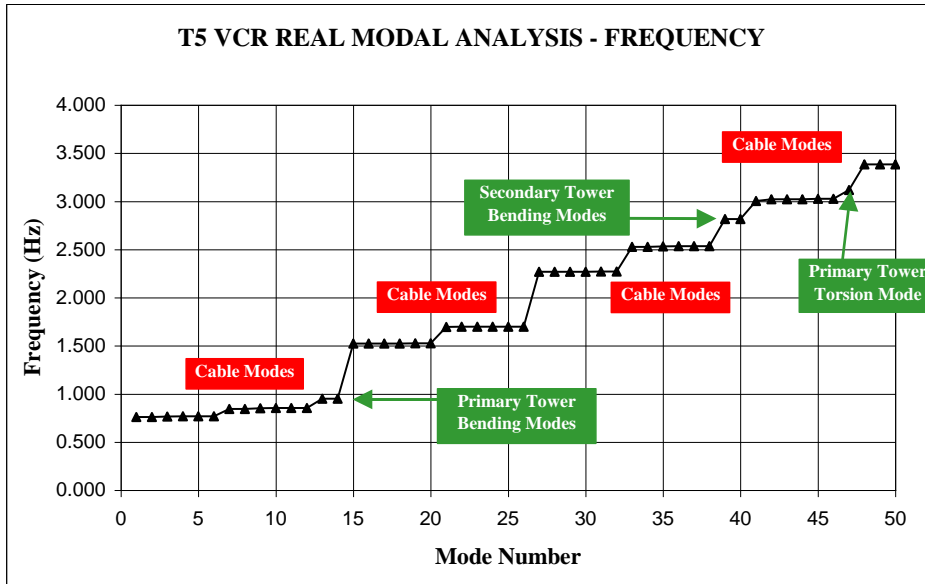
The Heathrow T5 Visual Control Tower was analyzed to a sudden brittle cable failure. An initial dynamic relaxation phase was performed (in LS-DYNA) in order to attain the static equilibrium position under gravity load with the correct pretension in the cables. The prestress in the cables was applied by a prescribed displacement at the cable anchorages in the direction along the cable axis during the dynamic relaxation phase until the force in cables reached a value of approximately 1.59MN. At this stage it is a good idea to confirm the natural frequency of the model by applying an impulsive force of say 0.3 seconds (knowing the fundamental mode to be approximately 0.95Hz) duration at the top of the tower. The frequency of the displacement response is observed to be approximately 0.95 Hz.



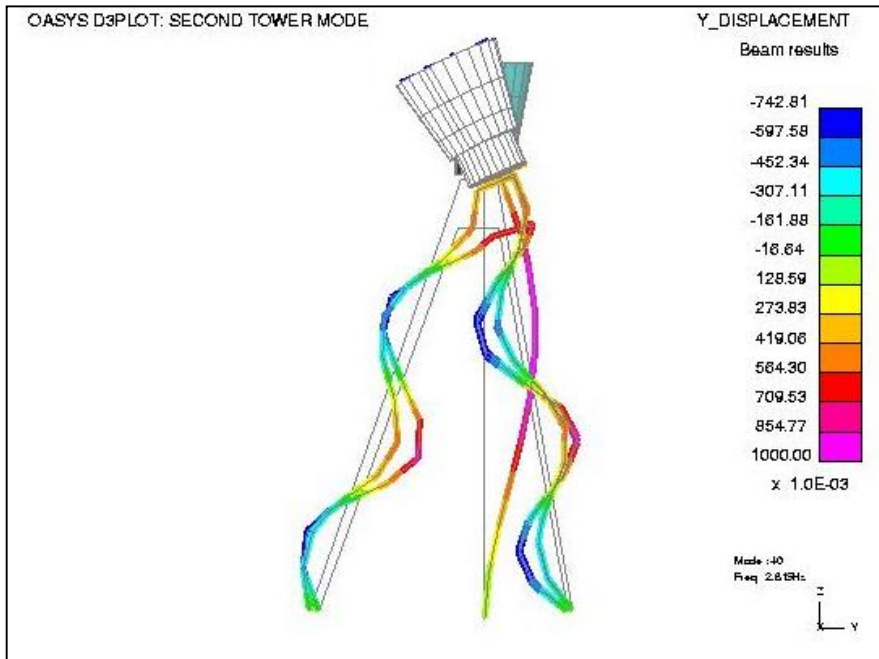
This correlates well with the natural modes analysis performed in previous linear NASTRAN analyses.



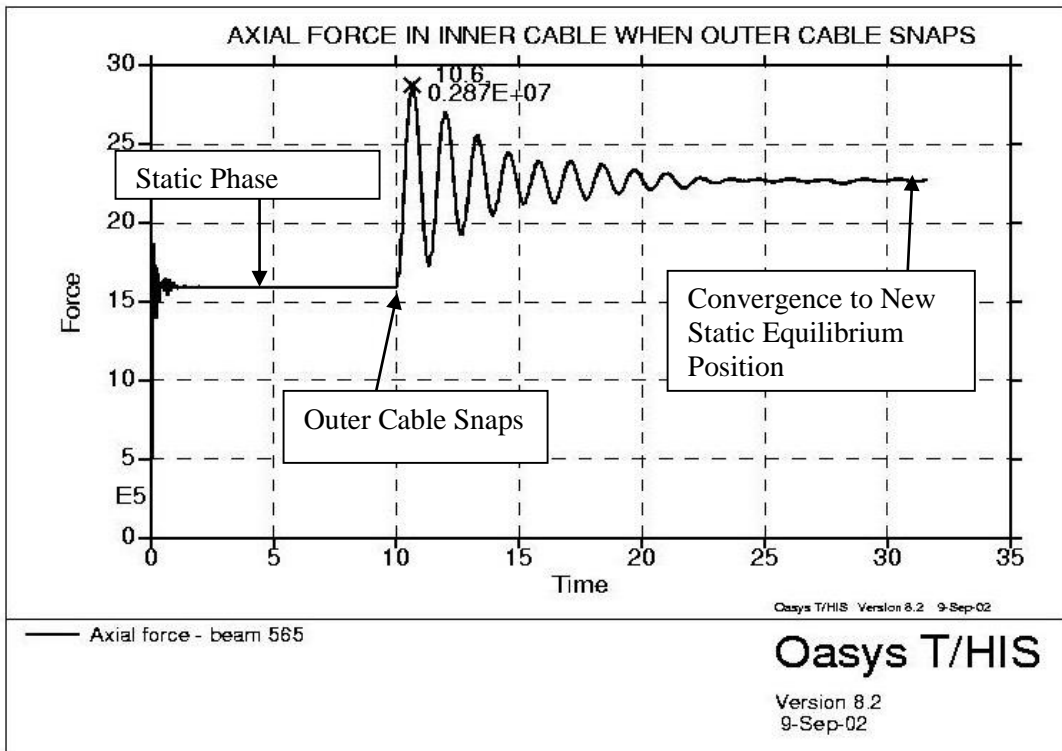
For reference, the natural frequencies of all modes up to 50Hz are presented as follows. The modal masses (normalized to MAX unity) are also presented for this elegant 680.9 tonne structure.



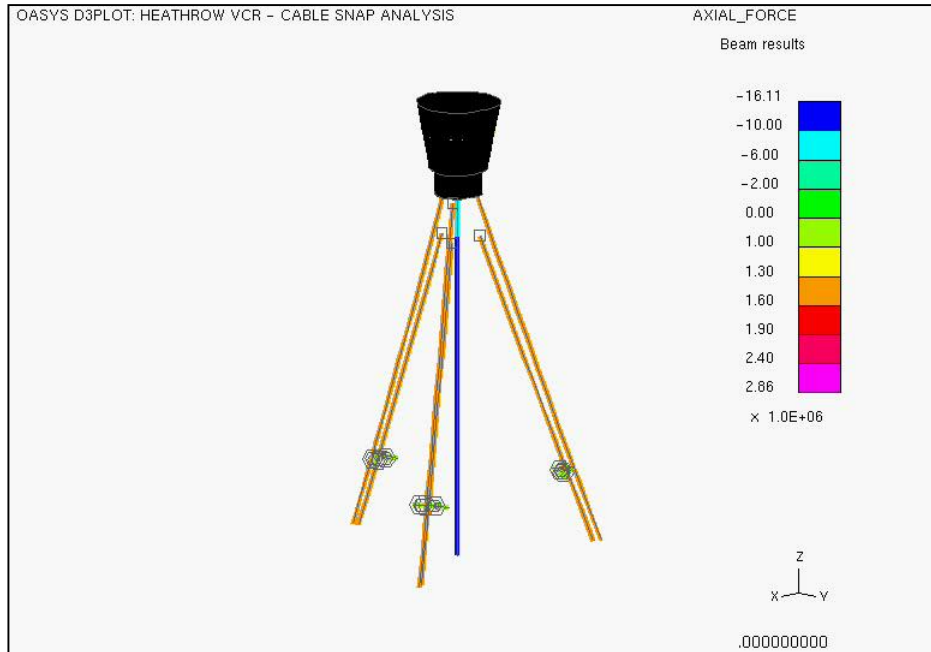
The static solution was followed by a transient dynamic phase where the displacement constraint in one of the cables was released, effectively modelling the consequence of a cable suddenly snapping. The resulting effect on the structure is of an impulse of certain duration. On animation of the displacement response (with or without a vector animation of the velocity response), it can be observed if higher modes were excited or not as this will affect the distribution of stresses within the system. Exciting the second tower mode (as actually occurred in this particular case) will certainly cause certain effects on the shaft which will not be captured from any static based analysis.



The axial force time history in an inner cable when the outer cable snaps is shown.



The time enveloped axial force within the 1D elements of the system is presented for design purposes. Of course, for completion, the time enveloped shear in 2 directions, bending about 2 axes and torsion would also have to be presented.



#### 4.9.5 GNL, MNL Explicit Central FD Scheme for Newton's Dynamic Equilibrium ODE (LS-DYNA)

##### 4.9.5.1 Solution of Partial or Ordinary Differential Equations Using Finite Difference (FD) Schemes

Finite difference mathematical methods are used to solve partial and ordinary differential equations (PDEs and ODEs) which are too complicated for exact analytical methods. Finite difference methods are thus numerical methods that are subjected to stability and accuracy requirements when solving the differential equations.

The only mathematics required is the elegant Taylor's theorem which states that for a function  $\phi(t)$ ,

$$\phi(t + \Delta t) = \phi(t) + \Delta t \frac{\partial \phi(t)}{\partial t} + \frac{(\Delta t)^2}{2} \frac{\partial^2 \phi(t)}{\partial t^2} + \dots$$

The expression will be exact if an infinite number of terms are taken and if  $\Delta t$  is small. We can also readily state that

$$\phi(t - \Delta t) = \phi(t) - \Delta t \frac{\partial \phi(t)}{\partial t} + \frac{(\Delta t)^2}{2} \frac{\partial^2 \phi(t)}{\partial t^2} - \dots$$

Finite difference schemes utilize the above two expressions to reduce the PDEs or the ODEs to a set of coupled or uncoupled equations with the same number of unknowns as the number of equations so that they can be solved. A set of coupled equations will require simultaneous solution algorithms (or inverting the matrix, which of course is not performed as is computationally too intensive). A finite difference scheme, which reduces the PDEs or ODEs to a set of coupled equations, is termed an implicit scheme. In an implicit scheme, the value for a variable at a particular grid at  $t+\Delta t$  is related to variables at adjacent grid points for the same time level. Conversely, a set of uncoupled equations do not require any simultaneous solution algorithms. A finite difference scheme, which reduces the PDEs or ODEs to a set of uncoupled equations, is termed an explicit scheme. An explicit scheme solves for unknowns at time  $t+\Delta t$  expressed directly in terms of known values at time  $t$  (or before) and already known values at  $t+\Delta t$ .

The **central (finite) difference scheme** subtracts and adds the two Taylor equations above to give the two expressions below for the first and second differential, both of which have an error in the order  $(\Delta t)^2$ .

$$\frac{\partial \phi(t)}{\partial t} = \frac{\phi(t + \Delta t) - \phi(t - \Delta t)}{2\Delta t} + O(\Delta t)^2$$

$$\frac{\partial^2 \phi(t)}{\partial t^2} = \frac{\phi(t + \Delta t) - 2\phi(t) + \phi(t - \Delta t)}{(\Delta t)^2} + O(\Delta t)^2$$

The **forward (finite) difference scheme** rearranges the first Taylor expression to give

$$\frac{\partial \phi(t)}{\partial t} = \frac{\phi(t + \Delta t) - \phi(t)}{\Delta t} + O(\Delta t)$$

The **backward (finite) difference scheme** rearranges the second Taylor expression to give

$$\frac{\partial \phi(t)}{\partial t} = \frac{\phi(t) - \phi(t + \Delta t)}{\Delta t} + O(\Delta t)$$

**These schemes in themselves are not implicit or explicit.** The application of these schemes to PDEs or ODEs will result in sets of equations that are implicit or explicit. The differential equation that concerns us is Newton's Dynamic Equilibrium Ordinary Differential Equation.

#### 4.9.5.2 Mathematical Formulation of Analysis – Explicit Central Finite Difference Scheme

Newton's Dynamic Equilibrium Ordinary Differential Equation at time  $t$  can be written as

$$[M]\{\ddot{u}(t)\} + [C(t)]\{\dot{u}(t)\} + [K(t)]\{u(t)\} - \{P(t)\} = \{0\}$$

or as follows

$$M\dot{v}_i + C\dot{v}_i + K v_i = f_i$$

Applying the central finite difference scheme

$$\frac{\partial u(t)}{\partial t} = \frac{u(t + \Delta t) - u(t - \Delta t)}{2\Delta t} + O(\Delta t)^2$$

$$\frac{\partial^2 u(t)}{\partial t^2} = \frac{u(t + \Delta t) - 2u(t) + u(t - \Delta t)}{(\Delta t)^2} + O(\Delta t)^2$$

or in other notations

$$\dot{v}_i = \frac{v_{i+1} - v_{i-1}}{2\Delta t} \quad \ddot{v}_i = \frac{\dot{v}_{i+1/2} - \dot{v}_{i-1/2}}{\Delta t} = \frac{v_{i+1} - 2v_i + v_{i-1}}{\Delta t^2}$$

we arrive to the finite difference expression

$$[M] \left\{ \frac{u(t + \Delta t) - 2u(t) + u(t - \Delta t)}{(\Delta t)^2} \right\} + [C(t)] \left\{ \frac{u(t + \Delta t) - u(t - \Delta t)}{2\Delta t} \right\} + [K(t)]\{u(t)\} - \{P(t)\} + O(\Delta t)^2 = \{0\}$$

The only unknown at time  $t + \Delta t$  in this expression is the displacement vector.

$$v_{i+1} = \left( M + \frac{C\Delta t}{2} \right)^{-1} \left[ \Delta t^2 (f_i - K v_i) + 2M v_i - \left( M - \frac{C\Delta t}{2} \right) v_{i-1} \right]$$

We need to know initial values  $\{u(t = 0)\}$  and  $\{u(t = -\Delta t)\}$  to begin computation. However, we usually only know the initial displacement  $\{u(t = 0)\}$  and velocity  $\{du/dt(t = 0)\}$ . One method is to define a fictitious quantity  $\{u(t = -\Delta t)\}$  with the following procedure.

$$\dot{v}_o = \frac{v_1 - v_{-1}}{2\Delta t} \quad \ddot{v}_o = \frac{v_1 - 2v_o + v_{-1}}{\Delta t^2}$$

Eliminating  $\{u(t = \Delta t)\}$ , hence solving for  $\{u(t = -\Delta t)\}$ ,

$$v_{-1} = v_o - \Delta t \dot{v}_o + \frac{\Delta t^2}{2} \ddot{v}_o$$

in which from equilibrium conditions we can deduce

$$\ddot{v}_o = \frac{1}{M} (f_o - C\dot{v}_o - K v_o)$$

Therefore, knowing the initial displacement  $\{u(t = 0)\}$  and velocity  $\{du/dt(t = 0)\}$ , we can obtain the fictitious quantity  $\{u(t = -\Delta t)\}$ . Now with  $\{u(t = 0)\}$  and  $\{u(t = -\Delta t)\}$  we can begin computation.

Note however, the expression for  $\{u(t)\}$  can only be written explicitly after inverting the  $[M]$  matrix. In order to avoid a complicated  $[M]$  matrix inversion (effectively solving the then coupled simultaneous equations), the mass matrix must be diagonal. This is thus a requirement in LS-DYNA for all elements to have lumped mass formulations instead of coupled (or consistent) mass matrix formulations. This effectively maintains the explicit solution scheme. Had the mass matrix been coupled, simultaneous equations need to be solved making the solution scheme implicit. Also note that the time step may vary from time to time. Thus, in the above finite difference approximation, for completion, it must be stressed that the term  $2\Delta t$  as the denominator in the velocity finite difference expression is the total time step over two steps, or the average multiplied by two.

It is crucial to remember that not all the terms within the Taylor's Expansion were utilized. In this case, the first 3 terms was utilized for the variation of displacement. This means that the displacement is **parabolic**, velocity is

**linear** and the acceleration is **constant** over the time step. Hence that the **displacement error** in the finite difference approximation of the ODE is of the order of the square of the time step,  $O(\Delta t)^2$ .

**The central finite difference solution scheme adopted in LS-DYNA is**

- IV. Conditionally stable as long as  $\Delta t < T_{\min}/\pi$**
- V. Second order accurate since  $O(\Delta t)^2$**

#### 4.9.5.3 Stability

The stability of any finite difference scheme can be investigated by the von Neumann Fourier method of stability analysis. Using this method, it can be shown for this case that for stability of Newton's undamped dynamic equilibrium ODE

$$\Delta t < \frac{2}{\omega_{\text{MAX}}}$$

For Newton's damped dynamic equilibrium ODE, the stability condition is

$$\Delta t < \frac{2}{\omega_{\text{MAX}}} \left( \sqrt{1 + \zeta^2} - \zeta \right)$$

Damping thus further reduces the critical time step.

The time step is limited by the largest natural frequency of the structure which in turn is limited by the highest natural frequency of any individual element in the finite element mesh. The solution technique is conditionally stable, which means that the timestep must be kept small enough for the solution to have a physical meaning. Physically, the timestep size has to be less than the time taken for a sound wave to traverse the smallest deformable (i.e. non-rigid) element in the model so that a stress wave which travels through the element will cause a stress to develop within the element and not jump across it. This is because the speed of the sound wave  $c$  through the element is some function of its natural frequency. Hence, the timestep,  $\Delta t$  has to be calculated for each and every element and the smallest governs the timestep for the whole analysis. Since we do not want the stress wave (at the speed of sound) to jump the element, the element must be less stiff, longer and/or of greater mass, thus of lower natural frequency. Since  $T=2\pi/\omega$ , the conditionally stable explicit solution algorithm requires that the time step subdivide the lowest period by  $\pi$  for stability (for the undamped case).

$$\Delta t < 2 / \omega_{\text{max}}$$

$$\Delta t < T_{\min} / \pi$$

Hence to have a large time step: -

- (i) avoid as far as possible short, light and stiff elements
- (i) make the relatively stiffer elements rigid
- (ii) employ mass scaling but ensure that the total mass added is not too much as to decrease the accuracy significantly; mass is added to elements so that their timestep is increased to the minimum set value; this automatic computation does not apply to spring elements, if which is the governing element, the user should manually add lumped masses to their nodes
- (iii) ensure limited hourglassing as distorted elements will decrease time step
- (iv) employ subcycling if there are relatively few small elements controlling the time step and the bulk of the elements have a stable time step at least twice that of the smallest element; subcycling divides elements into groups of timestep of  $\Delta t, 2\Delta t, 4\Delta t, 8\Delta t, 16\Delta t, 32\Delta t$  and so on.

For the Hughes-Liu (constant moment) beam and truss element, the critical time step is

$$\Delta t = L/c$$

where  $c$  = speed of sound wave  $(E/\rho)^{0.5}$ . This is as follows. We have said that

$$\Delta t < 2 / \omega_{\text{max}}$$

Now, for a truss

$$\omega_{\max} = 2c/L$$

Hence,

$$\Delta t < 2 / \omega_{\max} = L/c$$

For the Belytschko beam (linear moment), the critical time step is given

$$\Delta t = L/c$$

if the highest frequency is axial, but if the bending frequency is higher, then it is given by

$$\Delta t = \frac{0.5L}{c \sqrt{3I \left[ \frac{3}{12I + AL^2} + \frac{1}{AL^2} \right]}}$$

where I is the maximum moment of inertia and A the area.

For shell elements, the critical time step is

$$\Delta t = L/c$$

where L is the characteristic length and c is given by

$$c = \sqrt{\frac{E}{\rho(1-\nu^2)}}$$

For solid elements, the critical time step is

$$\Delta t = \frac{L}{\left\{ \left[ Q + \{Q^2 + c^2\}^{1/2} \right] \right\}}$$

where Q is a function of some bulk viscosity coefficients. For elastic materials with constant bulk modulus, the speed of sound c is given by

$$c = \sqrt{\frac{E(1-\nu)}{\rho(1+\nu)(1-2\nu)}}$$

The critical time step for a scalar spring is

$$\Delta t = 2 \sqrt{\frac{2M_1M_2}{k(M_1 + M_2)}}$$

From the critical time step equations, we can conclude that

- I. Since  $\Delta t \propto \rho^{1/2}$ , mass scaling is only marginally effective in increasing time step.
- II. Since  $\Delta t \propto L$ , increase the dimension of the element is very effective in increasing time step.
- III. Comparison of the critical time step for the truss element and the solid element shows that, for non-zero Poisson's ratio, the solid element gives considerably smaller time steps. The critical time step for shell elements is much more comparable to that of the truss element for non-zero Poisson's ratio.

#### 4.9.5.4 Accuracy

It is crucial to remember that not all the terms within the Taylor's Expansion were utilized. In this case, the first 3 terms was utilized for the variation of displacement. This means that the displacement is **parabolic**, velocity is **linear** and the acceleration is **constant** over the time step. Hence that the **displacement error** in the finite difference approximation of the ODE is of the order of the square of the time step,  $O(\Delta t)^2$ .

The time step size requirement to satisfy stability is usually sufficient to satisfy accuracy requirements. It is often mentioned that for good accuracy, the time step must subdivide the lowest period of *interest* by 10, a condition which is usually satisfied if the lowest period is subdivided by  $\pi$ . The order of error generated as detailed above must however be remembered.

#### 4.9.6 GNL, MNL Implicit Newmark Scheme for Newton's Dynamic Equilibrium ODE (MSC.NASTRAN)

##### 4.9.6.1 Mathematical Formulation of Analysis – Implicit Newmark Scheme

The Newmark method was proposed by Nathan Newmark and it is a general method that encompasses a family of different integration schemes including the linear acceleration and constant-average-acceleration methods. This method can be derived by considering the Taylor series expansions of the displacement and velocity at time  $t_{i+1}$  about  $t_i$  with some remainder terms.

$$v(t_{i+1}) = v(t_i) + \Delta t \left. \frac{dv}{dt} \right|_{t=t_i} + \frac{\Delta t^2}{2} \left. \frac{d^2v}{dt^2} \right|_{t=t_i} + \frac{\Delta t^3}{3!} \left. \frac{d^3v}{dt^3} \right|_{t=t_i+\theta_1}$$

$$\dot{v}(t_{i+1}) = \dot{v}(t_i) + \Delta t \left. \frac{d^2v}{dt^2} \right|_{t=t_i} + \frac{\Delta t^2}{2} \left. \frac{d^3v}{dt^3} \right|_{t=t_i+\theta_2}$$

where  $0 < \theta_{1,2} < 1$ . We can now approximate the displacement and velocity using truncated Taylor series.

$$v_{i+1} = v_i + \Delta t \dot{v}_i + \frac{\Delta t^2}{2} \ddot{v}_i + \Delta t^2 \beta (\ddot{v}_{i+1} - \ddot{v}_i)$$

$$\dot{v}_{i+1} = \dot{v}_i + \Delta t \ddot{v}_i + \Delta t \gamma (\ddot{v}_{i+1} - \ddot{v}_i)$$

where the terms containing  $\beta$  and  $\gamma$  represent the remainder terms in the Taylor series expansions. Since the exact values of the remainder terms are not known,  $\beta$  and  $\gamma$  are parameters to be chosen by the user to arrive at a numerical approximation. With some rearrangements of the above two equations, the Newark method comprises the following three equations

$$M \ddot{v}_{i+1} + C \dot{v}_{i+1} + K v_{i+1} = f_{i+1}$$

$$v_{i+1} = v_i + \Delta t \dot{v}_i + \Delta t^2 \left[ \left( \frac{1}{2} - \beta \right) \ddot{v}_i + \beta \ddot{v}_{i+1} \right]$$

$$\dot{v}_{i+1} = \dot{v}_i + \Delta t \left[ (1 - \gamma) \ddot{v}_i + \gamma \ddot{v}_{i+1} \right]$$

With some manipulation the following equivalent static equation is obtained.

$$\tilde{K} v_{i+1} = \tilde{f}_{i+1}$$

where

$$\tilde{K} = \frac{1}{\beta \Delta t^2} M + \frac{\gamma}{\beta \Delta t} C + K$$

$$\tilde{f}_{i+1} = f_{i+1} + \left( \frac{1}{\beta \Delta t^2} M + \frac{\gamma}{\beta \Delta t} C \right) v_i + \left[ \frac{1}{\beta \Delta t} M + \left( \frac{\gamma}{\beta} - 1 \right) C \right] \dot{v}_i + \left[ \left( \frac{1}{2\beta} - 1 \right) M + \frac{\Delta t}{2} \left( \frac{\gamma}{\beta} - 2 \right) C \right] \ddot{v}_i$$

The Newmark- $\beta$  method assumes some degree of contribution of acceleration from times  $t$  and  $t+\Delta t$ . When  $\gamma$  is anything other than 0.5, superfluous damping is introduced into the system. Hence it is usually taken as 0.5.  $\beta$  can vary from 1/6 to 1/2 although if  $\gamma=0.5$ ,  $\beta$  has got to be greater than 1/4 for unconditional stability. The general Newmark- $\beta$  scheme encapsulates the following schemes.

$\beta = 0, \gamma = 1/2 \rightarrow$  the explicit central difference scheme, but the above procedure inapplicable

$\beta = 1/2, \gamma = 1/2 \rightarrow$  the implicit linear acceleration scheme

$\beta = 1/4, \gamma = 1/2 \rightarrow$  the implicit constant-average-acceleration (a.k.a. trapezoidal) scheme

$\beta = 1/6, \gamma = 1/2 \rightarrow$  the implicit linear acceleration

$\beta = 1/12, \gamma = 1/2 \rightarrow$  the implicit Fox-Goodwin method which is 4<sup>th</sup> order accurate

The Newmark- $\beta$  scheme is unconditionally stable as long as  $\gamma \geq 0.5$  and  $\beta \geq 0.25 (\gamma + 0.5)^2$ . In general the Newmark- $\beta$  is second order accurate.

The Wilson- $\theta$  method is an extension of the linear acceleration method, but the acceleration is assumed to be linear from time  $t$  to  $t+\theta\Delta t$ . The scheme is unconditionally stable if  $\theta \geq 1.37$ . Usually  $\theta = 1.40$  is employed. When  $\theta = 1$ , the scheme is equivalent to the linear acceleration method.

The critical step size depends on the damping as well as the natural frequency of the structure. The values shown in the table assume that damping is zero. In general, the increase of damping increases the critical step sizes, although this effect is nullified as long as  $\gamma = 0.5$ .

Integration Method	Type of Method	Critical Step Size ( $\Delta t_{cr}$ )
Central Different	Explicit	$\frac{2}{\omega}$
Newmark Method $\gamma = \frac{1}{2}, \beta = \frac{1}{6}$ (Linear Acceleration)	Implicit	$\frac{3.464}{\omega}$
Newmark Method $\gamma = \frac{1}{2}, \beta = \frac{1}{4}$ (Constant-Average-Acceleration)	Implicit	Unconditionally Stable
Newmark Method $\gamma = \frac{1}{2}, \beta = 0$ (Central Difference)	Explicit	$\frac{2}{\omega}$
Wilson- $\theta$	Implicit	Unconditionally Stable when $\theta \geq 1.37$

The Newmark- $\beta$  ( $\beta=1/3$  default) (3-point integration scheme) implicit solution scheme adopted in MSC.NASTRAN SOL 109 is

- IV. Unconditionally stable
- V. Second order accurate since  $O(\Delta t)^2$

The Newmark- $\beta$  ( $\beta=1/3$  default) (3-point integration scheme) implicit solution scheme adopted in MSC.NASTRAN SOL 129 (AUTO or TSTEP) is

- I. Unconditionally stable
- II. Second order accurate since  $O(\Delta t)^2$

The Newmark- $\beta$  ( $\beta=1/4$  default) (2-point integration scheme) implicit solution scheme adopted in MSC.NASTRAN SOL 129 (ADAPT) is

- I. Unconditionally stable
- II. Second order accurate since  $O(\Delta t)^2$

The recommended default SOL 129 ADAPT scheme solves

$$M\ddot{u} + C\dot{u} + F(u) = P(t)$$

using the implicit constant-average-acceleration (a.k.a. trapezoidal) scheme such that

$$\left[ \frac{4}{\Delta t^2}M + \frac{2(1-\eta)}{\Delta t}C + \tilde{K} \right] \{ \Delta U^{j+1} \} = \{ R_{n+1}^j \}$$

where

$$\{ R_{n+1}^j \} = \{ P_{n+1}^j - F_{n+1}^j \} + \frac{4(1-\eta)}{\Delta t}M\{ \dot{U}_n \} + (1-2\eta)\{ P_n - F_n \} - \left[ \frac{4}{\Delta t^2}M + \frac{2(1-\eta)}{\Delta t}C \right] \{ U_{n+1}^j - U_n \}$$

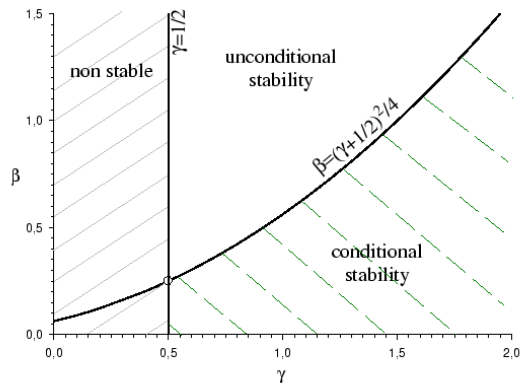
where  $\eta$  denotes numerical damping (PARAM, NDAMP). The ADAPT (default) is used to modify the integration time step automatically (within bounds) during the analysis to respond to changes in the frequency content of the loading on TLOADi and the response natural frequency.

#### 4.9.6.2 Stability

The implicit Newmark- $\beta$  scheme is unconditionally stable as long as  $\gamma \geq 0.5$  and  $\beta \geq 0.25 (\gamma + 0.5)^2$ . Hence, the time step can be as large as possible. However, the accuracy requirements will govern the size of the time step. The critical time step for Newmark- $\beta$  schemes is

$$\omega \Delta t_{cr} = \frac{\xi(\gamma - 1/2) + \left[ \gamma/2 - \beta + \xi^2(\gamma - 1/2)^2 \right]^{1/2}}{(\gamma/2 - \beta)}$$

From the above expression, we can see that when  $\gamma = 1/2$ , damping does not influence the critical step size. However, when  $\gamma > 1/2$ , the increase of damping tends to increase the critical step size.



#### 4.9.6.3 Accuracy

It is often mentioned that for good accuracy, the time step must subdivide the lowest period of interest by 10. For the purposes of illustration, let's consider the fundamental bending frequency (although in theory we should consider the higher frequencies of interest from all modes whether bending, axial or torsional) of a simply supported beam. Discretizing the beam as a lumped dynamic mass in the middle and assuming that the fundamental mode shape resembles the static deflected shape (because the  $\rho_0/K_i$  term is largest for the fundamental mode), and with the knowledge that the static deflection due to a unit point load on a simply supported beam is  $\Delta_1 = L^3/(48EI)$ , the unconditionally stable implicit solution algorithm requires that the time step subdivide (by at least 10 for good accuracy) the period of interest for accuracy

$$\begin{aligned} \Delta t &< 2\pi / 10\omega_1 \\ &< \pi/5 (m/k)^{1/2} \\ &< \pi/5 (\rho A L \Delta_1)^{1/2} \\ &< \pi/5 (\rho A L L^3 / (48EI))^{1/2} \\ &< \pi/5 L^2 (\rho A / (48EI))^{1/2} \end{aligned}$$

A small time step is necessary for accuracy. The following should be considered for accuracy: -

- (a) The time step should be smaller than 1/10 of the lowest natural period of interest of the system
- (b) The time step should be small enough to properly represent the variation of loading and capture all the significant peaks and troughs

#### 4.9.7 Comparison Between Implicit and Explicit Time Integration Schemes

The choice between employing an implicit or explicit time integration solution technique depends on the points listed below. These conditions are essential and must be considered for the physical problem being solved.

Implicit Time Integration	Explicit Time Integration
Requires <b>inversion of stiffness matrix</b> , which for nonlinear structures changes from time to time. Hence, the use of implicit methods for nonlinear structures requires a Newton-type iterative approach, which is not needed in explicit methods.	Does <b>not</b> require <b>inversion of stiffness matrix</b> , and stiffness matrix automatically updated at each time step.
The cost per timestep is large	The cost per time step is small
Element formulation should be complex as the matrix inversion dominates the cost	Element formulation should be simple as element processing dominates the cost
Coarser mesh as element formulation complex	Finer mesh as element formulation simple
Appropriate for <b>smaller models</b> as the computational cost of an implicit analysis varies proportionally to the 7 <sup>th</sup> power of a 3D model size. Hence the cost increase for doubling the mesh density of solid elements is x 128.	Appropriate for <b>larger models</b> as the computational cost of an explicit analysis varies proportionally to the 4 <sup>th</sup> power of a 3D model size. Hence the cost increase for doubling the mesh density of solid elements is x 16.
Extremely appropriate if the model is <b>materially linear, geometrically linear</b> and has <b>no contact</b> definitions, failing which the large time step no longer enables the perfectly accurate representation of the tangent stiffness matrix over a large range of strain increment. Nonlinear models can still be analyzed with implicit schemes but the <b>small time step requirement for accuracy</b> (not stability) means that it is more computationally beneficial to use an explicit scheme.	Extremely appropriate if the model is <b>materially highly nonlinear, geometrically highly nonlinear</b> and has <b>contact</b> definitions
The solution is <b>unconditionally stable</b> , hence a <b>large time step</b> can be employed, the size of which is <b>limited only by accuracy</b> of the solution; The time step for an implicit analysis is usually 100 – 1000 times greater than that of an explicit analysis. The time step needs to <b>subdivide the smallest period (highest frequency) of interest for accuracy</b> in the model.	The solution is <b>conditionally stable</b> , hence a small time step must be employed. The time step needs to <b>subdivide the smallest period (highest frequency) for stability</b> in the model. This automatically takes care of accuracy requirements, which also requires the subdivision of the smallest period.
Appropriate if the physics of the problem do not require a small time step, such as in stress wave transmission problems	Appropriate if the physics of the problem require a small time step, such as in stress wave transmission problems

The only way to check whether the time step for accuracy in an implicit analysis is adequate is to repeat the last part of the analysis with a reduced time step and check that the results are not significantly affected. The time step in both implicit and explicit analyses is limited by the highest frequency in the structure or the lowest period. But

the difference with implicit analysis is that since it is an unconditionally stable solution scheme, the time step is limited by the highest frequency *of interest*, in most instances that of only the first few initial modes of vibration. On the other hand, an explicit scheme requires that the time step subdivide the lowest period in the model as it is a conditionally stable algorithm. Thus, we are trying to minimize the largest frequency in the structure. Hence, short, stiff and light components are not computationally efficient for time integration analysis.

We have seen that the choice of employing an implicit or explicit scheme depends on a lot of parameters. The fundamental difference is the size of the time step, which directly affects the computational speed. The time step in an implicit scheme is governed by accuracy conditions ( $\Delta t$  must subdivide smallest period *of interest* by 10) and not by stability conditions of which there are none. The time step in an explicit scheme is governed by stability conditions ( $\Delta t$  must subdivide smallest period by  $\pi$ ) and not by the accuracy conditions ( $\Delta t$  must subdivide smallest period *of interest* by 10), which are usually automatically satisfied.

As mentioned, another clear indication of whether to employ an implicit or explicit scheme is the physics of the problem. If the system is highly nonlinear (geometrically, materially and due to contact definitions), then the requirement of a small time step for accuracy (as the stiffness, damping and external force within a time step is assumed constant) usually nullifies the benefit of the unconditionally stable large time step requirement for stability of an implicit scheme. Likewise in stress propagation problems. In these circumstances, it is prudent to employ an explicit time integration scheme, which has a small time step requirement for stability anyhow. The time taken to move one time step is much smaller in an explicit scheme than an implicit scheme due to the requirement of matrix inversion or simultaneous equation solving algorithms in the latter.

## 4.9.8 MSC.NASTRAN Decks

### 4.9.8.1 GNL, MNL Direct Forced (Implicit) Transient Response Analysis

All cards applicable to SOL 109 are also applicable to SOL 129.

<b>\$ EXECUTIVE CONTROL SECTION</b>
SOL 129
<b>\$ CASE CONTROL SECTION</b>
<b>\$ Sets defining grid ids or element ids</b> SET < Number > = 1 THRU 100, 211, 343, < etc > <b>\$ Grid output of displacement, velocity and acceleration with time</b> <b>\$ SORT1 lists the results by time whilst SORT2 lists the results by grid id</b> DISPLACEMENT(<SORT1/SORT2>,<PRINT,PUNCH,PLOT>) = ALL/<Grid Set ID> VELOCITY(<SORT1/SORT2>,<PRINT,PUNCH,PLOT>) = ALL/<Grid Set ID> ACCELERATION(<SORT1/SORT2>,<PRINT,PUNCH,PLOT>) = ALL/<Grid Set ID> <b>\$ Grid output of applied load vector</b> OLOAD(<SORT1/SORT2>,<PRINT,PUNCH,PLOT>) = ALL/<Grid Set ID> <b>\$ Grid output of d-set displacement, velocity and acceleration</b> SDISPLACEMENT(<SORT1/SORT2>,<PRINT,PUNCH>) = ALL/<Grid Set ID> SVELOCITY(<SORT1/SORT2>,<PRINT,PUNCH>) = ALL/<Grid Set ID> SACCELERATION(<SORT1/SORT2>,<PRINT,PUNCH>) = ALL/<Grid Set ID> <b>\$ Grid output of SPC forces</b> SPCFORCES(<SORT1/SORT2>,<PRINT,PUNCH,PLOT>) = ALL/<Grid Set ID> <b>\$ Element output of force, stress and strain</b> ELFORCE(<SORT1/SORT2>,<PRINT,PUNCH,PLOT>) = ALL/<Element Set ID> ELSTRESS(<SORT1/SORT2>,<PRINT,PUNCH,PLOT>) = ALL/<Element Set ID> STRAIN(<SORT1/SORT2>,<PRINT,PUNCH,PLOT>) = ALL/<Element Set ID> NLLOAD(PLOT) <b>SUBCASE 1</b> SPC = < ID of SPC Cards Defined in Bulk Data > DLOAD = < ID OF TLOAD1 or TLOAD2 > NONLINEAR = < ID OF NOLINi > TSTEPNL = < ID OF TSTEPNL > <b>SUBCASE 2</b> SPC = < ID of SPC Cards Defined in Bulk Data > DLOAD = < ID OF TLOAD1 or TLOAD2 > NONLINEAR = < ID OF NOLINi > TSTEPNL = < ID OF TSTEPNL > <b>\$ XY plot output</b> OUTPUT(XYPLOT) XYPUNCH <DISP/VELO/ACCE> RESPONSE <subcase>/<Grid ID>(<T1/T2/T3>) XYPUNCH <ELFORCE/ELSTRESS/STRAIN> RESPONSE <subcase>/<Element ID>(<Code Number>)
<b>\$ BULK DATA</b>
PARAM, AUTOSPC, NO           \$ AUTOSPC NO By Default PARAM, FOLLOWK, YES         \$ Includes Follower Force Stiffness PARAM, LGDISP, 1           \$ Includes Large Displacement Effects i.e. [T] not constant PARAM, LANGLE, 2           \$ Rotation Vector Approach for Large Rotations PARAM, K6ROT, 100          \$ Shell normal rotation restrained in nonlinear analysis

Mass-less DOFs should be avoided in SOL 129. The time step should be based on capturing the maximum frequency of interest. In linear analysis (SOL 109 and SOL 112) it is recommended that the time step, **DT** be a tenth of the period representing the highest frequency of interest (i.e. if 100Hz, then DT should be 0.001s) and that

DT should be small enough to accurately capture the highest frequency content of the excitation (i.e. if 1000Hz, then DT should be 0.001s or less). In nonlinear analysis SOL 129, if NOLINi is incorporated, DT should be 1/5 to 1/10 the size described above since NOLINi puts the structure out of equilibrium by one time step, so a very small integration time step is required to minimize this limitation. The TSTEPNL bulk data entry is as follows.

TSTEPNL	ID	NDT	DT	NO		KSTEP	MAXITER	CONV	
	EPSU	EPSP	EPSW	MAXDIV	MAXQN	MAXLS	FSTRESS		
	MAXBIS	ADJUST	MSTEP	RB	MAXR	UTOL	RTOLB		

Unlike linear analyses schemes, nonlinear analysis schemes (SOL 106 and SOL 129) employ subcases on an incremental basis, instead of separate load cases and boundary conditions. For SOL 129, the bulk data loads and prescribed motions are measured from the initial configuration at time zero. The following can be performed with multiple subcases:

- (i) Loads can be changed
- (ii) SPC cannot be changed. However, the change in boundary condition can more often than not be defined with prescribed motion load curves
- (iii) The initial time step size DT can be changed

The duration of the analysis is the number of time steps **NDT** times the time step size DT, which in general varies. **NO** is the time step interval for output.

**In this NONLINEAR TIME DOMAIN solution**, the static response must be added to the dynamic response if the dynamic analysis is performed about the initial undeflected (by the static loads) state with only the dynamic loads applied, hence causing the dynamic response to be measured relative to the static equilibrium position. **Hence, the total response = the dynamic response + the static response to static loads.** Time domain dynamic excitation functions should always be applied from the amplitude of 0.0 (and realistically de-ramped to 0.0 as well). This is because inherently, the dynamic excitation function has to be extrapolated within the analysis code to be from 0.0. Hence, that initial jolt should better be representative of reality irrespective of whether load excitations or enforced motion is being applied.

**Alternatively, in this NONLINEAR TIME DOMAIN solution**, if the dynamic analysis is performed with the deflected static shape as initial input and the static loads maintained throughout the dynamic excitations, the total or absolute response (static and dynamic) is obtained straight away from the dynamic analysis. **Hence total response = dynamic response (which already includes the static response to static loads).** Of course, if the transient dynamic analysis follows a static analysis (by say SOL 101, SOL 106, implicit dynamic relaxation by SOL 129 or explicit dynamic relaxation), then the dynamic excitation function should be ramped up from the static amplitude and not from 0.0 (and realistically de-ramped to the static load as well), so that again there would be no jolt unrepresentative of reality.

#### 4.9.8.1.1 Time Step and Stiffness Update Strategy (ADAPT with ADJUST, MSTEP, RB and MAXR, AUTO, TSTEP with KSTEP)

The load is divided up into time steps. Each time step is then divided into iteration steps. **METHOD** specifies the method for controlling **time step and stiffness** updates, whether **ADAPT (default)**, **AUTO** or **TSTEP**.

The **ADAPT** (default) is used to modify the integration time step automatically (within bounds) during the analysis to respond to changes in the frequency content of the **loading on TLOADi** and the **response natural frequency**. However, it may force the solution to solve for unnecessary high frequency modes. DT is used as an initial time step estimate. **ADJUST** controls the automatic time stepping, by default 5. If ADJUST = 0, then the automatic adjustment is deactivated. If ADJUST > 0, the time increment is continually adjusted for the first few steps until a

good value of DT is obtained. After this initial adjustment, the time increment is adjusted every ADJUST-th time step only. **MSTEP** and **RB** are used to adjust the time increment during analysis. MSTEP is the number of steps to obtain the dominant period response and RB defines bounds for maintaining the same time step for the stepping function during the adaptive process, default 0.75. The recommended value of MSTEP for nearly linear problems is 20. A larger value (e.g., 40) is required for highly nonlinear problems. By default, the program automatically computes the value of MSTEP based on the changes in the stiffness. The time increment adjustment is based on the number of time steps desired to capture the dominant frequency response accurately. The time increment is adjusted as follows.

$$\Delta t_{n+1} = f(r)\Delta t_n$$

where

$$r = \frac{1}{\text{MSTEP}} \left( \frac{2\pi}{\omega_n} \right) \left( \frac{1}{\Delta t_n} \right)$$

$$f = 0.25 \quad \text{for } r < 0.5 \cdot \text{RB}$$

$$f = 0.5 \quad \text{for } 0.5 \cdot \text{RB} \leq r < \text{RB}$$

$$f = 1.0 \quad \text{for } \text{RB} \leq r < 2.0$$

$$f = 2.0 \quad \text{for } 2.0 \leq r < 3.0/\text{RB}$$

$$f = 4.0 \quad \text{for } r \geq 3.0/\text{RB}$$

**MAXR** is the maximum ratio for the adjusted incremental time relative to DT allowed for time step adjustment, by default 16. MAXR is used to define the upper and lower bounds for adjusted time step size as follows.

$$\text{MIN} \left( \frac{\text{DT}}{2 \cdot \text{MAXBIS}}, \frac{\text{DT}}{\text{MAXR}} \right) \leq \Delta t \leq \text{MAXR} \cdot \text{DT}$$

ADAPT is the average acceleration scheme with  $\beta = 0.25$  and can be made to behave similarly to AUTO and TSTEP using MAXR set to 1.0 to prevent time step changes and possibly also set KSTEP to 1.

**AUTO** is analogous to AUTO in SOL 106. Time step is constant with AUTO.

**TSTEP** with **KSTEP** is analogous to ITER with KSTEP in SOL 106. Time step is constant with TSTEP.

The METHOD field selects an option for direct time integration and the stiffness matrix update strategies among ADAPT, AUTO and TSTEP. If the AUTO option is selected, MSC.Nastran automatically updates the stiffness matrix to improve convergence while the KSTEP value is ignored. If the TSTEP option is selected, MSC.Nastran updates the stiffness matrix every KSTEP-th increment of time. If the ADAPT option is selected, MSC.Nastran automatically adjusts the incremental time and uses the bisection algorithm in case of divergence. During the bisection process in the ADAPT option, stiffness is updated at every KSTEP-th successful bisection. The ADAPT method allows linear transient analysis, but AUTO or TSTEP will abort the run if the model does not have any data representing nonlinearity. The stiffness matrix is always updated for a new subcase or restart, irrespective of the option selected.

#### 4.9.8.1.2 Convergence Acceleration Techniques (Quasi-Newton MAXQN, Line Search using MAXLS, Bisection using MAXITER, RTOLB, MAXBIS and MAXDIV)

Quasi-Newton updates and line search is as SOL 106. In SOL 129, the default for MAXQN is 10 and MAXLS is 2.

**MAXITER** specifies the limit on number of iterations for each time step, 10 by default. The sign of MAXITER provides a control over the ultimate recourse (reiteration) in case of failure in convergence or bisection. If the MAXITER is negative, the analysis is terminated when the divergence condition is encountered twice during the same time step or the solution diverges for five consecutive time steps. If MAXITER is positive, the program computes the best attainable solution and continues the analysis on second divergence. If the solution does not converge at MAXITER iterations, the time step is **bisected** and the analysis is repeated. Bisection is also activated if **RTOLB**, by default 20.0 is exceeded. RTOLB is the maximum value of incremental rotation (in degrees)

allowed per iteration before bisection is activated. **MAXBIS** specifies the maximum number of bisections for each time step, 5 by default. If **MAXBIS** is positive and the solution does not converge after **MAXBIS** bisections, the best solution is computed and the analysis is continued to the next time step. If **MAXBIS** is negative and the solution does not converge in  $|\text{MAXBIS}|$  bisection, the analysis is terminated. **MAXDIV** provides control over diverging solutions, default 2. Depending on the rate of divergence, the number of diverging solutions (**NDIV**) is incremented by 1 or 2. The solution is assumed to diverge when **NDIV** reaches **MAXDIV** during the iteration. If the bisection option is used (allowed **MAXBIS** times) the time step is bisected upon divergence. Otherwise, the solution for the time step is repeated with a new stiffness based on the converged state at the beginning of the time step. If **NDIV** reaches **MAXDIV** again within the same time step, the analysis is terminated.

The number of iterations for a time step is limited to **MAXITER**. If the solution does not converge in **MAXITER** iterations, the process is treated as a divergent process; i.e., either a bisection or stiffness matrix update takes place based on the value of **MAXBIS**. The sign of **MAXITER** provides a control over reiteration in case of failure in convergence or bisection. If **MAXITER** is negative, the analysis is terminated when the divergence condition is encountered twice during the same time step or the solution diverges for five consecutive time steps. If **MAXITER** is positive, MSC.Nastran computes the best attainable solution and continues the analysis. The **MAXDIV** field provides control over diverging solutions. Depending on the rate of divergence, the number of diverging solutions (**NDIV**) is incremented by 1 or 2. The solution is assumed to be divergent when **NDIV** reaches **MAXDIV** during the iteration. If the bisection option is used with the **ADAPT** method, the time step is bisected upon divergence. Otherwise, the solution for the time step is repeated with a new stiffness based on the converged state at the beginning of the time step. If **NDIV** reaches **MAXDIV** twice within the same time step, the analysis is terminated with a fatal message.

#### 4.9.8.1.3 Convergence Criteria (**CONV**, **EPSU**, **EPSP**, **EPSW**)

**CONV** specifies the flags to select convergence criteria, **UPW** or any combination, note default **PW**. **EPSU** is the error tolerance for displacement error (U) convergence criteria, 1.0E-2 by default. **EPSP** is the error tolerance for load equilibrium error (P) convergence criteria, 1.0E-3 by default. **EPSW** is the error tolerance for work error (W) convergence criteria, 1.0E-6 by default. These correspond to the very high tolerance, **PARAM**, **NLTOL**, 0 unlike **SOL 106** which had engineering tolerance levels **PARAM**, **NLTOL**, 2.

#### 4.9.8.1.4 Nonlinear Transient Load

Nonlinear transient loads, which are functions of the displacement and/or velocity of the response, can be specified using **NOLINi** entries.

#### 4.9.8.1.5 Nonlinear Finite Elements, Nonlinear Material Definitions and Nonlinear Contact Interface

The nonlinear finite elements, the nonlinear material definitions and the nonlinear contact interface are as defined in the nonlinear static analysis **SOL 106** section.

#### 4.9.8.2 Nonlinear Static Analysis and Nonlinear Transient Analysis

Subcases can be employed to change the method of analysis from SOL 106 to SOL 129.

#### 4.9.8.3 Restart From Nonlinear Static Analysis SOL 106 Into Nonlinear Transient Analysis SOL 129

Restarts are allowed from end of subcases. A LOOPID is created after each converged load increment in static analysis and at the end of each converged subcase in nonlinear transient analysis. Only LOOPIDs written to the database and identified as such in the printed output can be used for a restart.

<b>\$ BULK DATA</b>
PARAM, SLOOPID, L \$ Load Step ID, L at the End of a Subcase of the SOL 106 Run

The initial transient loads should be identical to the static loads at the restart state. This is to ensure no sudden jump in load. The changes allowed in model are

- (i) Boundary conditions, i.e. SPC
- (ii) Direct input matrices
- (iii) Mass
- (iv) Damping

Note that when restarting a transient analysis from a static analysis, the static loads which have been applied must be maintained throughout the transient phase.

#### 4.9.8.4 Restart From Nonlinear Transient Analysis SOL 129 Into Nonlinear Transient Analysis SOL 129

Restarts are allowed from end of subcases.

<b>\$ FMS</b>
RESTART
<b>\$ BULK DATA</b>
PARAM, LOOPID, L \$ Loop Number on Printout, L
PARAM, STIME, T \$ Starting Value of Time, T

Note that when restarting a transient analysis from a static analysis (whether a Newton-Raphson nonlinear static analysis or dynamic relaxation), the static loads which have been applied must be maintained throughout the transient phase. Hence, when a transient phase dynamic analysis follows a dynamic relaxation analysis, it is prudent to define two curves for the static loads or prescribed motions, one ramped from zero to the static value in the dynamic relaxation phase and the other maintained at the same static throughout the transient dynamic analysis phase.

#### **4.9.8.5 Implicit Nonlinear (Static and) Dynamic Analysis SOL 400**

SOL 400 replaces SOL 106 and SOL 129 adding MSC.Marc's 3D contact routines, large rotation of rigid bodies and additional types of rigid mechanisms directly inside MSC.Nastran.

#### **4.9.8.6 Implicit Nonlinear (Static and) Dynamic Analysis SOL 600**

SOL 600 is the MSC.Marc implicit nonlinear static and dynamic analysis solver within MSC.NASTRAN.

#### **4.9.8.7 Explicit Nonlinear Dynamic Analysis SOL 700**

SOL 700 is the LS-DYNA explicit nonlinear dynamic analysis solver within MSC.NASTRAN.

### 4.9.9 LS-DYNA Decks

#### 4.9.9.1 GNL, MNL Direct Forced (Explicit) Transient Response Analysis

To specify termination time of the explicit dynamic analysis

\*CONTROL\_TERMINATION

<b>Termination Time Limit</b>	Termination Cycle Limit	Termination Min Time Step Size Limit	Termination Energy Ratio Limit	Termination Change in Total Mass From Mass Scaling			
-------------------------------	-------------------------	--------------------------------------	--------------------------------	--	--	--	--

To set structural timestep size control and invoke mass scaling

\*CONTROL\_TIMESTEP

Initial Time Step	<b>Factor For Time Step</b>	Basis	Shell Min Time Step	<b>Min Time Step For Mass Scaling</b>	Maximum Time Step Curve	Erosion Flag	Limit Mass Scaling
-------------------	-----------------------------	-------	---------------------	---------------------------------------	-------------------------	--------------	--------------------

To enable subcycling

\*CONTROL\_SUBCYCLE

To specify user-defined boundary conditions for the transient phase,

\*LOAD\_NODE\_<POINT, SET> (HM: forces, moments)

\*SET\_NODE

\*DEFINE\_CURVE with SIDR = 0 for transient phase

\*LOAD\_BEAM\_<ELEMENT, SET>

\*SET\_BEAM

\*DEFINE\_CURVE with SIDR = 0 for transient phase

\*LOAD\_SHELL\_<ELEMENT, SET> (HM: pressure → ShellPres)

\*SET\_SHELL

\*DEFINE\_CURVE with SIDR = 0 for transient phase

\*LOAD\_RIGID\_BODY

\*DEFINE\_CURVE with SIDR = 0 for transient phase

\*LOAD\_SEGMENT\_<SET> (HM: pressure → SegmentPre)

\*SET\_SEGMENT

\*DEFINE\_CURVE with SIDR = 0 for transient phase

To apply automatically computed gravitational loads, noting that by d-Alembert’s principle, applying accelerations in a certain direction results in inertial loads acting in the opposite direction. Hence, a downward gravity is applied as an upward acceleration.

\*LOAD\_BODY\_Z with sf = 9.81 ms<sup>-2</sup>

\*DEFINE\_CURVE with SIDR = 0 for transient phase

Do not apply gravity loads on soil elements because the in-situ measured soil properties already take into account its stiffness with gravity applied.

To prescribe displacements, velocity or accelerations (as in seismic analysis) on a node, on a set of nodes, on a rigid body in the global axes system or on a rigid body in the rigid body local axes system,

\*BOUNDARY\_PRESCRIBED\_MOTION\_<NODE, SET, RIGID, RIGID\_LOCAL> (HM: velocities → prcrbVel or HM: accels)

NID, NSID, or PART ID	DOF	Velocity, Acceleration or Displacement VAD	LCID	Load Curve Scale Factor SF	VID	DEATH	BIRTH
-----------------------	-----	--	------	----------------------------	-----	-------	-------

The vector ID, VID is used to specify a direction vector if imposed motion not in global axes system. DEATH and BIRTH can be used to specify deactivation and activation times of the imposed motion during the analysis.

\*SET\_NODE\_LIST

NSID	DA1	DA2	DA3	DA4			
NID	NID	NID	NID	NID	NID	NID	NID
NID	NID	NID	NID	...	...	...	...

\*DEFINE\_CURVE

LCID	SIDR	SFA	SFO	OFFA	OFFO	DATTYP	
Abscissa Values		Ordinate Values					
Abscissa Values		Ordinate Values					
...		...					

SIDR defines whether the curve is valid for the transient phase, stress initialization phase or both. Here obviously, SIDR = 0. Having said that, for every transient pair of \*BOUNDARY\_PRESCRIBED\_MOTION and \*DEFINE\_CURVE cards defined, it is generally necessary to define two corresponding cards that is valid for the stress initialization (dynamic relaxation) phase if dynamic relaxation is activated. For instance, if the earthquake acceleration time histories are to be applied in the transient phase, it is necessary to define zero velocity prescribed boundary conditions for the dynamic relaxation phase so that the structure is supported. The BOUNDARY\_PRESCRIBED\_MOTION card is useful to **change boundary conditions** during an analysis.

\*DEFINE\_VECTOR if DOF not global i.e. VID defined

VID	XTail	YTail	ZTail	Xhead	Yhead	ZHead	
-----	-------	-------	-------	-------	-------	-------	--

To prescribe initial conditions

\*INITIAL\_VELOCITY\_<BLANK, NODE, GENERATION> (HM: velocities → initVel)

\*SET\_NODE

or,

\*PART\_INERTIA

or,

\*CONSTRAINED\_NODAL\_RIGID\_BODY\_INERTIA

#### 4.9.10 Hand Methods Verification

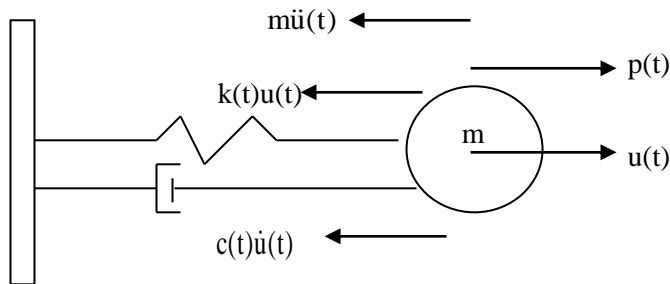
##### 4.9.10.1 Determination of Displacement Response Time History by Solving the SDOF Nonlinear (in Stiffness, Damping and Displacement) Equation of Motion ODE for Deterministic Time Domain Loading With/Without Initial Conditions by Implicit Newmark- $\beta$ Time Integration Schemes

Nonlinear time domain hand methods are capable of analyzing: -

##### SDOF or Single-Modal Response to Deterministic Non-Periodic Short Duration Impulse and Hence Random Non-Stationary Short Duration Impulse by Enveloping Deterministic Responses

Multi-modal nonlinear response cannot be performed because the superposition of nonlinear modal responses is not strictly valid for nonlinear systems where the physical coordinates (which includes all modes together) responds nonlinearly. Nonlinear analysis can be performed by the implicit Newmark- $\beta$  method (constant acceleration, linear acceleration etc.) or the implicit Wilson- $\theta$  method. Since hand computations are limited to SDOF system, all the algorithms are explicit as there is no need for matrix inversion (or solving of simultaneous equations).

The loading is divided into a sequence of time intervals. The response is evaluated at successive increments  $\Delta t$  of time, usually taken of equal lengths of time for computational convenience. At the beginning of each interval, the condition of dynamic equilibrium is established. Then, the response for the time increment  $\Delta t$  is evaluated approximately on the basis that the coefficients  $k$  and  $c$  remain constant during the interval  $\Delta t$ . The non-linear characteristics of these coefficients are considered in the analysis by re-evaluating these coefficients at the beginning of each time increment. The response is then obtained using the displacement and velocity calculated at the end of the time interval as the initial conditions for the next time step. Hence, basically the equation of motion (non-linear in that  $k$  and  $c$  changes at every time interval but constant within the interval) is solved for at each and every time step, the initial conditions at each time step being the displacement and velocity calculated at the end of the previous time interval. Also, the  $P(t)$  is unique for each and every time interval.



The general nonlinear Newton's dynamic equation of motion at time  $t_i$  can be written as

$$m\ddot{u}_i + c_i\dot{u}_i + k_i u_i = P_i$$

The incremental form of the equation of motion is then

$$m\Delta\ddot{u}_i + c_i\Delta\dot{u}_i + k_i\Delta u_i = \Delta P_i$$

The choice of the time integration scheme depends on the acceleration variation function across the time step. We shall describe the Newmark- $\beta$  method, which includes the constant acceleration and linear acceleration schemes within its formulation. The Newmark- $\beta$  method states the Newmark equations as

$$\Delta\dot{u}_i = \ddot{u}_i\Delta t + \gamma\Delta\ddot{u}_i\Delta t \quad \text{and} \quad \Delta u_i = \dot{u}_i\Delta t + \frac{1}{2}\ddot{u}_i\Delta t^2 + \beta\Delta\ddot{u}_i\Delta t^2$$

When  $\gamma$  is anything other than 0.5, superfluous damping is introduced into the system. Hence it is usually taken as  $\gamma = 0.5$ .  $\beta$  can vary from 1/6 to 1/2 but is unconditionally stable only as long as  $\beta \geq 0.25 (\gamma + 0.5)^2$ . When  $\beta$  is 1/4, the Newmark equations can be obtained from assuming the constant acceleration method (**unconditionally stable**)

$$\ddot{u}(t) = \frac{1}{2}(\ddot{u}_i + \ddot{u}_{i+1})$$

and when  $\beta$  is 1/6, the Newmark equations can be obtained from assuming the linear acceleration method (**conditional stability although implicit! note  $\beta \geq 0.25$  ( $\gamma + 0.5$ )<sup>2</sup> for unconditional stability**)

$$\ddot{u}(t) = \ddot{u}_i + \frac{\Delta \ddot{u}_i}{\Delta t} (t - t_i)$$

On rearranging the Newmark equations,

$$\Delta \ddot{u}_i = \frac{\Delta u_i}{\beta(\Delta t)^2} - \frac{\dot{u}_i}{\beta(\Delta t)} - \frac{1}{2\beta} \ddot{u}_i$$

$$\begin{aligned} \Delta \dot{u}_i &= \ddot{u}_i \Delta t + \gamma \left( \frac{\Delta u_i}{\beta(\Delta t)^2} - \frac{\dot{u}_i}{\beta(\Delta t)} - \frac{1}{2\beta} \ddot{u}_i \right) \Delta t \\ &= \frac{\gamma}{\beta(\Delta t)} \Delta u_i + \left( 1 - \frac{\gamma}{2\beta} \right) \ddot{u}_i \Delta t - \frac{\gamma}{\beta} \dot{u}_i \end{aligned}$$

**It is wise to choose**

**$\gamma = 0.5 \rightarrow$  No superfluous damping**

**$0.25 < \beta < 0.5 \rightarrow$  Unconditionally stable**

Replacing these rearranged Newmark equations into the incremental form of the equation of motion to yield only  $\Delta u_i$  as the unknown. This will be rearranged for  $\Delta u_i$ .

$$m \left( \frac{\Delta u_i}{\beta(\Delta t)^2} - \frac{\dot{u}_i}{\beta(\Delta t)} - \frac{1}{2\beta} \ddot{u}_i \right) + c_i \left( \frac{\gamma}{\beta(\Delta t)} \Delta u_i + \left( 1 - \frac{\gamma}{2\beta} \right) \ddot{u}_i \Delta t - \frac{\gamma}{\beta} \dot{u}_i \right) + k_i \Delta u_i = \Delta P_i$$

This can thus be implemented on a spreadsheet and looped over numerous time steps. The procedure is described as follows: -

- (a) Choose appropriate time step  $\Delta t$
- (b) Establish initial conditions noting that  $u(t)$  is relative to the static equilibrium position

$$u_0, \dot{u}_0, \ddot{u}_0$$

**For  $i = 0$  To Number of Increments**

- (c) Calculate incremental displacement from

$$\Delta u_i = \frac{\Delta P_i + \left( \frac{m}{2\beta} + \Delta t \left( \frac{\gamma}{2\beta} - 1 \right) c_i \right) \ddot{u}_i + \left( \frac{m}{\beta(\Delta t)} + \frac{\gamma}{\beta} c_i \right) \dot{u}_i}{\frac{1}{\beta(\Delta t)^2} m + \frac{\gamma}{\beta(\Delta t)} c_i + k_i}$$

- (d) Calculate incremental velocity from

$$\Delta \dot{u}_i = \frac{\gamma}{\beta(\Delta t)} \Delta u_i + \left( 1 - \frac{\gamma}{2\beta} \right) \ddot{u}_i \Delta t - \frac{\gamma}{\beta} \dot{u}_i$$

- (e) Compute displacement and velocity at new time  $i + 1$  as

$$u_{i+1} = u_i + \Delta u_i$$

$$\dot{u}_{i+1} = \dot{u}_i + \Delta \dot{u}_i$$

- (f) Compute the acceleration at the new time  $i + 1$  directly from differential equation noting that  $c$  and  $k$  may vary according to some condition on the velocity or displacement

$$\ddot{u}_{i+1} = \frac{1}{m} (P_{i+1} - c_{i+1} \dot{u}_{i+1} - k_{i+1} u_{i+1})$$

Next  $i$

## BIBLIOGRAPHY

1. BALFOUR, James A.D. *Computer Analysis of Structural Frameworks 2<sup>nd</sup> Edition*. Blackwell Scientific Publications, Oxford, 1992.
2. ZIENKIEWICZ, O.C. & TAYLOR, R.L. *The Finite Element Method. The Basis. Volume 1*. 5<sup>th</sup> Edition. Butterworth-Heinemann, Oxford, 2000.
3. COOK, Robert; MALKUS, David; PLESHA, Michael; WITT, Robert; *Concepts & Applications of Finite Element Analysis Fourth Edition*. John Wiley & Sons, Inc, United States of America, 2002.
4. FELIPPA, Carlos A. *Introduction to Finite Element Methods*. Center for Aerospace Structures, University of Colorado, 2001.
5. FELIPPA, Carlos A. *Advanced Finite Element Methods*. Center for Aerospace Structures, University of Colorado, 2001.
6. FELIPPA, Carlos A. *Nonlinear Finite Element Methods*. Center for Aerospace Structures, University of Colorado, 2001.
7. HARTOG, Den J.P. *Mechanical Vibrations 4<sup>th</sup> Edition*. McGraw-Hill Book Co., New York, 1934.
8. PAZ, Mario. *Structural Dynamics Theory and Computation*. Chapman and Hall, New York, 1997.
9. SPENCE, Dr. Peter. *What is 'Power Spectral Density'*. The Analyst.
10. WHITTAKER, Andrew. *Introduction to Earthquake Engineering Lecture Notes*. University of Buffalo, 2001.
11. Dr IZZUDDIN, Bassam. *Non-Linear Structural Mechanics*. Imperial College of Science Technology and Medicine, London, 2000.
12. Dr IZZUDDIN, Bassam. *Computational Engineering Analysis MEng Lectures*. Imperial College of Science Technology and Medicine, London, 1999.
13. Dr WADEE, M. *Structural Stability Systems Lecture Notes*. Imperial College of Science Technology and Medicine, London, 2000.
14. Dr LLYOD, Smith. *Plastic Collapse Analysis Lectures*. Imperial College of Science Technology and Medicine, London, 2000.
15. Dr LLYOD, Smith. *Aerodynamic Forces on Structures*. Imperial College of Science Technology and Medicine, London, 2000.
16. Prof HOBBS. *Virtual Work, Flexibility, Direct Stiffness Method, and Moment Distribution Method Lectures*. Imperial College of Science Technology and Medicine, London, 1999.
17. Dr IZZUDDIN, Bassam. *Computational Engineering Analysis MSC Lectures*. Imperial College of Science Technology and Medicine, London, 1999.
18. SITTON, Grant. *MSC.NASTRAN Basic Dynamic Analysis User's Guide*. The MacNeal-Schwendler Corporation, Los Angeles, U.S.A, July 1997.
19. MOORE, Gregory J. *MSC.NASTRAN Design Sensitivity and Optimization User's Guide*. The MacNeal-Schwendler Corporation, U.S.A, 1995.
20. KOMZSIK, Louis. *MSC.NASTRAN Numerical Methods User's Guide*. The MacNeal-Schwendler Corporation, U.S.A, 1998.
21. MILLER, Mark. *Getting Started With MSC.NASTRAN User's Guide*. 2<sup>nd</sup> Edition. The MacNeal-Schwendler Corporation, U.S.A, 1996.
22. MACNEAL-SCHWENDLER CORP. *MSC.NASTRAN Practical Dynamic Analysis Seminar Notes*.
23. BISHOP, Dr. Neil. *Fundamentals of FEA Based Fatigue Analysis & Vibration Fatigue in MSC.FATIGUE and MSC.NASTRAN Seminar Notes 2002*. MacNeal-Schwendler Corp., England, 2002.
24. LEE, John. *MSC.NASTRAN Linear Static Analysis User's Guide Version 69*. The MacNeal-Schwendler Corporation, U.S.A, May 1997.
25. MATINEZ, Angel. *Submodelling Techniques for Static Analysis*. MSC. Software First South European Technology Conference, 7-9 June 2000.
26. LEE, John M. *MSC.NASTRAN Common Questions and Answers*. 3<sup>rd</sup> Edition. The MacNeal-Schwendler Corporation, U.S.A, 1997.
27. DICKENS, J, NAKAGAWA, J, WITTBRODT. *A Critique of Mode Acceleration And Modal Truncation Augmentation Methods For Modal Response Analysis*. Elsevier Science Ltd., Computers and Structures Volume 62, No. 6, 1997.

28. MACNEAL-SCHWENDLER CORP. *MSC.NASTRAN Nonlinear Analysis Seminar Notes*. MacNeal-Schwendler Corp., Los Angeles, May 1994.
29. MACNEAL-SCHWENDLER CORP. *MSC.NASTRAN Reference Manual 2001*. MacNeal-Schwendler Corp., Los Angeles, 2001.
30. MACNEAL-SCHWENDLER CORP. *MSC.NASTRAN Release Guide 70.7*. The MacNeal-Schwendler Corporation, U.S.A.
31. MACNEAL-SCHWENDLER CORP. *MSC.NASTRAN Release Guide 2001*. The MacNeal-Schwendler Corporation, U.S.A, 2001.
32. MACNEAL-SCHWENDLER CORP. *MSC.NASTRAN Release Guide 2004*. The MacNeal-Schwendler Corporation, U.S.A, 2004.
33. HERTING, David. *MSC.NASTRAN Advanced Dynamic Analysis User's Guide*. The MacNeal-Schwendler Corporation, U.S.A, 1997.
34. MACNEAL-SCHWENDLER CORP. *MSC.NASTRAN Practical Finite Element Modelling Techniques Seminar Notes*.
35. BELLINGER, Dean. *Dynamic Analysis by the Fourier Transform Method with MSC.NASTRAN*. MacNeal-Schwendler Corp., Los Angeles, 1995.
36. MACNEAL-SCHWENDLER CORP. *MSC.NASTRAN Fatigue Analysis Quick Start Guide 2001*. MacNeal-Schwendler Corp., Los Angeles, 2001.
37. MACNEAL-SCHWENDLER CORP. *MSC.NASTRAN Fatigue Analysis User Guide 2001*. MacNeal-Schwendler Corp., Los Angeles, 2001.
38. MACNEAL-SCHWENDLER CORP. *MSC.NASTRAN Aeroelastic Analysis User Guide 2001*. MacNeal-Schwendler Corp., Los Angeles, 2001.
39. MACNEAL-SCHWENDLER CORP. *MSC.NASTRAN Superelement User's Guide 2001*. The MacNeal-Schwendler Corporation, U.S.A, 2001.
40. MACNEAL-SCHWENDLER CORP. *MSC 1995 World User's Conference Proceedings*. MacNeal-Schwendler Corp., Los Angeles, 1995.
41. LIVERMORE SOFTWARE TECHNOLOGY CORPORATION. *LS-DYNA Keyword User's Manual Version 950*. Livermore Software Technology Corporation, California, U.S.A, May 1999.
42. LIVERMORE SOFTWARE TECHNOLOGY CORPORATION. *LS-DYNA Theoretical Manual Version 950*. Livermore Software Technology Corporation, California, U.S.A, May 1999.
43. IZATT, Conrad. *Dynamic Relaxation in LS-DYNA*. Advanced Technology Ove Arup & Partners International Ltd., London.
44. HARGREAVES, James. *Modal Analysis, Forced Response And Optimization In MSC.NASTRAN For Vehicle NVH Applications*. Advanced Technology Ove Arup & Partners International Ltd., Coventry, 1998.
45. HARGREAVES, James. *Introduction to MSC.NASTRAN Training for ATG Graduates*. Advanced Technology Ove Arup & Partners International Ltd., Coventry.
46. OVE ARUP & PARTNERS INTERNATIONAL LTD. *Structural Modelling Manual*. Ove Arup & Partners International Ltd., London, 2002.
47. DALLARD, PAT. *Buckling – An Approach Based on Geometric Stiffness and Eigen Analysis*. Ove Arup & Partners International Ltd., London, June 1998.
48. MCKECHNIE, Steve. *Buckling Analysis Using the Dallard Method in GSA*. Ove Arup & Partners International Ltd., London, 2002.
49. OVE ARUP & PARTNERS INTERNATIONAL LTD. *Dynamics and Buckling in GSA*. Ove Arup & Partners International Ltd., London, 1999.
50. OVE ARUP & PARTNERS INTERNATIONAL LTD. *Nonlinear Analysis and Form-finding in GSA*. Ove Arup & Partners International Ltd., London, December 2002.
51. BANFI, Mike and FELTHAM, Ian. *Stability of Structures*. Ove Arup and Partners International Ltd., London, 2003.
52. BANFI, Mike and FELTHAM, Ian. *Preparing for the IStructE Part III Examinations*. Ove Arup and Partners International Ltd., London, 2003.
53. OVE ARUP & PARTNERS LTD. *An Arup Introduction to Structural Dynamics*. Ove Arup & Partners International Ltd., London.